Al-Mustansiriyah Journal of Science

ISSN 1814 - 635X

Vol. 24, No. 5, 2013

Special Issue: The Ninth Scientific Conference
College of Science (2013)

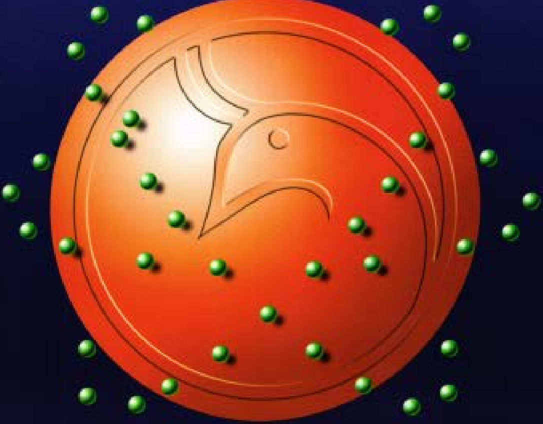

Issued by College of Science - Mustansiriyah University

Vol. 24
No. 5
2013

Al-Mustansiriyah Journal of Science

Issued by College of Science, Al-Mustansiriyah University, Baghdad, Iraq

Special Edition

The 9th Conference of the College Of Science, Al-Mustansiriyah University 6-7 May 2013

Mobile: 07711184399
e-mail: mustjsci@yahoo.com

INSTRUCTION FOR AUTHORS

1. The journal accepts manuscripts in Arabic and English languages. Which had not been published before.
2. Author (s) has to introduce an application requesting publication of his manuscript in the journal. Four copies (one original) of the manuscript should be submitted. Should be printed by on the computer by laser printer and re produced on A4 white paper in three coppice with floppy disc should be also submitted.
3. The title of the manuscript together with the name and address of the author (s) should typed on a separate sheet in both Arabic and English. Only manuscripts title to be typed again with the manuscript.
4. For manuscripts written in English, full name (S) of author (s) and only first letters of the words (except prepositions and auxiliaries) forming title of the manuscript should be written in capital letters. Author (s) address (es) to be written in small letters.
5. Both Arabic and English abstracts are required for each manuscript. They should be typed on two separate sheets (not more then 250 words each).
6. References should be denoted by a number between two bracket on the same level of the line and directly at the end of the sentence. A list of references should be given on a separate sheet of paper, following the interactional style for names and abbreviations of journals.
7. Whenever possible, research papers should follow this pattem: INTRODUCTION, EXPERIMENTAL (MATERIALS AND METHODS), RESULTS AND DISCUSSION, and REFERENCES. All written in capital letters at the middle of the page. Without numbers or underneath lines.
8. The following pattern should be followed upon writing the references on the reference sheet: Sumame (s), intials of author (s), title of the paper, name or abbreviation of the journal, volume, number, pages and (Year). For books give the author(s) name(s), the title, edition, pages, publisher, place of publication and (Year).
9. A publication fees in the amount of ID. 50 thousand is charged upon a Receipt of the paper and 25 thousand upon the acceptance for publication for their ID. 75 thousand should be paid for the editorial board.

CONTENTS

Fractal Dimension Based on Pixel Covering Method

Arkan J. Mohammed[1], Nadia M. G. Al-Saidi[2], and Adil M. Ahmed[3]
[1]Department of Mathematics-College of Science-Al-Mustansiriah University
[2]Applied Sciences Department-Applied Mathematics-University of Technology [3]Department of Mathematics, Ibn Al-Haytham College, University of Baghdad
Received 13/3/2013 – Accepted 15/9/2013

الخلاصة

البعد الكسوري هو احد الخصائص الاساسية التي تستخدم في تمييز الصور حيث يعتبر المفهوم الاساسي في هندسة الكسوريات والذي يستعمل لقياس نسبة التعقيد الهندسي للمجموعة الكسورية. التعريف الاساس للبعد الكسوري في هندسة الكسوريات هو من خلال البعد الهاوسدورفي والذي يصعب حسابه في أكثر الحالات. هناك العديد من الاتجاهات لحساب البعد الكسوري، قسم منها يعد غير كفوء حيث يعطي نتائج غير مقبولة عند استخدامه لتمييز الصفات المحلية للصورة. وللتغلب على هذا النوع من المشاكل قمنا في هذا البحث باقتراح خوارزميات جديدة تستخدم في تخمين البعد الكسوري والتي تعتبر خوارزميات موسعة للخوارزميتين التقليدية في حساب البعد الكسوري وهما (البعد التكعيبي وخوارزمية زمن الهروب) بالاعتماد على طريقة التغطية النقطية. الطرق المقترحة تستعمل كخاصية مهمة في العديد من التطبيقات في الطب،الهندسة والعلوم حيث انها تساعد على تحديد الخواص المحلية للصورة خلافا عن الطرق السابقة المصممة لايجاد البعد الكسوري للصورة بشكلها الكامل. الحسابات العددية تشير الى كفاءة هذة الطريقة مقارنة مع قسم من الطرق السابقة الواسعة الاستخدام.

ABSTRACT

Fractal dimension is an important feature of images, which is considered as a basic concept in fractal geometry used to measure the geometrical complexity of fractal set. In fractal geometry theory, the fundamental definition of fractal dimension have been based on Hausdorff dimension that is not easy to be estimated in most cases. There are many approaches to estimate the fractal dimension of an object, they compute inefficiently and the present of the local features of image invalidly. This paper addresses this problem by presenting a new estimated algorithm based on pixel covering method. The proposed approach will serve as an important characteristic for several applications in medical, engineering, and sciences, it helps to determine the local structure feature of image upon other conventional approaches used to determine the fractal dimension for the whole image. Experimental investigations indicate the efficiency of this approach compared with a well known widely used approaches such as; the box counting dimension, and the escape time dimension.

Keywords: Fractal Dimension (FD), Attractor, Box Counting Dimension (BCD), Escape Time Dimension (ETD), Pixel Covering Method (PCM).

1.Introduction

The description of irregular and random phenomenon in nature is performed through fractal that was established by B.B. Mandelbrot [1]. Fractal theory is a new system describe self-similarity, it has been studied by many researchers and successfully applied in many fields. Self-similarity could be also regarded as a measure of geometrical complexity of an object under discussion. Mandelbrot was the first that handled the irregularity of surfaces in an image through introducing the concept of FD, and described an approach to calculate it that is when he tried to estimate the length of the coastline. Although he did not give a precise definition of fractal, one can understand why, depends on the object studied, for this reason he give several non equivalent definitions of FD, that each problem should entail an appropriate notation of dimension [2].

Mandelbrot singled out "Hausdorff dimension", because most of the works of this subject was studied by Besicovitch, another type of dimension is belonging to the Bouligand-Minkowski dimension (Minkowski fractal dimension method) [3]. Some of them are equivalent but others are not. The most celebrated one is the Hausdorff (or Hausdorff–Besicovitch) dimension [4]. The most popular one is the box-counting dimension [4] a very similar method to Mandelbrot approach that is given by the Box-Counting theorem. There exist several equivalent definitions termed as a box-counting dimension. A capacity dimension (due to the definition given by Kolmogorov) and the Minkowski–Bouligand dimension are among them [4,5,6]. Although in many cases the Hausdorff dimension equals the box-counting dimension, in general the Hausdorff is used only in theoretical settings and is too subtle for practitioners [1,6]. Popular methods for estimating FD are also correlation dimensions [7] (Grassberger–Procaccia, Takens estimators) and information (or entropy) dimensions [8]. Bernsley [5] introduced the fractal interpolation method which applies iterated function system (IFS) to produce a fractal with known FD through N+1 points. These methods generate graphs which is attractor of the IFS of N contractive affine transformations. In the thesis of A. J. Mohammed [9], a new method to find the dimension of some fractals based on escape time principle was proposed using the method of spreading of the points inside a specific window with I=[-1,1]. In this paper a new estimated approach based on pixel covering method (PCM) is proposed. The proposed approach will serve as an important characteristic for several applications in image classification, object modeling, texture analysis and many other application in medical, engineering and sciences. It helps to determine the local structure feature of image upon other conventional approaches used to determine the FD for the whole image. Many other researchers proposed new approaches that used to improve the efficiency of FD estimation [8,10,11,12].

The material of this paper is arranged into six sections. Section 2 deals with the theoretical background of FD with some known types of fractal dimensions. Box-counting dimension with the proposed Box counting algorithm based on PCM is described in section 3. The ETD with the proposed escape time algorithm is presented in section 4. Section 5 is devoted to present the algorithm implementation with the numerical experiments. Finally, some conclusions are summarized in section 6.

2. Theoretical Background

Theory of fractal sets is a modern domain of research; whereas, the complexity of fractal set can be reflected using fractal dimension. This section presents an overview of major concepts and results that help to understand the FD and their counting methods, a more detailed review of the topics are as in [1,5,13,14].

Let (X,d) be a metric space, $Y \subseteq X$. Then Y is called totally bounded (precompact) if for each $\varepsilon > 0$, there exists a finite set of points $\{x_j\}_{j \in J_m} = \{x_1, x_2, \ldots, x_m\}$ such that $\bigcup_{j \in J_m} \overline{B}(x_j, \epsilon) \supseteq Y$ where $\overline{B}(x_j, \varepsilon) = \{x \in X : d(x, x_j) \leq \varepsilon\}$. When Y is totally bounded. Let $N_\varepsilon(Y) = min\{|J| : \bigcup_{j \in J} \overline{B}(x_j, \varepsilon) \supseteq Y\} = min\{m : \bigcup_{j \in J_m} \overline{B}(x_j, \varepsilon) \supseteq Y\}$.

Let C(Y) be the capacity (length, area, volume) of the subset Y of X. Therefore, $C(Y) = N_\varepsilon(Y)\varepsilon^{d(\varepsilon)}$. Then $d(\varepsilon)$ is a function of ε, where $d(\varepsilon) = \frac{ln(N_\varepsilon(Y))}{ln(1/\varepsilon)} - \frac{ln(C(Y))}{ln(1/\varepsilon)}$. If the $\lim_{\varepsilon \to 0} d(\varepsilon)$ exists, and equal to a real number d, then d is called the capacity dimension of Y. If the capacity dimension d not integer, then Y is called a fractal, and d is called a fractal dimension.

When $X = R^m$, and $Y \subseteq X = R^m$. Let $0 < r < 1$, and $r^n < \varepsilon \leq r^{n+1}$ for some positive integer n. Then $d = \lim_{\varepsilon \to 0} d(\varepsilon) = \lim_{n \to \infty} d(r^n)$.

Therefore $d = \lim_{\varepsilon \to 0} \frac{ln(N_\varepsilon(Y))}{ln(1/\varepsilon)} = \lim_{n \to \infty} \frac{ln(N_n(Y))}{n\,ln(1/r)}$. Then d is called box dimension, and the way to calculate d is called box counting dimension.

Let $X = R^m$, and $d(x,y) = (\sum_{j \in J_m}(x_j - y_j)^2)^{1/2}$ is a metric mapping defined on R^m. Then $(X,d) = (R^m, d)$ is a metric space. The mapping $f : X \to X$ is called contraction mapping when $d(f(x), f(y)) \leq sd(x,y)\ \forall$ $x, y \in X, s \in [0,1)$, which is a contractivity of f and similarity mapping when $d(f(x), f(y)) = sd(x,y)$ for all $x, y \in X, s \geq 0$, when $s = 1$, f is called isometry.

Let (R^m, d) be a complete metric space. Then $H(R^m)$ denote the set of all non-empty compact subsets of R^m and D is the Hausdorff metric on $H(R^m)$ defined by

$$D(A,B) = max\{\max_{b \in B}.\min_{a \in A} d(a,b), \max_{a \in A}.\min_{b \in B} d(a,b)\} \quad \text{for all } A, B \in H(R^m).$$

Then $(H(R^m), D)$ is a metric space.

Let $\{f_j\}_{j\in J_N}$ be the set of contraction mappings on R^m, with contractivity s_j $for\ j\in J_N$. Then $F(A)=\bigcup_{j\in J_N} f_j(A)$, for all $A\in H(R^m)$ is a contraction mapping on the complete metric space $(H(R^m),D))$ with contractivity $s=max\{s_j : j\in J_N\}$.By the contraction mapping theorem, there exists a fixed point $A\in H(R^m)$ such that $F(A)=A$,and $\lim_{n\to\infty} F^n(B)=A$ for all $B\in H(R^m)$. These fixed point A is called the attractor set. Let $B=I^m=[0,1]^m\in H(R^m)$, $F(I^m)=\bigcup_{j\in J_m} f_j(I^m)\subseteq I^m$ and

$I^m\supseteq F(I^m)\supseteq F^2(I^m)\supseteq\cdots\supseteq A$. Then $A=\bigcap_{n\in N} F^n(I^m)=\lim_{n\to\infty} F^n(I^m)$.

When f_j is a family of affine transformation $f_j(x)=s_jR_j(x)+b_j$, where R_j is an isometry and b_j is a transformation on I^m for $j\in J_N$, and for all $x\in I^m$. Then $A=f(A)$ is called self similarity in I^m, and d=dim A is the solution of $\sum_{j\in J_N} s_j^d=1$, is called similarity dimension of A it is calculated by $y=\sum_{j\in J_N} s_j^d$ when y=1.

Let (X,d) be a metric space, and $f:X\to X$ be a contraction mapping, then (X,f) is called dynamical system, when $f^{\circ}(x)=x, f^{n+m}(x)=f^n(f^m(x)), \forall x\in X$ and n,m are positive integers. Let $x_{n+1}=f(x_n)$ for all positive integer n.

Then $x=\lim_{n\to\infty} x_{n+1}=\lim_{n\to\infty} f(x_n)=f(\lim_{n\to\infty} x_n)=f(x)$. Let

$Y=\{x\in X : f(x)=x\}\subseteq$X. It is not easy to find Y, but

$Y=\{x\in X : \exists x_{\circ}\in X\ such\ that\ \lim_{n\to\infty} f^n(x_{\circ})=x\}$, when $X=I^m$ and

$f=(f_1,f_2,\ldots,f_m)$ where $f_j(x)=x_j$ for all $j\in J_m$. Then $x=(x_1,x_2,\ldots,x_m)$ implies $f(x)=x\in Y$.To find this x, let $x_n=(x_1^n,x_2^n,\ldots,x_m^n)$ and $x_j^{n+1}=f_j(x_n)$. Therefore $\lim_{n\to\infty} f_j(x_n)=x_j=\lim_{n\to\infty}(f^n(x_{\circ})$. This will form the escape time method.

3. Box Counting Dimension

Since the fractal dimension may be found by using the box counting dimension which is used on totally bounded sets by means of PCM for 2D monochrome images, which means that it is useful when we deals with fractals with dimension between 1 and 2, since we are aiming to find the dimension for the 3-dimentional object, this requires these images to be binarized in order to be estimated using pixel covering method; this may cause loss of information, which is not acceptable in many image processing applications, in addition, there is an underlying uncertainty accompanying of any estimation of FD according to the truncated error accrued as a result of iterative process and to using a sample of points for any object. To resolve this restriction the box counting method needs some modification to be general and suitable for all application based on 3- dimensional objects. Thus, a new approach is introduced in this work.[15]

Also, For computer applications, the data is usually discretized, the PCM is proposed to estimate the FD of fractal binarized images where points are represented by 1, while the background is represented by 0. The image Y is divided into squares with width ε, where $N_\varepsilon(Y)$ represents the minimum number of sets with radius less than or equals ε that covers Y. Hence, a group of data (-log δ_i, log $N_{\delta i}(Y)$) is obtained and the FD is estimated by changing the value of δ, it is the slop of the line derived from these data using the least squares linear regression. This is possible when the contraction mapping for the fractal Y is known, if not, so, it is not easy to calculate the box dimensions of a locally bounded subset $Y \subseteq I^m$, where $\delta(r^n) = \lim_{n\to\infty} \frac{ln(N_{(\frac{1}{2})^n}(Y))}{n\,ln2}$. Hence, we proposed a new estimation method to find δ, which is presented as follows:

3.1 The proposed algorithm to estimate FD

For a sufficiently large integer $n \in N$, let $S_n=\{0,1,2,\ldots,2^n-1\}$, and $p_n = \{\frac{0}{2^n}, \frac{1}{2^n}, \ldots, \frac{2^n-1}{2^n}\}$

Where $p_n \subseteq I = [0,1]$ with $|s_n|=|p_n|=2^n$.

Let $x^j = \frac{1}{2}(1 + \frac{(-1)^{j_1}}{2} + \frac{(-1)^{j_2}}{2^2} + \cdots + \frac{(-1)^{j_n}}{2^n})$, where $j_i \in \{0,1\}$.

Then $j=(j_1,j_2,\ldots j_n)=j_1+2j_2+\ldots+2^n j_n$, is a permutation of S_n and $x^j = (x_1^{j_1}, x_2^{j_2}, \cdots, x_m^{j_m}) \in I^m$ is a permutation of p_n.

Then $\hat{I}^m = \{x^j = (x_1^{j_1}, x_2^{j_2}, \cdots, x_m^{j_m}) : j_i \text{ is a permution of } p_n\}$, then we have $|\hat{I}^m| = 2^{nm}$ pixels, and these pixels will form partition of I^m as a small box region, where their vertices are these pixels.

Let $\hat{Y}\hat{Y} = \{x^j \in Y\}$ be the set of pixels in $Y \in H(I^m)$, since $N_{(1/2)^{n+1}}(Y) = min\{m : \bigcup_{j\in J_m} \hat{B}(x_j^j, (\frac{1}{2})^{n+1} \supseteq Y\} = N_{(1/2)^{n+1}}(\hat{Y})$.

Therefore, $\hat{\delta} = \frac{N_{(1/2)^{n+1}}(Y)}{n\,ln2} = \frac{N_{(1/2)^{n+1}}(\hat{Y})}{n\,ln2}$ is an approximate box dimension of $Y \in H(I^m)$.

The number of pixels in $\hat{Y}\hat{Y}$ can be calculated through the scanning way to all of these pixels in a given space, and as follows:
For each $x^j \in \hat{I}^m$, factorize $x^j = (x_1^{j_1}, x_2^{j_2}, \cdots, x_m^{j_m})$ into m collections of subsets, each has 2^n pixels that represent the value of $x=(x_1,x_2,\ldots,x_m)$. This can be performed using the recursive sequence of points $t_{i-1}=2^n t_i+k_i$, and $x_i=(k_i/2^n)\in[0,1]$ that scans all $\hat{I}^m$ pixels. Hence, it is easy to count the number of pixels $N_n(\hat{Y})$ in $\hat{Y}$. Then $\hat{\delta}=\frac{N_n(\hat{Y})}{n\ln 2}$ that represents the box dimension of the set $Y\in H(I^m)$, as in the following algorithm.

PCMD1 Algorithm

Input $m,n\in N$, where n is a large positive integer
$p=2^n$, $q=p^m-1$
Input $t_0\in Z_q$
Input Y
Factor $(t_0)=(k_1,k_2,\ldots k_m)\in Z_q^m$
  For $t_0=0 : 2^{nm}-1$
    For $i=1$: m
      $t_{i-1}=t_i p+k_i$
      $x_i=k_i/p$
    End i
      If $x=(x_1,x_2,\ldots,x_m)\in Y$, then $No=No+1$
  End t_0
Output $(x_1,x_2,\ldots,x_m)\in I^m$
Output $\hat{\delta}=\frac{N_0}{n\ln 2}$

Then $\hat{\delta}\hat{\delta}$ is a box dimension of Y, and if Y is a fractal, then $\hat{\delta}$ is called box dimension of the fractal Y.

Example 1

Let m=2, n=6, let Y is the given set as follows, where Dim(Y)=0.6813.
Y={(0.15625,0),(0.03125,0.03125),(0.125,0.5),(0,0.75),(0.5,0.03125), (0.28125,0.0635),(0.25,0.25),(0.96875,0.0625), (0.78125,0.09375),(0.5,0.125)(0.375,0.25),(0.25,0.3125), (0.25,0.4375),(0.375,0.5635), (0.875,0.625),(0.125,0.953125), (0.859357,0.156625) }.

Figure-1:A given set Y in I^2

For n=2 , $\hat{\delta}=\frac{\ln 2}{2\ln 2}=0.5$ For n=3, $\hat{\delta}=\frac{\ln 6}{3\ln 2}$=0.8617

For n=4, $\hat{\delta}=\frac{\ln 9}{4\ln 2}$ =0.7925   For n=5, $\hat{\delta}=\frac{\ln 15}{5\ln 2}=0.7814$

Then for large n, $\hat{\delta}=0.6813$.

4. Escape Time Dimension (ETD)

In this section, a new ETD is proposed, it is considered as a general algorithm whih is applicable for fractals generated using "Escape Time Algorithm", [5]. These fractals are generated by repeatedly applying a transformation to a given point in the plane, using an initial point; the resulted series of the transformed points is called the orbit of this point. The orbit is called diverges when its points grow further apart without bounds. In this case, a fractal can be defined as; "the set of points whose orbit does not diverge". With the existence of the same restriction mentioned in section 3, the proposed algorithm is considered useful, and also it is more efficient than the one proposed by [9], as we will show in the next section.

4.1Fractal generated by ETA

Let (X,d) be a metric space, for $f:X\to X$, $f^0(x)=x$, and $f^n(x)=f(f^{n-1}(x))$, for all $x\in X$. The sequence $\{x_n\}_{n=0}^{\infty}$ in X is generated as; $x_1=f(x_0)$, $x_2=f(x_1),\ldots,x_n=f(x_{n-1})$, where $x_n=f^n(x_0)$, for all $n\in N$, and $x_0\in X$. The convergence of the sequence $\{x_n\}$ in X is called *the attractor* of f in X, where $\{x=\lim\limits_{n\to\infty} x_n \in X\}=Y=\{x\in X : f(x)=x\}\subseteq X$.

4.2 The Proposed Escape Time Dimension (ETD)

Let (R^m, d') is a complete metric space where d' is the usual metric and $Y\in H(R^m)$ where Y is closed and totally bounded (i.e there exist $M>0$, such that $D(x,y)\le M$, for all $x,y\in Y$). Now if $M>1$, then the dimension of the attractor Y can be calculated by $\delta=\lim\limits_{\varepsilon\to\infty}\delta(\varepsilon)=\lim\limits_{\varepsilon\to 0}\frac{ln(N_\varepsilon(Y))}{ln(1/\varepsilon)}$, where $Y\subseteq I^m=[0,1]^m\subseteq R^m$, and $d(x,y)=(1/M)$ $d'(x,y)\le 1$.

Hence δ is the ETD of the attractor in the set Y and it can be calculated using the same proposed algorithm, and as follows.

PCMD2 Algorithm

Input $m,n\in N$, where n is a large positive integer

$p=2^n$, $q=p^m-1$

Input $t_0\in Z_q$, $S\in N$

Factor $(t_0)=(k_1,k_2,\ldots k_m)\in Z_q{}^m$

For $t_0=0 : 2^{nm}-1$

For $I=1: m$

$t_{i-1}=t_ip+k_i$

$x_i=k_i/p$

End I

For $j=0: S$

If $f^j(x)\in I^m$

End j
If $j>S$, then $x=(x_1,x_2,\ldots,x_m)\in Y$, and $No=No+1$
End t_0

Output Y, $\hat{\delta}=\dfrac{N_0}{n\ln 2}$

Then $\hat{\delta}\,\hat{\delta}$ is the ETD of Y, and if Y is a fractal, then $\hat{\delta}$ is called ETD of the fractal Y.

5. Experimental results and Implementation

The PCMD1 and PCMD2 algorithms with their graphic user interface (Figure 2) are carried out using Visual Basic. The results have been obtained by using a computer with the specifications 2.0 GHz Intel COR i5 CPU and 2 GB RAM.

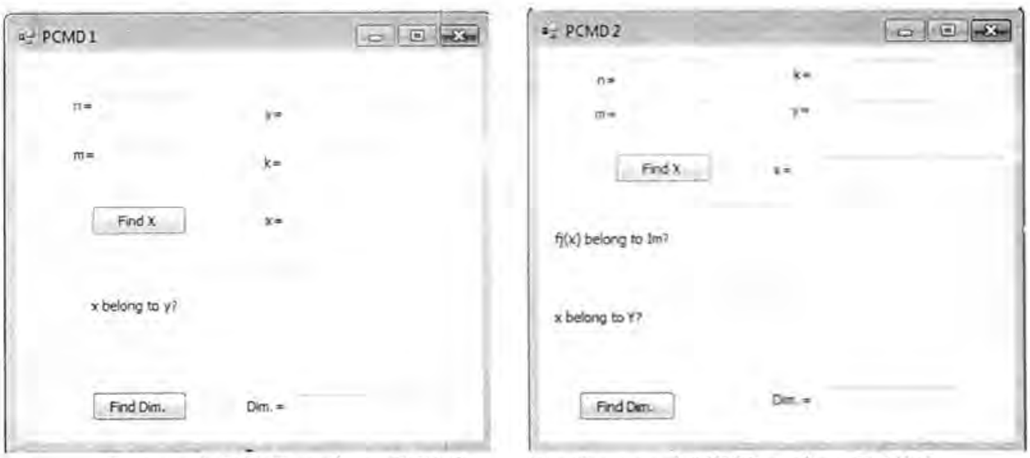

A. General BCD using PCM B. General ETD using PCM

Figure-2: User interface to calculate FD using PCMD1 and PCMD2

Table-1:Fractal Dimension comparison using the classical and proposed methods for some known fractal sets.

Iterated Function f	BCD	ETD	PCMD1	PCMD2
Sierpinski triangle	1.58496	1.58	1.58012	-
Filled Julia sets c=(0.2,0.7)	-	1.520263	-	1.51973
Cantor set	0.63093	0.63	0.629456	-
$Y=f(z)=z^2-1.25$	-	1.2845	-	1.27952

6.CONCLUSIONS

The fractal dimension is the basic concepts of fractal geometry and serves as an important feature of image. In many applications, the data sets do not strictly follow the definition of fractal, but only follow a certain range of scales. With the unavailability of a contraction mapping for many fractal images, the conventional methods that based on the using the coefficients in these mapping became useless, which motivating the researchers to always search for new methods to overcome these restrictions. In this paper, two new algorithms for the estimation of the FD are proposed. They are considered as a generalization for the well known and widely used algorithms; "*the box counting dimension*" and "the *escape time dimension*". It seems that from the experimental results, the proposed methods could be particularly useful to be applicable for various real world applications that based on gray scale and 3- dimensional levels in comparison with the corresponding classical methods used to estimate fractal dimension.

REFERENCES

1. Mandelbrot, B.B., "*The Fractal Geometry of Nature*", W.H. Freeman, NewYork, 1983.
2. Feng, Z.and Zhou, H., "*Computing method of fractal dimension of image and its application*". Journal of Jiangsu University of Science and Technology, No. 6, 2001, pp. 59-66.
3. Shuai, L.a, Xiangjiu, C.and Zhengxuan, W., "*Improvement of Escape Time Algorithm by No-Escape-Point*". Journal of Computers, Vol 6, No 8 (2011), pp. 1648-1653.
4. Falconer, K., "*Fractal Geometry Mathematical Foundations and Application*". John Wiley & Sons Ltd, 2nd edition, 2003.
5. Barnsley, M.F., "*Fractals everywhere*", 2ed. Academic Press Professional, Inc., San Diego, CA, USA, 1993.
6. Cherbit (Eds.), G., "*Fractals. Non-integral Dimensions and Applications*", Wiley, New York, 1990.
7. Grassberger, P.,"An Optimized Box-assisted al-gorithm for Fractal Dimensions" Phys. Lett. A 148 (1990),pp63-68.
8. Skubalska-Rafajłowicz, E., "*A new method of estimation of the box-counting dimension of multivariate objects using space-filling curves*". Nonlinear Analysis 63 (2005) e1281 – e1287.
9. Mohammed, A.J., "*On dimensions of some fractals*". Ph.D. thesis, Al- Mustansiriah University, 2005.
10. BÃlachowski ,A.and Ruebenbauer, K., "*Roughness Method to Estimate Fractal Dimension*". ACTA PHYSICA POLONICA A, Vol. 115 (2009).
11. André Backes, R.and Bruno Odemir, M., "*Fractal and Multi-Scale Fractal Dimension analysis: a comparative, study of Bouligand-Minkowski method*". CoRR abs/1201.3153: (2012).
12. Cholhui, Y., "*Box-Counting dimension of a kind of fractal interpolation surface on rectangular grids*". Romanian Journal of Mathematics and Computer science, 2(2)(2012), pp. 61-69

13. Peinke, J., Parisi,J., Rossler, O., E. and Stoop, R., "*Encounter with Chaos*". Springer, New York, 1992.
14. Peitgen, H., Jürgens, H.and Saupe, D. ,"*Chaos and Fractals: New Frontiers of Science*". 2ed, Springer, 2004.
15. Du, J. Gao, Y. Peng Qu, X. Xu, Zheng, Y., "*Multi- Multi-Feature Edge Extraction for Gray-Scale Images with Local Fuzzy Fractal Dimension*". Seventh International Conference on Fuzzy Systems and Knowledge Discovery (FSKD 2010), 2010.

Approximation of Unbounded Functions by Comonotone Polynomials

Saheb K. Jassim ، Israa Z. Shamkhi
Department of Mathematics- College of Science – Al-Mustansiriya University

Received 11/3/2013 – Accepted 15/9/2013

الخلاصة

الغرض من هذا البحث هو دراسة تقريب الدوال غيرالمقيدة في الفضاءات $L_{p,\alpha}[-1,1],\ 0 < p \le \infty$ بواسطة متعددات حدودية متساوية الرتابة . درجة افضل تقريب للدوال غير المقيدة وجدت بدلالة مقياس النعومة $\omega_2^{\varphi}(f,\delta)_{p,\alpha}$

ABSTRACT

The Purpose of this paper is to study the approximation of unbounded functions in the spaces $L_{p,\alpha}[-1,1]$, $0 < p \le \infty$ by comonotone polynomials. We find the degree of best approximation of unbounded functions in terms of the second Ditizian-Totik modulus of smoothness.

1. INTRODUCTION

In recent year the approximation by comonotone polynomial has been studied by [1] such that R.K.Beston and D.Leviatan obtain some results on the approximation of commonotone polynomials and N.M.Kassim [2] discussed approximation of bounded function by using comonotone and monotone polynomials in L_p-spaces ($0 < p < 1$) in terms modulus of smoothness.The main departure from these pervious works is that we shall prove direct estimates for the error of polynomial approximation in terms of the Ditizian Totick modules of smoothness .

2. Definition and notation

Let P_n denote the set of all algebraic polynomials of degree $\le$ n and $L_{p,\alpha}[-1,1]$ the set of all functions on $[-1,1]$ such that,

$$\|f\|_{p,\alpha} := \left(\int_a^b \left|f(x)e^{-\alpha x}\right|^p dx\right)^{\frac{1}{p}} < \infty \quad, \ 0 < p < \infty$$

Let $Y_r := \{y_1, \ldots, y_r \mid y_0 := -1 < y_1 < \ldots < y_r < 1 =: y_{r+1}\}$, $r \in N$. Denote by $\Delta^1(Y_r)$ the set of all nondecreasing functions f on $[y_{r-2k}, y_{r-2k+1}]$ and is nonincreasing on$[y_{r-2k-1}, y_{r-2k}]$, $(k \in N)$ that is mean those have r monotonicity changes at the points in Y_r and are nondecreasing near 1.

Let $\Delta^1 := \Delta^{(1)}(Y_0)$ denote the set of all nondecreasing functions on $[-1,1]$. Function from the class $\Delta^{(1)}(Y_r)$ are said to be comonotone with one another, comonotone polynomial approximation is the approximation of function $f \in \Delta^1(Y_r)$ by polynomial which are comonotone with it.

For $f \in L_{p,\alpha}[-1,1]$ let us define the degree of comonotone polynomial approximation of f by

$$E_n^{(1)}(f, Y_r)_{p,\alpha} := \inf_{p_n \in P_n \cap \Delta^1(Y_r)} \|f - p_n\|_{p,\alpha} \quad \text{, if exist} \qquad \ldots(2.1)$$

The m-th order Ditizian-Totik modulus of smoothness $\omega_m^{\varphi}(f, \delta)_{p,\alpha}$ is given by

$$\omega_m^{\varphi}(f, \delta)_{p,\alpha} := \sup_{0<h\le\delta} \left\|\Delta_{h\varphi(\cdot)}^m (f, \cdot) e^{-\alpha x}\right\|_p,$$

where $\varphi(x) = \sqrt{1-x^2}$ and

$$\Delta_{h\varphi(x)}^m (f, x) := \begin{cases} \sum_{i=0}^{m} (-1)^{m-i} \binom{m}{i} f(x - \frac{m}{2}\eta + i\eta) & , \ x \mp \frac{m}{2}\eta \in [-1,1] \\ 0 & , \ \text{o.w} \end{cases}$$

Define d(r) by,

$d(r) := \min\{y_1, y_2 - y_1, \ldots, y_r - y_{r-1}, 1 - y_r\}$

Now, in [3] for sufficiently large $\mu = \mu(r)$, there exists polynomials $v_n(x)$ and $w_n(x)$ of degree $\le c(r)\, n$ such that the polynomial

$$p_n(x) := (q_n(x) - q_n(y_1))\, v_n(x) + q_n(y_1) w_n(x) \qquad \ldots(2.2)$$

is comonotone with f, and the following inequalities are satisfied

$$\begin{aligned} |\operatorname{sgn}(x - y_1) - v_n(x)| &\le c(r)\psi_j^{\mu}(x), \\ |\operatorname{sgn}(x - y_1) - w_n(x)| &\le c(r)\psi_j^{\mu}(x), \end{aligned} \qquad \ldots(2.3)$$

Where $\psi_j(x) = \dfrac{h_j}{|x - x_j| + h_j}$ (recall that $y_1 \in [x_j, x_{j-1}]$).

3-The Main Results

It is found that the degree of approximation of a comonotone polynomial are in stages. In the first approximant $f \in L_{p,\alpha}[-1,1] \cap \Delta^1(Y_r)$ by continuous piecewise linear spline $s \in \Delta^1(Y_r)$ that is

$$\|f - s\|_{p,\alpha} \le c\,\omega_2^{\varphi}(f, n^{-1})_{p,\alpha},$$

where

$$\omega_2^{\varphi}(f, n^{-1}) := \sup_{0<h\le s} \left\|\Delta_{h\varphi(x)}^2 (f, \cdot) e^{-\alpha x}\right\|_p$$

Then the study shows how to approximate s by a polynomial in $\Delta^1(Y_r)$,use [4] for formation the partition of the interval [–1,1] by the nodes x_k ,k = 0, …, n with Y_r then delete x_i and x_{i-1} for which there is a y_j , j = 1, …, r such that $x_{i-1} \le y_j \le x_i$ and end up a new partition which denote $Z_{r,n}$ by :

$$Z_{r,n} := Y_r \cap \left(\{x_k\}_{k=0}^{n} \setminus \{x_i, x_{i-1} : x_{i-1} \le y_j \le x_i \text{ for some } j = 1,\ldots,r\}\right) \quad (3.1)$$

And can be chose $\overline{s}$ for every interval [-1,1] of the partition $Z_{r,n}$ the restriction of $\overline{s}$ to I is a near-best linear approximant to f in $L_{p,\alpha}(I)$.

Let $\overline{y} \in [x_{i-1}, x_i]$, say and suppose that p_1 is non decreasing and p_2 is non increasing.

Now define s in $[x_{i-3}, x_{i-2}]$ as the piecewise linear continuous spline $s(x) = \overline{s}(x)$ for $x \notin (x_{i-2}, x_{i+1})$ and $s(\overline{y}) = p_1(\overline{y})$, if $p_2(x_{i-2}) \le p_1(x_{i+1})$ or $s(\overline{y}) = p_2(\overline{y})$ if $p_2(x_{i-2}) > p_1(x_{i+1})$. A continuous piecewise linear spline s $\in \Delta^1(Y_r)$ is obtained [4].

Lemma (3.1):

Let a function $f \in L_{p,\alpha} \cap \Delta^1(Y_r)$, $0 < p \le \infty$, then for every $n \ge c(r)/d(r)$ $(d(r) \ne 0)$there exists a continuous piecewise linear spline $s \in \Delta^1(Y_r)$ on the knot sequence $Z_{r,n}$ satisfying

$$\|f - s\|_{p,\alpha} \le c\,\omega_2^{\varphi}(f, n^{-1})_{p,\alpha} \quad \ldots(3.2)$$

and

$$\omega_2^{\varphi}(s, n^{-1})_{p,\alpha} \le c\,\omega_2^{\varphi}(f, n^{-1})_{p,\alpha} \quad \ldots(3.3)$$

Proof:

First proof (3.3) by using (3.2)

$$\omega_2^{\varphi}(s, n^{-1})_{p,\alpha} = \omega_2^{\varphi}(s - f + f, n^{-1})_{p,\alpha}$$
$$\le c_1\omega_2^{\varphi}(s - f, n^{-1})_{p,\alpha} + c_2\omega_2^{\varphi}(f, n^{-1})_{p,\alpha}$$
$$\omega_2^{\varphi}(s, n^{-1})_{p,\alpha} = c\|s - f\|_{p,\alpha} + c_2\omega_2^{\varphi}(f, n^{-1})_{p,\alpha}$$
$$\le c_3\omega_2^{\varphi}(f, n^{-1})_{p,\alpha} + c_2(r)\omega_2^{\varphi}(f, n^{-1})_{p,\alpha}$$

Hence,

$$\omega_2^{\varphi}(s, n^{-1})_{p,\alpha} \le c\,\omega_2^{\varphi}(f, n^{-1})_{p,\alpha}$$

Now to prove (3.2) construct a spline $\overline{s}$ which satisfies the condition for each $n > c(r) / d(r)$ such that

$$E_n^{(1)}(f, Y_r)_{p,\alpha} \le c(r)\omega_2^{\varphi}(f, n^{-1})_{p,\alpha}$$

Consider the case where $p_2(x_{i-2}) \le p_1(x_{i+1})$, the other case is analogous, all are shows as follows :

$$\|f - s\|^p_{p,\alpha[x_{i-2},\overline{y}]} = \|f - p_2 + p_2 - s\|^p_{p,\alpha[x_{i-2},\overline{y}]}$$
$$\|f - s\|^p_{p,\alpha[x_{i-2},\overline{y}]} \le \|f - p_2\|^p_{p,\alpha[x_{i-2},\overline{y}]} + \|s - p_2\|^p_{p,\alpha[x_{i-2},\overline{y}]}$$

To estimate the term $\|s - p_2\|^p_{p,\alpha[x_{i-2},\overline{y}]}$. Indeed

$$\|s-p_2\|_{p,\alpha[x_{i-2},\bar{y}]}-|s(\bar{y})-p_2(\bar{y})|-|p_1(\bar{y})-p_2(\bar{y})|$$
$$\le\|s-p_2\|_{p,\alpha[x_{i-2},\bar{y}]}-|s(\bar{y})-p_2(\bar{y})-p_1(\bar{y})+p_2(\bar{y})|$$
$$=\|s-p_2\|_{p,\alpha[x_{i-2},\bar{y}]}-|s(\bar{y})-p_1(\bar{y})|$$
$$\|s-p_2\|_{p,\alpha[x_{i-2},\bar{y}]}-|s(\bar{y})-p_2(\bar{y})|-|p_1(\bar{y})-p_2(\bar{y})|$$
$$\le c|s(\bar{y})-p_2-s(\bar{y})+p_1(\bar{y})|$$
$$=c\|p_1-p_2\|_{p,\alpha[x_{i-2},\bar{y}]}$$

Therefore,

$$\|s-p_2\|_{p,\alpha[x_{i-2},\bar{y}]}-|s(\bar{y})-p_2(\bar{y})|-|p_1(\bar{y})-p_2(\bar{y})|$$
$$\le c\,h_i^{-1/p}\|p_1-p_2\|_{p,\alpha[x_{i-2},\bar{y}]}\le c_1\|p_1-p_2\|_{p,\alpha[x_{i-2},\bar{y}]} \qquad \ldots(3.4)$$

where $h_i=|x_{i-1}-x_i|$

Then from (3.4)

$$\|f-s\|^p_{p,\alpha[x_{i-2},\bar{y}]}\le\|f-p_2\|^p_{p,\alpha[x_{i-2},\bar{y}]}+\|s-p_2\|^p_{p,\alpha[x_{i-2},\bar{y}]}$$
$$\le\|f-p_1\|^p_{p,\alpha[x_{i-2},\bar{y}]}+\|p_1-p_2\|^p_{p,\alpha[x_{i-2},\bar{y}]}$$
$$\le\|f-p_1\|^p_{p,\alpha[x_{i-2},\bar{y}]}+\|f-f+p_1-p_2\|^p_{p,\alpha[x_{i-2},\bar{y}]}$$
$$\le\|f-p_1\|^p_{p,\alpha[x_{i-2},\bar{y}]}+c_1\|f-p_1\|^p_{p,\alpha[x_{i-2},\bar{y}]}+c_2\|f-p_2\|^p_{p,\alpha[x_{i-2},\bar{y}]}$$

Hence

$$\|f-s\|^p_{p,\alpha[x_{i-2},\bar{y}]}\le c\|f-p_1\|^p_{p,\alpha[x_{i-2},\bar{y}]}+\|f-p_2\|^p_{p,\alpha[x_{i-2},\bar{y}]}$$

Now in this part, prove that f is going to be a continuous piecewise linear function on the Knot sequence $Z_{r,n}$ which belongs to $\Delta^1(Y_r)$ and satisfying $f(y_1)=0$.

Lemma (3.2):

Let $y_1\in I_j:=[x_{j-1},x_j]$ and set $h_j:=|I_j|=x_j-x_{j-1}$. Show that

$$\|f\|_{L_{p,\alpha[y_1-\frac{h_j}{6},y_1+\frac{h_j}{6}]}}\le c\omega_2(f,h_j,J_j)_{p,\alpha}$$

where

$J_j=[x_{j-2},x_{j+2}]$

Proof:

In the first, take L to be the straight line such that $L|_{[x_{j-2},\bar{y}]}=f|_{[x_{j-2},\bar{y}]}$, and get

$$\|f\|_{L_{p,\alpha[y_1-\frac{h_j}{6},y_1]}} \le \|f-L\|_{L_{p,\alpha[y_1-\frac{h_j}{6},y_1]}}$$

$$= \left\| f(x)-L(x)+2L(x)-2L(x)+\frac{Lh_j}{3}-\frac{Lh_j}{3} \right\|_{p,\alpha[y_1-\frac{h_j}{6},y_1]}$$

$$= \left\| f(x)-L(x)+L(x)+L(x)-2L(x)+\frac{Lh_j}{3}-\frac{Lh_j}{3} \right\|_{p,\alpha[y_1-\frac{h_j}{6},y_1]}$$

$$= \left\| f(x)-L(x+\frac{h_j}{3})-2L(x+\frac{h_j}{6}) \right\|_{p,\alpha[y_1-\frac{h_j}{6},y_1]}$$

$$= \left\| \Delta^2_{\frac{h_j}{6}} f \right\|_{p,\alpha[y_1-\frac{h_j}{6},y_1]}$$

$$= \sup_{0<h<\frac{h_j}{6}} \left\| \Delta^2_{\frac{h_j}{6}} f \right\|_{p,\alpha[y_1-\frac{h_j}{6},y_1]}$$

$$\|f\|_{L_{p,\alpha[y_1-\frac{h_j}{6},y_1]}} \le c\omega_2(f,h_j,I_j)_{p,\alpha}$$

Similarly, can show that

$$\|f\|_{L_{p,\alpha[y_1,y_1+\frac{h_j}{6}]}} \le c\omega_2(f,h_j,J_j)_{p,\alpha}$$

Then

$$\|f\|_{L_{p,\alpha[y_1-\frac{h_j}{6},y_1+\frac{h_j}{6}]}} \le c\omega_2(f,h_j,J_j)_{p,\alpha} \qquad \ldots(3.5)$$

And, while $I_j \subset J_j$ have $|I_j| \le c|J_j| - ch_j$, and for $n \ge c(r) / d(r)$, with sufficiently large c(r) the result is :

$$\omega_2(f,h_j,J_j)_{p,\alpha} \le c\,\omega_2^{\varphi}(f,n^{-1})_{p,\alpha} \qquad (3.6)$$

And (3.5) become,

$$\|f\|_{L_{p,\alpha}} \le c\omega_2^{\varphi}(f,h_j,J_j)_{p,\alpha}$$

Now, to prove the following theorem the following notations are necessary.

Define the function $\hat{f}(x)$ by:

$$\hat{f}(x) := \begin{cases} -f(x) & \text{if } x < y_1 \\ f(x) & \text{if } x \ge y_1 \end{cases}$$

The function $\hat{f}$ is continuous piecewise linear spline from the class $\Delta^1(Y_r/\{y_1\})$ and (3.6) implies that for $n \geq \frac{c(r)}{d(r)}$

$$c\,\omega_2^{\varphi}(\hat{f}, n^{-1})_{p,\alpha} \leq \omega_2^{\varphi}(f, n^{-1})_{p,\alpha} \qquad ...(3.7)$$

Lemma (3.3):[3]

Let q_n be a polynomial which is comonotone with $\hat{f}$ such that

$$\left\|\hat{f} - q_n\right\|_p \leq c\,\omega_2^{\varphi}(\hat{f}, n^{-1})_p$$

Lemma (3.4):

Let $f \in L_{p,\alpha}[-1,1]$,$(0 < p \leq \infty)$ and q_n be comonotone polynomial we have

$$\left\|\hat{f} - q_n\right\|_{p,\alpha} \leq c\,\omega_2^{\varphi}(\hat{f}, n^{-1})_{p,\alpha}$$

Proof:

$$\left\|\hat{f} - q_n\right\|_{p,\alpha} = \left\|\left(\hat{f} - q_n\right)e^{-\alpha x}\right\|_p$$
$$= \left\|\hat{f}\, e^{-\alpha x} - q_n e^{-\alpha x}\right\|_p$$

Let $\hat{f}\, e^{-\alpha x} = F$ and $q_n\ e^{-\alpha x} = p_n$ where F is bounded function and p_n comonotone polynomial then by using lemma (3.3) ,

$$\left\|\hat{f}\, e^{-\alpha x} - q_n e^{-\alpha x}\right\|_p = \left\|F - p_n\right\|_p$$
$$\leq c\,\omega_2^{\varphi}(F, n^{-1})_p$$
$$= c\,\omega_2^{\varphi}(\hat{f}, n^{-1})_{p,\alpha}$$

Lemma (3.5):

If $c\int_{-1}^{1} \psi_j^{\mu p}(x)dx \leq c\,h_j$ and that q_n is monotone near y_1 then

$$\int_{-1}^{1} \left|q_n(y_1)e^{-\alpha x}\right|^p \psi_j^{\mu p}(x)dx \leq c\,\omega_2^{\varphi}(f, n^{-1})_{p,\alpha}^{\varphi}$$

Proof: by using (3.7) and lemma (3.4) ,

$$\int_{-1}^{1} \left|q_n(y_1)e^{-\alpha x}\right|^p \psi_j^{\mu p}(x)dx \leq c\,h_j \left|q_n(y_1)e^{-\alpha x}\right|^p$$
$$\leq c\left\|q_n\right\|_{p,\alpha}^p$$
$$\leq c\left\|\hat{f} - \hat{f} + q_n\right\|_{p,\alpha}^p$$

$$\le \left\|\hat{f}-q_n\right\|_{p,\alpha}^{p}+c\left\|\hat{f}\right\|_{p,\alpha}$$
$$\le c\,\omega_2^{\varphi}(\hat{f},n^{-1})_{p,\alpha}^{p}+c\|f\|_{p,\alpha}$$
$$\le c\,\omega_2^{\varphi}(f,n^{-1})_{p,\alpha}^{p}+c^*\omega_2(f,n^{-1})_{p,\alpha}^{p}$$

Hence

$$\int_{-1}^{1}\left|q_n(y_1)e^{-\alpha x}\right|^{p}\varphi_j^{\mu p}(x)dx\le c\,\omega_2^{\varphi}(f,n^{-1})_{p,\alpha}^{p}$$

Lemma (3.6):[4]

Let $i\in Z_{r,n}(y_1,x)$ and $\hat{h}_i:=z_{i-1}-z_i$ then

$$|f'(z_{i+})-f'(z_{i-})|\le c\,\hat{h}_i^{(p+1)/p}\omega_2^{\varphi}(f,n^{-1})_p$$

Lemma (3.7):

Let $f\in L_{p,\alpha}[-1,1]$ and $0<p\le\infty$ have

$$\left|\left(f'(z_{i+})-f'(z_{i-})\right)e^{-\alpha x}\right|\le c\,\hat{h}_i^{(p+1)/p}\omega_2^{\varphi}(f,n^{-1})_{p,\alpha}$$

Proof:

$$\left|\left(f'(z_{i+})-f'(z_{i-})\right)e^{-\alpha x}\right|=\left|f'(z_{i+})e^{-\alpha x}-f'(z_{i-})e^{-\alpha x}\right|$$

Let

$F'(z_{i+})=f'(z_{i+}e^{-\alpha x})$

$F'(z_{i-})=f'(z_{i-}e^{-\alpha x})$

where F' is bounded then by using lemma (3.6) ,

$$\left|\left(f'(z_{i+})-f'(z_{i-})\right)e^{-\alpha x}\right|=\left|F'(z_{i+})-F'(z_{i-})\right|$$
$$\le c\,\hat{h}_i^{(p+1)/p}\omega_2^{\varphi}(f,n^{-1})_p$$
$$\le c\,\hat{h}_i^{(p+1)/p}\omega_2^{\varphi}(f,n^{-1})_{p,\alpha}$$

Lemma (3.8):

Let $f\in\Delta^1(Y_r)$ be a continuous piecewise linear spline on the $Z_{r,n}$, $y_1\in[x_{j-1},x_j]$ and $f(y_1)=0$ then for all $x\in[-1,1]$

$$\left|f(x)e^{-\alpha x}\right|\le c\left(1+\frac{|x-x_j|}{\delta(x,x_j)}\right)^{2}\delta_n(x,x_j)^{-\frac{1}{p}}\omega_2^{\varphi}(f,n^{-1})_{p,\alpha}$$

where

$\delta_n(x,x_j)=\min\{\Delta_n(x),\Delta_n(x_j)\}\ne 0$ for all i

Proof:

Set $Z_{r,n}=\{-1=z_m<z_{m-1}<\ldots<z_1<z_0=1\}$ and $\hat{h}_i:=z_{i-1}-z_i$, Fix $x>y_1$ (and similar case when $x\le y_1$) and denote $Z_{r,n}(y_1,x):=\{i\,|\,z_i\in Z_{r,n}:y_1\le z_i<x\}$.

Since f is piecewise linear, then

$$|f(x)e^{-\alpha x}| = |(f(x)-0)\,e^{-\alpha x}|$$
$$= |(f(x)-f(y_1))\,e^{-\alpha x}|$$
$$= |(f'(\zeta))\,e^{-\alpha x}|(x-y_1) \quad \text{, for some } \zeta \in (y_1,x)$$

Now,

$$\left|f'(\zeta)e^{-\alpha x}\right| \le \left|(f'(\zeta)-f'(y_{1+}))e^{-\alpha x}\right| + \left|f'(y_{1+})e^{-\alpha x}\right|$$
$$\le \left|(f'(\zeta)-f'(y_{1+}))e^{-\alpha x}\right| + \left|(f'(y_{1+})-f'(y_{1-}))e^{-\alpha x}\right|$$
$$\le \sum_{i\in Z_{r,n}(y_1,\zeta)} \left|(f'(z_i)-f'(z_i))e^{-\alpha x}\right|$$
$$\le \sum_{i\in Z_{r,n}(y_1,x)} \left|(f'(z_i)-f'(z_i))e^{-\alpha x}\right|$$
$$\le c\left(1+\frac{|x-x_j|}{\delta_n(x,x_j)}\right)|x-x_j| \max_{i\in Z_{r,n}(y_1,x)} \left|(f'(z_i)-f'(z_i))e^{-\alpha x}\right|$$

Since $\hat{h}_i \ge \delta_n(x,x_j)$ then

$\hat{h}_i^{(p+1)/p} \ge \delta_n^{(p+1)/p}(x,x_j)$ and $\hat{h}_i^{-(p+1)/p} \le \delta_n^{-(p+1)/p}(x,x_j)$

and by lemma (3.7) get,

$$\left|f(x)e^{-\alpha x}\right| \le c\,\hat{h}_i^{(p+1)/p}\left(1+\frac{|x-x_j|}{\delta_n(x,x_j)}\right)|x-x_j|\,\omega_2^{\varphi}(f,n^{-1})_{p,\alpha}$$

$$\le c\left(1+\frac{|x-x_j|}{\delta_n(x,x_j)}\right)|x-x_j|\,\delta_n^{-(p+1)/p}(x,x_j)\,\omega_2^{\varphi}(f,n^{-1})_{p,\alpha}$$

$$= c\left(|x-x_j|+\frac{|x-x_j|^2}{\delta_n(x,x_j)}\right)\delta_n^{-1}(x,x_j)\,\delta_n^{-1/p}(x,x_j)\,\omega_2^{\varphi}(f,n^{-1})_{p,\alpha}$$

$$= c\left(\frac{|x-x_j|}{\delta_n(x,x_j)}+\frac{|x-x_j|^2}{\delta_n(x,x_j)}\right)\delta_n^{-1/p}(x,x_j)\,\omega_2^{\varphi}(f,n^{-1})_{p,\alpha}$$

$$\le c\left(1+2\frac{|x-x_j|}{\delta_n(x,x_j)}+\left(\frac{|x-x_j|}{\delta_n(x,x_j)}\right)^2\right)\delta_n^{-1/p}(x,x_j)\,\omega_2^{\varphi}(f,n^{-1})_{p,\alpha}$$

$$\le \left(1+\frac{|x-x_j|}{\delta_n(x,x_j)}\right)^2 \delta_n^{-1/p}(x,x_j)\,\omega_2^{\varphi}(f,n^{-1})_{p,\alpha}$$

Theorem (3.9):

Let $f \in \Delta^{(1)}(Y_r)$ be a continuous piecewise spline then for each $n \geq c(r)/d(r)$ there is a polynomial $p_n \in P_n$ such that

$$\|f - p_n\|_{p,\alpha} \leq c(r)\omega_2^{\varphi}(f, n^{-1})_{p,\alpha}$$

Proof:

From (2.2), (2.3) get,

$$\|f - p_n\|_{p,\alpha}^{p} = \|f - (q_n(x) - q_n(y_1))v_n(x) + q_n(y_1)w_n(x)\|_{p,\alpha}^{p}$$

$$= \|f - q_n(x)v_n(x) + q_n(y_1)v_n(x) - q_n(y_1)w_n(x)\|_{p,\alpha}^{p}$$

$$= \|f - q_n \operatorname{sgn}(x-y_1) + q_n \operatorname{sgn}(x-y_1) - q_n(y_1)v_n(x) + q_n(y_1)v_n(x) - q_n(y_1)w_n(x)\|_{p,\alpha}^{p}$$

$$= \left\|\hat{f}\operatorname{sgn}(x-y_1) - q_n \operatorname{sgn}(x-y_1) + q_n \operatorname{sgn}(x-y_1) - q_n(y_1)v_n(x) + q_n(y_1)v_n(x) - q_n(y_1)w_n(x)\right\|_{p,\alpha}^{p}$$

$$= \left\|(\hat{f} - q_n)\operatorname{sgn}(x-y_1) + q_n(\operatorname{sgn}(x-y_1) - v_n(x)) + q_n(y_1)(v_n(x) - w_n(x))\right\|_{p,\alpha}^{p}$$

$$\leq \left\|(\hat{f} - q_n)\operatorname{sgn}(x-y_1)\right\|_{p,\alpha}^{p} + \left\|q_n(\operatorname{sgn}(x-y_1) - v_n(x))\right\|_{p,\alpha}^{p} + \left\|q_n(y_1)(v_n(x) - w_n(x))\right\|_{p,\alpha}^{p}$$

$$\leq \left\|(\hat{f} - q_n)\operatorname{sgn}(x-y_1)\right\|_{p,\alpha}^{p} + c\int_{-1}^{1}\left|f(x)e^{-\alpha x}\right|^{p}\psi_j^{\mu p}(x)dx + c\int_{-1}^{1}\left|q_n(y_1)e^{-\alpha x}\right|^{p}\psi_j^{\mu p}(x)dx$$

Using lemmas (3.2), (3.4) and (3.8) we get,

$$\|f - p_n\|_{p,\alpha}^{p} \leq \left\|(\hat{f} - q_n)\operatorname{sgn}(x-y_1)\right\|_{p,\alpha}^{p} + c\int_{-1}^{1}\left|f(x)e^{-\alpha x}\right|^{p}\psi_j^{\mu p}(x)dx + c\int_{-1}^{1}\left|q_n(y_1)e^{-\alpha x}\right|^{p}\psi_j^{\mu p}(x)dx$$

$$\leq c\omega_2^{\varphi}(\hat{f}, n^{-1})_{p,\alpha}^{p} + c\int_{-1}^{1}\left(1 + \frac{|x - x_j|}{\delta_n(x, x_j)}\right)^{2p}\delta_n^{-1}\omega_2^{\varphi}(f, n^{-1})_{p,\alpha}^{p}\psi_j^{\mu p^2}(x)dx + c\omega_2^{\varphi}(f, n^{-1})_{p,\alpha}^{p}$$

Then,

$$\|f - p_n\|_{p,\alpha}^{p} \leq c\omega_2^{\varphi}(f, n^{-1})_{p,\alpha}^{p}$$

Conclusions

Suppose that f is unbounded function and used moduli of smoothness to found equivalence relation between the degree of best approximation of this function and the moduli of smoothness in the weight $L_{p,\alpha}$- space and found approximation by spline function by comonotone polynomial .

REFERENCES

1. R.K.Beston and D.Leviatan, "On Comonotone Approximation", Canada, Math., Bull, 26, 220-224(1993).
2. N.M.Kassim, , "On The Monotone and Comonotone Approximation", M.Sc. Thesis, Kufa University, Mathematical Department, College of Education(2004).
3. Kopotun.K.A."Coconvex Polynomial Approximation of Twice Differentiable Functions", J.Approx., 83, 141-156,(1995).
4. Kopotun.K.A. and Leviatan.D. " Comonotone Polynomial Approximation in L_p $[-1,1]$, $0 < p \leq \infty$",Acta. Math. Hunger, 77(4), 301-310 , (1997).

On Rational Solutions for the Class $\beta u_{tt} + \alpha u_t = (f(u)u_x)_x + \lambda u(1 - u^n)$

I. A. Malloki, and N. A. Al-Khairalla
Department of Mathematics- College of Science – Al-Mustansiriya University
Received 31/3/2013 – Accepted 15/9/2013

الخلاصة

في هذا العمل، استخدم نشر متسلسلة لورانت بالمقارنة مع تعريف الدالة النسبي من الأقطاب البسيطة لبعض المعادلات التفاضلية الجزئية اللاخطية N لإيجاد الحلول النسبية ب

ABSTRACT

In this work , Laurent series expansion compared with definition of rational function is used to find rational solutions with N simple poles for some nonlinear partial differential equations.

INTRODUCTION

During the last three decades, there has been a great deal of interest in rational solution of integrable nonlinear evolution equations: This began with studies of the rational solutions of the Korteweg-de Vries (KdV) and Kadomtsev-Petviashvilli (KP) equations, but soon similar results were obtained concerning the Benjamin-Ono equation and the classical Boussinesq and AKNS systems, [1 , 2].

Rational solutions were found in the majority of the equations of mathematical physic that possess a rich algebraic structure: an infinite set of symmetries and related commuting flows. It was the rational solutions of such equations are special limiting forms of exponential "multisoliton" solutions and can be obtained from the latter once by long-wave degeneration, [3].

Further applications of rational solutions to soliton equations include the description of explode-decay waves and vortex solutions of the complex sine-Gordon equation, [2].

The direct methods for the construction of rational solutions have great importance in mathematical physics. For instance, such methods are based on the transformation of various forms of the τ function to the equation of interest, or on the group theory, or on the analytic properties of the Baker-Akhiezer function, [3].

The goal of this work is to present a method for finding rational solutions with N simple poles for the nonlinear partial differential equations.

$$\beta u_{tt} + \alpha u_t = (f(u)u_x)_x + \lambda u(1 - u^n) \qquad \ldots(1.1)$$

which has a lengthy history of analysis, both analytically and numerically,

For various combinations of the parameters n, α, β and λ, the above class may respects many nonlinear PDEs:[4]

(i) When $n = 1$, $\alpha = 1$, $\beta = 0$ and $f = 1$, we have the fisher equation which arises in the study of reaction-diffusion waves in biology.
(ii) The case $n = 2$, $\alpha = 0$, $\beta = 1$ and $f = 1$ gives the ϕ^4 model equation.
(iii) With $\lambda = 0$, $\alpha = 1$ and $\beta = 0$, we have the nonlinear diffusion equation.
(iv) When $\lambda = 0$, $\alpha = 0$ and $\beta = 1$, we have the nonlinear (1-1) wave equation whose long wave speed is given by $f(u)$. In some studies, the speed is assumed to be a function of u_x, i.e., f is replaced by $g(u_x)$.
(v) In (iv) above, if α is assumed to be nonzero but small, then the wave equation is construed as a wave equation with a damping term.
(vi) The Telegraph equation is also obtained with $n = 1$ and $\alpha, \beta \neq 0$.

Description of the Method

Consider a given nonlinear PDE, say in two variables x and t

$$\frac{\partial u}{\partial t} = F(x, t, u, \frac{\partial u}{\partial x}, \frac{\partial^2 u}{\partial x^2}, \ldots, \frac{\partial^n u}{\partial x^n}) , \ x \in \text{£} , \ t \in \text{¡} \qquad \ldots(2.1)$$

In order to apply this method, we need the following steps:

Step 1: We assume that $u(x,t)$ is a rational solution of the equation (2.1) with N simple poles, we use

$$u(x, t) = \frac{R_1(t)}{x - x_1(t)} + a_0(t) + a_1(t)(x - x_1(t)) \qquad (2.2)$$

where $R_1(t)$ is the residue of $u(x,t)$ near $x_1(t)$ and

$$a_0(t) = \sum_{k=2}^{N} \frac{R_k(t)}{x_1(t) - x_k(t)} \ , \ x_1(t) \neq x_k(t)$$

$$a_1(t) = \sum_{k=2}^{N} \frac{-R_k(t)}{(x_1(t) - x_k(t))^2}, \ x_1(t) \neq x_k(t).$$

Step 2: Letting $x - x_1$ to be ε, then Substitute the following derivatives of $u(x,t)$ with respect the variables x and t in the equation

$$\frac{\partial u}{\partial t} = \frac{\dot{R}_1}{\varepsilon} + \frac{R_1 \dot{x}_1}{\varepsilon^2} + H(\varepsilon) \qquad (2.3a)$$

$$\frac{\partial^2 u}{\partial t^2} = \frac{\ddot{R}_1}{\varepsilon} + \frac{2\dot{R}_1 \dot{x}_1 + R_1 \ddot{x}_1}{\varepsilon^2} + \frac{2R_1 \dot{x}_1^2}{\varepsilon^3} + G(\varepsilon) \qquad (2.3b)$$

$$\frac{\partial u}{\partial x} = \frac{-R_1(t)}{\varepsilon} + a_1(t)$$

$$\frac{\partial^n u}{\partial x^n} = \frac{(-1)^n n! R_1}{\varepsilon^{n+1}} \qquad n=2,3,\ldots \qquad \ldots(2.3c)$$

Where H(ε) and G(ε) are analytic functions of ε:

$$\mathrm{H}(\varepsilon) = a_0^{g} + a_1^{g}\varepsilon - a_1 x_1^{g}$$

$$\mathrm{G}(\varepsilon) = a_0^{gg} - 2a_1^{g} x_1^{g} + a_1^{gg}\varepsilon - a_1 x_1^{gg}$$

Step 3: Equating the coefficients of ε^i to zero, to have a nonlinear system of algebraic or differential equations and then solve the system.

Remarks*:*

(i) Our method is based on the comparison of the usual assumption for function with N simple poles

$$\mathrm{u}(x,\mathrm{t}) = \sum_{k=1}^{N} \frac{\mathrm{R}_k}{x - x_k}, \ x \in £ \qquad \ldots(2.4)$$

and expand of functions by formal Laurent series near a specified pole (say x_1):

$$\mathrm{u}(x,\mathrm{t}) = \sum_{n=-1}^{\infty} a_n (x - x_1)^n \qquad \ldots(2.5)$$

Denote a_{-1} by R_1. We can see that

$$\sum_{n=0}^{\infty} a_n(\mathrm{t})(x - x_1(\mathrm{t}))^n = \sum_{k=2}^{N} \frac{\mathrm{R}_k(\mathrm{t})}{x - x_k(\mathrm{t})} \qquad \ldots(2.6)$$

(ii) THe coefficients $a_0(\mathrm{t})$, $a_1(\mathrm{t})$, … in (2.6) carry information about the poles $x_2, \ldots, x_N$.

(iii) The ansatz that we adopt, is:

$$\mathrm{u}(x,\mathrm{t}) = \frac{\mathrm{R}_1(\mathrm{t})}{x - x_1(\mathrm{t})} + \sum_{n=0}^{\infty} a_n(\mathrm{t})\left(x - x_k(\mathrm{t})\right)^n \qquad \ldots(2.7)$$

and because of the difficulty of equating coefficients for $(x - x_1(\mathrm{t}))$ of the nonlinear from PDE. Hence we will write the form (2.7) as (2.2) which we have directly in the first step of the method.

The ϕ^4-Model Equation and Rational Solution

In this section, we consider ϕ^4-model equation of mathematical physics

$$\frac{\partial^2 \mathrm{u}}{\partial \mathrm{t}^2} = \frac{\partial^2 \mathrm{u}}{\partial x^2} + \lambda \mathrm{u}(1 - \mathrm{u}^2) \qquad \ldots(3.1)$$

which arises in many contexts and is often used as a phenomenological model, this equation is nonintegrable.

By substituting (2.2) and their derivatives (2.3) in equation(3.1) we obtain the following identity:

$$2R_1\dot{x}_1^2\varepsilon^{-3} + R_1\ddot{x}_1\varepsilon^{-2} + 2\dot{R}_1\dot{x}_1\varepsilon^{-2} + \ddot{R}_1\varepsilon^{-1} + \ddot{a}_0 - 2\dot{a}_1\dot{x}_1 - a_1\ddot{x}_1 + \ddot{a}_1\varepsilon =$$
$$2R_1\varepsilon^{-3} + \lambda(R_1\varepsilon^{-1} + a_0 + a_1\varepsilon) - \lambda[R_1^3\varepsilon^{-3} + 3a_0R_1^2\varepsilon^{-2} + 3a_1R_1^2\varepsilon^{-1} + 2a_0^2R_1\varepsilon^{-1} + 6a_0a_1R_1 + 3a_1^2R_1\varepsilon +$$
$$a_0^2R_1^2\varepsilon^{-1} + a_0^3 + 3a_0^2a_1\varepsilon + 3a_0a_1^2\varepsilon^2 + a_1^3\varepsilon^3]$$

Collecting all terms with the powers in ε^i ($i = -3, \ldots, 3$) and setting each of the obtained coefficients of ε^i to zero yields the following set of equations with respect to $R_1(t)$, $x_1(t)$, $a_0(t)$ and $a_1(t)$

(α) $\quad 2R_1\dot{x}_1^2 = 2R_1 - \lambda R_1^3$

(b) $\quad R_1\ddot{x}_1 + 2\dot{R}_1\dot{x}_1 = -3\lambda a_0R_1^2$

(c) $\quad \ddot{R}_1 = \lambda R_1 - 3\lambda a_1R_1^2 - 2\lambda a_0^2R_1 - \lambda a_0^2R_1^2$

(d) $\quad \ddot{a}_0 - 2\dot{a}_1\dot{x}_1 - a_1\ddot{x}_1 = \lambda a_0 - 6\lambda a_0a_1R_1 - \lambda a_0^3$

(e) $\quad \ddot{a}_1 = \lambda a_1 - 3\lambda a_1^2R_1 - 3\lambda a_0^2a_1$

(f) $\quad -3\lambda a_0a_1^2 = 0$

(g) $\quad -\lambda a_1^3 = 0$

For which we have the following cases:

Case 1: when $\lambda = 0$ then

$x_1(t) = \pm t + c_1$

$R_1(t) = c_2$

$a_0(t) = c_3t^2 + c_5t + c_6$

$a_1(t) = c_3t + c_4$

where c_i ($i = 1, \ldots, 6$) are arbitrary constants.

The solution will be of the form:

$$u(x,t) = \frac{c_2}{x \mp t - c_2} + c_3t^2 + c_5t + c_6 + (c_3t + c_4)(x \mp t - c_1)$$

Case 2: when $a_1(t) = 0$: if $a_0 = 0$ then $\lambda = 0$ and hence $u = \dfrac{c_2}{x \pm t - c_2}$.

if $a_0 \neq 0$, from eq. b and c we get that $R_1(t) = \dfrac{-B \pm \sqrt{B^2 - 4AC}}{2A}$ where $A = \pm 3\lambda a_0$, $B = \pm 2a_0^2 + 3\dot{a}_0$, $C = \pm 2(1 - 2a_0^2)$

Notice that A,B and C depend on λ and a_0. Multiply eq. d by $\dot{a}_0$ to be reduced to $\dot{a}_0^2 = \lambda(a_0^2 - \frac{1}{2}a_0^4) + const$. This eq. can be solved for several values of λ:

$\lambda=-2$. Take const. to be 1 then $\dot{a}_0^{2}=(a_0^{2}-1)^2$ hence $a_0(t)=\dfrac{k_1e^{\pm 2t}-1}{k_1e^{\pm 2t}+1}$.

$\lambda=2$. Take const. to be -1 then $\dot{a}_0^{2}=-(a_0^{2}-1)^2$ hence $a_0(t)=\dfrac{k_1e^{\pm 2it}-1}{k_1e^{\pm 2it}+1}$

$\lambda=-(1+k^2)$, $0<k^2<1$, rescale eq. d as $a_0(t)=Aw(t)$ to get that $\dot{w}^{2}=(1-w^2)(1-k^2w^2)$ and $w=sn(t,k)$ Jacobian elliptic function.

The Nonlinear Wave Equation

In this section, we consider the nonlinear wave equation given by

$$\frac{\partial^2 \mathrm{u}}{\partial \mathrm{t}^2}=\frac{\partial}{\partial x}(f(\mathrm{u})\frac{\partial \mathrm{u}}{\partial x}) \qquad \ldots(4.1)$$

where $f(\mathrm{u})$ is a polynomial, i.e

$$f(\mathrm{u})=\sum_{\mathrm{i}=0}^{\mathrm{l}}\gamma_\mathrm{i}\mathrm{u}^\mathrm{i}\ ,\ \mathrm{l}\geq 1 \qquad \ldots(4.2)$$

When (2.2) and (2.3) are substituted in (4.1) we have the following identity:

$$\mathrm{R}_1\ddot{x}_1\varepsilon^{-2}+2\dot{\mathrm{R}}_1\dot{x}_1\varepsilon^{-2}+2\mathrm{R}_1\dot{x}_1^{2}\varepsilon^{-3}+\ddot{\mathrm{R}}_1\varepsilon^{-1}+\ddot{a}_0-2\dot{a}_1\dot{x}_1+\ddot{a}_1\varepsilon-a_1\ddot{x}_1=$$
$$[\gamma_0+\gamma_1(\mathrm{R}_1\varepsilon^{-1}+a_0+a_1\varepsilon)+\ldots+\gamma_\mathrm{l}(\mathrm{R}_1\varepsilon^{-1}+a_0+\mathrm{R}_1\varepsilon)^\mathrm{l}][2\mathrm{R}_1\varepsilon^{-3}]+[\gamma_1+2\gamma_2(\mathrm{R}_1\varepsilon^{-1}+a_0+a_1\varepsilon)+\ldots+$$
$$\mathrm{l}\gamma_\mathrm{l}(\mathrm{R}_1\varepsilon^{-1}+a_0+a_1\varepsilon)^{\mathrm{l}-1}][-\mathrm{R}_1\varepsilon+a_1]^2$$

By [5], balancing the higher powers of ε leads to $\ell=0$

Collecting all terms with the powers in ε^i (i = – 3, …, 1) and setting each of the obtained coefficients of ε^i to zero yields the following set of equations with respect to $\mathrm{R}_1(\mathrm{t})$, $x_1(\mathrm{t})$, $a_0(\mathrm{t})$ and $a_1(\mathrm{t})$

$$2\mathrm{R}_1\dot{x}_1^{2}=2\gamma_0\mathrm{R}_1$$
$$\mathrm{R}_1\ddot{x}_1+2\dot{\mathrm{R}}_1\dot{x}_1=0$$
$$\ddot{\mathrm{R}}_1=0$$
$$\ddot{a}_0-2\dot{a}_1\dot{x}_1-a_1\ddot{x}_1=0$$
$$\ddot{a}_1=0$$

For which we have the following:

$$x_1(t) = \pm\sqrt{\gamma_0}\, t + c_1$$

$$R_1(t) = c_2$$

$$a_0(t) = \pm c_3\sqrt{\gamma_0}\, t^2 + c_5 t + c_6$$

$$a_1(t) = c_3 t + c_4$$

c_i ($i = 1,\dots,6$) are arbitrary constants.

The solution will be of the form:

$$u(x,t) = \frac{c_2}{x \mp \sqrt{\gamma_0}\,t - c_1} \pm c_3\sqrt{\gamma_0}\,t^2 + c_5 t + c_6 + (c_3 t + c_4)(x \mp \sqrt{\gamma_0}\,t - c_1)$$

The Telegraph Equation

In this section, we consider the telegraph equation is given by

$$\beta\frac{\partial^2 u}{\partial t^2} + \alpha\frac{\partial u}{\partial t} = \frac{\partial}{\partial x}\left(f(u)\frac{\partial u}{\partial x}\right) + \lambda u - \lambda u^2 \qquad \dots(5.1)$$

where $f(u)$ is as in (4.2).

when (2.2) and (2.3) are substituted in (5.1) we have the following identity:

$$\beta(R_1\ddot{x}_1\varepsilon^{-2} + 2\dot{R}_1\dot{x}_1\varepsilon^{-2} + 2R_1\dot{x}_1^2\varepsilon^{-3} + \ddot{R}_1\varepsilon^{-1} + \ddot{a}_0 - 2\dot{a}_1\dot{x}_1 + \ddot{a}_1\varepsilon - a_1\ddot{x}_1) +$$

$$\alpha(R_1\dot{x}_1\varepsilon^{-2} + \dot{R}_1\dot{x}_1\varepsilon^{-1} + \dot{a}_0 + \dot{a}_1\varepsilon - a_1\dot{x}_1)$$

$$= [\gamma_0 + \gamma_1(R_1\varepsilon^{-1} + a_0 + a_1\varepsilon) + \dots + \gamma_l(R_1\varepsilon^{-1} + a_0 + a_1\varepsilon)^l][2R_1\varepsilon^{-3}] +$$

$$[\gamma_1(-R_1\varepsilon^{-2} + a_1) + 2\gamma_2(R_1\varepsilon^{-1} + a_0 + a_1\varepsilon) + \dots + \gamma_l(R_1\varepsilon^{-1} + a_0 + a_1\varepsilon)^{l-1}]$$

$$1[-R_1\varepsilon^{-2} + a_1] + \lambda(R_1\varepsilon^{-1} + a_0 + a_1\varepsilon) - \lambda(R_1\varepsilon^{-1} + a_0 + a_1\varepsilon)^2$$

By [4], balancing the higher powers of ε leads to $\ell = 0$

Collecting all terms with the powers in ε^i ($i = -3, \dots, 2$) and setting each of the obtained coefficients of ε^i to zero yields the following set of equations with respect to $R_1(t)$, $x_1(t)$, $a_0(t)$ and $a_1(t)$

(α) $\quad 2\beta R_1\dot{x}_1^2 = 2\gamma_0 R_1$

(b) $\quad \beta R_1\ddot{x}_1 + 2\beta\dot{R}_1\dot{x}_1 + \alpha R_1\dot{x}_1 = -\lambda R_1^2$

(c) $\quad \beta\ddot{R}_1 + \alpha\dot{R}_1\dot{x}_1 = \lambda R_1 - 2\lambda a_0 R_1$

(d) $\quad \beta\ddot{a}_0 - 2\beta\dot{a}_1\dot{x}_1 - \beta a_1\ddot{x}_1 + \alpha\dot{a}_0 - \alpha a_1\dot{x}_1 = \lambda a_0 - \lambda a_0^2 - 2\lambda a_1 R_1$

(e) $\quad \beta\ddot{a}_1 + \alpha\dot{a}_1 = \lambda a_1 - 2\lambda a_0 a_1$

(f) $\quad -\lambda a_1^2 = 0$

For which we have the following:

Case 1: when $\lambda = 0$ then

$$x_1(t) = \pm\sqrt{\frac{\gamma_0}{\beta}}\,t + c_1$$

$$R_1(t) = c_2 e^{\frac{-\alpha}{2\beta}t}$$

$$a_0(t) = \frac{2c_3\beta^2}{\alpha^2}\sqrt{\gamma_0\beta}\, e^{\frac{-2\alpha}{\beta}t}$$

$$a_1(t) = c_3 e^{\frac{-\alpha}{\beta}t} + c_4$$

where γ_0, c_n $(n = 1,\ldots,4)$ are arbitrary constants.
The solution will be of the form:

$$u(x,t) = \frac{c_2 e^{\frac{-\alpha}{2\beta}t}}{x \mp \sqrt{\frac{\gamma_0}{\beta}}\,t - c_1} + \frac{2c_3\beta^2}{\alpha^2}\sqrt{\gamma_0\beta}\, e^{\frac{-2\alpha}{\beta}t} + (c_3 e^{\frac{-\alpha}{\beta}t} + c_4)(x \mp \sqrt{\frac{\gamma_0}{\beta}}\,t - c_1)$$

Case 2: when $a_1(t) = 0$ then it is enough to solve the eq.

$\beta\ddot{a}_0 + \alpha\dot{a} = \lambda(a_0 - a_0^2)$ $\quad\quad \dot{a}_0 = p(a_0)$ then $pp' + \frac{\alpha}{\beta}p = \frac{\lambda}{\beta}(a_0 - a_0^2)$

Upon the transformations $p = \frac{1}{y}, a_0 = x$ the eq. becomes

$y' - \frac{\alpha}{\beta}y^2 = \frac{\lambda}{\beta}(x - x^2)$ then let $y(x) = -\frac{1}{tx'(t)}$ we have

$t^2x'' = \frac{\lambda}{\beta}x(1-x)$ let $x(t) = t^k u(z)$, $z = t^r$ we can choose k, r and other parameters so that we have the eq. in the form $u'' = Azu^2$ which has the solution $u(z) = \frac{6}{Az^2}$

CONCLUSION

In this method for obtaining rational solutions with simple poles using Laurent series expansion, the exact solution for nonlinear PDE using the whole Laurent series expansion may be difficult to be evaluated especially in nonlinear term . We expect there is a relation between the number of poles and the number of terms of using power series expansion.

REFERENCES

1. Clarkson, P.A., Rational Solutions of the Classical Bossinesq System, Nonlinear Analysis:Real World Application, 2008.
2. Hone, A.N., Crum Transformation and Rational Solutions of the Non-Focusing Nonlinear Schrödinger Equation, J.Phys, 1413-1483, 1997.
3. Pelinovsky, D., Rational Solutions of the Kadomtsev-Petviashvili Hierarchy and Dynamics of Their Poles.1.New Form of a General Rational Solution, J.Math.Phys., Vol.35, No.11, 1994.
4. Kara, A.H., Bokhari, A.H., and Zaman, F.D., On the Exact Solutions of the Nonlinear Wave and ϕ^4-Model Equations, Journal of Nonlinear Mathematical Physics, Volume 15, Supplement 1, pp.105-111, 2008.
5. Malloki, I.A., Poles Order of Rational Solutions for Evolution Equation, Al-Mustansariya J.Sci., Vol.20, No.3, 2009.

Some generalization of Banach 's contraction principle in complete cone metric space

Tamara Shehab Ahmed
Department of mathematics, Ibn Al-Haytham college of education, Baghdad University
Received 17/3/2013 – Accepted 15/9/2013

الخلاصة

في هذا البحث قدمنا بعض مبرهنات النقطة الصامدة لتطبيقات انكماشية ذاتية وحيدة القيمة تحقق شروطا خاصة والتي تمثل تعميما لنظرية بناخ الانكماشية في فضاء كون المتري الكامل مع افتراض ان الكُون منتظمة ..

ABSTRACT

In this paper we present some fixed point theorems for single –valued self contractive mappings satisfying special conditions that are generalization of Banachs contraction principle in complete cone metric space under the assumption that the cone is regular .our results are new.

1- INTRODUCTION

It is well known that the classical contraction mapping principle of Banach is a fundamental result in fixed point theory . several authors have obtained various extensions and generalizations of Banachs theorem by considering contractive mapping on many different metric spaces , see , [1],[2],[3],[4],[5],[6],[7],[8] and others .

Recently,Huang and zhang [9] generalized the notion of metric spaces by replacing the real numbers by ordered Banach space and define cone metric space . They have proved the Banach contraction mapping theorem and some other fixed point theorems of contractive type mappings in cone metric spaces . Sub sequantly , Rezapour and Haml barani [10],Hic and Rakocevic[11] studied fixed point theorems for contractive type mappings in cone metric spaces.

The main purpose of this paper is to prove some fixed point theorems for single –valued self contractive type mapping satisfying special conditions which are generalization of Banach contraction principle in complete cone metric space with the assumption that the cone is regular.

2- Preliminaries

Through out this paper , we denote the set of Banach space by E , The set of positive integers by N and The set of real numbers by R .

Definition (2.1):[9]

Let P be a subset of E , P is called a cone if and only if :

- p is closed , non empty and satisfies $p \neq \{0\}$.
- $a,b \in R$, $a,b \geq 0$, $x,y \in p$ implies that $ax+by \in p$
- $x \in p$ and $-x \in p$ then $x = 0$

Given a cone $p \subseteq E$, we define a partial ordering " $\leq$ " with respect to p by $x \leq y$ if and only if $y-x \in p$, we shall write $x < y$ if $x \leq y$ and $x \neq y$ and $x << y$ if $y-x \in \text{int}\, p$,where int p is the interior points of p .

Definition (2.2):[10]
The cone p is called normal if there is a number $k > 0$ such that for all $x,y \in E$, $0 \le x \le y$ implies $\|x\| \le k \|y\|$, the least positive number satisfying the previous inequality is then called the normal constant of p .

Definition (2.3):[10]
The cone p is called regular if every increasing sequence which is bounded from above is convergent. That is if $< x_n >_{n\ge1}$ is a sequence such that $x_1 \le x_2 \le \ldots\ldots \le y$ for some $y \in E$, then there is $x \in E$ such that $\lim\limits_{n\to\infty} \|x_n - x\| = 0$ equivalently , The cone p is regular if and only if every decreasing sequence which is bounded from below is convergent .
The following lemma shows the relation between normal cone and regular cone ,this lemma was mentioned in [9] , but it was proved in [10] .
Lemma (2.4): Every regular cone is normal cone . For the proof ,we can see lemma (1.1)[10]
Remark (2.5): The converse of lemma (2.2) is not true in general , the following example shows that :
Example (2.6)[10]: Let $E = C_R([0,1])$ which is the set of all real continous function define on [0,1] with the supremum norm and $p = \{f \in E : f(x) \ge 0\}$
Then , p is normal cone with normal constant of $k = 1$,but p is not regular cone .

Example(2.7):
Let $k > 1$ be given . consider the real vector space $E = \{ax + b : a,b \in R ; x \in [1-\frac{1}{k},1]\}$ with the supremum norm and the cone $p=\{ax+b \in E : a \le 0 , b \ge o\}$ in E . We show that p is regular and so is normal.
Let $<a_n x+b_n>_{n\ge1}$ be an increasing sequence which is bounded from above , that is , there is an element $cx + d \in E$ such that $a_1 x+b_1 \le a_2 x+b_2 \le \ldots \le a_n x+b_n \le \ldots \le cx+d$, for all $x \in [1-\frac{1}{k},1]$, then $<a_n>_{n\ge1}$ and $<b_n>_{n\ge1}$ are two sequences in R such that : $b_1 \le b_2 \le \ldots \le d$, $a_1 \ge a_2 \ge \ldots \ge c$
Thus , $<a_n>_{n\ge1}$ and $<b_n>_{n\ge1}$ are convergent ,
Let $a_n \to a$ and $b_n \to b$, then $ax+b \in p$ and $a_n x + b_n \to ax+ b$, there for , p is regular .
Definition (2.8) [9] :

Let X be a non –empty set .Suppose that the mapping $d: X\times X \to E$ satisfying the following axioms for all x,y,z in X

- $0\leq d(x,y)$ and $d(x,y)=0$ if and only if $x=y$
- $d(x,y)=d(y,x)$ (symmetry)
- $d(x,y)\leq d(x,z)+d(z,y)$ (triangular inequality) .

Then d is called a cone metric on X and (X,d) is called a cone metric space .

This definition is more general than that a metric space .

Example(2.9)[9]:

Let $E=R^2$, $P=\{(x,y)\in E: x,y\geq 0\}$, X=R and $d: X\times X\to E$ defined by $d(x,y)=(|x-y|, \lambda|x-y|)$, where $\lambda\geq 0$ is a constant . Then (X,d) is a cone metric space .

Definition (2.10) [9]:

Let (X,d) be a cone metric space , A sequence $<x_n>_{n\geq 1}$ in X is said to be:

- A convergent sequence if for every $c\in E$ with $0 << c$, there is $n_0 \in N$ such that for all $n\geq n_0$, $d(x_n,x)<< c$ for some x in X .We denote this by $\lim_{n\to\infty} x_n = x$ or $x_n \to x$ as $(n\to\infty)$ or $\lim_{n\to\infty} d(x_n,x)=0$
- A Cauchy sequence if for every $c\in E$ with $0<<c$, there is $n_1\in N$ such that for all $n,m\geq n_1$, $d(x_n,x_m)<< c$. We denote this by $\lim_{n,m\to\infty} d(x_n,x_m)=0$
- A cone metric space (X,d) is said to be complete if every Cauchy sequence is convergent in X.

3- Main result

In this section , we give some generalizations of Banach contraction principle in complete cone metric space with the assumption that the cone p is regular .

Theorem (3.1):

Let (X,d) be a complete cone metric space with regular cone p such that $d(x,y)\in p$ for $x,y\in X$. let $T: X\to X$ be a mapping on X , satisfy the following condition

$d(T(x),T(y))\leq k\, d(x,y)$ …….. (3.1) for all x,y in X , where $k\in[0,1)$ is a constant .

Then T has a unique fixed point .

Proof :

Fix $x\in X$ and let $x_n=T^n(x)$, n = 1,2,….. to show that $<x_n>$ is a Cauchy sequence .

$$d(x_n,x_{n+1}) = d(T^n(x),T^{n+1}(x)) = d(T(T^{n-1}(x)),T(T^n(x)))$$
$$\leq kd(T^{n-1}(x),T^n(x))$$
$$= kd(x_{n-1},x_n)$$

So, $d(x_n,x_{n+1}) \leq kd(x_{n-1},x_n) < d(x_{n-1},x_n)$

Therefore the sequence $< d(x_n,x_{n+1}) >$ is monotone decreasing and bounded below ,

but p is regular cone , so $< d(x_n,x_{n+1}) >$ is convergent sequence and there exists r ∈P such that $< d(x_n,x_{n+1}) > \to r$ (as $n \to \infty$) ,

$\lim_{n\to\infty} d(x_n,x_{n+1}) = r$

Now , Assume $r \neq 0$, then by condition (3.1) and taking $n \to \infty$ to both sides we have :

$d(x_{n+1},x_{n+2}) \leq kd(x_n,x_{n+1}), n = 1,2,.....$

$r \leq kr \Rightarrow r - kr \leq 0 \Rightarrow r(1-k) \leq 0 \Rightarrow r \leq 0.$

So $r = 0$, therefore $\lim_{n\to\infty} d(x_n,x_{n+1}) = 0$

Now we will show that $< x_n >$ is Cauchy sequence in X , since $\lim_{n\to\infty} d(x_n,x_{n+1}) = 0$ and

P is closed hence for every c $\in$ int p then $\frac{c}{m} \in \text{int}\, p$ for all positive integer $m \geq 1$

So , There exists $n_0 \in N$ such that ; $d(x_n ,x_{n+1}) << \frac{c}{2}$ for all $n > n_0$

hence by triangular inequality we have : $d(x_n,x_{n+2}) \leq d(x_n ,x_{n+1}) + d(x_{n+1} ,x_{n+2})$

$$<< \frac{c}{2} + \frac{c}{2}$$
$$= c \quad , \text{ for all } n > n_0$$

Similarly by induction , $d(x_n,x_m) << c$ for all $m > n > n_0$

Hence $< x_n>$ is a Cauchy sequence , By completeness of X , it must be convergent in X,

Hence $\lim_{n\to\infty} x_n = u$ for some u $\in$X .

Now , we will show that u is a fixed point of T .By traingular inequality we have :

$d(T(u),u) \leq d(T(u),x_{n+1}) + d(x_{n+1},u)$, by condition (3.1) we have :

$d(T(u),x_{n+1})=d(T(u),T^{n+1}(x)) = d(T(u),T(T^n(x))$
$\leq k\ d(u,T^n(x))$
$= k\ d(u,x_n)$

Thus : $d(T(u),u) \leq k\ d(u,x_n)+d(x_{n+1}, u)$

Now , Taking $n \to \infty$ to both sides we have : $d(T(u),u)=0$ and $T(u) = u$.

Therefore , T has a fixed point .
For the uniqueness of fixed point , suppose Z is another fixed point of T ;
(i.e) T(Z) = Z , so by condition (3.1) we have :
$d(z,u) = d(T(z),T(u)) \le k\ d(z,u)$, so we have
$d(z,u) - k\ d(z,u) \le 0 \Rightarrow (1-k)\ d(z,u) \le 0 \Rightarrow d(z,u) \le 0$ and we obtain that
$d(z,u) = 0$ and then $z = u$
Therefore , T has a unique fixed point .

Now , As a consequence of theorem (3.1) , we have the following corollary :

Corollary(3.2):
Let (X,d) be a complete cone metric space , with regular cone p such that $d(x,y) \in p$ for $x,y \in X$. let $T: X \to X$ be a mapping on X , Satisfy the following condition for some $n \in N$; $d(T^n(x), T^n(y)) \le k\ d(x,y)$ ……(3.2) for all x,y in X , where $k \in [0,1)$ is a constant . Then T has a unique fixed point .

Proof :
By theorem (3.1) , we conclude that T^n has a unique fixed point say x .
(i.e) $T^n(x) = x$ for some positive integer n .
Now , $T^{n+1}(x) = T^n(T(x)) = T(x)$
So , T(x) is also fixed point of T^n , but T^n has a unique fixed point which is x , therefore T(x) = x so , T has a fixed point which is x .
To show the uniqueness of x , suppose z is another fixed point of T ,
(i.e) T(z) = z and $T^n(z) = z$ for some positive integer n .
$d(x,z) = d(T(x),T(z)) = d(T^n(x),T^n(z)) \le k\ d(x,z)$
So , $d(x,z) - k\ d(x,z) \le 0 \Rightarrow (1-k)\ d(x,z) \le 0 \Rightarrow d(x,z) \le 0$
Thus , we get $d(x,z) = 0$ and $x = z$.

Therefore , T has a unique fixed point .
Now , we generalize theorem (3.1) into following theorems which are another generalizations of Banach contraction principle in complete cone metric space by using some contractive conditions .

Theorem (3.3):
Let (X,d) be complete cone metric space with a regular cone p such that $d(x,y) \in p$ for $x,y \in X$.let $T:X \to X$ be a mapping on X , suppose there

exists $\alpha \in S$ which is the class of functions $\alpha : \text{int}\, p \to [0,1)$ satisfying the simple condition (if $\alpha(t_n) \to 1$ then $t_n \to 0$), Such that for each x,y in X :
$d(T(x),T(y)) \leq \alpha(d(x,y))\, d(x,y)$ ......(3.3) then , T has a unique fixed point .

Proof :
Fix $x \in X$ and let $x_n = T^n(x)$, n = 1,2,....... To show that $<x_n>$ is a Cauchy sequence .

$$\begin{aligned} d(x_n, x_{n+1}) &= d(T^n(x),T^{n+1}(x)) = d(T(T^{n-1}(x)),T(T^n(x))) \\ &\leq \alpha(d(T^{n-1}(x),T^n(x)))\, d(T^{n-1}(x),T^n(x)) \\ &= \alpha(d(x_{n-1}, x_n))\, d(x_{n-1}, x_n) \\ &< d(x_{n-1}, x_n) \end{aligned}$$

So , $d(x_n , x_{n+1}) < d(x_{n-1} , x_n)$.
Therefore the sequence $< d(x_n , x_{n+1}) >$ is monotone decreasing and bounded below , but p is regular cone , so $<d(x_n ,x_{n+1}) >$ is convergent sequence and there exist $r \in P$ such that $d(x_n , x_{n+1}) \to r$ (as $n \to \infty$) or $\lim_{n\to\infty} d(x_n, x_{n+1}) = r$.

Now , Assume $r \neq 0$, Then by condition (3.3) we have :
$\frac{d(x_{n+1}, x_{n+2})}{d(x_n, x_{n+1})} \leq \alpha(d(x_n, x_{n+1})), n = 1,2,......$ letting $n \to \infty$, we see that
$1 \leq \lim_{n\to\infty}[\alpha(d(x_n, x_{n+1})]$

So, By properties of α , we have $\lim_{n\to\infty} d(x_n, x_{n+1}) = 0$

Now , To show that $< x_n >$ is a Cauchy sequence , if not assume $\lim_{n,m\to\infty} \sup d(x_n, x_m) > 0$,

By the triangular inequality and by the condition (3.3) we have :

$$\begin{aligned} d(x_n,x_m) &\leq d(x_n,x_{n+1}) + d(x_{n+1} , x_{m+1}) + d(x_{m+1} , x_m) \\ &\leq d(x_n , x_{n+1}) + \alpha(d(x_n , x_m)) .d(x_n , x_m) + d(x_{m+1} , x_m) \end{aligned}$$

$d(x_n,x_m) - \alpha(d(x_n , x_m)) .d(x_n , x_m) \leq d(x_n,x_{n+1}) + d(x_{m+1} , x_m)$
$[\, 1-\alpha(d(x_n , x_m))\,]\, d(x_n , x_m) \leq d(x_n,x_{n+1}) + d(x_{m+1} , x_m)$
$d(x_n,x_m) \leq [\, 1-\alpha(d(x_n , x_m))\,]^{-1} [d(x_n,x_{n+1}) + d(x_{m+1} , x_m)\,]$,
under the assumption $\lim_{n,m\to\infty} \sup d(x_n, x_m) > 0$, we have

$$\lim_{n,m\to\infty} \sup[1-\alpha(d(x_n, x_m))]^{-1} = \lim_{n,m\to\infty} \sup \frac{1}{1-\alpha(d(x_n, x_m))} = \frac{1}{1-1} = \frac{1}{0} = {}^{+}\infty$$

From which $\lim_{n,m\to\infty} \sup \alpha(d(x_n, x_m)) = 1$

By properties of α , $\lim_{n,m\to\infty} \sup d(x_n, x_m) = 0$ which is again contradiction

Hence , $< x_n >$ is cauchy sequence in (X,d) , By completeness of X , It must be convergent in X , So $\lim_{n\to\infty} x_n = z$ for some z in X .

Now ,we will show that z is a fixed point of T .

By triangular inequality we have : $d(T(z),z) \leq d(T(z), x_{n+1}) + d(x_{n+1}, z)$

By condition (3.3) we have : $d(T(z), x_{n+1}) = d(T(z), T^{n+1}(x)) = d(T(z), T(T^n(x)))$

$\leq \alpha(d(z,T^n(x)))\, d(z,T^n(x))$

$= \alpha(d(z,x_n))\, d(z,x_n)$

Thus , $d(T(z),z) \leq \alpha(d(z,x_n))\, d(z,x_n) + d(x_{n+1}, z)$

Now , taking $n \to \infty$ to both sides we have :

$d(T(z),z) \leq \lim_{n\to\infty} \alpha(d(z,x_n)).\lim_{n\to\infty} d(z,x_n) + \lim_{n\to\infty} d(x_{n+1},z)$

So, $d(T(z),z) \leq \lim_{n\to\infty} \alpha(d(z,x_n)).0 + 0$

Thus , $d(T(z),z) \leq 0$ and we obtain $d(T(z),z) = 0$, So $T(z) = z$

Now , To show the uniqueness of fixed point of T , Suppose u is another fixed point of T ,

So , $T(u) = u$, Thus by condition (3.3) we have :

$d(z,u) = d(T(z),T(u)) \leq \alpha(d(z,u))\, d(z,u)$

But $\alpha(d(z,u)) \in [0,1)$, So we get that $\alpha(d(z,u)) < d(z,u)$ and we obtain that $d(z,u) < d(z,u)$

Which is a contradiction .

Therefore , T has a unique fixed point .

As a consequence of theorem (3.3) , we have the following corollary :

Corollary (3.4) :

If X , P, T as in theorem (3.3) and $\alpha : \text{int}\, p \to [0,1)$ defined by $\alpha(t) = k$ For all t , Then theorem (3.1) will be obtained .

Theorem (3.5):

Let (X,d) be complete cone metric space with a regular cone p such that $d(x,y) \in p$ for $x,y \in X$. let $T: X \to X$ be a mapping on X satisfies :

$d(T(x),T(y)) \leq \varphi\, d(x,y)$...... (3.5)

for each x,y in X , where $\varphi : \{o\} \cup \text{int}\, p \to \{0\} \cup \text{int}\, p$ is continuos and satisfies the following properties :

i. $\varphi(t) = 0$ if and only if $t=0$

ii. $\varphi(t) < t$ for all $t \in \text{int}\, p$.

Then T has a unique fixed point .

Proof:

Fix $x \in X$ and let $x_n = T^n(x)$, $n = 1,2,\ldots\ldots$, To show that $< x_n >$ is a Cauchy sequence

$d(x_n, x_{n+1}) = d(T^n(x), T^{n+1}(x)) = d(T(T^{n-1}(x)), T(T^n(x))) \leq \varphi(d(T^{n-1}(x),T^n(x))) = \varphi(d(x_{n-1},x_n))$

So , By properties of φ , (2) , we get that : $d(x_n, x_{n+1}) \leq \varphi(d(x_{n-1},x_n)) < d(x_{n-1},x_n)$

Thus , the sequence $< d(x_n, x_{n+1}) >$ is monotone decreasing and bounded below , but p is regular cone, so $< d(x_n, x_{n+1}) >$ is convergent sequence and there exists $r \in P$ such that $d(x_n, x_{n+1}) \to r$ (as $n \to \infty$) or $\lim_{n\to\infty} d(x_n, x_{n+1}) = r$

Now , Assume $r \neq 0$, then by condition (3.5) we have: $d(x_{n+1},x_{n+2}) \leq \varphi(d(x_n, x_{n+1}))$,n=1,2,….

Now , letting $n \to \infty$ to both sides and by the continuity of φ we obtained that $r \leq \varphi(r)$, but by properties of φ , (2) , we have $\varphi(r) < r$ for all $r \in \text{int } p$, so we get that $\varphi(r) = r$ and by properties of φ , (2) we obtain that r = 0 which is contradiction , So , $\lim_{n\to\infty} d(x_n, x_{n+1}) = 0$

Now , To show that $< x_n >$ is a Cauchy sequence , If not , suppose that there exists $c \in E$ with

$0 << c$ such that for any $k \in N$, there exists $m_k > n_k > k$ such that : $d(xm_k, xn_k) \geq c$….(a)

Further more assume that for each k , m_k , is the smallest number greater than n_k for which the inequalities (a) holds . In view of the first part of proof , There exists k_0 such that $k \geq k_0$ and that implies $d(x_k,x_{k+1}) << \frac{c}{2}$, For such k , we have by triangular inequality :

$c \leq d(xm_k, xn_k) \leq d(xm_k, xm_{k-1}) + d(xm_{k-1} , xn_k)$

$\leq d(x_k , x_{k-1}) + d(x_{k-1} , x_k) << \frac{c}{2}+\frac{c}{2}=c$. So , $c \leq d(xm_k, xn_k) << c$

This proved $\lim_{k\to\infty} d(xm_k, xn_k) = c$. on the other hand ,

$d(xm_k, xn_k) \leq d(xm_k, xm_{k+1}) + d(xm_{k+1} , xn_{k+1}) + d(xn_{k+1} , xn_k)$

$\leq 2\, d(x_k,x_{k+1}) + \varphi(d(xm_k,xn_k))$ .Now , letting $k \to \infty$ to both sides , we have that

$c \leq \varphi(c)$, So we get by properties of φ that c=0 which is a contradiction with the inequality of (2) . So , $< x_n >$ is a Cauchy sequence in (X,d) , Therefore by completeness of (X,d) we obtained that $< x_n >$ is a convergent sequence , So there exists $z \in X$ such that $\lim_{n\to\infty} x_n = z$

Now , we will show that z is a fixed point of T . By triangular inequality we have :

$d(T(z),z) \leq d(T(z),x_{n+1}) + d(x_{n+1},z)$. By condition (3.5) we have :
$d(T(z),x_{n+1}) = d(T(z),T^{n+1}(x)) \leq \varphi(d(z,T^n(x))) = \varphi(d(z,x_n))$
Thus , $d(T(z),z) \leq \varphi(d(z,x_n)) + d(x_{n+1},z)$. Now , letting $n \to \infty$ to both sides we have :
$d(T(z),z) \leq \varphi(0)$, So by properties of φ we obtain that $d(T(z),z) \leq 0$ and then $d(T(z),z) = 0$,
Thus $T(z)= z$. To prove the uniqueness of fixed point , suppose u is another fixed point of T ,
So , $T(u) = u$, Thus ; $d(z,u) = d(T(z),T(u)) \leq \varphi(d(z,u))$. So , by properties of φ ,(2) , we have
$\varphi(d(z,u)) < d(z,u)$. Therefore we get $d(z,u) \leq \varphi(d(z,u)) < d(z,u)$.
So , we obtain that $\varphi(d(z,u)) = d(z,u)$ .Thus , by property of φ ,(1) , we have $d(z,u) = 0$ and $z=u$. Therefore , T has a unique fixed point .

REFERENCES

1. Grabiec,M.,"Fixed points in fuzzy metric space ,fuzzy sets and systems ",27,385- 389,1988
2. Hicks ,T.L. and Rhoades ,B.E., "Fixed point theory in symmetric spaces with applications to probabilistic spaces " ., Non linear Anal .36,331-344,1999.
3. I seki,K., "Fixed point theorems in 2-metric spaces ", Math – sem-Notes , Kobe univ .3,133-136,1975.
4. Jackymski,J.Matkowski,J.and swiat kowski ,T.," Non linear contraction on semi – metric spaces" , J.Appl.Anal .1,125-134,1995.
5. Kada,O., Suzuki,T.and Takashashi,w.,"Non convex minimization theorems and fixed point theorems in complete metric spaces ,"Math .Japan .44,381-391,1996.
6. Nadler,S.B.,"multi – valued contraction mapping ,pacific J. Math . 30, 475-488,1969.
7. Reilly,I.L., Subrahmanyam, P.v. and Vamanamurthy,M.K.,"Cauchy sequences in quasi –pseudo-metric spaces " Monatsh . Math .93,127-140,1982.
8. Sehgal,V.M.and Bharucha-Reid,A.T.,"Fixed points of contraction mappings on probabilistic metric spaces " ,Math ,system theory , 6,97 -102,1972.
9. Huang Long –Guang and Zhang xian ., " Cone metric spaces and fixed point theorems of contractive mapping" ,J. Math .,Anal . Appl.332,1468-1476,2007.

10. Rezapour,Sh. and Hamlbarani, R ., "Some notes on the paper ; cone metric spaces and fixed point theorems of contractive mapping " , J.Math.Anal .Appl.345,719-724,2008.
11. D. Ili´c and V. Rakocevi´c, Common fixed points for maps on cone metric space, J. Math. Anal. Appl . 341 (2008), 876–882.

The Direct and Inverse Problems for the Hyperbolic Boundary Value Problem

Jamil Amir Ali Al-Hawasy[1] and Halah Rahman Jaber[2]
[1,2]Deparment of mathematics, College of Science, University of Al-Mustansiriyah
Received 6/3/2013 – Accepted 15/9/2013

الخلاصة

يتناول هذا البحث حل المسألة المباشرة لمعادلة تفاضلية جزئية من النوع الزائدي مع شروط ابتدائية و حدودية باستخدام طريقة العناصر المحددة ويتناول ايضا حل المسألة العكسية لمسألة القيم الابتدائية المذكورة اعلاه لايجاد الشرط الابتدائي المصاحب لمسألة القيم الابتدائية من النوع الزائدي بتحويلها الى مسألة امثلية غير خطية والتي يتم حلها باستخدام طريقة هوك وجيفز غير مشروطة.اعطيت النتائج على شكل جداول او رسومات حيث اظهرت كفاه الطريقتين في الحل.

ABSTRACT

This paper deals with solving the direct problem for partial differential equation of hyperbolic type with initial conditions and boundary conditions using finite element method. Also it deals with the direct method for solving the inverse problem to determine the initial condition which associates the hyperbolic partial differential equation when the solution of the equation is given at finite number of points of the domain that the solution is defined. This problem is transformed to a nonlinear optimization problem which is solved by the unconstraint Hook and Jives method. The results are given by tables and/or figures and show the efficiency of these methods.

INTRODUCTION

During the last three decades, inverse problems have been studied from many researchers. Warin S. and Suabsagun Y. used the iterative method for Levenberg-Marquardt method to estimate the model parameters of conductivity variation of the ground [1]. Liao W. applied TAMC tool to solve the optimization problem which obtained from the formulation of inverse problem to determine the unknown acoustic coefficient (coefficient of 2D wave equation) [2]. Rashedi K. and Yousefi S.A., used a technique on the Ritz-Galrekin method to solve the inverse problem to determine the coefficient of a parabolic equation [3]. Al-Hawasy Ali, J. A. used the direct method to solve the inverse problem to determine the unknown region that the equation is defined [4]. In fact the differenence between the direct method which is used in [4] and which is used here are , first the varational method is used there to solve the direct problem while the finite elements method is used here , second the inverse problem is used there to find the region that the equation is defined while here the inverse problem is used to find the initial condition.

Since the inverse problems for hyperbolic partial differential equations arise naturally in geophysics, oil prospecting, in the design of optical devise, and in many other area. Hence our interest in this paper to study the inverse problem of hyperbolic differential equations to determine an initial condition.

The paper consists of two parts, in the first part, the direct problem is to solve the hyperbolic partial differential equation when the initial and the boundary conditions are given using the finite elements method. While the second part deals with the direct method for solving the inverse problem to determine the initial condition associated with hyperbolic differential equation when the solution of this equation are given at finite numbers of points of the domain that the equation is defined. This inverse problem is transformed to a nonlinear optimization problem which is solved by using the unconstraint Hook and Jives method. The results for both direct and inverse problems are given in tables and/or figures which show the efficiency of both methods.

STATEMENT OF THE DIRECT PROBLEM

Let $\Omega \in R^d$ be an open and bounded region with Lipischitz boundary $\Gamma=\partial\Omega$ and let I= (0, T) $0 < T < \infty$ and Q=Ω×I. The hyperbolic equation is given by:

$$y_{tt} + A(t)y = f(\vec{x}, t) \text{ in Q}, \vec{x} = (x_1, x_2, \ldots, x_d) \qquad \ldots(1)$$

with the boundary condition

$$y(x,t) = 0, \text{ in } \Sigma, \text{ where } \Sigma = \Gamma \times \mathrm{I} \qquad \ldots(2)$$

and the initial conditions

$$y(x,0) = y^0(x), \text{ in } \Omega \qquad \ldots(3)$$

$$y_t(x,0) = y^1(x), \text{ in } \Omega \qquad \ldots(4)$$

where A(t) is the 2nd order elliptic differential operator i.e.:

$$A(t)y = -\sum_{i,j=1}^{d} \frac{\partial}{\partial x_i}\left[a_{ij}(x,t)\frac{\partial y}{\partial x_i}\right]$$

Now, we denote by (,.) ,and $.\|.\|_1$ the inner product and norm in Sobolev space $V=H_0^1(Q)$ by $<.,.>$ the duality bracket between V and its dual $V^*$and by $\|.\|_Q$ the norm in $L^2(Q)$.

The weak form of the problem (1-4) is given by:

$$< y_{tt}, v > + a(t,y,v) = (f(t), v) \text{ , almost everywhere on I} \qquad \ldots(5)$$

$$y(0) = y^0 \text{ ,in } \Omega \qquad \ldots(6)$$

$$y_t(0) = y^1 \text{,in } \Omega \qquad \ldots(7)$$

with

$$a(t,y,v) = \sum_{i,j=1}^{d} aij(x,t)\frac{\partial y}{\partial x_j}\frac{\partial v}{\partial x_i} \qquad \ldots(8)$$

where the initial conditions make sense if $y^0 \in$ V, $y^0 \in L^2(\Omega)$,and $a(t,.,.)$ is the usual bilinear form associated with A(t),we suppose $a(t,v,w)$ is symmetric and for some positive constants $\alpha_1, \alpha_2, \forall\, v, w \in V \;\&\; t \in \bar{I}$, satisfies $|a(t,v,w)| \le \alpha_1 \|v\|_1 \|w\|_2$ and $a(t,v,w) \ge \alpha_1 \|v\|_1^2$.

We can rewrite equation (5) by

$< z_t, v > +a(t,y,v) = (f(t),v)$, almost everywhere on ...(5a)

$< y_{tt}, v >=< z_t, v >$ ...(5b)

DESCRTIZATION OF THE CONTINUOUS EQUATION

In this section we discrtize the weak form (5-7) by using the finite elements method. We suppose for simplicity the operator $a(t,.,.)$ is independent of t, the domain Ω is polyhedron. For every integer n, let $\{S_i^n\}_{i=1}^{m(n)}$ be an admissible regular triangulation of $\bar{\Omega}$ into closed disimplices [5],$\{I_j^n\}_{j=0}$ be subdivision of the interval $\bar{I}$ into N (n) intervals, where $t_j^n = [t_j^n, t_{j+1}^n]$ of equal lengths equal $lengths\, \Delta t = T/_N$. Set $Q_{ij} = S_i^n \times I_j^n$, Let $V_n \subset V = H_0^1(\Omega)$ be the space of continuous pricewise affine in Ω .

Hence, the discrete state equations, for each $v \in V_n$ is written in the form:

$(z_{j+1}^n - z_j, v) + \Delta t a(y_{j+1}^n, v) = \Delta t(f(t_j^n), v)$, $j = 0,1, ..., N-1$... (9)

$y_{j+1}^n - y_j^n = \Delta t Z_{j+1}^n$, $j = 0,1, ..., N-1$ ...(10)

$(y_0^n, v) = (y^0, v)$ ... (11)

$(z_0^n, v) = (y^1, v)$ ... (12)

Where $y^0 \in V, y^1 \in L^2(\Omega)$ are given, and $y_j^n = y(t_j^n), z_j^n = z(t_j^n), \in V$ for $j = 0,1,..,N$

Now, suppose the function f is defined on $S_i^n \times I_j^n$,$(i = 1,2, ..., m)$ continuous w.r.t. t_j^n, x_j.

form here and up and for brevity we will drop some times the agreement t_j^n of dependent variable y_j^n, Z_j^n and any others terms which contain this independent variable.

SOLUTION OF THE WAVE EQUATION BY FINITE ELEMENT METHOD

To find the solution $y^n = (y_0^n, y_1^n, ..., y_N^n)$ for fixed any j $(0 \le j \le N-1)$, the procedure utilized here, can be described by using the following steps: **Step 1:** for fixed any j,$(0 \le j \le N-1)$, let $\{v_i, i = 1,2, ... M(n)\}$ be a finite basis of V_n (where $V_i(x)$,for $i = 1,2, ..., n$ are continuous pricewise affine in Ω with $v_i(x)$ are zero on the boundary Γ), then equations(9-12) for any $i = 1,2, ..., M$ and $y_j^n, Z_j^n, y_{j+1}^n, Z_{j+1}^n \in V_n$, can be written in the form:

$(z_{j+1}^n - z_j, v_i) + \Delta t a(y_{j+1}^n, v_i) = \Delta t(f(t_j^n), v_i)$, $j = 0,1, ..., N-1$ (13)

$y_{j+1}^n - y_j^n = \Delta t Z_{j+1}^n$, $j = 0,1, ..., N-1$ ... (14)

$(y_0^n, v_i) = (y^0, v_i)$, ... (15)

$(z_0^n, v_i) = (y^1, v_i)$ ... (16)

Step2: Rewriting (14) in the form

$Z_{j+1}^{n} = \frac{y_{j+1}^{n} - y_{j}^{n}}{\Delta t}$ ... (17)

Substituting (17) in (13), we have:

$(y_{j+1}^{n} -, v_i) + \Delta t^2 a(y_{j+1}^{n}, v_i) = (y_j^n -, v_i) + \Delta t(z_j{}^n, v_i) + \Delta t^2 (f(t_j^n), v_i)$ ... (18)

Step3: From the basis of V_n, using Galerkin method we write $y_0^n = \sum_{k=1}^{m} c_k^0 v_k$

$y_j^n = \sum_{k=1}^{m} c_k^j v_k$, $y_{j+1}^n = \sum_{k=1}^{m} c_k^{j+1} v_k$, $Z_0^n = \sum_{k=1}^{m} d_k^0 v_k$, $Z_j^n = \sum_{k=1}^{m} d_k^1 v_k$, and

$Z_{j+1}^n = \sum_{k=1}^{m} d_k^{j+1} v_k$.

Where, $c_k^j = c_k(t_j^n)$, and, $d_k^j = d_k(t_j^n)$, are unknown constants, for each

$j = 0,1,\dots,N$.

Step4: Substituting $y_0^n, y_j^n, y_{j+1}^n, Z_0^j, Z_j^n$ and Z_{j+1}^n in equations (17,18,15,&16) we get the following linear system of ordinary differential equations:

$(A+(\Delta t)^2 B)C^{j+1} = AC^j + \Delta t A D^j + (\Delta t)^2 \vec{b}(t_j)$, $j = 0,1,\dots,N-1$ .. (19)

$D^{j+1} = \frac{1}{\Delta t}(C^{j+1} - C^j)$, $j = 0,1,\dots,N-1$ ... (20)

$AC^0 = e^0$ ... (21)

$AD^0 = e^1$ ... (22)

Where $A = (a_{ik})_{M\times M}$, $a_{ik} = (v_k, v_i)$, $B = (b_{ik})_{M\times M}$, $b_{ik} = a(t, v_k, v_i)$

$C_{M\times 1}^j = \left(c_1^j, c_2^j, \dots, c_M^j\right)^T$, $D_{M\times 1}^j = \left(d_1^j, d_2^j, \dots, d_M^j\right)$, $\vec{b} = (b_i)_{M\times 1}$, $b_i = (f(t_j), v_i)$

$\vec{V} = (v_i)_{M\times 1}$, $e^0 = (e_j^0)_{M\times 1}$, $e^1 = (e_j^1)_{M\times 1}$, $e_i^0 = (y^0, v_i)$ and $e_i^1 = (y^1, v_i)$, for each $i, k = 1,2,\dots,M$

The above linear system has a unique solution [6]. To solve the linear systems (19) and (20), first we solve the linear systems (21) and (22) to get the unknowns C^0 and D^0 , then we set $j = 0$ in (19) and (20) to get C^1 and D^1 , then we repeat this procedure to solve (19) and (20) , for $j = 2,\dots,N-1$ to get the unknowns C^j and D^j (solution of the direct problem).

THE INVERSE PROBLEM OF THE WAVE EQUATION
DESCRIPTION OF THE INVERSE PROBLEM

The previous section is devoted to the solution of the direct problem for the wave equation in $Q \subset R^3$, in which the solution of the problem

(discrete wave form) is found over the region Q , when the initial condition y$(x_1, x_{2,}0)$is given, while the inverse problem is to determine the initial condition $y_0(\vec{x}, 0)$when the solution of the wave equation is given on Δ (where Δ contains a finite number of the points of Q).
Where
$\Delta = \{(x_{1i}, x_{2i}): x_{1i} = x_{10} + ih, x_{2i} = x_{20} + ih, i = 0,1, \dots, M, \bar{t} = o.3 \in I\}$
In general the unknown initial condition can be expressed by the polynomial

$$y(x, 0) = \sum_{i=0}^{p} a_i x^i \quad \dots (23)$$

where a_i $(i = 0,1, \dots, p)$ are unknown constants)

MATHEMATICAL STATEMENT OF THE INVERSE PROBLEM FOR THE WAVE EQUATION

Before solving the inverse problem to find the unknown initial condition, the region of space variable Ω is assumed be a square, hence the unknown initial condition (23) must be in the form:

$$y(x, 0) = (x_1 - a)(x_2 - a)(x_1 - b)(x_2 - b) \quad \dots (24)$$

Therefore, our problem becomes to find the unknowns constants (a and b). Now, to solve this problem by using the direct method to find these unknowns the problem is transformed to the following discrete least-square approximation

$$\text{Min } H(a, b) = \sum_{i=0}^{M} \left[u(x_{1i}, x_{2i}, \bar{t}) - u_{ap}(x_{1i}, x_{2i}, \bar{t})\right]^2 \quad \dots (25)$$

where $u(x_{1i}, x_{2j}, \bar{t})$ are the given values of solution of the discrete wave equation at the point $(x_{1i}, x_{2i}, \bar{t}) \in \Delta$ with $\bar{t} = 0.3$ when all the initial and boundary conditions are known (solution of the direct problem) , $u_{ap}(x_{1i}, x_{2i}, \bar{t})$ are the values of the approximate solution of the same problem but when $y(\vec{x}, 0)$ has the form (24), i.e., the problem becomes to find the unknowns a and b which are in (24), the unconstrained Hook and Jives method [7], used to determine these values.

NUMERICAL EXAMPLES

EXAMPLE (1)

Consider the following wave equation :

$y_{tt} - \Delta y = f(\vec{x}, t)$, where $\vec{x} = (x_1, x_2)$

associated with the initial and boundary conditions

$y(\vec{x}, t) = 0$ on $\Sigma = \Gamma \times I$

$y(\vec{x}, 0) = x_1 x_2 (x_1 - 1)(x_2 - 1)$

$y_t(\vec{x}, 0) = -2(x_1^2 - x_1)(x_2^2 - x_2)$

where

$$f(\vec{x},t) = [4(x_1^2 - x_1)(x_2^2 - x_2) - 2(x_1^2 - x_1) - 2(x_2^2 - x_2)\,]e^{-2t}$$

The exact solution of this problem is:

$$y(x_1, x_2) = x_1 x_2 (x_1 - 1)(x_2 - 1)e^{-2t}$$

By using the finite element method for M=9, N=100, we get the results which are shown in Table (1) and Figure (1) at $\bar{t}$=0.3, the table shows the approximate solution $u_{ap}(x_{1i}, x_{2j}, \bar{t})$ and the exact solution $u(x_{1i}, x_{2j}, \bar{t})$ and the absolute error at x_1 and x_2.

Table-1: Comparison between exact and approximation solutions

X_{1i}	X_{2i}	*Exact solution*	*Approximate solution*	*Absolute Error*
0.2	0.2	0.0140	0.0136	4×10^{-4}
0.4	0.2	0.0211	0.0208	3×10^{-4}
0.6	0.2	0.0211	0.0211	10^{-4}
0.8	0.2	0.0140	0.0141	1×10^{-4}
0.2	0.4	0.0211	0.0208	3×10^{-4}
0.4	0.4	0.0316	0.0317	1×10^{-4}
0.6	0.4	0.0316	0.0318	2×10^{-4}
0.8	0.4	0.0211	0.0211	10^{-4}
0.2	0.6	0.0211	0.0211	10^{-4}
0.4	0.6	0.0316	0.0318	2×10^{-4}
0.6	0.6	0.0316	0.0317	1×10^{-4}
0.8	0.6	0.0211	0.0208	3×10^{-4}
0.2	0.8	0.0140	0.0141	1×10^{-4}
0.4	0.8	0.0211	0.0211	10^{-4}
0.6	0.8	0.0211	0.0208	3×10^{-4}
0.8	0.8	0.0140	0.0136	4×10^{-4}

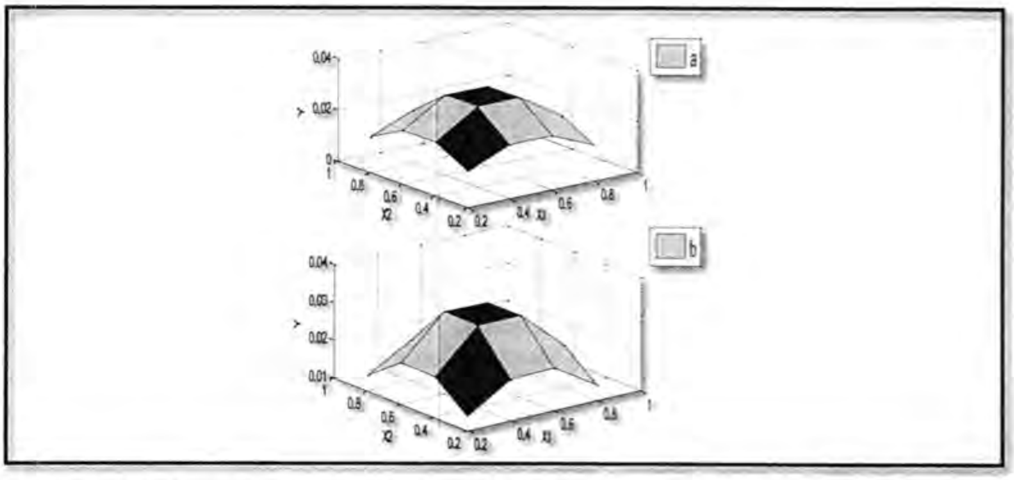

Figure-1: (a) shows the exact solution (b) shows the approximation solution

EXAMPLE (2)

Consider the following wave equation:

$$y_{tt} - \Delta y = f(\vec{x},t), \text{ where } \vec{x} = (x_1, x_2)$$

associated with the initial and boundary conditions

$$y(\vec{x},t) = 0 \text{ on } \Sigma = \Gamma \times I$$
$$y(\vec{x},0) = (x_1^2 - 4x_1 + 3)(x_2^2 - 4x_2 + 3)$$
$$y_t(\vec{x},0) = -(x_1^2 - 4x_1 + 3)(x_1^2 - 4x_2 + 3)$$

Where

$$f(\vec{x},t) = [(x_1^2 - 4x_1 + 3)(x_2^2 - 4x_2 + 3) - 2(x_1^2 - 4x_1 + 3) - 2(x_2^2 - 4x_2 + 3)]e^{-t}$$

The exact solution of this problem is:

$$y(x_1,x_2) = (x_1^2 - 4x_1 + 3)(x_2^2 - 4x_2 + 3)e^{-t}$$

By using the finite elements method for M=19, N=100, we get the results which are shown in Table (2) and Figure (2) at $\bar{t}$=0.3, which shows the approximate results $u_{ap}(x_{1i},x_{2i},t)$ and the exact solution $u(x_{1i},x_{2j},\bar{t})$ and the absolute error at the values of x_1 and x_2 which are given in the table.

Table-2: Comparison between exact and approximation solution

X_{1i}	X_{2i}	*Exact solution*	*Approximate solution*	*Absolute Error*	X_{1i}	X_{2i}	*Exact solution*	*Approximate solution*	*Absolute Error*
1.2	1.4	0.0901	0.089	1.1×10^{-3}	1.2	2.2	0.1351	0.1345	0.6×10^{-3}
1.4	1.4	0.2418	0.2404	1.4×10^{-3}	1.4	2.2	0.3627	0.3614	1.3×10^{-3}
1.6	1.4	0.3556	0.3558	0.2×10^{-3}	1.6	2.2	0.5334	0.5319	1.5×10^{-3}
1.8	1.4	0.4315	0.4308	0.7×10^{-3}	1.8	2.2	0.6472	0.6452	2×10^{-3}
2	1.4	0.4694	0.4684	1×10^{-3}	2	2.2	0.7041	0.7019	2.2×10^{-3}
2.2	1.4	0.4694	0.4681	1.3×10^{-3}	2.2	2.2	0.7041	0.7020	2.1×10^{-3}
2.4	1.4	0.4315	0.4301	1.4×10^{-3}	2.4	2.2	0.6472	0.6455	1.7×10^{-3}
2.6	1.4	0.3556	0.3540	1.6×10^{-3}	2.6	2.2	0.5334	0.5325	0.9×10^{-3}
2.8	1.4	0.2418	0.2417	1×10^{-3}	2.8	2.2	0.3627	0.3612	1.5×10^{-3}
1.2	1.8	0.1351	0.1344	0.7×10^{-3}	1.2	2.6	0.0901	0.0902	0.1×10^{-3}
1.4	1.8	0.3627	0.3612	1.5×10^{-3}	1.4	2.6	0.2418	0.2417	1×10^{-3}
1.6	1.8	0.5334	0.5325	0.9×10^{-3}	1.6	2.6	0.3556	0.3540	1.6×10^{-3}
1.8	1.8	0.6472	0.6455	1.7×10^{-3}	1.8	2.6	0.4315	0.4301	1.4×10^{-3}
2	1.8	0.7041	0.7020	2.1×10^{-3}	2	2.6	0.4694	0.4681	1.3×10^{-3}
2.2	1.8	0.7041	0.7019	2.2×10^{-3}	2.2	2.6	0.4694	0.4684	1×10^{-3}
2.4	1.8	0.6472	0.6452	2×10^{-3}	2.4	2.6	0.4315	0.4305	1×10^{-3}
2.6	1.8	0.5334	0.5319	1.5×10^{-3}	2.6	2.6	0.3556	0.3558	0.2×10^{-3}
2.8	1.8	0.3627	0.3614	1.3×10^{-3}	2.8	2.6	0.2418	0.2404	1.4×10^{-3}

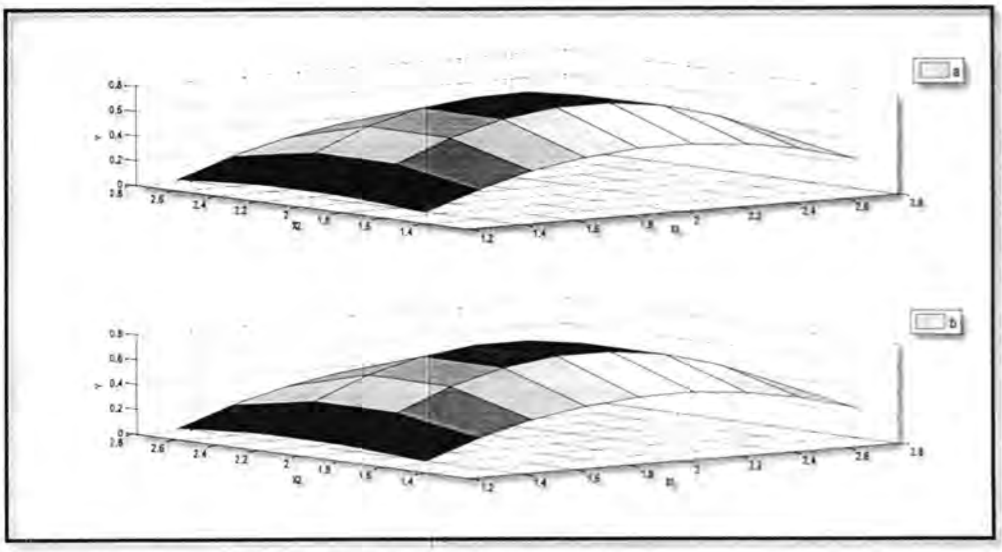

Figure-2: (a) shows the exact solution (b) shows the approximation solution

EXAMPLE (3)

Consider the following hyperbolic equation:

$$y_{tt} - \Delta y = f(\vec{x}, t), \text{ where } \vec{x} = (x_1, x_2)$$

With the boundary condition

$$y(\vec{x}, t) = 0 \text{ on } \Gamma = I \times \partial\Omega$$

And the initial conditions

$$y(\vec{x}, 0) = (x_1 - a)(x_2 - a)(x_1 - b)(x_2 - b)$$

$$y_t(\vec{x}, 0) = -2(x_1^2 - x_1)(x_2^2 - x_2)$$

Where

$$f(x, t) = [4(x_1^2 - x_1)(x_2^2 - x_2) - 2(x_1^2 - x_1) - 2(x_2^2 - x_2)]e^{-2t}$$

In this example the inverse problem is to find the unknown (a and b) using the method of Hook and Jives when the solution of the direct method is given at the points of the set Δ . By using the unconstraint Hook and Jives method with step length k=0.5,1 and different initial values of (a and b). the results are shown in table (3).

Table-3: Different initial values of unknowns (a and b) and their final values

K=0.5,1					
Initial Values		$Z = \sum_1^n (approximate - exact)^2$	*Final Values*		$Z = \sum_1^n (approximate - exact)^2$
a	b		a	b	
-2	3	0.0424	1	0	1×10^{-9}
2	5	1.5245	1	0	1×10^{-9}
3	6	10.3975	1	0	1×10^{-9}
4	8	94.1536	1	0	1×10^{-9}

EXAMPLE (4)

Consider the following hyperbolic equation:

$$y_{tt} - \Delta y = f(\vec{x}, t), \text{ where } \vec{x} = (x_1, x_2)$$

With the boundary condition

$$y(\vec{x}, t) = 0 \text{ on } \Gamma = I \times \partial\Omega$$

And initial conditions

$$y(\vec{x}, 0) = (x_1 - a)(x_2 - a)(x_1 - b)(x_2 - b)$$
$$y_t(\vec{x}, 0) = -(x_1^2 - 4x_1 + 3)(x_2^2 - 4x_2 + 3)$$

Where

$$f(x,t) = [(x_1^2 - 4x_1 + 3)(x_2^2 - 4x_2 + 3) - 2(x_1^2 - 4x_1 + 3) - 2(x_2^2 - 4x_2 + 3)]e^{-t}$$

By using the method of Hook and Jives with step length k=1 and different initial values of (a and b). The results are shown in table (4).

Table-4: Different initial value of unknowns (a and b) and their final values

K=1					
Initial Values		$Z=\sum_1^n(approximate - exact)^2$	*Final Values*		$Z=\sum_1^n(approximate - exact)^2$
a	b		a	b	
-3	1	194.4597	1	3	7×10^{-9}
3	6	0.1447	1	3	7×10^{-9}
4	8	20.0892	1	3	7×10^{-9}
5	7	12.7818	1	3	7×10^{-9}

CONCLUSION

In this paper we conclude that the finite elements method is suitable and efficient to solve the direct problem and in the other hand the finite elements method associated with unconstraint Hook and Jives method for solving a nonlinear optimization problem at certain time $\bar{t}$ with different values of space variable is efficient to determine initial condition associated with the given partial differential equation. It is important to mention here that the value of $\bar{t}$ is chose arbitral in the interval I, one can take any other value of $\bar{t}$ provided this value belong to I.

REFERENCES

1. Warin S., and Subsagun Y., 'Mathematical Inverse Problem of Magnetic Field from Exponentially Varying Conductive Ground', Applied Mathematic Science, Vol. 16, No. 113, 2012.
2. Lio W., 'An Accurate and Efficient Algorithm for Parameter Estimation of 2D Acoustic Wave Equation', International Journal of Applied Physics, Vol. 1 No. 2, 2011.

3. Rashedi k., and Yousefi S. A., 'Ritz Galerkin Method for Solving a Class of Inverse Problem in the Parabolic Equation', International Journal of Nonlinear Science, Vol. 12 No. 4, 2011.
4. Al-Hawasy J. A., 'On the Mathematical Inverse Problems with Applications to the Acoustic Wave Scattering', College of Science, Al-Nahrain University, M. Sc. Thesis, 1994.
5. Thomee V., 'Galerkin Finite Element methods for Parabolic Problem', 1997 Springer Verlag Berlin Heidelberg, New York.
6. Al-Hawasy J. A., 'The Discrete Classical Optimal Control Problem of Nonlinear Hyperbolic Partial Differential Equation (DCOCP)' Journal Al-Nahrain, Vol.13 , No 2. 2010.
7. Rao S. S., 'Optimization: Theory and Application', 2^{nd}, 1984, Wiely, New York.

Modules Whose Submodules Are Strongly Stable Relative To An Ideal

Mehdi S. Abbas[1] and Khalid A. Khudair[2]
Department of Mathematics, College of Science, Mustansiriya University, Baghdad, Iraq.
Received 6/3/2013 – Accepted 15/9/2013

الخلاصة

في هذا العمل، مفهوم مقاسات تامة الاستقرارية بقوة بالنسبة الى مثالي عَرّض و دُرّس و هو اقوى من مفهومي مقاسات تامة الاستقرارية و مقاسات تامة الاستقرارية بالنسبة الى مثالي. أعطينا عديد من الخواص و التوصيفات. درسنا حلقة التشاكلات الذاتية لهذا النوع من المقاسات و أعطينا فيصلية لكي تكون حلقة التشاكلات الذاتية تامة الاستقرارية بقوة بالنسبة الى مثالي باستخدام مفاهيم نظرية الفئات. أعطينا توصيف للمقاسات الجزئية بدلالة شرط البواقي و خاصية كل مقاس جزئي متحايد بالنسبة الى مثالي.

ABSTRACT

In this work, the notion of fully strongly stable modules relative to an ideal has been introduced and studied which is stronger than those of fully stable modules and fully stable modules relative to an ideal. Several properties and characterizations have been given. Endomorphism ring of this class of modules has been studied and criteria given, that an endomorphism ring is fully strongly stable relative to an ideal by using categorical concepts.characterization of submodules have been given in terms of some residual condition, and the property that each submodule is idempotent relative to an ideal.

INTRODUCTION

Throughout, R represents an associative ring with identity, unless otherwise stated and M a unitary right R-module. Let M be an R-module , a submodule N of M is called stable if $\alpha(N) \subseteq N$ for each R-homomorphism $\alpha : N \rightarrow M$. In case each submodule of M is stable, then M is called fully stable [1]. The relativity manners are usually applicable in mathematics, especially in module theory. Let M be an R-module and A a right ideal of R. A submodule N of M is called stable relative to A if $\alpha (N) \subseteq N + MA$ for each R-homomorphism $\alpha : N \rightarrow M$, and M is called fully stable relative to A,if each submodule of M is stable relative to A [2]. It is clear that the class of fully stable modules is contained in that of fully stable module relative to an ideal A. In fact, M is fully stable if and only if it is fully stable relative to the zero ideal.
In this paper, we consider a strong view of fully stable and hence fully stable modules relative to an ideal. Let M be an R-module and A a non-zero right ideal of R. M is called fully strongly stable relative to A if $\alpha (N) \subseteq N \cap MA$ for each submodule N of M and R-homomorphism α of N into M. It is shown that an R-module M is fully strongly stable relative to A if and only if each cyclic submodule of M is strongly stable relative to A. Several properties and characterizations of this class of module were considered. Among others, we proved the following : An R-module M is fully strongly stable relative to A if and only if $\ell_M (r_R(x)) = xR \cap MA$ for each x in M if and only if for each R-

homomorphism α of xR into M, there is an element r in R such that α (x) = xr $\in$ MA where x in M. We study conditions under which fully strongly stable modules relative to A are equivalent that the double annihilator condition holds for each submodules.

We studied the endomorphism ring of these modules. We show that over commutative ring, fully strongly stable modules relative to an ideal have endomorphism rings with strong view of commutativty. Further, we give the following: Let M be an R-module with endomorphism ring S and M generates ker(β) for each β in S. Then S is a right fully strongly stable ring relative to an ideal A of S if and only if ker(β) $\subseteq$ ker(α) implies that $\alpha \in \beta S \cap SA$.

An R-module M is called multiplication if each submodule of M is of the form MA for some ideal A of R [3]. We consider the following residual condition $[r_R(M):r_R(x)] = [xR \cap MA : M]$ where $x \in M$.

We proved that an R-module M is fully strongly stable relative to A if and only if the residual condition holds for each x in M under multiplication modules.

Finally, we introduced the concept of idempotent submodules relative to an ideal and consider modules in which all submodules are idempotent relative to an ideal, and show that an R-module M is fully strongly stable relative to A if and only if each submodule of M is idempotent relative to A where M is a prime module.

FULLY STRONGLY STABLE MODULES RELATIVE TO AN IDEAL.

In this section we introduce a concept which stronger than that of fully stable modules

Definition 2.1: Let M be an R-module and A a non-zero right ideal of R. A submodule N of M is called strongly stable relative to A (simply strongly A-stable). if $f(N) \subseteq N \cap MA$ for each R-homomorphism f of N into M. M is called fully strongly A-stable, if each submodule of M is strongly A-stable. If R as a right R-module is fully strongly A-stable, then R is called fully strongly A-stable ring.

It is clear that, if a submodule N of an R-module M is strongly A-stable, then it is strongly B-stable for each right ideal B of R containing A. Hence, if N is strongly A-stable submodule of M, then it is strongly R-stable, and this is equivalent to saying that N is stable in M. Thus every fully strongly A-stable R-module is fully stable, while the converse may not be true generally, for example, the Z_6-module Z_6 is fully stable, but it is not fully strongly A-stable for each proper ideal A of Z_6. If M is a fully stable R-module and M= MA for some non-zero right ideal A of R, then M is fully strongly A-stable. If M is projective R-module, then

M = Mtr(M) where tr(M) is the trace of M [4, proposition(2.40)], so if M is a fully stable projective R-module, then M is fully strongly tr(M)-stable. In particular, every fully stable ring R is fully strongly tr(R)-stable. The Z-module Z as well as Q and Q/Z are not fully strongly (mZ)-stable for each non-negative integer m. If $\{N_i \mid i \in I\}$ is a family of strongly A-stable submodules of an R-module M, then so is $\Sigma_{i\in I} N_i$.
Fully strongly A-stable modules are not closed under submodules. For example, the Z-module Z_{p^∞} is fully strongly (nZ)-stable for each positive integer n, if $\alpha: Z_{p^k} \rightarrow Z_{p^\infty}$ is a Z-homomorphism, then $\alpha(Z_{p^k}) \subseteq Z_{p^k} \cap Z_{p^\infty}$. It is well known that Z_{p^∞} is divisible, so $nZ_{p^\infty} = Z_{p^\infty}$ for each positive integer n and hence $\alpha(Z_{p^k}) \subseteq Z_{p^k} \cap Z_{p^\infty}(nZ)$. We claim that the submodule $Z_{p^{2k}}$ of Z_{p^∞} is not fully strongly $(Z_{p^{2k}})$-stable, for each $k > 1$, let $f : Z_{p^k} \rightarrow Z_{p^{2k}}$ be the inclusion mapping, so $f(Z_{p^k}) = Z_{p^k}$, but $Z_{p^k} \cap (Z_{p^{2k}} \cdot p^{2k}Z) = 0$. This shows that $Z_{p^{2k}}Z$ is not fully strongly $(Z_{p^{2k}}Z)$-stable.
Let M be an R-module and A a non-zero right ideal of R. We say that a submodule N of M is A-pure, if $NA = N \cap MA$.
In the following we show that certain submodules inherit the property of full strong stability relative to a non-zero ideal.
Proposition 2.2: Let M be a fully strongly A-stable module. Then every A-pure submodule of M is fully strongly A-stable. In particular, every pure (and hence direct summand) submodule of fully strongly A-stable module is fully strongly A-stable.
Proof: Let N be A-pure submodule of M. For each submodule K of N and R-homomorphism $f : K \rightarrow N$, put $g = i_N \circ f : K \rightarrow M$ where i_N is the inclusion mapping of N into M, then $f(K) = g(K) \subseteq K \cap MA \subseteq K \cap N \cap MA = K \cap NA$. Thus N is fully strongly A-stable.
The proof of following proposition is immediate
Proposition 2.3: Let M be an R-module and non-zero right ideal A of R. Then
1- M is fully strongly A-stable if and only if each cyclic submodule of M is strongly A-stable.
2- M is fully strongly A-stable for each non-zero right ideal of R. if and only if it is fully strongly (aR)-module for each non-zero element a in R.
Next, we discuss the direct sums of fully strongly A-stable modules. The Z-module Q / Z is not fully strongly A-stable for each ideal A of Z, while $Q / Z \cong \oplus_p Z_{p^\infty}$ where the sum has been taken over all primes. This shows that fully strongly A-stable modules are not closed under direct

sum. In the following we consider conditions which guarantee full strong A-stability of finite direct sum.

Proposition 2.4 : Let $M = \oplus_{i=1}^{n} M_i$ where M_i is an R-module for each i with $r_R(M_i) + \cap_{j\neq i} r_R(M_j) = R$ and A a non-zero right ideal of R. Then M is fully strongly A-stable if and only if each M_i is fully strongly A-stable.

Proof: we shall prove the case $M = M_1 \oplus M_2$ and the proposition then follows by induction on n. Let K be a submodule of M. The condition $r(M_1) + r(M_2) = R$ implies that there are submodules N_1 of M_1 and N_2 of M_2 such that $K = N_1 \oplus N_2$ [1]. Let $\theta: K \to M$ be an R-homomorphism. put $\theta_i = \pi_i\theta\, j_i$ $(i = 1,2)$ where $j_i : N_i \to M$ is the injection mapping and $\pi_i : M \to M_i$ is the natural projection. Hence $\theta = \theta_1 + \theta_2$ and $\theta(K) = \theta_1(N_1) \oplus \theta_2(N_2) \subseteq (N_1 \cap M_1A) \oplus (N_2 \cap M_2A) \subseteq (M_1 \oplus M_2)A = K \cap MA$. This implies that M is fully strongly A-stable. The converse follows from proposition (2.2).

Next we note characterizations of fully strongly A-stable modules.

Theorem 2.5: Let M be an R-module and non-zero right ideal A of R. Then the following conditions are equivalent:

1- M is fully strongly A-stable,
2- Each cyclic submodule of M is strongly A-stable,
3- $\ell_M(r_R(x)) = xR \cap MA$ for each x in M,
4- $r_R(x) \subseteq r_R(y)$ implies $y \in xR \cap MA$ for each x in M and y in MA,
5- $\ell_M(aR + r_R(x)) = \ell_M(aR) \cap xR \cap MA$ for each x in M and a in R.
6- For each R-homomorphism $\alpha: xR \to M$, there is r in R such that $\alpha(x) = xr \in MA$.

Proof: (1) $\Leftrightarrow$ (2): Follows from Proposition (2.3)

(4) $\Rightarrow$ (3): It always $xR \cap MA \subseteq xR \subseteq \ell_M(r_R(x))$. If $y \in \ell_M(r_R(x))$, then $r_R(x) \subseteq r_R(y)$, so $y \in xR \cap MA$, by (4), and hence $\ell_M(r_R(x)) \subseteq xR \cap MA$.

(3) $\Rightarrow$ (4): Let $x \in M$ and $y \in MA$. If $r_R(x) \subseteq r_R(y)$, then $\ell_M(r_R(y)) \subseteq \ell_M(r_R(x))$ so by (3), $yR \cap MA \subseteq xR \cap MA$, but $y \in yR \cap MA$, then $y \in xR \cap MA$.

(3) $\Rightarrow$ (5): $\ell_M(aR + r_R(x)) = \ell_M(aR) \cap \ell_M(r_R(x)) = \ell_M(aR) \cap xR \cap MA$

(5) $\Rightarrow$ (6): Let $\alpha: xR \to M$ be an R-homomorphism. Then $\alpha(x)R \subseteq \ell_M(r_R\alpha(x)) \subseteq \ell_M(r_R(x)) = xR \cap Ma$, by take $a = 0$ in (5), so $\alpha(x) = xr \in MA$ for some r in R.

(6) $\Rightarrow$ (2): Let $\alpha: xR \to M$ be an R-homomorphism. Then by (6), there is r in R such that $\alpha(x) = xr \in MA$. For each $u = xt \in xR$, where t in R,

so $\alpha(u) = \alpha(xt) = \alpha(x)t = (xr)t \in xR \cap MA$ and hence $\alpha(xR) \subseteq xR \cap MA$. This shows that xR is strongly A-stable submodule in M.

As we have mentioned that an R-module M is fully stable if and only if it is fully strongly R-stable, so by take A = R and M = R in Theorem (2.5) we the following corollaries respectively.

Corollary2.6: ([1], theorem (3.6)) Let M be an R-module. Then the following conditions are equivalent:

1- M is fully stable,

2- Each cyclic submodule of M is stable,

3- $\ell_M(r_R(x)) = xR$ for each x in M,

4- $r_R(x) \subseteq r_R(y)$ implies $y \in xR$ for each x, y in M ,

5- Each R-homomorphism $\alpha: xR \to M$ is a right multiplication by an element of R.

Corollary 2.7: The following are equivalent for a ring R and a non-zero right (respt. left) ideal A of R.

1- R is right (respt. left) fully strongly A-stable,

2- Each right (respt. left) principal ideal of R is strongly A-stable,

3- $\ell_R(r_R(x)) = xR \cap RA$ (respt. $r_R(\ell_R(x)) = Rx \cap AR$) for each x in R,

4- $r_R(x) \subseteq r_R(y)$ implies $y \in xR \cap RA$ (respt. $\ell_R(x) \subseteq \ell_R(y)$) implies $y \in Rx \cap AR$)for each x in R and y in RA,

5- $\ell_R(aR + r_R(x)) = \ell_R(aR) \cap xR \cap MA$ (respt. $r_R(Ra + \ell_R(x)) = r_R(Ra) \cap Rx \cap AR$) for each x , a in R.

6- For each R-homomorphism $\alpha : xR \to M$ (respt. $\alpha : Rx \to M$), there is r in R such that $\alpha(x) = xr \in RA$ (respt. $\alpha(x) = rx \in AR$).

We direct our attention for conditions (3) and (6) of Theorem (2.5) for each submodule. We have proved that an R-module M is fully strongly A-stable if and only if for each cyclic submodule xR and R-homomorphism α: $xR \to M$, there is an element r in R such that $\alpha(x) = xr \in MA$ if and only if $\ell_M(r_R(x)) = xR \cap MA$ for each x in M.

Proposition 2.8 : Let M be an R-module and A a non-zero right ideal of R with $r_R(N \cap K) = r_R(N) + r_R(K)$ for each finitely generated submodules N and K of M. Then the following statements are equivalent:

1- M is fully strongly A-stable,

2- For each R-homomorphism $\alpha: x_1R + x_2R + \ldots + x_nR \to M$, there is t in R such that $\alpha(\sum_{i=1}^{n} x_i r_i) = (\sum_{i=1}^{n} x_i r_i)t \in MA$ where $r_1, r_2, \ldots, r_n$ in R.

Proof : (2) $\Rightarrow$ (1) : follows from Theorem (2.5)

(1) $\Rightarrow$ (2): Let $N = x_1R + x_2R + \ldots + x_nR$ be a finitely generated submodule of M and $\alpha: N \to M$ be an R-homomorphism. We use

induction on n. For n = 1, this is just theorem (2.5). Suppose that the statement holds for m < n, there exist two element r, s in R such that $\alpha(\sum_{i=1}^{n-1} x_i r_i) = (\sum_{i=1}^{n-1} x_i r_i)r \in MA$ and $\alpha(x_n r_n) = x_n r_n s \in MA$. Now, let $y = \sum_{i=1}^{n-1} x_i r_i = x_n r_n$, then $\alpha(y) = yr = ys$, so $r - s \in r_R(y)$, but $y \in \sum_{i=1}^{n-1} x_i R \cap x_n R$, there exist $u \in r_R(\sum_{i=1}^{n-1} x_i R)$ and $v \in r_R(x_n R)$ such that $r - s = u + v$. Put $t = r - u = s + v$. let $z = \sum_{i=1}^{n-1} x_i r_i$. Then

$\alpha(z) = \alpha(\sum_{i=1}^{n-1} x_i r_i) + \alpha(x_n r_n) = (\sum_{i=1}^{n-1} x_i r_i)r + (x_n r_n)s = (\sum_{i=1}^{n-1} x_i r_i)r - (\sum_{i=1}^{n-1} x_i r_i)u + (x_n r_n))s + (x_n r_n)v = (\sum_{i=1}^{n-1} x_i r_i)t + (x_n r_n))t = zt \in MA$

Corollary 2.9: Let M be a noetherian R-module and A a non-zero right ideal of R with $r_R(N \cap K) = r_R(N) + r_R(K)$ for each two submodules N and K of M. Then the following statements are equivalent:

1- M is fully strongly A-stable,

2- Given a submodule N of M and R-homomorphism $\alpha : N \to M$, for each x in N, there exists an element r in R such that $\alpha(x) = xr \in MA$

Lemma 2.10: Let M be a fully strongly A-stable R-module such that for given x in M and right ideal I of R, each R-homomorphism of xI into M can be extended to one from xR into M. Then if a submodule N of M satisfies $\ell_M(r_R(N)) = N \cap MA$, then so does N+xR.

Proof: Denote $r_R(N)$ and $r_R(xR)$ by B and C respectively. Then by Theorem (2.5) and assumption, we have $\ell_M(C) = xR \cap MA$ and $\ell_M(B) = N \cap MA$. Since $r_R(N + xR) = B \cap C$, it is enough to show that $\ell_M(B \cap C) \subseteq (N + xR) \cap MA$. Let $y \in \ell_M(B \cap C)$. $\theta: xB \to M$ is well-defined by $\theta(xb) = yb$. The hypothesis implies that θ can be extended to $\alpha: xR \to M$, so $\alpha(x) \in xR \cap MA$. For each b in B, $\alpha(x)b = \alpha(xb) = yb$ implies that $\alpha(x) - y \in \ell_M(B) = N \cap MA$, so $\alpha(x) - y = n$ for some $n \in N \cap MA$ or $y = -n + \alpha(x) \in N \cap MA + Rx \cap MA \subseteq (N + xR) \cap MA$.

Proposition 2.11: Let M be an R-module and non-zero ideal A of R, such that for given x in M and right ideal I of R, each R-homomorphism of xI into M can be extended to one of xR into M. Then the following are equivalent:

1- M is fully strongly A-stable,

2- $\ell_M(r_R(N)) = N \cap MA$ for each finitely generated submodule N of M.

Proof: (1) ⇒ (2): Let $N = \sum_{i=1}^{n} x_i R$ be a finitely generated submodule of M. we use induction on n. Theorem (2.5) implies that (2) is true for n = 1. Suppose that $\ell_M(r_R(K) = K \cap MA$ for m -generated submodule K of M where m < n. Then lemma (2.10) implies (2) for (m+1)-generated submodule of M.

(2) ⇒ (1) Follows from Theorem (2.5).

Note that quasi-injective modules ([4],definition (6.70)) are satisfying the extension condition of Proposition (2.11). Then, we have the following corollary.

Corollary 2.12: Let M be a Noetherian quasi-injective R-module and A a non-zero right ideal of R. Then M is fully strongly A-stable if and only if $\ell_M(r_R(N)) = N \cap MA$ for each submodule N of M.

ENDOMORPHISM RING

Let M be an R-module with $S=End_R(M)$, its endomorphism ring and A a non-zero right ideal of R. Suppose R is commutative and M is fully strongly A-stable. Then for each α, β in S and x in M, there are s, t in R such that $\alpha(x) = xs \in MA$ and $\beta(x) = xt \in MA$, so $\alpha\beta = \beta\alpha$. Since MA is a fully invariant submodule of M, then $\alpha\beta(x) = \beta\alpha(x) = \beta(xs) \in \beta(MA) \subseteq MA$.

The above suggest the following:

Let M be an R-module and S be its endomorphism ring. We say that S is Strongley commutative relative to a right ideal A of R (simpley strongly A-commutative, if $\alpha\beta(x) = \beta\alpha(x) \in MA$ for each α, β in S and x in M.

Proposition 3.1: Let R be a commutative ring, and M a fully strongly A-stable R-module. Then S is strongly A-commutative.

The converse of the above proposition may not be true for example, it is well known that $End_Z(Q) \cong Q$ ([5], page 216) which is a commutative. Since $Q(mZ) = Q$ for each nonzero m in Z, thus $End_Z(Q)$ is strongly (mZ)-commutative for each non-zero m in Z, while Q is not fully strongly (mZ)-stable for each ideal mZ of Z.

Now, we discuss the converse in certain class of modules.

Proposition 3.2: Let M be an R-module in which every cyclic submodule is direct summand. If $S = End_R(M)$ is strongly A-commutative, then M is fully strongly A-stable, where A is a non-zero right ideal of R.

Proof : Let $N = xR$ be a cyclic submodule of M and $\alpha : N \rightarrow M$ be an R-homomorphism. Then $M = N \oplus L$ for some submodule L of M. α can be extended to $\beta \in S$, by putting $\beta(L) = 0$. For each $w = x+y \in M$ where $x \in N$ and $y \in L$, define $h: M \rightarrow M$ by $h(x+y) = x$. Put $\alpha(x) = u+v$ for some $u \in N$ and $v \in L$. Now $(h\circ\beta)(w) = h(\beta(x+y)) = h(\alpha(x)) = h(u+v) = u$, but $\beta \circ h(w) = u+v$. Strong A-commutative of S implies $u = u+v \in MA$, so $v = 0$ and hence $f(x) = u \in N \cap MA$. This shows that N is strongly A-stable, so by Theorem (2.5), M is fully strongly A-stable.

Recall that an R-module M is regular if for each $m \in M$, there is $\alpha \in M^*=Hom_R(M,R)$ such that $m = m\alpha(m)$. In regular modules each cyclic submodule is direct summand [6, Theorem(1.6)]. Then we have.

Corollary 3.3: Let M be a regular R-module (R is commutative ring) and A a non-zero ideal of R. Then M is fully strongly A-stable if and only if $S = End_R(M)$ is strongly A-commutative.

In ([6],theorem(5.2)), Zelmanowitz proved that for a regular R-module M, M is quasi-injective if and only if $End_R(M)$ is self-injective ring. We shall regard this as a motivation for the following

Theorem 3.4: Let M be a regular R-module (R is commutative ring) and A a non-zero ideal of R. Then M is fully strongly A-stable, if and only if $S = End_R(M)$ is right fully strongly $Hom_R(M,MA)$-stable.

First we need the following lemma.

Lemma 3.5: Let M be an R-module in which every cyclic submodule is direct summand and A a non-zero right ideal of R. If $S = End_R(M)$ is fully strongly $Hom_R(M,MA)$-stable, then M is fully strongly A-stable.

Proof: Let N be a cyclic submodule of M and $\alpha : N \to M$ an R-homomorphism. $I = Hom_R(M,N)$ is a right ideal of S. $\theta: I \to S$ is well defined by $\theta(f) = \alpha\circ f$, for each $f \in I$. full strong $K = Hom_R(M,MA)$ -stability of S implies that θ(I)\subseteq I ∩ KS=I ∩ K, that is for each $f \in I$, $\alpha \circ f \in I \cap K$, so $\alpha \circ f : M \to N \cap MA$. Since N is direct summand, then $\alpha \circ \pi_N: M \to N \cap MA$ where π_N is the natural projection of M onto N. Since π_N is onto, then $\alpha(N) = \alpha(\pi_N(N)) = (\alpha \circ \pi_N)(N)$ so, $\alpha : N \to N \cap MA$. Then $\alpha(N) \subseteq N \cap MA$, this shows that M is fully strongly A-stable, Theorem (2.5).

Corollary 3.6: Let M be a regular R-module and A a non-zero right ideal of R. If $S = End_R(M)$ is a right fully strongly $Hom_R(M,MA)$-stable, then M is fully strongly A-stable.

Proof of theorem (3.4): Let $K = Hom_R(M,MA)$ and M a regular fully strongly A-stable R-module. Then by [6, theorem (3.4)], cent(S) is a regular ring, Proposition (3.1) implies that S is strongly A-commutative, and so commutative ring. Thus S is fully stable ring [1, proposition (1.2.2)]. For each $\alpha \in S$ and S-homomorphism $\beta : (\alpha) \to S$, we have $\beta(\alpha S) \subseteq \alpha S$, but $\beta(\alpha) \in S$ and since S is strongly A-commutative, then $\alpha\circ\beta = \beta \circ \alpha$ and $Im(\beta\, \alpha) \subseteq MA$, so $\beta\circ \alpha \in K$, that is $\beta(\alpha) \in K$ and hence $\beta(\alpha) \subseteq \alpha S \cap K = \alpha S \cap KS$, this shows that S is fully strongly K-stable. The other direction follows from Corollary (3.6)

We conclude this section with some conditions that an endomorphism ring is fully strongly stable relative to an ideal.

Recall that, for two R-modules B and C, B generates C if $C = \Sigma Im(\varphi)$ where the sum runs over all R-homomorphism $\varphi : B \to C$. Dually, C cogenerates B if $0 = \cap \ker(\varphi)$ where the intersection runs over all R-homomorphism $\varphi : B \to C$. This is equivalent to saying that for each non-zero R-homomorphism $\lambda: L \to B$, there exists an R-homomorphism $\varphi: B \to C$ such that $\varphi \lambda \neq 0$([7], theorem(3.3.3)).

Theorem 3.7: Let M be an R-module, $S = End_R (M)$ and W a non-zero right ideal of S. Then

1- Assume that M generates $\ker(\beta)$ for each β in S. Then S is a right fully strongly W-stable if and only if $\ker(\beta) \subseteq \ker(\delta)$ implies that $\delta \in \beta S \cap SW$.

2- Assume that M cogenerates $M/\beta(M)$ for each $\beta \in S$. Then S is a left fully strongly W-stable if and only if $\delta(M) \subseteq \beta(M)$ implies that $\delta \in S\beta \cap WS$.

Proof : 1- For each $\alpha \in r_S(\beta)$, then $Im(\alpha) \subseteq \ker(\beta) \subseteq \ker(\delta)$, so $\alpha \in r_S(\delta)$. Thus $r_S(\beta) \subseteq r_S(\delta)$ implies that $\delta \in \beta S \cap SW$, corollary 2.7. Conversely, if $\delta \in \ell_S(r_S(\beta))$ and $x \in \ker(\beta)$, then $\beta(x) = 0$ and $x = \sum_{i=1}^{n} \alpha_i (m_i)$ where $m_i \in M$ and $\alpha_i : M \to \ker(\beta)$, hence $0 = \sum_{i=1}^{n} \beta\alpha_i (m_i)$, thus $\beta\, \alpha_i = 0$ for each i, then $\alpha_i \in r_S(\beta)$, so $\delta\alpha_i = 0$ for each i. Then $\delta(x) = \sum_{i=1}^{n} \delta\alpha_i (m\ \ ) = 0$ implie that $x \in \ker(\delta)$ Thus $\ker(\beta) \subseteq \ker(\delta)$. The hypothesis implies that $\delta \in \beta S \cap SW$,so by Corollary (2.7), S is right fully strongly W-stable.

2- For each $\alpha \in \ell_S(\beta)$, then $\alpha\beta = 0$, $Im(\delta) \subseteq Im(\beta) \subseteq \ker(\alpha)$ implies that $Im(\delta) \subseteq \ker(\alpha)$ and $\alpha \in \ell_S(\delta)$. Hence $\ell_S(\beta) \subseteq \ell_S(\delta)$. Corollary (2.7) implies that $\delta \in S\beta \cap WS$. Conversely, if $\delta \in r_S(\ell_S(\beta))$ and $\delta(M) \not\subseteq \beta(M)$, then there is $m_0 \in M$ such that $\delta (m_0) \notin \beta(M)$, thus the natural epimorphism $\upsilon: M \to M / \beta(M)$ is non-zero. The cogeneration hypotheses implies there is an R-homomorphism $\sigma : M \to M$ such that $\sigma\upsilon \neq 0$, so $\sigma(\delta(m_0) + \beta(M)) \neq 0$. $f : M \to M$ is well defined by $f(m) = \sigma(m + \beta(M))$ for $m \in M$. Then $f(\delta(m_0)) = f\,\delta(m_0) = \sigma(\delta(m_0) + \beta(M)) \neq 0$, so $f\,\delta \neq 0$, while $f\,\beta = 0$, hence $f \notin \ell_S(\beta)$, but $f\,\delta \neq 0$ which is a contradiction. Thus $\delta(M) \subseteq \beta(M)$,so the hypothesis implies that $\delta \in S\beta \cap WS$, and then $r_S(\ell_S(\beta)) = S\beta \cap WS$. Corollary (2.7) implies that S is left fully strongly W-stable.

RESIDUAL CONDITION

Let R be a ring with identity and A a non-zero ideal of R.Then by theorem (2.5). R is fully strongly A-stable if and only if $\ell_R(r_R(a)) = aR \cap RA$ for each $a \in R$. If R is commutative ring, then the last condition is equivalent to the condition $[r_R(R): r_R(a)] = [aR \cap RA: R]$ for each $a \in R$ while for arbitrary R-module M, the residual condition does not equivalent to full strong A-stability of M, for example, the Z-module Q satisfies the condition $[r_R(Q) : r_R(x)] = [xZ \cap Q(mZ) : Q]$ where x in Q, but Q is not fully strongly (mZ) -stable for each non-zero $m \in Z$.

First, we prove the following

Prpopostion 4.1: Let M be an R-module and A a non-zero right ideal of R. If M is fully strongly A-stable, then $[r_R(M): r_R(x)] = [xR \cap MA : M]$ for each $x \in M$.

Proof : Let $w \in [r_R(M) : r_R(x)]$ and $m \in M$. Define $\theta : xR \to M$ by $\theta(xr) = mrw$, for $r \in R$. If $xr = 0$ and since $r_R(w) \subseteq r_R(m)$, then $mrw = 0$, thus θ is well defined. It is clear that θ is R-homomorphism. Then Theorem (2.5) implies that there is $t \in R$ such that $\theta(x) = xt \in MA$, thus $mw \in xR \cap MA$. Therefor $w \in [xR \cap MA : M]$ and hence $[r_R(M) : r_R(x)] \subseteq [xR \cap MA : M]$. The other inclusion is always true.

We need the following lemma which appears in ([1], lemma(3.2.4)), before considering the converse of Proposition (4.1)

Lemma 4.2: Let M be a multiplication R-module (R is a commutative ring) and N a submodule of M. For each R-homomorphism $\theta: N \to M$ we have

1- $[\theta(N) : M] \subseteq [r_R(M) : r_R(N)]$

2- $\theta(N) \subseteq M[r_R(M) : r_R(N)]$

Theorem 4.3: Let M be a multiplication R-module, (R is a commutative ring) and A a non-zero ideal of R. If $[r_R(M): r_R(x)] \subseteq [xR \cap MA : M]$ for each $x \in M$, then M is fully strongly A-stable.

Proof: Let xR be a cyclic submodule of M. For each $m \in M$ and $e \in [r_R(M) : r_R(x)]$, $\alpha_{(m,e)} : xR \to M$ is well defined by $\alpha_{(m,e)}(xr) = mre$, for $r \in R$. By the choice of e, m and the condition $[r_R(M) : r_R(x)] \subseteq [xR \cap MA : M]$ we have $\alpha_{(m,e)}(xR) \subseteq xR \cap MA$. Now for each R-homomorphism $\alpha : xR \to M$, by Lemma (4.3) we get $\alpha(xR) \subseteq M[r_R(M) : r_R(x)]$, thus $\alpha(xr) = \alpha(x)r = \sum_{i=1}^{n} m_i r e_i$ for some $m_i \in M$ and $e_i \in [r_R(M):r_R(x)]$ so $\alpha(xr) = \sum_{i=1}^{n} \alpha_{(m_i,e_i)}(xr)$. Therefore $\alpha = \sum_{i=1}^{n} \alpha_{(m_i,e_i)}$ and hence hence $\alpha(xR) \subseteq xR \cap MA$. That is M is fully strongly A-stable.

Then we have the following corollary which gives a characterization of fully strongly A-stable modules in terms of residual condition.

Corollary 4.4: Let M be a multiplication R-module and A a non-zero ideal of R. Then M is fully strongly A-stable if and only if $[r_R(M):r_R(x)] = [xR \cap MA : M]$ for each $x \in M$.

As every cyclic module over a commutative ring R is multiplication, in the following we have the motivation that mentioned at beginning of this section.

Corollary 4.5: Let A be a non-zero ideal of a ring R. Then R is fully strongly A-stable if and only if $[r_R(R): r_R(x)] = [xR \cap A: R]$ for each $x \in R$.

There is no comparison between multiplication modules and the residual condition, for example Z is a multiplication Z-module which does not satisfy the residual condition while Z_{p^∞} is a fully strongly A-stable Z-module for each non-zero ideal A of Z and hence by Proposition (4.1) satisfies the residual condition, but Z_{p^∞} is not multiplication.

Definition 4.6: Let M be an R-module and A a non-zero ideal of R. A submodule N of M is called A-idempotent in M if $N = N[N \cap MA : N]$

Next, we consider modules in which each submodule is A-idempotent this is equivalent to saying that each cyclic submodule is A-idempotent.

Proposition 4.7: Let M be an R-module and A a non-zero ideal of R. If each submodule of M is A-idempotent, then M is fully strongly A-stable.

Proof: Let N be a submodule of M and $\alpha: N \rightarrow M$ an R-homomorphism. For each $n \in N = N[N \cap MA:M]$, then $n = \sum_{i=1}^{n} n_i r_i$ for some $n_i \in N$ and $r_i \in [N \cap MA : M]$. Thus $\alpha(n_i)r_i \in Mr_i \subseteq N \cap MA$ for each i and so $\alpha(N) \subseteq N \cap MA$.

The Z-module Z_8 is fully strongly (3Z)-stable, Theorem (2.5). Consider the submodule $N = \{\bar{0}, \bar{4}\}$ of Z_8. $N[N \cap Z_8(3Z) : Z_8] = N[N : Z_8] = N(4Z) = 0 \neq N$. This shows Z_8 has a submodule which is not (3Z) -idempotent.

For the converse of Proposition (4.7), recall that an R-module M is prime if $r_R(M) = r_R(N)$ for each non-zero submodule N of M.

Theorem 4.8: Let M be a prime R-module and A a non-zero ideal of R. Then the following statements are equivalent

1- M is fully strongly A-stable

2- $[r_R(M) : r_R(x)] = [xR \cap MA:M]$ for each $x \in M$

3- Every submodule of M is A-idempotent.

Proof: (1) $\Rightarrow$ (2): Follows from Proposition (4.1)

(2) $\Rightarrow$ (3): Let N be a submodule of M, and a non-zero element n in N (no loss of generality if we assume that N is non-zero). Then by (2), $R = [r_R(M) : r_R(n)] = [nR \cap MA : M] \subseteq [N \cap MA:M] \subseteq R$, so $R = [N \cap MA : M]$ and hence $N = N[N \cap MA:M]$

(3) $\Rightarrow$ (1): Follows from Proposition (4.7)

REFRENCESS

1. Abbas, M. S., On fully stable modules, Ph.D. Thesis, Univ. of Baghdad, 1990.
2. Abbas M. S. and A. M. Sharky, Fully stable modules relative to an ideal, Al-Mustansiriya J. Sc. Vol. (21).No. 6, 2010, 392-400.
3. Barnard, A. Multiplication modules, Algebra, 71, 174-178, (1981).
4. Lam, T. y., Lectures on Modules and Rings, Springer-Verlag, Berlim, New York, 1998
5. Fuchs, L. Abelian Group, Academic press, 1960.
6. Zelmanowitz, J., Regular modules, Trans. Amer. Math. Soc., 163 (1972), 341-355.
7. Kasch, F. Modules and Rings, Academic Press, Lordon, New York, 1982.

Input-Output Stabilization Problem For Some Nonlinear Dynamical Systems With Bifurcation

Radhi A. Zaboon[1] and Anwar A. Yahea[2]
Department of Mathematics, College of Science, Al-Mustansiriyah University
Received 13/3/2013 – Accepted 15/9/2013

الخلاصة

في هذه البحث، تم دراسة التشعب لانظمة سيطرة ديناميكية غير خطية ذات معلمات. اعتمد نظام لورنز غير الخطي إنموذجاً لمسألة غير خطية تمتلك سلوكية تشعب. تم ايجاد الصيغة القياسية شبه الخطية لهذا النظام باستخدام منهجية ادخال-اخرج المحسنة. تم ايجاد دالة ليابانوف لتلك الصيغة القياسية و استخدامها لتصميم مسيطر غير خطي للمنظومة الاصلية. وفي نهاية هذا العمل تم محاكات نظام لورنز غير الخطي لمختلف المعلمات و شروط ابتدائية مختلفة ومسيطره.

ABSTRACT

In this paper the control methodology of bifurcation for a nonlinear control system with parameter has been studied. The controlled Lorenz system is treated as a model of nonlinear control system with bifurcation. The normal form of this control system has been found by modifying the input-output methodology. Lyapunov function for the normal form which equivalent to the original system are found and used to design the controller for the original control system. A numerical simulations of Lorenz system with different parameters and initial conditions and its controller and graphs are shown in the end of this work.

1.INTRODUCTION

The input-output methodology is an approach to nonlinear control design which has attracted a great deal of research interest in recent years. Where this approach is to algebraically transform a nonlinear system dynamics into a exactly or partially linear form. For the normal form of the nonlinear control system and its connection to the bifurcation problem one can consult **[1]**, **[2]**, **[3]**, **[4]**, and **[5]**. In this work, The controlled Lorenz system as model of a nonlinear control system depending on parameter with bifurcation has been adapted. Some theoretical justifications to design and analyze some classes of nonlinear dynamical systems with bifurcation have been developed based on some previous literature a normal form for the controlled Lorenz system with output function has been driven via input-output method. Some numerical simulations are given to show the behavior and the stability for the closed-loop system.

2. Mathematical concepts

In this section some mathematical concepts which important in the study of nonlinear control systems with output function have been introduced.

Definition (1) : [6]

Let $h: R^n \to R$ be a smooth scalar function, and $f: R^n \to R^n$ be a smooth vector field on R^n, then the Lie derivative of h with respect to f

is a scalar function defined by $L_f h = \nabla h \cdot f$, Repeated Lie derivatives can be defined recursively $L_f^i h = L_f(L_f^{i-1} h) = \nabla(L_f^{i-1} h) f$ for $i = 1,2,\cdots$

Similarly, if g is another vector field, then the scalar function $L_g L_f h$ is

$$L_g L_f h = \nabla(L_f h) \cdot g$$

Definition (2) : [7]

Let f and g be two vector fields on R^n. The Lie bracket of f and g is the vector field defined by $[f, g] = \nabla g . f - \nabla f . g$. Repeated Lie brackets can be defined as $ad_f^i\, g = [f, ad_f^{i-1}\, g]$ for $i = 1,2,\cdots$

Definition (3) : [7]

A function φ: $R^n \to R^n$ defined in a region Ω , is called a diffeomorphism if it is smooth, and if its inverse φ^{-1} exists and smooth.

Lemma (1) : [6]

Let $\varphi(x)$ be a smooth function defined in a region Ω in R^n. If the Jacobian matrix $\nabla\varphi$ is non-singular at a point $x = x_0$ of Ω , then $\varphi(x)$ defines a local diffeomorphism in a sub-region of Ω .

Remark(1) : [6]

A single input nonlinear control system $\dot{x} = f(x) + g(x)u$ where f, g being smooth vector fields on R^n, $x \in R^n$ and the control function $u \in R$. This system is said to be input-state linearizable if there exists a region Ω in R^n, a diffeomorphism $\varphi: \Omega \to R^n$ and a nonlinear feedback control law $u = \alpha(x) + \beta(x)v$ such that the new state variables $z = \varphi(x)$ and the new input v satisfy a linear time invariant relation $\dot{z} = Az + Bv$.

where $z = \begin{bmatrix} z_1 \\ z_2 \\ \vdots \\ z_n \end{bmatrix}$, $A = \begin{bmatrix} 0 & 1 & \cdots & 0 \\ 0 & 0 & \ddots & 0 \\ \vdots & \vdots & & 1 \\ 0 & 0 & \cdots & 0 \end{bmatrix}$ and $B = \begin{bmatrix} 0 \\ \vdots \\ 0 \\ 1 \end{bmatrix}$.

The form of system $\dot{z} = Az + Bv$ is called the Brounovsky normal form.

Definition (4) : [8]

The single input single output nonlinear control system (1) is said to have relative degree (or strong relative degree) r in the region Ω if :

$$L_g h(x) = L_g L_f h(x) = \cdots = L_g L_f^{r-2} h(x) = 0$$

And $\qquad L_g L_f^{r-1} h(x) \neq 0 \qquad \forall x \in \Omega.$

Lemma(2):[9]

Consider the autonomous nonlinear dynamical system $\dot{x} = f(x)$ with the equilibrium point of interest being the origin, and let $A(x) = \nabla f(x)$ denote the Jacobian matrix of the system. If there exist a symmetric positive definite matrix P and a symmetric semi-positive definite matrix Q, such that $\forall x \neq 0$ and if the matrix $F(x) = A^T P + PA + Q$, is negative semi-definite in some neighborhood Ω of the origin. Then the function $V(x) = f^T P f$ is a Lyapunov function for this system.

3. Problem formulation

Consider the following control system $\dot{x} = f(x,\mu) + g(x,\mu)u$, where f, g are smooth vector fields, $x \in R^n$ is the state variable, $u \in R^m$ is the control input, $\mu \in R$ is the parameter. The performance of the system depends on the values of μ and u. The following is the controlled Lorenz system: $\dot{X} = \begin{bmatrix} a(y-x) \\ cx - zx - y \\ xy - bz \end{bmatrix} + \begin{bmatrix} 0 \\ 1 \\ 0 \end{bmatrix} u$, where $X = \begin{bmatrix} x \\ y \\ z \end{bmatrix}$, and x is proportional to the intensity of convective motion, y is proportional to the temperature difference between ascending and descending currents, z is proportional to the distortion of the vertical temperature profile. a, b are positive parameters and the parameter c depends on the difference between the temperature in the top and the temperature in the bottom, in general we have assumed that $c > 0$ **[10]**. Figure(1) show the classical Lorenz system when the control $u = 0$.

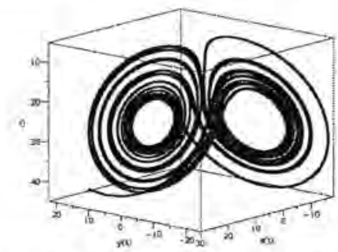

Figure-1:the trajectory of the Lorenz system with the initial conditions $x(0) = 2$, $y(0) = 1$, $z(0) = 4$, and $a = 10$, $b = \frac{8}{3}$, $c = 28$

Remark (2):

Lorenz system represent a wide variety of physical and engineering phenomena like electrical circuit and ocean navigation **[2]**. Systems like these need a specific output functions and these output functions are differs by the difference of the physical problem. The general form of the output function for any nonlinear control system can be defined as

$h(x) = \sum_{i=1}^{n} \alpha_i x_i$, where $x = \begin{bmatrix} x_1 \\ x_2 \\ \vdots \\ x_n \end{bmatrix}$ is the state space and $\alpha_i, i = 1, \dots, n$

So in this work, And the input output controlled Lorenz system would be

$$\dot{X} = \begin{bmatrix} a(y-x) \\ cx - zx - y \\ xy - bz \end{bmatrix} + \begin{bmatrix} 0 \\ 1 \\ 0 \end{bmatrix} u \qquad (1)$$

$$h(X) = \alpha_1 x + \alpha_2 y + \alpha_3 z$$

where $X = \begin{bmatrix} x \\ y \\ z \end{bmatrix}$ is the state vector and a, b, c are real positive parameters.

since our aim is to study and control the Lorenz system as a nonlinear dynamical system with bifurcation, the following is necessary.

4. The Input-Output Stabilization of The Lorenz system

In this section the main theorem has been introduced, with the following aims

1. find out a transformations family which are transforming the nonlinear controlled Lorenz system into a simpler nonlinear normal form.
2. Design a nonlinear controller u for the original nonlinear system.

Next we give a remarks which is important to the proof of the main theorem.

Remark (3)

Based on the natural structure of Lorenz system, there are three general cases for the relative degree of system (1)

1. $r = 3$: the system(1) is input-state linearizable. This case has been studied in our previous work which have been sending for publishing.
2. $r = 2$: based on definition (4), then the following is hold $L_g h(X) = 0$

implies $\alpha_2 = 0$, and $L_g L_f h(X) = \alpha_1 a + \alpha_3 x \neq 0$, which means for $r = 2$ there are some necessary next conditions hold:

i. $\alpha_2 = 0$

ii. for $a \neq 0$ (given):

If $\alpha_1 \neq 0$ and $\alpha_3 \neq 0$, then the controlled Lorenz system (1) have relative degree $r = 2$ if and only if $x \neq -\frac{\alpha_1 a}{\alpha_3}$.

If $\alpha_3 = 0$and $\alpha_1 \neq 0$, then the controlled Lorenz system (1) have relative degree $r = 2$ for any x.

3. $r = 1$: the normal form has relative degree $r = 1$, which is again nonlinear control system , it may complicated more than the original system. So this case had been ignored and the case when $r = 2$ has been adapted.

Based on remark(3) the following is developed.

Theorem(1): (The Main Theorem)

Consider the controlled Lorenz system(1), If $x \neq -\frac{\alpha_1 a}{\alpha_3}$ then:

1. There are a family of single input single output normal forms that could be driven by using The state transformations family

$$\begin{bmatrix} z_1 \\ z_2 \\ z_3 \end{bmatrix} = \begin{bmatrix} \alpha_1 x + \alpha_3 z \\ \alpha_1 a(y-x) + \alpha_3(xy - bz) \\ \varphi_3(X,c) \end{bmatrix} \tag{2.a}$$

Where $\varphi_3(X,c)$ is any scalar function satisfied the conditions

i. $L_g\varphi_3(X,c) = 0$

ii. $\alpha_1 \frac{\partial\varphi_3(X,c)}{\partial z} \neq \alpha_3 \frac{\partial\varphi_3(X,c)}{\partial x}$

And the control transformation $v = L_f^2 h(X) + L_g L_f h(X) \cdot u$ (2.b)

The normal form of the system(1) via transformation (2) is defined as

$$\begin{bmatrix} \dot z_1 \\ \dot z_2 \\ \dot z_3 \end{bmatrix} = \begin{bmatrix} z_2 \\ v \\ \left.\left(\frac{\partial\varphi_3(X,c)}{\partial x} a(y-x) + \frac{\partial\varphi_3(X,c)}{\partial z}(xy - bz)\right)\right|_{X=\varphi(Z)^{-1}} \end{bmatrix}$$

2. The nonlinear controller of the original system is as the following

$$u = -\frac{\left(L_f^2\, h(X) + k_1 h(X) + k_2 L_f h(X) + k_3\varphi_3(x)\right)}{L_g\, L_f\, h(X)}$$

where $L_g\, L_f\, h(X) \neq 0$ and $K = [k_1 \quad k_2 \quad k_3]$ is the gain vector, that will be designed later on.

Proof:

1. Since $x \neq -\frac{\alpha_1 a}{\alpha_3}$ and $\alpha_2 = 0$ and based on remark(3) then the system (1) have relative degree $r = 2$. We are Looking for a family of diffeomorphisms so that consider the vector function

$$Z = \begin{bmatrix} z_1 \\ z_2 \\ z_3 \end{bmatrix} = \begin{bmatrix} \varphi_1(X,c) \\ \varphi_2(X,c) \\ \varphi_3(X,c) \end{bmatrix} = \varphi(X,c)$$

On using $h(X) = \alpha_1 x + \alpha_3 z$, and let $\varphi(X,c) = \begin{bmatrix} h(X) \\ L_f\, h(X) \\ \varphi_3(X,c) \end{bmatrix}$, then

$$\varphi(X,c) = \begin{bmatrix} \alpha_1 x + \alpha_3 z \\ \alpha_1 a(y-x) + \alpha_3(xy - bz) \\ \varphi_3(X,c) \end{bmatrix}$$

and to prove that the vector function $\varphi(X,c)$ defines a diffeomorphism, then based on proposition(1) we have to prove that the matrix $\nabla\varphi(X,c)$ is nonsingular

$$|\nabla\varphi(X,c)| = \begin{vmatrix} \alpha_1 & 0 & \alpha_3 \\ -\alpha_1 a + \alpha_3 y & \alpha_1 a + \alpha_3 x & -\alpha_3 b \\ \frac{\partial\varphi_3(X,c)}{\partial x} & \frac{\partial\varphi_3(X,c)}{\partial y} & \frac{\partial\varphi_3(X,c)}{\partial z} \end{vmatrix} \neq 0 \tag{4}$$

Since $L_g\varphi_3(X,c) = 0$, then $\frac{\partial\varphi_3(X,c)}{\partial y} = 0$ (5)

On substitution (5) in (4), then

$$|\nabla\varphi(X,c)\,| = \alpha_1 a + \alpha_3 x\left(\alpha_1\frac{\partial\varphi_3(X,c)}{\partial z} - \alpha_3\frac{\partial\varphi_3(X,c)}{\partial x}\right) \neq 0$$

For $\alpha_1\frac{\partial\varphi_3(X,c)}{\partial z} \neq \alpha_3\frac{\partial\varphi_3(X,c)}{\partial x}$. Thus $\varphi(X,c)$ is nonsingular. Based on definition(3), the diffeomorphism $\varphi(X,c)$ has a smooth inverse, and since $r = 2$, then the following is true

$$\dot{z}_1 = \ = L_f\varphi_1(X,c) = z_2 \qquad (6)$$

and $\dot{z}_2 \ = L_f^2h(X) + L_gL_fh(X)\cdot u$ (7)

By the control transformation (2.b) in (7), one gets $\dot{z}_2 = v$ (8)

and $\dot{z}_3 = L_f\varphi_3(X,c) + L_g\varphi_3(X,c)u$

By the condition $L_g\varphi_3(X,c) = 0$, then we have

$$\dot{z}_3 = \left(\frac{\partial\varphi_3(X,c)}{\partial x}a(y-x) + \frac{\partial\varphi_3(X,c)}{\partial z}(xy-bz)\right)\Big|_{X=\varphi(Z)^{-1}} \qquad (9)$$

By (6), (8) and (9), the normal form is as the following

$$\begin{bmatrix}\dot{z}_1\\ \dot{z}_2\\ \dot{z}_3\end{bmatrix} = \begin{bmatrix} z_2 \\ v \\ \left(\frac{\partial\varphi_3(X,c)}{\partial x}a(y-x) + \frac{\partial\varphi_3(X,c)}{\partial z}(xy-bz)\right)\Big|_{X=\varphi(Z)^{-1}}\end{bmatrix}$$

2. On using the equation (2.b) $v = L_f^2h(X) + L_gL_fh(X)\cdot u$

And set $v = -KZ$, where K is the gain vector $K = [k_1 \quad k_2 \quad k_3]$, in (2.a) , the controller is found to be

$$u = -\frac{\left(L_f^2\,h(X)+k_1h(X)+k_2L_fh(X)+k_3\varphi_3(x)\right)}{L_g\,L_f\,h(X)}, \text{ where } L_g\,L_f\,h(X) \neq 0.$$

Proposition(2)

Consider the controlled Lorenz system(1)

$$\dot{X} = \begin{bmatrix} a(y-x) \\ cx - zx - y \\ xy - bz\end{bmatrix} + \begin{bmatrix}0\\1\\0\end{bmatrix}u$$

$$h(X) = \alpha_1 x + \alpha_3 z$$

where $X = \begin{bmatrix}x\\y\\z\end{bmatrix}$ is the state vector and a, b, c are real positive parameters. If we set $\alpha_1 = 1$ and $\alpha_3 = 0$, and based on the state and control transformation (2) in the main theorem, then

1. there exists a state transformations family can be defined as:

$$\begin{bmatrix}z_1\\z_2\\z_3\end{bmatrix} = \begin{bmatrix} x \\ a(y-x) \\ c_1x^2 + c_2z\end{bmatrix}, c_1 \text{ and } c_2 \text{ are nonzero constant} \qquad (10.a)$$

with the condition $L_g\varphi_3(X,c) = 0$, and the control transformation

$$v = L_f^2 h(X) + L_g L_f h(X) \cdot u \tag{10.b}$$

2. the transformation family (10) which transforms the nonlinear control system (1) into the following nonlinear normal form

$$\begin{aligned} \dot{z}_1 &= z_2 \\ \dot{z}_2 &= v \\ \dot{z}_3 &= -bz_3 + \left(2c_1 + \tfrac{c_2}{a}\right) z_1 z_2 + (c_1 b + c_2){z_1}^2 \end{aligned} \tag{11}$$

3. The nonlinear control law of the original system is then

$$u = \frac{1}{a}(-k_1 x - k_2 a(y-x) - k_3(c_1x^2 + c_2 z) - (a^2 + ac)x) \\ +(a^2 + a)y + axz \tag{12}$$

Proof: the proof can be obtained directly from the proof of theorem(1).

5.Design analysis

In this section, some concepts which is useful in the nonlinear analysis have been introduced. The normal form (11) which introduced in proposition(2) is nonlinear and also it's linearization (as a control system) is uncontrollable so we can not use the linear system design control to define the nonlinear control. So a Lyapunov function has been developed for that normal form to get some information and conditions to determine the gain matrix K for the linear control v. The next remark is important.

Remark(4)

1. The Lyapunov theory have been adapted to find some conditions and relation between the element of the gain vector K. On using $v = -KZ$ in the normal form (11) we have the linear approximation the closed-loop system at the origin

$$\begin{bmatrix} \dot{z}_1 \\ \dot{z}_2 \\ \dot{z}_3 \end{bmatrix} = \begin{bmatrix} 0 & 1 & 0 \\ -k_1 & -k_2 & -k_3 \\ 0 & 0 & -b \end{bmatrix} \cdot \begin{bmatrix} z_1 \\ z_2 \\ z_3 \end{bmatrix} \tag{13}$$

The characteristic equation of (13) is

$$|A - \lambda I| = -\lambda^3 - (k_2 + b)\lambda^2 - (k_1 + bk_2)\lambda - k_1 b = 0$$

The system have three eigenvalue:

$\lambda_1 = -b$, $\lambda_2 = -\frac{k_2}{2} + \frac{\sqrt{{k_2}^2 - 4k_1}}{2}$ and $\lambda_3 = -\frac{k_2}{2} - \frac{\sqrt{{k_2}^2 - 4k_1}}{2}$. Then one conclude the following conditions on the elements of the gain vector:

i. k_1 and k_2 are positive real and $\left(\frac{k_2}{2}\right)^2 < k_1$.

ii. Since the eigenvalue do not depend on k_3 i.e k_3 does not effect on the stability of system (11) , so we can set $k_3 = 0$.

2.To simplifying the calculation in the next proposition one can set $c_1 = -\frac{1}{2a}$ and $c_2 = 1$ in the transformation(10), then the normal form is

$$\dot{z}_1 = z_2$$

$$\dot{z}_2 = -k_1 z_1 - k_2 z_2 \qquad (14)$$
$$\dot{z}_3 = -bz_3 + \varepsilon {z_1}^2$$

where $\varepsilon = \left(\frac{2a-b}{2a}\right)$ and $b \neq 2a$, A Lyapunov function which is stabilize the normal form will be found by the next proposition.

Proposition (3):

Consider the nonlinear closed-loop system (14)

$$\dot{z}_1 = z_2$$
$$\dot{z}_2 = -k_1 z_1 - k_2 z_2$$
$$\dot{z}_3 = -bz_3 + \varepsilon {z_1}^2$$

If P_1, P_2, and P_3 are positive real and satisfies the conditions :

$$q_2 - 2k_2 P_2 > 0 \text{ , and } q_3 - 2bP_3 > 0 \qquad (15)$$

Then the stabilizing Lyapunov function of system (14) is obtained to be $V(Z) = P_1 {z_2}^2 + P_2(k_1 z_1 + k_2 z_2)^2 + P_3(-bz_3 + \varepsilon {z_1}^2)^2$.

Proof:

On using lemma(2) . consider the function $V(Z) = \mathcal{F}^T P \mathcal{F}$, where $\mathcal{F} = \begin{bmatrix} z_2 \\ -k_1 z_1 - k_2 z_2 \\ -bz_3 + \varepsilon {z_1}^2 \end{bmatrix}$ and P is 3×3 positive definite matrix. Since the origin is the only critical point then $V(0) = \mathcal{F}(0)^T P \mathcal{F}(0) = 0$

Let $P = \begin{bmatrix} P_1 & 0 & 0 \\ 0 & P_2 & 0 \\ 0 & 0 & P_3 \end{bmatrix}$, where $P_i > 0$, $i = 1,2,3$

Set $Q = \begin{bmatrix} q_1 & 0 & 0 \\ 0 & q_2 & 0 \\ 0 & 0 & q_3 \end{bmatrix}$, where $q_i \geq 0$, $i = 1,2,3$

because P positive definite matrix then $V(Z) > 0$, $\forall Z \neq 0$, then

$$\dot{V}(Z) = \mathcal{F}^T P \dot{\mathcal{F}} + \dot{\mathcal{F}}^T P \mathcal{F} \text{ ; } \dot{\mathcal{F}} = \left(\frac{\partial \mathcal{F}}{\partial z}\right) = A(Z)$$
$$= \mathcal{F}^T (PA(Z) + A(Z)^T P + Q - Q)\mathcal{F} \text{ ,}$$

then $\dot{V}(Z) = \mathcal{F}^T F(Z) \mathcal{F} - \mathcal{F}^T Q \mathcal{F}$, where $F(Z) = A(Z)^T P + PA(Z) + Q$

$$\text{Then } F(Z) = \begin{bmatrix} q_1 & P_1 - k_1 P_2 & 2\varepsilon z_1 P_3 \\ P_1 - k_1 P_2 & q_2 - 2k_2 P_2 & 0 \\ 2\varepsilon z_1 P_3 & 0 & q_3 - 2bP_3 \end{bmatrix}$$

Using Sylvester criterion (see reference [11]), then $D_1 = q_1$,

$$D_2 = \begin{vmatrix} q_1 & P_1 - k_1 P_2 \\ P_1 - k_1 P_2 & q_2 - 2k_2 P_2 \end{vmatrix} = q_1(q_2 - 2k_2 P_2) - (P_1 - k_1 P_2)^2,$$

$$D_3 = \begin{vmatrix} q_1 & P_1 - k_1 P_2 & 2\varepsilon z_1 P_3 \\ P_1 - k_1 P_2 & q_2 - 2k_2 P_2 & 0 \\ 2\varepsilon z_1 P_3 & 0 & q_3 - 2bP_3 \end{vmatrix}$$
$$= q_1(q_2 - 2k_2 P_2)(q_3 - 2bP_3) - (q_2 - 2k_2 P_2)(2\varepsilon z_1 P_3)^2$$
$$-(q_3 - 2bP_3)(P_1 - k_1 P_2)^2$$

Since Q is semi-positive definite matrix then we can set $q_1 = 0$
On using the conditions(15) above, then
$D_1 = 0, D_2 = -(P_1 - k_1P_2)^2 < 0$, and
$D_3 = -\left((q_2 - 2k_2P_2)(2\varepsilon z_1P_3)^2 + (q_3 - 2bP_3)(P_1 - k_1P_2)^2\right) < 0$
That mean $F(Z)$ is semi-negative definite and since Q is semi-negative definite then $\dot{V}(Z)$ is semi-negative definite, so that the function $V(Z)$ is a Lyapunov function and defined as

$$V(Z) = P_1{z_2}^2 + P_2(k_1z_1 + k_2z_2)^2 + P_3(-bz_3 + \varepsilon {z_1}^2)^2.$$

6. Numerical Illustrations

The following are the numerical simulations for the controlled Lorenz system (1) and the Lyapunov approaches which has been modified in proposition(3) and remarks(4).

6.1 control design

To complete the control design chose the matrices P and Q satisfied the conditions (15). then $P = \begin{bmatrix}1 & 0 & 0\\0 & 1 & 0\\0 & 0 & 1\end{bmatrix}$ and $Q = \begin{bmatrix}0 & 0 & 0\\0 & 1 & 0\\0 & 0 & 6\end{bmatrix}$

The gain vector can be chosen as $[k_1 \quad k_2 \quad k_3] = [0.3 \quad 0.4 \quad 0]$ (16)
On using the nonlinear controller (12) which is given by proposition(2)

$$u = \frac{1}{a}(-k_1x - k_2a(y - x) - k_3(c_1x^2 + c_2z) - (a^2 + ac)x) + (a^2 + a)y + axz$$

If we set $a = 10$, $b = \frac{8}{3}$, and $c = 28$. And obtain the value of the gain vector K (16), then the nonlinear control law of the original control system is $u = \frac{1}{10}(-0.3x - 4(y - x) - 380x) + 110y + 10xz$ (17)
the figures (2) show the stability of the single input single output controlled Lorenz system using the nonlinear control law (17)

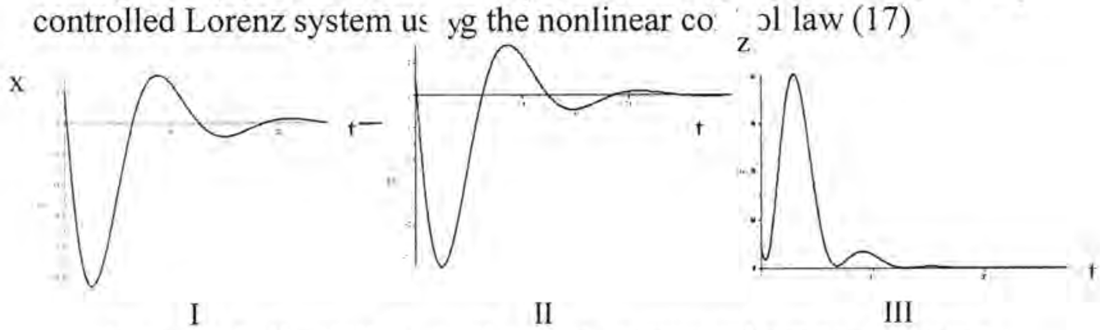

Figure -2: I , II and III shows the x-state, y-state and z-state versus time respectively of controlled Lorenz system with the initial conditions $x(0) = 2$, $y(0) = 1$, and $z(0) = 4$, and $a = 10$, $b = \frac{8}{3}$, and $c = 28$

6.2 Control bifurcations

The bifurcation problems for the control system is invariant under change of coordinates (diffeomorphisms) then we can study the bifurcation of dynamical systems by focusing on bifurcation of their normal forms.

The local bifurcation is the change of the stability of the dynamical system as the parameter varied. To study the bifurcation of the classical Lorenz system If the parameter $c < 1$ then the origin is the only critical point, while if $c > 1$ then in addition to the origin there are two critical points

$P_1 = (\sqrt{b(c-1)}, \sqrt{b(c-1)}, (c-1))$ and

$P_2 = (-\sqrt{b(c-1)}, -\sqrt{b(c-1)}, (c-1))$ **[12]**.

1. If $0 < c < 1$: The origin is the only critical point and hyperbolic and all of the eigenvalues have negative real part then the origin is asymptotically stable. **[12]**
2. if $c = 1$: The equilibrium point at the origin bifurcates into two equilibria p_1 and p_2 .The origin is nonhyperbolic equilibrium point and the system experience a pitchfork bifurcation.
3. if $1 < c < \frac{a(a+b+3)}{a-b-1}$: In general the system has one real positive eigenvalue and two complex eigenvalue with negative real part. The equilibrium points p_2 and p_3 are asymptotically stable and the origin is unstable.
4. $c = \frac{a(a+b+3)}{a-b-1}$: The system experience a Hopf bifurcation**[13]**
5. $c > \frac{a(a+b+3)}{a-b-1}$: All the eigenvalue have positive real part, so all the equilibria are unstable **[13]**. See figure(3)

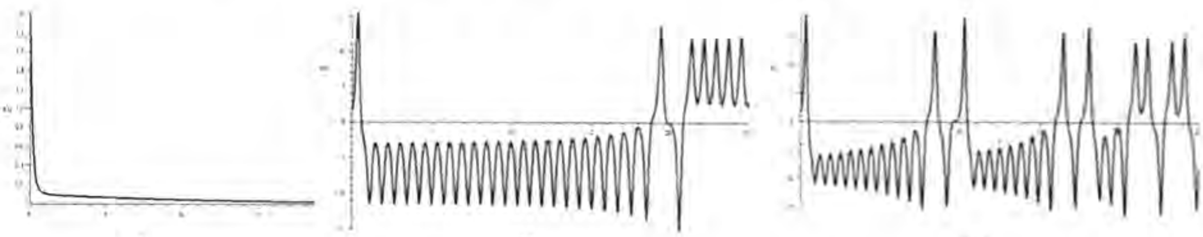

I II III

Figure-3:(Bifurcation of Lorenz system):I,II III shows x-state versus time of Lorenz system **when** $c < 1$, $1 < c < 24.737$ and $c > 24.737$ respectively with the I.P (2,1,4) and parameters $a = 10$, $b = \frac{8}{3}$

Therefore the Lorenz system have two bifurcations value at $c = 1$ and $c = \frac{a(a+b+3)}{a-b-1}$. As we mention before the parameters a and b do not effect on the stability of the Lorenz system, therefore this system is belong to bifurcation of one parameter family. in order to control the bifurcation of Lorenz system with respect the parameter c. In order to show that the nonlinear controller (12) will controlled the bifurcations we will graph the closed-loop system with different values of the parameter c which represent the bifurcation values in the classical Lorenz system.

Let $a = 10$, $b = \frac{8}{3}$, and k_1, k_2 as in (12) ,then

$$u = \frac{1}{10}(-0.3x - 4(y - x) - (100 + 10\,c)x) + 110y + 10xz \quad (18)$$

we can see that the nonlinear control law is parameterized controller, i.e., depend on the state X, as well as the parameter c. The control(18) $u(X, c)$ will control the bifurcation. Lorenz system have two bifurcations value at $c = 1$ and $c = \frac{a(a+b+3)}{a-b-1}$, when $a = 10$ and $b = \frac{8}{3}$. Then $c = 1$ and $c = 24.737$. Table (1) the behavior of nonlinear controlled Lorenz system has no bifurcation when the parameter c varied and pass through the bifurcation values of the Lorenz system.

Table-1:

The parameter value	The associated control law with respect the parameter value	The figure number
$c < 1$ (c = 0.5)	$u = \frac{1}{10}(-0.3x - 4(y - x) - 105x) + 110y + 10xz$	Figure (4)
$1 < c < 24.737$ (c = 20)	$u = \frac{1}{10}(-0.3x - 4(y - x) - 300x) + 110y + 10xz$	Figure (5)
c > 24.73 (c = 28)	$u = \frac{1}{10}(-0.3x - 4(y - x) - 380x) + 110y + 10xz$	Figure (2)

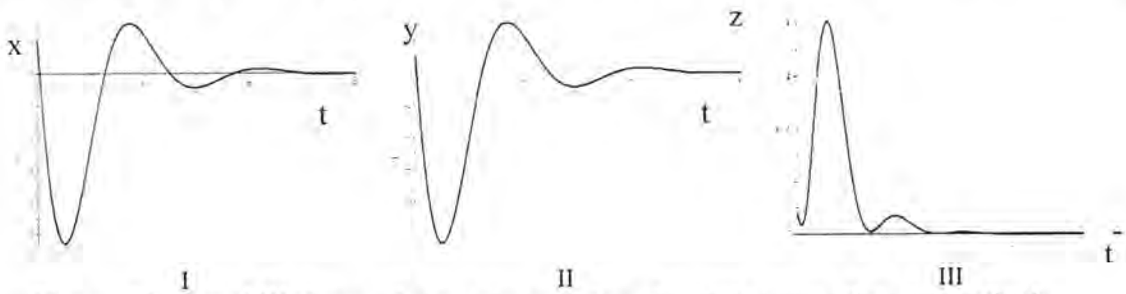

Figure-4:I , II and III shows the x-state, y-state and z-state versus time respectively of controlled Lorenz system with the initial conditions $x(0) = 2$, $y(0) = 1$, and $z(0) = 4$, and $a = 10$, $b = \frac{8}{3}$, and $c < 1$

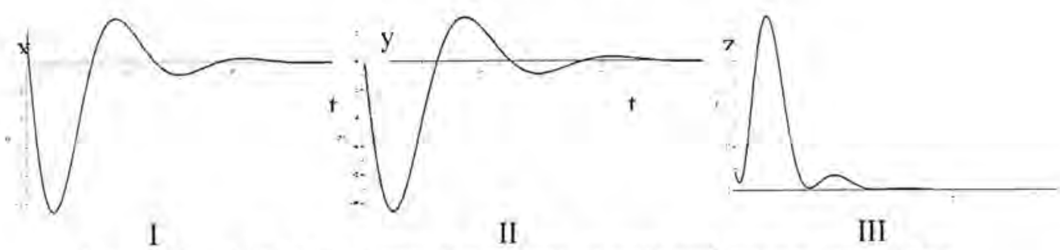

Figure-5: I , II and III shows the x-state, y-state and z-state versus time respectively of controlled Lorenz system with the initial conditions $x(0) = 2$, $y(0) = 1$, and $z(0) = 4$, and $a = 10$, $b = \frac{8}{3}$, and $c > 24.73$

7. CONCLUSIONS

From the present study, the following conclusions may be drawn: The Lyapunov function which stabilize the normal form is employed to design the controller. The Input-Output Stabilization Design method is applicable to stabilize the systems with bifurcation. The design control methods for these systems suggest that we can find a feedback control law depend on these parameters.

8. REFERENCES

1. Kang W. and Krener A., Normal form of nonlinear control systems, int. J. of chaos and control, pp. 345-376 , 2006
2. Kang W., Bifurcation and Normal form of nonlinear control systems, PartI , SIAM J. Cont. Optim., Vol. 36, No.1, pp 213-232, 1998
3. Kang W., Bifurcation and Normal form of nonlinear control systems, PartII , SIAM J. Cont. Optim., Vol. 36, No.1, pp 213-232, 1998
4. Kang W., The stability and invariants of control systems with pitchfork or cusp bifurcations , IEEE Conf. on decision and control, pp. 378-383, 1997
5. Kang W., Invariants and stability of control systems with transcritical and saddle-node bifurcations , IEEE Conf. on decision and control, pp. 1162-1167, 1997
6. Slotine E. and Li W. , Applied Nonlinear control , 1991.
7. Lu Q. , Sun Y. , and Mei S. , Nonlinear Control Systems and Power System Dynamics , 2001.
8. Sastry S. and Isidori A. , adaptive control of linearizable systems, IEEE Transaction on Automatic control, Vol. 34, No. 11, pp.1123-1131, 1989.
9. Krasovskii, N. N., Problems of the Theory of Stability of Motion, Stanford Univ. Press, 1963; translation of the Russian edition, Moscow (1959).
10. Lorenz Edward N. , Deterministic non-periodic flow , 1963.
11. Farina L. and Rinaldi S. , Positive Linear Systems : Theory and Applications , 2000
12. Gulick D. , Encounters with chaos , 1992
13. C. Sparrow. The Lorenz equations: bifurcations, chaos, and strange attractors. Applied Mathematical Sciences, 41, 1982.

Cryptanalysis of Complement Product Generator by Solving Linear Equations System of the Generated Sequence

Sahar Ahmed Mohammed
Mathematical Dept./College of Scince/ Al-Mustansiriya University
Received 17/3/2013 – Accepted 15/9/2013

الخلاصة

في هذا البحث، اولا تم عرض طريقة كولومب لانشاء نظام معادلات خطية لمسجل زاحف منفرد. ثانيا، تم تطوير هذه الطريقة لانشاء نظام معادلات خطية لمولد مفاتيح (منظومة مسجلات زاحفة) والتي يظهر فيها جليا تأثير الدالة المركبة. واخيرا، وقبل الشروع بحل ذلك النظام الخطي ،علينا اختبار توفر ووحدانية الحل لهذا النظام ومن ثم حل هذا النظام باستخدام احدى الطرق التقليدية المعروفة مثل طريقة كاوس للحذف. ان حل نظام المعادلات الخطية يعني ايجاد القيم الابتدائية للمسجلات الزاحفة المشتركة في المولد. احد المولدات المعروفة، مثل المولد الضربي المتمم، كان المثال العملي لهذا البحث.

ABSTRACT

In this paper, firstly, a Golomb's method is introduced to construct a linear equations system of a single linear feedback shift register. Secondly, this method is developed to construct a linear equation system of key generator (a linear feedback shift register system) where the effect of combining function of linear feedback shift register is obvious. Lastly, before solving the linear equations system, the uniqueness of the solution must be tested, then solving the linear equations system using one of the classical methods like Gauss elimination. Finding the solution of linear equations system means finding the initial values of the generator. One of the known generators; Complement generator, treated as a practical example of this work.

INTRODUCTION

A Linear Feedback Shift Register (LFSR) System (LFSRS) consists of two main basic units. First, is a feedback function and initial state values [1]. The second one is, the Combining Function (CF), which is a Boolean function [2]. Most of all Stream Cipher System's are depending on these two basic units. Figure1 shows a simple diagram of LFSRS consists of n LFSR's.

This paper aims to find the initial values of every LFSR in the system depending on the following information:

1. The length of every LFSR and its feedback function are known.
2. The CF is known.
3. The sequence S (keystream) generated from the LFSRS is known, or part of it, practically, that means, a probable word attack be applied [1].

This work consists of three stages, constructing linear equations system, test the uniqueness of the solution of this system, and lastly, solving the linear equations system.

CONSTRUCTING A LINEAR EQUATIONS SYSTEM FOR SINGLE LFSR

Before involving in solving the Linear Equations System (LES), it should show how could be the LES of a single LFSR constructed, since its considered a basic unit of LFSRS. Let's assume that all LFSR that are used are maximum LFSR, that means, Period (P)=2^r-1, where r is LFSR length. Let SR_r be a single LFSR with length r, let $A_0=(a_{-1},a_{-2},\ldots,a_{-r})$ be the initial value vector of SR_r, s.t. a_{-j}, $1\le j\le r$, be the component j of the vector A_0, in another word, a_{-j} is the initial bit of stage j of SR_r, let $C_0^T=(c_1,\ldots,c_r)$ be the feedback vector, $c_j\in\{0,1\}$, if c_j=1 that means the stage j is connected. Let S=$\{s_i\}_{i=0}^{m-1}$ be the sequence (or S=$(s_0,s_1,\ldots,s_{m-1})$ read "S vector") with length m generated from SR_r. The generation of S depending on the following equation:

$$s_i = a_i = \sum_{j=1}^{r} a_{i-j}c_j \quad i=0,1,\ldots \qquad \ldots(1)$$

Equation (1) represents the linear recurrence relation (see [3]).
The objective is finding the A_0, when r, C_0 and S are known.
Let M be a r×r matrix, which is describes the initial phase of SR_r
$M=(C_0|I_{r\times r-1})$, where M^0=I.
Let A_1 represents the new initial of SR_r after one shift, s.t.

$$A_1=A_0\times M=(a_{-1},a_{-2},\ldots,a_{-r})\begin{pmatrix} c_1 & 1 & \cdots & 0 \\ c_2 & 0 & \cdots & 0 \\ \vdots & \vdots & \vdots & \vdots \\ c_r & 0 & \cdots & 0 \end{pmatrix} = (\sum_{j=1}^{r} a_{-j}c_j, a_{-1},\ldots,a_{1-r}).$$

In general,

$$A_i=A_{i-1}\times M,\ i=0,1,2,\ldots \qquad \ldots(2)$$

Equation (2) can be considered as a recurrence relation, so we have:

$$A_i=A_{i-1}\times M=A_{i-2}\times M^2=\ldots=A_0\times M^i \qquad \ldots(3)$$

The matrix M^i represents the i phase of SR_r, equations (2-3) can be considered as a Markov Process s.t., A_0, is the initial probability distribution, A_i represents probability distribution and M be the transition matrix (see [4]). Notice that:
$M^2=[C_1C_0|I_{r\times r-2}]$ and so on until get $M^i=[C_{i-1}\ldots C_0|I_{r\times r-i}]$, where $1\le i<r$.
When $C_P=C_0$ then M^{P+1}=M.
Now let's calculate C_i (see [4]) s.t.

$$C_i=M\times C_{i-1},\ i=1,2,\ldots \qquad \ldots(4)$$

Equation (1) can be rewritten as:

$$A_0\times C_i=s_i,\ i=0,1,..,r-1 \qquad \ldots(5)$$

When i=0 then $A_0\times C_0=s_0$ is the 1st equation of the LES,

$i=1$ then $A_0 \times C_1 = s_1$ is the 2^{nd} equation of the LES, and

$i=r-1$ then $A_0 \times C_{r-1} = s_{r-1}$ is the r^{th} equation of the LES.

In general:

$$A_0 \times \mathbf{C} = S \qquad \ldots(6)$$

C represents the matrix of all C_i vectors s.t.

$$\mathbf{C} = (C_0 C_1 \ldots C_{r-1}) \qquad \ldots(7)$$

The LES can be formulated as:

$$Y = [\,\mathbf{C}^T | S^T] \qquad \ldots(8)$$

Y represents the extended matrix of the LES.

Example (1)

Let the SR_4 has $C_0^T=(0,0,1,1)$ and $S=(1,0,0,1)$, by using equation(4), get:

$$C_1 = M \times C_0 = \begin{pmatrix} 0 & 1 & 0 & 0 \\ 0 & 0 & 1 & 0 \\ 1 & 0 & 0 & 1 \\ 1 & 0 & 0 & 0 \end{pmatrix} \begin{pmatrix} 0 \\ 0 \\ 1 \\ 1 \end{pmatrix} = \begin{pmatrix} 0 \\ 1 \\ 1 \\ 0 \end{pmatrix}, \text{ in the same way, } C_2 = \begin{pmatrix} 1 \\ 1 \\ 0 \\ 0 \end{pmatrix}, C_3 = \begin{pmatrix} 1 \\ 0 \\ 1 \\ 1 \end{pmatrix}$$

From equation (6) we have:

$$A_0 \begin{pmatrix} 0 & 0 & 1 & 1 \\ 0 & 1 & 1 & 0 \\ 1 & 1 & 0 & 1 \\ 1 & 0 & 0 & 1 \end{pmatrix} = (1,0,0,1), \text{ this system can be written as equations:}$$

$a_{-3}+a_{-4}=1$

$a_{-2}+a_{-3}=0$

$a_{-1}+a_{-2}=0$

$a_{-1}+a_{-3}+a_{-4}=1$

Then the LES after using formula (8) is:

$$Y = \left[\begin{array}{cccc|c} 0 & 0 & 1 & 1 & 1 \\ 0 & 1 & 1 & 0 & 0 \\ 1 & 1 & 0 & 0 & 0 \\ 1 & 0 & 1 & 1 & 1 \end{array}\right] \qquad \ldots(9)$$

COMPLEMENT PRODUCT GENERATOR (N-CPSCG)

The Product generator is defined by n-maximum-length LFSRs whose lengths $r_1, r_2, \ldots, r_n$, where $n \in Z^+$ are pair wise relatively prime, with AND combining function [1]:

$$F_n(x_1, x_2, .., x_n) = x_1 \otimes x_2 \otimes \ldots \otimes x_n = \prod_{i=1}^{n} x_i \qquad \ldots(10)$$

Where $\otimes$ is the usual product operation.

In this paper the complement product generator will be discussed. The generator takes the complement of the output of every LFSR. So, equation (10) can be written as follows:

$$F_n(x_1,x_2,..,x_n)=\prod_{i=1}^{n}(x_i \oplus 1) \qquad ...(11)$$

Where $\oplus$ is the exclusive OR (XOR).

This generator considered weak, despite of his good linear complexity, because of his weak randomness (see Figure 1).

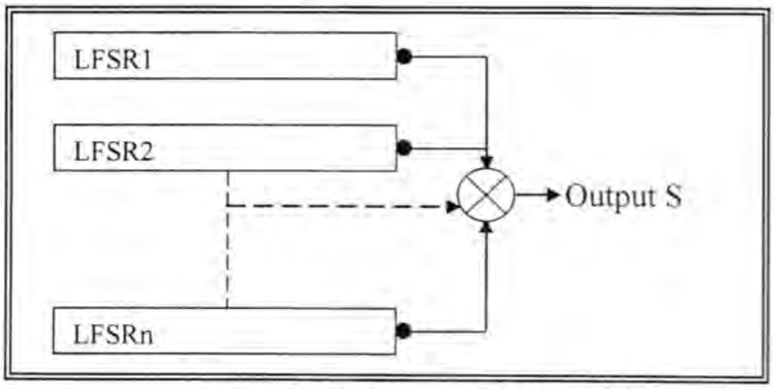

Figure-1:Complement Product CSG.

Where • is the complement of the output of LFSRi.

For n=3 the truth table of this generator will be shown in table (1).

Table-1: The truth table of Complement Product CSG.

x_1	x_2	x_3	$x_1\oplus 1$	$x_2\oplus 1$	$x_3\oplus 1$	F_n
0	0	0	1	1	1	1
0	0	1	1	1	0	0
0	1	0	1	0	1	0
0	1	1	1	0	0	0
1	0	0	0	1	1	0
1	0	1	0	1	0	0
1	1	0	0	0	1	0
1	1	1	0	0	0	0

The linear complexity (LC) of this generator is $LC(S_P)=\prod_{i=1}^{n}(r_i+1)$

Where S_P is the sequence generate from n-CPSCG.

Assuming the degrees of the all combined primitive feedback polynomials are relatively primes.

The correlation probability $CP(S_i)$ of the sequences S_i generated from of output of $LFSR_i$ which is combined in the n-CPSCG. It can be calculated by the following Lemma (1).

Lemma (1): for all inputs of the complement product function consists of n-LFSR's, the CP=0.5+1/2^n.

Proof:

Since the complement product function gives output zero's everywhere accept for the state when all inputs are zeros's the corresponding output is one, then for all zero's and all one's inputs are identical to the corresponding output of the product function, then the CP_1

$$CP_1(S) = 2/2^n \qquad \ldots(a)$$

Where n is the number of combined LFSR's.

Half of the rest inputs is 2^n-2 are zero's, so they are identical to the corresponding output of the product function, then the CP_2 is:

$$CP_2 = \frac{\frac{2^n - 2}{2}}{2^n} = \frac{2^{n-1} - 1}{2^n} \qquad \ldots(b)$$

The final CP is the sum of the CP's in equations (a) and (b), then

$$CP = \frac{2}{2^n} + \frac{2^{n-1} - 1}{2^n} = \frac{2^{n-1} + 1}{2^n} = 0.5 + \frac{1}{2^n} \qquad \ldots(12)$$

And this is ending the proof. ■

Table (2) shows some values of correlation probability for n=2...8 depending on equation (11).

Table-2: some values of CP for n=2...8 using on equation (12).

n	2	3	4	5	6	7	8
CP	0.75	0.625	0.5625	0.53125	0.515625	0.5078125	0.507421875

Form table (2), when the value of n=2,3,4,5 then the complement product system can be attacked by correlation or fast correlation attack, otherwise the system is immune.

Constructing A Linear Equations System for n-CPSCG

As known, the outputs of every LFSR of the complement product system are multiply with each other to gain the sequence S which is generating from this system.

Since SR_{r_j} has r_j number of unknown initial values, then m=$\prod_{j=1}^{n}(r_j + 1)$

.

Now, all the vectors A_{0j} are extended from r_j to m as follows:

$$A_0=\prod_{j=1}^{n}(A_{0_j}\oplus 1)=(A_{01}\oplus 1).(A_{02}\oplus 1)\ldots(A_{0n}\oplus 1)$$

For simplicity without losing generality, let n=3.
Then:

$$A_0=\prod_{j=1}^{3}(A_{0_j}\oplus 1)=(A_{01}.A_{02}.A_{03})\oplus(A_{01}A_{02}\oplus A_{01}A_{03}\oplus A_{02}A_{03})$$
$$\oplus(A_{01}\oplus A_{02}\oplus A_{03})\oplus 1$$

$A_0=(p_0,p_1,\ldots,p_{m-1})$, where:
$p_0=a_{11}\cdot a_{12}\cdot a_{13}$, $p_1=a_{11}\cdot a_{12}\cdot a_{23},\ldots$, $p_k=a_{11}\cdot a_{12}$, $p_{k+1}=a_{11},\ldots$, $p_j=a_{11}\cdot a_{12}$, $p_{j+1}=a_{11},\ldots$, $p_{m-1}=1$.

The same process will be done on the feedback vectors C_{ij} which must be found first from equation (4), therefore, C_i will be:

$$C_i=\prod_{j=1}^{3}(C_{ij}\oplus 1)$$
$$=(C_{i1}.C_{i2}.C_{i3})\oplus(C_{i1}C_{i2}\oplus C_{i1}C_{i3}\oplus C_{i2}C_{i3})\oplus(C_{i1}\oplus C_{i2}\oplus C_{03})\oplus 1$$

Where, i=0,1,…,m-1.

Since the CF is AND, then S can be gotten from multiply all unknowns S_j. Since m equations are needed, that means every LFSR shifts m movements, then:

$$s_i=\prod_{j=1}^{3}(s_{ij}\oplus 1)=(s_{i1}.s_{i2}.s_{i3})\oplus(s_{i1}s_{i2}\oplus s_{i1}s_{i3}\oplus s_{i2}s_{i3})\oplus(s_{i1}\oplus s_{i2}\oplus s_{03})\oplus 1,$$

where i=0,1,…,m-1, and, $S_j=(s_{0j},s_{1j},\ldots,s_{m-1,j})$, j=1,2,…,n.
while S can be found by following equation:

$$S=\prod_{j=1}^{3}(s_j\oplus 1)=(s_0,s_1,\ldots,s_{m-1}).$$

Figure 2 describes the sequence S generated from the product system.

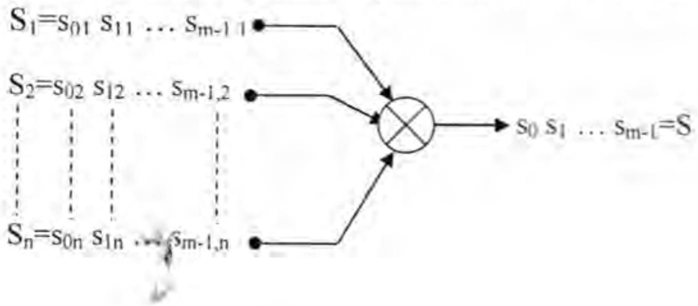

Figure -2:Complement Product system.

So **C** can be obtained from equation (7) and by applying equation (6), the LES can be constructed depending on b_i values.

Example (2)

Let's have the following feedback vectors for 3 LFSR with length 2,3 and 4:

$$C_{01}=\begin{pmatrix}1\\1\end{pmatrix},\ C_{02}=\begin{pmatrix}1\\0\\1\end{pmatrix}\ \text{and}\ C_{03}=\begin{pmatrix}1\\0\\0\\1\end{pmatrix}.$$

Notice that $\mathbf{m=\prod_{j=1}^{3}(r_j+1)=60}$

S=(0,0,0,0,0,0,0,0,0,0,0,0,0,0,0,0,0,0,0,0,0,0,0,0,0,0,0,0,0,0,0,0,0,0,0,0,0,0,0,0,0,0,0,0,0,0,0,0,0,0,0,0,0,0,0,0,0,0,0,1)

Let's denote $v_{01}=\begin{pmatrix}1\\1\end{pmatrix}$, $v_{11}=\begin{pmatrix}0\\1\end{pmatrix}$ and $v_{21}=\begin{pmatrix}1\\0\end{pmatrix}$ then,

$C_{i1}=\ldots=C_{j1}=\ldots=C_{57+i,1}=v_{i1}$, $i=0,1,2$, $j=3*k+i$, $k=1,\ldots,18$.

Let's denote $v_{02}=\begin{pmatrix}1\\0\\1\end{pmatrix}$, $v_{12}=\begin{pmatrix}1\\1\\1\end{pmatrix}$, $v_{22}=\begin{pmatrix}0\\1\\1\end{pmatrix}$, $v_{32}=\begin{pmatrix}1\\1\\0\end{pmatrix}$, $v_{42}=\begin{pmatrix}0\\0\\1\end{pmatrix}$, $v_{52}=\begin{pmatrix}0\\1\\0\end{pmatrix}$,

and $v_{62}=\begin{pmatrix}1\\0\\0\end{pmatrix}$ then, $C_{i2}=\ldots=C_{j2}=\ldots=C_{56+i,2}=v_{i2}$, $i=0,1,\ldots,6$ $j=7*k+i$, $k=1,\ldots,7$.

Let's denote $v_{03}=\begin{pmatrix}1\\0\\0\\1\end{pmatrix}$, $v_{13}=\begin{pmatrix}1\\0\\1\\1\end{pmatrix}$, $v_{23}=\begin{pmatrix}1\\1\\1\\1\end{pmatrix}$, $v_{33}=\begin{pmatrix}0\\1\\1\\1\end{pmatrix}$, $v_{43}=\begin{pmatrix}1\\1\\1\\0\end{pmatrix}$, $v_{53}=\begin{pmatrix}0\\1\\0\\1\end{pmatrix}$,

and $v_{63}=\begin{pmatrix}1\\0\\1\\0\end{pmatrix}$, $v_{73}=\begin{pmatrix}1\\1\\0\\1\end{pmatrix}$, $v_{83}=\begin{pmatrix}0\\0\\1\\1\end{pmatrix}$, $v_{93}=\begin{pmatrix}0\\1\\1\\0\end{pmatrix}$, $v_{10,3}=\begin{pmatrix}1\\1\\0\\0\end{pmatrix}$, $v_{11,3}=\begin{pmatrix}0\\0\\0\\1\end{pmatrix}$, $v_{12,3}=$ $\begin{pmatrix}0\\0\\1\\0\end{pmatrix}$, $v_{13,3}=\begin{pmatrix}0\\1\\0\\0\end{pmatrix}$, $v_{14,3}=\begin{pmatrix}1\\0\\0\\0\end{pmatrix}$ then, $C_{i2}=\ldots=C_{j2}=\ldots=C_{56+i,2}=v_{i3}$, $i=0,1,\ldots,14$, $j=15*k+i$, $k=1,2$.

$A_0=(a_{11}\cdot a_{12}\cdot a_{13}, a_{11}\cdot a_{12}\cdot a_{23},\ldots, a_{21}\cdot a_{32}\cdot a_{43})=(p_0, p_1,\ldots, p_{23})$

Where $p_0 = a_{11} \cdot a_{12} \cdot a_{13}$, $p_1 = a_{11} \cdot a_{12} \cdot a_{23}, \ldots, p_{23} = a_{21} \cdot a_{32} \cdot a_{43}$.
by applying equation (4), C_0^T will be:
C_0^T=(1,0,0,1,0,0,0,0,1,0,0,1,1,0,0,1,0,0,0,0,1,0,0,1,1,0,1,1,0,1,1,0,1,1,0,1 ,1,0,0,1,1,0,0,1,1,0,0,1,1,0,0,1, 1,0,0,1,0,0,0,0,1,0,0,1,1,1,1,0,1,1,0,0,1,1)

Therefore,

$$Y = \left(\begin{array}{l} 1\,0\,0\,1\,0\,0\,0\,0\,1\,0\,0\,1 \ldots 0\,0\,1\,1\,1\,1\,0\,1\,1\,0\,0\,1\,1 \mid 1 \\ 0\,0\,0\,0\,0\,0\,0\,0\,0\,0\,0\,0 \ldots 0\,1\,1\,0\,1\,1\,1\,1\,1\,0\,0\,1\,1 \mid 0 \\ \vdots \\ 0\,0\,0\,0\,0\,0\,0\,0\,0\,0\,0\,0 \ldots 1\,0\,0\,0\,1\,0\,1\,1\,1\,0\,0\,1\,1 \mid 0 \\ 1\,0\,0\,0\,1\,0\,0\,0\,0\,0\,0\,0 \ldots 0\,0\,0\,1\,0\,1\,1\,0\,1\,0\,0\,1\,1 \mid 1 \end{array} \right) \quad \ldots(13)$$

Test The Uniqueness of The Solution of LES

Since the system consists of m variables, then there are 2^m-1 equations, but only m independent equations are needed to solve the system. If the system contains dependent equations, then the system has no unique solution. So first it should test the uniqueness of solution of the system by many ways like calculating the rank of the system matrix ($r(\mathbf{C}^T)$) or by finding the determinant of the matrix. If the rank equal the matrix degree ($\deg(\mathbf{C}^T)$), then the system has unique solution, else ($r(\mathbf{C}^T) < \deg(\mathbf{C}^T)$) the system has no unique solution.

In order to calculate the $r(\mathbf{C}^T)$ it should to use the elementary operations to convert the $\mathbf{C}^T$ matrix to a simplest matrix by making, as many as possible of, the matrix elements zero's. The elementary operations should be applied in the rows and columns of the matrix $\mathbf{C}^T$, if it converts to Identity matrix then $r(\mathbf{C}^T)=\deg(\mathbf{C}^T)=m$, then we can judge that $\mathbf{C}^T$ has unique solution [5].

<u>Example (3)</u>

Let's have the matrix $\mathbf{C}^T=\begin{pmatrix} 0 & 0 & 1 & 1 \\ 0 & 1 & 1 & 0 \\ 1 & 1 & 0 & 0 \\ 1 & 0 & 1 & 1 \end{pmatrix}$, by using the elementary operations, the matrix can be converted to the matrix $\mathbf{C}^{T^*}=$ $\begin{pmatrix} 1 & 0 & 0 & 0 \\ 0 & 1 & 0 & 0 \\ 0 & 0 & 1 & 0 \\ 0 & 0 & 0 & 1 \end{pmatrix}$, this matrix has rank =4=deg($\mathbf{C}^T$) then the matrix has unique solution.

SOLVING THE LES

After be sure that the LES has unique solution, the LES can be solved by using one of the most common classical methods, its Gauss Elimination method. This method chosen since it has lower complexity than other methods. As its known, this method depending in two main stages, first, converting the matrix Y to up triangular matrix, and the second one, is finding the converse solution [5]. Example (4) shows the solving of a single LES for one LFSR.

Example (4)

Let's use the matrix Y of equation (9), after applying the elementary operations, and then the up triangular matrix is:

$$Y' = \left[\begin{array}{cccc|c} 1 & 1 & 0 & 0 & 0 \\ 0 & 1 & 1 & 0 & 0 \\ 0 & 0 & 1 & 1 & 1 \\ 0 & 0 & 0 & 1 & 1 \end{array}\right]$$

Now applying the backward solution to get the initial value vector: A_0=(0,0,0,1).

The LES of n-LFSR's is more complicated than LES of a single LFSR, specially, if the CF is high order (non-linear) function. First, it should solve the variables which are consists of multiplying more than one initial variable bits of the combined LFSR's. As an example of complement Product Generator, its going to solve the variables d_k, $1 \le k \le m-1$, then solving the initial values a_{-ij} since d_k is represented by multiplying two initial bits. In another word, every system has its own LES system because of the CF, so it has own solving method.

Example (5)

When solving the LES of equation(12), then the solved vector of solution:

$X=A_0=(x_0,x_1,\ldots x_{59})$=(0,0,0,0,0,0,0,0,0,0,0,0,0,0,0,0,0,0,0,0,0,0,0,1,0,0,0, 0,0,1,0,0,0,0,0,0,0,1,0,0,0,0,0,0,0,0,0,1,0,1,0,0,1,0,0,0,1,1).

There are many strategies to find the initial of the combined LFSR's, like:

1. Notice that :$a_1=x_{50}=0$, $a_2=x_{51}=1$, $b_1=x_{52}=0$, $b_2=x_{53}=0$, $b_3=x_{54}=1$, $c_1=x_{55}=0$, $b_2=x_{56}=0$, $c_3=x_{57}=0$, $c_3=x_{58}=1$, then: $A_{01}=(0,1)$, $A_{02}=(0,0,1)$, $A_{03}=(0,0,0,1)$.
2. Notice that:$x_{23}=a_2b_3c_4=1$, $x_{29}=a_2b_3=1$, $x_{37}=a_2c_4=1$, $x_{47}=b_3c_4=1$, $x_{51}=a_2=1$,
$x_{54}=b_3=1$,$x_{58}=c_4=1$,Then:$A_{01}=(a_1,a_2)=(a_1,1)$,$A_{02}=(b_1,b_2,b_3)=(b_1,b_2,1)$,

$A_{03}=(c_1,c_2,c_3,c_4)= (c_1,c_2,c_3,1)$. Now we look at combinations of product of two known values product with unknown one, for example $a_2b_3c_1=x_{20}=0$, then $c_1=0$, since $a_2=b_3=1$, and so on until found all unknowns.

CONCLUSIONS

1. If we change our attack from known plain attack to cipher attack only, which means, changing in the sequence S (non-pure absolute values), so we shall find a new technique to isolate the right equations in order to solve the LES.
2. It is not hard to construct a LES of any other LFSR systems; of course, we have to know all the necessary information (CF, the number of combined LFSR's and their lengths and tapping).
3. Notice that m is high because of the non-linearity of the combining function CF, and because of changing the non-linear variables to new variables, so we think that it can keep m as number of non-linear variables and solving the non-linear system by using methods like Newton-Raphson.

REFERENCES

1. Schneier, B., "Applied Cryptography (Protocol, Algorithms and Source Code in C." Second Edition, John Wiley & Sons Inc. 1997.
2. Whitesitt, J. E., "Boolean Algebra and its Application", Addison-Wesley, Reading, Massachusetts, April, 1995.
3. Golomb, S.W., "Shift Register Sequences" San Francisco: Holden Day, Reprinted by Aegean Park Press in 1982.
4. Papoulis, A. "Probability Random Variables, and Stochastic Process", McGraw-Hill College, October, 2001.
5. Zaraowski, C. J., "An Introduction to Numerical Analysis for Electrical and Computer Engineers", John Wiley & Sons Inc. Publication, 2004.

Stable (quasi-) Continuous Modules

Mehdi Sadik Abbas and Saad Abdulkadhim Al-Saadi
Department of Mathematics, College of Science, Al- Mustansiriyah University, Iraq
Received 15/3/2013 – Accepted 15/9/2013

الخلاصة

في هذا البحث، تم تقديم و دراسة مفهوم المقاسات (شبه) المستمرة المستقرة كتعميم فعلي للمقاسات (شبه) المستمرة. تم أعطاء العديد من النتائج و الخواص للمقاسات (شبه) المستمرة المستقرة. برهنا ان مقاس Mيكون مقاس (شبه) مستمر بشدة اذا و فقط اذا كان M تام الاستقراري من النمط cl و M يكون (شبه) مستمر مستقر. أثبتنا أن بعض النتائج المعروفة جيدا في المقاسات المستمرة تبقى متحققة في المقاسات المستمرة المستقرة. على سبيل المثال، برهنا ان اي مقاس مستمر مستقر و مباشر منتهي يكون كوهوفيني.

ABSTRACT

In this paper, we introduce and study stable (quasi)- continuous modules as a proper generalization of (quasi)- continuous modules. Many results and properties of stable (quasi-)continuous modules are obtained. An R-module M is strongly (quasi-)continuous if and only if M is cl-fully stable and M is stable (quasi-)continuous. We verify some properties well-known for continuous modules still hold under Stable continuous modules. For instance, a directly finite stable continuous module is cohophfian.

1-INTRODUCTION

Continuous modules and quasi-continuous modules were introduced and studied by S. Mohamed and T. Bouhy [1], Jeremy [2] and Goel and Jain [3] as a generalization of quasi-injective modules. They showed that some properties known for quasi-injective modules still hold under weaker assumption of continuity.

Throughout this paper all rings have an identity and modules are unitary. Let R be a ring and M be a left R-module. A submodule N of M is essential if every non-zero submodule of M intersects N nontrivially. Also, a submodule N of M is closed in M, if it has no proper essential extensions in M [4] .By Zorn's lemma any submodule of M is contained in a maximal essential extension (a closed submodule) in M. An R-module M is continuous, if it satisfies the conditions (C_1): Every subomdule of M is essential in a direct summand of M; and (C_2): Every submodule of M which is isomorphic to a direct summand of M is a direct summand of M. Also, an R-module M is quasi-continuous if it satisfies the conditions (C_1) and (C_3): If two direct summands of M have zero intersection, then their sum is a direct summand of M.

Recall that a submodule N of an R-module M is fully invariant if $f(N)\subseteq N$ for each $f\in \mathrm{EndR}(M)$ [5]). On the other hand, M. S. Abbas introduced and studied stable submodules which are properly stronger than that of fully invariant submodules [6]. A submodule N of an R-module M is called stable if, $f(N)\subseteq N$ for each R-homomorphism f:

$N \longrightarrow M$. An R-module M is called fully stable if each submodule of M is stable.

2- Stable (quasi-) continuous modules.

We introduce and study the concept of stable (quasi-) continuous modules as a proper generalization of (quasi-) continuous modules. Firstly, we introduce the following conditions for an R-module M:

(S_1): Every closed stable submodule of M is a direct summand.

(S_2): Every submodule of M which is isomorphic to a stable direct summand of M is a direct summand of M.

(S_3): If two stable direct summands of M have zero intersection, their sum is a direct summand of M.

Definition (2.1): An R-module M is called stable continuous (shortly, S-continuous), if M satisfies the conditions (S_1) and (S_2).

Definition (2.2): An R-module M is called stable quasi-continuous (shortly, S-quasi-continuous), if M satisfies the conditions (S_1) and (S_3).

Examples and Remarks (2.3):

(1) Clearly, every continuous module is S-continuous, while the converse is not true in general (see (8)).

(2) Also, every quasi-continuous module is S-quasi-continuous, while the converse is not true in general (see (8)).

(3) If an R-module M has (S_2), then it satisfies the condition (S_3).

Proof: Let A and B are stable direct summands of M such that $A \cap B = 0$. Write $M = A \oplus C$, where C is a submodule of M, and let π be the projection of $A \oplus C$ onto C. Since $b = (1-\pi)b + \pi b \in A \oplus \pi B$ for all $b \in B$, and $\pi b = b - (1-\pi)b \in A \oplus \pi B$, it follows that $A \oplus B = A \oplus \pi B$. Since $A \cap B = 0$, then $\pi|_B : B \longrightarrow C$ is a monomorphism. Hence, $\pi B \cong B$, it follows that by (S_2) condition of M; that πB is a direct summand of M. Write $M = \pi B \oplus D$, where D is a submodule of M. Since $\pi B \subseteq C \subseteq M$, by modular law; we have $C = \pi B \oplus X$. Thus $M = A \oplus \pi B \oplus (C \cap X) = A \oplus B \oplus (C \cap X)$; and hence $A \oplus B$ is a direct summand of M.

(4) As a consequence of (3), we have every S-continuous module is S-quasi-continuous, while the converse is not true in general (see (6)).

(5) Recall that an R-module M is stable uniform if every stable submodule of M is essential [7]. It is clear that, every S-uniform (and hence uniform) module is S-quasi-continuous.

(6) The Z-module Z is S-quasi-continuous (from (5)) since Z as Z-module is uniform which is not continuous. In fact, Z_Z does not satisfy the (S_2) condition since $2Z \cong Z$ where Z is a stable direct summand of Z_Z, but $2Z$ is not direct summand of Z_Z (since $2Z \xrightarrow{e} Z$).

(7) The converse of (5) is not true in general, for example Z_6 as Z-module is S-quasi-continuous which is not S-uniform since the submodule $N = \{\bar{0}, \bar{3}\}$ is a stable submodule of Z_6 as Z-module , but it is not essential of Z_6 (since N is a direct summand of Z_6).

(8) For any prime number p, the Z-module $M = (Z/Z_p) \oplus Q$ has $M_1 = Z/Z_p \oplus 0$ and $M_2 = 0 \oplus Q$ both uniform and thus M_1 and M_2 are satisfies the (S_1) condition and hence, by theorem (3.2.1), M satisfies the (S_1) condition. By [8, Example 4.2] M satisfies the (C_2) condition and so M satisfies the (S_2) condition. Therefore, M is S-(quasi-)continuous Z-module. While M does not satisfies (C_1), because $K = Z_p(1 + Z_p, 1)$ is a complement submodule which is not direct summand of M where Z_p is local ring (see [9, Example 10]. Hence M is not (quasi-)continuous Z-module.

(9) Every S-extending module (recall that a module M is S-extending if every stable submodule of M is essential in a direct summand of M [7]) satisfies the (S_1) condition. In fact, assume that an R-module M is S-extending and let N be a stable closed submodule of M. so there is a direct summand D such that N is essential in D. But N is closed, hence N=D. so M has (S_1) condition.

(10) Let M be an SS-module (recall that an R-module is SS-module if every direct summand of M is stable) , then M has (C_2) (respectively,(C_3)) if and only if M has (S_2) (respectively,S_3).

(11) By [10, Lemma (2.1.6)] , every fully invariant direct summand is stable. So we have:

(a) An R-module M has (S_2) if and only if every submodule of M which is isomorphic to a fully invariant direct summand of M is a direct summand.

(b) An R-module M has (S_3) if and only if direct sum of any two fully invariant direct summands of M with zero intersection is a direct summand of M.

(12) Recall that an R-module is S-indecomposable if (0) and M the only stable direct summand of M. One can easily prove that every S-indecomposable module has the (S_3) condition. Moreover, by (9) every S-extending S-indecomposable module is S-quasi-continuous.

In following proposition we give a characterization of the condition (S_2).

Proposition (2.4): An R-module M has (S_2) if and only if for each submodule N of M which is isomorphic to a stable direct summand of M, each R-homomorphism $f: N \longrightarrow M$ can be extended to an R-endomorphism of M.

Proof: ($\Leftarrow$). Let N be a submodule of M which is isomorphic to a direct summand D of M. Let $i: N \longrightarrow M$ be the inclusion homomorphism, and $g: N \longrightarrow D$ be an isomorphism, $\pi: M \longrightarrow D$ the natural projection of M onto D, $i_1: D \longrightarrow M$ inclusion map, then $\pi \circ i_1: D$

$\longrightarrow D$ and $(\pi\circ i_1)(d) = \pi(i_1(d)) = \pi(d) = d$ for each $d \in D$, hence $\pi\circ i_1 = I_D$.

$$\begin{tikzcd}
0 \arrow[r] & N \arrow[r] \arrow[d, "g"'] & M \arrow[ddl, dotted, "h"] \\
 & D \arrow[d, shift right, "i"'] & \\
 & M \arrow[u, shift right, "\pi"'] &
\end{tikzcd}$$

By hypothesis, the R-homomorphism $i_1\circ g\colon N \longrightarrow M$ extends to an R-endomorphism $h\colon M\longrightarrow M$, hence $(h\circ i_1)(n)= h(i_1(n)) = h(n) = (i_1\circ g)(n)$ for each n in N, hence $(i_1\circ g) = (h\circ i)$, then $(g^{-1}\circ\pi\circ h\circ i)\colon N\longrightarrow N$ and $(g^{-1}\circ\pi\circ h\circ i)(n) =(g^{-1}\circ\pi)\circ(h\circ i)(n) = (g^{-1}\circ(\pi\circ i_1)\circ g)(n) = (g^{-1}\circ g)(n) = n$ for each $n \in N$, hence $(g^{-1}\circ\pi\circ h\circ i)= I_N$. Take $\alpha = g^{-1}\circ\pi\circ h$, then $\alpha\circ i=I_N$, thus $Im(i)$ is a direct summand of M, therefore N is a direct summand of M, hence M has the (S_2) condition.

($\Rightarrow$). Let N be a submodule of M which isomorphic to a stable direct summand D of M and $f\colon N\longrightarrow M$ be any R-homomorphism. By hypothesis, M has the (S_2) condition, and then N is a direct summand of M. Hence it easily checks that f can be extended to an R-homomorphism $g\colon M\longrightarrow M$.

Corollary (2.5): An R-module M is S-continuous if and only if M has the (S_1) condition and for each submodule N of M which is isomorphic to a stable direct summand of M, each R-homomorphism $f\colon N\longrightarrow M$ can be extended to an R-endomorphism of M.

In following results, we give a characterization of strongly (quasi-) continuous by using conditions reducer than conditions in result ([10], propositions (2.3.14),(2.3.15)). Following [10], recall the following conditions for an R-module M:

(SC_1) Every submodule of M is essential in a stable direct summand of M

(SC_2) Every submodule of M which is isomorphic to a direct summand of M is a stable direct summands of M.

(SC_3) If two direct summands of M have zero intersection, then their sum is a stable direct summand of M.

An R-module M is called strongly continuous if it satisfies the conditions (SC_1) and (SC_2). An R-module M is called strongly quasi-continuous if it satisfies the conditions (SC_1) and (SC_3) [10].

Proposition (2.6): The following statements are equivalent for an R-module M:
(1) M is strongly continuous;
(2) M satisfies the conditions (SC_1) and (C_2);
(3) M satisfies the conditions (SC_1) and (S_2).
Proof: **(1) $\Rightarrow$(2)**. [10, proposition (2.3.6)].
(2) $\Rightarrow$(3). It is obvious.
(3) $\Rightarrow$(1). Let N be a submodule of M which isomorphic to a direct summand D of M (i.e. $N\cong D$). Since every module has the (SC_1) is SS-module [10, (Lemma (2.3.4))], then D is a stable. So, by (S_2) property of M, N is a direct summand of M. Again by SS-module property of M, N is a stable direct summand of M. Then, M has (SC_2). So M is strongly continuous.
Proposition (2.7): The following statements are equivalent for an R-module M:
(1) M is quasi-strongly continuous;
(2) M satisfies the conditions (SC_1) and (C_3);
(3) M satisfies the conditions (SC_1) and (S_3).
Proof: The proof essentially the same as that the proof of proposition (2.6), so omitted. □

Recall that an R-module M is cl-fully stable, if for each closed submodule N of M, $\alpha(N)\subseteq N$ for each R-homomorphism $\alpha: N\longrightarrow M$ [12]. Clearly, every fully stable module is cl-fully stable and every cl-fully stable is SS-module.

We obtain the next lemmas which are useful to get more examples of cl-fully stable modules and establish a relationship between S-(quasi)continuous modules and strongly (quasi-)continuous modules.
Lemma (2.8): An R-module M is cl-fully stable if and only if every submodule of M is essential in a stable submodule of M.
Proof : **($\Rightarrow$)**. Let N be a submodule of M. Since, by Zorn's lemma, N is essential in a closed submodule of M (say) C. Thus, by hypothesis C is a stable submodule of M.
($\Leftarrow$). Let N be a closed submodule of M. By hypothesis, there exists a stable submodule H of M such that N is essential in H. But N is closed in M, hence N =H and so N is a stable of M. Then, M is cl-fully stable.
Lemma (2.9): An R-module M is uniform if and only if M is S-uniform and M is cl-fully stable.
Proof : **($\Rightarrow$)**. Clearly, every uniform module is S-uniform and by lemma (2.8), every uniform module is cl-fully stable.
($\Leftarrow$). Let N be a submodule of M. Since M is cl-fully stable (by lemma (2.8)), N is essential in a stable submodule H of M. But, by S-uniformity of M, H is essential in M. Hence, N is essential in M. Thus, M is uniform.

By using above lemmas, we give a sufficient and necessarily condition for strongly (quasi-)continuous modules.

Proposition (2.10): An R-module M is strongly (quasi-)continuous if and only if M is cl-fully stable and M is S-(quasi-)continuous.

As an application of Zorn's lemma, each submodule N of an R-module M has a relative complement. In particular every direct summand of M has a relative complement. In fact, if N is a direct summand of M, then in general there are various complements of N in M. For example, consider the vector space $V = F^{(2)}$ over a field F. Let $S = \{(\alpha, 0) \mid \alpha \in F\}$, $S' = \{(0, \beta) \mid \beta \in F\}$ and $W = \{(\lambda, \lambda) \mid \lambda \in F\}$, then S, S', W are subspaces of V. It is easy to check that S is a direct summand of V and S', W are two different complements of S in V.

We need to introduce the following concepts:

Definition (2.11): An R-module M is called DUC-module if, every direct summand of M has a unique complement.

Definition (2.12): An R-module M is called comstable if, every submodule of M has a stable complement.

It is clear that uniform modules, cl-fully stable moduels and strongly extending modules are some examples of comstable modules. Moreover, every comstable module is DUC-module.

Motivate by Ming's ideas [13, theorems 1, 2], we investigate a characterization of S-(quasi-) continuous modules under some conditions.

Proposition (2.13): Let M be a DUC-module. Then, the following statements are equivalent:

(1) M is S-quasi-continuous R-module;

(2) For any stable complement submodule K of M, any relative complement of K in M, any submodule N of M containing $K \oplus C$, every R-homomorhism of N into M extends to an R-endomorphism of M.

Proof: **(1)⇒(2)**. Let K be stable complement submodule of M, C is a relative complement of K in M. Then $K \oplus C$ is essential in M (by Lemma (1.1.8)). Let N be a submodule of M containing $K \oplus C$. By the (S_1) condition of M, K is a direct summand of M. But M is DUC-module, so K has a unique complement and hence by [6, theorem (4.8)], C is a stable submodule of M. Again, by the (S_1) condition of M, C is a direct summand of M. Since $K \cap C = 0$, so by the (S_3) of M, $K \oplus C$ is a direct summand of M. Therefore, by [14, p.75], $K \oplus C = N = M$. Then, (2) is valid.

(2)⇒(1). Let K be a stable closed (complement) submodule of M. If C is a relative complement of K in M, let $E = K \oplus C$, $\pi: E \longrightarrow K$ the natural projection. The set $S = \{(L, \alpha) \mid E \hookrightarrow L \hookrightarrow M, \alpha: L \longrightarrow K\}$, clearly $S \neq \phi$ and by Zorn's lemma S has a maximal element (L, α). Now, let

$\alpha: L \longrightarrow K$ be the extension of π to L. If $i: K \longrightarrow M$ is the inclusion map, then $(i \circ \alpha): L \longrightarrow M$ and by hypothesis, $i \circ \alpha$ extends to an R-endomorphism $h: M \longrightarrow M$ of M. Suppose that $h(M) \not\subset K$. Since K is a relative complement of C in M, then $(h(M) + K) \cap C \neq 0$. If $0 \neq c \in (h(M) + K) \cap C$, $c = h(m) + k$, $m \in M$ and $k \in K$. Define $F = \{u \in M \mid h(u) \in E\}$, it is an easy to see that F is a submodule of M. Moreover, F properly contains L, in fact, if $x \in L$, then $h(x) = \alpha(x) \in K \subseteq E$, hence $x \in F$, on the other hand, $h(m) = c - k \in E$, thus $m \in F$, now if $m \in L$, then $h(m) = k + c$, so $\alpha(m) = (i \circ \alpha)(m) = h(m) = k + c \in K$, thus $c = \alpha(m) - k \in C \cap K$ which is contradiction, hence $m \notin L$. Define $\beta: F \longrightarrow E$ by $\beta(x) = h(x)$ for each $x \in F$, then $(\pi \circ \beta): F \longrightarrow K$ and $(\pi \circ \beta)(x) = \pi(\beta(x) = \pi(\alpha(x)) = \pi(\pi(x)) = \pi(x)$ for all $x \in L$. Hence $(\pi \circ \beta)$ is an extension of π to F which contradicts the maximally of L, thus $h(M) \subseteq K$ which implies that $h(M) = K$. Now if $k \in K \cap ker(h)$, then $0 = h(k) = \pi(k) = k$, therefore $K \cap ker(h) = (0)$. Also, $h(b - h(b)) = h(b) - h(h(b)) = 0$ for each $b \in M$, thus if $b \in M$, $b = h(b) + b - h(b) \in K + ker(h)$. Hence, $M = K \oplus ker(h)$. Since C is a relative complement of K, then $h(c) = \alpha(c) = \pi(c) = 0$, this implies that $C \subseteq ker(h)$, by maximalty of C, $C = ker(h)$ and hence $M = K \oplus C$. Thus, M satisfies the (S_1) condition.

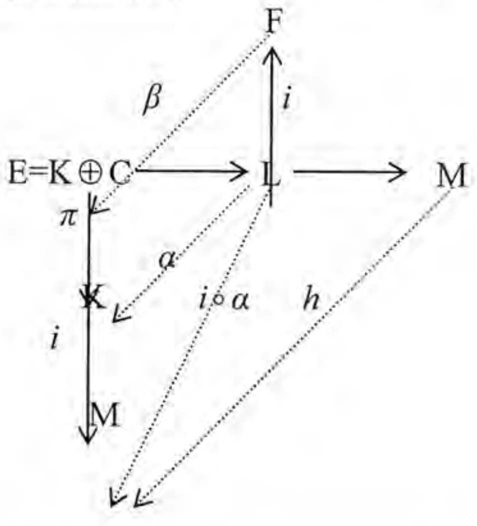

Let D and K are two stable direct summands of M with $D \cap K = (0)$. By Zorn's lemma, the set of submodules of M containing D and having zero intersection with K has a maximal member V which is a relative complement of K in M. We have, as above, $M = K \oplus V$. Since $D \subseteq V$, D is a direct summand of M, then $V = D \oplus U$ which yields $M = K \oplus V \oplus U$. Thus M has (S_3). Therefore, M is S-quasi-continuous.

Proposition (2.14): Let M be an DUC-module. Then, the following statements are equivalent:

(1) M is S-continuous R-module;

(2) For any isomorphic image K of a stable complement submodule of M, any relative complement C of K in M, any submodule N containing $K\oplus C$, any R-homomorhism of N into M extends to an R-endomorphism of M.

(3) M is S-quasi-continuous such that for each submodule N of M which is isomorphic to a stable direct summand of M, each R-homomorphism $f: N \longrightarrow M$ can be extended to an R-endomorphism of M.

Proof: **(1)$\Rightarrow$(2)**. Let K be a non-zero isomorphic image of a stable complement submodule of M, C a relative complement of K in M, N a submodule of M containing $K\oplus C$. By S-continuity of M, K is a direct summand of M and since M is DUC-module, C is a stable submodule of M, so C is a direct summand of M. Since $K\cap C=(0)$, then $K\oplus C$ is a direct summand of M (M has (S_3)). But $K\oplus C$ is essential of M which implies that $K\oplus C=M$ and so $N=M$. Thus, (1) implies (2).

(2)$\Rightarrow$(3). By proposition (2.13), we get M is S-quasi-continuous. Now, let N be a submodule of M which is somorphic to a stable direct summand of M. Let D be a relative complement of N in M, and $f: N \longrightarrow M$ be any R-homomorphism, $g: D\oplus N \longrightarrow N$ the natural projection, then $f\circ g: D\oplus N \longrightarrow N$ and by hypothesis, $f\circ g$ extends to an R-endomorphism h of M. Clearly, h is an extension of f and hence (2) implies (3).

(3)$\Rightarrow$(1). By using Corollary (2.5). □

Remarks (2.15): The concepts of DUC-modules and S-continuous modules are different. For example, the vector space $V=F^{(2)}$ over a field F is S-continuous F-module which it is not DUC-module. On other hand, Z as Z-module is DUC-module which it is not S-continuous.

Recall that an R-module M is directly finite if, M is not isomorphic to a proper direct summand of itself [15]. Also, an R-module M is cohopfian (or M has (M-I) property), if every monomorphism endomorphism of M is an isomorphism [9].

It is well- known that directly finite continuous modules are cohopfian [16, p.53]. In the next result, we generalize this result for S-continuous modules.

Proposition (2.16): Every directly finite S-continuous module is cohopfian.

Proof: Let M be directly finite S-continuous R-module and $\alpha: M\longrightarrow M$ be a monomorphism. Then, $\alpha M\cong M$, but M is a stable direct summand of M. So by S-continuity of M, we have αM is a direct summand of M. Now, since M is directly finite, it follows that $\alpha M=M$ and hence α is isomorphism. Therefore, M is cohopfian.

Corollary (2.17): A directly finite S-continuous module can not be embedded in a proper submodule.

Proof: Let $\alpha: M \longrightarrow N$ be a monomorphism. If $N \subsetneq M$, then $M \xrightarrow{\alpha} N \xrightarrow{i} M$ is a monomorphism, hence by Proposition (2.16), it is an isomorphism which contradicts directly finite property of M.

Remark (2.18):

(1) The concepts of directly finite modules and S-continuous modules are different concepts. For example, Z as Z-module is directly finite which is not S-continuous. On other hand, consider any continuous (or quasi-) injective module which does not having the cancellation property [16].

(2) A directly finite S-continuous modules need not be continuous. For example, as we have seen in (Examples and Remarks (2.3) (8)) the Z-module $M = (Z/Z_p) \oplus Q$ (p a prime number) is S-continuous which it is not continuous. Other direction, since Z/Z_p and Q are indecomposable Z-modules, hence they are directly finite. Also, Z/Z_p and Q are quasi-injective Z-modules. Since, by [15, corollary (6.21)], any direct sum of directly finite quasi-injective modules is directly finite. So $M = (Z/Z_p) \oplus Q$ is directly finite Z-module.

It is well-known that if M is a continuous R-module and if S denotes the endomorphism ring of M, and J denotes the Jacobson radical of S, then the following valid: (1) $J(S) = \{\alpha \in S \mid ker\ \alpha \xrightarrow{e} M\}$; (2) $S/J(S)$ is a regular ring [16, proposition (3.5)].

In the following proposition, we study the endomorphism ring of S-continuous modules and show that the properties (1), (2) above still for S-continuous modules under an additional condition.

It is known that, if M be an arbitrary module and $\Delta = \{\alpha \in S \mid ker\ \alpha \xrightarrow{e} M\}$, then Δ is a two sided ideal of S [16].

Proposition (2.19): Let M be a comstable S-continuous R-module, then S/Δ is a regular ring and $J(S) = \Delta$.

Proof: Let $h \in S$, and denotes $ker(h)$ by K. By comstability of M, let L be a stable complement of K in M. By the (S_1) condition of M, we have L is a direct summand of M. Since $L \cap K = (0)$, then $h_{|L}: L \longrightarrow M$ is a monomorphism. Hence $hL \cong L$, and the (S_2) condition of M implies that hL is a direct summand of M. Write $M = hL \oplus X$, and let π be the projection of M onto hL. For any $\ell \in L$, $(h^{-1}\pi h)(\ell) = (h^{-1}h)(\ell) = \ell$. Let $\alpha := h^{-1}\pi$, hence $(\alpha h)_{|L} = I_L$. It follows that $(h - h\alpha h)L = 0$. Consequently, $L \oplus K \subseteq ker(h - h\alpha h) \subseteq M$. Since $L \oplus K \xrightarrow{e} M$, then by Proposition (1.1.2) ; $ker(h - h\alpha h) \xrightarrow{e} M$. Hence, $h - h\alpha h \in \Delta$, and thus $h \equiv h\alpha h$ modulo Δ. Therefore, S/Δ is a regular ring. Now, let $\beta \in \Delta$. By essentiality of $ker(\beta)$ in M, and since $ker(\beta) \cap ker(1-\beta) = 0$, we have that $ker(1-\beta) = 0$. Thus $(1-\beta)M \cong M$, and by the (S_2) condition of M, $(1-$

$\beta)M$ is a direct summand of M. However, $ker(\beta) \subseteq (1-\beta)M \subseteq M$ and so $(1-\beta)M \xrightarrow{e} M$, by [11,Proposition (1.1.2)]. Consequently, $(1-\beta)M = M$, and hence $(1-\beta)$ is unit in S. So it follow that $\beta \in J(S)$ and hence $\Delta \subseteq J(S)$. On other hand, S/Δ is a regular ring, thus we have J $(S/\Delta) = 0$ and so $J(S) \subseteq \Delta$. Therefore, $J(S) = \Delta$.□

REFERENCES

1. Mohamed S. H. and Bouhy T.: Continuous modules, Arabian J. Sci. Eng. 2, 107- 122 (1977).
2. Jeremy L.:Modules Et Anneaux Quasi-Continuus, Canad. Math.Bull. 17(2), 158- 173 (1972).
3. Goel V. K. and Jain S. K.: π-injective modules and rings whose cyclics are π-injective, Comm. Algebra 6, 59- 73 (1978).
4. Ahmed A. A.: On submodules of multiplication modules, M.Sc. Thesis, Univ. of Baghdad, 1992.
5. Harmanci A.; Smith P. F.; Tercan A. and Tiras Y.: Direct sums of CS modules, Vol. 22, No.1, 61- 71 (1996).
6. Abbas M. S.: On fully stable modules, Ph.D. Thesis, Univ. of Baghdad, 1991.
7. Abbas M. S. and Alsaadi saad A.: Stable extending modules, Journal of Basarh Researches (Sciences), V.37 , N. 4 , D(2011),
8. Smith P.F. and Tercan A.: Generalizations of CS modules, Comm. Algebra, 21(6), 1809- 1847 (1993).
9. Birkenmeier G.F.: On the cancellation of quasi-injective modules, Comm. Algebra 4, 101-109 (1976).
10. Abbas M. S. and Alsaadi saad A.: Modules whose direct summands are stable, AL. Mustansiriya J. Sci., Vol.21, No. 5, 411-420 (2010)
11. Al-saadi Saad A., S-extending module and related concept, Ph.D. Thesis,Al-Mustansiriya Univ., Iraq, 2007.
12. Abbas M. S. : Semi-injectivity and continuity, to appear
13. Yue Chi Ming R.: On generalizations of injectivity, Arch. Math. 28, 215- 220(1992).
14. Anderson F. W. and Fuller K. R.: Rings and Categories of Modules, Springer-Verlag. New York 1973.
15. Goodearl K. R.: Ring theory: Non-singular rings and modules, Marcel Dekker, INC. New York and Basel 1976.
16. Goodearl S. H. and Muller B. J.: Continuous and Discrete modules, London Math. Soc., LN 147, Cambridge, Univ. Press 1990.

Special Quasi-Injective Modules and Special Principally Quasi- Injective Modules

Mehdi Sadiq Abbas and Shaymaa Noori Abd-Alridha
Department of Mathematics, university of Mustansiriyah, Baghdad, Iraq
Received 18/3/2013 – Accepted 15/3/2013

الخلاصة

في هذا البحث قدمنا مفهوم مقاسات شبه الغامرة الخاصة والمقاسات شبه الغامرة الرئيسية الخاصة وهي اعمام الى المقاسات شبه الغامرة والمقاسات شبه الغامرة الرئيسية . قدمنا بعض الخواص الاساسية لهذه الموديولات

ABSTRACT

In this paper we introduce the concept of Special quasi-injective modules and Special PQ-injective modules which generalize the concept of Special injective modules, quasi-injective modules and PQ-injective modules. It gives some of the basic properties of these modules.

INTRODUCTION

Let R be a commutative ring with 1, and M be a unitary left R-module. M is said to be quasi-injective if for each R-homomorphism f: N→M (where N is a submodule of M) there exists an R-homomorphism g:M→M such that g(n)=f(n) for all n in N. And an R-module M is called special injective modules relative to N (or special N-injective) (where N is an R-module) if for each R-monomorphism f: K →N (where K is an R-module) and each R-homomorphism g: K→M there is an R- homomorphism. h:N →M such that h of (x)-g(x)∈ L(M) {where L(M) is the prime radical of M}for each x in K .An R-module M is called special injective if M is special injective relative to all R-modules. In this work we introduce the concept of special quasi-injective modules which is generalization of both quasi-injective modules and special injective module. An R-module M is called special quasi-injective module if for each R-homomorphism f: N →M {where N is a submodule of M} there exists an R-homomorphism g:M→M such that g(n)-f(n)∈ L(M),for all n in N .Also the concept of special PQ-injective modules is introduced here as a generalization of both PQ-injective module and special quasi-injective modules. Given two R-module M and N. An R-module M is called special principally N-injective module if for cyclic R-submodule A of N and ever R-homomorphism

f:A→M. There exists an R-homomorphism g:M→M such that g(a)-f(a)∈L(M) ,for all a in A. An R-module M is called special principally quasi-injective if M is special principally M-injective. Many characterizations and properties on direct sum of special PQ-injective modules are given. Finally new characterizations of semi-simple Artinian rings in terms of special PQ-injective is introduced.

Definition (1) : An R-module M is said to be special quasi-injective, if M is Special M-injective that is for each R-submodule N of M and each R-homomorphism $f:N \to M$, there exists an R-homomorphism $g:M \to M$ such that $g(x)-f(x) \in L(M)$ for all x in N.

Examples and Remarks (2):-

a) Every quasi-injective R-module is Special quasi-injective.

b) It is clear that every special injective R-module is Special quasi-injective, but the converse is not true in general, for example Z_p : as Z-module is Special quasi-injective, but not Special injective since Z_p is quasi-injective and by (a), then Z_p is Special quasi-injective but Z_p is not Special injective by [1].

c) Every semi-simple (simple) R-module is Special quasi-injective.

d) The following statements are equivalent for an R-module M:

1) M is special quasi-injective.

2) For each diagram with exact row (where N be a submodule of an R-module M)

$$\begin{tikzcd} 0 \arrow[r] & N \arrow[r, "\alpha"] \arrow[d, "f"'] & M \arrow[dl, dashed, "g"] \\ & M & \end{tikzcd}$$

There exists an R-homomorphism $g:M \to M$ such that $(g \circ \alpha)(x)-f(x) \in L(M)$ for all x in N. □

Proposition (3):- Direct summands of special quasi-injective R-modules are special quasi-injective.

Proof: Let M be any special quasi-injective R-module and N be any direct summand R- submodule of M. Thus there exists an R-submodule N_1 of M such that $M = N \oplus N_1$. Let B be any R-submodule of N and $f : B \to N$ be any R-homomorphism. Define $g : B \to M = N \oplus N_1$ by $g(b)=(f(b),0)$ for all b in B. It is clear that g is an R-homomorphism and since M is special quasi-injective, thus there exists an R-homomorphism $h : M \to M$ such that $h(x)-g(x) \in L(M)$ for all x in B. Let π_N be the natural projection R-homomorphism of $M = N \oplus N_1$ into N and i_N be the inclusion map from N into M.Put $h_1 = \pi_N \circ h \circ i_N : N \to N$. Thus h_1 is an R-homomorphism and for each b in B.Then

$$h_1(b)-f(b)=\pi_N \circ h \circ i_N(b)-f(b)=\pi_N \circ h \circ i_N(b)-\pi_N((f(b),0))$$
$$=\pi_N(h \circ i(b)-\pi_N(g(b))=\pi_N(h \circ i(b)-g(b)$$

$=\pi_N(h(b)-g(b)) \in L(N)$ [2].Therefore, N is special quasi-injective. □

Recall that an R-module M is semi-simple, if each submodule B of M is a direct summand of M (i.e. $M=B\oplus K$ for some submodule K of M).A ring R is semi-simple, if it is a semi-simple R-module.Also an R-module M is called Artinian, if for each descending sequence $S_1 \supseteq S_2 \supseteq \ldots \supseteq S_n \supseteq \ldots$ of submodules of M, there exists $k \in Z^+$, such that $S_k=S_{k+i}$ for all $i \geq 0$. A ring R is Artinian, if it is Artinian as R-module.It is well-known that, a ring R is semi-simple Artinian if and only if, R is regular and Neotherian ring [3]. The following theorems give new characterizations of semi-simple Artinian rings in term of special injectivity.

Theorem (4): The following statements are equivalent for a commutative ring R:

1) R is semi-simple Artinian ring.
2) Every R-module is special injective.
3) Every cyclic R-module is special injective.

Proof : $(1)\Rightarrow(2)$. Since every module over semi-simple Artinian ring R is injective [4], then every R-module is special injective.

$(2)\Rightarrow(3)$. It is obvious.

$(3)\Rightarrow(1)$. Assume that every cyclic R-module is special injective. Let M be any simple R-module. By our assumption, M is a special injective R-module. Since J(M)=0 by [5] and L(M) $\leq$ J(M)=0 then L(M)=0. Thus M is an injective R-module, [1] Therefore every simple R-module is injective and this implies that R is a regular ring, by [5] . Therefore the Jacobson radical of every cyclic R-module is zero [5] and since L(M) $\leq$ J(M)=0 then L(M)=0 and hence every cyclic R-module is injective. Thus R is semi-simple Artinian ring [6].□

As it has been mentioned (Examples and Remarks ((2), b), that every special injective module is Special quasi-injective, the following theorem shows that the converse is true under the condition that R is semi-simple Artinian.

Theorem (5): The following statements are equivalent for a ring R

1) R is semi-simple Artinian ring.
2) The direct sum of any two special quasi-injective R-modules is special quasi-injective.
3) Every special quasi-injective R-module is special injective.

Proof: $(1)\Rightarrow(2)$. Assume that R is semi-simple Artinian ring. Thus every R-module is special injective by Theorem (4) and this implies that every R-module is special quasi-injective, by example and remark ((2), b).Therefore, the direct sum of any two special quasi-injective R-module is special quasi-injective.

$(2)\Rightarrow(3)$. Let M be any a special quasi-injective R-module and E=E(M) be the injective envelope of M [1]. It is enough to show that M is a special direct summand of E. Consider diagram (1) with exact row.

$$\begin{tikzcd} 0 \arrow[r] & M \arrow[r, "\beta"] \arrow[d, "I_M"'] & E \\ & M & \end{tikzcd}$$

(Diagram (1))

Let i_1 be the injection R-homomorphism of E into $M\oplus E$ and i_2 be the injection R-homomorphism of M into $M\oplus E$, thus diagram (1) implies diagram (2).

$$\begin{tikzcd} 0 \arrow[r] & M \arrow[r, "\beta"] \arrow[d, "I_M"'] & E \arrow[r, "i_1"] \arrow[dl, dotted] & M\oplus E \arrow[ddll, dotted, "f"] \\ & M \arrow[d, shift left, "i_2"] & & \\ & M\oplus E \arrow[u, shift left, "P"] & & \end{tikzcd}$$

(Diagram (2))

By (2), $M\oplus E$ is a special quasi-injective R-module. Thus by proposition ((2), d). There exists an R-homomorphism $f: M\oplus E\rightarrow M\oplus E$ such that $(f\circ i_1\circ\beta)(m)-(i_2\circ I_M)(m)\in L(M\oplus E)$, for all m in M. Put $g=p\circ f\circ i_1: E\rightarrow M$, where p be the projection of $M\oplus E$ onto M such that $p\circ i_2=I_M$, it is clear that g is an R-homomorphism for all m in M. We have $(g\circ\beta)(m)-I_M(m)=(p\circ f\circ i_1\circ\beta)-(p\circ i_2\circ I_M)(m)$ $p((f\circ i_1\circ\beta)(m)-(i_2\circ I_M)(m))$. Since $(f\circ i_1\circ\beta)(m)-(i_2\circ I_M)(m))\in L(M\oplus E)$, for all m in M, thus $p((f\circ i_1\circ\beta)(m)-(i_2\circ I_M)(m))\in L(M)$, for all m in M, [2] then for $(g\circ\beta)(m)-I_M(m)\in L(M)$ for all m in M. Return to diagram (1) we have just shown there exists an R-homomorphism g: $E\rightarrow M$ such that $(g\circ\beta)(m)-I_M(m)\in L(M)$ for all m in M.

$$\begin{tikzcd} 0 \arrow[r] & M \arrow[r, "\beta"] \arrow[d, "I_M"'] & E \arrow[dl, dotted, "g"] \\ & M & \end{tikzcd}$$

Hence [1] implies that M is a special direct summand of E, therefore M is a special injective R-module.Thus every special quasi-injective R-module is special injective.

$(3) \Rightarrow (1)$. Assume that every special quasi-injective R-module is special injective. Since J(M)=0 for any semi-simple R-module M [5], and since every semi-simple R-module is special quasi-injective by example ((2),c). Thus by (3) every semi-simple R-module is special injective. Since L(M) $\leq$ J(M)=0 then L(M)=0, thus every semi-simple R-module is injective, [1] since every simple R-module is semi-simple, then every simple R-module is injective and this implies that R is regular ring [5] . Let M_1 be any countable direct sum of injective hulls of simple R-modules. Since every simple R-module is injective, thus M_1 is a countable direct sum of simple R-modules. Therefore by [5], M_1 is semi-simple R-module. Since every semi-simple R-module is injective, thus M_1 is injective R-module. Hence every countable direct sum of injective hulls of simple R-modules is injective and this implies that R is a Neotherian ring [5], therefore R is regular and Neotherian ring and this implies that R is a semi-simple Artinian ring, by [3]. □

Recall that a ring R is fully stable if $\alpha(I) \subseteq I$ for each ideal I of R and for each R-homomorphism $\alpha : I \to R$ [7].

Here we are introduced a special fully stable ring.

Definition (6): Let R be a ring, R is called special fully stable ring if $\alpha(I) \subseteq I + L(R)$ for each ideal I of R and each R-homomorphism $\alpha : I \to R$.

Example and Remark (7):

It is clear that every fully stable ring is special fully stable but the converse may not be true in general. For Let $R = Z_2[x, y]/\langle x^2, y^2, xy \rangle$ (the polynomial ring in two indeterminate x and y over Z_2 modulo the ideal $\langle x^2, y^2, xy \rangle$. R is special fully stable ring but not fully stable.

Proof : The only ideals of R are $(\bar{0}), (\bar{x}), (\bar{y}), (\bar{x}, \bar{y})$ and R, the zero ideal $(\bar{0})$ is not prime since $x^2 \in (\bar{0})$ but $x \notin (\bar{0})$ $(\bar{x})$ is not prime ideal since $(\bar{x}) = R\bar{x} = \{\bar{0}, \bar{x}\}$ and $y^2 \in (\bar{x})$ but $y \notin (\bar{x})$ similarly $(\bar{y})$ is not

prime ideal, and since $(\bar{x},\bar{y})$ is maximal ideal and every maximal is prime in commutative ring then $(\bar{x},\bar{y})$ is prime and $(\bar{x},\bar{y})$ is the only prime ideal in R. Thus $L(R)=(\bar{x},\bar{y})$. Then $L(R)=J(R)=(\bar{x},\bar{y})$.
Since R is fully J-stable by [8], then R is fully L-stable (i,e) R is special fully stable ring. But R is not fully stable ring since $anna_R(anna_R(\bar{x}))=anna_R((\bar{x},\bar{y}))=(\bar{x},\bar{y})\neq(\bar{x})$ [7]. □

Recall that an R-module M is called principally N-injective if for any cyclic R-submodule A of N, every R-homomorphism from A into M can be extended to an R-homomorphism from N into M. An R-module M is called principally quasi-injective (in short, PQ-injective) if M is principally M-injective.

Definition (8): Let M and N be two R-modules. M is said to be special principally N-injective (in short, special P-N-injective) if for any cyclic R-submodule A of N and any R-homomorphism $f:A\longrightarrow M$ there exists an R-homomorphism $g:N\rightarrow M$ such that $g(a)-f(a)\in L(M)$, for all a in A. an R-module M is called special PQ-injective, if M is special principally M-injective. A ring R is called special PQ-injective, if R special PQ-injective R-module.

Examples and Remarks (9) :
1) It is clear that every special quasi-injective module (resp., PQ-injective module) is special PQ-injective module.
2) The concept of special PQ-injective modules is a proper generalization of both, special quasi-injective modules and PQ-injective modules: as it has been shown in the following examples
i) Let R be the ring of all continuous function from the set of rational numbers Q to Z_2. R is a PQ-injective R-module [9], thus by remark (1) R is a special PQ-injective R-module. Since R is a regular ring and not self-injective, then L(R)=0 and this implies that R is not special quasi-injective R-module. Since if not, that is R is special quasi-injective R-module then (by remark ((2),d) for each diagram with exact row (where I be any ideal of R),

$$\begin{tikzcd} 0 \arrow[r] & I \arrow[r, "\alpha"] \arrow[d, "f"'] & R \arrow[dl, dotted, "g"] \\ & R & \end{tikzcd}$$

there exists an R-homomorphism $g:R\rightarrow R$ such that $(g\circ\alpha)(x)-f(x)\in L(M)=0$, for all x in I (i,e) $(g\circ\alpha)(x)=f(x)$ for all x in I, and this contradiction since R is not self-injective. Thus R is not special quasi-injective R-module.

ii) Let $R = Z_2[x,y]/<x^2,y^2,xy>$ (the polynomial ring into indeterminate x and y over Z_2 module the ideal $<x^2,y^2,xy>$, R is fully L-stable but it is not fully stable ring by (Example (7)).R is special quasi-injective ring, let I be any ideal of R and let $f : I \to R$ be any R-homomorphism if $I = R$, then put $g = f$. Now if $I \neq R$, since R is fully L-stable ring, thus $f(I) \subseteq I + L(R)$. Since $(\bar{0}),(\bar{x}),(\bar{y}),(\bar{x},\bar{y})$ and R are the only ideals of R and since $L(R) = (\bar{x},\bar{y})$, thus $I \subseteq L(R)$ for all ideal $I \neq R$ and this implies that $f(I) \subseteq L(R)$.Define $g : R \to R$ by $g(r) = r\bar{x}$ for all r in R. It is clear that g is an R-homomorphism. Since $\bar{x} \in L(R)$, thus $g(r) \in L(R)$ for all r in R, therefore $g(r) - f(r) \in L(R)$ for all r in I. Hence R is a special quasi-injective ring and by remark (1) R is special PQ-injective ring. Since R is not fully stable ring since $ann_R(ann_R(\bar{x})) = ann_R((\bar{x},\bar{y})) = (\bar{x},\bar{y}) \neq (\bar{x})$ .Thus R is not self-injective ring [7] and hence R is not PQ-injective [7].Therefore R is a special PQ-injective but it is not PQ-injective R-module.

3) i) If M is special principally N-injective and $K \square M \Rightarrow K$ is special principally N-injective.

ii) If M is special principally N-injective and $K \square N \Rightarrow M$ is special principally K-injective.

In general there is the following implication

special injective $\Rightarrow$ special quasi-injective $\Rightarrow$ special PQ-injective
modules modules modules
$\Uparrow$ $\Uparrow$ $\Uparrow$
Injective modules $\Rightarrow$ quasi-injective modules $\Rightarrow$ PQ-injective modules

The following theorem gives many characterizations of special P-N-injective modules.

Theorem (10): Let M and N be two R-modules and $S = End_R(M)$ then the following statements are equivalent:

1) M is special P-N-injective R-module.

2) For each m in M, n in N such that $ann_R(n) \subseteq ann_R(m)$, there exists an R-homomorphism $g : N \to M$ such that $g(n) - m \in L(M)$.

3) For each m in M, n in N such that $ann_R(n) \subseteq ann_R(m)$, we have $Sm \subseteq Hom_R(N,M)(n) + L(M)$.

4) For each R-homomorphism $f : A \to M$ (where A be any R-submodule of N) and each a in A, there exists an R-homomorphism $g : N \to M$ such that $g(a) - f(a) \in L(M)$.

Proof : $(1)\Rightarrow(2)$. Let M be a special P-N-injective R-module. Let $m \in M$, $n \in N$ such that $ann_R(n) \subseteq ann_R(m)$. Define $f : Rn \to M$ by $f(rn) = rm$ for all r in R. It is clear that f is well-defined R-homomorphism. Since M is special P-N-injective R-module, thus there exists an R-homomorphism $g : N \to M$ such that $g(x) - f(x) \in L(M)$, for each $x \in R_n$. Therefore $g(n) - m \in L(M)$.

$(2)\Rightarrow(3)$. Let $m \in M$, $n \in N$ such that $ann_R(n) \subseteq ann_R(m)$. By hypothesis there exists an R-homomorphism $g : N \to M$ such that $g(n) - m \in L(M)$. Put $g(n) - m = \ell$, where $\ell \in L(M)$. Let $\alpha \in S$, thus $\alpha(m) = \alpha(g(n) - \ell) =$
$\alpha(g(n)) + \alpha(-\ell) = \alpha \circ g(n) + \alpha(-\ell)$ since $\alpha \circ g \in Hom_R(N,M)$ and $\alpha(-\ell) \in L(M)$. Thus $\alpha(m) \in Hom_R(N,M) + L(M)$ therefore $Sm \in Hom_R(N,M)(n) + L(M)$.

$(3)\Rightarrow(4)$ Let $f : A \to M$ be any R-homomorphism where A be any R-submodule of N, and let $a \in A$, put $m = f(a)$, since $m \in M$ and $ann_R(a) \subseteq ann_R(m)$, thus by hypothesis we have $S_m \in Hom_R(N,M)_n + L(M)$. Let $I_M : M \to M$ be the identity map since $I_M \in S$, thus there exists an R-homomorphism $g \in Hom_R(N,M)$ such that $I_M(m) = g(a) + \ell$ where $\ell \in L(M)$. Thus $g(a) - m \in L(M)$ and hence $g(a) - f(a) \in L(M)$.

$(4)\Rightarrow(1)$. Let A=Ra be any cyclic R-submodule of M, and $f : A \longrightarrow M$ be an R-homomorphism , thus by hypothesis there exists an R-homomorphism $g : N \to M$ such that $g(a) - f(a) \in L(M)$ for each x in A, x=ra for some r in R, we have that $g(x) - f(x) = g(ra) - f(ra) = r(g(a) - f(a)) \in L(M)$.

Therefore M is special P-N-injective R-module. □

As an immediate consequence of theorem (10) there is the following corollary in which many characterizations of special PQ-injective modules have been given.

Corollary (11): The following statements are equivalent for an R-module M:

1) M is special PQ-injective.

2) For each $n,m \in M$ such that $ann_R(n) \subseteq ann_R(m)$, there exists an R-homomorphism $g : M \to M$ such that $g(n) - m \in L(M)$.

3) For each $n,m \in M$ such that $ann_R(n) \subseteq ann_R(m)$, we have $Sm \subseteq Sn + L(M)$ where $S = End_R(M)$.

4) For each R-homomorphism $f:A \to M$ (where A be any R-submodule of M) and each a in A, there exists an R-homomorphism $g:M \to M$ such that $g(a)-f(a) \in L(M)$.□

Proposition (12): Let M and N be two R-modules. If M is special P-N-injective then M is special P-A-injective for each R-submodule A of N.

Proof : Let A be an R-submodule of N, B be a cyclic R-submodule of A and $f:B \longrightarrow M$ be an R-homomorphism. Let i_B be the inclusion R-homomorphism from B into A and i_A be the inclusion R-homomorphism from A into N. Since B is a cyclic R-submodule of N and M is special P-N-injective thus there exists an R-homomorphism $h:N \to M$ such that $(h \circ i_A \circ i_B)(b)-f(b) \in L(M)$ for all b in B. Put $g:h \circ i_A : A \to M$, then for each b in B we have that $g(b)-f(b)=(h \circ i_A)(b)-f(b)=(h \circ i_A)(i_B(b))-f(b)$
$=(h \circ i_A \circ i_B(b)-f(b) \in L(M)$.Therefore M is special P-A-injective for each R-submodule.□

As an immediate consequence of proposition (12) there is the following corollary

Corollary (13): Let N be a submodule of an R-module M. If N is special P-M-injective then N is special PQ-injective.□

Proposition (14): Direct summands of special P-N-injective R-module are special P-N-injective.

Proof: Let M be any special P-N-injective R-module and A be any direct summand R-submodule of M. Thus there exists an R-submodule A_1 of M such that $M=A \oplus A_1$.

Let B be any cyclic R-submodule of N and $f:B \to A$ be any R-homomorphism. Define $g:B \to M = A \oplus A_1$ by $g(b)=(f(b),0)$ for each b in B. It is clear that g is an R-homomorphism and since M is special P-N-injective R-module, thus there exists an R-homomorphism $h:N \to M$ such that $h(b)-g(b) \in L(M)$ for all b in B. Let π_A be the natural projection R-homomorphism of $M=A \oplus A_1$ into A. Put $h_1=\pi_A \circ h : N \to A$. Thus h_1 is an R-homomorphism and for each b in B. Then

$h_1(b)-g(b)=(\pi_A \circ h)(b)-\pi_A((f(b),0)=\pi_A(h(b)-\pi_A(g(b)$
$=\pi_A(h(b)-g(b)) \in L(A)$. [7] Therefore A is special P-N-injective R-module. □

By proposition (14) and corollary (11) we have the following corollary

Corollary (15): Any direct summand of special PQ-injective R-module is also special PQ-injective. □

Theorem (16) : Let $M=\bigoplus_{i=1}^{n} M_i$. If M_j is a special P-M_i-injective R-modules for each i,j=1,…,n, then M is special PQ-injective.

Proof : Let N=Rm be a cyclic R-submodule of an R-module M, then we can write $m=(m_1,m_2,\dots,m_n)$ where $m_i \in M_i$ (i =1,…,n). Let $f:N\to M$ be any R-homomorphism and put $f_{ij}=\pi_j \circ f_i$ for each (i,j=1,…,n) where f_i be the restriction of f to Rm_i and π_j be the projection of M onto M_j. Then $f_{ij}:Rm_i \to M_j$. Since for each i,j=1,…,n, M_j is a special P-M_i-injective. Then there exists an R-homomorphism $g_{ij}:M_i\to M_j$ such that $g_{ij}(x)-f_{ij}(x)\in L(M_j)$ for each $x\in Rm_i$. Put $g=\sum_{i=1}^{n}\sum_{j=1}^{n}\alpha_j\circ g_{ij}\circ\pi_i$ where α_j is the injection R-homomorphism from M_j into M and π_i is the projection R-homomorphism from M onto M_i, then $g\in End_R(M)$. Therefore,

$$g(m)-f(m)=(\sum_{i=1}^{n}\sum_{j=1}^{n}\alpha_j\circ g_{ij}\circ\pi_i)(m)-$$

$$\sum_{i=1}^{n}f_i(m_i)=(\sum_{i=1}^{n}\sum_{j=1}^{n}\alpha_j\circ g_{ij}\circ\pi_i)(m)-\sum_{i=1}^{n}(I_M(f_i(m_i))$$

$$=(\sum_{i=1}^{n}\sum_{j=1}^{n}\alpha_j\circ g_{ij}\circ\pi_i)(m)-\sum_{i=1}^{n}[\sum_{j=1}^{n}\alpha_j\circ\pi_j)(f_i(m_i)]$$

$$=(\sum_{i=1}^{n}\sum_{j=1}^{n}\alpha_j\circ g_{ij}\circ\pi_i)(m)-\sum_{i=1}^{n}[(\sum_{i=1}^{n}\alpha_i\circ\pi_i)(f_i\circ\pi_i(m))]$$

$$=\sum_{i=1}^{n}\sum_{j=1}^{n}\alpha_j\circ g_{ij}\circ\pi_i(m)-\sum_{i=1}^{n}\sum_{j=1}^{n}(\alpha_i(\pi_i\circ f_i)\circ\pi_i)(m)$$

$$=\sum_{i=1}^{n}\sum_{j=1}^{n}\alpha_j\circ g_{ij}\circ\pi_i(m)-\sum_{i=1}^{n}\sum_{j=1}^{n}(\alpha_i\circ f_{ij}\circ\pi_i)(m)$$

$$=\sum_{i=1}^{n}\sum_{j=1}^{n}\alpha_j(g_{ij}(\pi_i(m)))-f_{ij}(\pi_i(m)))$$

$$=\sum_{i=1}^{n}\sum_{j=1}^{n}\alpha_j(g_{ij}(m_i)-f_{ij}(m_i))=\sum_{i=1}^{n}\sum_{j=1}^{n}\alpha_j(a_j)$$

where $a_j=g_{ij}(m_i)-f_{ij}(m_i)\in L(M$) for each i,j=1,…,n.

since $\alpha_j : M_i \to M$ is an R-homomorphism, thus by [2]. $\alpha_j(a_j) \in L(M)$, for each j=1,...,n, hence $\sum_{i=1}^{n}\sum_{j=1}^{n}\alpha_j(a_j) \in L(M)$. Therefore, $g(m) - f(m) \in L(M)$ and this implies that $g(x) - f(x) \in L(M)$, for each x in Rm. Hence $M = \bigoplus_{i=1}^{n} M_i$ is a special PQ-injective R-module. □

By Theorem (16) and Corollary (15) we have the following corollary Corollary (17): For each R-module M and $n \in Z^+$, then M is a special PQ-injective if and only if, M^n is a special PQ-injective R-module. □

The direct sum of any two special PQ-injective modules need not be special PQ-injective module. However the following proposition we give a condition on which direct sum of any two special PQ-injective R-module is special PQ-injective.

Proposition (18): The following statements are equivalent for a ring R.
1) Direct sum of any two special PQ-injective R-module is special PQ-injective.
2) Every cyclic special PQ-injective R-module is special injective.

Proof: $(1) \Rightarrow (2)$. Let M be any special PQ-injective R-module, let E=E(M) be the injective envelope of M, $\alpha : M \to E$ be any R-monomorphism i_1 be the injection R-homomorphism of E into $M \oplus E$ and i_2 be the injection R-homomorphism of M into $M \oplus E$, thus we have the following diagram with exact row :

$$\begin{tikzcd}
0 \arrow[r] & M \arrow[r, "\alpha"] \arrow[d, "I_M"'] & E \arrow[r, "i_1"] \arrow[dl, dotted, "f"] & M \oplus E \arrow[ddll, dotted, "g"] \\
 & M \arrow[d, shift left, "i_2"] & & \\
 & M \oplus E \arrow[u, shift left, "P"] & &
\end{tikzcd}$$

By hypothesis $M \oplus E$ is a special P-Q-injective R-module and thus by corollary (11) we have that for each m in M, there exists an R-homomorphism $g : M \oplus E \to M \oplus E$ such that $(g \circ i_1 \circ \alpha)(m) - (i_2 \circ I_M)(m) \in L(M \oplus E)$. Put $f = p \circ g \circ i_1 : E \to M$ where p is the projection R-homomorphism of $M \oplus E$ onto M such that $p \circ i_2 = I_M$. Since

$(g \circ i_1 \circ \alpha)(m) - (i_2 \circ I_M)(m) \in L(M \oplus E)$, thus $p((g \circ i_1 \circ \alpha)(m) - (i_2)(m)) \in L(M)$[2]., therefore each R-monomorphism $\alpha : M \to E$ and for each m in M, there exists an R-homomorphism $f : E \to M$ such that $(f \circ \alpha)(m) - m \in L(M)$ and this implies that α is special split R-homomorphism[1], thus M is special injective R-module[1].

$(2) \Rightarrow (1)$. Let M_1 and M_2 be any two cyclic special PQ-injective R-modules. By hypothesis M_1 and M_2 are special injective R-modules, thus $M_1 \oplus M_2$ is special injective by corollary [1].and hence $M_1 \oplus M_2$ is special PQ-injective R-module. □

The following example shows that the direct sum of any two special PQ-injective dose not need to be special PQ-injective module.

Example (19): Let $M_1 = Q$ as Z-module, $M_2 = Z_p$ as Z-module. Since M_1 is an injective and M_2 is a quasi-injective, thus $M_1$and M_2 are special PQ-injective Z-modules.Let $M = M_1 \oplus M_2 = Q \oplus Z_p$, then M is not special PQ-injective Z-module. Since suppose M is special PQ-injective Z-module then by proposition (18), every cyclic special PQ-injective is special injective, then $M_2 = Z_p$ is special injective Z-module and this contradiction with example [1].Therefore, $M = Q \oplus Z_p$ is not special principle quasi-injective Z-module. □

Corollary (20): if direct sum of any two special PQ-injective R-modules is special PQ-injective, then R is a regular ring.

Proof: Let M be any simple R-module. Since M is a special PQ-injective R-module, thus by proposition (18) M is special injective R-module. Since L(M)=0, thus M is injective R-module, since every injective module is P-injective, then M is P-injective R-module. Hence every simple R-module is P-injective and this implies that R is a regular ring [10]. □

Corollary (21): If direct sum of any two special PQ-injective R-modules is special PQ-injective, then every cyclic special PQ-injective R-module (and hence simple R-module) is injective R-module.

Proof: Let M be any cyclic special PQ-injective. By proposition (18), then M is special injective R-module. Since R is a regular ring by corollary (20) thus J(M)=0 and since $L(M) \hookrightarrow J(M)=0$. Then L(M)=0 and this implies that M is injective R-module. [1].□

By corollary (20) and corollary (21) we have the following corollary:
Corollary (22): If direct sum of any two special PQ-injective R-modules special PQ-injective, then the following statements are equivalent:

1. R is a self-injective ring.
2. R is a self P-injective ring.
3. R is a special PQ-injective ring.
4. If R is principal, R is a self special injective ring. □

Faith and Utumi in [11] were proved that a ring R is a semi-simple Artinian if and only if, every R-module is quasi-injective.

The following proposition gives a new characterization of semi-simple Artinian ring in terms of special PQ-injective R-modules which is a generalization of Faith's and Utumi's reslts.

Proposition (23): The following statements are equivalent for a ring R.

1) R is a semi-simple Artinian ring.
2) Every R-module is special PQ-injective.
3) Every cyclic R-module is special PQ-injective and direct sum of any two special PQ-injective R-modules is special PQ-injective.

Proof: $(1) \Rightarrow (2)$. And $(2) \Rightarrow (3)$. Are obvious.
$(3) \Rightarrow (1)$. Let M be any cyclic R-module. By (3) M is special PQ-injective R- module and by corollary (21), then M is injective R-module. Hence every cyclic R- module is injective therefore R is a semi-simple Artinian ring, by [6].

The following corollary is immediately from proposition (23).

Corollary(24):- (Faith's and Utumi's results) [12]

A ring R is a semi- simple Artinian if and only if every R- module is quasi- injective.
Proof:- Let R is semi-simple Artinian ring, then by proposition (23) every cyclic R-module is special PQ-injective and direct sum of any two special PQ-injective R modules is special PQ-injective, then by corollary (21), M is injective R-module, thus M is quasi-injective.

Corollary(25): - The following statements are equivalent for a ring R:-
1) R is a semi- simple Artinian ring.
2) An R-module M is P- injective if, and only if, M is special PQ-injective .

Proof: $(1)\Rightarrow(2)$. It is obvious by proposition (23).
$(2)\Rightarrow(1)$. Let M be any simple R- module. Thus M is a special PQ-injective and by hypothesis M is P-injective. Hence every simple R-module is P-injective and this implies that R is a regular ring [10]. Hence every R-module is P- injective [10] and by hypothesis we are every R- module is special PQ- injective. Therefore R is a semi-simple Artinian ring, by proposition (23). □

B. L. Osofsky has noted that a ring R is a semi- simple Artinian if, and only if, for each R- module M. if N_1 and N_2 are injective R- sub modules of M, then $N_1 \cap N_2$ is also injective R- module [13]in the following proposition we give a new characterization of semi- simple Artinian rings which is a generalization of Osofsky's result in [13].

Proposition (26):-The following statements are equivalent for a ring R:-
1) R is a semi- simple Artinian ring.
2) For each R- module M, if N_1 and N_2 are special PQ- injective R-submodules of M, then $N_1 \cap N_2$ is special PQ- injective.
3) For each R- module M, if N_1 and N_2 are special quasi- injective R-sub modules of M, then $N_1 \cap N_2$ is a special PQ- injective R-module.
4) For each R-module M, if N_1 and N_2 are quasi- injective R-submodules of M, then $N_1 \cap N_2$ is a special PQ- injective R- module.
5) For each R- module M, if N1 and N_2 are injective R- sub modules of M, then $N_1 \cap N_2$ is a special PQ- injective R- module.

Proof: $(1)\Rightarrow(2)$ It follows from Proposition (23)
$(2)\Rightarrow(3), (3)\Rightarrow(4)$and $(4)\Rightarrow(5)$are obvious.
$(5)\Rightarrow(1)$Let M be any R- module and $E=E(M)$is the injective envelope of M, let $Q=E\oplus E$, $K=\{(x,x)\in Q \mid x\in M\}$K is a submodule of Q and let $\bar{Q}=Q/K$. Also put

$M_1=\{y+k\in\bar{Q}/y\in E\oplus(0)\}$ and $M_2=\{y+k\in\bar{Q}/y\in(0)\oplus E\}$. It is clear that $\bar{Q}=M_1+M_2$. Define $\alpha_1:E\to M_1$ by $\alpha_1(y)=(y,0)+K$, for all $y\in E$ and $\alpha_2: E\to M_2$ by $\alpha_2(y)=(0,y)+K$, for all $y\in E$. Since $(E\oplus(0))\cap K=(0)$ and $((0)\oplus E)\cap K=(0)$, thus we have α_1 and α_2 are R-isomorphisms. Since E is an injective R-module therefore M_i is injective R-submodule of $\bar{Q}$. For $i=1,2$,see [13] and thus by (5), we have $M_1\cap M_2$ is a special PQ-injective R-module. Define by $f(m)=(m,0)+K$, for all $m\in M$. Since $M_1\cap M_2=\{y+k\in\bar{Q}/y\in M\oplus(0)\}$, thus it is easy to prove that f is an R-isomorphism. Thus M is a special PQ-injective R- module, by remark. Hence every R- module is special PQ-injective and this implies that R is a semi-simple Artinian ring, by proposition (23). □

REFRANCES

1. Abbas, M.S. and Abd-Alridha, S.N: Special Injective Modules and Their Endomorphism Ring, vol. (21), No.6, 2010,AL-Mustansiriya J.Sci. ,482-500
2. Saeed, A.B.: L-Regular Modules, M.Sc.thesis, Univ.of Al-Mustansiriyah, 2000.
3. Anderson, F.W.; Fuller, K.R.: Rings and Categories of Modules, Springer-verlag, Berlin, Heidelberg, New York, 1974.
4. Hungerford, T.W.: Algebra, Springer-verlag, New York Heidelblerg, Berlin, 1974.
5. kasch, F. :Modules and Rings ,Academic press ,London ,New York ,1982.
6. Osofsky,B.L.: Rings all whose Finitely Generated Modules are Injective, pac.J.Math.14 (1964), 645-650
7. Abbas, M.S.: On fully Stable Modules, Ph .D. thesis , Univ. of Baghdad, 1990
8. Abbas, M.S.: Semi-regular and fully J-stable modules, Iraqi J. science, vol(41)D,No.1,2000.
9. Tiwary, A.K.; paramhans, S.A. and pandey, B.M.: Generalization of Quasi-injectivity, progr.Math. (Allahabad), Vol. (13), (1-2)1979, 31-40.
10. Chi Ming, R.yu: On von Neumann Regular Rings, Proc.Edinburagh Math.Soc.19 (1974), 89-91.
11. Faith, C.; Utumi, Y.: Quasi-injective Modules and TheirEndomorphisms rings, Archiv.Math., 15(1964),166-174.

12. Alok, M.K., and Atul Gaur, p. Anand: Prime submodules inMultiplication Modules, Inter.Jour. Of Algebra,V01.1, 2007, No.8, 375-380.
13. Faith, C.: Lectures on Injective Modules and Quotient Rings, No.49, Springer-verlag,Berlin,Heidelberg,NewYourk ,1967.

Convex Approximation by q- Meyer-König-Zeller Durrmeyer Operators

Saheb K. Al-Saidy[1] and Nadia M.J. Ibrahim[2]
[1]University of Al-Mustansrya, College of Science, Department of Mathematics
[2]University of Baghdad , College of Science for Women, Department of Mathematics
Received 13/3/2013 – Accepted 15/9/2013

الخلاصة

في هذا البحث و بمساعدة مفاهيم q-calculus ندرس صفات التقريب المحدب لعائلة المؤثرات (q-Meyer-König and Zeller Durrmeyer operators) والمعروفة بأنها مؤثرات خطية موجبة وذلك بتحويلها الى نوع جديد من انواع q-Meyer-König and Zeller operators والتي تكون مؤثرات خطية موجبة محدبة.

ABSTRACT

In this paper, the convex approximation properties of a general family of q-Meyer-König and Zeller Durrmeyer operators has been studied based on q-calculus concepts .Thus operators are well-known positive linear operators. The aim of this work is to convert them into a new type of convex positive q-Meyer-König and Zeller operators.

1-Introduction

Many works on q-calculus are available in literature of different branches of mathematics and physics. Recent studies show that the theory of q-calculus plays an important role on analytic number theory and theoretical physics. For example, various applications of this theory have appeared in the study of hypergeometric series [5], in the approximation theory [6,15,17] while other important applications have been related with the quantum theory [10,11,13].

We recall some notations and concepts of q-calculus. All of the results can be found in [8] and [10]. In what follows, q is a real number satisfying $0 < q < 1$.

The classical Meyer-König and Zeller (MKZ) operators defined on C[0,1]:

$$M_n(f;x)=\begin{cases}(1-x)^{n+1}\sum_{k=0}^{\infty} f\left(\frac{k}{k+n+1}\right)\binom{n+k}{k}x^k, & \text{if } x\in[0,1) \\ f(1) & \text{if } x=1\end{cases}$$

were introduced in 1960 [10].

Abel et al. [1] present the Meyer-Konig-Zeller Durrmeyer operators as:

$$M_n(f;x)=\sum_{k=0}^{\infty}\binom{n+k-1}{k}x^k(1-x)^n\int_0^1 n\binom{n+k}{k}t^k(1-t)^{n-1}f(t)dt, \qquad 0\le x<1$$

Also, H.Wang [18], O. Dogru and V. Gupta [7], A. Altin, O. Dogru and M.A. Ozarslan [4] and T. Trif [17] studied the q-Meyer-Konig-Zeller operators.

Before introducing the operators, we mention some definitions that concern us in this search that based on q-integers.

For each non-negative integer k, the q-integer $[k]$ and the q-factorial $[k]!$ respectively defined by:

$$[k]=\begin{cases}\dfrac{1-q^k}{1-q} & q\neq 1\\ k & q=1\end{cases} \quad \text{and} \quad [k]!=\begin{cases}[k][k-1]...[1] & k\geq 1\\ 1 & k=0\end{cases} \qquad (1.1)$$

For the integer n, k satisfying $n \geq k \geq 0$, the q- binomial coefficients defined by:

$$\binom{n}{k}=\frac{[n]!}{[k]![n-k]!}$$

We use the following notations:

$$[k+1]=q[k]+1 \quad , \frac{[k]}{[n+k-1]}=x \ , \quad [n]=[k]+q^k[n-k] \ ,$$
$$[k+2]=q^2[k]+q+1$$
$$(a+b)_q^n=\prod_{s=0}^{n-1}(a+q^s b)=(a+b)(a+qb)...(a+q^{n-1}b)$$

and $\quad (t,q)_0=1, \quad (t,q)_n=\prod_{s=0}^{n-1}(1-q^s t), \qquad (t,q)_\infty=\prod_{s=0}^{\infty}(1-q^s t)$

Also it can be seen that :

$(a,q)_n=\dfrac{(a,q)_\infty}{(aq^n,q)_\infty}$ such that $(aq^n,q)_\infty \neq 0$

For $m,n \in$ N, the q-Beta function is defined as:

$$B_q(m,n)=\int_0^1 t^{m-1}(1-qt)_q^{n-1}d_q t$$

and

$$B_q(m,n)=\frac{[m-1]![n-1]!}{[m+n-1]!}$$

It can easily cheek that:

$$\prod_{s=0}^{n-1}(1-q^s x)\sum_{k=0}^{\infty}\binom{n+k-1}{k} x^k=1 \qquad (1.2)$$

In 2009, Sharma [16] introduce the q-Meyer-Konig-Zeller Durrmeyer operator as follows:

$$M_{n,q}(f;x)=\sum_{k=0}^{\infty}m_{n,k,q}(x)\int_0^1 b_{n,k,q}(t)f(qt)d_q t, \qquad 0\leq x<1 \text{ and } 0<q<1 \qquad (1.3)$$

where $m_{n,k,q}(x)=P_{n-1}(x)\binom{n+k-1}{k}x \quad , \quad P_{n-1}(x)=\prod_{s=0}^{n-1}(1-q^s x) \qquad (1.4)$

and $\quad b_{n,k,q}(t)=\dfrac{[n+k]!}{[k]![n-1]!}t^k(1-qt)_q^{n-1} \qquad (1.5)$

For the interval U $\subseteq$ R , the continuous function ρ : U $\rightarrow$ (0, ∞) is called *weight*. We call *weighted space* $L_{p,\rho}$, the set which represents the space of all functions f : U $\rightarrow$ R, for which there exist $M > 0$, such that

$|f(x)| \le M\rho(x)$, for every $x \in$ U. This space can be endowed with the norm ρ - norm [2]:

$$\|f\|_{L_{p,\rho}} = \|f\|_{p,\rho} = \begin{cases} \left\{ \int_{-1}^{1} \left| \frac{f(x)}{\rho(x)} \right|^p dx \right\}^{1/p} & 1 \le p < \infty \\ ess \sup_{x \in U} \left| \frac{f(x)}{\rho(x)} \right| & p = \infty \end{cases} \quad (1.6)$$

If the set is convex, closed, bounded, and m-dimensional, it is called an *m-dimensional convex body* , let K^m denote the set of all convex bodies in R^m. For $U \in \mathrm{K}^m$, by $Lip_\lambda(U)$, $\lambda > 0$, we denote the set of all functions on U satisfying the *weighted Lipschitz condition*:

$$\left| \frac{f(x)}{\rho(x)} - \frac{f(y)}{\rho(y)} \right| \le \lambda |x - y|$$

The function $f : U \to R$, $U \in \mathrm{K}^m$, is *convex* if :

$f(\alpha x + (1-\alpha)y) \le \alpha f(x) + (1-\alpha) f(y)$ $\quad \forall x, y \in U$ and $0 \le \alpha \le 1$

The following Lemma on convex extension of Lipschitz functions:

Lemma 1.1 [12]:Let $U \in \mathrm{K}^m$ and $f \in Lip_1(U)$. Then, f can be extended to a function (i.e. $\tilde{f}(x) = f(x), \forall x \in U$) which convex on R^m, and satisfies the Lipschitz condition on R^m with the constant $\sqrt{2}$.

We note that it was shown in [12] that can be defined as follows:

$$\tilde{f}(x) := \inf \{ y \in R : (x, y) \in CO\{(x, g(x)) \in R^m \times R : x \in R^m\}\}$$

where $g(x) := f(P(x)) + |x - P(x)|$, $P(x) := \arg\min_{y \in U} |y - x|$, $x \in R^m$, and CO(A) denotes the convex hull of A.

Now we smooth $\tilde{f}$ by considering its first steklov mean:

$$\tilde{f}_\varepsilon(x) = \varepsilon^{-1} \int_{-\varepsilon/2}^{\varepsilon/2} (f/\rho)(x + t_1)\, dt_1, \qquad x, t_1 \in U \qquad (1.7)$$

for sufficiently small $\varepsilon > 0$.

As usual, throughout the paper we use the test functions $e_i(x) = x^i$ for $i = 0, 1, 2$.

In the present paper we first introduce a new sequence of convex positive linear operators and then investigate their approximation properties. Mainly, we obtain a Korovkin-type approximation theorem and compute the rates of convergence of these operators by means of modulus of continuity.

2-Auxiliary Lemmas

Lemma 2.1 : [16] For the integer n, k satisfying $n \ge k \ge 0$, $q > 0$ and for $g_s(t) = t^s$,

s = 0, 1, 2, . . .,we have:

$$\int_0^1 b_{n,k,q}(t)\, g_s(qt)\, d_q t = q^s \frac{[n+k]![k+s]!}{[k]![k+s+n]!} \qquad (2.2)$$

Lemma 2.2 : [9] For $r = 0, 1, 2, \ldots, n > r$, and $k \geq 0$, we have:

$$P_{n-1}(x)\sum_{k=0}^{\infty}\binom{n+k-1}{k}\frac{x^k}{[n+k-1]^r} = \frac{\prod_{s=1}^{r}(1-q^{n-s}x)}{[n-1]^r} \tag{2.3}$$

where $[n-1]^r = [n-1][n-2]\ldots[n-r]$.

Lemma 2.3 :[9]

For $r \geq 0$ and $n > r$, the identity :

$$\frac{1}{[n+k+r]} \leq \frac{1}{q^{r+1}[n+k-1]}, \tag{2.4}$$

holds.

Lemma 2.4:[3] For $\widetilde{f}_\varepsilon$ defined on (1.7) and $\forall x \in U$:

1- if $f(x) = 1$ then $\widetilde{f}_\varepsilon(x) = 1$

2- if $f(x) = x$ then $\widetilde{f}_\varepsilon(x) = x$

3- if $f(x)=x^2$ then $\widetilde{f}_\varepsilon(x) = x^2$

3-The Main Result

Now, we construct a new type of q-Meyer-Konig-Zeller Durrmeyer operators which are convex linear positive operators as follows:

$$\widetilde{M}_{n,q}(f;x) = \sum_{k=0}^{\infty} m_{n,k,q}(x)\int_0^1 b_{n,k,q}(t)\,\widetilde{f}_\varepsilon(qt)\,d_qt, \qquad 0 \leq x < 1 \text{ and } 0 < q < 1 \tag{3.1}$$

where $m_{n,k,q}(x)$, $b_{n,k,q}(t)$ and $\widetilde{f}_\varepsilon$ are given in (1.4), (1.5) and (1.7) respectively.

Theorem 3.1:

For all $x \in [0, 1]$, $n \in N$ and $q \in (0, 1)$, we have:

1- $\widetilde{M}_{n,q}(e_0;x) = 1$

(3.2)

2- $(1-\frac{(1+q^{n-2})}{[n+1]})x + q^{n-2}(1-q)x^2 \leq \widetilde{M}_{n,q}(e_1;x) \leq x + \frac{(1-q^{n-1}x)}{q[n-1]}$

(3.3)

3-

$$\widetilde{M}_{n,q}(e_2;x) \leq x^2 + \frac{(1+q)^2}{q^3}\frac{(1-q^{n-1}x)}{[n-1]}x + \frac{(1+q)}{q^4}\frac{(1-q^{n-1}x)(1-q^{n-2}x)}{[n-1][n-2]} \qquad n \neq 1, n \neq 2$$

(3.4)

proof:

1- From Lemma 2.4 (1), we get $\widetilde{f}_\varepsilon(x) = e_0 = 1$.

Therefore by using (1.2) and *Lemma* 2.1 (when s=0), we have:

$$\widetilde{M}_{n,q}(e_0;x)=\sum_{k=0}^{\infty}m_{n,k,q}(x)\int_0^1 b_{n,k,q}(t)\ d_qt\ =1$$

2- From *Lemma* 2.4 (2) , we get $\widetilde{f}_1(x)=e_1=x$ then $\widetilde{f}_1(qt)=qt$

Therefore by *Lemma* 2.1 (when $s=1$) and (1.4), we have:

$$\widetilde{M}_{n,q}(e_1;x)=\sum_{k=0}^{\infty}m_{n,k,q}(x)\int_0^1 b_{n,k,q}(t)\,qt\,d_qt\ =\sum_{k=0}^{\infty}P_{n-1}(x)\binom{n+k\text{-}1}{k}x^k(q\frac{[n+k]![k+1]!}{[k]![k+n+1]!})$$

$$=qP_{n-1}(x)\sum_{k=0}^{\infty}\binom{n+k\text{-}1}{k}\frac{[n+k]![k+1][k]!}{[k]![k+n+1][n+k]!}\ x^k$$

$$=qP_{n-1}(x)\sum_{k=0}^{\infty}\binom{n+k\text{-}1}{k}\frac{[k+1]}{[k+n+1]}\ x^k$$

by *Lemma* 2.3 (when $r=1$),and where $k\neq n\text{-}1$, we get:

$$\widetilde{M}_{n,q}(e_1;x)\leq qP_{n-1}(x)\sum_{k=0}^{\infty}\binom{n+k\text{-}1}{k}\frac{q[k]+1}{q^2[k+n-1]}\ x^k$$

$$\leq qP_{n-1}(x)\sum_{k=0}^{\infty}\binom{n+k\text{-}1}{k}\frac{q[k]}{q^2[k+n-1]}\ x^k+qP_{n-1}(x)\sum_{k=0}^{\infty}\binom{n+k\text{-}1}{k}\frac{1}{q^2[k+n-1]}\ x^k$$

$$\leq P_{n-1}(x)\sum_{k=0}^{\infty}\binom{n+k\text{-}1}{k}\frac{[k]}{[k+n-1]}\ x^k+P_{n-1}(x)\sum_{k=0}^{\infty}\binom{n+k\text{-}1}{k}\frac{1}{q[k+n-1]}\ x^k$$

$$\leq xP_{n-1}(x)\sum_{k=0}^{\infty}\binom{n+k\text{-}1}{k}\ x^k+\frac{P_{n-1}(x)}{q}\sum_{k=0}^{\infty}\binom{n+k\text{-}1}{k}\frac{x^k}{[k+n-1]}$$

By using (1.2) and *Lemma* 2.2 (when $r=1$), we get:

$$\widetilde{M}_{n,q}(e_1;x)\leq x+\frac{(1-q^{n-1}x)}{q[n-1]} \tag{3.5}$$

Also $\widetilde{M}_{n,q}(e_1;x)=qP_{n-1}(x)\sum_{k=0}^{\infty}\binom{n+k\text{-}1}{k}\frac{[k+1]}{[k+n+1]}\ x^k$

from definitions of $\binom{n}{k}$ and $[k]!$, we have:

$$\widetilde{M}_{n,q}(e_1;x)=qP_{n-1}(x)\sum_{k=1}^{\infty}\binom{n+k\text{-}1}{k-1}\frac{[k+n-1]}{[k]}\frac{[k+1]}{[k+n+1]}\ x^k$$

from property $[n]=[j]+q^j[n\text{-}j]$, we get:

$$\widetilde{M}_{n,q}(e_1;x)=P_{n-1}(x)\sum_{k=1}^{\infty}\binom{n+k\text{-}1}{k-1}\frac{[k+1]}{[k]}\frac{[k+n]-1}{[k+n+1]}\ x^k$$

$$\geq P_{n-1}(x)\sum_{k=0}^{\infty}\binom{n+k\text{-}1}{k}(\frac{[k+n+1]-1}{[k+n+2]})\ x^{k+1}$$

$$=P_{n-1}(x)\sum_{k=0}^{\infty}\binom{n+k\text{-}1}{k}(\frac{[k+n+1]}{[k+n+2]}-\frac{1}{[k+n+2]})\ x^{k+1}$$

$$\geq P_{n-1}(x)\sum_{k=0}^{\infty}\binom{n+k\text{-}1}{k}\left(\frac{[k+n+1]}{[k+n+2]}-\frac{1}{[n+1]}\right)x^{k+1}$$

$$=P_{n-1}(x)\sum_{k=0}^{\infty}\binom{n+k\text{-}1}{k}\left(\frac{[k+n+1]}{[k+n+2]}\right)x^{k+1}-\left(\frac{1}{[n+1]}\right)xP_{n-1}(x)\sum_{k=0}^{\infty}\binom{n+k\text{-}1}{k}x^{k}$$

$$=P_{n-1}(x)\sum_{k=0}^{\infty}\binom{n+k\text{-}1}{k}\left(\frac{[k+n+2]-q^{k+n+1}}{[k+n+2]}\right)x^{k+1}-\frac{1}{[n+1]}x$$

$$=P_{n-1}(x)\sum_{k=0}^{\infty}\binom{n+k\text{-}1}{k}\left(1\text{-}\frac{q^{k+n+1}}{[k+n+2]}\right)x^{k+1}-\frac{1}{[n+1]}x$$

$$=P_{n-1}(x)\sum_{k=0}^{\infty}\binom{n+k\text{-}1}{k}\left(1\text{-}\frac{q^{n-2}(1-(1-q)[k])}{[k+n-1]}\right)x^{k+1}-\frac{1}{[n+1]}x$$

$$=xP_{n-1}(x)\sum_{k=0}^{\infty}\binom{n+k\text{-}1}{k}x^{k}-P_{n-1}(x)\sum_{k=0}^{\infty}\binom{n+k\text{-}1}{k}\frac{(q^{n-2}-q^{n-2}(1-q)[k])}{[k+n-1]}x^{k+1}-\frac{1}{[n+1]}x$$

$$=x-q^{n-2}xP_{n-1}(x)\sum_{k=0}^{\infty}\binom{n+k\text{-}1}{k}\frac{1}{[k+n-1]}x^{k}+q^{n-2}(1-q)xP_{n-1}(x)\sum_{k=0}^{\infty}\binom{n+k\text{-}1}{k}\frac{[k]}{[k+n-1]}x^{k}-\frac{1}{[n+1]}x$$

$$=x-\frac{q^{n-2}x}{[n+1]}+q^{n-2}(1-q)x^{2}P_{n-1}(x)\sum_{k=0}^{\infty}\binom{n+k\text{-}1}{k}x^{k}-\frac{1}{[n+1]}x$$

$$=x\left(1-\frac{q^{n-2}}{[n+1]}-\frac{1}{[n+1]}\right)+q^{n-2}(1-q)x^{2}$$

Therefore
$$\widetilde{M}_{n,q}(e_1;x)\geq\left(1-\frac{q^{n-2}+1}{[n+1]}\right)x+q^{n-2}(1-q)x^{2}\qquad(3.6)$$

Then from (3.5) and (3.6), we get (3.3).

3- To obtain (3.4), since if $f=x^2$ then $\widetilde{f}_{\varepsilon}(x)=e_2=x^2$ and , we get: $\widetilde{f}_{\varepsilon}(qt)=(qt)^2$

$$\widetilde{M}_{n,q}(e_2;x)=\sum_{k=0}^{\infty}m_{n,k,q}(x)\int_0^1 b_{n,k,q}(t)\,(qt)^2\,d_qt$$

By lemma 2.1, (where s =2), we get:

$$\widetilde{M}_{n,q}(e_2;x)==\sum_{k=0}^{\infty}P_{n-1}(x)\binom{n+k\text{-}1}{k}x^{k}\left(q^{2}\frac{[n+k]![k+2]!}{[k]![k+n+2]!}\right)$$

$$=q^{2}\sum_{k=0}^{\infty}P_{n-1}(x)\binom{n+k\text{-}1}{k}x^{k}\left(\frac{[n+k]![k+2][k+1][k]!}{[k]![k+n+2][k+n+1][n+k]!}\right)$$

$$=q^{2}\sum_{k=0}^{\infty}P_{n-1}(x)\binom{n+k\text{-}1}{k}x^{k}\left(\frac{[k+1][k+2]}{[k+n+1][k+n+2]}\right)$$

by *Lemma* 2.3 and $[k+2]=q^2[k]+q+1$, we have:

$$\widetilde{M}_{n,q}(e_2;x)\leq q^{2}\sum_{k=0}^{\infty}P_{n-1}(x)\binom{n+k\text{-}1}{k}x^{k}\left(\frac{(1+q[k])(q^{2}[k]+q+1]}{q^{6}[k+n-1][k+n-2]}\right)$$

$$=\frac{1}{q^{4}}\sum_{k=0}^{\infty}P_{n-1}(x)\binom{n+k\text{-}1}{k}x^{k}\left(\frac{(1+q[k])(q^{2}[k]+q+1]}{[k+n-1][k+n-2]}\right)$$

$$=\frac{1}{q^4}\sum_{k=0}^{\infty}P_{n-1}(x)\binom{n+k\text{-}1}{k}\left(\frac{q^3[k]^2+q^2[k]+q[k]+q^2[k]+q+1}{[k+n-1][k+n-2]}\right)x^k$$

$$=\frac{1}{q^4}\sum_{k=0}^{\infty}P_{n-1}(x)\binom{n+k\text{-}1}{k}\left(\frac{q^3[k]^2+q[k](1+2q)+q+1}{[k+n-1][k+n-2]}\right)x^k$$

$$=\frac{1}{q}P_{n-1}(x)\sum_{k=0}^{\infty}\binom{n+k\text{-}1}{k}\left(\frac{[k]^2}{[k+n-1][k+n-2]}\right)x^k+\frac{(1+2q)}{q^3}P_{n-1}(x)\sum_{k=0}^{\infty}\binom{n+k\text{-}1}{k}\left(\frac{[k]}{[k+n-1][k+n-2]}\right)x^k+$$

$$\frac{(q+1)}{q^4}P_{n-1}(x)\sum_{k=0}^{\infty}\binom{n+k\text{-}1}{k}\left(\frac{1}{[k+n-1][k+n-2]}\right)x^k \tag{3.7}$$

Since:

$$\binom{n+k\text{-}1}{k}\left(\frac{[k]^2}{[k+n-1][k+n-2]}\right)=\frac{[n+k-1]!}{[k]![n-1]!}\left(\frac{[k]^2}{[k+n-1][k+n-2]}\right)$$

$$=\frac{[n+k-1][n+k-2][n+k-3]!}{[k][k-1]![n-1]!}\ \frac{[k]^2}{[k+n-1][k+n-2]}$$

where k=k+1 then:

$$\binom{n+k\text{-}1}{k}\left(\frac{[k]^2}{[k+n-1][k+n-2]}\right)=\frac{[n+k-2]![k+1]}{[k]![n-1]!}=\frac{[n+k-2]!}{[k]![n-1]!}(q[k]+1) \tag{3.8}$$

and

$$\binom{n+k\text{-}1}{k}\left(\frac{[k]}{[k+n-1][k+n-2]}\right)=\frac{[n+k-1]!}{[k]![n-1]!}\frac{[k]}{[k+n-1][k+n-2]}=\frac{[n+k-1][n+k-2]![k]}{[k][k-1]![n-1]![k+n-1][k+n-2]}$$

$$=\frac{[n+k-2]!}{[k-1]![n-1]![n+k-2]}$$

where k=k+1 then:

$$\binom{n+k\text{-}1}{k}\left(\frac{[k]}{[k+n-1][k+n-2]}\right)=\frac{[n+k-1]!}{[k]![n-1]![n+k-1]}=\binom{n+k\text{-}1}{k}\frac{1}{[n+k-1]} \tag{3.9}$$

and since $[n\text{-}1]^r$=$[n\text{-}1][n\text{-}2]\ldots[n\text{-}r]$ then

$$\frac{1}{[k+n-1][n+k-2]}=\frac{1}{[n+k-1]^2}$$

(3.10)

By substituting 3.8,3.9 and 3.10 in 3.7, we get:

$$\widetilde{M}_{n,q}(e_2;x)\le\frac{P_{n-1}(x)}{q}\sum_{k=0}^{\infty}\frac{[n+k-2]!}{[k]![n-1]!}(q[k]+1)x^{k+1}+\frac{x(2q+1)P_{n-1}(x)}{q^3}\sum_{k=0}^{\infty}\binom{n+k\text{-}1}{k}\frac{1}{[n+k-1]}x^k$$

$$+\frac{(q+1)P_{n-1}(x)}{q^4}\sum_{k=0}^{\infty}\binom{n+k\text{-}1}{k}\frac{1}{[n+k-1]^2}x^k$$

By Lemma 2.2 , we get:

$$\widetilde{M}_{n,q}(e_2;x) \le \frac{P_{n-1}(x)}{q} x \sum_{k=0}^{\infty} \frac{[n+k-2]!q[k]}{[k][k-1]![n-1]!} x^k + \frac{x}{q} P_{n-1}(x) \sum_{k=0}^{\infty} \frac{[n+k-2]!}{[k]]![n-1]!} x^k \left(\frac{[n+k-1]}{[n+k-1]}\right)$$
$$+ \frac{x(2q+1)}{q^3} \frac{(1-q^{n-1}x)}{[n-1]} + \frac{(q+1)}{q^4} \frac{(1-q^{n-1}x)(1-q^{n-2}x)}{[n-1][n-2]}$$
$$= x^2 P_{n-1}(x) \sum_{k=0}^{\infty} \binom{n+k-1}{k} x^k + \frac{x}{q} P_{n-1}(x) \sum_{k=0}^{\infty} \binom{n+k-1}{k} x^k \left(\frac{1}{[n+k-1]}\right) + \frac{(2q+1)(1-q^{n-1}x)x}{q^3[n-1]} +$$
$$\frac{(q+1)}{q^4} \frac{(1-q^{n-1}x)(1-q^{n-2}x)}{[n-1][n-2]}$$

Therefore

$$\widetilde{M}_{n,q}(e_2;x) \le x^2 + \frac{x}{q}\left(\frac{1-q^{n-1}x}{[n-1]}\right) + \frac{(2q+1)(1-q^{n-1}x)}{q^3[n-1]} x + \frac{1+q}{q^4} \frac{(1-q^{n-1}x)(1-q^{n-2}x)}{[n-1][n-2]}$$
$$= x^2 + x\left(\frac{1-q^{n-1}x}{[n-1]}\right)\left(\frac{1}{q} + \frac{2q+1}{q^3}\right) + \frac{1+q}{q^4} \frac{(1-q^{n-1}x)(1-q^{n-2}x)}{[n-1][n-2]}$$
$$= x^2 + x \frac{1-q^{n-1}x}{[n-1]} \left(\frac{q^2+2q+1}{q^3}\right) + \frac{1+q}{q^4} \frac{(1-q^{n-1}x)(1-q^{n-2}x)}{[n-1][n-2]}$$
$$= x^2 + \frac{(q+1)^2}{q^3} \frac{(1-q^{n-1}x)}{[n-1]} x + \frac{1+q}{q^4} \frac{(1-q^{n-1}x)(1-q^{n-2}x)}{[n-1][n-2]} \qquad \text{for } n \ne 1,2$$

Theorem 3.2: The sequence $M_{n,q_n}(f)$ converges to f on $C_\rho[0,1]$ for each $f \in C_\rho[0,1]$ iff $q_n \to 1$ as $n \to \infty$.

proof: By the Korovkin Theorem, $M_{n,q_n}(f,x)$ converges to f uniformly on $[0,1]$ as $n \to \infty$ for $f \in C_\rho[0,1]$ iff $M_{n,q_n}(t^i,x) \to x^i$ for i=1,2 uniformly on $[0,1]$ as $n \to \infty$.

Moreover, as $q_n \to 1$, then $[n]_{q_n} \to \infty$, therefore by Theorem 3.1, we get:

$$M_{n,q_n}(t^i,x) \to x^i \qquad \text{for } i = 0,1,2$$

Hence, $M_{n,q_n}(f)$ converges to f on uniformly $C_\rho[0,1]$.

Conversely, Let $M_{n,q_n}(f)$ converges to f uniformly on $C_\rho[0,1]$ and q_n does not tend to 1 as $n \to \infty$, then there exist a sequence $\{q_{nk}\}$ of $\{q_n\}$ such that: $q_{nk} \to q_0 \quad (q_0 \ne 1)$.

$$\text{as } k \to \infty \qquad , \qquad \frac{1}{[n]_{q_{nk}}} = \frac{1-q_{nk}}{1-q_{nk}^n} \to (1-q_0) \qquad \text{s.t. } q_{nk}^n \ne 1$$

Take $n=n_k$ and $q=q_{nk}$ in $M_{n,q}(e_2,x)$, we have:

$$M_{n,q}(e_2,x) \le x + \frac{(1-q_{n_k}^{n-1}x)(1-q_0)}{q_{n_k}} \ne x \qquad \text{s.t.} q_{n_k} \ne 0$$

This is contradiction. Therefore: $q_n \to 1$ as $n \to \infty$.

Theorem 3.3: Let $(q_n)_n$ be a sequence satisfying $st-\lim_n q_n = 1, q_n \in (0,1)$, then:

$$|\widetilde{M}_{n,q}(f,x)-\widetilde{f}_{\varepsilon}|\leq 2w_{p,\rho}(f,\sqrt{\delta_n})$$

for all $f\in C_{\rho}[0,1]$, where $\delta_n=\widetilde{M}_{n,q}((qt-x)^2,x)$

proof:

By the linearity and monotonicity of $\widetilde{M}_{n,q}$, we get:

$$|\widetilde{M}_{n,q}(f,x)-\widetilde{f}_{\varepsilon}|\leq \widetilde{M}_{n,q}(|f(t)-\widetilde{f}_{\varepsilon}(x)|,x)$$

$$=\sum_{k=0}^{\infty}m_{n,k,q}(x)\int_0^1 b_{n,k,q}(t)|\widetilde{f}_{\varepsilon}(qt)-\widetilde{f}_{\varepsilon}(x)|\,d_qt,$$

Also $|\widetilde{f}_{\varepsilon}(qt)-\widetilde{f}_{\varepsilon}(x)|=|\frac{1}{\varepsilon}\int_{-\varepsilon/2}^{\varepsilon/2}\frac{f}{\rho}(qt+t_1)dt_1-\frac{1}{\varepsilon}\int_{-\varepsilon/2}^{\varepsilon/2}\frac{f}{\rho}(x+t_1)dt_1$ s.t. $\varepsilon>0$

$$\leq\frac{1}{\varepsilon}\int_{-\varepsilon/2}^{\varepsilon/2}|\frac{f}{\rho}(qt+t_1)-\frac{f}{\rho}(x+t_1)dt_1$$

$$\leq\frac{1}{\varepsilon}\int_{-\varepsilon/2}^{\varepsilon/2}|\omega_p(\frac{f}{\rho},\delta(qt+t_1-x-t_1)|dt_1 \qquad s.t.\ |qt-x|\leq\delta,\ \delta>0$$

$$=\omega_{p,\rho}(f,\delta(\frac{qt-x}{\lambda\delta}))[\frac{\varepsilon}{2}\int_{-\varepsilon/2}^{\varepsilon/2}dt_1] \qquad s.t.\ \lambda>0$$

$$=\omega_{p,\rho}(f,\delta)\,(1+\frac{qt\text{-}x}{\delta})$$

Then

$$|\widetilde{f}_{\varepsilon}(qt)-\widetilde{f}_{\varepsilon}(\mathrm{x})|\leq(1+\frac{(qt-x)^2}{\delta^2})\,\omega_{p,\rho}(f,\delta) \qquad \text{s.t.}|\,qt\text{-}x\,|\leq\delta$$

Therefore $|\widetilde{M}_{n,q}(f,x)-\widetilde{f}_{\varepsilon}|\leq\sum_{k=0}^{\infty}m_{n,k,q}(x)\int_0^1 b_{n,k,q}(t)\,(1+\frac{(qt-x)^2}{\delta^2})\,\omega_{p,\rho}(f,\delta)\,d_qt$

$$=(\widetilde{M}_{n,q}(e_0,x)+\frac{1}{\delta^2}M_{n,q}((qt-x)^2,x))\,\omega_{p,\rho}(f,\delta) \qquad (3.11)$$

and

$$\widetilde{M}_{n,q}((qt-x)^2,x)=\widetilde{M}_{n,q}(q^2t^2-2xqt+x^2,x)$$

$$=q^2\widetilde{M}_{n,q}(e_2,x)+x^2\widetilde{M}_{n,q}(e_0,x)-2xq\,\widetilde{M}_{n,q}(e_1,x)$$

By Theorem 3.1,we get:

$$\widetilde{M}_{n,q}((qt-x)^2,x)\leq q^2(x^2+\frac{(1+q)^2}{q^3}\frac{(1-q^{n-1}x)}{[n-1]}x+\frac{1+q}{q^4}\frac{(1-q^{n-1}x)(1-q^{n-2}x)}{[n-1][n-2]}+x^2-2xq\,(\mathrm{x}+\frac{(1\text{-}q^{n-1}x)}{q[n-1]})$$

$$-2xq((1-\frac{(1+q^{n-2}x)}{[n+1]})x+q^{n-2}(1-q)x^2)$$

$$=x^2(q^2-2q+1)+x(\frac{(1+q)^2(1-q^{n-1}x)}{q[n-1]}-\frac{2q(1-q^{n-1}x)}{q[n-1]})+\frac{(1+q)(1-q^{n-1}x)(1-q^{n-2}x)}{q^2[n-1][n-2]}$$

$$=(q-1)^2x^2+(\frac{(1+q)^2-2q)(1-q^{n-1}x)}{q[n-1]})x+\frac{(1+q)(1-q^{n-1}x)(1-q^{n-2}x}{}$$

$$=(1-q)^2x^2+\frac{(1+q^2)(1-q^{n-1}x)}{q[n-1]}x+\frac{(1+q)}{q^2}\frac{(1-q^{n-1}x)(1-q^{n-2}x)}{[n-1][n-2]}-2x^2q+2x^2q\frac{1+q^{n-2}}{[n+1]}-2x^3q^{n-1}(1-q)$$

From the condition of this Theorem, we get:

$$\lim_{\substack{n\to\infty\\ q_r\to 1}}\widetilde{M}_{n,q}((qt-x)^2,x)=0$$

Let $\delta_n=\widetilde{M}_{n,q}((qt-x)^2,x)$, and $\delta_n>0$ for all n and $\delta=\sqrt{\delta_n}$, by substituting in 3.11 we get:

$$|\widetilde{M}_{n,q}(f,x)-\widetilde{f}_\varepsilon|\le(1+\frac{\delta_n}{\delta_n})\omega_{p,\rho}(f,\delta)$$

Then $$\|\widetilde{M}_{n,q}(f,x)-\widetilde{f}_\varepsilon\|_{p,\rho}\le 2\omega_{p,\rho}(f,\delta)$$

Theorem 3.4:

For all $f\in C_\rho[0,1]$ and $\widetilde{f}_\varepsilon(1)=0$,we have:

$$|A_{n,k,q}(\widetilde{f}_\varepsilon)|\le A_{n,k,q}(|\widetilde{f}_\varepsilon|)\le\omega_{p,\rho}(f,q^n)(1+q^{-n})\qquad 0\le k\le n$$

proof:

$$|\widetilde{f}_\varepsilon(qt)|=|\widetilde{f}_\varepsilon(qt)-\widetilde{f}_\varepsilon(1)|\ \le\omega_{p,\rho}(f,q^n(1-qt))\ \le\omega_{p,\rho}(f,q^n)(1+\frac{(1-qt)}{q^n})$$

Thus $|A_{n,k,q}(f)|\le A_{n,k,q}(|f|)=\int_0^1 b_{n,k,q}(t)|\widetilde{f}_\varepsilon(qt)|\,d_qt$

$$\le\omega_{p,\rho}(f,q^n)\int_0^1 b_{n,k,q}(t)(1+\frac{1-qt}{q^n})d_qt$$

Since $1+\frac{1-qt}{q^n}=1+\frac{1}{q^n}-\frac{1}{q^n}qt$, then:

$$|A_{n,k,q}(f)|\le\omega_{p,\rho}(f,q^n)((1+\frac{1}{q^n})\int_0^1 b_{n,k,q}(t)d_qt-\frac{1}{q^n}\int_0^1 b_{n,k,q}(t)\,qt\,d_qt$$

By using Lemma 2.1:

$$|A_{n,k,q}(f)|\le\omega_{p,\rho}(f,q^n)((1+\frac{1}{q^n})-\frac{1}{q^n}\frac{q[k+1]}{[k+n+1]})=\omega_{p,\rho}(f,q^n)(1+\frac{1}{q^n}-\frac{1}{q^{n-1}}\frac{[k+1]}{[k+n+1]})$$

$$\le\omega_{p,\rho}(f,q^n)(1+q^{-n})$$

4-Conclusions

From the results we conclude that, we can convert a positive linear operators which satisfying Korovkin Theorem into convex operators by using the convex function $\widetilde{f}_\varepsilon$.

In addition, this new operators $M_{n,q_n}(f)$ satisfying Korovkin Theorem therefore converges to f on $C_\rho[0,1]$ for each $f \in C_\rho[0,1]$ iff $q_n \to 1$ as $n \to \infty$ and $|\widetilde{M}_{n,q}(f,x) - \widetilde{f}_\varepsilon| \le 2w_{p,\rho}(f, \sqrt{\delta_n})$.

REFERENCES

1. Abel U., Ivan M. and Gupta V., "On the rate of convergence of a Durrmeyer variant of Meyer Konig and Zeller operators", *Archives Inequal. Appl.*,(2003),1–9.
2. AlSaaedy S.K. and Ibrahem N.M.J, "Approximation by Convex Linear Positive Operator", *Qadisiyah Journal for Computer Science and Mathematics*,(to appear) ,(2012).
3. AlSaaedy S.K. and Ibrahem N.M.J, " Approximation by Convex Polynomials in Weighted Spaces", *Int. J. Contemp. Math. Sciences*, Vol. 7, no. 40, (2012), 1963 - 1972.
4. Altin A., Dogru O. and M.A. Ozarslan, " Rate of convergence of Meyer-Konig and Zeller operators based on q-integer", *WSEAS Transactions on Mathematics*, 4(4) (2005), 313–318.
5. Andrews GE, Askey R and Roy R, "*Special functions*", Cambridge: Cambridge University Press, 1999.
6. Dogru O. and Duman O., "Statistical approximation of Meyer-König and Zeller operators based on q-integers", *Publ Math Debrecen* (2006);68:199–214.
7. Dogru O. and Gupta V., " Korovkin-type approximation properties of bivariate q–Meyer-Konig and Zeller operators", *Calcolo*, 43(1) (2006), 51–63.
8. Ernst, T , " *The history of q-calculus and a new method* ", U.U.D.M Report 2000, 16, ISSN 1101-3591, Department of Mathematics, Upsala University (2000)
9. Gupta V. and Sharma H., "Statistical approximation by q-integrated Meyer-Konig-Zeller and Kantrovich operators", *Creative Mathematics and Informatics*, in press.
10. Kac V. and Cheung P., *Quantum Calculus*, Universitext, Springer-Verlag, NewYork, (2002).
11. Kundu A., " Origin of quantum group and its application in integrable systems", *Chaos, Solitons & Fractals* (1995);12:2329–44.
12. Lu X.G., " Convex approximation by multivariate polynomial", *Math. Numer. Sinica* 12, no. 2, (1990), 186-193.
13. Majid S., " *Foundations of quantum group theory*", Cambridge: Cambridge University Press; (2000).
14. Özarslan , M.A. and , Duman ,O., "Approximation theorems by Meyer-König and Zeller type operators", Chaos, *Solitons and Fractals* 41 (2009) 451-456.

15. Phillips GM., "On generalized Bernstein polynomials" , *Numerical analysis. River Edge, NJ: World Sci. Publ.*; (1996).
16. Sharma H., "Properties of q–Meyer-König-Zeller Durrmeyer Operators", *J. Inequal. Pure and Appl. Math.*, 10(4) (2009), Art. 105, 10 pp.
17. Trif T., "Meyer-Konig and Zeller operators based on q-integers", *Revue d'Analysis Numerique et de Theorie de l' Approximation*, 29(2) (2000), 221–229.
18. Wang H., "Properties of convergence for q–Meyer Konig and Zeller operators", *J. Math. Anal. Appl.* 335 (2007) 1360–1373 .

Equivalent between Weighted Earliness and Weighted Tardiness Problems On A single Machine

Tariq S. Abdul-Razaq, Manal G. Ahmed Al-Ayoubi and Manal H. Ibrahim
Mathematic Dept College of science Al- Mustansiriyah University
Received 2/4/2013 – Accepted 15/9/2013

الخلاصة

في هذا البحث تناولنا مسألة جدولة n من الاعمال على ماكنة واحده لمناقشة العلاقة بين مسألة التبكير والتأخير الموزونين .وبما ان هاتان المسألتان من النوع Np الصعب ، برهنا نتيجه جيده ان قاعدة EDD والتي فيها $E_i \le P_i$ تعطي حل امثل للمسألة $1/C_i \le d_i / \Sigma W_i E_i$.وكذلك برهنا ان E^W_{max} و T^W_{max} متكافئتان لمسألتي $1/C_i \le d_i / E^W_{max}$ و $1/C_j \ge d_j / T^W_{max}$.الخواص بين مسألتي التبكير الموزون والتأخير الموزون اعطي مع بعض الامثلة .

ABSTRACT

In this paper we consider the problem of scheduling n jobs on a single machine to discuss the relationship between weighted earliness and weighted tardiness problems (i.e., the problems $1/c_i \le d_i / \sum W_i E_i$ and $1/C_j \ge d_j / \sum W_j T_j$). These two problems are NP-hard ,for special case we proved a good result that EDD rule with $E_i \le P_i$ is optimal for $1/c_i \le d_i / \sum W_i E_i$ problem .

Also we proved that E^W_{max} and T^W_{max} are equivalent for $1/C_i \le d_i / E^W_{max}$ problem and $1/C_j \ge d_j / T^W_{max}$ problem. The properties between weighted earliness and weighted tardiness problems are given with some examples.

INTRODUCTION

Scheduling problems are one of the most studied problems in combinatorial optimization. It can be defined as a decision making process that is used on a regular basis in many manufacturing and services industries. It deals with the allocation of resources to task over given time periods and its goal is to minimize one or more objectives [1]. In the scheduling literature, the objective is generally to minimize functions such as makespan, tardiness, flow time, etc.

The two objectives $\sum E_i$ and $\sum T_i$ that are important in practice as well . The $1//\sum T_i$ problem has received an enormous amount of attention in the literature [1] ,[2],[3] . It is well know that the problems $1//\sum W_i E_i$ and $1//\sum W_i T_i$ and their generalizations $1//\sum W_i E_i$ and $1//\sum W_i T_i$ are NP-hard problems. Since the earliness objectives are non regular functions, hence there are a few studies to earliness problems.

The scheduling problem under consideration can be described as follows: there are n jobs to be scheduled on a single machine, which can handle one job at a time , each job i has positive integer processing time P_i and positive integer due date d_i .Job i (i=1,2,..,n) becomes available for processing at time zero . The main object of this paper to prove the equivalence of the following problems :

$1/C_i \le d_i / \sum W_i E_i$ and $1/C_i \ge d_i / \sum W_i T_i$, $1/C_i \le d_i / E^W_{max}$ and $1/C_i \ge d_i / T^W_{max}$ where

E^W_{max} = W_i Max{E_i} = W_i Max{d_i-c_i ,0 } and T^W_{max} = W_i Max {T_i} = W_i Max {C_i-d_i ,0 }.

In this paper in section one, we proved that $1/c_i \leq d_i/E^W_{max}$ is equivalent to $1/c_j \geq d_j/T^W_{max}$ and we proved that EDD schedule with $E_i \leq P_i$ is optimal for $1/c_i \leq d_i/\sum W_i E_i$ .In section two we show some properties of weighted earliness and weighted tardiness problems with some examples for each case is given. In section three we show the conclusion and future work.

The following lemma shows that the total weighted earliness problem is equivalent to the total weighted tardiness problem.

Lemma (1)

The following measures are equivalent:

$$1\text{-} \sum_{i=1}^{n} W_i E_i ,\quad 2\text{-} \sum_{j=1}^{n} W_j T_j .$$

Proof

Let $C = \sum_{j=1}^{n} p_j$, consider an instance of the total weighted tardiness ($\sum_{j=1}^{n} W_j T_j$) problem where $p'_i = p_i$ and $d'_j = C - d_i + p_i$ for j = 1, 2,...,n. Suppose S is an optimal schedule for this instance. Define a new schedule S' as follows:

If a job j is the k-th job scheduled in S, then j' is the (n-k+1)th job scheduled in S'. Clearly, we have $C'_j = C - C_j + p_j$ and hence

$W_jT_j = W_j \max \{ C'_j - d'_j, 0 \} = W_j \max \{(C - C_j + P_j) - (C - d_j + P_j), 0 \}$
$= W_j \max \{ d_j - C_j, 0 \} = W_j E_j$.

Therefore, the minimum total weighted earliness is the same as the minimum total weighted tardiness. Hence, as we know that the total weighted tardiness problem on one machine is NP-hard [5], then the total weighted earliness must also NP-hard.

It should be noted that in our problem $1/c_i \leq d_i/\sum_{i=1}^{n} W_i E_i$ every job i is either early or on time, but in the total weighted tardiness problem $1/c_j \geq d_j/\sum_{j=1}^{n} W_j T_j$, every job j is either tardy or on time.

Lemma (2)

E^W_{max} is equivalent to T^W_{max} in case of complexity

Proof:

Let $\sum_{j=1}^{n} p_j$,consider an instance of the maximum weighted tardiness Max{W_iT_i }problem where $p'_j = p_j$ and $d'_j = C - d_j + p_j$ for j = 1, 2,…,n. Suppose S is an optimal schedule for this instance. Define a new schedule S' as follows:
If a job j is the k-th job scheduled in S, then j' is the (n-k+1)th job scheduled in S'. Clearly, we have $C'_j = C - C_j + p_j$ and hence

$T^W_{\max}$ = W_j max{T_j} = W_j max{max{ $c'_j - d'_j$, 0 } } = W_j max {max(C–C_j+P_j) –(C – d_j + P_j), 0 } = W_j max { max{d_j – C_j , 0 }} = $E^W_{\max}$.

Hence, as we know that the $1//T^W_{\max}$ problem is solved by Lawler algorithm , then the $1//E^W_{\max}$ problem is also solved by sequencing the jobs in non –decreasing order of
$w_is_i = w_i(d_i-p_i)$.

The following result shows the equivalent of $1/c_i \le d_i/\sum_{i=1}^{n} W_iE_i$ problem and $1/c_i \ge d_i/\sum_{j=1}^{n} W_iT_i$ problem.

Theorem (1)

If the EDD schedule with $T_j \le P_j$ for each job j is optimal for $1/c_j \ge d_j/\sum_{j=1}^{n} W_jT_j$, then the EDD schedule with $d_i = C - d_j + P_j$ and with $E_i \le P_i$ is optimal for $1/c_i \le d_i/\sum_{i=1}^{n} W_iE_i$ problem.

Proof

Let S be the optimal schedule for $1/c_j \ge d_j/\sum_{j=1}^{n} W_jT_j$ problem obtained by EDD rule for the due date d_j and with $T_j \le P_j$ for each j.
Now construct a schedule S' by EDD rule for $d_i = C - d_j + P_j$, where $C = \sum_{j=1}^{n} P_j$ and the completion time for each job i is given by $C_i = C - C_j + P_j$. From lemma (1) the measures $\sum_{i=1}^{n} W_iE_i$ and $\sum_{j=1}^{n} W_jT_j$ are equivalent.

For the optimal schedule S, we have $T_j \le P_j$. Hence $C_j - d_j \le P_j$, using the definition of d_i and C_i in the schedule S' we have for each job i
$T_j = C_j - d_j = (C + P_j - C_i) - (C + P_j - d_i) = d_i - C_i = E_i \le P_j$ and $P_i = P_j$
Then $E_i \le P_i$.

Hence the EDD schedule with $E_i \le P_i$ for each job i is optimal for 1 $/c_i \le d_i/ \sum_{i=1}^{n} W_i E_i$.

Now we will give some examples to show some of the important properties for the weighted earliness and tardiness problem which is given in the above results.

Example (1) Consider the weighted earliness problem with four job. We now show that the weighted earliness and weighted tardiness equivalence with the following four -job, for which the processing times and due dates are shown in the following table (1). The jobs are already numbered in EDD order.

Table-1:data for 1 $/c_i \le d_i/ \sum W_i E_i$ problem is arbitrary.

EDD	1	2	3	4
P_i	6	5	3	4
d_i	10	14	15	18
W_i	3	4	5	1
C_i	6	11	14	18
E_i	4	3	1	0
W_i Ei	12	12	5	0

is clear from table(1) that C =18 and the minimum $\sum_{i=1}^{4} W_i E_i$ = 29 and $E_i \le P_i$ for each i , $E^W_{max} = 12$.

Table-2: data for $1/c_j \ge d_j/ \sum W_j T_j$ problem.

EDD	4	3	2	1
P_j	4	3	5	6
D_j	4	6	9	14
W_j	1	5	4	3
C_j	4	7	12	18
T_j	0	1	3	4
W_j	1	5	4	3
$W_j T_j$	0	5	12	12

It is clear from table(2) that minimum $\sum_{j=1}^{6} W_j T_j = 29$ and $T_j \le P_j$ for each j , T^W_{max} = 12 .

Example (2) shows that, if the EDD rule is optimal for 1 $/c_i \le d_i/ \sum W_i E_i$ problem, but there exists a job i with $E_i > P_i$, then there exists an optimal schedule for $1 / c_j \geq d_j / \sum W_j T_j$ problem with $\sum W_i E_i = \sum W_j T_j$ and with same job j with $T_j > P_j$.

Table-3: data for $1 / c_i \leq d_i / \sum W_i E_i$ problem

EDD	1	2	3	4
P_i	4	3	6	2
d_i	8	12	13	16
W_i	2	3	1	4
C_i	4	7	13	15
E_i	4	5	0	1
W_i Ei	8	15	0	4

It is clear from table (3) that EDD rule is optimal with $E_2 = 5 > P_2 = 3$,

C= 15, $\sum_{i=1}^{4} W_i E_i = 27$.

Table -4:data for $1 / c_j \geq d_j / \Sigma W_j T_j$ problem.

J	4	3	2	1
P_j	2	6	3	4
d_j	1	8	6	11
W_j	4	1	3	2
C_j	2	8	11	15
T_j	1	0	5	4
$W_j T_j$	4	0	15	8

It is clear from table(4) that the schedule(4,3,2,1) is optimal, but it is not EDD schedule, and $\Sigma W_j T_j = \Sigma W_i E_i = 27$ and $T_2 = 5 > P_2 = 3$.

Properties

(1) If SWPT rule gives maximum value for $1 / c_i \leq d_i / \Sigma W_i E_i$ problem, then LWPT rule gives maximum value for $1 / c_j \geq d_j / \Sigma W_j T_j$ problem.

Example (3) Shows that SWPT rule is maximum for $1 / c_i \leq d_i / \Sigma w_i E_i$ problem and LWPT rule is maximum for $1 / c_j \geq d_j / \Sigma W_j T_j$ problem.

Table-5:data for the example (3) for $1 / c_i \leq d_i / \Sigma W_i E_i$ problem

SWPT	1	2	3	4	5
P_i	2	3	4	5	6
d_i	6	5	12	20	22
W_i	4	6	2	2	2
C_i	2	5	9	14	20
E_i	4	0	3	6	2
$W_i E_i$	16	0	6	12	4

It is clear from table (5) that C = 20, and $\sum_{i=1}^{5} W_i E_i$ = 38 (maximum)

Table-6:data for $1 / c_j \geq d_j / \Sigma W_j T_j$ problem

LWPT	5	4	3	2	1
P_j	6	5	4	3	2
d_j	4	5	12	18	16
W_j	2	2	2	6	4
C_j	6	11	15	18	20
T_j	2	6	3	0	4
$W_j T_j$	4	12	6	0	16

It is clear from table (6) that $\sum_{j=1}^{5} W_j T_j = 38$ (maximum).

The other feasible schedules for $1 / c_j \geq d_j / \Sigma W_j T_j$ are: (5,4,3,1,2) with $\Sigma W_j T_j = 38$, (4,5,3,2,1) with $\Sigma W_j T_j = 36$,(4,5,3,1,2) with $\Sigma W_j T_j = 36$.

It is clear from theorem(1) and property(1) above, if LWPT rule gives minimum value for $1 / c_i \leq d_i / \Sigma W_i E_i$ problem, then SWPT rule gives minimum value for $1 / c_j \geq d_j / \Sigma W_j T_j$ problem, see property (2).

(2) If for each job i $\mathbf{d_i = d} = \sum_{j=1}^{n} P_j$, then LWPT rule is optimal for $1 / c_i \leq d_i / \Sigma W_i E_i$ problem, and the optimal schedule for $1 / c_j \geq d_j / \Sigma W_j T_j$ problem is obtained directly by setting $d_j = P_j$ for each job j.

Example(4) Shows that if $\mathbf{d_i = d} = \sum_{j=1}^{n} P_j$ for each job i for the $1 / c_i \leq d_i = d / \Sigma Wi\, E_i$ problem and LWPT schedule is optimal and if $\mathbf{d_j = P_j}$ for each job j, then SWPT schedule is optimal for the $1 / c_j \geq d_j / \Sigma W_j T_j$ problem.

Table-7: data for $1 / c_i \leq d_i / \Sigma W_i E_i$ problem

i	1	2	3	4	5
P_i	5	4	3	2	1
d_i	15	15	15	15	15
W_i	2	2	2	6	4
C_i	5	9	12	14	15
E_i	10	6	3	1	0
$W_i E_i$	20	12	6	6	0

It is clear that C = 15, and $\sum_{i=1}^{5} W_i E_i$ =44.

Table-8:data for $1 / c_j \geq d_j / \Sigma W_j T_j$ problem

j	5	4	3	2	1
P_j	1	2	3	4	5
d_j	1	2	3	4	5
W_j	4	6	2	2	2
C_j	1	3	6	10	15
T_j	0	1	3	6	10
$W_j T_j$	0	6	6	12	20

It is clear from table (8) that $d_j = P_j$, and $\sum_{j=1}^{5} W_j T_j = 44$.

(3) If for each job i $\mathbf{P_i = P}$, then LWPT is optimal for $1 / c_i \leq d_i / \Sigma W_i E_i$ problem and SWPT is optimal for $1 / c_j \geq d_j / \Sigma W_j T_j$ problem .

Example (5) Shows that if $\mathbf{P_i = P}$ for each job i for $1 / c_i \leq d_i / \Sigma W_i E_i$ problem and $\mathbf{P_j = P}$ for $1 / c_j \geq d_j / \Sigma W_j T_j$ problem .

Table-9:data for $1 / c_i \leq d_i / \Sigma W_i E_i$ problem

I	1	2	3	5	4
P_i	2	2	2	2	2
d_i	5	8	7	12	10
W_i	1	2	3	4	5
C_i	2	4	6	8	10
E_i	3	4	1	2	2
$W_i E_i$	3	8	3	16	0

It is clear that C= 10, and $\sum_{i=1}^{5} W_i E_i = 30$.

Table (10) data for $1 / c_j \geq d_j / \Sigma W_j T_j$ problem

j	4	5	3	2	1
P_j	2	2	2	2	2
d_j	2	0	5	4	7
W_j	5	4	3	2	1
C_j	2	4	6	8	10
T_j	0	4	1	4	3
$W_j T_j$	0	16	3	8	3

It is clear from table (10) that $\sum_{j=1}^{5} W_j T_j = 30$.

(4) If in the optimal solution for $1 / c_i \leq d_i / \Sigma W_i E_i$ problem, all the jobs completed on times (i.e., $C_i = d_i$ the ideal solution) then the optimal solution for $1 / c_j \geq d_j / \Sigma W_j T_j$ problem all the jobs completed on times.

Example (6) Shows that all jobs completed on their due dates(ideally solution) for $1 / c_i \leq d_i / \Sigma W_i E_i$ and $1 / c_j \geq d_j / \Sigma W_j T_j$ problems.

Table-11:data for $1 / c_i \le d_i / \Sigma W_i E_i$ problem

i	1	2	3	4	5
P_i	4	3	1	2	5
d_i	4	7	8	10	15
W_i	1	6	2	8	7
C_i	4	7	8	10	15
E_i	0	0	0	0	0
$W_i E_i$	0	0	0	0	0

Hence it is clear that C =15, and $\sum_{i=1}^{5} W_i E_i = 0$.

Table-12: data for $1 / c_j \ge d_j / \Sigma W_j T_j$ problem

j	5	4	3	2	1
P_j	5	2	1	3	4
d_j	5	7	8	11	15
W_j	7	8	2	6	1
C_j	5	7	8	11	15
T_j	0	0	0	0	0
$W_j T_j$	0	0	0	0	0

Hence it is clear that $\sum_{j=1}^{5} W_j T_j = 0$.

Conclusions and Future Work

The study shows the relationship between earliness and tardiness problems. These two problems are NP-hard , then we proved a very good result that the EDD rule with $E_i \le P_i$ is optimal for $1 / c_i \le d_i / \Sigma W_i E_i$ problem.

An interesting future research topic would involve experimentation discuss the relationship between

$F2/C_i \le d_i/\sum W_i E_i$ and $F2/C_i \ge d_i/\sum W_i T_i$

REFERENCES

1. Pinedo M. L Scheduling , Theory , algorithms and systems . Spring 2008
2. Abdul - Razaq T. S., Potts C. N. and Van wassenhove L.N A survey of algorithms for single machine total weighted tardiness scheduling problem ,Discrete Applied mathematics 26 (1990), 235-253.
3. Su ,L. H and Chen, C.J., Minimizing total tardiness on a single machine with un equal release date .European Journal of operation Research 186 (2008),no. 2, 496-503 .
4. Batzewicz J., Ecker K.H., Pesch E., Schmidt G. and Weglarz J. "Scheduling Computer and Manufacturing Process" Springer - verlay Berlin. Heidelberg 1996.
5. Du J. and Leung, Minimizing total tardiness on one processor is NP-hard, Mathematics of Operations Research 15 (1990), 483-495.

Discrete Point Symmetry for the BBM Equation

Mallaki I.A .[1] and Aldhlki T. $Jassim$[2]
Department of Mathematics, College of Science, AL-Mustansiriyah University
Department of Mathematics, College of Basic Education, AL-Mustansiriyah University
Received 31/3/2013 – Accepted 15/9/2013

الخلاصة

يقدم هذا البحث خوارزمية لحساب كل التماثلات المتقطعة النقطية لمعادلة تفاضلية تمتلك تماثلات مستمرة (تماثلات لي النقطية) من خلال تطبيق طريقة هايدن. لقد حصلنا على كل التماثلات متشاكلة لمعادلة بي بي ام الى Z_2

ABSTRACT

This paper introduces an algorithm for calculating all discrete point symmetries for a given differential equation with a known nontrivial group of Lie point symmetries by applying Hyden's method. We have obtained discrete symmetry isomorphic to Z_2, of BBM equation.

1- INTRODUCTION

Symmetries of all kinds (point, contact, generalized, nonlocal) are valuable in the study of differential equations. Many DE's of physical importance have (Local) Lie groups of point symmetries (continuous symmetries) that can be obtained fairly easily by linearizing the symmetry condition about the identity transformation to derive the Lie algebra of point symmetry generators. Each generator can be exponentied to yield a one-parameter (Local) Lie group of symmetries [1, 5, 9, 12, 13, 14, 18].

The set of all such "continuous" symmetries is a normal (invariant), N, subgroup of the group, G, of all point symmetries, when the continuous symmetries are factored out, the remaining point symmetries form a discrete group,G/N.

Many differential equations have discrete symmetries which can not be founded by Lie's method, such symmetries are important in many applications, for example they are used to reduce the domain on which an ODE is solved numerically, thereby computational efficiency. This is possible if the ODE, the computational domain and the boundary conditions are invariant [8].

Sometimes it is possible to obtain exact solutions that are invariant under a discrete symmetries [10]. Discrete symmetries involving charge conjugation, parity change and time – reversal symmetries play a key role in quantum field theories. Also they are used in the bifurcation analysis of nonlinear systems [16].

The main difficulty to find discrete symmetry is that it cannot reduce to study the infinitesimal action of vector field (as continuous symmetry). Therefore; when applying symmetry condition we get determining equations for discrete symmetries typically form a highly – coupled nonlinear system. Some discrete symmetries (such as reflections) may be founded by inspection or by using an ansatz [3]. Hydon[6, 7, 8, 9,10] gave a new approach (indirect method) to the problem of finding all discrete point symmetries of differential equation which has Lie continuous symmetries. The technique is based on the observation that every point symmetry yields an automorphism of the Lie algebra of Lie point symmetry generators. This results in a set of auxiliary equations that are satisfied by all point symmetries. These equations can be considerably simplified to give the DE's discrete symmetries.

The aim of the present work is to present Hydon's method by an algorithm to obtain discrete symmetries of the Benjamin-Bona- Mahony (BBM) equation (which is sometime called the regularized long wave (RLW) equation). It was proposed by Benjamin et.al in 1972, it boasts a wide range of applications in the unidirectional propagation of weakly long dispersive waves in inviscid fluids

$$u_t = uu_x + u_{txx} \qquad t,x \in \square \qquad (1)$$

2- Methodology (Indirect method) [2,9]

A point symmetry of a given system of DE

$$\Delta(x,u) = 0 \qquad (2)$$

where $x \in R^n,\ u \in R^m$ is a diffeomorphism

$$\Gamma: (x,u) \longmapsto \big(\hat{x}(x,u), \hat{u}(x,u)\big)$$

maps the set of solutions of the equation to itself. This happens if

$$\Delta(\hat{x},\hat{u}) = 0 \ when \ \Delta(x,u) = 0 \qquad (3)$$

the symmetry condition (3) can be split into a system of determining equations for $(\hat{x},\hat{u})$ (cannot be solved by a direct approach)

In [9], Hydon state that,

Every arbitrary point symmetry Γ of the given differential equation (2) induces an automorphism of the Lie algebra $\mathcal{L}$ of all generators of one parameter Lie point symmetries of (2). For each Γ there exists a constant non-singular $r \times r$ matrix $B = \left(b_i^\ell\right)$ such that

$$X_i = \textstyle\sum_{\ell=1}^{r} b_i^\ell \hat{X}_\ell \qquad (4)$$

All structure constants are preserved by the automorphsim.

The basic method to find the discrete symmetries can be described by the following steps:-

1- Create a system of determining equations by using lemma (2.1) to obtain the following system of first order quasilinear PDES

$$X_i\hat{z} = \textstyle\sum b_i^\ell \hat{X}_\ell \hat{z} \ , \ i = 1,\dots,r \qquad (5)$$

may be solves by the method of characteristic or (if $r \geq 3$) by algebra means.

The solutions of $\hat{z}$ are obtained in terms of z, b_i^ℓ and constants of integration, Note that not every solution of (5) need be a symmetry.

2- Find discrete point symmetries, the symmetry condition is used to factor out the unwanted solutions that may exists from the previous step that do not correspond to a symmetry transformation or if the given differential equation (2) holds so must $\Delta(\hat{x}, \hat{u}) = 0$

The above two-steps basic method works in principle but it has serveral disadvantages:-

1- Differential equations without a Lie symmetry algebra can not be considered since the method require such an algebra.

2- The calculations are fairly simple for lower dimensional $\mathcal{L}$ but not for higher dimensional $\mathcal{L}$, since more coefficients b_i^ℓ of $r \times r$ matrix B must be considered and we get a larger system of determining equations.

when the Lie algebra $\mathcal{L}$ is non-abelian the elements of B satisfy the nonlinear constrains

$$\sum_{\ell=1}^{r}\sum_{m=1}^{r} C_{\ell m}^{n}\, b_i^\ell b_j^m = \sum_{k=1}^{r} C_{ij}^{k} b_k^n \,, 1 \le i < j \le r, 1 \le n \le r \quad (6)$$

The nonlinear constrains (6) by themselves provide some simplification of the matrix elements b_i^ℓ. But a combination of the nonlinear constrains together with equivalence transformation is even more powerful as we shall see. The equivalence transformations enable us to factor out the Lie symmetries of the non-abelian Lie algebra $\mathcal{L}$, before trying to solve the system of (5). The adjoint action was defined as,

If $X_i \in \mathcal{L}$, the adjoint action (adjoint representation) is an operator that maps Y_j to $[X_i, Y_i]$

$$Ad(X_i)_{Y_i} \mapsto [X_i, Y_i]$$

or a linear transformation of $\mathcal{L}$ onto itself.

The adjoint action of the one-parameter Lie group of point transformations generated by X_j on the set $X_1, \dots, X_r$ of basis generators, can be described by matrix

$$A(\varepsilon, j) = e^{\varepsilon C(i)} \quad where \quad (C(i))_i^k = C_{ij}^k \quad (7)$$

therefore, we have an equivalent transformation, generated by X_j, to group generated by

$$\tilde{X}_i = Ad(e^{\varepsilon X_j})X_i = X_i - \varepsilon[X_j, X_i] + \frac{\varepsilon^2}{2!}[X_j, [X_j, X_i] \dots \equiv \sum_{p=0}^{\infty} A(\varepsilon, j)_i^p X_p$$

and the relation (4) can be written as

$$\tilde{X}_i = \sum_{\ell=1}^{r} \tilde{b}_i^\ell \hat{X}_\ell \quad with\, \tilde{b}_i^\ell = (A(\varepsilon, j))_i^p b_p^\ell$$

in other words the previous equation is equivalent to

$$X_i = \sum_{\ell=1}^{r} \tilde{b}_i^\ell \hat{X}_\ell$$

under the group generated by X_j. The matrix B can now be replaced by $A(\varepsilon, j)B, or\ BA(\varepsilon, j)$, and we have the freedom to choose ε to be a value which simplifies the replaced matrix.

3- Algorithm

In this section, Hydon's method including its improvements is explained by the following steps, assuming that the given DE has a nontrivial continuous symmetries $X_1, X_2, \dots, X_r$.

Step I: Check if $\mathcal{L}$ is abelian or not, if $\mathcal{L}$ is abelian go to step IV

Step II: Calculate each (ε, i) , given by $A(\varepsilon, j) = e^{\varepsilon C(j)}$ corresponding to each basis of the Lie algebra $\mathcal{L}$.

Step III: Construct the matrix B from (5), then simplify the matrix B by using (6).

Step IV: Create the determining equations of $\hat{z}$ by (5).

Step V: Determine the discrete point symmetries by using symmetry condition (3).

Step VI: Factor out the remaining central Lie symmetries.

4- Calculating discrete symmetries of BBM equation

In this section we will derive the discrete symmetries of equation (1) which has a 3-dimensional Lie algebra $\mathcal{L}^3$: $\{X_1, X_2, X_3\}$ [5] where

$$X_1 = \frac{\partial}{\partial t}, X_2 = \frac{\partial}{\partial x}, X_3 = t\frac{\partial}{\partial t} - u\frac{\partial}{\partial u}$$

Note that the model considered here is (time-space) reversible, i.e if u(t,x) is a solution of (1) then so is u(-t,-x) [11]

By the commutator relation

$$[X_i, X_j] = \sum_{k=1}^{3} C_{ij}^k X_k \qquad i, j = 1, 2, 3$$

we get the commutator table

$[X_i, X_j]$	X_1	X_2	X_3
X_1	0	0	X_1
X_2	0	0	0
X_3	$-X_1$	0	0

then the structure constants C_{ij}^k are

$[X_1, X_2] = 0 \Rightarrow C_{11}^1 = 0, C_{11}^2 = 0, C_{11}^3 = 0$

$[X_2, X_1] = 0 \Rightarrow C_{21}^1 = 0, C_{21}^2 = 0, C_{21}^3 = 0$

$[X_3, X_1] = -X_1 \Rightarrow C_{31}^1 = -1, C_{31}^2 = 0, C_{31}^3 = 0$

$[X_1, X_2] = 0 \Rightarrow C_{12}^1 = 0, C_{12}^2 = 0, C_{12}^3 = 0$

$[X_2, X_2] = 0 \Rightarrow C_{22}^1 = 0, C_{22}^2 = 0, C_{22}^3 = 0$

$[X_3, X_2] = 0 \Rightarrow C_{32}^1 = 0, C_{32}^2 = 0, C_{32}^3 = 0$

$[X_1, X_3] = X_1 \Longrightarrow C_{13}^1 = 1, C_{13}^2 = 0, C_{13}^3 = 0$
$[X_2, X_3] = 0 \Longrightarrow C_{23}^1 = 0, C_{23}^2 = 0, C_{23}^3 = 0$
$[X_3, X_3] = 0 \Longrightarrow C_{33}^1 = 0, C_{33}^2 = 0, C_{33}^3 = 0$
The matrices $C\,(j)$ are

$$C\,(1) = \begin{bmatrix} 0 & 0 & 0 \\ 0 & 0 & 0 \\ -1 & 0 & 0 \end{bmatrix}, C\,(2) = \begin{bmatrix} 0 & 0 & 0 \\ 0 & 0 & 0 \\ 0 & 0 & 0 \end{bmatrix}, C\,(3) = \begin{bmatrix} 1 & 0 & 0 \\ 0 & 0 & 0 \\ 0 & 0 & 0 \end{bmatrix}$$

Note that X_2 belong to centre of Lie algebra.
The next step is to calculate the matrices $A\,(\varepsilon, j)$ by using Exponentiation of the matrices C (j) , by adjoin representation or by solving I.V.P.

$$\frac{d\,v(\varepsilon)}{d\varepsilon} = [v(\varepsilon), X]\,, v(0) = v_{\,0}$$

$Ad(e^{\varepsilon xj})Xi$	X_1	X_2	X_3
X_1	X_1	X_1	$e^{\varepsilon}X_1$
X_2	X_2	X_2	X_2
X_3	$X_3{}^{-\varepsilon x_1}$	X_3	X_3

Adjoint representations table

$[X_1, X_1] = X_1 \Longrightarrow a_{11}^1 = 1, a_{11}^2 = 0, a_{11}^3 = 0$
$[X_2, X_1] = X_2 \Longrightarrow a_{21}^1 = 0, a_{21}^2 = 1, a_{21}^3 = 0$
$[X_3, X_1] = X_3{}^{-\varepsilon x_1} \Longrightarrow a_{31}^1 = -\varepsilon, a_{31}^2 = 0, a_{31}^3 = 1$
$[X_1, X_2] = X_1 \Longrightarrow a_{12}^1 = 1, a_{12}^2 = 0, a_{12}^3 = 0$
$[X_2, X_2] = X_2 \Longrightarrow a_{22}^1 = 0, a_{22}^2 = 1, a_{22}^3 = 0$
$[X_3, X_2] = X_3 \Longrightarrow a_{32}^1 = 0, a_{32}^2 = 0, a_{32}^3 = 1$

$[X_1, X_3] = e^{\varepsilon}X_1 \Longrightarrow a_{13}^1 = e^{\varepsilon}, a_{13}^2 = 0, a_{13}^3 = 0$
$[X_2, X_3] = X_2 \Longrightarrow a_{23}^1 = 0, a_{23}^2 = 1, a_{23}^3 = 0$
$[X_3, X_3] = X_3 \Longrightarrow a_{33}^1 = 0, a_{33}^2 = 0, a_{33}^3 = 1$

$$A\,(1,\varepsilon) = \begin{bmatrix} 1 & 0 & 0 \\ 0 & 1 & 0 \\ -\varepsilon & 0 & 0 \end{bmatrix}, A\,(2,\varepsilon) = \begin{bmatrix} 1 & 0 & 0 \\ 0 & 1 & 0 \\ 0 & 0 & 1 \end{bmatrix}, A\,(3,\varepsilon) = \begin{bmatrix} e^{\varepsilon} & 0 & 0 \\ 0 & 1 & 0 \\ 0 & 0 & 1 \end{bmatrix}$$

from the non-linear constraints

$$\sum_{l=1}^{3}\sum_{m=1}^{3} C_{lm}^{n}\, b_i^l b_j^m = \sum_{k=1}^{3} C_{ij}^{k}\, b_k^n \quad 1 \le i < j \le 3\,, 1 \le n \le 3$$

for = 2 , we obtain

$$\sum C_{ij}^k b_k^2 = 0$$

for $(i,j) = (1,3)$ *we get* $b_1^2 = 0$ (8)
for = 3 , we obtain

$$\sum C_{ij}^k b_k^3 = 0$$

for $(i,j) = (1,3)$ *we get* $b_1^3 = 0$ (9)

Therefore $= \begin{pmatrix} b_1^1 & 0 & 0 \\ b_2^1 & b_2^2 & b_2^3 \\ b_3^1 & b_3^2 & b_3^3 \end{pmatrix}$, where $b_1^1 \neq 0$ (since $|B| \neq 0$)

For = 1 , we obtain

$$C^1_{lm} b^l_i b^m_j = C^k_{ij} b^1_k$$

for $(i\,,j) = (1\,,2) we\ get\ b^1_1 b^3_2 - b^3_1 b^1_2 = 0$ (10)

for $(i\,,j) = (2\,,3) we\ get\ b^1_2 b^3_3 - b^3_2 b^1_3 = 0$ (11)

for $(i\,,j) = (1\,,3) we\ get\ b^1_1 b^3_3 - b^3_1 b^1_3 = b^1_1$ (12)

solve (8), (9),(10), (11) and (12) we get

$b^3_2 = 0\ and\ b^1_2 = 0\ \ b^2_2 \neq 0$ (since $|B| \neq 0$)

$and\ b^3_3 = 1$

We simplify B to the following:-

$$B = \begin{pmatrix} b^1_1 & 0 & 0 \\ 0 & b^2_2 & 0 \\ b^1_3 & b^2_3 & 1 \end{pmatrix}$$

Now using the adjoint matrices $A(i, \varepsilon), i = 1\,,3$

$$A(1,\varepsilon)B = \begin{bmatrix} 1 & 0 & 0 \\ 0 & 1 & 0 \\ -\varepsilon & 0 & 1 \end{bmatrix}\begin{bmatrix} b^1_1 & 0 & 0 \\ 0 & b^2_2 & 0 \\ b^1_3 & b^2_3 & 1 \end{bmatrix} = \begin{bmatrix} b^1_1 & 0 & 0 \\ 0 & b^2_2 & 0 \\ -\varepsilon b^1_1 + b^1_3 & b^2_3 & 1 \end{bmatrix}$$

so (by choosing $\varepsilon = \frac{b^1_3}{b^1_1}$ $, since\ b^1_1 \neq 0$) this equivalence transformation enables us to replace b^1_3 by zero. Similarly, post multiplying B by $A\left(3\,, ln\left|\frac{1}{b^1_1}\right|\right), \varepsilon = ln\left|\frac{1}{b^1_1}\right|$ is equivalent to setting $b^1_1 = \mp 1$

In summary, we have factored out the die symmetries by using the adjoin action, and the inequivalent discrete symmetries are those solution of $X_{i(\hat{x},\hat{u})} = b^l_i \hat{X}_{l(\hat{x},\hat{u})}$, with

$$B = \begin{bmatrix} \propto & 0 & 0 \\ 0 & b^2_2 & 0 \\ 0 & b^2_3 & 1 \end{bmatrix} \qquad \propto \in \{1, -1\}$$

that also satisfies the symmetry condition.

The system $X_{i(\hat{x},\hat{u})} = b^l_i \hat{X}_{l(\hat{x},\hat{u})}$ with B as above, amounts to

$$\begin{bmatrix} X_1\hat{t} & X_1\hat{x} & X_1\hat{u} \\ X_2\hat{t} & X_2\hat{x} & X_2\hat{u} \\ X_3\hat{t} & X_3\hat{x} & X_3\hat{u} \end{bmatrix} = \begin{bmatrix} \propto & 0 & 0 \\ 0 & b^2_2 & 0 \\ 0 & b^2_3 & 1 \end{bmatrix}\begin{bmatrix} 1 & 0 & 0 \\ 0 & 1 & 0 \\ \hat{t} & 0 & -\hat{u} \end{bmatrix}$$

$$\Rightarrow \begin{bmatrix} \hat{t}_t & \hat{x}_t & \hat{u}_t \\ \hat{t}_x & \hat{x}_x & \hat{u}_x \\ t\hat{t}_t - u\hat{t}_u & t\hat{x}_t - u\hat{x}_u & t\hat{u}_t - u\hat{u}_u \end{bmatrix} = \begin{bmatrix} \propto & 0 & 0 \\ 0 & b^2_2 & 0 \\ \hat{t} & b^2_3 & -\hat{u} \end{bmatrix}$$

This system of first – order PDEs has the general solution

$$\left.\begin{aligned} \hat{t} &= \propto t + \frac{A}{u} \\ \hat{x} &= b^2_2 x - b^2_3 ln u + c_1 \\ \hat{u} &= c\, u \end{aligned}\right\} \qquad (13)$$

Now we factor out the one – parameter Lie group generated by X_2 setting $c_1 = 0$, and since (1) is homogeneous PDE take $c = 1$, therefore (13) becomes

$$\left.\begin{array}{l}\hat{t} = \propto t + \frac{A}{u} \\ \hat{x} = b_2^2 x - b_3^2 lnu \\ \hat{u} = u\end{array}\right\} \quad (14)$$

where $\propto \in \{1,-1\}$, A is an arbitrary constant. All that remains is to substitute (14) in to the symmetry condition

$\hat{u}_{\hat{t}} = \hat{u}\hat{u}_{\hat{x}} + \hat{u}_{\hat{t}\hat{x}\hat{x}}$ when $u_t = uu_x + u_{txx}$

(for the sake of brevity, the details of this straight forward calculation are omitted) It turns out that the symmetry condition imposes the further constraints

$$A = b_3^2 = 0 \ , \ b_2^2 = \propto$$

Therefore we have

$$\begin{array}{ll}\hat{t} = \propto t & \\ \hat{x} = \propto x & \propto \in \{1,-1\} \\ \hat{u} = u & \end{array}$$

Therefore there are two classes of discrete symmetries, namely those that are equivalent to

$$\Gamma_1 : (t, x, u) \mapsto (-t, -x, u)$$

And those that equivalent to ${\Gamma_1}^2 = \text{I}$ (Identity), In other words the factor group of in equivalent discrete symmetries is isomorphic to the cyclic group Z_2 and is generated by Γ_1. Thus we have derive the following result.

4.1. Theorem: -

BBM equation's discrete symmetry group is cyclic of order 2, generated by Γ.

4.2. Corollary:-

The maximal real point symmetry group of the PDE (1) consists of all point transformation of the form $\gamma\Gamma^i$ $i = 1,2$ and γ is continuous symmetry.

5- CONLUSION

In this paper, we have found discrete symmetries of the BBM equation. By applying Lie group method. We get group of discrete symmetry isomorphic to Z_2.

REFERENCE

1. Bulman G.W. and Kumei S. Symmetries and Differential Equations, Vol. 81, 1989 Springer, New York.
2. Christlan T., Discrete Symmetries of Nonlinear Ordinary Differential Equations, Thesies,2003 Lulea University of Technology.

3. Gaeta G. and Rodriguez M.A., Determining Discrete Symmetries of Differential Equation, Nuovo Cimen Vol.111,p 879-891 (1996).
4. Hamad M.A.A, Hassanien I.A. and Elnahary H., Discrete Symmetries Analysis of Burgers Equation with Time Dependent Flux at the Origin, World Applied Sciences, p. 2291-2300 (2011).
5. Ibragmov N.H., Symmetries Exact Solutions and Conservation Laws, Vol. I, 1994, CRC Press.
6. Hydon P.E., Discrete Point Symmetries of ODE. , Proc. Soc. Lond. A 454 p. 1961-1972 (1997).
7. Hydon P.E., Discrete Point to Construct the Discrete Symmetries of P.D.E., Applied Mathematics, Vol 11, No.5, p 515-527 (1998).
8. Hydon P.E., How to use Lie Symmetries to find Discrete Symmetries, Modern Group Analysis VII, Mars publishers, p. 141-147 (1999).
9. Hydon P.E., Symmetry Methods for Differential Equations : Aleginner's Guide, 2000, Gambridge University Press.
10. Hydon P.E., How to Construct the Discrete Symmetries of Partial Eur. J. Appl. Math, Vol 11, p. 515-527 (2000).
11. Martel Y. Multi-solutions and large time dynamics of the subcritical generalized KdV equations.
12. Olver P.J., Application of Lie Group to Differential Equations, 1993, Springer-Verlag, New York.
13. Olver P.J., Equivalence, Invariants and Symmetry,1995 Cambridge, University Press.
14. Ovsiannikov, L.V., Group Analysis of Differential Equations, 1982, Academic Press, New York.
15. Papal, Applications of Lie Classical Method to some Nonlinear Partial Differential Equations,thesies, 2010, Thapar University, India.
16. Rachal S., Bifurcations with Spherical Symmetries; Thesies 2010, University Of Nottingham.
17. Stephani H., Differential Equation: Their Solution using Symmetries 1989, Combridge, University Press.
18. Yang H., Shi Y., Yin B. and Dong H., Discrete Symmetries Analysis and Exact Solutions of the Inviscid Burger's Equations, Discrete Dynamics in Nature and Society VOl.56, P. 1-15 (2012).

Approximate Solution Of The Linear Mixed Volterra-Fredholm Integro Differential Equations Of Second kind By Using Variational iteration Method

Fadhel subhi Fadhel[1], Abdul khaliq owaid mezaal[2] and Shymaa hussain salih[3]
[1] Department Mathmatice, Collage science, Al-Nahrain University
[2] Department Mathmatice, Collage science, Al-Mustansiriyah University
[3] Department Mathmatice, Collage science, Al-Technology University
Received 18/3/2013 – Accepted 15/9/2013

الخلاصة

في هذا العمل وظفت طريقة التغاير التكرارية ((VIM))لايجاد الحل التقريبي للمعادلات التفاضلية التكاملية الخطية التي تدعى فولتيرا -فريدهوم من النوع الثاني حيث هذه الطريقة استخدمت مضارب لاكرانج (λ)للحصول على امثلية الحل من خلال نظرية التغاير. وتم برهان نظرية تقارب حلول تقريبية الى حل المضبوطة واخيراً ظهرت النتائج في الجداول والأشكال وتم احتساب الخطأ لكل مثال.

ABSTRACT

In this work, the variatioal iteration method (VIM) is employed to finding the approximation solution of the linear mixed Volterra-Fredholm integro differential equation of second kind (V-FIEs) .The (VIM) is to construct correction functional using general Lagrange multipliers(λ) identified optimally via the variational theory. We proving theorm study the convergence approximate solutions to the exact solutions, Finlly ,two examples are given and their results are given in tables and are shown in figures, the error estimate ,in each examples is calculated.

INTRODUCTION

A mixed Volterra- Fredholm integro differential equation contain mixed Volterra and Fredholm integral equations where the Fredholm integral is the interior integral ,whereas the volterra integral is the exterior one.Moreover , the unknown function u(x,y) appears inside the integral ,whereas the derivative $\frac{\partial u}{\partial y}(x,y)$ appears outside the integral. These types of equations playing an important role in many branches of linear and nonlinear functional analysis and their applications in the theory of elasticity, engineering and mathematical physics[1,2,3,4].

A discussion of the formulation of these models is given in wazwaz[4] and the references therein.

In this work, we consider the following the linear mixed Volterra-Fredholm differential equation of second kind:

$$\frac{\partial u}{\partial y}(x,y) = g(x,y) + \int_0^x \int_\Omega k(x,y,z,m)u(z,m)dz\,dm \quad (x,y) \in [0,T] \times \Omega \tag{1}$$

where u(x,y) is an unknown function, the known functions g(x,y) and k(x,y,z,m) are continuous of x and y on D=[0,T]×Ω and (S×R) where (S={(x,y,z,m)},0≤ z, m ≤T,(x,y)⊂Ω×Ω}) and (Ω is a closed subset of R^n (n=1,2,3,...)).

The existences and uniqueness to Eq.(1) are given in [5].Many research are used the linear mixed Volterra-Fredholm integral and integro differential equation by Brunner H.[6] ,Shazad S.[7] and wazwaz A. [4]. In this work we propose procedure for solving the linear mixed Volterra-Fredholm integro equation of second kind using varaitional iteration method.

Variational Iteration Method:

The variational iteration method was porposed by Ji-Huan He in 1999[8,9], and yet powerful method for solving a wide class of linear and nonlinear problems. The (VIM) gives rapidly convergent successive approximation of the exact solution if such a solution exists[9]. This method is based on use of lagrange multipliers for identification of optimal value of a parameter in a functional [10, 11].

To illustrate the basic idea of the (VIM), we consider the following general functional equation given in operator form:

$$L(u(x,y)) + N(u(x,y)) = g(x,y) \qquad \dots (2)$$

where L is a linear operator. N is a nonlinear operator and g(x,y) is any given function which is called the nonhomogeneous term. According to the (VIM), we can construct the following correction functional

$$u_{n+1}(x,y) = u_n(x,y) + \int_0^y \lambda\{ L(x,y) + N\tilde{u}(x,y) - g(x,y)\}$$

where λ is a general lagrange multiplier which can be identified optimally via variation theory[10,11,12], u_0 is an initial approximation in this work knowns functions, and $\tilde{u}$ consider as restricted variation

which means $\delta\,\tilde{u} = 0$.Therefor, we first determine the lagrange multiplier

λ that will be $u_{n+1}(x,y) \geq 0$ of the solution u(x,y) will be readily obtained

upon using the lagrange multiplier obtained by using any selective

function $u_0(x,y)$,consequently the solution $u(x,y)=\lim_{n\to\infty}u_n(x,y)$.

Variational Iteration Method Solving The Linear Mixed Volterra-Fredholm Integro Differential Equation Of Second Kind(V-FIEs):-

Now, we consider the linear mixed Volterra-Fredholm integro differential equation of of second kind:-

$$\frac{\partial u}{\partial y}(x,y) = g(x,y) + \int_0^x \int_a^b k(x,y,z\,,m)u(z,m)dz\,dm \qquad \dots(3)$$

Then we have the following iteration sequence

$$u_{n+1}(x,y)=u_n(x,y)+\int_0^y \lambda(\xi)\{u_n(\xi,y)-g(\xi,y) - \int_0^x \int_a^b k(\xi,y,z,m)u_n(\xi,m)\,dzdm\}d\xi \qquad \dots(4)$$

To find the optimal λ ,we procced as follows :

$$\delta u_{n+1}(x,y)=\delta u_n(x,y)+\delta \int_0^y \lambda(\xi)\{\acute{u}_n(\xi,y)-g(\xi,y)-\int_0^x \int_a^b k(\xi,y,z,m)u_n(\xi,m)\,dzdm\}d\xi = 0 \quad ...(5)$$

and upon using the method of integration by parts,then Eq.(5)will be reduced to:

$$\delta u_{n+1}(x,y) = \delta u_n(x,y) + \int_0^y \lambda(\xi)\delta(\,\acute{u}\,(\xi,y))$$
$$=\delta u_n\,(x,y) + \lambda(x,y)\delta u_n(x,y) + \int_0^x \acute{\lambda}\,(\xi)\delta\, u_n\,(x,y) = 0$$

Then the following stationary conditiones are obtained:

$$\acute{\lambda} = 0 \qquad , \qquad \lambda + 1 = 0$$

The general Lagrange multipliers therefor ,can be readily identified : λ=-1 and by substituting in Eq.(4), The following iteration formula $n \geq 0$ is obtained

$$u_{n+1}(x,y)=u_n(x,y)-\int_0^y\{\acute{u}_n(\xi,y)\; g(\xi,y)-\int_0^x \int_a^b k(\xi,y,z,m)u_n(\xi,m)\,dzdm\}d\xi \quad ...(6)$$

Theorem:- Let $u \in (C^2[a, b], \|\,.\,\|_\infty)$ be the exact solution of the linear mixed Volterra-Fredolm integro differential equation of (3) and $u_n \in C^2[a, b]$ be the obtained solution of the sequence defined by eq.(4). If $E_n(x) = u_n(x,y) - u(x,y)$ and $|k| \leq c$, $0 < c < 1$, then the sequence of approximate solutions $\{u_n\}$, n = 0, 1, ...; converges to the exact solution u(x,y).

Proof:-

Consider the linear mixed Voltrrra-Fredholm integro differential equation of second:-

$$\frac{\partial}{\partial y}u(x,y) = g(x,y) + \int_a^x \int_a^b K(x,y,z,m)u(z,m)dzdm$$

Where the approximate solution using the VIM is given by

$$u_{n+1}(x,y) = u_n(x,y) - \int_0^y [\tfrac{\partial}{\partial s} u_n(x,s) - g(x,s) - \int_a^x \int_a^b k(x,s,z,m)u_n(z,m)dzdm]ds \quad ...(7)$$

And since u is exact solution of the linear mixed VFIEs, have

$$u(x,y) = u(x,y) - \int_0^y [\tfrac{\partial}{\partial s} u(x,s) - g(x,s) - \int_a^x \int_a^b k(x,s,z,m)u(z,m)dzdm]ds \quad ...(8)$$

Now, subtracting Eq.(8) from Eq.(7) to get:

$$E_{n+1}(x,y) =$$
$$E_n(x,y) - \int_0^y [E_n(x,s) - g(x,s) + g(x,s) \int_a^x \int_a^b k(x,s,z,m) E_n(z,m)\,dzdm]ds$$
$$E_{n+1}(x,y) = E_n(x,y) - \int_0^y \frac{\partial}{\partial s} E_n(x,s)ds + \int_0^y \int_a^x \int_a^b k(x,s,z,m) E_n(z,m)\,dzdmds$$
$$E_{n+1}(x,y) =$$
$$E_n(x,y) - E_n(x,y) - E_n(x,0) - \int_0^y \int_a^x \int_a^b k(x,s,z,m) E_n(z,m)\,dzdmds$$

And since $E_n(x,0) = u_n(x,0) - u(x,0)$, which have the initial condition of the VFIEs, the $E_n(x,0) = 0. Hance$

$$E_{n+1}(x,y) = \int_0^y \int_a^x \int_a^b k(x,s,z,m) E_n(z,m)\,dzdmds \qquad \ldots(9)$$

Now, taking the maximum-norm on both sides of Eq.(9), yields to :

$$\|E_{n+1}(x,y)\|_\infty = \left\| \int_0^y \int_a^x \int_a^b k(x,s,z,m) E_n(z,m)\,dzdmds \right\|_\infty$$
$$\|E_{n+1}(x,y)\|_\infty \leq \int_0^y \int_a^x \int_a^b \|k\|_\infty \|E_n(z,m)\|_\infty\, dzdmds$$

since K is function bounded by c, c$\in$ (0,1), then

$$\|E_{n+1}(x,y)\|_\infty \leq c\int_0^y \int_a^x \int_a^b \|k\|_\infty \|E_n(z,m)\|_\infty\, dzdmds$$
$$\|E_{n+1}(x,y)\|_\infty = cy\int_a^x \int_a^b \|E_n(z,m)\|_\infty\, dzdm$$

Therefor

$$\|E_{n+1}(x,y)\|_\infty \leq cy\int_a^x \int_a^b \|E_n(z,m)\|_\infty\, dzdm, \forall n = 0,1, \qquad \ldots(10)$$

Now, if n=0, then inequality (10) yield to

$$\|E_1(x,y)\|_\infty \leq cy\int_a^x \int_a^b \|E_0(z,m)\|_\infty\, dzdm$$
$$\|E_1(x,y)\|_\infty \leq cy\int_a^x \int_a^b \underset{(z,m)}{Max} |E_0(z,m)|dzdm$$
$$\|E_1(x,y)\|_\infty = cy\,(x-a)(b-a)Max|E_0| \qquad \ldots(11)$$

Also, if n=1, then from inequality (10) and (11) we have

$$\|E_2(x,y)\|_\infty \leq cy\int_a^x \int_a^b \|E_1(z,m)\|_\infty\, dzdm$$

Substituting (11) ,in this inequality we get

$$\|E_2(x,y)\|_\infty \leq cy\int_a^x \int_a^b cy\,(x-a)(b-a)Max|E_0|$$
$$\|E_2(x,y)\|_\infty = c^2y^2\,\frac{(x-a)^2}{2}\,(b-a)^2\ Max|E_0| \qquad \ldots(12)$$

Similarly, for n=2 and from inequality (10) and(12) ,we have

$$\|E_3(x,y)\|_\infty \leq cy\int_a^x \int_a^b \|E_2(z,m)\|_\infty\, dzdm$$

Substituting (12) ,in this inequality we get

$$\|E_3(x,y)\|_\infty \leq cy\int_a^x \int_a^b c^2y^2\,\frac{(x-a)^2}{2}\,(b-a)^2\ Max|E_0|dzdm$$
$$\|E_3(x,y)\|_\infty = c^3y^3\,\frac{(x-a)^3}{3!}\,(b-a)^3\ Max|E_0|$$

And so on, in general and using mathematical induction we get:

$$\|E_n(x,y)\|_\infty \leq c^ny^n\,\frac{(x-a)^n}{n!}\,(b-a)^n\ Max|E_0| \qquad \ldots(13)$$

And since $c \in (0,1)$ and as $n \to \infty$, then we will have the right hand side of inequality (13) tends to zero, i.e, $\|E_n(x,y)\|_\infty \to 0$ as $n \to \infty$

Which implies to $u_n(x,y) \to u(x,y)$ as $n \to \infty$

i.e., the sequence of solutions obtaind from the VIM converge of the exact solution u(x,y).

Numerical Examples:-

In the section, we used the (VIM) which is discussed of the previous section for solve two examples.

Example (1):-

Consider the linear mixed Volterra-Fredholm integro differential equation of second kind

$$\frac{\partial}{\partial y}u(x,y) = x - \frac{1}{10}x^3y + \int_0^x\int_0^1 z^3xy\,u(z,m)dz\,dm$$

With exact solution u(x,y)=xy

The corresponding iterative formula (6) for this example can be constructed as follows:

$$u_{n+1}(x,y)=u_n(x,y)-\int_0^y\{\acute{u}_n(\xi,y)-g(\xi,y)-\int_0^x\int_a^b k(\xi,y,z,m)u_n(\xi,m)\,dzdm\}d\xi$$

Let the initial approximate solution $u_0(x,y) = x - \frac{1}{10}y\,x^3$,we get:

$$u_1(x,y)=u_0(x,y)-\int_0^y\{\acute{u_0}(x,y)-(x-\frac{1}{10}yx^3)-\int_0^x\int_0^1 z^3\,x\,y\,u_0(z,m)dzdm\}d\xi$$

$$=\frac{1}{240}[-12y^2x^3 - yx^3 + 20ytx^2 + 240yx + 240x]$$

$$u_2(x,y)=u_1(x,y)-\int_0^y\{\acute{u_1}(x,y)-\left(x-\frac{1}{10}x^3y\right)-\int_0^x\int_0^1 z^3\,x\,y\,u_1(z,m)dzdm\}d\xi$$

$$=\frac{1}{240}[-12y^2x^3 - yx^3 + 20yx^2 + 240yx + 240x] - \frac{1}{40320}[63x^4y - 2561]$$

And so on ,we may compute u_9,u_{11},u_{13}; which be more complicated .

The exact solution and the approximate solution u_N with different N and the absolute error $|e_N| = |u_{exact}-u_N|$, Table(1)and Figure(1)&(2) are shown exact and approximate solutions by using variational iteration Method.

Table-1 :The results of Example(1)

x	y	exact	Approximate Sol.atN=9	error	Approximate Sol.atN=10	error	Approximate Sol.atN=11	error	Approximate Sol.atN=13	error
0	0	0	0		0	0	0	0	0	0
0.1	0.1	0.01	0.01	0	0.01	0	0.01	0	0.01	0
0.2	0.2	0.0400	0.0400	0	0.0400	0	0.0400	0	0.0400	0
0.3	0.3	0.0900	0.0900	0	0.0900	0	0.0900	0	0.0900	0
0.4	0.4	0.1600	0.1600	0	0.1600	0	0.1600	0	0.1600	0
0.5	0.5	0.2500	0.2500	0	0.2500	0	0.2500	0	0.2500	0
0.6	0.6	0.3600	0.3600	0	0.3600	0	0.3600	0	0.3600	0
0.7	0.7	0.4900	0.4900	0	0.4900	0	0.4900	0	0.4900	0
0.8	0.8	0.6400	0.6400	0	0.6400	0	0.6400	0	0.6400	0
0.9	0.9	0.8100	0.8099	0.0001	0.8100	0	0.8100	0	0.8100	0
1	1	1.000	0.9998	0.0002	1.000	0	1.000	0	1.000	0
L.S.E			3.38e-08		1.968e-011		7.53e-15		4.75e-022	

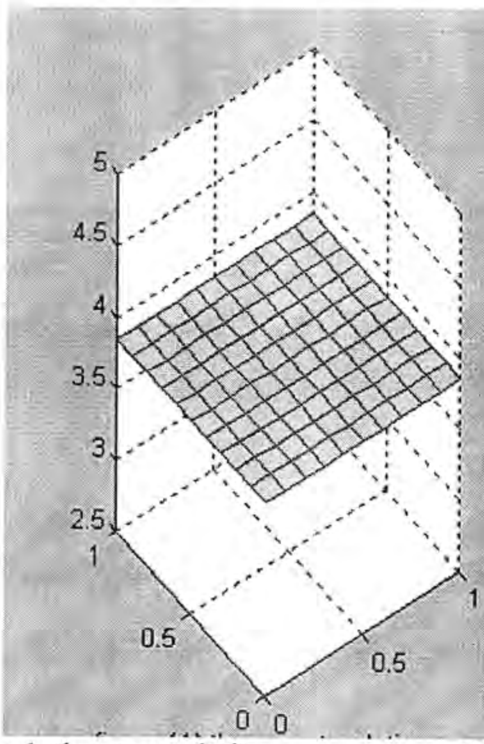

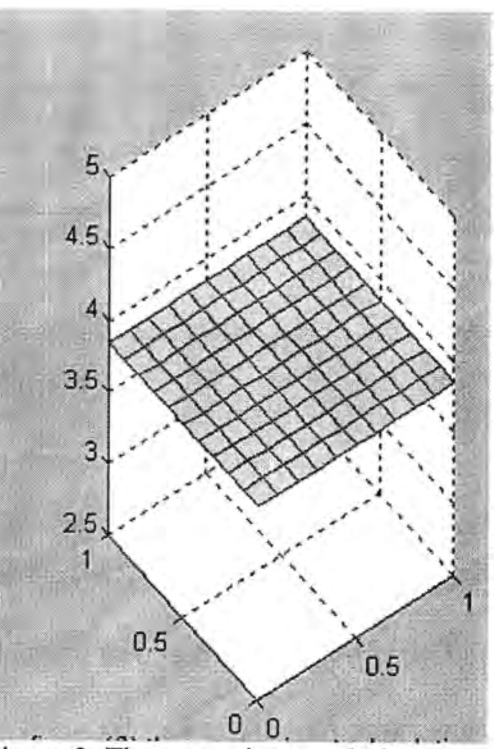

Figure-1: the exact solution

Figure-2: The approximate solution

Example (2):-

Consider the Linear mixed Volterra-Fredholm integro differential equation of second kind

$$u'(x,y) = 2ye^x - (x^2e^{-1}e^x - x^2e^{-1})(e^2-5)+\int_0^x\int_{-1}^1 x^2e^{-z}\,u(z,m)dz\,dm$$

With exact solution $u(x,y)=y^2e^x$

The corresponding iterative formula (6) for this example can be constr as follows:

$$u_{n+1}(x,y)=u_n(x,y)-\int_0^y\{\acute{u}_n(\xi,y)-g(\xi,y)-\int_0^x\int_a^b k(\xi,y,z,m)u_n(\xi,m)\,dzdm\}d\xi$$

Let the initial approximate solution $u_0(x,y) = 2ye^x - (x^2e^{-1})(e^2-5)$ we get:-

$$u_1(x,y)=u_0(x,y)-\int_0^y\{\acute{u}_0(x,y)-(2ye^x-(x^2e^{-1})(e^2-5))-\int_0^x\int_{-1}^1 x^2\,e^{-z}\,u_0(z,m)dzd$$

$$= y^2e^x - 0.8788x^2e^x + 0.8788x^2y - 0.58592yx^3 + 2yx^4 + 0.8788x^2 -$$

$$4.3944yx^3e^{-1} + 0.8788yx^3e^1 - 0.8788yx^2e^x$$

$$u_2(x,y) = u_1(x,y)-\int_0^y\{\acute{u}_1(x,y)\left(2ye^x-(x^2e^{-1})(e^2-5)\right)-\int_0^x\int_{-1}^1 x^2\,e^{-z}\,u_1(z,m)dz$$

$$= y^2e^x - 0.8788x^2e^x + 0.8788x^2y - 0.58592yx^3 + 2yx^4 + 0.8788x^2$$

$$4.3944yx^3e^{-1} + 0.8788yx^3e^1 - 0.8788yx^2e^x + xye^{-2}(0.89e^3 + 13.$$

$$62.5e^1 + 0.878e^4 + 0.666xe^2 + 35.155)$$

The exact solution and the approximate solution u_N with different N and the absolute error $|e_N| = |u_{exact}-u_N|$, Table(1)and Figure(3)&(4) are shown exact and approximate solutions by using variational iteration Method.

Table-2:The results of Example(2)

x	y	exact	Approximate Sol.atN=9	error	Approximate Sol.atN=11	error	Approximate Sol.atN=13	error	Approximate Sol.atN=15	error
0	0	0	0	0	0	0	0	0	0	0
0.1	0.1	0.0111	0.0111	0	0.0111	0	0.0111	0	0.0111	0
0.2	0.2	0.0489	0.0489	0	0.0489	0	0.0489	0	0.0489	0
0.3	0.3	0.1215	0.1215	0	0.1215	0	0.1215	0	0.1215	0
0.4	0.4	0.2387	0.2386	0.001	0.2387	0	0.2387	0	0.2387	0
0.5	0.5	0.4122	0.4120	0.002	0.4122	0	0.4122	0	0.4122	0
0.6	0.6	0.6560	0.6552	0.008	0.6560	0	0.6560	0	0.6560	0
0.7	0.7	0.9867	0.9846	0.0021	0.9867	0	0.9867	0	0.9867	0
0.8	0.8	1.4243	1.4189	0.054	1.4243	0	1.4243	0	1.4243	0
0.9	0.9	1.9923	1.9800	0.0123	1.9921	0	1.9923	0	1.9923	0
1	1	0.7183	2.6925	0.258	2.7178	0.0005	2.7183	0	2.7183	0
L.S.E		8.48e-004			2.6e-007		2.85e-011		1.35e-015	

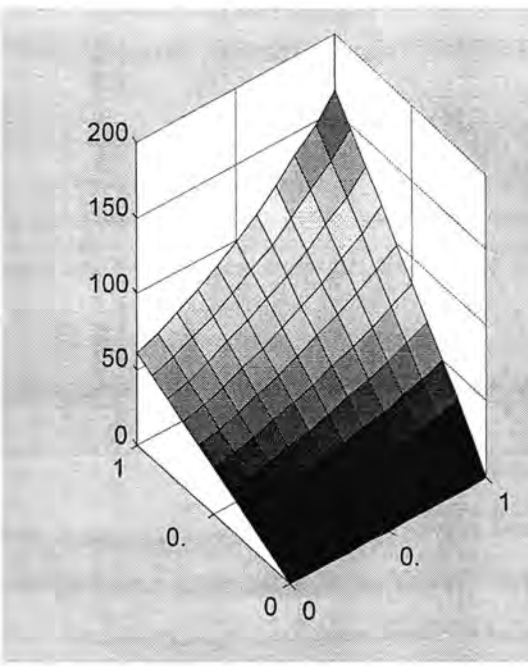

Figure-3: Approximate solution using VIM

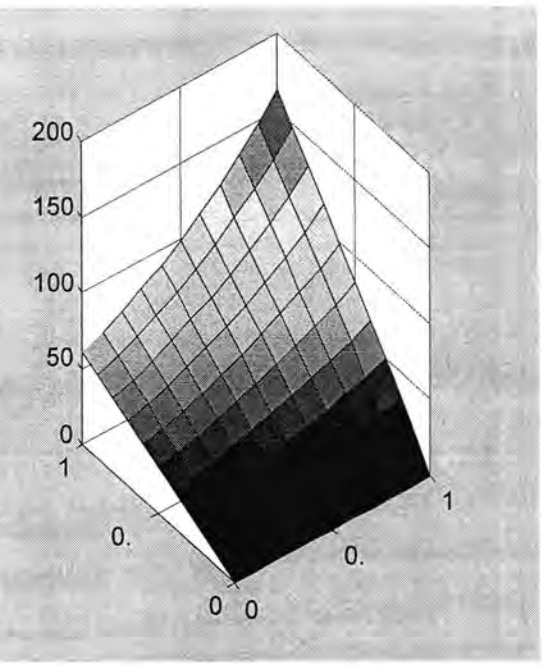

Figure-4:Exact solution

CONCLUSION

In this paper the variational iteration method is used to solve the linear mixed Volterra-Fredholm integro diferential equation with second kind .The reasults showed that the convergence and accuracy of variational iteration method for numerically solution for (V-FIE)were in a good argreement with analytical solutions.The computations associated with examples and graphing in this paper performed using matlab (v 6.5).

REFERENCES

1. Hadizadeh M. and Yazdani S. ,"Piecewise constant bounds for the solution of nonlinear Volterra-Fredholm integral equations,comput.Appl.Math. ,31:1-18 ,(2012)
2. Avaji M.,Hafshejani J.S,,Dehcheshmesh S.S. and Ghahfarokhi D.F.,"Solution of Delay Volterra integral Equation Using the Variational iteration method ",J.Appl.sci.,12:196-200,(2012).
3. Shadan S.B.,"The Use of Iterative method to solve Two-dimensional Nonlinear Volterra-Fredholm Integro-Differential Equations,J. of communication in Numerical Analysis ,2012:1-20,(2012).http//www.ivsl.org.
4. Wazwaz A. M., "Linear and Nonlinear Integral Equations Method and Application ",HEP and spring-Verlag Heidelberg,303-309,2011,London,NewYork.
5. Akram H.M.and Lamymaa H.S.,"Existence of solution of certain volterra-Fredholm integro differential equations ",J.Edu.&Sci.,vol.(25),No.(3),2012.
6. Brunner H. ," On the numerical solution of nonlinear Volterra-Fredholm integralequation bycollocation methods", SIAM J. Numer. Anal., 27:987-1000(1997).
7. Shazad S.A.," Numerical Solution for Volterra-Fredholm integral Equation of Second kind by using Least Squares Technique",*Iraqi J. of Scie.,52:.504-512*(2011).
8. Hendi F.A. and Bakodah H.O.,"Discrete Adomian Decomposition Solution of Nonlinear Mixed Integral Equation",J.Amercian Sci.,7:1081-1084(2011).
9. He,J.H.,"Variational iteration method akind of non-linear analytical technique",Int.J.nonlinear Mech,34:699-708,(1999).
10. Behzad G.and Mehdi G.P. ,"Variational Iteration Method for Solving Volterra and Fredholm Integral Equations of the Second Kind", *Gen. Math. Notes,2: pp. 143-148(2011).*
11. Maryam H.W.,"Numerical Solution of Fractional Order Integral Equations",M.Sc. Thesis ,college of Eduction ,Al-Mustansiriyah University,2012.
12. Sekine H. , Inokuti M. and Mura T., "General use of the Lagrange multiplier in nonlinear mathematical physics, in:S.Nemat-Nasser (Ed.), Variational Method in the Mechanics of solids, *Pergamon Press*, New York,156-16(1978).

Efficient solutions for multicriteria problems

Adawiyah A. Mahmood Al-Nuaimy[1] and Tariq S. Abdul-Razaq[2]
[1]Mathematics Department, College of Science, Dayala University
[2]Mathematics Department, College of Science, Al-Mustansiriyah University
Received 25/3/2013 – Accepted 15/9/2013

الخلاصة

درسنا مسألة جدولة n من الاعمال على ماكنة واحدة. هدفنا تصغير دالة الهدف والتي تكون دالة لمقياسين أو ثلاثة والمسألة هي ايجاد مجموعة الحلول الكفوءة بالنسبة الى المقاييس (2) أو (3) والتي هي (مجموع تأخير لوحدات عمل متأخر مع اكبر تأخير لوحدات عمل متأخر) و(مجموع أوقات الاتمام للاعمال مع اكبر تأخير لاسالب واكبر تأخير لوحدات عمل متأخر).

اقترحنا خوارزمية لكلا المسألتين وتم بحث كفاءة هذه الخوارزمية على هذه المسائل المتعددة الاهداف وتبين ان هذه الخوارزمية عامة وكفوءة ويمكن استخدامها لايجاد مجموعة الحلول الكفوءة لمسائل اخرى. النتائج التجريبية تشير الى ان الخوارزمية المقترحة تجد كل الحلول الكفوءة في معظم الحالات.

ABSTRACT

We study the problem of scheduling n jobs on a single machine. We wish to minimize an objective function that is a function of 2 or 3 performance criteria. The problem is to find the set of efficient solutions (Pareto optimal points) with respect to these performance criteria 2 and 3, i.e., (total late work with maximum late work) and (total completion time with maximum tardiness and maximum late work). We propose algorithm for both problems and investigate its performance on these two multicriteria problems, this algorithm is efficient and general one and can be used to find the set of efficient solutions for other problems. Our experiment results indicate that the proposed algorithm finds all efficient solutions in most cases.

1.INTRODUCTION

In general, the scheduling problem is defined as a problem of assigning a set of jobs to a set of machines in time under given constraints ([2,5,9]). Jobs are mainly characterized by processing times (p_j), due dates (d_j) define expected completion times (C_j) for particular jobs.

The quality of an assignment, a schedule, can be evaluated from different points of view, which are represented by different performance measures. Most objective functions based on due dates are regular ones, i.e. non-decreasing with increase in completion times of jobs. This group includes criteria based on lateness($L_j=C_j - d_j$),tardiness($T_j=\max\{0,C_j - d_j\}$) or the number of tardy jobs($U_j=1$,if $C_j > d_j$, otherwise $U_j=0$). The criteria based on earliness($E_j=\max\{0,d_j - C_j\}$) are non-regular ones.

The late work criterion estimates the quality of a solution on the basis of the duration of late parts of particular jobs. Late work combines the features of two parameters: tardiness and the number of tardy jobs. Formally speaking, in the non-preemptive case the late work parameter is defined as $V_j=\min\{\max\{0,C_j - d_j\},p_j\}=\min\{T_j , p_j\}$ or, in a more extensive way, as

$$V_j = \begin{cases} 0 & \text{if } C_j \le d_j \quad j=1,2,\ldots,n \\ C_j - d_j & \text{if } d_j < C_j < d_j + p_j \quad j=1,2,\ldots,n \\ p_j & \text{if } d_j + p_j \le C_j \quad j=1,2,\ldots,n \end{cases}$$

In the preemptive case durations of particular tardy parts of a job have to be summed up. The quality of a schedule (with n jobs) is expressed

with the total late work ($\sum_{j=1}^{n} V_j$).

The parameter V_j was first introduced by Blazewicz [3], who called it " information loss ", reffering to a possible application of the performance measures based on it. The phrase " late work " was proposed by Potts and Van Wassenhove [10]. Some researchers, e.g. Hochbaum and Shamir [6], use a descriptive name for this schedule parameter-the number of tardy job units.

The relation between late work and other performance measures was established by Blazewicz et al. [4].

Applications of the late work minimization problems arise in control systems [3,10], where the accuracy of control procedures depends on the amount of information provided as their input. A job represents a message carrying a certain amount of information, which determines the job length. All information received by the system after a given due date is useless. The information exposed after the time required (called the information loss) is modeled with the late work and should be minimized in order to increase the efficiency (the precision) of the control process.

The late work parameter appears to be important in production planning both from the customer's point of view and from the manager's point of view. If the customer orders are interpreted as jobs to be executed, then minimizing the late work is equivalent to minimizing those parts of orders which are not executed on time. Obviously, every customer is interested in minimizing these late parts. The manager is also interested in minimizing orders delays, which cause financial loss.

Interesting applications of the late work criteria arise in agriculture, where performance measures based on due-dates are especially useful [1]. Late work criteria can be applied in any situation where a perishable commodity is involved [10]. For example, if crops that might be collected from different stretches of cultivated land are represented by jobs, then the process of harvesting can be modeled by the late work minimization problem.

This paper begins with a notation and basic concepts of multicriteria scheduling in section 2.Formulation of the simultaneous multicriteria (P) problem and special cases are described in section 3. An algorithm (ADA) for finding efficient solutions of the (P and P1) problems is presented in section 4. The formulation of the simultaneous multicriteria (P1) problem is presented in section 5. Computational experiments are presented in section 6. Conclusions and areas for future research are described in section 7.

2. Notation and basic concepts of multicriteria scheduling

n : number of jobs.
p_j : processing time for job j.
d_j : due date for job j.
C_j : completion time for job j.
V_j : late work for job j.
V_{max} : maximum late work.
$\sum V_j$: total late work.
$\sum U_j$: number of tardy jobs.
EDD : earliest due date.

Definition [7]:

A feasible solution (schedule) σ is efficient (Pareto optimal, or non- dominated) with respect to the performance criteria f and g if there is no feasible solution (schedule) π such that both $f(\pi)\leq f(\sigma)$ and $g(\pi)\leq g(\sigma)$
,where at least one of the inequalities is strict.

Lawler's algorithm (LA) which solves the $1/prec/f_{max}$ problem or $1//f_{max}$ problem where $f_{max} \in \{ C_{max}, L_{max}, T_{max}, v_{max} \}$ [9]. Lawler's algorithm (LA) is described by the following steps:
Step (1): Let N= $\{1,2,\dots,n\}$, and F is the set of all jobs with no Successors, $\pi = \varphi$.
Step (2): Let j^* such that $f_{j^*}(\sum_{i\in N} p_i) = \min_{j\in F}\{f_j(\sum_{i\in N} p_i)\}$.
Step (3): Set $N = N - \{j^*\}$ and sequence job j^* in last position of π, i.e. $\pi = (\pi, j^*)$.
Step (4): Modify F with respect to the new set of schedulable jobs.
Step (5): If $N = \varphi$ stop, otherwise go to step (2).

Moore's algorithm (MA) [9] which solves the problem $1//\sum U_j$ to find minimum number of late jobs, is described as follows :
Step(1): Order the jobs by EDD rule , let $E = L = \varphi$, $k = t = 0$.
Step(2): $k = k+1$, if $k > n$ go to step(4) .

Step(3): $t = t + p_k$, $E = E \cup \{k\}$, if $t \le d_k$ go to step(2) , otherwise (i.e., if $t > d_k$) then find a job $j \in E$ with p_j as large as possible and let $t = t - p_j$, $E=E-\{j\}$, $L = L \cup \{j\}$ and go to step(2) .
Step(4): E is the set of early jobs and L is the set of late jobs .

3.Formulation of the (P) problem

The simultaneous multicriteria problem of total late work and maximum late work (P) is formulated as follows:

$$\left.\begin{array}{l} \text{Min}\left\{\begin{array}{c} \sum_{j=1}^{n} V_j \\ V_{max} \end{array}\right\} \\ \text{subject to} \\ V_j = \text{Min}\{T_j , p_j\}, \ j=1,2,\ldots,n \\ V_j = \left\{\begin{array}{ll} 0 & C_j \le d_j \\ C_j - d_j & d_j < C_j < d_j + p_j \\ p_j & d_j + p_j \le C_j \end{array}\right. \end{array}\right\} \quad (P)$$

This problem is NP-hard since $1//\sum V_j$ the non-preemptive total late work problem is NP-hard [10].

3.1 Special cases for the problem (P)

Case (1): The $1/d_j = d/\text{Lex}(\sum V_j , V_{max})$ problem is solved by Lawler's algorithm (LA) , where $j=1,2,\ldots,n$.
Proof: Let V_{max}^* is the minimum value of maximum late work (i.e. $\min\{ \max\{ V_j \}\}$, $j = 1,2,\ldots,n$) obtained by Lawler's algorithm for the schedule σ. Since any schedule is optimal for $1//\sum V_j$ if $d_j = d$. Hence this schedule σ is optimal also for $\sum V_j$. This means that the schedule σ is optimal for $1/d_j = d/\text{Lex}(\sum V_j , V_{max})$ problem.□

Case (2): The problems $1/d_j = d/ \sum V_j + V_{max}$ and $1/d_j = d/(\sum V_j , V_{max})$are solved by Lawler's algorithm .
Proof: Similar to proof of case (1).□

Case (3): If for any schedule $C_j \ge d_j + p_j \ \forall j$ ($j=1,2,\ldots,n$) , then the $1//(\sum V_j , V_{max})$ problem is solved by Lawler's algorithm (LA) .
Proof: If for any schedule $C_j \ge d_j + p_j \ \forall j$ ($j=1,2,\ldots,n$) , then $V_j = p_j \ \forall j$ ($j=1,2,\ldots,n$) . Hence $\sum V_j = \sum p_j$ which is constant .

Thus Lawler's algorithm (LA) solves $1//(\sum V_j , V_{max})$ problem.□

Case (4): If Moore's algorithm (MA) gives a schedule with $\sum U_j = 0$, then this schedule gives $(\sum V_j , V_{max}) = (0 , 0)$.
Proof: Since Moore's algorithm (MA) gives a schedule with $\sum U_j = 0$, then this means that all jobs j are early and $C_j \le d_j$, j=1,2,…,n . Hence $V_j = 0$. Thus the schedule which is obtained by Moore's algorithm (MA) gives $(\sum V_j , V_{max}) = (0 , 0)$.□

Case (5): If EDD rule gives a schedule with $T_{max} = 0$, then this schedule gives $(\sum V_j , V_{max}) = (0 , 0)$.
Proof: Since the EDD schedule gives $T_{max} = 0$, then $T_j = 0$ for each job j, j=1,2,…,n . Since $V_j \le T_j$, $\forall j$ (j=1,2,…,n) and $V_j \ge 0$, then $V_j = 0$. Hence the EDD schedule gives $(\sum V_j , V_{max}) = (0 , 0)$.□

4. Algorithm (ADA) for finding efficient solutions for the problem (P)

This algorithm depends on the branch and bound (BAB) algorithm without reset the upper bound (UB) as follows:
Step(1): Find the first upper bound (UB1) by the (EDD) rule ,that is, sequencing the jobs in non-decreasing order of their due dates d_j, j=1,…,n, for this order σ compute $\sum V_j(\sigma)$,$V_{max}(\sigma)$ and put $UB1=\sum V_j(\sigma) + V_{max}(\sigma)$.
Step(2): Find the second upper bound (UB2) by Lawler's algorithm (LA), suppose that (LA) gives the sequence σ', for this order σ' compute $\sum V_j(\sigma')$, $V_{max}(\sigma')$ and put $UB2= \sum V_j(\sigma') + V_{max}(\sigma')$, j=1,…,n.
Step(3): Set the upper bound UB = min{UB1,UB2} at the parent node of the search tree.
Step(4): For each node IN in the search tree , compute the lower bound LB(IN) = cost of sequencing jobs + cost of unsequencing jobs , where the cost of unsequencing jobs is obtained by EDD rule for $\sum V_j$ and LA for V_{max}.
Step(5): Branch each node IN with LB(IN) ≤ UB.
Step(6): At the last level of the (BAB) algorithm we get a set of solutions, for this set eliminate the dominated solutions and the remaining solutions is the set of efficient solutions.

5. Formulation of the (P1) problem

The simultaneous multicriteria problem of total completion time with maximum tardiness and maximum late work (P1) is formulated as follows:

$$
\text{Min}\begin{Bmatrix}\sum_{j=1}^{n} C_j \\ T_{max} \\ V_{max}\end{Bmatrix}
$$

Subject to

$$
C_j = \sum_{i=1}^{j} p_i \qquad , j=1,\ldots,n
$$

$$
T_j = \max\{C_j - d_j , 0\} \quad , j=1,\ldots,n
$$

$$
V_j = \min\{T_j , p_j\} \qquad , j=1,\ldots,n
$$

(P1)

We see that the algorithm (ADA) is still applicable if the number of criteria is 3 as in problem P1.

Hence algorithm (ADA) is adopted to be used for finding efficient solutions for the problem (P1) such that (UB1) is obtained by (SPT) rule , that is , sequencing the jobs in non-decreasing order of their processing times p_j . (UB2) is obtained by EDD rule and the third upper bound (UB3) is obtained by LA. In step(3) set UB = min{UB1,UB2,UB3}. In step(4) the cost of unsequencing jobs is obtained by SPT rule for the $\sum C_j$, EDD rule for the T_{max} and LA for the V_{max} .

5.1 Analysis of number of efficient solutions

As our aim is to identify the set of all efficient solutions, we should try to hold the entire set. It is clear that if the objectives can be optimized individually, we can deduce that the set of efficient solutions have no more elements only one with extreme values of the individual objective functions. Because we are using (ADA) algorithm which depends on BAB algorithm, we can be sure that a solution is truly an efficient solution. However, we can determine if some solutions of the (ADA) algorithm is dominated by other solutions. It should be noted that the SPT schedule is one of the efficient solutions for the problem (P1).

6. Computational experiments

The ADA algorithm is tested on problems (P and P1) for generating efficient solutions by coding it in Matlab R2009b and running on a personal computer hp with Ram 2.50 GB. Test problems are generated as follows : for each job j, an integer processing time p_j is generated from the discrete uniform distribution [1,10]. Also, for each job j, an integer due date is generated from the discrete uniform distribution

[P(1-TF-RDD/2),P(1-TF+RDD/2)], where $P = \sum_{j=1}^{n} p_j$, depending on the relative range of due date (RDD) and on the average tardiness factor (TF). For both parameters, the values 0.2,0.4,0.6,0.8,1.0 are considered. For each selected value of n, two problems are generated for each of the five values of parameters producing 10 problems for each value of n, where the number of jobs n=5,10,15,20.

For the problem (P) average computation times in seconds and average number of efficient points are given in table (6.1).

Table-1:Average computation time in seconds and average number of efficient points.

Number of jobs (n)	Average computation time	Average number of efficient points
5	0.0098	2.8
10	0.1997	6
15	0.5676	9
20	40.6897	12

For the problem (P1) average computation times in seconds and average number of efficient points are given in table (6.2).

Table-2:Average computation time in seconds and average number of efficient points.

Number of jobs (n)	Average computation time	Average number of efficient points
5	0.0192	3
10	0.2989	7
15	0.7874	11
20	43.9593	14

From the above results we can conclude that the average number of efficient points is very small when compared to the number of permutation schedules and the average computation times rapidly increase with problem size $n \geq 15$. The objective of the experimental work reported here was to obtain some idea of the computational performance of the (ADA) algorithm. Also we solved the problems (P) and (P1) by complete enumeration method to find efficient solutions set, and programmed in Matlab R2009b, and implemented on the same above personal computer and we get the same results when compared the results with (ADA) algorithm with size number n = 4, 5, 6 and 7 jobs. But this method is not practically, since the scheduling problem is defined on finite set of candidate schedules. This set is usually so large such that finding the efficient schedules by complete enumeration within a reasonable time is not possible.

8. Conclusions

In this paper, an algorithm (ADA) is presented to multicriteria optimization and investigated its performance on a specific single machine multicriteria scheduling problem(P and P1). Since we are using

(ADA) algorithm which is depend on a BAB algorithm, we can be sure that a solution for problem P or P1 is truly an efficient solution. Hence the algorithm (ADA) is a general one and can be used for many multicriteria scheduling problems to find the set of efficient solutions. As a result of our experiments, we conclude that the (ADA) algorithm performs quite well for the multicriteria problems (P and P1). The research presented here contributes to the multi-objective scheduling literature by adapting (ADA) algorithm to multi-objective problems. For future research, we recommend the topic that would involve experimentation with the following machine scheduling problems:

1. $1//F(T_{max}, V_{max}, \sum V_j)$.
2. $1//F(\sum C_j, \sum V_j, V_{max})$.
3. $1//F(\sum C_j, \sum V_j, T_{max})$.

REFERENCES

1. Alminana M, Escudero LF, Landete M, Monge JF, Rabasa A, Sanchez-Soriano J. WISCHE; A DSS for water irrigation scheduling. Omega 2010; 38 (6): 492-500.
2. Blazewicz J, Ecker K, Pesch E, Schmidt G, Weglarz J. Handbook on scheduling. From theory to applications. Berlin-Heidelberg-New York: Springer; 2007.
3. Blazewicz J. Scheduling preemptible tasks on parallel processors with information loss. Technique et Science Informatiques 1984; 3(6): 415-20.
4. Blazewicz J, Pesch E, Sterna M, Werner F. Total late work criteriafor shop scheduling problems. In: Inderfurth K, Schwoediauer G, Domschke W, Juhnke F, Kleinschmidt P, Waescher G. editors. Operations Research Proceedings 1999. Berlin: Springer; 2000. P. 354-9.
5. Brucker P. Scheduling algorithms. Berlin-Heidelberg-New York:Springer; 2007.
6. Hochbaum DS, Shamir R. Minimizing the number of tardy job units under release time constraints. Discrete Applied Mathematics 1990; 28(1): 45-57.
7. Hoogeveen J. A. Invited Review. Multicriteria scheduling. European Journal of Operational Research 167(2005) 592-623.
8. Leung JY-T. Minimizing total weighted error for imprecise computation tasks and related problems. In: JY-T Leung. editor. Handbook of scheduling: algorithms, models and performance analysis. Boca Raton: CRC Press; 2004. P. 34.1-16.
9. Pinedo M. Scheduling: theory, algorithms and systems. New York:Springer; 2008.
10. Potts CN. Van Wassenhove LN. Single machine scheduling to minimize total late work. Operations Research 1991; 40(3): 586-95.

New Types of Minimal and Maximal Sets via Preopen Sets

Qays Rashid Shakir
Operations Management Techniques Depart.-Technical College of Management
Received 12/3/2013 – Accepted 15/9/2013

الخلاصة

في هذا البحث تم تقديم ودراسة المجموعة قُبيل مفتوحة الاصغرية و المجموعة قُبيل مفتوحة الاكبرية وكذلك تم تعريف فضاءات جديدة باستخدام المجموعة قُبيل مفتوحة الاصغرية و المجموعة قُبيل مفتوحة الاكبرية . بالاضافة الى ذلك، تم تعريف نوعين من الدوال المستمرة سُميت الدالة قُبيل مستمرة الاصغرية و الدالة قُبيل مستمرة الاكبرية.

ABSTRACT

In this paper, minimal preopen and maximal preopen are introduced and studied. And new spaces defined by using the minimal preopen and maximal preopen sets. Furthermore, new types of continuous maps depending on minimal and maximal preopen sets introduced and investigated which called minimal precontinuous and maximal precontinuous.

1. INTRODUCTION

The minimal and maximal open sets introduced in [1] and [2] and these sets used to investigate many topological properties. In this paper we introduced the notion of minimal preopen and maximal preopen and their complements.

Definition (1.1)[1]: A proper nonempty open subset O of a topological space X is said to be minimal open set if any open set which is contained in O is ϕ or O.

Definition (1.2)[2]: A proper nonempty open subset O of a topological space X is said to be maximal open set if any open set which is contains O is O or X.

Definition (1.3)[3]: A proper nonempty closed subset F of a topological space X is said to be minimal closed set if any open set which is contained in F is ϕ or F.

Definition (1.4)[3]: A proper nonempty closed subset O of a topological space X is said to be maximal closed set if any open set which is contains O is O or X.

Definition (1.5)[4]: A subset A of a space X is called a preopen set $A \subseteq \overline{A}^{o}$ .The complement of a preopen set is defined to be a preclosed set.

Definition (1.6)[4]: Let X and Y be topological spaces and f:X→Y is a map then f is called a precontinuous function if $f^{-1}(A)$ is a preopen set in X for every open set A in Y.

2. Minimal and Maximal Preopen Sets

Definition (2.1): A proper preopen subset B of a topological space X is said to be a minimal preopen set if any preopen set which is contained in B is ϕ or B.

Remark (2.2): Minimal open set is minimal preopen set but the converse is not true in general as in the following example.

Example (2.3): Let X={a, b, c}, and $\tau = \{\phi, \{a,b\}, X\}$ then {a} is minimal preopen but not minimal open.

Definition (2.4): A proper nonempty preopen subset B of a topological space X is said to be a maximal preopen set if any preopen set which is contains B is X or B.

Remark (2.5): Maximal open set is maximal preopen set but the converse is not true in general as in the following example.

Example (2.6): In (2.3) {a, c} is maximal preopen but not maximal open.

Definition (2.7): A proper nonempty preclosed subset F of a topological space X is said to be a minimal preclosed set if any preclosed set which is contained in F is ϕ or F.

Remark (2.8): Minimal closed set is minimal preclosed set but the converse is not true in general as in the following example.

Example (2.9): In (2.3) {B} is minimal preclosed but not minimal closed.

Definition (2.10): A proper nonempty preclosed subset F of a topological space X is said to be a maximal preclosed set if any preclosed set which is contains F is X or F.

Remark (2.11): Maximal closed set is maximal preclosed set but the converse is not true in general as in the following example.

Example (2.12): In (2.3) {b, c} is maximal preclosed but not maximal closed.

Remarks (2.13):

(1) The family of all minimal preopen (resp. minimal preclosed) set of a topological space X is denoted by $M_iPO(X)$ (resp. $M_iPC(X)$).

(2) The family of all maximal preopen (resp. maximal preclosed) set of a topological space X is denoted by $M_aPO(X)$ (resp. $M_aPC(X)$).

Remark (2.14): The concept of minimal preopen, maximal preopen, minimal preclosed and maximal preclosed are independent of each other as in the following example.

Example (2.15): let X = {a, b, c} and $\tau = \{\phi, \{a\}, \{a, b\}, X\}$ so $PreO(X)=\{\phi,\{a\},\{a,b\},X\}$, $M_i\,PreO(X)=\{\{a\}\}$, $M_i\,PreC(X)=\{\{c\}\}$, $M_a\,PreO(X)=\{\{a,b\}\}$, $M_a\,PreC(X)=\{\{b,c\}\}$

Table (1)

	{a}	{c}	{a,b}	{b,c}
Minimal preopen	Yes	No	No	No
Maximal preopen	No	Yes	No	No
Minimal preclosed	No	No	Yes	No
Maximal preclosed	No	No	No	Yes

Theorem (2.16): let F be a subset of a topological space X, then F is a minimal preclosed if and only if X-F is maximal preopen set.

Proof: $\Rightarrow$ let F is a minimal preclosed, so X-F is preopen. We have to show that X-F is maximal preopen suppose not, so there is a preopen subset D of X such that $X-F \subset D$ hence $X-D \subset F$ and this contradict being F is minimal preclosed.

$\Leftarrow$ let F be an preclosed subset of X, suppose that there is an preclosed $K \neq \phi$ such that $K \subset F$ thus $X-F \subset X-K$ but X-K is proper preopen set. Contradiction to the assumption of being X-F is maximal preopen.∎

Theorem (2.17): Let U and V be maximal preopen subsets of a Topological space X, then $U \cup V = X$ or U=V.

Proof: if $U \cup V = X$ then the proof is complete.

If not, i.e. $U \cup V \neq X$ so we have to show that U=V.

Since $U \cup V \neq X$ so $U \subset U \cup V$ and $V \subset U \cup V$.

But U is maximal preopen set, so $U \cup V = X$ or $U \cup V = U$

Thus $U \cup V = U$ and so $V \subset U$.

Now since $V \subset U \cup V$ and V is maximal preopen set, so $U \cup V = X$ or $U \cup V = V$, but $U \cup V \neq X$ so $U \cup V = V$ and hence $U \subset V$

Therefore U=V.∎

Theorem (2.18): Let U be a maximal preopen and V be an preopen subsets of a Topological space X then $U \cup V = X$ or $V \subset U$.

Proof: If $U \cup V = X$ then the proof is complete.

If $U \cup V \neq X$ so $U \subset U \cup V$ and $V \subset U \cup V$.

Since U is maximal preopen and $U \subset U \cup V$ so by definition of maximal preopen we have that $U \cup V = X$ or $U \cup V = U$ but $U \cup V \neq X$ so $U \cup V = U$ and hence $V \subset U$.∎

Theorem (2.19): Let U be a maximal preopen subset of a Topological space X with $x \in X/U$ then $X/U \subset V$ for any preopen subset of X with $x \in V$.

Proof: Let $x \in X/U$ and $x \in V$, so $V \not\subset U$, thus by (2.18) we have that $U \cup V = X \Rightarrow (X \setminus U) \cap (X \setminus V) = \phi$

$\Rightarrow X \setminus U \subset V$.∎

Theorem (2.20): let F be a minimal preclosed and K be an preclosed subsets of a Topological space X then $F \cap K = \phi$ or $F \subset K$.

Proof: If $F \cap K = \phi$ then the proof is complete.

If $F\cap K\neq\phi$ then we have to show that $F\subset K$.
Since $F\cap K\neq\phi$ then $F\cap K\subset F$ and $F\cap K\subset K$.
But F is minimal preclosed, so we have $F\cap K=F$ or $F\cap K=\phi$.
Thus $F\cap K=F$
So $F\subset K$.■

Theorem (2.21): let F and K be minimal preclosed subsets of a Topological space X then $F\cap K=\phi$ or $F=K$.

Proof: If $F\cap K=\phi$ then the proof is complete.
If $F\cap K\neq\phi$ then we have to show that $F=K$.
Since $F\cap K\neq\phi$ so $F\cap K\subset F$ or $F\cap K\subset K$.
Since F is minimal preclosed so we have $F\cap K=F$ or $F\cap K=\phi$. But $F\cap K\neq\phi$ hence $F\cap K=F$ which means $F\subset K$.
Now since K is minimal preclosed so we have $F\cap K=K$ or $F\cap K=\phi$. But $F\cap K\neq\phi$ hence $F\cap K=K$ which means $K\subset F$. Therefore F=K. ■

Theorem (2.22): Let U, V and W be maximal preopen subsets of a Topological space X such that $U\neq V$, if $U\cap V\subset W$, then either U=W or V=W.

Proof: Suppose that $U\cap V\subset W$, if U=W then the proof is complete.
If $U\neq W$ we have to show that V=W

$V\cap W=V\cap(X\cap W)$ *Set Theory*
$=V\cap[W\cap(U\cup V)]$ by (2.17)
$=V\cap[(W\cap U)\cup(W\cap V)]$ *Set Theory*
$=(V\cap W\cap U)\cup(V\cap W\cap V)$ *Set Theory*
$=(U\cap V)\cup(V\cap W)$ since $U\cap V\subset W$
$=(U\cup W)\cap V$ Set Theory
$=X\cap V$ since $U\cup W=X$ Thus $V\cap W=V$ implies $V\subset W$ but V is
$=V$
maximal preopen therefore V=W or $V\cup W=X$ but $V\cup W\neq X$ so V=W. ■

Theorem (2.23): U, V and W be maximal preopen subsets of a Topological space X which are different from each other, then $U\cap V\not\subset U\cap W$

Proof:

Let $U\cap V\subset U\cap W$
$\Rightarrow(U\cap V)\cup(W\cap V)\subset(U\cap W)\cup(W\cap V)$
$\Rightarrow(U\cap W)\cup V\subset(U\cap V)\cup W$
$\Rightarrow X\cup V\subset X\cup W$
$\Rightarrow V\subset W$

But V is maximal preopen and W is a proper subset of X so V=U, this result contradicts the fact that U, V and W are different from each other.
Hence $U\cap V\not\subset U\cap W$ ■

Theorem (2.24): Let F be a minimal preclosed subset of a Topological space X , if $x \in F$ then $F \subset K$ for any preclosed subset K of X containing x.

Proof: Suppose $x \in K$ and $F \not\subset K$ so $F \cap K \subset F$ and $F \cap K \neq \phi$ since $x \in F \cap K$

But F is minimal preclosed so $F \cap K = F$. or $F \cap K = \phi$.

hence $F \cap K = F$ which contract the relation $F \cap K \subset F$. Therefore $F \subset K$.■

Theorem (2.25): Let F and $F_\alpha\,(\alpha \in A)$ be minimal β-closed sets if $F \subset \bigcup_{\alpha \in A} F_\alpha$ then there exists $\alpha_O \in A$ such that $F = F_{\alpha_0}$.

Proof: First we have to show that $F \cap F_{\alpha_0} \neq \phi$, suppose that $F \cap F_{\alpha_0} = \phi$ then $F_{\alpha_0} \subset X \setminus F$ and so $F \subset \bigcup_{\alpha \in A} F_\alpha \subset X \setminus F$ which is a contradiction. So $F \cap F_{\alpha_0} \neq \phi$. and hence $F \cap F_{\alpha_0} \subset F$ and $F \cap F_{\alpha_0} \subset F_{\alpha_0}$

since $F \cap F_{\alpha_0} \subset F$ and F is minimal preclosed then $F \cap F_{\alpha_0} = F$ or $F \cap F_{\alpha_0} = \phi$

thus $F \cap F_{\alpha_0} = F$ and hence $F_{\alpha_0} \subset F$. Now since $F \cap F_{\alpha_0} \subset F_{\alpha_0}$ and F_{α_0} is minimal preclosed then $F \cap F_{\alpha_0} = F_{\alpha_0}$ or $F \cap F_{\alpha_0} = \phi$. Thus $F \cap F_{\alpha_0} = F_{\alpha_0}$ and hence $F \subset F_{\alpha_0}$. Therefore $F = F_{\alpha_0}$.■

3. $\mathbf{T_{premin}}$ and $\mathbf{T_{premax}}$ space

Definition (3.1): A topological space X is said to be $T_{pre\min}$ space if every nonempty proper preopen subset of X is minimal preopen set.

Definition (3.2): A topological space X is said to be $T_{pre\max}$ space if every nonempty proper preopen subset of X is maximal preopen set.

Example (3.3): Let X={a, b, } and $\tau = \{\phi, \{a\}, \{b\}, X\}$ thus $\mathrm{Pre}\,O(X) = \tau$, it is clear that {a} and {b} are maximal and minimal preopen sets thus the space X is both $T_{pre\max}$ and $T_{pre\max}$.

Remark (3.4): $T_{pre\min}$ and $T_{pre\max}$ spaces are identical.

Theorem (3.5): A space X is $T_{pre\min}$ if and only if it is $T_{pre\max}$.

Proof: $\Rightarrow$ Let X is $T_{pre\min}$ space. Suppose that X is not $T_{pre\max}$, so there is a proper preopen subset K of X which is not maximal, this mean there exist a preopen subset of X with $K \subset H \neq \phi$. Thus we get that H is not minimal which is contradict of being X is $T_{pre\max}$.

$\Leftarrow$ Let X is $T_{pre\max}$ space. Suppose that X is not $T_{pre\min}$, so there is a proper preopen subset K of X which is not minimal, this mean there exist an preopen subset of X with $\phi \neq H \subset K$. Thus we get that H is not maximal which is contradict of being X is $T_{pre\,max}$. ■

Theorem (3.6): A topological space X is $T_{pre\,min}$ space if and only if every nonempty proper preclosed subset of X is maximal preclosed set in X.

Proof: $\Rightarrow$ let F be a proper preclosed subset of X and suppose F is not maximal.

So there exists an preclosed subset K of X with $K \neq X$ such that $F \subset K$.

Thus $X - K \subset X - F$. Hence X-F is a proper preopen which is not minimal and this contradicts of being X is $T_{pre\,min}$ space.

$\Leftarrow$Suppose U is a proper preopen subset of X. thus X-U is a proper preclosed subset of X, so X-U is maximal preclosed subset of X. and by (2.16) U is minimal preopen . thus X is $T_{pre\,min}$ space. ■

Theorem (3.7): A topological space X is $T_{pre\,max}$ space if and only if every nonempty proper preclosed subset of X is minimal preclosed set in X.

Proof:

$\Rightarrow$ let F be a proper preclosed subset of X, suppose F is not minimal preclosed in X, so there is a proper preclosed subset of X such that $K \subset F$

Thus $X - F \subset X - K$ but X-K is proper preopen in X so X-F is not maximal in X. Contradiction to the fact X-F is maximal preopen.

$\Leftarrow$let U be a proper preopen subset of X, then X-U is a proper preclosed subset of X and so it is minimal preclosed set. By (2.16) we get that U is maximal preopen. ■

Theorem (3.8): Every pair of different minimal preopen sets of $T_{pre\,min}$ are disjoint.

Proof: Let U and V be minimal preopen subsets of $T_{pre\,min}$ space X such that $U \neq V$ to show that $U \cap V = \phi$ suppose not i.e. $U \cap V \neq \phi$.

So $U \cap V \subset U$ and $U \cap V \subset V$. Since $U \cap V \subset U$ and U is minimal preopen then $U \cap V = U$ or $U \cap V = \phi$ thus $U \cap V = U$.

Now since $U \cap V \subset V$ and V is minimal preopen then $U \cap V = V$ or $U \cap V = \phi$ thus $U \cap V = V$.

Hence we get that U=V this result contradicts the fact that U and V are different. Therefore $U \cap V = \phi$. ■

Theorem (3.9): Union of every pair of different maximal preopen sets in $T_{pre\,max}$ space X is X.

Proof: Let U and V be maximal preopen subsets of $T_{pre\,max}$ space X such that $U \neq V$ to show that $U \bigcup V = X$ suppose not i.e. $U \bigcup V \neq X$.

So $U \subset U \bigcup V$ and $V \subset U \bigcup V$.

Since $U \subset U \bigcup V$ and U is maximal preopen then $U \bigcup V = U$ or $U \bigcup V = X$.

Thus $U \bigcup V = U \ldots (1)$.

Now since $V \subset U \bigcup V$ and V is maximal preopen then $U \bigcup V = V$ or $U \bigcap V = X$

thus $U \bigcup V = V \ldots (2)$

Hence from (1) and (2) we get that U=V this result contradicts the fact that U and V are different. Therefore $U \bigcap V = X$.■

4. Continuity with Minimal and Maximal Preopen Sets

Definition (4.1): Let X and Y be topological spaces, a map $f : X \rightarrow Y$ is called minimal precontinuous if $f^{-1}(U)$ is minimal preopen in X for any open subset U of Y.

Example (4.2): Let X = Y = {a, b, c} and $f : (X, \tau) \rightarrow (Y, \sigma)$ is the identity map, where τ={ϕ, {a}, {a, c}, X} and σ={ϕ, {a}, Y} then f is minimal precontinuous since the only proper open subset of Y is {a} and $f^{-1}(\{a\}) = \{a\}$ is minimal preopen in X.

Definition (4.3): Let X and Y be topological spaces, a map $f : X \rightarrow Y$ is called maximal precontinuous if $f^{-1}(U)$ is maximal preopen in X for any open subset U of Y.

Example (4.4): Let X = Y = {a, b, c} and $f : (X, \tau) \rightarrow (Y, \sigma)$ is the identity map, where τ={ϕ, {a}, {b},{a, b}, X} and σ={ϕ, {a, b}, Y} then f is maximal precontinuous since the only proper open subset of Y is {a, c} and $f^{-1}(\{a, b\}) = \{a, b\}$ is maximal preopen in X.

Theorem (4.5): Every minimal precontinuous map is precontinuous.

Proof: Let $f:X\rightarrow Y$ be a minimal precontinuous map and U be open subset of Y. then $f^{-1}(U)$ is minimal preopen in X and so $f^{-1}(U)$ is preopen subset of X.■

Remark (4.6): The converse is not true in general as in the following example.

Example (4.7): Let X = Y = {a, b, c} and $f:(X,\tau)\rightarrow(Y,\sigma)$ is the identity map, where $\tau=\{\phi, \{a\}, \{c\}, \{a, c\}, X\}$ and $\sigma=\{\phi, \{a, c\}, Y\}$ then f is precontinuous but f is not minimal precontinuous since $f^{-1}(\{a,c\})=\{a,c\}$ is not minimal preopen since $\{a\}\in PreO(X)$ and $\phi\neq\{a\}\subset\{a,c\}$.

Theorem (4.8): Let X and Y be topological spaces, if $f:X\rightarrow Y$ is a precontinuous onto map and X is $T_{pre\min}$ space then f is minimal precontinuous.

Proof: It is clear that the inverse image of ϕ and Y are preopen subsets of X. So let U be a proper open subset of Y. Since f is precontinuous so $f^{-1}(U)$ is proper preopen subset of X, but X is $T_{pre\min}$ so $f^{-1}(U)$ minimal preopen.■

Remark (4.9): the converse is not true in general as in the following example.

Example (4.10): In (4.2) f is minimal f-continuous but X is not $T_{pre\min}$.

Theorem (4.11): Let X and Y be topological spaces, if $f:X\rightarrow Y$ is a precontinuous onto map and X is $T_{pre\max}$ space then f is maximal precontinuous.

Proof: It is clear that the inverse image of ϕ and Y are preopen subsets of X. So let U be a proper open subset of Y. Since f is precontinuous so $f^{-1}(U)$ is a proper preopen subset of X but X is $T_{pre\max}$ so $f^{-1}(U)$ is maximal preopen.■

Remark (4.12): the converse is not true in general as in the following example.

Example (4.13): In (4.4) f is maximal precontinuous but X is not $T_{pre\max}$ space.

Theorem (4.14): Every maximal precontinuous map is precontinuous.

Proof: Let $f: X \to Y$ be a maximal precontinuous map and U be open subset of Y. then $f^{-1}(U)$ is maximal preopen in X and so $f^{-1}(U)$ is preopen subset of X.■

Remark (4.15): The Converse is not true in general as in the following example.

Example (4.16): Let X = Y = {a, b, c} and $f:(X,\tau) \to (Y,\sigma)$ is the identity map, then where $\tau=\{\phi, \{a\}, \{a, c\}, X\}$ and $\sigma=\{\phi, \{a\}, Y\}$ then f is precontinuous but f is not maximal precontinuous since $f^{-1}(\{a\}) = \{a\}$ is not maximal preopen since $\phi \neq \{a,c\} \supset \{a\}$.

Remark (4.17): Minimal precontinuous and maximal precontinuous maps are independent of each other and the following examples show that.

Example (4.18): In (4.4) f is maximal precontinuous since $f^{-1}(\{a,c\}) = \{a,c\}$ is preopen but f is not minimal precontinuous.

Example (4.19): In (4.2) f is minimal precontinuous but it is not maximal precontinuous
since $f^{-1}(\{a\}) = \{a\}$ is not maximal preopen in X.

Theorem (4.20): Let $f: X \to Y$ be a map and X and Y be topological spaces, then f is maximal (resp. minimal) precontinuous if and only if $f^{-1}(F)$ is minimal (resp. maximal) preclosed subset of X for each closed subset F of Y.

Proof: $\Rightarrow$ let F be a closed set in Y. thus Y-F is open and so $f^{-1}(Y-F)$ is maximal (resp. maximal) preopen. but $f^{-1}(Y-F) = X - f^{-1}(F)$ so $f^{-1}(F)$ is minimal (resp. maximal) preclosed.■

Theorem (4.21): Let X,Y and Z be topological spaces, if $f: X \to Y$ is a minimal (respect. maximal) precontinuous map and $g: Y \to Z$ is a continuous map then $g \circ f: X \to Z$ is a minimal (resp. maximal) precontinuous map.

Proof: Let U be an open subset of Z, since g is continuous so $g^{-1}(U)$ is an open subset of Y. But f is minimal (respect. maximal) precontinuous thus $f^{-1}(g^{-1}(U)) = (g \circ f)^{-1}$ is a minimal (respect. maximal) preopen subset of X.■

5. Conclusion

In this paper we get some theorems presented to explore many various properties of the minimal preopen and maximal preopen and their complements and we defined two types of topological spaces and finally we defined continuity over the new sets which produced here.

REFERENCES

1. Nakaoka F., and Oda N., " Some applications of minimal open sets", Int. J. Math. Sci. 27-8, 471-476 (2001).
2. Nakaoka F., and Oda N., " Some properties of maximal open sets", Int. J. . Math. Sci. 21, 1331-1340 (2003).
3. Nakaoka F., and Oda N., " On minimal closed sets", Proceeding of Topological Spaces and its Applications, 5, 19-21 (2003).

4. Mashhour, M. E., Abd El-Monsef M. E., El-Deeb S. N., "On pre-continuous and weak pre-continuous mappings", Proc. Math. Phys. Soc. Egypt, 53, 47-53 (1982)

Contrast Enhancement of Different Types Dark Medical Images

Layla H.Abass and Anwar H.Mahdy
Al-Mustansriyah University, College of science Dep. Comp.science
Received 24/3/2013 – Accepted 15/9/2013

الخلاصة

تحسين التغاير هي طريقة لتوضيح التغاير لمعالم الصورة لذلك تحسين الصورة يؤدي الى زيادة وضوحية عناصر الصورة بدون تشويه معالم الاخرى وزيادة جودتها. المشكلة في الصور الطبية هي كيفية معالجة وتحليل تلك الصور (لانها مهمة في المجال التشخيص الطبي)بحيث يمكن ان نحصل على جودة عالية للصورة ومعلومات كافية والتي تفيد في التشخيص والمعالجة.لتقديم طريقة لتحسين التغايرتغطي كل الصورة بما في ذلك المناطق ذات شدة الاضاءة الواطنة(المظلمة)وتحسين الجودة المرئية للصورة.في هذا البحث تم
2-هي اظهار التفاصيل المخفية في الصورة. unsharp masking تحسين التغاير في خطوتين هما 1-
من الصور الطبية . بمدى واسع من التغاير للمعالم وزيادة الوضوحية والتفاصيل باستخدام انواع مختلفة للصور.كل ذلك تتميزبه صور النتائج.

ABSTRACT

Contrast enhancement is a method to expand the contrast of features of interest so that they occupy a larger portion of the displayed gray level range without distortion to other features and the overall image quality. The problem in medical images is how to process and analyze of images (because it is important in medical diagnosis field) so that high quality information can be produced for satisfy disease and treatment. To produce a contrast enhancement recover an image within a given area darkness, also improve visual quality of it. In this paper we proposed a method of contrast enhancement which consists of two steps unsharp masking step and contrast enhancement step then bring out hidden details. We provide experimental results using different kind of medical images, which are hard to be contrasted by other conventional techniques. The output images show a wide variety of features, visible and interpretable to the human eye. Many more details become visible. The resulting images after applying the new proposed contrast are enhanced.

1. INTRODUCTION

Image enhancement processes consist of a collection techniques that seek to enhance the visual appearance of an image or to mutate convert the image to a form better suited for analysis by a human or machine. Image enhancement is applied in every field where images are ought to be understood and analyzed. The principle objective of image enhancement techniques is to process an image so that the result is more suitable than the original image for a specific application [1]. During this process, one or more attributes of the image are modified. The choice of attributes and the method they are modified are specific to a given task [2]. Contrast enhancement is a method to expand the contrast of features of interest so that they occupy a larger portion of the displayed gray level range without distortion to other features and the overall image quality. The goal of contrast enhancement techniques is to determine an optimal transformation function relating original gray level and the displayed intensity such that contrast between adjacent structures in an image is maximally portrayed [3].

Medical imaging modalities such as computed tomography (CT), magnetic resonance imaging (MRI), and digital radiography often contain 12 bit or more significant contrast information .Anatomical tissues may occupy significantly different dynamic ranges on display due to difference of X-ray attenuation .By comparison, the human visual system can only perceive less than 100 different gray levels [4] .Thus, contrast enhancement is usually needed for clinical readings. In some CT radiographs, the features of interest occupy only a relatively narrow range of the gray scale.

The problem of enhancing contrast of images enjoys much attention and spans a wide gamut of applications, ranging from improving visual quality of photographs acquired with poor illumination to medical imaging [5][6] .Common techniques for global contrast enhancements like global stretching and histogram equalization do not always produce good results, especially for images with large spatial variation. A review of traditional contrast enhancement methods for digital radiography can be found in [7].

Medical image processing has experienced dramatic expansion, and has been an interdisciplinary research field attracting expertise from applied mathematics, computer sciences, engineering, statistics, physics, biology and medicine. Computer-aided diagnostic processing has already become an important part of clinical routine. Accompanied by a rush of new development of high technology and use of various imaging modalities, more challenges arise; for example, how to process and analyze of images so that high quality information can be produced for disease diagnoses and treatment. The influence and impact of digital images on modern society is tremendous, and image processing is now a critical component in science and technology. The rapid progress in computerized medical image reconstruction, and the associated developments in analysis methods and computer-aided diagnosis, has propelled medical imaging into one of the most important sub-fields in scientific imaging [8].

1.1 Type of Medical Images

During the past few decades, with the increasing availability of relatively inexpensive computational resources computed tomography (CT), magnetic resonance imaging (MRI), doppler ultrasound and various imaging techniques based on nuclear emission (PET) (positron emission tomography)etc have all been valuable additions to the radiologists arsenal of imaging tools towered ever more detection and diagnosis of disease. Imaging principles are rooted in physics, mathematics, computer science and engineering [9].Some type of medical Image are

1. (MRI). In medicine radio waves are used in magnetic resonance imaging (MRI).This technique places a patient in a powerful magnet and passes radio waves through his or her body in short pulses. Each pulse causes a responding pulse of radio waves to be emitted by the patient's tissues. The location from which these signals originate and their strength is determined by a computer, which produces a two-dimensional picture of a section of the patient. MRI can produce pictures in any plane. MRI images of a human knee and spine [10].

2. X-rays are among the oldest sources of EM (electro magnetic) radiation used for imaging. The best known use of X-rays is medical diagnostics, but they also are used extensively in industry and other areas, like astronomy. X-rays for medical and industrial imaging are generated using an X-ray tube, an X-ray contrast medium is injected through the catheter. This enhances contrast of the blood vessels and enables the radiologist to see any irregularities or blockages. The catheter can be seen being inserted into the large blood vessel on the lower left of the picture. Note the high contrast of the Perhaps the best known of all uses of X-rays in medical imaging is computerized axial tomography. Due to their resolution [10].

3. CAT (computer axial tomography) or CT (computer tomography) scans revolutionized medicine from the moment and CAT image is a "slice" taken erpendicularly through the patient. Numerous slices are generated as the patient is moved in a longitudinal direction. The ensemble of such images [11].

4. Ultrasound imaging is used routinely in manufacturing, the best known applications of this technique are in medicine, especially in obstetrics, and where unborn babies are imaged to determine the health of their development byproduct of this examination is determining the sex of the baby. Ultrasound images are generated using the following basic procedure:

1. The ultrasound system (a computer, ultrasound probe consisting of a source and receiver, and a display) transmits high-frequency (1 to 5 MHz) sound pulses into the body.

2. The sound waves travel into the body and hit a boundary between tissues (e.g., between fluid and soft tissue, soft tissue and bone). Some of the sound waves are reflected back to the probe, while some travel on further until they reach another boundary and get reflected.

3. The reflected waves are picked up by the probe and relayed to the Computer.

4. The machine calculates the distance from the probe to the tissue or organ boundaries using the speed of sound in tissue (1540 m_s) and the time of the each echo's return.

5. The system displays the distances and intensities of the echoes on the screen, forming a two-dimensional image [11].

1.2 Properties of Medical Images

It is generally desirable for image brightness (or film density) to be uniform except where it changes to form an image. There are factors, however, that tend to produce variation in the brightness of a displayed image even when no image detail is present. This variation is usually random and has no particular pattern. In many cases, it reduces image quality and is especially significant when the objects being imaged are small and have relatively low contrast [12].

2- Implementation of Enhancement Technique

In proposed enhancement technique, we used these steps:

The steps of our enhancement technique are as following:

1. Unsharp masking step: Enhances small structures and bring out the hidden details in the image by using unsharp masking. It only sharpens the areas, which have edges or lots of details. Unsharp masking performed by generating

A blurred copy of the original image by using laplacian filter [13], subtracting it from the original image

$$I(i,j) = I_0(i,j) - I_b(i,j) \ldots\ldots\ldots\ldots\ldots\ldots\ldots\ldots\ldots\ldots (1)$$

Where

I (i,j) unsharp masking image, and $I_b(i,j)$ blurred copy image

Multiply the unsharp masking image by a fractional contrasted. In this step, the large features are not changed by much, but the small ones are enhanced. The result is a sharper, more detailed image.

$$g(i,j) = I_0(i,j) + kI(i,j) \ldots\ldots\ldots\ldots\ldots\ldots\ldots\ldots\ldots\ldots (2)$$

Where: g (i, j) is output image

k is scaling constant. Logical values for k vary between 0.2 and 0.7. Recently there was an attempt to perform the sharpening by local analysis of gradients [13].

2. Contrast enhancement step: For a grey scale image sliding 3x3 map mask moves from the left side to the right side of original image horizontally in steps starting from the image's upper right corner. A pixel value in the enhanced widow dependents only on its value that's mean

a. If the interest pixel exceeds a certain value (threshold) its value remain unchanged
b. If the value of the pixel is under the threshold then it will be the process can be described with the mapping function O =*M* (i),

Where

O the new pixel values
i old pixel values
The form of the mapping function M that determines the effect of the operation is:

$$M = i * \frac{c}{1+e^{-i}} \quad \dots\dots\dots\dots\dots\dots\dots\dots\dots\dots\dots\dots\dots (3)$$

According to (eq. 3) mapping function the new value of corresponding pixel will be

$$O = \begin{cases} i & if\ i > t \\ i + \left(i * \dfrac{c}{1+e^{-i}}\right) & if\ i < t \end{cases} \quad \dots\dots (4)$$

Where

c is a contrast factor determines the degree of the needed contrast. After map window reaches the right side, it returns to the left side and moves down a step. The process is repeated until the sliding window reaches the right-bottom corner of the image. Then apply the slider map window as where c is a contrast factor determines the degree of the needed contrast. After map window reaches the right side, it returns to the left side and moves down a step.

3. Results

We have use a robust method for contrast enhancement of dark medical images. The technique is based on the pixels of sharpened version of original image the sharpened version is obtained by using unsharp masking. Then a 3x3-sliding window passes over the sharpened version,. All pixels values go over the threshold remain unchanged, other pixels will remapped according to equation (4). Using two ways to calculated of contrast of (input image and image after implantation algorithm) the values are shown in Table (1). And figers (1, 2, 3, 4) show the enhancement technique applied on different type of medical images.

Table-1:values of contrast for in and out images using two ways to calculated of contrast

Image kind	Image in $Contrast = \frac{L_{max}-L_{min}}{L_{max}+L_{min}}$	Image in $Contrast = \mu/\sigma$	Image out $Contrast = \frac{L_{max}-L_{min}}{L_{max}+L_{min}}$	Image out $Contrast = \mu/\sigma$
Ultrasound1	0.8012	0.7412	0.5777	0.57011
Ultrasound2	0.9616	0.84321	0.4760	0.45255
X-ray1	0.823	0.873	0.643	0.723
X-ray2	0.446	0.423	0.1471	0.1028
MRI1	0.235	0.1854	0.528	0.234
MRI2	0.1764	0.5388	0.1484	0.533
CAT	0.2240	0.226	0.197	0.1706

Discussion

The results from applying our approach on grey scale; medical images show that the technique is robust and able to recover even too dark images from blurring and darkness and form table(1) noted that the values of images contrast decreased after implementation the algorithm and there are several advantages of using this algorithm, including

1-The ability to enhance the performance of any still image regardless of its construction.

2-Provide enhancements that are physically impossible to achieve, beside its ideal for enhancement of all types of medical images

Future Wore

We suggest applying the technique in an iterative manner and show the results on real remote sensing panchromatic images.

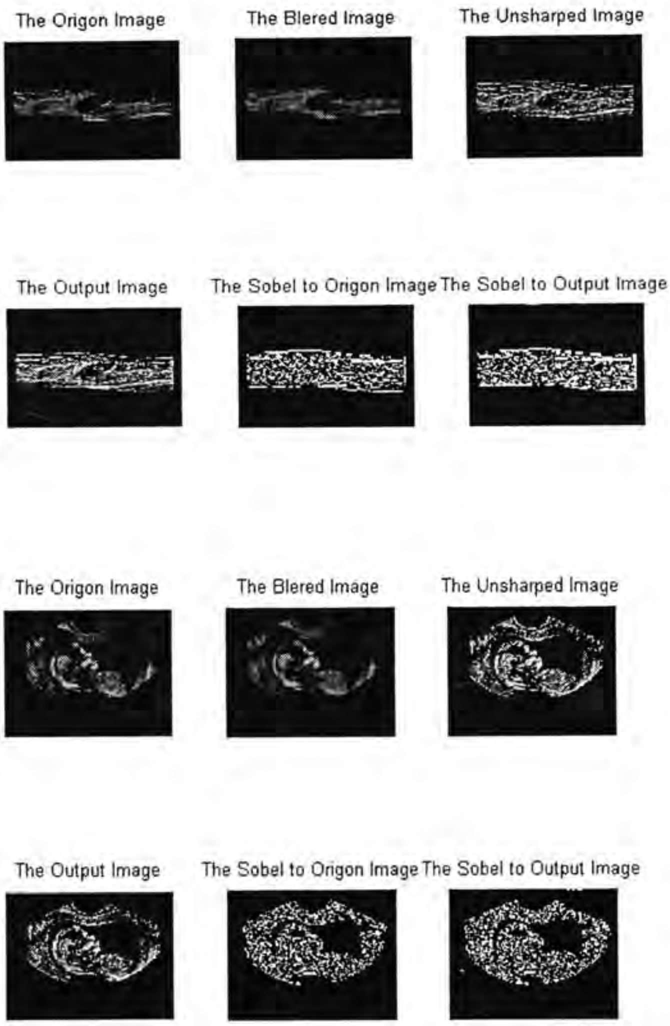

Figure-1: The result of our method ultrasound image.

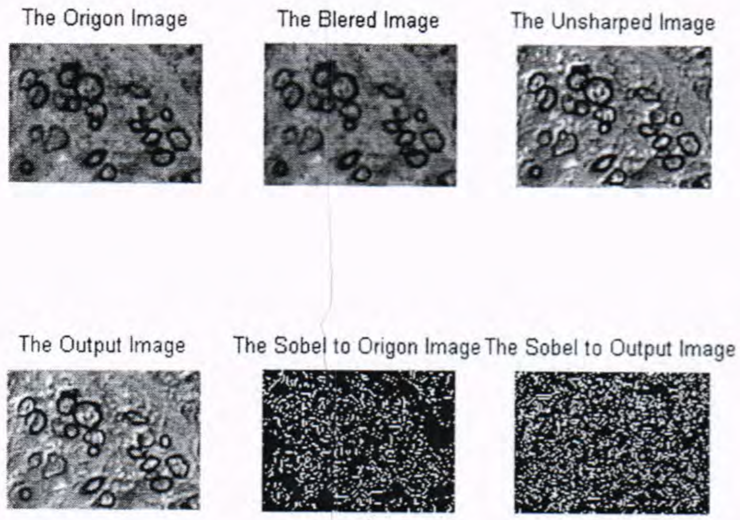

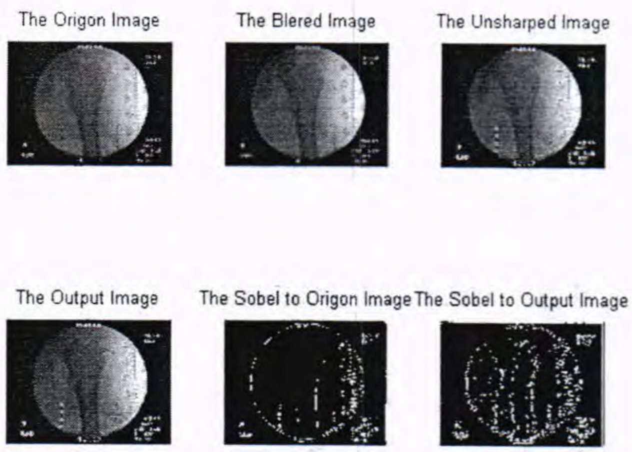

Figure-2: The result of our method on An X-ray images

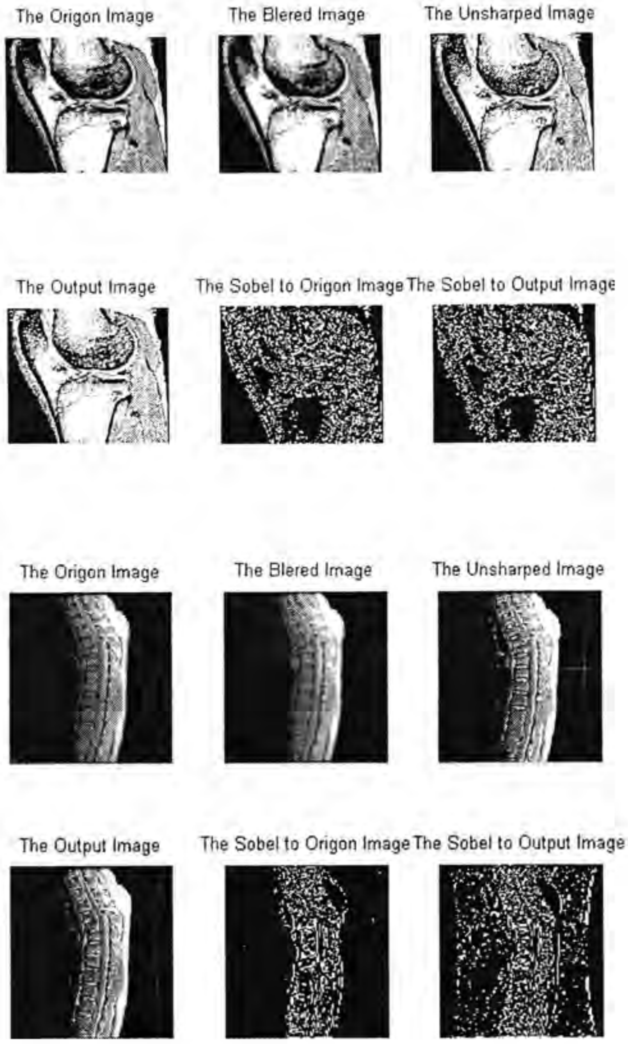

Figure-3: The result of our method on MRI images

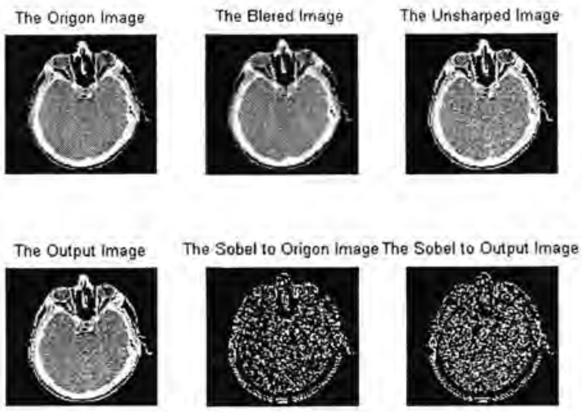

Figure-4: The result of our method on CAT images.

REFERENCES

1. John C. Russ, "The Image Processing Handbook", 3rd Edition CRC Press, LLC ISBN: 1998.
2. Bhabatosh Chanda and Dwijest Dutta Majumder, "Digital Image Processing and Analysis", Book , Second Edition, 2002
3. J. B. Zimmerman, S. B. Cousins, K. M. Hartzell, M. E. Frisse, and M. G. Kahn, "A Psychophysical Comparison of Two Methods for Adaptive Histogram Equalization." Journal of Digital Imaging, vol. 2, pp. 82-91, 1989.
4. J. E. Barnes, "Characteristics and control of contrast in CT.," *Radiographics*, vol. 12, pp. 825-837, 1992.
5. 5. A. K. Jain, Fundamentals of Digital Image Processing. Englewood Cliffs, NJ: Prentice-Hall, 1989.
6. Barten, P. G. 1999,"Contrast sensitivity of the human eye and its effects on image quality", SPIE - The International Society for Optical Engineering, 1999.
7. Boccignone, G., and Picariello, A." Multiscale contrast enhancement of medical images", Proceedings of ICASSP, 1997.
8. DG Nishimura, Principles of Magnetic Resonance Imaging, 1996.
9. Z-P Liang and PC Lautenberg, Principles of Magnetic Resonance Imaging: a signal processing perspective, IEEE press series in biomedical engineering, 1999.
10. N Bloembergen, EM Purcell, and RV Pound, "Relaxation effects in nuclear magnetic resonance absorption," Phys. Rev. vol. 73, pp 679-712, 1948.
11. H. Haubecker, H. Tizhoosh Computer Vision and Application, Academic press, 2000.
12. J.S. Lim, Two-Dimensional Signal and Image processing, Prentice Hall, New Jersey, 1990.
13. J G Leu." Edge sharpening by ramp width reduction", Image and Vision Computing, PAMI-18,, pp. 501-514,2000

Scheduling 0n Single Machine with Release date to Minimize Total Completion times and Maximum Lateness

Manal Ghassan Ahmed, Hanan Ali Cheachan, Tariq S. Abdul-Razaq
Dep. of Mathematics, College of Sciences, University of Mustansiriyah
Received 18/3/2013 – Accepted 15/9/2013

الخلاصه

في هذا البحث قمنا بدراسة مسألة جدولة n من الاعمال على ماكنه واحده لتصغير الكلفة الكلية لمجموع اوقات الاتمام الكلية واكبر تأخير لكل الاعمال مع وقت التحضير . كل عمل i له وقت تحضير r_i ووقت العمل p_i والزمن المثالي d_i لاتمام العمل i .وقمنا بأشتقاق عدة قيود عليا وقيد ادنى واستخدمت هذه القيود في طريقة التفرع والتقييد .ولصعوبة االتعقيدات الحسابيه طورت خوارزميات للحصول على حلول قريبه من الحل الامثل. كل الخوارزميات تم اختبارها والنتأئج التجريبية مدونه بجداول.

ABSTRACT

In this paper, we study the problem of scheduling n jobs on a single machine to minimize total cost of total completion times and maximum lateness of all jobs with release date. Each job i has a release date r_i, processing time p_i and due date d_i. We derive several upper bounds and a lower bound, these bounds are used in a branch and bound solution method. Because of the computational complexity of the problem, near optimal solutions are obtained by developed algorithms. All algorithms are tested and computational experiment are given in tables.

INTRODUCTION

Scheduling theory appeared in 1950. Since this time, problems became more and more complex due to the numerous practical constraints they want to take into account. Surprisingly the most important part of literature on scheduling problems, in practice, is the use of multiple criteria which often allows to compute a more realistic solution for the decision maker. A survey on multicriteria one-machine scheduling problems can be found in [1]. They show that three kinds of problems have been talked. The first one deals with problems in which a lexicographical order of criteria is minimized. The second class of problems considers a convex combination of criteria. The third class of problems concerns the determination of all strict Pareto optima [2].

Scheduling is a decision-making process that plays an important role in most manufacturing and service industries. It is used in procurement and production, in transportation and distribution, and in information processing and communication. The scheduling function in a company uses mathematical techniques or heuristic methods to allocate limited resources to the processing of tasks. A proper allocation of resources enables the company to optimize its objectives and achieve its goals.

Research on multiple and bicriteria scheduling has been scarce, especially when compared to research in single criterion scheduling [3]. Recently, much research has been directed to scheduling problems with multiple criteria. Van Wassenhove and Gelder [4], Hoogeveen [5], Abbas [6].

In this paper, we study bicriteria scheduling problem belong to the second class. In section (2) problem formulation and analysis are given. In section(3), we propose a branch and bound algorithm for optimal solution for the problem. Special cases for the problem is given in section (4). Near optimal solution for the problem obtained by using some algorithms σ given in section(5).In section (6) computational experience is given. The conclusion is given in section(7). Future work is given in section (8).

Formulation of the problem and analysis

The general problem of scheduling jobs on a single machine to minimize the total cost can state as follows: A set of n independent jobs N={1,2,3,…,n} which has to be scheduled without preemption on a single machine that can handle at most one job at a time. The machine is assumed to be continuously available from time zero onwards and no precedence relationship exists between jobs. Each job j, $j \in N$ has an positive integer processing time P_j, a release date r_j and ideally should be completed at its due date d_j. For any given schedule (1,2,…,n), $c_1=r_1+p_1$, $c_j=\max\{r_j, c_{j-1}\}+p_j$ for j=2,3,…,n and $L_{max}=\max_{1\le j\le n}\{l_j\}$, $L_j= c_j - d_j$, j=1,2,…,n. The objective is to find the schedule that minimize the sum of total completion times and maximum lateness costs of all jobs with release dates on a single machine (i.e. minimize the multiple objective function(MOF)denotedby $(\sum_{j=1}^{n} c_j + L_{max})$.

Our scheduling problem can be stated as follows:

Given a schedule δ=(1,2,…,n), then for each job $j \in \boldsymbol{\delta}$ can be calculated the completion time C_j and the lateness L_j. The objective is to find a schedule , $\boldsymbol{\sigma} = (\boldsymbol{\sigma}(\mathbf{1}), \boldsymbol{\sigma}(\mathbf{2}), \dots\dots, \boldsymbol{\sigma}(\boldsymbol{n}))$ that minimize the total cost $Z(\boldsymbol{\sigma})$ where

$$\boldsymbol{Z(\sigma) = \sum_{j=1}^{n} C_\sigma(j) + L_{max}(\sigma)}.$$

Let S be a set of all schedules, then we can formulate our problem in mathematical form as :

$$\left.\begin{array}{ll}
\underset{\sigma\in S}{Min}\{Z(\sigma)\} = \min\limits_{\sigma\in S}\{\sum_{j=1}^{n} C_{\sigma}(j) + L_{max}(\sigma)\} & \\
\text{s.t.} & \\
C_{\sigma(j)} \ge r_{\sigma(j)} + P_{\sigma(j)} & j=1,2,\dots,n \\
C_{\sigma(j)} \ge C_{\sigma(j-1)} + P\sigma(j) & j=2,3,\dots,n \\
C_{\sigma(j)} = \max\{\{C_{\sigma(j-1)}, r_{\sigma(j)}\} + P_{\sigma(j)}\} & j=2,3,\dots,n \\
L\,\sigma(j) \ge C\sigma(j) - d\sigma(j) & j=1,2,3,\dots,n \\
P\,\sigma(j) > 0 & j=1,2,\dots,n \\
r_{\sigma(j)} > 0 & j=1,2,3,\dots,n
\end{array}\right\} \quad (P)$$

The aim of problem (p) is to find a processing order of σ of the jobs on a single machine to minimize the sum of total completion times and maximum lateness (i.e., to minimize $\sum_{j=1}^{n} C\sigma(j) + L\max(\sigma)$, $\sigma \in S$).

The problem (p) is decomposed into two subproblems (sp1) and (sp2) with a simple structure as follows:

$$\left.\begin{array}{ll}
Z1=\min\limits_{\sigma\in S}\{\sum_{j=1}^{n} C\sigma(j)\} & \\
\text{s.t.} & \\
C_{\sigma(j)} \geq r_{\sigma(j)} + P_{\sigma(j)} & j=1,2,..,n \\
C_{\sigma(j)} \geq C\,\sigma(j-1) + P\sigma(j) & j=2,3,\ldots,n \\
C_{\sigma(j)} = \max\{\{C_{\sigma(j-1)}, r_{\sigma(j)}\} + P_{\sigma(j)}\} & j=2,3,\ldots,n
\end{array}\right\} \text{(sp1)}$$

It is clear that subproblem (sp1) is NP-hard [7].

$$\left.\begin{array}{ll}
Z2=\min\limits_{\sigma\in S}\{\max\{L\sigma(j)\}\} & \\
\text{s.t.} & \\
C\,\sigma(j) \geq r\,\sigma(j) + P\sigma(j) & j=1,2,\ldots,n \\
C\,\sigma(j) \geq C\,\sigma(j-1) + P\sigma(j) & j=2,3,\ldots,n \\
L\,\sigma(j) \geq C\sigma(j) - d\sigma(j) & j=1,2,3,\ldots,n \\
P_{\sigma(j)} > 0 & j=1,2,\ldots,n \\
r_{\sigma(j)} > 0 & j=1,2,3,\ldots,n
\end{array}\right\} \text{(sp2)}$$

It is clear that subproblem (sp2) is NP-hard [8].

Then $1/r_i/(\sum_{j=1}^{n} c_{j}+ L_{max})$ is NP-hard.

Theorem 1[6]

If Z1 , Z2 and M are the minimum objective function values of (sp1),(sp2) and (P) respectively then Z1 +Z2 ≤ M .

Branch and Bound (BAB) Method to find Optimal Solution

Our branch and bound algorithm uses a forward sequencing branching rule for which nodes at level (L) of the search tree correspond to initial partial sequenced in the first (L) position .First step in BAB is to calculate upper bound (UB).

Derivation of upper bound

We can find upper bound for our problem (P) by using :

Heuristic 1

Sorting the jobs (1,2,3,…,n) by non-decreasing order of r_j (i.e. $r_1 \leq r_2 \leq \ldots \leq r_n$).

If σ = (σ(1),σ(2),…,σ(n)) is obtained by heuristic 1

Then $UB1=\sum_{j=1}^{n} C\sigma(j)+L\max(\sigma)$.

Heuristic 2

Sorting the jobs by non-decreasing order of r_j+p_j (i.e. $r_1+p_1 \leq r_2+p_2 \leq \ldots\ldots \leq r_n+p_n$).

If $\sigma=(\sigma(1),\sigma(2),\ldots,\sigma(n))$ is obtained by heuristic 2

Then $UB2=\sum_{j=1}^{n} C\sigma(j)+L\max(\sigma)$.

Heuristic3

Choose minimum r_1+p_1 and sorting (n-1) jobs by SPT rule (i.e. $p_1 \leq p_2 \leq \ldots\ldots \leq p_n$).

If $\sigma=(\sigma(1),\sigma(2),\ldots,\sigma(n))$ is obtained by heuristic 3

Then $UB3=\sum_{j=1}^{n} C\sigma(j)+L\max(\sigma)$.

Heuristic 4 [9]

Let t be a time at which a machine is available

$R_j(t)=\max(t,r_j)$ the earliest beginning time of job j at time t.

$C_j(t)=R_j(t)+P_j$ the earliest completion time of job j at time t.

$G(j,t)=R_j(t)+C_j(t)$

Given a set of jobs $N=\{1,2,\ldots,n\}$

Step 1: Initialized t=0, $A=\{1,2,\ldots,n\}$ and $\sigma=\emptyset$.

Step 2: Select job j with $\min_{\sigma\in A} G(j,t)$.Break ties by choosing j within{min $R_j(t)$}, and further ties by choosing j with min d_j.

Step 3: Update t, A and σ, such that $t=C_j(t)$, $A=A-\{j\}$, $\sigma=(\sigma,\sigma(j))$

Step 4: If $A\neq\emptyset$, return to step 2.

Step 5: Compute $UB4=\sum_{j=1}^{n} C\sigma(j)+L\max(\sigma)$

Then $UB=\min\{UB1,UB2,UB3,UB4\}$.

The second step in BAB method is calculate lower bound (LB).

Derivation of lower bound

A lower bound for problem (P) is based on decomposition (P) into two subproblems (sp1) and (sp2) as shown in section (2), then calculate Z1 to be the lower bound for sp1 and Z2 to be the lower bound for sp2 , then applying (theorem 1) to get a lower bound (LB) for our problem (P).

For subproblem (sp1) we obtained the lower bound by using the lower which proposed by Al-Zuwaini(2000)[10] depend on relaxation of the constrained on the jobs, that is relaxed the release date, then

$$LB(sp1)=nr^*+\alpha-R$$

Where $r^* = \min_{j \in N}\{r_j\}$, $R = \sum_{j=1}^{n} r_j$ and α be an optimal solution for $1/r_i=0/\sum C_i$ (i.e. α is obtained by SPT rule).

For the subproblem sp2 , we relaxed the release date and the problem become $1/r_i=0/L_{max}$, then sorting the jobs by EDD rule (i.e. $d_1 \leq d_2 \leq \ldots \leq d_n$) and calculate $L_{max} = \max\{L_i\} = \max\{C_i - d_i\}$, $LB(SP2) = L_{max}$.

Then $LB = LB(sp1) + LB(sp2)$.

Special cases for the problems

1- If $r_i = r$, $d_i = d$ $\forall i=1,2,3,\ldots,n$ then the optimal solution for the resulting problem obtained by SPT rule , L_{max}= constant for all sequences = $(\sum P_i + r - d)$.

2- If $r_i=r$, $p_i=p$, $d_i=d$ then any schedule is optimal for our problem.

3- If $r_i=r$, $p_i=p$ $\forall i=1,2,3,\ldots,n$, then $\sum C_i$= constant for all sequences , EDD schedule gives optimal L_{max} .

4- If $r_i=r$ $\forall i=1,2,3,\ldots,n$ then SPT,EDD schedule gives optimal for our problem.

and max $L_{max} = r + \sum P_i - d_{min}$

min $L_{max} = r + \sum P_i - d_{max}$.

5- If $r_i=r$, d_i= constant = $\sum P_i + r$ then $L_{max}=0$ for all sequences and the optimal solution is obtained by SPT rule .

6- If r = constant , $d = np_i$ $n > 1$, then SPT rule is optimal for $\sum ci$ and L_{max}.

Local Search Heuristic Method

In this section we study local search techniques which are useful tools for solving single machine scheduling problem

Local search is an iterative algorithm that moves from one solution s to another s' according to some neighborhood structure. Local search provides a robust approach to obtain high quality solutions to problems of a realistic size in reasonable time.

Local search procedure usually consists of the following steps.

1. Initialization. Choose an initial schedule s to be the current solution and compute the value of the objective function $F(s)$.
2. Neighbor Generation. Select a neighbor s' of the current solution s and compute $F(s')$.
3. Acceptance Test. Test whether to accept the move from s to s'. If the move is accepted, then s' replaces s as the current solution; otherwise s is retained as the current solution.
4. Termination Test. Test whether the algorithm should terminate. If it terminates, output the best solution generated; otherwise, return to the neighbor generation step.

We assume that a schedule is represented as a permutation of job numbers $(j_1, j_2, \ldots, j_n)$. This can always be done for a single machine processing system or for permutation flow shop; for other models more complicate structures are used.

In Step(1), a starting solution can be specified by a random job permutation. If local search procedure is applied several times, then it is reasonable to use random initial schedules.

To generate a neighbor s' in Step(2), a neighborhood structure should be specified beforehand. Often the following types of neighborhoods are considered:

- *transpose neighborhood* in which two jobs occupying adjacent positions in the sequence are interchanged:
$(1, 2, 3, 4, 5, 6, 7) \rightarrow (1, 3, 2, 4, 5, 6, 7)$;
- *swap neighborhood* in which two arbitrary jobs are interchanged:
$(1, 2, 3, 4, 5, 6, 7) \rightarrow (1, 6, 3, 4, 5, 2, 7)$;
- *insert neighborhood* in which one job is removed from its current position and inserted elsewhere:
$(1, 2, 3, 4, 5, 6, 7) \rightarrow (1, 3, 4, 5, 6, 2, 7)$.

Neighbors can be generated randomly, systematically, or by some combination of the two approaches.

In Step (3), the acceptance rule is usually based on values $F(s)$ and $F(s')$ of the objective function for schedules s and s'. In some algorithms only moves to 'better' schedules are accepted (schedule s' is better than s if $F(s') < F(s)$); in others it may be allowed to move to 'worse' schedules. Sometimes "wait and see" approach is adopted.

The algorithm terminates in Step(4) if the computation time exceeds the prespecified limit or after completing the prespecified number of iterations.

Threshold Acceptance Method (TH)[11]:

A variant of simulated annealing is the threshold acceptance method (Brucker [11]). It differs from simulated annealing only by the acceptance rule for the randomly generated solution $s' \in N$. s' is accepted if the difference $F(s') - F(s)$ is smaller than some non-negative threshold t. t is a positive control parameter which is gradually reduced.

The threshold acceptance method has the advantage that they can leave a local minimum. They have the disadvantage that it is possible to get back to solutions already visited. Therefore oscillation around local minima is possible and this may lead to a situation where much computational time is spent on a small part of the solution set. For details of threshold acceptance structure see [11].

Tabu Search (TS)[12]:

The use of the tabu search was pioneered by Glover [12] who from 1994 onwards has published many articles discussing its numerous applications. Others were quick to adopt the technique which has been used for such purposes as sequencing, scheduling, oil exploration and routing.

The properties of the tabu search can be used to enhance other procedure by preventing them becoming stuck in the regions of local minima. The tabu search utilizes memory to prevent the search from returning to a previously explored region of the solution space too quickly. This is achieved by retaining a list of possible solutions that have been previously encountered. These solutions are considered tabu-hence the name of the technique. The size of the tabu list is one of the parameters of the tabu search.

The tabu search also contains mechanism for controlling the search. The tabu list ensures that some solution will be unacceptable; however, the restriction provided by the tabu list may become too limiting in some cases causing the algorithm to become trapped at a locally optimum solution. The tabu search introduces the notion of aspiration criteria in order to overcome this problem. The aspiration criteria over-ride the tabu restrictions making it possible to broaden the search for the global optimum.

An initial solution is generated (usually randomly). The tabu list is initialized with the initial solution. A number of iterations are performed which attempt to update the current solution with a better one, subject to the restriction of the tabu list. A list of candidate solution is proposed in every iteration. The most admissible solution is selected from the candidate list. The current solution is updated with the most admissible one and the new current solutions added to the tabu list. The algorithm stops after a fixed number of iterations or when a better solution has been found for a number of iterations. For more details of a generic tabu search see [12].

Memetic Algorithm Approach (MA)[13]:

Memetic algorithms (MA), combines the recognized strength of the population-based methods with the intensification capability of a local search. In an MA, all individuals of the population evolve solutions until they become a local minima of a certain neighborhood (or highly evolved solutions of individual search strategies), i.e., after the recombination and mutation steps, a local search is applied to the resulting solutions. A more formal introduction to MA and polynomial merger algorithms can be found in Moscato [13].

The initialization part begins at initialize Population and ends just before the repeat command. This part is responsible for the generation, optimization and evaluation of the initial population (*Pop*). The second part includes the so-called 'generation loop'. At each step, two parent configurations are selected for recombination and an offspring is produced and, if selected to mutate, it suffers a mutation process. The next steps are local search, evaluation and insertion of the new solution into the population. If the population is considered to have lost diversity, a mutation process is applied on all individuals except the best one. Finally, a termination condition is checked. For more details of pseudo-code of a memetic algorithm can found in [13].

The local search methods (TH), (TS) and (MA) stopped when iteration =500 iterations.

Computational experience

An intensive work of numerical experimentations has been performed. We first present how instances (tests problem) can be randomly generated.

There exists in the literature a classical way to randomly generate tests problem of scheduling problems.

- The processing time P_i is uniformly distributed in the interval [1,10].
- The release date r_i is uniformly distributed in the interval [1,10].
- The due dates d_i are uniformly distributed in the interval $[P(1-TF-RDD/2), P(1+TF+RDD/2)]$; where $P=\sum P_i$, depending on the relative range of due date (RDD) and on the average tardiness factor (TF). For both parameters, the values 0.2 , 0.4 , 0.6 , 0.8 ,1.0 are considered. For each selected value of n two problems were generated for each of the values of parameters producing 10 problems for each values of n.

The BAB algorithm was tested in Fortran Power Station and local search methods (Threshold Acceptance Method (TH) Tabu Search (TS) Memetic Algorithm Approach (MA)) were tested by coding then in Matlab R2009b and running on Pentium (R) at 2.20 GHz with Ram 2 GB computer processor-type PDCT 4400. In table (1) n = 8 jobs and 11 jobs we list 10 problems for each value of n. Test problems are tested to show the efficiency of our lower bound (LB) used in BAB algorithm to obtain the optimal solution. Results of comparing the lower bound , upper bounds and the optimal solutions are given in table (1). The first column is the number of problems. The second column gives the value of an optimal solution found by using BAB algorithm. The third column gives the value of the initial lower bound (ILB). The fourth, fifth, six, seven columns give the value of our upper bounds (UB1,UB2,UB3,UB4). The eight column gives the number of nodes (Nodes). The nine column gives the time in seconds (Time).

Table-1:The performance of initial lower bound, upper bounds, number of nodes and computational time in seconds of BAB algorithm.

N	Number	Opt.	ILB	UB1	UB2	UB3	UB4	Nodes	Time
8	1	135	89	169	143	166	152	22692	0.1598
	2	118	66	134	132	160	128	21792	0.00083
	3	170	121	219	195	205	188	23104	0.00066
	4	275	219	286	296	299	283	28960	0.000666
	5	242	194	309	265	257	255	28320	0.00050
	6	117	69	133	127	180	136	17757	0.04933
	7	153	104	188	170	175	182	19323	0.01433
	8	204	148	247	213	212	212	260076	0.01766
	9	191	124	232	210	243	194	26969	0.000833
	10	274	211	285	286	288	288	28960	0.00900
11	1	253	205	380	313	355	291	17132069	0.409000
	2	387	305	477	429	395	388	27607860	0.63200
	3	216*	216	331	308	282	297	15787054	0.38600
	4	367	278	482	453	394	367	23622829	0.544333
	5	397	284	518	489	512	405	20628934	0.4826667
	6	173	116	225	184	211	194	11255923	0.28750
	7	285	214	394	327	391	305	15461978	0.37800
	8	340	281	426	359	355	358	22235133	0.52366
	9	259	162	334	278	319	291	11423946	0.290166
	10	324	234	443	400	411	325	21960225	0.528333

Opt. = The optimal value obtained by BAB algorithm.
ILB = Initial lower bound.
UB1,UB2,UB3,UB4 = Upper bounds.
Nodes = The number of generated nodes.
Time = Computational time in seconds.
* = The optimal value equal to initial lower bound.

Table (1) shows that the lower and upper bounds, the number of nodes and computational time for the 10 problems of n=8 , n=11 jobs, we observe that whenever n increases the number of nodes and computational time increase.

Table-2: comparison optimal solutions in BAB with Threshold Acceptance Method, Tabu Search and Memetic Algorithm.

N	Number	Optimal	TH	TS	MA
10	1	328	340	340	340
	2	210	246	246	210
	3	271	300	300	280
	4	213	224	224	224
	5	263	283	284	284
	6	260	300	300	263
	7	251	292	292	251
	8	211	212	212	212
	9	257	265	265	257
	10	336	380	378	354
No. of optimal			-	-	3

Optimal = Optimal solution in BAB.
TH = Threshold Acceptance Method .
TS=Tabu Search.
MA= Memetic Algorithm.

Comparative Results for Local Search Methods

Table (3) shows the comparative of local search methods which are TH, TS and MA .

The results in table (3) show that (MA) has good performance results, followed by (TH) and (TS).

Table-3: comparison between Local Search Methods

N = 50				
N	MA	TH	TS	Best
1	4525	4664	4484	4525
2	5129	5256	5185	5129
3	6636	6791	6859	6636
4	5220	5304	5229	5220
5	5379	5390	5325	5325
6	5043	5181	5126	5043
7	5694	5901	5923	5694
8	5276	5464	5435	5276
9	5031	5120	5127	5031
10	4451	4610	4681	4451
No. of best	9	-	1	-
Av. time	0.282623	0.009904	0.014296	-
N = 200				
1	83844	84856	86453	83844
2	87318	91275	88264	87318
3	87825	89450	87417	87417
4	88496	87028	89707	87028
5	90988	89366	90079	89366
6	84250	84056	86412	84056
7	84473	85929	85617	84473
8	85334	90175	88939	85334
9	93733	93789	93939	93733
10	82144	83803	83566	82144
No. of best	6	3	1	-
Av. time	1.265881	0.01451	0.030966	-
N = 1000				
1	2492995	2490916	2516663	2490916
2	2496571	2567825	2549667	2496571
3	2488072	2476684	2490617	2476684
4	2473856	2493724	2497602	2473856
5	2486050	2533676	2537109	2486050
6	2448095	2523447	2504914	2448095
7	2523077	2618261	2574040	2523077
8	2375832	2423735	2418723	2375832
9	2418306	2404481	2417588	2404481
10	2550317	2539757	2521801	2521801
No. of best	6	3	1	-
Av. time	7.962432	0.037203	0.196053	-
N = 2000				
1	10180780	10451115	10428029	10180780
2	10492722	10622499	10503469	10492722
3	10640560	10742138	10701567	10640560
4	10595684	10597336	10641069	10595684
5	10470588	10508482	10606767	10470588
6	10571121	10769029	10706307	10571121
7	10144201	10325587	10366143	10144201
8	10626555	10660926	10657006	10626555
9	10355671	10658294	10663512	10355671
10	10305168	10427466	10410195	10305168
No. of best	10	-	-	-
Av. time	22.74968	0.06635	0.466959	-

N=5000				
1	67160733	67096125	67313807	67096125
2	66594548	67080140	67084417	66594548
3	67230227	67491103	67286350	67230227
4	67099756	67579581	67581732	67099756
5	66919533	68159105	67892903	66919533
6	67390319	67445367	67340144	67340144
7	67292694	67618130	67480314	67292694
8	67166577	67288419	67332743	67166577
9	66543462	68262964	68278332	66543462
10	67079040	68339866	68247116	67079040
No. of best	8	1	1	-
Av. time	114.9944	0.153073	1.256968	-

MA= Memetic Algorithm.
TH = Threshold Acceptance Method .
TS=Tabu Search.
Best = The best solution by using MA, TH and TS.
No. of best = Number of best solutions.
Av. time = Average time of ten examples.

It is clear from the results in table (2) and (3) algorithm MA is the best in case of number of best as well as average time.

CONCLUSIONS

In this study, the problem of scheduling jobs on one machine to minimize bi-criteria with release date is considered. The two criteria to be minimized are $\sum C_i$ and L_{max}.

We present a Branch and Bound algorithm to find optimal solution for the problem of minimizing a linear function (i.e., $\sum C_i + L_{max}$). A computational experiment for BAB algorithm on a large set of test problems are given and BAB algorithm solve our test problem up to (11) jobs . The NP–hardness of this problem and the optimal solutions of the BAB algorithm are not always quickly. Hence , this problem is solved by using local search methods Memetic Algorithm , Threshold Acceptance Method and Tabu Search. Also , we report on the results of extensive computations test of local search methods.

The main conclusion to be drawn for our computation results is that MA is more effective method for our problem followed by TH and TS. Whereas the computational time of (TH) is very small followed by the computational times of (TS) and (MA).

Future Work

An interesting future research topic would involve experimentation with the following problems:

$F2/ r_i / \sum C_i + L_{max}$.

$1 /r_i / \sum C_i + L_{max} + E_{max}$.

REFRENCES

1. Hoogeveen, J.A., "Single machine bi-criteria scheduling", PhD Dissertation, Center for mathematics and Computer science, Amsterdam. The Netherlands, (1992).
2. T'kindt, V. and Billaut, J.C., "Some guidelines to solve multicriteria scheduling problems", IEEE , 463-468 (1999).
3. Ozgur Uysal and Serol Bulkan " Comparison of Genetic Algorithm and Particle Swarm Optimization for Bicriteria Permutation Flowshop Scheduling Problem" International Journal of Computational Intelligence Research. ISSN 0973-1873 Vol.4, No. 2, pp.159-175, (2008).
4. Van Wassenhove L.N ana Gelder L.F. "Solving a bicriterion scheduling problem" European Journal of Operation Research, 4,42-48 (1980).
5. Hoogeveen J.A. "Invited Review Multicriteria Scheduling" European Journal of Operation Research,167,592-623 (2005).
6. Abbas, I.T., "The performance of multicriteria scheduling in one machine", M.Sc. Thesis Univ.of Al-Mustansiriyah,Colloge of Science, Dept. of Mathematiccs (2009).
7. Lee C.V, Vairaktarakis GL.," Complexity of single machine Hierarchical scheduling : a survey complexity in numerical optimization" , 19, 269-298, world scientific (1993).
8. Lenstra J.K.,Rinnooy Kan A.H.G and Brucker P."Complexity of machine scheduling problems, Annals of Discrete Mathematics 1,343-362.
9. Husein N.A. "Machine Scheduling Problem to Minimize Multiple Objective Function" . MSc. Thesis. College of Education, Ibn AL-Haitham, University of Baghdad, (2012).
10. Al-Zuwaini M. K., "Single machine scheduling to minimize total cost of flow time with unequal ready times", Journal of Basrah Researches, V.25,Par.3,94-108 (2000).
11. Brucker P., "Scheduling Algorithms", Springer Berlin Heidelberg New York, Fifth Edition , 2007.
12. Glover, F., "A user's guide to tabu search", Annals of Operations Research, Vol.41, PP.3-28, 1994.
13. Moscato, P. "On evolution, search, optimization, genetic algorithm and martial arts: toward memetic algorithms", Caltech concurrent computation program c3p Technical Report, California, 826(1989).

Purely Baer Modules

Mehdi S. Abbas and Ali H. Al-saadi
Department of Mathematics, College of Science, Mustansiriya University
Received 27/3/2013 – Accepted 15/9/2013

الخلاصة

في هذا العمل، عرضنا مفهوم خاصية بير النقية على المقاسات كأعمام لخاصية بير. هذا المفهوم يقوم على دراسة العلاقة بين المقاسات وحلقات تشاكلاتها الذاتية من خلال نقاوة التالفات. بينا أن مركبات الجمع المباشر تتوارث هذه الخاصية، وأن كل زمرة أبدالية منتهية التولد تكون بير أذا وفقط أذاكانت بير نقية أذا وفقط أذا كانت أما شبه بسيطة أو عديمة الألتواء. وفرنا أمثلة تبين أن الجمع المباشرلمقاسات بير النقية لا تكون كذلك. لكن الجمع المباشر لمقاسات بير نقية المتشاكلة تقابليا تبادليا تكون بير نقية، وأن كل مقاس طليق على حلقة بير نقية يكون بير نقيا. أعطينا عديد من الخواص والتوصيفات لمقاسات بير النقية. قمنا بتوسيع بعض النتائج المفيدة على حلقات بير الى المقاسات.

ABSTRACT

In this work, we introduced the notion of purely Baer property of modules as a generalization to that of Baer property. This notion depends on studying the relation between the modules and their endomorphism rings through the purity of annihilators. We show that direct summands inherit this property and that, every finitely generated abelian group is purely Baer if and only if it is semi-simple or torsionfree. We provided examples to show that direct sums of purely Baer modules are not so. But arbitrary direct sum of matually subisomorphic purely Baer modules is purely Baer, and that every free module over purely Baer ring is purely Baer. We give number of characterizations and properties of purely Baer modules and extend some useful results of Baer rings to the general module theoretic setting.
(2010) Mathematics Subject Classification: 16D10 , 16D50

INTRODUCTION

All the rings are assumed to be with unit, and not necessarily commutative. The modules are unital right modules. We usually denote the base ring by R, the module by M and its endomorphism ring by $S = \mathrm{End}_R(M)$. The right annihilator of $X \subseteq M$ in R (i.e. all elements $r \in R$ so that $Xr = \mathbf{0}$) is denoted by $r_R(X)$, the left annihilator of $X \subseteq M$ in S (i.e. all elements $\alpha \in S$ so that $\alpha X = 0$) is denoted by $l_S(X)$; the right annihilator of $T \subseteq S$ in M (i.e. all elements $m \in M$ so that $Tm = \mathbf{0}$) is denoted by $r_M(T)$ and the left annihilator of $P \subseteq R$ in M (i.e. all elements $m \in M$ so that $mP = \mathbf{0}$) is denoted by $l_M(P)$.

A submodule N of an R-module M is called essential in M (or M is essential extension of N), if N has non-trivial intersection with every non-zero submodule of M. N is closed in M, if N has no proper essential extension in M.

C.S.Roman in [1] introduced and studied Baer modules as a generalized case of Baer rings. An R-module M is called Baer module, if for each left ideal A of S, $r_M(A)$ is a direct summand in M. He gave a number of very interesting properties of Baer modules.

The notion of purity for abelian groups was generalized to modules over arbitrary rings in several ways, of which the best-known is Cohns purity [2]. A submodule N of M is pure if the sequence $0 \rightarrow N \otimes E \rightarrow M \otimes E$ is exact for every R-module E. This is equivalent to saying that for each $n_j = \Sigma m_i r_{ji} \in N$ where $r_{ji} \in R$, $m_i \in M$, $j = 1,\ldots,k$, there exist $x_i \in N$, $i = 1,\ldots,n$ such that $n_j = \Sigma x_i r_{ji}$ for each j. It is well-known that every direct summand of a module is pure [3].

In this work, we introduced and studied purely Baer modules as a generalization of Baer modules. An R-module M is purely Baer, if the right annihilator in M of any left ideal of S is pure. It is clear that Baer

For properties and characterizations of purely Baer property of modules More generally, we introduced purely Baer module relative to a submodule, we proved that an R-module M is purely Baer if and only of for every direct summands A and B of M with A is a subset of B, A is purely Baer relative to B. Conditions are investigated under which purely Baer property is equivalent to the regular property in the sense of Fieldhouse [5]. Direct summands inherit the property of purely Baer, unlike for direct sums, so conditions are considered under which finite direct sums have this property. Regular rings are characterized as those every module is purely Baer. Finally we describe purely Baer modules in the case of finitely generated modules over principal ideal domains.

$N \leq M$ means N is a submodule of M, $N \overset{e}{\leq} M$ means N is essential in M, $N \overset{c}{\leq} M$ means N is closed in M, $N \leq^{\oplus} M$ means N is direct summand of M, $N \overset{P}{\leq} M$ means N is pure in M.

PURELY BAER PROPERTY

Firstly we introduce the following generalization of Baer modules.

Definition (2.1) : An R-module M is called purely Baer if for each left ideal I of $S = End_R(M)$, $r_M(I) \leq^P M$. A ring R is called purely Baer ring if R_R is purely Baer R-module.

All Baer modules are purely Baer. The converse is not true by the following example which is appear in([3].Example7.54) and we list it as a counter example. Of course, a Baer ring (e.g., a domain) need not be von Neumann regular. We construct here a ring R that is von Neumann regular and hence it is purely Baer, but not Baer. But R is necessarily neither right self-injective nor left self-injective . Let F be a field, and $A = F \times F \times \ldots$. This ring is commutative, von Neumann regular, and is Baer ring by ([3],Examples(7.47)-(4)). Now let R be the subring of A consisting of "sequences" $(a_1, a_2, \ldots) \in A$ that are eventually constant, that is there exist a positive integer k such that $a_n = b\ \forall n \geq k$. For any $(a_1, a_2, \ldots) \in R$, define $x = (x_1, x_2, \ldots)$ by : $x_n = a_n^{-1}$ *if* $a_n \neq 0$, and $x_n = 0$ if $a_n = 0$. Then $x \in R$ and $a = a\,x\,a$. Therefore, R is von Neumann regular and hence R is purely Baer. Let $e_i \in R$ denote the i^{th} "unit vector" $(0,0,\ldots,0,1,0,\ldots)$, and let $N = \{e_1, e_3, e_5, \ldots\}$, that is N consists of e_i with i is odd. Then $r_R(N)$ consists of sequences $a = (a_1, a_2, \ldots)$ which are eventually zero, and such that $a_n = 0$ for n odd. Now to show that $r_R(N)$ cannot be principal ideal of R. Suppose that $r_R(N) = bR$ for some $b = (b_1, b_2, \ldots) \in r_R(N)$, then there exist a big integer k_0 such that $b_n = 0$ for $n \geq k_0$. now for each $i = 2, 4, \ldots$, the i^{th} "unit vector" $e_i \in r_R(N)$. In particular $e_{2k0} \in r_R(N)$, thus $e_{2k0} = br$ for some $r \in R$, implies that $1 = b_{2k0}\, r_{2k0} = 0$, a contradiction, hence $r_R(N)$ can not generated by an idempotent so $r_R(N)$ can not be a direct summand. Thus R is purely Baer ring which is not Baer, so the purely Baer property is a proper generalization of Baer property.

Recall that an R-module M is F-regular, if each submodule of M is pure [4]. It is clear that every F-regular module is purely Baer. The converse is not true for example $\mathbf{Z}$ as $\mathbf{Z}$-module.

A submodule of purely Baer module may not to be purely Baer module. Let M be a nonsingular module over a commutative ring R such that M is not purely Baer (see below) and let $E(M)$ be the injective hull of M and M is essential submodule of $E(M)$. Then $E(M)$ is nonsingular([5],proposition 1.22), but $E(M)$ is injective and hence $E(M)$ is extending, thus $E(M)$ is Baer module by ([1],theorem 2.2.2) and hence $E(M)$ is purely Baer while M is not purely Baer. As an application of above let K be any field, consider the factor ring $R = K[x,y]/(xy)$, where $K[x,y]$ is the polynomial ring of two commuting indeterminates x, y, and (xy) is the ideal of $K[x,y]$ generated by xy . R is nonsingular and $r_R(\bar{x}) = (\bar{y})$ is not pure in R.

It is an easy matter to show that isomorphic R-module of purely Baer R-module is purely Baer, but homomorphic image may not, Z as Z-module is purely Baer, but Z_4 is not, since for the endomorphism of Z_4, f which defined by f(x)=2x for x in Z_4, we have 2Z, which the annihilator of f in Z_4, which is not pure in Z_4.

In the following we characterize purely Baer modules:

Theorem (2.2) : *An R-module M is purely Baer iff for each family* $\{\alpha_\lambda\}_{\lambda \in \Lambda}$ *of endomorphisms of M, where* Λ *be an index set,* $\bigcap_{\lambda \in \Lambda} Ker(\alpha_\lambda) \leq^P M$.

Proof: Given M is purely Baer and let $\{\alpha_\lambda\}_{\lambda \in \Lambda}$ be a family of endomorphisms of M, where Λ be an index set . Let I be the left ideal of $S = End_R(M)$ generated by the family $\{\alpha_\lambda\}_{\lambda \in \Lambda}$, since M is purely Baer then $r_M(I) \leq^P M$, but each $\alpha_\lambda \in I$, then $r_M(I) \leq r_M(\alpha_\lambda) = Ker(\alpha_\lambda)$, thus

$r_M(I) \leq \cap_{\lambda\in\Lambda}\ Ker(\alpha_\lambda)$. Now if $m \in \cap_{\lambda\in\Lambda}\ Ker(\alpha_\lambda)$ then $\alpha_\lambda(m) = 0$ for each $\lambda \in \Lambda$, if $\psi \in I$ implies $\psi = \sum_{i=1}^{n} s_i\alpha_i$ where $s_i \in S$ and $\alpha_i \in \{\alpha_\lambda\}_{\lambda \in \Lambda}$, for each $i = 1, \ldots, n$, then $\psi(m) = \sum_{i=1}^{n} s_i\alpha_i(m) = \sum_{i=1}^{n} s_i(0) = 0$ implies $m \in r_M(I)$, Then we have $r_M(I) = \cap_{\lambda\in\Lambda}\ Ker(\alpha_\lambda) \leq^P M$.
Conversely, let I be a left ideal of S, then $r_M(I) = \cap_{\alpha\in I} Ker(\alpha)$. By hypothesis $r_M(I) \leq^P M$.

Corollary (2.3) : *If M is purely Baer R-module and $\{A_\alpha\}_{\alpha\in\Lambda}$ be a family of direct summands of M, where Λ be an index set, then $\cap_{\alpha\in\Lambda} A_\alpha \leq^P M$*
***Proof* :** Since for each $\alpha \in \Lambda$ there is a submodule B_α of M such that $M = A_\alpha \oplus B_\alpha$. Now consider $\pi_\alpha : M \longrightarrow M$ be the projection map onto B_α, since M is purely Baer then by Theorem(2.2) we have that $\cap_{\alpha\in\Lambda} Ker(\pi_\alpha) = \cap_{\alpha\in\Lambda} A_\alpha \leq^P M$.
From Theorem(2.2) we can deduce that an R-module M is purely Baer if and only if for each subset X of $S = End_R(M)$, $r_M(X) \leq^P M$.

1) The converse of Corollary(2.3) is not true in general. For example consider $\mathbf{Z}p\infty$ as $\mathbf{Z}$-module, its indecomposable so the only direct summands are 0 and $\mathbf{Z}p\infty$, then $0 \cap \mathbf{Z}p\infty = 0 \leq^P \mathbf{Z}p\infty$ (in fact the only pure submodules are 0 and $\mathbf{Z}p\infty$), but $\mathbf{Z}p\infty$ is not purely Baer. Consider the $\mathbf{Z}$-homomorphism $\alpha : \mathbf{Z}p\infty \longrightarrow \mathbf{Z}p\infty$, define by $\alpha(t/p^k + \mathbf{Z}) = t/p^{k-1} + \mathbf{Z}$ for each $t \in \mathbf{Z}$, $k \in \infty$, then then $Ker(\alpha) = (t/p + \mathbf{Z})$which is not pure submodule of $\mathbf{Z}p\infty$.

Recall that an R-module M is said to have summand pure intersection property if the intersection of two direct summands is pure submodule of M [6]. So from corollary (2.3) we can deduce that purely Baer modules have summand pure intersection property.
More generally, we consider the following
Definition (2.4) : Let M be an R-module and let N be a submodule of M, M is called N-purely Baer or M is purely Baer module relative to N, if for each sub set I of $Hom_R(M,N)$, $r_M(I) \leq^P M$.
Examples and Remarks:

1) It is clear that M is purely Baer iff M is purely Bear module relative to M.
2) Every module is purely Baer relative to the zero submodule of itself.
3) $\mathbb{Q}$ as $\mathbf{Z}$-module is purely Baer module relative to each submodule A of itself. Since each subset I of $Hom_R(\mathbb{Q}, A)$, $r_A(I) = A \cap r_{\mathbb{Q}}(I) = A \cap \mathbf{0} = \mathbf{0}$ is pure in A.
4) For each prime number p and integer $n > 2$, $\mathbf{Z}p^n$ as $\mathbf{Z}$-module is not purely Baer module relative to $\mathbf{Z}p^{n-1}$. Consider the $\mathbf{Z}$-homomorphism $f : \mathbf{Z}p^n \longrightarrow \mathbf{Z}p^{n-1}$ define by $f\,(t/p^k + \mathbf{Z}) =$

$t/p^{k-1}+\mathbf{Z}$ for each $t\in \mathbf{Z}$, $k \in\infty$, then $r_{\mathbf{Z}_{p^{n-1}}}(f) = (t/p+\mathbf{Z}) = \mathbf{Z}p$ which is not pure in $\mathbf{Z}p^{n-1}$.

Proposition (2.5): *For any R-module M, the following are equivalent:*

1) *M is purely Baer,*
2) *For any two direct summands A and B with $B \leq A$, A is B-purely Baer.*
3) *M is purely Baer module relative to any direct summand of itself.*

Proof: (1)$\Rightarrow$(2) Let I be a subset of $Hom_R(A,B)$, since A and B are direct summands of M then there are a submodules C and D of M such that $M = A \oplus C = B \oplus D$, now consider π_C and π_D are the projection maps onto C and D respectively, since for each $\alpha \in I$, α can be extended to $\acute{\alpha}$ by putting $\acute{\alpha}(C) = \mathbf{0}$,since M is purely Baer then by Theorem(2.2) we have $Ker\pi_C \cap Ker\pi_D \cap (\cap_{\alpha\in I} Ker\acute{\alpha}) = A \cap B \cap (\cap_{\alpha \in I} Ker\acute{\alpha}) \leq^P M$ where $Ker\pi_C = A$ and $Ker\pi_D = B$. Now to check that $Ker\acute{\alpha} = C \oplus ker\alpha$, it's clear that $C \oplus Ker\alpha \leq Ker\acute{\alpha}$, let $m \in Ker\acute{\alpha}$, then $m = a + c$ for some $a \in A$ and $c \in C$, but $0 = \acute{\alpha}(m) = \acute{\alpha}(a + c) = \alpha(a) + 0 = \alpha(a)$, thus $a \in Ker\alpha$ implies that $m \in C\oplus Ker\alpha$. By the help of modular law we have $A \cap Ker\acute{\alpha} = A \cap C + A \cap Ker\alpha = Ker\alpha$, then $B \cap (\cap_{\alpha\in I} Ker\alpha) = B \cap A\cap (\cap_{\alpha\in I} Ker\acute{\alpha}) \leq^P M$. But $r_B(I) = B \cap (\cap_{\alpha\in I} Ker\alpha)$. Thus $r_B(I) \leq^P M$.

(2) $\Rightarrow$ (3) $\Rightarrow$ (1). It is clear.

Proposition(2.6): *An R-module M is purely Baer if and only if for any two direct summands A and B of M and for each subset I of $Hom_R(A,B)$, $r_A(I) \leq^P M$.*

Proof: Since A is a direct summand of M, then there is a submodule C of M such that $M = A\oplus C$, since for each $\alpha \in I$, α can be extended to $\acute{\alpha}$ by putting $\acute{\alpha}(C) = \mathbf{0}$, now consider π_C be the projection map onto C, and by the similar way of the proof of Proposition(2.5) we have $r_A(I) = \cap_{\alpha\in I} Ker\alpha = A \cap (\cap_{\alpha\in I} Ker\acute{\alpha}) = Ker\pi_C \cap (\cap_{\alpha\in I} Ker\acute{\alpha}) \leq^P M$.

Conversely : put $A = B = M$.

Corollary (2.7): *Let M be a purely Baer R-module . Any decomposition $M = A\oplus B$ and any subset I of $Hom_R(A,B)$, $r_A(I) \leq^P A$.*

Corollary(2.8): *Let M be a purely Baer R-module. Any decomposition $M = A \oplus B$ and any R-homomorphism $\alpha: A \rightarrow B$, $Ker\alpha \leq^P A$.*

Recall that an R-module M is called quasi-Dedekind if each non-zero R-endomorphism of M is a monomorphism [7]. It is an easy matter, to show that every quasi-Dedekind R-module is purely Baer, but the converse may not true, for example, the Z-module $Z_2\oplus Z_2$ is semisimple, so M is purely Baer, but M is not quasi-Dedekind, since the projection mapping onto Z_2 is not monomorphism. However, the converse is true if M is pure-simple(the trivial submodules are only pure in M).

Recall that an R-module M is cogenerator, if for any R-module A,*(0)= ∩ker(f), where the intersection runs over all R-homomorphism of A into M [3].*

In the following we consider conditions under which purely Baer modules are equivalent to regular modules in the sense of Fieldhouse.

Proposition(2.9): *Let M be a cogenerator R-module. Then*

(1) **A= $r_M(l_S$(A) for each submodule A of M.**

(2) **M is purelt Baer if and only if M is regular.**

Proof: It is clear that A $\subseteq r_M(l_S(A))$. Let m$\notin$ A. Since M is cogenerator, then A=∩ ker(f), where the intersection runs over all R-homomorphism of M/A into M.Then there is f_0:M/A→ M such that $f_0(m+A) \neq 0$. Now let π: M→ M/A be the natural epimorphism, then $f_0(\pi(A))=0$, thus $f_0\,\pi \in l_S(A)$, but $f_0\ \pi(m)=f_0(m+A) \neq 0$, then m$\notin$ $r_M(l_S(A))$, therefore A = $r_M(l_S(A))$.

(2)Let N be a submodule of M. Then $l_S(N)$ is a left ideal of S, Since M is purely Baer, $r_M(l_S(N)) \leq^P M$. By (1), N is pure in M and hence M is regular. The other direction is trivial.

Recall that an R-module M is purely extending, if each submodule of M is essential in a pure submodule of M. This is equivalent to saying that every closed submodule of M is pure. A ring R is called purely extending, if R is purely extending R- module[8].

Remark: *A right nonsingular purely extending ring R is purely Baer.*

Proof: Let A be a left ideal of R. By ([1], lemma (1.2.12)), r_R(A) is closedright ideal of in R. But R is purely extending, then r_R(A) is pure in R.

DIRECT SUMS (SUMMANDS) OF PURELY BAER MODULES

In any algebraic concept, a natural question arise is whether the concept is inherit by direct summands or direct sums. The following result shows that direct summands of purely Baer modules inherit the concept.

Theorem (3.1): *A direct summand of purely Baer module is purely Baer.*

Proof: Let *M* be a purely Baer *R*-module and let *A* be a direct summand of *M*. Now let *I* be a left ideal of $End_R(A)$ to show that $r_A(I) \leq^P A$, since there is a submodule *B* of *M* such that $M = A \oplus B$, then for each $\alpha \in I$, α can be extended to $\acute{\alpha} \in S = End_R(M)$ by put $\acute{\alpha}(B) = \mathbf{0}$. But *M* is purely Baer then by Theorem (2.2) we have that $A \cap (\cap_{\alpha\in I} Ker\acute{\alpha}) = Ker\pi_B \cap (\cap_{\alpha\in I} Ker\acute{\alpha}) \leq^P M$, where π_B be the projection map onto *B*. Now for each $\alpha \in I$, $Ker\acute{\alpha} = Ker\alpha \oplus \oplus B$ and by the help of modular law then $A \cap Ker\acute{\alpha} = A \cap (Ker\alpha \oplus B) = A \cap Ker\alpha \oplus A \cap B = Ker\alpha$, therefore $\cap_{\alpha\in I} Ker\alpha = \quad A \cap (\cap_{\alpha\in I} Ker\acute{\alpha}) \leq^P M$. But $r_A(I) = \cap_{\alpha\in I} Ker\alpha \leq^P M$ and $r_A(I) \leq A$, thus $r_A(I) \leq^P A$. Then *A* is purely Baer.

The following corollary provides a source of example of purely Baer modules

Corollary (3.2): *Let R be a purely Baer ring, and let* $e^2 = e \in R$ *be any idempotent of R. Then* $M = eR$ *is an R-module which is purely Baer.*

Proposition(3.3): *If a purely Baer module can be decompose into a finite direct sum of pure simple summands, then any arbitrary direct decomposition is a finite.*

Proof: Let $M = M_1 \oplus M_2 \oplus \ldots \oplus M_n$, where $n \in \infty$, be a finite direct sum of pure simples. Assume now that M also decompose as $M = \oplus_{i\in I} N_i$, let $0 \neq m_j \in M_j$, $j = 1, \ldots, n$, then $m_j = \sum_{i\in I_j} n_i^{(j)}$, where $n_i^{(j)} \in N_i$, $\forall\, i \in I_j$, and I_j is finite subset of I, $\forall\ j = 1, \ldots, n$, thus $m_j \in M_j \cap (\oplus_{i\in I_j} N_i)$ since M_j and $\oplus_{i\in I_j} N_i$ are direct summands of M then by Corollary(2.3) we have that $M_j \cap (\oplus_{i\in I_j} N_i)$ is pure submodule of M, thus $0 \neq M_j \cap (\oplus_{i\in I_j} N_i) \leq^P M_j$, but M_j is pure simple then $M_j \cap (\oplus_{i\in I_j} N_i) = M_j$ implies that $M_j \leq \oplus_{i\in I_j} N_i$, then we have $M = \oplus_{i=1}^{n} M_i \leq \oplus_{i\in \bigcup_{j=1}^{n} I_j} N_i$, hence we actually have equality, but the union of $I_1, I_2, \ldots, I_n$ is finite set, hence only finitely many N_i are non zero, $i \in I$.

Proposition(3.4): *Let* $\{M_i\}_{i\in I}$ *be a class of R-modules, where I be an index set. If* $\oplus_{i\in I} M_i$ *is purely Baer, then the following hold :*

1) *M_i is purely Baer,* $\forall\ i \in I$.
2) $\forall\ i, j \in I$ *and for each family* $\{\alpha_\lambda\}_{\lambda\in\Lambda}$ *of an R-homomorphisms of* $Hom_R(M_i, M_j)$*, where* Λ *be an index set,* $\cap_{\lambda\in\Lambda} Ker\alpha_\lambda \leq^P M_i$.
3) $\forall\ i \neq j \in I$, $\forall$ *R-monomorphism* $\varphi : M_i' \leq^{\oplus} M_i \longrightarrow M_i$ *and R-monomorphism* $\psi : M_j' \leq^{\oplus} M_j \longrightarrow M_i$ *. Then the set* $A = \{(\varphi^{-1}(a), -\psi^{-1}(a)) \mid a \in Im(\varphi) \cap Im(\psi)\}$ *is a pure submodule of* $M_i' \oplus M_j'$.

Proof: The elements of the endomorphism ring of $\oplus_{i\in I} M_i$ are matrices, for which the (i,j) entries are homomorphisms $M_j \longrightarrow M_i$. *(1) follows from theorem(3.1).* (2) Set $I = \{\alpha_\lambda\}_{\lambda\in\Lambda}$ then by Proposition(2.7) we have $r_{M_i}(I) = \cap_{\lambda\in\Lambda} Ker\alpha_\lambda \leq^P M_i$

(3) Observe that as φ is defined on a summand of M_i, it can be extended to the whole M_i, by considering $\varphi\pi$, where π is the canonical projection of M_i onto M_i'; similarly with ψ. To simplify notation, we use the same symbols for these new homomorphism. Consider the following matrix $(\alpha_{i'j'})_{i',j' \in I}$, with: 1) $\alpha_{i'j'} = 0, \forall\ (i', j') \neq (i, j), (i, i)$; 2) $\alpha_{ii} = \varphi$; 3) $\alpha_{ij} = \psi$. Then $Ker((\alpha_{i'j'})) = K = \{(b,c) \mid \varphi(b) + \psi(c) = 0\}$. Notice that $Ker(\varphi) \oplus Ker(\psi) \leq K$. Moreover, since both the kernels of φ and ψ are direct summands, we have $M_i = Ker(\varphi) \oplus M_i'$ and $M_j = Ker(\psi) \oplus M_j'$. Note

that φ is monomorphism on M_i' and ψ is monomorphism on M_j'. We have $\varphi(b) + \psi(c) = 0$ only if $\varphi(b) = -\psi(c) \in Im(\varphi) \cap Im(\psi)$. For $(b, c) \in (M_i' \oplus M_j') \cap K$, we get $(b, c) \in \{((\varphi_{|Mi'})^{-1}(a), -(\psi_{|Mj'})^{-1}(a)) | a \in Im(\varphi) \cap Im(\psi)\} = A$. Now $(Ker(\varphi) \oplus Ker(\psi)) \cap A = \{(0,0)\}$, obviously. Given the fact that any pair $(b,c) \in K$ can be written uniquely as $(b,c) = (b',c') + (b'',c'')$ with $(b',c') \in Ker(\varphi) \oplus Ker(\psi)$ and $(b'',c'') \in (M_i' \oplus M_j')$. we have that $K = Ker(\varphi) \oplus Ker(\psi) \oplus A$, since $\oplus_{i\in I} M_i$ is purely Baer then $K = Ker((\alpha_i{}'_j{}'))$ is pure submodule of $\oplus_{i\in I} M_i$ but $K \leq M_{i'} \oplus M_{j'}$, then $K \leq^P M_{i'} \oplus M_{j'}$ and $A \leq^{\oplus} K$ implies $A \leq^P K \leq^P M$, thus $A \leq^P M_{i'} \oplus M_{j'}$.

Finite direct sums of purely Baer modules are not necessarily purely Baer modules. The $\mathbf{Z}$-module $\mathbf{Z} \oplus \mathbf{Z}_2$ is not purely Baer, even though $\mathbf{Z}$ and $\mathbf{Z}_2$ both are purely Baer $\mathbf{Z}$-modules, since define $f: \mathbf{Z} \to \mathbf{Z}_2$ by $f(x) = \bar{x}\ \forall\ x \in \mathbf{Z}$. If $\mathbf{Z} \oplus \mathbf{Z}_2$ is purely Baer, by corollary(2.8), $Ker f = 2\mathbf{Z} \leq^P \mathbf{Z}$, a contradiction.

Theorem(3.5): *Let M_1 and M_2 be a purely Baer R-modules. If we have the conditions*:

1) $\forall\ N \leq M_1 \oplus M_2$ *implies that* $N = N_1 \oplus N_2$, *where,* $N_i \leq M_i\ \forall\ i = 1,2$.
2) $\bigcap_{\alpha \in Hom_R(M_i, M_j)} Ker(\alpha) = \mathbf{0}$ $(i \neq j,\ i, j = 1,2)$.

Then $M_1 \oplus M_2$ is purely Baer.

Proof: Let $S = End(M_1 \oplus M_2)$, and let I be a left ideal of S. Then by (1), $r_M(I) = N_1 \oplus N_2$ where, $N_i \leq M_i (i=1,2)$. By similar way of the proof of ([1],theorem(3.3.2)) we can show that $N_1 = N_1' \cap (\cap_{\psi \in I_{12}} Ker\psi) = N_1' = r_{M_1}(I_1) \leq^P M_1$ because M_1 is purely Baer also $N_2 = N_2' \cap (\cap_{\psi \in I_{21}} Ker\psi) = N_2' = r_{M_2}(I_2) \leq^P M_2$. Then we have $r_{M_1 \oplus M_2}(I) = N_1 \oplus N_2 \leq^P M_1 \oplus M_2$. Then $M_1 \oplus M_2$ is purely Baer.

Even though there is no connection between purely Baer modules and modules which satisfy the pure intersection property (intersection of pure submodules is pure). In the following, we show that they share in many properties.

Proposition (3.6):*Llet M be a pure simple R-module and let N be any R-module. If $M \oplus N$ is purely Baer then*

1) *$Hom_R(M,N) = \mathbf{0}$ or Every non zero R-homomorphism from M to N is monomorphism.*
2) *M is Quasi Dedekind.*

Proof:(1) Assume $Hom_R(M,N) \neq \mathbf{0}$, then let $f: M \to N$ be a nonzero R-homomorphism, since $M \oplus N$ is purely Baer then by Corollary(2.8) we have $Ker f \leq^P M$, but M is pure simple and $f \neq 0$, then $Ker f = \mathbf{0}$, thus f is monomorphism .

(2) M is direct summand of ($M \oplus N$), then by Theorem (3.1) M is purely Baer. If $f(\neq 0)$:M$\longrightarrow$M, then $Kerf \leq^{P} M$, since M is purely Baer. But M is pure simple and $f\neq 0$, thus $Kerf=0$. *This shows that* M is Quasi Dedekind.

Proposition(3.7): *Let M be an R-module. If $R\oplus M$ is purely Baer R-module, then every cyclic submodule of M is flat.*

Proof: Let $0 \neq m \in M$. Now consider the following short exact sequence

$$0 \longrightarrow Kerf \xrightarrow{i_1} R \xrightarrow{f} mR \longrightarrow 0$$

Where i_1 is the inclusion homomorphism and f is defined as follows $f(r) = mr$, for each $r \in R$. Let $i_2 : mR \rightarrow M$ be the inclusion homomorphism, now consider $i_2 \circ f : R \rightarrow M$. Since $R\oplus M$ is purely Baer then by corollary(2.8), $Ker(i_2 \circ f)$ is pure in R. But i_2 is monomorphism therefore $Kerf = Ker\ i_2 \circ f$, since R is flat R-module and $R/Kerf \cong mR$. we have mR is flat.

Recall that a ring R is flat if every finitely generated ideal is flat [9]

Proposition (3.8): *Let R be a ring. If $\oplus_{i=1}^{n} R$ is purely Baer R-module, $\forall\, n \in$ □, then R is flat ring.*

Proof: Let $I = \sum_{i=1}^{n} a_i R$ be a finitely generated ideal of R. Define f: $\oplus_{i=1}^{n+1} R \rightarrow R$ by $f((r_i)_{i=1}^{n}) = \sum_{i=1}^{n} a_i r_i$, it is clear that f is an R-homomorphism and $Im(f) = I$. Since $\oplus_{i=1}^{n+1} R$ is purely Baer R-module, then by Corollary (2.8), $Kerf \leq^{P} \oplus_{i=1}^{n} R$, but $\oplus_{i=1}^{n} R$ is flat R-module and $\oplus_{i=1}^{n} R/Kerf \cong I$, so I is flat and hence R is flat ring.

Proposition (3.9): *Let R be a ring such that every finitely generated flat R-module is purely Baer. Then R is flat.*

Proof: Let I be a finitely generated ideal of R. Then there is a finitely generated free R-module F and an epimorphism $f : F \rightarrow I$, now consider $i : I \rightarrow R$ be the inclusion map, then $i \circ f : F \rightarrow R$ and $F\oplus R$ is flat R-module. By hypothesis $F\oplus R$ is purely Baer, then $Ker(i \circ f) \leq^{P} F$, but i is monomorphism then $Ker(i \circ f) = Kerf$ and $F/Kerf \cong Imf = I$, but F is flat then I is flat ideal. Thus R is flat ring.

In the following we characterize regular rings in terms of purely Baer modules.

Theorem(3.10) : *Let R be a ring. Then the following statements are equivalent:*

1) *R is regular,*
2) *All R-modules are F-regular,*

3) All R-modules are purely Baer.

Proof:(1) $\Leftrightarrow$ (2) See [10]

(2) $\Rightarrow$ (3) It is clear.

(3) $\Rightarrow$ (2) Let M be an R-module and let N be a submodule of M. Consider $\pi: M \rightarrow M/N$ be the natural epimorphism, now by assumption $M \oplus M/N$ is purely Baer and by Corollary(2.8) we have $N = Ker\pi \leq^{p} M$. Thus M is F-regular, in particular R is regular.

Let R be a regular ring which is not semisimple then there is a purely Baer module that it is not Baer. For, since R is not semisimple, there exists an R-module M (say) which is not Baer ;([1],proposition(2.4.14)), but R is regular, then theorem (3.10) implies that M is purely Baer.

Theorem(3.11): *Let R be a principal ideal domain. The following statements are equivalent:*

1) *R is field.*
2) *All R-modules are purely Baer.*
3) *All divisible R-modules are purely Baer.*

Proof: Since every regular and principal ideal domain ring is field, so by Theorem(3.10), we have (1)$\Leftrightarrow$ (2).

(2) $\Rightarrow$ (3) It is clear.

(3) $\Rightarrow$ (2) Let M be an R-module, then there is an injective R-module E and a monomorphism $\mu: M \rightarrow E$. Let $\pi: E \rightarrow M/Im\mu$ be the natural epimorphism, since E is an injective then E is a divisible and the epimorphic image of divisible is a divisible and hence $E \oplus M/Im\mu$ is a divisible R-module, thus $E \oplus M/Im\mu$ is purely Baer. Now by Corollary (2.8), $Ker\pi$ is a pure in E, but $Ker\pi = Im\mu$, so $Im\mu$ is a pure in E, Thus $\forall r(\neq 0) \in R$ we have $(Im\mu)r = Mr \cap Im\mu$, but M is divisible then $Mr = M$, and hence $(Im\mu)r = Im\mu$ is divisible, but R is principal ideal domain then $Im\mu$ is injective, thus $Im\mu$ is a summand of E. Since E is purely Baer, then by Theorem (3.1) we have that $Im\mu$ is purely Baer. But $M \cong Im\mu$, then M is purely Baer.

Proposition(3.12): *Let $\{R_\lambda\}_{\lambda \in \Lambda}$ be a family of rings, where Λ be an index set. Then $R = \oplus_{\lambda \in \Lambda} R_\lambda$ is purely Baer ring if and only if R_λ is purely Baer ring for each $\lambda \in \Lambda$.*

Proof: It is clear that R_λ is a direct summand of R and R is purely Baer then by Theorem (3.1), R_λ is purely Baer ring.

Conversely, Let I be a left ideal of R. Now consider $\pi_\lambda : R \rightarrow R_\lambda$ be the projection map onto R_λ, for each $\lambda \in \Lambda$, since I is a left ideal of R then $\pi_\lambda(I)$ is a left ideal of R_λ, since R_λ is purely Baer then $r_{R_\lambda}(\pi_\lambda(I))$ is a pure right ideal of R_λ. Now we claim that $r_R(I) = \oplus_{\lambda \in \Lambda} r_{R_\lambda}(\pi_\lambda(I))$, let $a = (a_\lambda)_{\lambda \in \Lambda} \in r_R(I)$ then $Ia = \mathbf{0}$ implies that $\pi_\lambda(I)a_\lambda = \mathbf{0}$ for each $\lambda \in \Lambda$, thus $a_\lambda \in r_{R_\lambda}(\pi_\lambda(I))$, so $a \in \oplus_{\lambda\in\Lambda} r_{R_\lambda}(\pi_\lambda(I))$. Now let $b = (b_\lambda)_{\lambda\in\Lambda} \in \oplus_{\lambda\in\Lambda} r_{R_\lambda}(\pi_\lambda(I))$, then we have $\pi_\lambda(I)\, b_\lambda = \mathbf{0}$ $\forall$ $\lambda\in\Lambda$. Now $1_R = \sum_{\lambda\in\Lambda}\pi_\lambda$, then $I\,b = 1_R(I\,b) = \sum_{\lambda\in\Lambda}\pi_\lambda(Ib) = \sum_{\lambda\in\Lambda}\pi_\lambda(I)\, b_\lambda = \mathbf{0}$, thus $b\in r_R(I)$. Then $r_R(I) = \oplus_{\lambda\in\Lambda} r_{R_\lambda}(\pi_\lambda(I))$. But $r_{R_\lambda}(\pi_\lambda(I))$ is a pure right ideal of R_λ, $\forall$ $\lambda\in\Lambda$, so by Lemma(1.1.4), $r_R(I)$ is a pure in R_R.

In the following we characterize purely Baer modules in the class of finitely generated modules.

Theorem(3.13): *Let M be a finitely generated module over principal ideal domain R. The following statements are equivalent:*

1) *M is purely Baer.*
2) *M is semisimple or torsion-free.*

Proof:

(1) $\Rightarrow$ (2) Assume that M is finitely generated purely Baer module which is not semisimple to show that M is torsion-free. Now by ([11], Corollary 8.3), we can always decompose $M = t(M)\oplus f(M)$ where $t(M)$ is the torsion submodule of M and $f(M)$ is the torsion-free submodule of M. Assume $t(M) \neq \mathbf{0}$ and $f(M) \neq \mathbf{0}$, and by ([11]Theorem 8.14) we have $t(M) = \oplus_{p\in P} Mp^{n(p)}$, where $P \subseteq R$ is a finite collection of primes (irreducibles) and $Mp^{n(p)}$ is a non-trivial cyclic modules of prime power order $p^{n(p)}$ where $n(p)\in\square$. Also by ([11], Lemma 8.17) we have the only submodules of $Mp^{n(p)}$ are: $\mathbf{0} = p^{n(p)}\, Mp^{n(p)} \leq p^{n(p)-1}\, Mp^{n(p)} \leq \ldots. \leq p\, Mp^{n(p)} \leq Mp^{n(p)}$. Let p_0 be a prime so that $n(p_0)\neq 0$ and let $\varphi : R\rightarrow Mp_0^{n(p_0)}$ be the R-homomorphism define by $\varphi(x) = \bar{x}$, for $x \in R$, then $\mathbf{0} \neq Ker(\varphi) = p_0^{n(p_0)}R$ is not pure in R_R, but M is purely Bear and by Corollary(2.8) then $Ker(\varphi)$ is pure in R_R, a contradiction. Then $t(M) = \mathbf{0}$ or $f(M) = \mathbf{0}$. Assume $f(M) = \mathbf{0}$.Then $M = t(M)$; it is a direct sum of modules of the form $Mp^{n(p)}$which is describe as above,therefore by Theorem(3.1) $Mp^{n(p)}$ must be purely Baer. Since M is not semisimple, then M can not decomposition as a direct sum of simple modules, then there is a prime number p such that $n_0(p) > 1$. Let $\theta : Mp^{n_0(p)} \rightarrow Mp^{n_0(p)}$ define by $\theta(\bar{x}) = p\bar{x}$, thus $\theta \neq 0$ because $\theta(Mp^{n_0(p)}) = p\,Mp^{n_0(p)} \neq 0$, since $Mp^{n_0(p)}$ is purely Baer, then $Ker(\theta) = p^{n_0(p)-1}\, Mp^{n_0(p)}$is pure in $Mp^{n_0(p)}$ which is contradiction because $Mp^{n_0(p)}$ is pure simple. Then we have $t(M) = \mathbf{0}$, thus $M = f(M)$.

(2)$\Rightarrow$(1) If M is semisimple then M is obviously Baer and hence purely Baer. If M is finitely generated and torsion-free then $M \cong R^n$ for some n

∈□ , thus by proposition(3.12), R^n is purely Baer ring and hence *M* is purely Baer.

REFERENCES

1. C. S. Roman, "Baer and quasi-Baer modules", *Ph.D. Thesis, The Ohio State University*, 2004.
2. P. M. Cohn, "On the free product of associative rings", *Math. Z.* 71 : 380–398, 1959
3. T.Y. Lam, "Lectures On Modules and Rings", *Springer -Verl* [21]
4. D. J. Fieldhouse: Aspects of purity , In ring theory, proceeding of the Oklahoma Conference, Mercel Dekker, INC, New York (1974)
5. K.R.Goodearl: Ring theory, non-singular rings and modules, Mercel Dekker, INC, New York(1976)
6. N. S. Al-Mothafar: " Sums and intersections of submodules", *Ph.D. Thesis, University of Baghdad*, 2002
7. A. S. Mijbass, "Quasi-Dedekind Modules", *Ph.D. Thesis, University of Baghdad,* 1997*.ag*, 1999. [27]
8. J. Clark, "On purely extending modules", *The proceeding of the International Conference on Abelian Group and Modules,* 353–358, 1999.
9. F. H. Al-Alwan, "Modules on flat rings", *M.Sc. Thesis, University of Baghdad*, 1985.
10. S.M.Yassen:F-regular modules, M. Sc.thesis, University of Baghdad,1993
11. B. Hartely and T. O. Haekes, "Rings, Modules and Linear Algebra", *London* 1970.

Comparison of Classical and Bayesian Estimations for Shape Parameter in Burr Type XII Distribution under the Jeffrey's and modified Jeffrey's Priors

Nadia H. Al-Noor[1] and Huda A. Abd Al-Ameer[2]
[1]Dept. of Mathematics / College of Science / AL- Mustansiriya University
[2]Dept. of Mathematics / College of Science / Diyala University
Received 1/4/2013 – Accepted 15/9/2013

الخلاصة

اهتم البحث الحالي بتقدير معلمة الشكل لتوزيع بيور نوع XII. تم مناقشة المقدرات الكلاسيكية المتمثلة بـ (مقدر الامكان الاعظم، المقدر المنتظم غير المتحيز ذو الاصغر تباين) ومقدرات بيز. تم الحصول على مقدرات بيز بأعتماد توزيعي جيفري وجيفري المعدل كتوزيعات اولية تحت دوال خسارة متماثلة وغير متماثلة "دالة الخسارة التربيعية ودالة الخسارة الوقائية". تم احتساب ومقارنة متوسط مربعات الخطأ للبيانات المولدة باعتماد المحاكاة لعينات صغيرة، متوسطة وكبيرة. لوحظ ان المقدر المنتظم غير المتحيز ذو الاصغر تباين قد اعطى اصغر القيم لـ MSE يليه مقدر بيز تحت دالة الخسارة التربيعية مع جيفري المعدل وبالتالي فهي المقدرات المفضلة لجميع احجام العينات كما لوحظ ان اداء دوال الخسارة باعتماد جيفري المعدل كتوزيع اولي كان افضل مقارنة مع اعتماد جيفري.

ABSTRACT

The current paper considers the estimation of shape parameter in Burr type XII distribution. The classical estimators "Maximum Likelihood estimator, Uniformly Minimum Variance Unbiased estimator" and Bayesian estimators are discussed. Bayes estimators are obtained using Jeffrey's and modified Jeffrey's Priors under symmetric and asymmetric loss functions "squared error and precautionary". Mean squared error (MSE) of the estimators are calculated and compared for small, moderate and large samples using simulated data sets. It is observed that Uniformly Minimum Variance Unbiased estimator gives smallest values of MSE followed by the Bayes estimator under squared error loss function with modified Jeffrey's prior information and hence they are preferred estimators for all sample sizes, also It is observed that performances of loss functions with modified Jeffrey's prior are better comparing with Jeffrey's prior.

1. INTRODUCTION

Burr introduced twelve different forms of cumulative distribution functions for modeling lifetime data or survival data [1]. Out of those twelve distributions, Burr Type XII and Burr Type X have received the maximum attention due to its application in the study of biological, industrial, reliability and life testing, and several industrial and economic experiments [10].

The Burr Type XII has the following distribution function for X > 0 :

$$F(x;\theta,\lambda) = 1 - \frac{1}{(1+x^{\lambda})^{\theta}} \ ; \ \theta > 0, \lambda > 0 \qquad (1)$$

Therefore, the Burr Type XII has the density function for X > 0 as :

$$f(x;\theta,\lambda) = \theta\,\lambda\ x^{\lambda-1}\,\frac{1}{(1+x^{\lambda})^{\theta+1}} \ ; \ \theta > 0, \lambda > 0 \qquad (2)$$

where θ and λ are the shape parameters of the distribution.

Inferences on the Burr type XII distribution have been studied by many authors. Evans and Ragab (1983) [2] obtained Bayes estimates for shape parameter, θ, and reliability function on type II censored samples. Mousa (1995) [5] obtained empirical Bayes estimation of the shape parameter and reliability function based on accelerated type II censored data. Mousa and Jaheen (2002) [6] obtained Bayes approximate estimates for the two parameters and reliability function based on progressive type II censored samples. Soliman (2005) [13] investigated properties of Bayesian estimates of reliability and hazard functions. Yarmohammadi and Pazira (2010) [14] compared the classical estimators of the shape parameter with the minimax estimators under weighted balanced squared error, squared log error and special case of precautionary loss functions. Makhdoom and Jafari (2011) [4] compared empirically using Monte-Carlo simulation the point and interval Bayesian estimators for the shape parameter with the special form of the distribution when ($\lambda = 1$) using grouped and un-grouped data. Nasir and Al-Anber (2012) [7] did comparative study for the maximum likelihood estimator, median estimator and Bayesian estimators for estimation the reliability function under Jeffrey , modified Jeffrey and extension of Jeffrey priors information with squared error loss function. Also, Rastogi and Tripathi (2012) [10] obtained several Bayesian estimates against different symmetric and asymmetric loss functions such as squared error, linex and general entropy considered on the basis of a progressively type II censored sample.

2. Different Estimators of Parameter

In this section classical and Bayes estimators of the shape parameter, θ, has been determined with the assumption that the other shape parameter, λ , is known.

2.1 Maximum Likelihood Estimator (MLE) of θ

Let $x_1, x_2, \dots\dots, x_n$ be a random sample of size n drawn from the Burr type XII distribution defined by (2). Then the Likelihood function for the given random sample is given by:

$$L(\theta,\lambda|\underline{x}) = \prod_{i=1}^{n} f(x_i|\theta,\lambda) = \frac{\theta^n \lambda^n \prod_{i=1}^{n} x_i^{\lambda-1}}{\prod_{i=1}^{n}\left(1+x_i^{\lambda}\right)^{\theta+1}} \qquad (3)$$

From which we calculate the log-likelihood function:

$$l(\theta,\lambda|\underline{x}) = n\ln\theta + n\ln\lambda + (\lambda-1)\sum_{i=1}^{n}\ln(x_i) - (\theta+1)\sum_{i=1}^{n}\ln\left(1+x_i^{\lambda}\right)$$

Finding the maximum with respect to θ by taking the derivative and setting it equal to zero yields the maximum likelihood Estimator of the θ parameter, denoted by $\hat{\theta}_{ML}$:

$$\hat{\theta}_{ML} = \frac{n}{\sum_{i=1}^{n} \ln(1 + x_i^{\lambda})} \tag{4}$$

2.2 Uniformly Minimum Variance Unbiased Estimator (UMVUE) of θ

The function of Burr type XII distribution is belongs to exponential family. Therefor $\sum_{i=1}^{n} \ln(1 + x_i^{\lambda})$ is a complete sufficient statistic for θ [14]. If X has a Burr type XII distribution, then:

$\sum_{i=1}^{n} ln(1 + x_i^{\lambda}) \sim Gamma\ (n,\ \theta)$

Now, depending on the theorem of Lehmann-Scheffe [3], taking the mathematical expected of the complete sufficient statistic yields the Uniform Minimum Variance Unbiased Estimator of the θ parameter, denoted by $\hat{\theta}_{UMVUE}$:

$$\hat{\theta}_{UMVU} = \frac{n-1}{\sum_{i=1}^{n} \ln(1 + x_i^{\lambda})} \tag{5}$$

2.3 Bayes Estimation

In this subsection we studied Bayes estimators under two loss functions. One is symmetric "squared error loss function" and the second is asymmetric "precautionary loss function". The squared error loss function associates equal importance to the losses due to overestimation and underestimation of equal magnitude. However, in real applications, the estimation of the parameters "or function as reliability function" an overestimation is more serious than the underestimate; thus, the use of a symmetrical loss function is inappropriate. In this case, an asymmetric loss functions must be considered.

2.3.1 Prior and Posterior Density Function of θ

For Bayesian estimation we need to specify a prior distribution for the parameter. We consider two different prior distributions for θ [7]:

- J effrey's Prior Information: $g(\theta) \propto \frac{1}{\theta}$ (6)
- Modified Jeffrey's Prior Information: $g(\theta) \propto \frac{1}{\sqrt{\theta^3}}$ (7)

Now the Posterior density function of θ for the given random sample X with Jeffrey's prior information is given by:

$$\pi(\theta|\underline{x})_J = \frac{\prod_{i=1}^{n} f(x_i;\theta)\ g(\theta)}{\int_0^{\infty} \prod_{i=1}^{n} f(x_i;\theta)\ g(\theta) d\theta}$$

$$= \frac{\dfrac{\theta^n \lambda^n \prod_{i=1}^n x_i^{\lambda-1}}{\prod_{i=1}^n (1+x_i^\lambda)^{\theta+1}} \dfrac{1}{\theta}}{\int_0^\infty \dfrac{\theta^n \lambda^n \prod_{i=1}^n x_i^{\lambda-1}}{\prod_{i=1}^n (1+x_i^\lambda)^{\theta+1}} \dfrac{1}{\theta}\, d\theta}$$

$$= \frac{\theta^{n-1} \prod_{i=1}^n (1+x_i^\lambda)^{-(\theta+1)}}{\int_0^\infty \theta^{n-1} \prod_{i=1}^n (1+x_i^\lambda)^{-(\theta+1)}\, d\theta}$$

$$= \frac{\theta^{n-1}\, e^{-(\theta+1)\sum_{i=1}^n \ln(1+x_i^\lambda)}}{\int_0^\infty \theta^{n-1}\, e^{-(\theta+1)\sum_{i=1}^n \ln(1+x_i^\lambda)}\, d\theta}$$

$$= \frac{\theta^{n-1}\, e^{-\theta\sum_{i=1}^n \ln(1+x_i^\lambda)}}{\int_0^\infty \theta^{n-1}\, e^{-\theta\sum_{i=1}^n \ln(1+x_i^\lambda)}\, d\theta}$$

$$\Rightarrow \pi(\theta|\underline{x})_J = \frac{\left(\sum_{i=1}^n \ln(1+x_i^\lambda)\right)^n}{\Gamma(n)} \theta^{n-1} e^{-\theta\sum_{i=1}^n \ln(1+x_i^\lambda)} \qquad (8)$$

which implies that: $(\theta|\underline{x})_J \sim Gamma\left(n\,,\ \sum_{i=1}^n ln(1+x_i^\lambda)\right)$

By the same way, the posterior density function of θ for the given random sample X with modified Jeffrey's prior information is given by:

$$\pi(\theta|\underline{x})_{MJ} = \frac{\prod_{i=1}^n f(x_i;\theta)\ g(\theta)}{\int_0^\infty \prod_{i=1}^n f(x_i;\theta)\ g(\theta) d\theta}\ .$$

$$= \frac{\dfrac{\theta^n \lambda^n \prod_{i=1}^n x_i^{\lambda-1}}{\prod_{i=1}^n (1+x_i^\lambda)^{\theta+1}} \dfrac{1}{\sqrt{\theta^3}}}{\int_0^\infty \dfrac{\theta^n \lambda^n \prod_{i=1}^n x_i^{\lambda-1}}{\prod_{i=1}^n (1+x_i^\lambda)^{\theta+1}} \dfrac{1}{\sqrt{\theta^3}}\, d\theta}$$

$$\pi(\theta|\underline{x})_{MJ} = \frac{\theta^{n-\frac{3}{2}} \prod_{i=1}^n (1+x_i^\lambda)^{-(\theta+1)}}{\int_0^\infty \theta^{n-\frac{3}{2}} \prod_{i=1}^n (1+x_i^\lambda)^{-(\theta+1)}\, d\theta}$$

$$= \frac{\theta^{n-\frac{3}{2}}\, e^{-(\theta+1)\sum_{i=1}^n ln(1+x_i^\lambda)}}{\int_0^\infty \theta^{n-\frac{3}{2}}\, e^{-(\theta+1)\sum_{i=1}^n ln(1+x_i^\lambda)}\, d\theta}$$

$$= \frac{\theta^{n-\frac{3}{2}}\, e^{-\theta\sum_{i=1}^n ln(1+x_i^\lambda)}}{\int_0^\infty \theta^{n-\frac{3}{2}}\, e^{-\theta\sum_{i=1}^n ln(1+x_i^\lambda)}\, d\theta}$$

$$\Rightarrow \pi(\theta|\underline{x})_{MJ} = \frac{\left(\sum_{i=1}^n ln(1+x_i^\lambda)\right)^{n-\frac{1}{2}}}{\Gamma\left(n-\frac{1}{2}\right)} \theta^{n-\frac{3}{2}}\, e^{-\theta\sum_{i=1}^n ln(1+x_i^\lambda)} \qquad (9)$$

which implies that: $(\theta|\underline{x})_{MJ} \sim Gamma\left(n-\frac{1}{2}\ ,\ \sum_{i=1}^n ln(1+x_i^\lambda)\right)$

2.3.2 Loss Functions

Here we have determined Bayes estimators of θ for squared error and precautionary loss functions.

Squared error loss function defined as [10]:

$$L(\hat{\theta},\theta) = (\hat{\theta}-\theta)^2 \qquad (10)$$

For squared error loss function Bayes estimator is the mean of posterior density function. From (8) posterior density function is a Gamma distribution with parameters $\left(n, \sum_{i=1}^{n} ln\left(1+x_i^{\lambda}\right)\right)$. Hence the mean of posterior density function is $\frac{n}{\sum_{i=1}^{n}\ln(1+x_i^{\lambda})}$. Therefore the Bayes estimator of θ under squared error loss function with Jeffrey's prior information is:

$$\hat{\theta}_{JS} = \frac{n}{\sum_{i=1}^{n}\ln\left(1+x_i^{\lambda}\right)} \qquad (11)$$

From (9) posterior density function is a Gamma distribution with parameters $\left(n-\frac{1}{2}\ ,\ \sum_{i=1}^{n} ln\left(1+x_i^{\lambda}\right)\right)$. Therefore the Bayes estimator of θ under squared error loss function with modified Jeffrey's prior information is:

$$\hat{\theta}_{MJS} = \frac{n-\frac{1}{2}}{\sum_{i=1}^{n}\ln\left(1+x_i^{\lambda}\right)} \qquad (12)$$

Now suppose the loss function is precautionary, which is defined as [8]:

$$L(\hat{\theta},\theta) = \frac{\left(\hat{\theta}-\theta\right)^2}{\hat{\theta}} \qquad (13)$$

The Bayes estimator under this asymmetric loss function is denoted by $\hat{\theta}_{\mathrm{P}}$ and may be obtained by solving the following equation [8]:

$$\hat{\theta}_P^2 = \mathrm{E}\left(\theta^2|\underline{x}\right) \Rightarrow \hat{\theta}_P = \sqrt{\mathrm{E}\left(\theta^2|\underline{x}\right)}$$

For (8) posterior density function the Bayes estimator of θ is obtained as:

$$\mathrm{E}\left(\theta^2|\underline{x}\right)_{JP} = Var\left(\theta|\underline{x}\right)_{JP} + \left(\mathrm{E}\left(\theta|\underline{x}\right)_{JP}\right)^2$$

$$= \frac{n}{\left(\sum_{i=1}^{n}\ln\left(1+x_i^{\lambda}\right)\right)^2} + \left(\frac{n}{\sum_{i=1}^{n}\ln\left(1+x_i^{\lambda}\right)}\right)^2$$

$$= \frac{n+n^2}{\left(\sum_{i=1}^{n}\ln\left(1+x_i^{\lambda}\right)\right)^2}$$

$$\Rightarrow \hat{\theta}_{JP}^2 = \mathrm{E}\left(\theta^2|\underline{x}\right)_{JP} = \frac{n(n+1)}{\left(\sum_{i=1}^{n}\ln\left(1+x_i^{\lambda}\right)\right)^2}$$

Therefore the Bayes estimator of θ under precautionary loss function with Jeffrey's prior information is:

$$\hat{\theta}_{JP} = \frac{\sqrt{n(n+1)}}{\sum_{i=1}^{n} \ln(1 + x_i^{\lambda})} \tag{14}$$

Now, for (9) posterior density function the Bayes estimator of θ is obtained as:

$$\mathrm{E}(\theta^2|\underline{\mathrm{x}})_{MJP} = Var(\theta|\underline{\mathrm{x}})_{MJP} + \left(\mathrm{E}(\theta|\underline{\mathrm{x}})_{MJP}\right)^2$$

$$= \frac{n - \frac{1}{2}}{\left(\sum_{i=1}^{n} \ln(1 + x_i^{\lambda})\right)^2} + \left(\frac{n - \frac{1}{2}}{\sum_{i=1}^{n} \ln(1 + x_i^{\lambda})}\right)^2$$

$$= \frac{\left(n + \frac{1}{2}\right)\left(n - \frac{1}{2}\right)}{\left(\sum_{i=1}^{n} \ln(1 + x_i^{\lambda})\right)^2}$$

$$\Rightarrow \hat{\theta}_{MJP}^2 = \mathrm{E}(\theta^2|\underline{\mathrm{x}})_{MJP} = \frac{n^2 - \frac{1}{4}}{\left(\sum_{i=1}^{n} \ln(1 + x_i^{\lambda})\right)^2}$$

Therefore the Bayes estimator of θ under precautionary loss function with modified Jeffrey's prior information is:

$$\hat{\theta}_{MJ\mathrm{P}} = \frac{\sqrt{n^2 - \frac{1}{4}}}{\sum_{i=1}^{n} \ln(1 + x_i^{\lambda})} \tag{15}$$

3. Simulation Study and Results

To compare the estimators $\hat{\theta}_{ML}$, $\hat{\theta}_{UMVU}$, $\hat{\theta}_{JS}$, $\hat{\theta}_{JP}$, $\hat{\theta}_{MJS}$ and $\hat{\theta}_{MJP}$ we have considered Mean Squared Errors (MSE) of the estimator. The MSE of an estimator is defined as:

$$MSE(\hat{\theta}) = \frac{\sum_{i=1}^{R} (\hat{\theta}_i - \theta)^2}{R} \; ; \; R \; is \; the \; number \; of \; replication \tag{16}$$

The number of replication used was R = 3000 samples from the Burr type XII distribution of sizes n = 5, 10, 15, 30, 50, 100 to represent small, medium, and large dataset. The values of the parameters chosen were $\lambda = 2$, θ = 1.5 and 3. The results of simulation study are summarized in the tables 1, 2 and figures 1, 2.

From results we observed that MSE of the Bayes estimator of θ under precautionary loss function with Jeffrey's prior information, $\hat{\theta}_{JP}$, is high for small sample but declining and becoming closer to other estimators with increasing sample size. Among Bayes estimators, the Bayes estimator of θ under squared error loss function with modified Jeffrey's prior information, $\hat{\theta}_{MJS}$, gives smaller value of MSE. Also, the performances of loss functions with modified Jeffrey's prior are better comparing with Jeffrey's prior. Among classical estimators, we note that the performance of $\hat{\theta}_{UMVU}$ is better than $\hat{\theta}_{ML}$ for all sample sizes. Among classical and Bayesian estimators $\hat{\theta}_{UMVU}$ gives smallest values of MSE followed by $\hat{\theta}_{MJS}$ and hence they are preferred respectively for all n. Also, we notice that the formula of the Bayes estimator of θ under squared error loss function with Jeffrey's prior information, $\hat{\theta}_{JS}$, is the same as $\hat{\theta}_{ML}$, so , the Bayes estimator may give the classical estimator in some cases. When θ=1.5 and $n \geq 30$, the MSE values of $\hat{\theta}_{MJP}$ are equal to that values for $\hat{\theta}_{JS}$ and $\hat{\theta}_{ML}$, while with θ=3 we notice that $\hat{\theta}_{MJP}$=$\hat{\theta}_{ML}$=$\hat{\theta}_{JS}$ when n=100. For all cases, as the sample size increases the mean squared error decrease. From tables 1 and 2 we see that all methods give estimated values greater than true value of θ exception UMVU where give estimated values smaller than true value of θ with ≤ 15 .

Table-1: Estimated value and MSE of different estimators of the shape parameter of Burr Type XII distribution when λ=2, θ=1.5

n	*Criteria*	$\hat{\theta}_{ML}$	$\hat{\theta}_{UMVU}$	$\hat{\theta}_{JS}$	$\hat{\theta}_{JP}$	$\hat{\theta}_{MJS}$	$\hat{\theta}_{MJP}$
5	*Estimated value*	1.8470	1.4776	1.8470	2.0232	1.6623	1.8377
	MSE	1.1016	0.6285	1.1016	1.4513	0.8212	1.0855
10	*Estimated value*	1.6517	1.4865	1.6517	1.7323	1.5691	1.6496
	MSE	0.3611	0.2740	0.3611	0.4259	0.3099	0.3596
15	*Estimated value*	1.6002	1.4935	1.6002	1.6527	1.5469	1.5993
	MSE	0.2092	0.1735	0.2092	0.2357	0.1883	0.2088
30	*Estimated value*	1.5529	1.5012	1.5529	1.5786	1.5271	1.5527
	MSE	0.0912	0.0826	0.0912	0.0975	0.0862	0.0912
50	*Estimated value*	1.5321	1.5015	1.5321	1.5474	1.5168	1.5320
	MSE	0.0532	0.0501	0.0532	0.0555	0.0515	0.0532
100	*Estimated value*	1.5153	1.5001	1.5153	1.5228	1.5077	1.5153
	MSE	0.0237	0.0229	0.0237	0.0242	0.0233	0.0237

Table-2: Estimated value and MSE of different estimators of the shape parameter of Burr Type XII distribution when λ=2, θ=3

n	Criteria	$\hat{\theta}_{ML}$	$\hat{\theta}_{UMVU}$	$\hat{\theta}_{JS}$	$\hat{\theta}_{JP}$	$\hat{\theta}_{MJS}$	$\hat{\theta}_{MJP}$
5	*Estimated value*	3.6939	2.9551	3.6939	4.0465	3.3245	3.6754
	MSE	4.4066	2.5141	4.4066	5.8052	3.2846	4.3420
10	*Estimated value*	3.3034	2.9730	3.3034	3.4646	3.1382	3.2992
	MSE	1.4444	1.0962	1.4444	1.7035	1.2397	1.4386
15	*Estimated value*	3.2004	2.9870	3.2004	3.3054	3.0937	3.1986
	MSE	0.8366	0.6939	0.8366	0.9428	0.7530	0.8350
30	*Estimated value*	3.1059	3.0023	3.1059	3.1572	3.0541	3.1055
	MSE	0.3648	0.3304	0.3648	0.3901	0.3448	0.3646
50	*Estimated value*	3.0643	3.0030	3.0643	3.0947	3.0336	3.0641
	MSE	0.2130	0.2006	0.2130	0.2220	0.2058	0.2129
100	*Estimated value*	3.0306	3.0003	3.0306	3.0457	3.0154	3.0305
	MSE	0.0947	0.0919	0.0947	0.0968	0.0931	0.0947

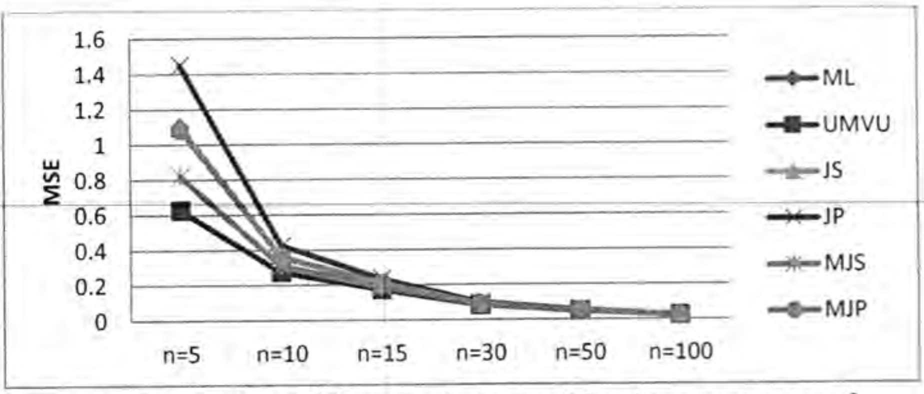

Figure-1: MSE of different estimators of the shape parameter of Burr Type XII distribution when λ=2, θ=1.5

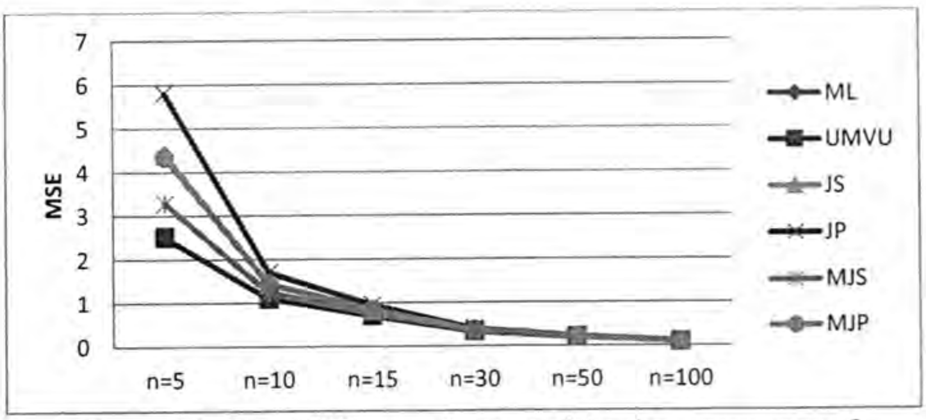

Figure-2: MSE of different estimators of the shape parameter of Burr Type XII distribution when λ=2, θ=3

4. Conclusions

In this paper, we have addressed the problem of Bayesian estimation for the Burr type XII distribution, under symmetric "squared error" and asymmetric "precautionary" loss functions with different prior distribution "Jeffrey's and modified Jeffrey's" and that of classical estimators "maximum likelihood estimation and Uniformly Minimum Variance Unbiased estimator". A simulation study was conducted to examine and compare the performance of the estimates for different sample sizes with respect to their MSE. From the results, we observed that in all cases, $\hat{\theta}_{UMVU}$ estimator and $\hat{\theta}_{MJS}$ have the smallest mean squared error values respectively. As the sample size increases the mean squared error decrease. From the above results of simulation study according to the values of MSE the relation among the estimators is:

From table (1) when θ=1.5:

$$\hat{\theta}_{UMVU} < \hat{\theta}_{MJS} < \hat{\theta}_{MJP} < \hat{\theta}_{ML} = \hat{\theta}_{JS} < \hat{\theta}_{JP} \qquad for\, n \leq 15$$

$$\hat{\theta}_{UMVU} < \hat{\theta}_{MJS} < \hat{\theta}_{ML} = \hat{\theta}_{JS} = \hat{\theta}_{MJP} < \hat{\theta}_{JP} \qquad for\, n \geq 30$$

From table (2) when θ=3:

$$\hat{\theta}_{UMVU} < \hat{\theta}_{MJS} < \hat{\theta}_{MJP} < \hat{\theta}_{ML} = \hat{\theta}_{JS} < \hat{\theta}_{JP} \qquad for\, n \leq 50$$

$$\hat{\theta}_{UMVU} < \hat{\theta}_{MJS} < \hat{\theta}_{ML} = \hat{\theta}_{JS} = \hat{\theta}_{MJP} < \hat{\theta}_{JP} \qquad for\, n = 100$$

REFERENCES

1. Burr, I.W. (1942), Cumulative frequency distribution, Annals of Mathematical Statistics, Vol.13, PP.215-232.
2. Evans, I.G. and Ragab, A.S. (1983), Bayesian inferences given a type-2 censored sample from Burr distribution, Comm. Statist, Theory Methods, Vol.12, PP.1569–1580.
3. Hogg, R. V.; McKean, J. W. and Craig, A. T. (2005), Introduction to Mathematical Statistics, Sixth Edition, Pearson Prentice Hall.
4. Makhdoom, I. and Jafari, A. (2011), Bayesian Estimations on the Burr Type XII Distribution Using Grouped and Un-grouped Data. Australian Journal of Basic and Applied Sciences, Vol.5, No.6, PP.1525-1531
5. Mousa, M.A.M.A. (1995), Empirical Bayes estimators for the burr type XII accelerated life testing model based on type-2 censored data. J. Stat. Comput. Simul., Vol.52, PP. 95-103.
6. Mousa, M.A.M.A. and Jaheen, Z.F. (2002), Statistical inference for the Burr model base on progressively censored data, Comput. Math. Appl., Vol.43, PP.1441–1449.
7. Nasir, S. A. and Al-Anber, N. J. (2012), A Comparison of the Bayesian and Other Methods for Estimation of Reliability Function for Burr-XII Distribution, Journal of Mathematics and Statistics Vol.8, No.1, PP.42-48,

8. Norstrom, J.G. (1996), The use of precautionary loss function in risk analysis, IEEE Trans. on Reliab. 45(3): 400-403.
9. Panahi, H. and Asadi, S. (2009), Burr Type XII Distribution: Different Method of Estimations, The Tenth Islamic Countries Conference on Statistical Sciences, Egypt.
10. Rastogi, M. K. and Tripathi, Y. M. (2012), Estimating the parameters of a Burr distribution under progressive type II censoring. Statistical Methodology, Vol. 9, PP.381-391.
11. Singh, S.K.; Singh, U. and Kumar, D. (2011), Bayes Estimation of the Exponentiated Gamma Parameter and Reliability Function under Asymmetric Loss Function. REVSTAT Statistical Journal, Vol. 9, No.3, PP.247-260.
12. Soliman, A.A. (2002), Reliability Estimation in a Generalized Life Model with Application to the Burr-XII. IEEE Trans. Reliab. , Vol.51, PP.337-343.
13. Soliman, A.A. (2005), Estimation of parameters of life from progressively censored data using Burr-XII model. IEEE Trans. Reliab. , Vol.54, PP.34–42.
14. Yarmohammadi, M. and Pazira, H. (2010), Minimax Estimation of the Parameter of the Burr Type XII Distribution, Australian Journal of Basic and Applied Sciences, Vol. 4, No.12, PP.6611-6622.

Adomian Decomposition Method Applied to Nonlinear System of Fractional Fredholm Integro-Differential Equations

Nabaa N. Hasan
Department of Mathematics, College of Sciences, Al-Mustansiriya University
Received 17/3/2013 – Accepted 15/9/2013

الخلاصة

في هذا البحث تم تطبيق طريقة (Adomian Decomposition) لحل نظام معادلات فريدهولم التكاملية-التفاضلية اللاخطية عند الرتب الكسورية. صيغة (Leibniz) استخدمت لحل التكامل لقيم مختلفة من الرتبة الكسورية التي اعطيت في الامثلة العددية.

ABSTRACT

In this paper, Adomain decomposition method use to solve system of nonlinear Fredholm integro-differential equations with fractional order. Leibniz formulation is used to solve the integral for different values of fractional order are given in numerical examples.

INTRODUCTION

System of integral equations are used as mathematical models for many physical situations, recently a great deal of interest has been focused on application of the Adomian decomposition method to solve a wide variety of problems. Convergence theorem of Adomian decomposition method for nonlinear Fredholm integral equations is presented in, [1]. A computational method for solving a class of nonlinear Fredholm integro-differential eqations of fractional order which is based on cosine and sine wavelets presented in, [2]. Discrete Adomian decomposition method used to solve two dimensional Fredholm-Volterra integral equations in, [3]. Homotopy perturbation method is applied to solve nonlinear Fredholm integro-differential equations of fractional order in, [4].

In this paper, fractional calculus about fractional integral operator with its properties are given in preliminaries. Adomian decomposition method is used to approximate nonlinear system of fractional Fredholm integro-differential problems, by substituting Adomian polynomials to solve nonlinear part of the problem is presented in section 2. Numerical results show the approach of the method to exact solutions is described in section 3.

1. Preliminaries

In this section we introduce some basic definitions and properties of fractional integral which are used in this paper.

Definition(1),[5]:

A rea fnction *f(x)* is said to be in the space $C_\beta, \beta \in \mathbb{R}$ if there exists a real number $p > \beta$, such that $f(x) = x^p f_1(x)$, where $f_1 \in C[0, \infty)$, and it is said to be in the space C_β^n iff $f^{(n)} \in C_\beta$, $n \in N$.

Definition(2), [5]:

The Riemann-Liouville fractional integral operator of order $\alpha > 0$, of function $f \in C_\beta$, $\beta \geq -1$, is defined as :

$$I^\alpha f(x) = \frac{1}{\Gamma(\alpha)} \int_0^x (x-t)^{\alpha-1} f(t)dt < \infty$$

where $\Gamma(.)$ is the Euler gamma function.

this integral operator has the following properties:

(i) $I^0 f(x) = f(x)$

(ii) $I^\alpha I^\beta = I^{\alpha+\beta} = I^\beta I^\alpha$, $\alpha, \beta > 0$

(iii) $I^\alpha (x-a)^\gamma = \frac{\Gamma(\gamma+1)}{\Gamma(\alpha+\gamma+1)} (x-a)^{\alpha+\gamma}$, $\alpha > 0$, $\gamma > -1$

Definition(3), [2]: Fractional Leibniz Formula

$I_x^\alpha D_x^\alpha f(x) = f(x) - f(0)$, $0 < \alpha \leq 1$

$D_x^\alpha I_x^\alpha f(x) = f(x)$, $0 < \alpha < 1$

2. The Adomian Decomposition Method

In this section we extend the work presented in, [1] to solve system of nonlinear Fredholm integro-differential equations with fractional order. Fractional calculus is used to solve the fractional derivative and Adomian polynomials to solve the nonlinear part of the problem.

Consider the nonlinear system of fractional Fredholm integro-differential equations:

$$D^\alpha F(x) = G(x) + \int_a^b V(x,t,F(t))dt, \quad x \in [a,b], \alpha \in [0,1] \quad \ldots(1)$$

where:

$V(x,t,F(t)) = (v_1(x,t,F(t)), v_2(x,t,F(t)), \ldots, v_n(x,t,F(t)))^T$

$F(t) = (f_1(t), f_2(t), \ldots, f_n(t))^T$

$G(t) = (g_1(t), g_2(t), \ldots, g_n(t))^T$

Consider the i^{th} equation of (1):

$$D^\alpha f_i(x) = g_i(x) + \int_a^b v_i(x,t,f_1(t),f_2(t),\ldots,f_n(t))dt \quad \ldots(2)$$

Leibinz formula (definition(3)) of fractional integral for (2), we have:

$$f_i(x) - f_i(0) = I^\alpha g_i(x) + I^\alpha \int_a^b v_i(x,t,f_1(t),f_2(t),\ldots,f_n(t))dt \quad \ldots(3)$$

The Adomian equations can be written as, [1], [6]:

$$f_i(x) - f_i(0) = g_i(x) + N_i(x) \quad \ldots(4)$$

where:

$$N_i(x) = N_i(f_1, f_2, \ldots, f_n)(x) + I^\alpha \int_a^b v_i(x,t,f_1(t),f_2(t),\ldots,f_n(t))dt \quad \ldots(5)$$

Let: $f_i(x) = \sum_{m=0}^{\infty} f_{im}(x)$ and $N_i(x) = \sum_{m=0}^{\infty} A_{im}$
where A_{im}, $m = 0,1,2,...$ are the Adomian polynomials. Hence (4) can be written as
$\sum_{m=0}^{\infty} f_{im}(x) = g_i(x) + \sum_{m=0}^{\infty} A_{im}(f_{10}, f_{11}, \dots, f_{1m}, \dots, f_{n0}, \dots, f_{nn})$
...(6)
Define $f_{i0}(x) = g_i(x) - f_i(0)$
$f_{i,m+1}(x) = A_{im}(f_{10}, \dots, f_{1m}, \dots, f_{n0}, \dots, f_{nm})$ $i = 1,2,\dots,n$; $m = 0,1,2,\dots$ ...(7)
The approximation of the solution $f_i(x) = \sum_{m=0}^{\infty} f_{im}(x)$, truncated by the following series $u_{ik}(x) = \sum_{m=0}^{k-1} f_{im}(x)$, with:
$\lim_{k\to\infty} u_k(x) = f_i$
...(8)

To determine the Adomian polynomials, [7]:
$f_{i\lambda}(x) = \sum_{m=0}^{\infty} f_{im}(x)\lambda^m$
...(9)
and
$N_{i\lambda}(f_1, f_2, \dots, f_n) = \sum_{m=0}^{\infty} A_{im}\,\lambda^m$
...(10)
where λ is a parameter introduced for convenience. From (10), we obtain
$A_{im}(x) = \frac{1}{m!}\left[\frac{d^m}{d\lambda^m} N_{i\lambda}(f_1, f_2, \dots, f_n)\right]_{\lambda=0}$
...(11)

For example, the following two nonlinear functions, (which are used in numerical results) applied (11) to compute Adomian polynomials.
Assume the nonlinear part of (1), is f^2, then:
$A_0 = f_0^2$, $A_1 = 2f_0\, f_1$, $A_2 = 2f_0\, f_2 + f_1^2$, $A_3 = 2f_0\, f_3 + 2f_1 f_2$, ...
Assume the nonlinear part of (1), is f^3, then:
$A_0 = f_0^3$, $A_1 = 3f_0^2 f_1$, $A_2 = 3f_1^2 f_0 + 3f_0^2 f_2$, $A_3 = f_1^3 + 3f_0^2 f_3 + 6f_1 f_2 f_0$, ...

3. Numerical Results

In this section, we applied the presented method in this paper for solving nonlinear system of Fredholm integral equations of the second kind with fractional order and solved some examples. The computations associated with the examples were performed using MathCad14 software.

Example(1):

$$D^{\alpha} f_1(x) = g_1(x) + \int_0^1 f_1(t) f_2(t)\,dt$$

$$D^{\alpha} f_2(x) = g_2(x) + \int_0^1 f_1^2(t) f_2(t) dt$$

where $= 0.5$, $f_1(0) = f_2(0) = 0$

$$g_1(x) = \frac{\Gamma(2)}{\Gamma(1.5)} x^{0.5} - \frac{1}{4}$$

$$g_2(x) = \frac{\Gamma(3)}{\Gamma(2.5)} x^{1.5} - \frac{1}{5}$$

By fractional Leibniz formulation of integral:

$$f_1(x) = x - \frac{1}{4\Gamma(1.5)} x^{0.5} + I^{\alpha} \int_0^1 f_1(t) f_2(t) dt$$

$$f_2(x) = x^2 - \frac{1}{5\Gamma(1.5)} x^{0.5} + I^{\alpha} \int_0^1 f_1^2(t) f_2(t) dt$$

Now let, $f_{10}(x) = I^{\alpha} g_1(x)$ and $f_{20}(x) = I^{\alpha} g_2(x)$, then:

$$f_{10}(x) = x - \frac{1}{4\Gamma(1.5)} x^{0.5}$$

$$f_{20}(x) = x^2 - \frac{1}{5\Gamma(1.5)} x^{0.5}$$

By Adomian decomposition method, for the first iteration, we have:

$$f_{11}(x) = A_{10}(f_{10}, f_{20})$$

$$= I^{\alpha} \int_0^1 f_{10}(t) f_{20}(t) dt = I^{\alpha}(0.110962)$$

$$= 0.110962 \frac{1}{\Gamma(1.5)} x^{0.5}$$

$$f_{21}(x) = A_{20}(f_{10}, f_{20})$$

$$= I^{\alpha} \int_0^1 f_{10}^2(t) f_{20}(t) dt = I^{\alpha}(0.065297)$$

$$= 0.065297 \frac{1}{\Gamma(1.5)} x^{0.5}$$

For the second iteration, we have:

$$f_{12}(x) = A_{11}(f_{10}, f_{11}, f_{20}, f_{21})$$

$$= I^{\alpha} \int_0^1 f_{10}(t) f_{21}(t) + f_{20}(t) f_{11}(t) dt = I^{\alpha}(0.040725)$$

$$= 0.040725 \frac{1}{\Gamma(1.5)} x^{0.5}$$

$$f_{22}(x) = A_{21}(f_{10}, f_{11}, f_{20}, f_{21})$$
$$= I^{\alpha}\int_{0}^{1} f_{10}^{2}(t)f_{21}(t) + 2f_{10}(t)f_{20}f_{11}(t)dt$$
$$= I^{\alpha}(0.035067) = 0.035067\frac{1}{\Gamma(1.5)}x^{0.5}$$

For the third iteration, we have:

$$f_{13}(x) = A_{12}(f_{10}, f_{11}, f_{12}, f_{20}, f_{21}, f_{22})$$
$$= I^{\alpha}\int_{0}^{1} 2f_{10}(t)f_{22}(t) + 2f_{11}(t)f_{21}(t) + 2f_{20}(t)f_{12}(t)dt$$
$$= I^{\alpha}(0.045609) = 0.045609\frac{1}{\Gamma(1.5)}x^{0.5}$$
$$f_{23}(x) = A_{22}(f_{10}, f_{11}, f_{12}, f_{20}, f_{21}, f_{22})$$
$$= I^{\alpha}\int_{0}^{1} 2f_{10}^{2}(t)f_{22}(t) + 4f_{10}(t)f_{21}(t)f_{11}(t)$$
$$+ f_{20}(2f_{11}^{2}(t)4f_{10}f_{12}(t))dt = I^{\alpha}(0.042129)$$
$$= 0.042129\frac{1}{\Gamma(1.5)}x^{0.5}$$

The solutions after three iterations are:

$$u_1(x) = f_{10}(x) + f_{11}(x) + f_{12}(x) + f_{13}(x) = x - 0.059\sqrt{x}$$
$$u_2(x) = f_{20}(x) + f_{21}(x) + f_{22}(x) + f_{23}(x) = x^2 - 0.065\sqrt{x}$$

where the exact solutions are:

$f_1(x) = x$ and $f_2(x) = x^2$

Table(1) and figures(1) and (2) illustrate the results of example(1):

Table:1- Results of Example (1)

x	$f_1(x)$	$u_1(x)$	$\lvert f_1(x)- u_1(x)\rvert$	$f_2(x)$	$u_2(x)$	$\lvert f_2(x)- u_2(x)\rvert$
0	0	0	0	0	0	0
0.1	0.1	0.081	0.019	0.01	0.011	0.021
0.2	0.2	0.173	0.027	0.04	0.011	0.029
0.3	0.3	0.267	0.033	0.09	0.054	0.036
0.4	0.4	0.362	0.038	0.16	0.119	0.041
0.5	0.5	0.458	0.042	0.25	0.204	0.046
0.6	0.6	0.554	0.046	0.36	0.310	0.050
0.7	0.7	0.650	0.050	0.49	0.436	0.054
0.8	0.8	0.747	0.053	0.64	0.582	0.058
0.9	0.9	0.844	0.056	0.81	0.748	0.062
1	1	0.941	0.059	1	0.935	0.065

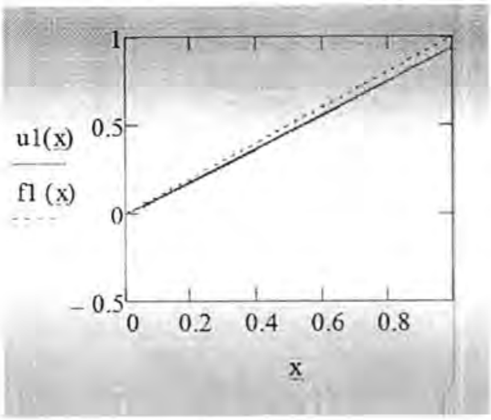

Figure-1

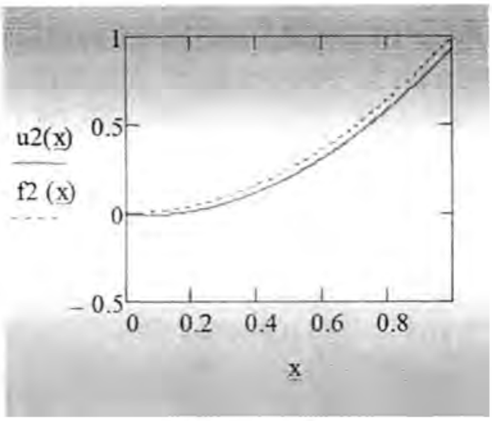

Figure-2

Example(2):

$$D^{\alpha_1} f_1(x) = g_1(x) + \int_0^1 xtf_1^2(t) + t^2 f_2^3(t)dt$$

$$D^{\alpha_2} f_2(x) = g_2(x) + \int_0^1 tf_1^3(t) - xf_2(t)dt$$

where $\alpha_1 = 0.5$ and $\alpha_2 = 0.75$, $f_1(0) = f_2(0) = 0$

$$g_1(x) = \Gamma(1.5) - \frac{x}{2}$$

$$g_2(x) = \frac{\Gamma(2)}{\Gamma(1.25)} x^{0.25} + \frac{x}{2} - \frac{2}{7}$$

By using fractional Leibniz formulation of integral and Adomian decomposition method, after three iterations, the solutions are:

$$u_1(x) = f_{10}(x) + f_{11}(x) + f_{12}(x) + f_{13}(x) = 1.183\sqrt{x} - 0.134x^{1.5}$$

$$u_2(x) = f_{20}(x) + f_{21}(x) + f_{22}(x) + f_{23}(x)$$
$$= x - 0.027x^{0.75} + 0.013x^{1.75}$$

where the exact solutions are:

$f_1(x) = \sqrt{x}$ and $f_2(x) = x$

Table(2) and figures(3) and (4) illustrate the results of example(2):

Table2-Results of Example (2)

x	$f_1(x)$	$u_1(x)$	$\lvert f_1(x)- u_1(x)\rvert$	$f_2(x)$	$u_2(x)$	$\lvert f_2(x)- u_2(x)\rvert$
0	0	0	0	0	0	0
0.1	0.316	0.370	0.054	0.1	0.095	4.57e10^{-3}
0.2	0.447	0.517	0.070	0.2	0.193	7.301e10^{-3}
0.3	0.548	0.626	0.078	0.3	0.291	9.374e10^{-3}
0.4	0.632	0.714	0.082	0.4	0.389	0.011
0.5	0.707	0.789	0.082	0.5	0.488	0.012
0.6	0.775	0.854	0.079	0.6	0.587	0.013
0.7	0.837	0.911	0.074	0.7	0.686	0.014
0.8	0.894	0.962	0.068	0.8	0.786	0.014
0.9	0.949	1.008	0.059	0.9	0.886	0.014
1	1	1.049	0.049	1	0.986	0.014

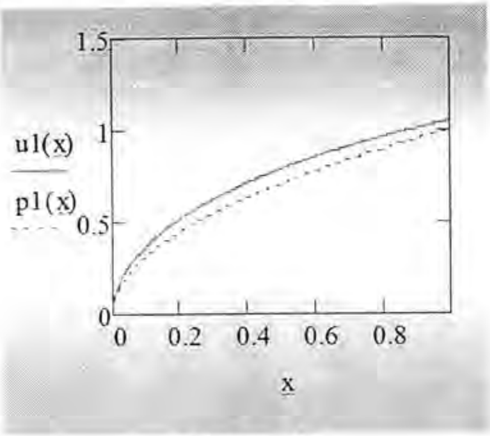

Figure-3

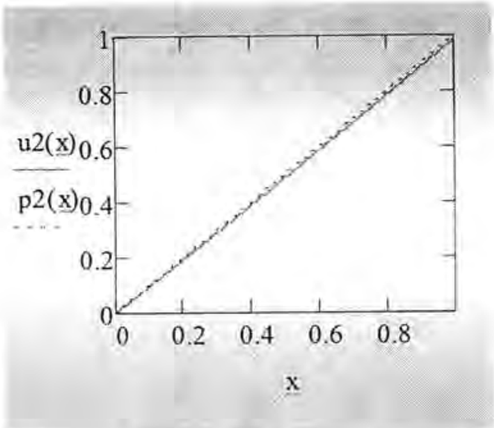

Figure-4

Conclusion

System of nonlinear Fredholm integral equations with fractional order is usually difficult to solve analytically. In many cases, it is required to obtain the approximate solutions. For this purpose, the presented method can be proposed. We approximate the nonlinear parts by Adomian polynomials. The method gave better approximations with less iterations when applied to solve the problem presented in this paper, As shown by numerical examples, the accuracy of this method is reasonable.

REFERENCES

1. Bakodah H. O., "Some Modifications of Adomian Decomposition Method Applied to Nonlinear System of Fredholm Integral Equations of the Second Kind", Int. J. Contemp. Math. Sciences, vol.7, no.19, pp.929-942, 2012.
2. Saeedi H. and Mohseni M., "A CAS Wavelet Method for Solving Nonlinear Fredholm Integro-Differential Eqations of Fractional Order", Max-Planck-Institut., preprint no.4, pp. 1-16, 2010.
3. Hendi F.A. & Bakodah H.O., "Numerical Solution of Fredholm-Volterra Integral Equation in two Dimensional Space by Using Discrete Adomian Decomposition Method", IJRRAS, vol.10, no.3, pp.466-471, 2012.
4. Saeedi H. and Samimi F., "He's Homotopy Perturbation Method for Nonlinear Fredholm Integro-Differential Equations of Fractional Order", International Jornal of Engineering Research and Applications, vol.2, no.5, pp.052-056, 2012.
5. Balachandran K. and Kiruthika S., "Existence of Solutions of Abstract Fractional Impulsive Semilinear Evolution Equations", electric journal of qualitative theory of differential equations, no.4, pp.1-12, 2010.

6. Biazar J. and Shafior S., "A Simple Algorithm for Calculating Adomian Polynomials", Int. J. Contemp. Math. Sciences, vol.2, no.20, pp. 975-982, 2007.
7. Hooman F. and Hossein A., "On Calculation of Adomian Polynomials by Matlab", J. of applied computer science & mathematics, vol.5, no.11, pp.85-88, 2011.

The Geometry of The Line of Order Seventeen and its Application to Error-Correcting Codes

J.W.P. Hirschfeld [1]and N.A.M. Al-seraji[2]
[1]School of Mathematical and Physical Sciences, University of Sussex, Brighton, United Kingdom
[2]Department of Mathematics, College of Science, Al-Mustansiriya University
Received 19/2/2013 – Accepted 15/9/2013

الخلاصة

الهدف من هذا البحث هو تصنيف تشكيل هندسي معين يدعى k-set وبالوضع الخاص يدعى خط الإسقاط من الرتبة السابعة عشر. الاداوات الأساسية هي نظرية خط الإسقاط الهندسي . يوجد إسقاطي وحيد لخط الإسقاط ينقل ثلاث نقاط إلى إي ثلاث نقاط أخرى . كل واحدة k-sets تعطي تصحيح اكبر خطا للرمز والتي تصحح النهايات العظمى من الإعداد الممكنة من الأخطاء لأطوالها .

ABSTRACT

The main of this paper is to classify certain geometric structures, called k-sets, in a particular setting, namely the projective line of order seventeen $PG(1,17)$. The basic tool is the fundamental theorem of projective geometry; there is a unique projectivity of the projective line transforming three points to any three other points. Each of these k-sets gives rise to an error-correcting code that corrects the maximum possible number of errors for its length.

1. INTRODUCTION

On $PG(1,q)$, a $(k;1)$-arc is just an unordered set of k distinct points simply called a k-set. A 4-set is called a tetrad, a 5-set a pentad, a 6-set a hexad, a 7-set a heptad, an 8-set a octad, a 9-set a nonad. A $(k;2)$-arc in projective plane $PG(2,q)$ is a set of k points no three of which are collinear.

k-sets in $PG(1,q)$ for $q = 2,3,4,5,7,8,9,11,13$ have been classified; see [3] and k-sets in $PG(1,16)$ are classified see [4], k-sets in $PG(1,19)$ are classified see [5]. We are looking at the line of order seventeen, as it is the next in the sequence, see [1].

We answer the equestion: How many projectively inequivalent k-sets in $PG(1,q)$ are there and what is the stabilizer group of each one?

Associated to any topic in mathematics is its history. Arcs were first introduced by Bose (1947) in connection with designs in statistics. In 1981 Goppa found important applications of curves over finite fields to coding theory. As to geometry over a finite field, it has been thoroughly studied in the major treatise of Hirschfeld 1979-1985 and of Hirschfeld and Thas 1991) and Hirschfeld, G. Korchmáros and F. Torres (2007).

The 18 points of $PG(1,17)$ are $P(x_0,x_1)$, $x_i \in \mathbb{F}_{17}$. So

$$PG(1,17) = \{U_0 = P(1,0)\} \cup \{P(x,1) | x \in \mathbb{F}_{17}\}.$$

Each point $P(x_0,x_1)$ with $x_1 \neq 0$ is determined by the non-homogeneous coordinate x_0/x_1; the coordinate for U_0 is ∞. Then, with

$\mathbb{F}_{17} \cup \{\infty\}$, each point of $PG(1,17)$ is represented by a single element of $\mathbb{F}_{17} \cup \{\infty\}$. Thus

$$PG(1,17) = \{P(t,1) | t \in \mathbb{F}_{17} \cup \{\infty\}\};$$

Here, $P(\infty,1) = P(1,0)$. A projectivity $\xi = M(T)$ of $PG(1,16)$ is given by $Y = XT$, where $X = (x_0, x_1)$, $Y = (y_0, y_1)$ and

$$T = \begin{pmatrix} a & b \\ c & d \end{pmatrix}.$$

Let $s = y_0/y_1$ and $t = x_0/x_1$; then $s = (at + c)/(bt + d)$. If $Q_i = P_i\xi$ for $i = 2,3,4$ and P_i and Q_i have the respective coordinate t_i and s_i, then ξ is given by

$$\frac{(s - s_3)(s_2 - s_4)}{(s - s_4)(s_2 - s_3)} = \frac{(t - t_3)(t_2 - t_4)}{(t - t_4)(t_2 - t_3)}$$

2. PREVIOUS RESULTS

Definition(2.1): Let S and S^* be two subspaces of $PG(n,K)$, A *projectivity* $\beta: S \to S^*$ is a bijection given by a matrix T, necessarily non-singular, where $P(X^*) = P(X)\beta$ if $tX^* = XT$, with $t \in K$. Write $\beta = M(T)$; then $\beta = M(\lambda T)$ for any λ in K. The group of projectivities of $PG(n,K)$ is denoted by $PGL(n+1,K)$.

Definition(2.2): A group G acts on a set Λ if there is a map $\Lambda \times G \to \Lambda$ such that given g, g′ elements in G and 1 its identity, then

1. $x1 = x$,
2. $(xg)g' = x(gg')$ for any x in Λ.

Definition(2.3): The orbit of x in Λ under the action of G is the set

$$xG = \{xg | g \in G\}.$$

Definition(2.4): The stabilizer of x in Λ under the action of G is the group

$$G_x = \{g \in G | xg = x\}.$$

Theorem(2.5)[3]: There is a unique projectivity of $PG(1,q)$ transforming three points to any three other points.

Definition(2.6): An $[n,k,d]_q$ code C is a subspace of $V(n,q) = (\mathbb{F}_q)^n$, where the dimension of C is dim $C = k$, and the minimum distance is $d(C) = d = \min d(x,y)$.

Definition(2.7): For any $[n,k,d]_q$ code we have $d \leq n - d + 1$.

Definition(2.8): Let the group G act on the set Λ.

1. If $y = xg$, for $x, y \in G$, then
   - $yG = xG$;
   - $G_y = g^{-1}G_x g$.
2. $|G_x| = |G|/|xG|$.

Definition(2.9): A *finite field* is a field with only a finite number of elements. The characteristic of a finite field K is the least positive integer p, and hence a prime, such that

$$pz = \underbrace{z + \cdots + z}_{p} = 0$$

For all $z \in K$.

Definition(2.10): The set denoted by $\mathbb{F}_P$, with P prime, consists of the residue classes of the integers modulo P under the natural addition and multiplication.

Theorem(2.11)[3]: There exists a projective $[n, k, d]_q$ −code if and only if there exists an $(n; n - d)$-arc in $PG(k - 1, q)$.

3. Results and Discussion

3.1 The Algorithm for Classification of the k -Sets in $PG(1, q)$

On $PG(1,17)$, a k-set can be constructed by adding to any $(k - 1)$- set one point from the other $q - k + 2$ points. According to the Fundamental Theorem of Projective Geometry, Theorem (2.5), any three distinct points on a line are projectively equivalent; so choose a fixed triad A. A 4-set is formed by adding to A one point from the other $q - 2$ points on $PG(1, q)$; that is, from $PG(1, q) - A = A^c$. A 5-set is formed by adding to any tetrad B one point from the other $q - 3$ points on $PG(1, q)$.

The stabilizer group G_B fixes B and splits the other $q - 3$ points into a number of orbits; so, different 5-sets are formed by adding one point from each different orbit. The procedure can be extended to construct $6,7,8,9, \cdots, (\frac{q+1}{2})$-sets in $PG(1, q)$. The (n − 1)-subsets of an n-set are classified according to their projective type.

Let K and K' be two pentads. To check they are equivalent the following steps are used.

1. Classify tetrads in both pentads.
2. If the classifications of K and $K'$are different then they are projectively inequivalent.
3. If the classifications of K and $K'$are the same, then the transformations matrices A_α are constructed from a tetrad T with highest recurrence in the algebraic structure of K to tetrads T_α in K with same types of T.
4. If the action of one A_α on the remaining points of T are equal to the remaining points of T', then K and K' are projectively equivalent. If not, it means they are projectively inequivalent.

This procedure can be extended to check the equivalence between k-sets,

$k = 6,7,8,9,\cdots,(\frac{q+1}{2})$ and also can be used to calculate the stabilizer group of each k-set, for more details see [6].

3.2 Preliminary to $PG(1,17)$

On $PG(1,17)$, the projective line over Galois field of order 17, there are 18 points. The points of $PG(1,17)$ are the elements of the set

$$\mathbb{F}_{17} \cup \{\infty\} = \{\infty, 0, \pm 1, \pm 2, \pm 3, \pm 4, \pm 5, \pm 6, \pm 7, \pm 8\}.$$

The order of the projective group $PGL(2,17)$ is 18.17.16=4896. This is the number of ordered sets of three points. In the following sections, the k-sets in $PG(1,17)$, $k = 4,\cdots,9$; are classified by giving the projectively inequivalent k -sets with their stabilizer groups.

3.3 The Tetrads

Let S be the set of all different tetrads in $PG(1,17)$. Then the order of S

$$\text{is } |S| = \binom{18}{4} = 3060.$$

The cross-ratio of four ordered points P_1, P_2, P_3, P_4 with coordinate t_1, t_2, t_3, t_4 is

$$\{P_1, P_2; P_3, P_4\} = \{t_1, t_2; t_3, t_4\} = \frac{(t - t_3)(t_2 - t_4)}{(t - t_4)(t_2 - t_3)}.$$

If P_1, P_2, P_3, P_4 are distinct points, then P_1 and P_2 separate P_3 and P_4 harmonically, written $h(P_1, P_2; P_3, P_4)$, if $\{t_1, t_2; t_3, t_4\} = -1$.
So,

$$h(P_1, P_2; P_3, P_4) \Leftrightarrow h(P_2, P_1; P_3, P_4).$$

In this case, the permutations of the points only give three values of the cross-ratio, -1,2,1/2. Let ω be the cross-ratio of a tetrad in a given order. The tetrad is called *harmonic* (H) if $\omega = 1 - \omega, \omega/(\omega - 1)$ or $\omega = 1/\omega$. It is called *equianharmonic* (E) if $\omega = 1/(1 - \omega)$ or $\omega = (\omega - 1)/\omega$, and it is neither harmonic nor equianharmonic (N) if the cross-ratio is another value. Consider the tetrad $\{\infty, 0, 1, t\}$ with $t \in \mathbb{F}_{17}\{0,1\}$.
Let

$$X_1 = \{\text{ class of } H \text{ tetrads }\},$$
$$X_2 = \{\text{ class of } E \text{ tetrads }\},$$
$$X_3 = \{\text{ class of } N \text{ tetrads }\}.$$

Since $17 \not\equiv 0,1 (\text{mod } 3)$, there are no equianharmonic tetrads. So X_2 is empty. The tetrad $\{\infty, 0, 1, a\} \in X_1$ for $a = -1, 2, -8$. The tetrad $\{\infty, 0, 1, c\} \in X_3$ for

$$c = -2, 3, -3, 4, -4, 5, -5, 6, -6, 7, -7, 8.$$

As a tetrad of type N has six possible values of its cross-ratio, the class X_3 is partitioned into two subclasses C_2 with $c = -2,3,-5,6,-7,8$. and the other C_3 with $c = -3,4,-4,5,-6,7$. If we now call the three classes C_1, C_2 and C_3 where $C_1 = X_1$, $C_2 \cup C_3 = X_3$, then the tetrads within each class C_i are projectively equivalent. So there are three projectively distinct tetrads: one of type H and two of type N, called N_1 and N_2.

1. Consider the tetrad $H = \{\infty, 0, 1, -1\}$ chosen from the class C_1. Then the projective group of H is isomorphic to dihedral group of order 8.
2. the tetrad $N_1 = \{\infty, 0, 1, -2\}$ chosen from the class C_2. Then the projective group of N_1 is isomorphic to the direct product of $\mathbf{Z}_2$ and $\mathbf{Z}_2$.
3. the tetrad $N_2 = \{\infty, 0, 1, -3\}$ chosen from the class C_3. Then the projective group of N_2 is isomorphic to the direct product of $\mathbf{Z}_2$ and $\mathbf{Z}_2$.

3.4 The Pentads

To construct the pentad in $PG(1,17)$, it is enough to add one point from each orbit that comes from the action of the projective group of the tetrad G_T on the complement of T, where $T = H, N_1, N_2$. All orbits of the tetrads are given in Table 1.

Table -1: Partition of $PG(1,17)$ by the projectivities of tetrads

T	G_T	Partition of T^c
H	$\langle \frac{1}{x}, \frac{x-1}{x+1} \rangle$	1. {2,-2,3,-3,6,-6,8,-8} 2. {4,-4} 3. {5,-5,7,-7}.
N_1	$\langle \frac{x+2}{x-1}, \frac{-2}{x} \rangle$	1. {-1,2,4,8} 2. {3,5,6,-6} 3. {-3,-4,-5,-8} 4. {7,-7}.
N_2	$\langle \frac{x+3}{x-1}, \frac{-3}{x} \rangle$	1. {-1,3} 2. {2,-4,5,7} 3. {-2,-6,-7,-8} 4. {4,-5,6,8}.

According to Table 3.1, there are thirteen pentads constructed by adding one point from each orbit to the corresponding tetrad. Each pentad contains five tetrads. In Table 3.2, for each pentad $\{a_1, a_2; a_3, a_4, a_5\}$ the classification of its tetrads in the order $\{a_1, a_2, a_3, a_4\}$, $\{a_1, a_2, a_3, a_5\}$, $\{a_1, a_2, a_4, a_5\}$, $\{a_1, a_3, a_4, a_5\}$, $\{a_2, a_3, a_4, a_5\}$ is given. Also the stabilizer group of each pentad is given.

Table-2: Pentads on $PG(1,17)$

No.	The pentads	Types of tetrads	Stabilizer
1	$\{\infty,0,1,-1,2\}$	$HHN_1N_1N_2$	$\mathbf{Z}_2=\langle\frac{1-x}{1}\rangle$
2	$\{\infty,0,1,-1,4\}$	$HN_2N_2N_2N_2$	$\mathbf{Z}_4=\langle\frac{x-1}{x+1}\rangle$
3	$\{\infty,0,1,-1,5\}$	$HN_2N_1N_1N_2$	$\mathbf{Z}_2=\langle\frac{1-x}{1+x}\rangle$
4	$\{\infty,0,1,-2,-1\}$	$N_1HHN_1N_2$	$\mathbf{Z}_2=\langle\frac{-x-1}{1}\rangle$
5	$\{\infty,0,1,-2,3\}$	$N_1N_1N_2N_2N_1$	$\mathbf{Z}_2=\langle\frac{1-x}{1}\rangle$
6	$\{\infty,0,1,-2,-3\}$	$N_1N_2N_1N_2H$	$\mathbf{Z}_2=\langle\frac{-x-2}{1}\rangle$
7	$\{\infty,0,1,-2,7\}$	$N_1N_2N_2N_1N_1$	$\mathbf{Z}_2=\langle\frac{-2}{x}\rangle$
8	$\{\infty,0,1,-3,-1\}$	$N_2HN_1HN_1$	$\mathbf{Z}_2=\langle\frac{x+3}{x-1}\rangle$
9	$\{\infty,0,1,-3,2\}$	$N_2HN_2N_2N_2$	$\mathbf{Z}_4=\langle\frac{2x-2}{x}\rangle$
10	$\{\infty,0,1,-3,-2\}$	$N_2N_1N_1N_2H$	$\mathbf{Z}_2=\langle\frac{-x-2}{1}\rangle$
11	$\{\infty,0,1,-3,4\}$	$N_2N_2N_1N_1N_1$	$\mathbf{Z}_2=\langle\frac{1-x}{1}\rangle$

According to the types of the five tetrads, the pentads fall into four sets, $\{1,4,8\},\{2,9\},\{3,6,10\},\{5,7,11\}$. The pentads 6 and 10 are the same. For those pentads with an equivalent sets of tetrads, Table 3 gives the projectivities between them.

Table-3: The equivalence of pentads

No.	Equivalent pentads	Projective equation
1	1⟶4	$(\frac{-x}{1})$
2	1⟶8	$(\frac{1+x}{1-x})$
3	2⟶9	$(\frac{1+x}{x})$
4	3⟶6	$(\frac{1+x}{8x-6})$
5	5⟶7	$(\frac{x+2}{5x+2})$
6	5⟶11	$(\frac{7x-3}{1})$

Table 3 gives the following conclusion.

Theorem (3.1): On $PG(1,17)$ there are precisely four projectively distinct pentads, given with their stabilizer groups in Table 4.

Table -4: Inequivalent pentads on $PG(1,17)$

Type	The pentad	Stabilizer
P_1	$\{\infty,0,1,-1,2\}$	$\mathbf{Z}_2=\langle\frac{1-x}{1}\rangle$
P_2	$\{\infty,0,1,-1,4\}$	$\mathbf{Z}_4=\langle\frac{2x-2}{x}\rangle$
P_3	$\{\infty,0,1,-1,5\}$	$\mathbf{Z}_2=\langle\frac{1-x}{1+x}\rangle$
P_4	$\{\infty,0,1,-2,3\}$	$\mathbf{Z}_2=\langle\frac{1-x}{1}\rangle$

3.5 The Hexads

The projective group G_{P_i} splits $P_i{}^c, i=1,2,3,4$ into a number of orbits. The hexads are constructed by adding one point from each orbit to the corresponding pentads. All orbits are listed in Table 3.5.

Table -5: Partition of $PG(1,17)$ by the projectivities of pentads

P_i	Partition of $P_i{}^c$
P_1	1. {-2,3} 2. {-3,4} 3.{-4,5} 4. {-5,6} 5. {-6,7} 6.{-7,8} 7. {-8}
P_2	1. {-2,3,-6,-8} 2. {2,6,-3,-8} 3. {-4} 4. {5,-5,-7,7}
P_3	1. {2,-6} 2. {-2,-3} 3. {3,8} 4. {4,-4} 5. {-5,7} 6. {6,-8} 7. {-7}
P_4	1. {-1,2} 2. {-3,4} 3. {-4,5} 4. {-5,6} 5.{-6,7} 6. {-7,8} 7.{-8}

Therefore, 25 hexads can be formed (the total number of all orbits) by adding
one point from each orbit to the corresponding pentad.

According to the types of the six pentads, the hexads fall into ten sets. This gives the following conclusion.

Theorem 3.2: On $PG(1,17)$ there are precisely 10 projectively distinct hexads, given in Table -6.

Table -6: The distinct hexads

Type	The hexad	Types of pentads	Stabilizer
H_1	$\{\infty,0,1,-1,2,-2\}$	$P_1P_1P_1P_1P_3P_3$	$\mathbf{Z}_2\times\mathbf{Z}_2=\langle\frac{-x}{1},\frac{2}{x}\rangle$
H_2	$\{\infty,0,1,-1,2,-3\}$	$P_1P_1P_2P_4P_3P_4$	$\mathbf{I}=\langle x\rangle$
H_3	$\{\infty,0,1,-1,2,-4\}$	$P_1P_2P_3P_1P_3P_2$	$\mathbf{Z}_2=\langle\frac{2x+2}{x-2}\rangle$
H_4	$\{\infty,0,1,-1,2,-6\}$	$P_1P_1P_3P_4P_4P_3$	$\mathbf{Z}_2=\langle\frac{1-x}{1+x}\rangle$
H_5	$\{\infty,0,1,-1,2,-7\}$	$P_1P_3P_1P_4P_3P_4$	$\mathbf{Z}_2=\langle\frac{x-2}{x-1}\rangle$
H_6	$\{\infty,0,1,-1,2,-8\}$	$P_1P_1P_1P_1P_1P_1$	$\mathbf{D}_6=\langle\frac{1+x}{2-x},\frac{2-x}{x+1}\rangle$
H_7	$\{\infty,0,1,-1,4,-4\}$	$P_2P_2P_2P_2P_2P_2$	$\mathbf{S}_4=\langle\frac{1+x}{4-4x},\frac{x+1}{1-x}\rangle$
H_8	$\{\infty,0,1,-1,4,5\}$	$P_2P_3P_2P_4P_4P_3$	$\mathbf{Z}_2=\langle\frac{1-x}{1+4x}\rangle$
H_9	$\{\infty,0,1,-1,5,-5\}$	$P_3P_3P_3P_3P_4P_4$	$\mathbf{Z}_2\times\mathbf{Z}_2=\langle\frac{-x}{1},\frac{5}{x}\rangle$
H_{10}	$\{\infty,0,1,-2,3,-6\}$	$P_4P_4P_4P_4P_4P_4$	$\mathbf{S}_3=\langle\frac{x+2}{x-1},\frac{x+6}{6x-1}\rangle$

3.6 The Heptads

The projective group G_{H_i} splits ${H_i}^c, i=1,\cdots,10$ into a number of orbits. The heptads are constructed by adding one point from each orbit to the corresponding hexads. All orbits are listed in Table 7.

Table -7: Partition of $PG(1,17)$ by the projectivities of hexads

H_i	Partition of ${H_i}^c$
H_1	1. {3,-3,5,-5} 2.{4,-4,8,-8} 3.{6,-6} 4.{7,-7}
H_2	G_{H_2} splits ${H_2}^c$ 5 into 12 orbits of single points
H_3	1. {-2,-8} 2.{3,8} 3. {-3,-6} 4.{4,5} 5. {-5,6} 6.{7,-7}
H_4	1. {-2,-3} 2.{3,8} 3.{4,-4} 4.{5} 5.{-5,7} 6.{6,-8} 7.{-7}
H_5	1. {-2,7} 2.{3,-8} 3.{-3} 4.{4,-5} 5.{-4,8} 6.{5} 7.{6,-6}
H_6	G_{H_6} fixes ${H_6}^c$
H_7	G_{H_7} fixes ${H_7}^c$
H_8	1. {2,-2} 2. {3,-8} 3.{-3,-5} 4.{-4,-6} 5.{6,-7} 6.{7,8}
H_9	1. {2,-2,6,-6} 2.{3,-3,4,-4} 3.{7,-7,8,-8}
H_{10}	1. {-1,-5,5,6,8,-8} 2.{ 2,-3,4,-4,7,-7}

Therefore, 49 heptads can be formed by adding one point from each orbit to the corresponding hexad.
According to the types of the seven hexads, the heptads fall into ten sets. This gives the following conclusion.
Theorem 3.3: On $PG(1,17)$ there are precisely 10 projectively distinct heptads, given in Table8.

Table -8: The distinct heptads

Type	The hetad	Types of hexads	Stabilizer
T_1	$\{\infty,0,1,-1,2,-2,-3\}$	$H_1H_2H_1H_3H_2H_3H_4$	$\mathbf{Z}_2=\langle -x-1\rangle$
T_2	$\{\infty,0,1,-1,2,-2,-8\}$	$H_1H_6H_4H_2H_3H_2H_4$	$\mathbf{I}=\langle x\rangle$
T_3	$\{\infty,0,1,-1,2,-2,6\}$	$H_1H_2H_4H_2H_4H_8H_8$	$\mathbf{Z}_2=\langle \frac{2}{x}\rangle$
T_4	$\{\infty,0,1,-1,2,-2,-7\}$	$H_1H_4H_4H_4H_4H_9H_9$	$\mathbf{Z}_2=\langle \frac{-2}{x}\rangle$
T_5	$\{\infty,0,1,-1,2,-3,4\}$	$H_2H_2H_2H_2H_4H_4H_4$	$\mathbf{Z}_2=\langle 1-x\rangle$
T_6	$\{\infty,0,1,-1,2,-3,-4\}$	$H_2H_3H_3H_8H_4H_9H_2$	$\mathbf{I}=\langle x\rangle$
T_7	$\{\infty,0,1,-1,2,-3,5\}$	$H_2H_3H_2H_7H_8H_3H_8$	$\mathbf{Z}_2=\langle \frac{x+3}{x-1}\rangle$
T_8	$\{\infty,0,1,-1,2,-3,6\}$	$H_2H_2H_4H_8H_{10}H_9H_8$	$\mathbf{I}=\langle x\rangle$
T_9	$\{\infty,0,1,-1,2,-3,-7\}$	$H_2H_4H_4H_2H_{10}H_4H_{10}$	$\mathbf{Z}_2=\langle \frac{x-2}{x-1}\rangle$
T_{10}	$\{\infty,0,1,-1,2,-4,-7\}$	$H_3H_4H_8H_4H_4H_3H_8$	$\mathbf{Z}_2=\langle \frac{2x-3}{x-2}\rangle$

3.7 The Octads

The projective group G_{T_i} splits $T_i{}^c, i=1,\cdots,10$ into a number of orbits. The octads are constructed by adding one point from each orbit to the corresponding heptads. All orbits are listed in Table 9.

Table-9: Partition of $PG(1,17)$ by the projectivities of heptads

T_i	Partition $T_i{}^c$
T_1	1. {3,-4} 2.{4,-5} 3.{5,-6} 4.{6,-7} 5.{7,-8} 6.{8}
T_2	G_{T_2} splits $T_2{}^c$ into 11 orbits of single points.
T_3	1. {3,-5} 2.{-3,5} 3.{4,-8} 4.{-4,8} 5.{-6} 6.{7,-7}
T_4	1. {3,5} 2.{-3,-5} 3.{4,8} 4.{-4,-8} 5.{6,-6} 6.{7}
T_5	1. {-2,3} 2.{-4,5} 3.{-5,6} 4.{-6,7} 5.{-7,8} 6.{-8}
T_6	G_{T_6} splits $T_6{}^c$ into 11 orbits of single points.
T_7	1. {-2,-6} 2.{3} 3.{4,8} 4.{-4,7} 5.{-5,6} 6.{-7,-8}
T_8	G_{T_8} splits $T_8{}^c$ into 11 orbits of single points.
T_9	1. {-2,7} 2.{3,-8} 3.{4,-5} 4.{-4,8} 5.{5} 6.{6,-6}
T_{10}	1.{-2,6} 2.{3} 3.{-3,-5} 4.{4,-6} 5.{5,8} 6.{7,-8}

Therefore, 75 octads can be formed by adding one point from each orbit to the corresponding heptad.
According to the types of the eight heptads, the octads fall into 17 sets. This gives the following conclusion.
Theorem 3.4: On $PG(1,17)$ there are precisely 17 projectively distinct octads, given in Table 10.

Table -10: The distinct octads

Type	The octad	Type of heptads	Stabilizer
O_1	$\{\infty,0,1,-1,2,-2,-3,-4\}$	$T_1T_2T_6T_1T_{10}T_2T_6T_5$	$\mathbf{Z}_2=\langle -x-1\rangle$
O_2	$\{\infty,0,1,-1,2,-2,-3,4\}$	$T_1T_2T_5T_1T_2T_5T_2T_2$	$\mathbf{Z}_2=\langle\frac{x+3}{-x-1}\rangle$
O_3	$\{\infty,0,1,-1,2,-2,-3,5\}$	$T_1T_1T_7T_3T_7T_3T_{10}T_{10}$	$\mathbf{Z}_2=\langle\frac{2}{x}\rangle$
O_4	$\{\infty,0,1,-1,2,-2,-3,-7\}$	$T_1T_4T_9T_3T_6T_8T_6T_8$	$\mathbf{I}=\langle x\rangle$
O_5	$\{\infty,0,1,-1,2,-2,-3,-8\}$	$T_1T_2T_2T_4T_6T_6T_1T_4$	$\mathbf{Z}_2=\langle\frac{2x-1}{x-2}\rangle$
O_6	$\{\infty,0,1,-1,2,-2,-3,8\}$	$T_1T_2T_8T_2T_7T_8T_7T_9$	$\mathbf{Z}_2=\langle -x-1\rangle$
O_7	$\{\infty,0,1,-1,2,-2,-8,-4\}$	$T_2T_2T_2T_9T_9T_2T_9T_9$	$\mathbf{Z}_2\times\mathbf{Z}_2=\langle\frac{-x+2}{x+1},\frac{x+1}{-8x-1}\rangle$
O_8	$\{\infty,0,1,-1,2,-2,-8,6\}$	$T_2T_3T_2T_4T_5T_6T_6T_{10}$	$\mathbf{I}=\langle x\rangle$
O_9	$\{\infty,0,1,-1,2,-2,-8,-6\}$	$T_2T_3T_2T_8T_6T_6T_3T_8$	$\mathbf{Z}_2=\langle\frac{-x+2}{-2x+1}\rangle$
O_{10}	$\{\infty,0,1,-1,2,-2,-8,7\}$	$T_2T_4T_2T_{10}T_8T_{10}T_8T_4$	$\mathbf{Z}_2=\langle\frac{x+1}{2x-1}\rangle$
O_{11}	$\{\infty,0,1,-1,2,-2,-8,8\}$	$T_2T_2T_2T_2T_7T_7T_3T_3$	$\mathbf{Z}_2\times\mathbf{Z}_2=\langle\frac{1}{x},\frac{-1}{x}\rangle$
O_{12}	$\{\infty,0,1,-1,2,-2,6,-7\}$	$T_3T_4T_5T_9T_9T_5T_8T_8$	$\mathbf{I}=\langle x\rangle$
O_{13}	$\{\infty,0,1,-1,2,-2,-7,7\}$	$T_4T_4T_4T_4T_4T_4T_4T_4$	$\mathbf{D}_8=\langle\frac{-x+7}{5x+1},\frac{x+2}{x+1}\rangle$
O_{14}	$\{\infty,0,1,-1,2,-3,4,5\}$	$T_5T_7T_6T_8T_7T_8T_{10}T_6$	$\mathbf{I}=\langle x\rangle$
O_{15}	$\{\infty,0,1,-1,2,-3,-4,5\}$	$T_6T_7T_7T_6T_7T_6T_6T_7$	$\mathbf{Z}_2\times\mathbf{Z}_2=\langle\frac{x-5}{-x-1},\frac{-x+1}{-4x+1}\rangle$
O_{16}	$\{\infty,0,1,-1,2,-3,-4,-7\}$	$T_6T_9T_{10}T_{10}T_8T_9T_6T_8$	$\mathbf{Z}_2=\langle\frac{x+7}{-x-1}\rangle$
O_{17}	$\{\infty,0,1,-1,2,-3,6,8\}$	$T_8T_8T_8T_8T_8T_8T_8T_8$	$\mathbf{D}_8=\langle\frac{x+1}{-x+1},\frac{2x+1}{x-2}\rangle$

3.8 The Nonads

The projective group G_{O_i} splits ${O_i}^c, i=1,\cdots,17$ into a number of orbits. The nonads are constructed by adding one point from each orbit to the corresponding octads. All orbits are listed in Table 11.

Table -11: Partition of $PG(1,17)$ by the projectivities of octads

O_i	Partition of O_i^c
O_1	1. {3,-5} 2.{4,-6}3.{5,-7}4.{6,-8}5.{7,8}
O_2	1. {3,7}2.{-4,-6}3.{5,-7}4.{-5,8}5.{6}7.{8}
O_3	1. {3,-5}2.{4,-8}3.{-4,8}4.{6}5.{-6}6.{7,-7}
O_4	G_{O_4} splits $O_4{}^c$ into 10 orbits of single points
O_5	1. {3,5}2.{4,-5}3.{-4,-7}4.{6,7}5.{-6,8}
O_6	1. {3,-4}2.{4,-5}3.{5,-6}4.{6,-7}5.{7,-8}
O_7	1. {-3,-5,6,-6}2.{3,4,5,8}3.{7,-7}
O_8	G_{O_8} splits $O_8{}^c$ into 10 orbits of single points
O_9	1. {-3,8}2.{3,7}3.{4,-7}4.{-4,-5}5.{5,6}
O_{10}	1. {-3,-7}2.{3,-6}3.{4,8}4.{-4,6}5.{5,-5}
O_{11}	1. {3,-3,6,-6}2.{4,-4}3.{5,-5,7,-7}
O_{12}	$G_{O_{12}}$ splits $O_{12}{}^c$ into 10 orbits of single points
O_{13}	1. {3,-3,4,-4,5,-5,8,-8}2.{6,-6}
O_{14}	$G_{O_{14}}$ splits $O_{14}{}^c$ into 10 orbits of single points
O_{15}	1. {-2,-5,6,-7}2.{3,-6,8,-8}3.{4,7}
O_{16}	1. {-2,5}2.{3,6}3.{4,8}4.{-5,-8}5.{-6,7}
O_{17}	1. {-2,3,5,-5,-6,7,-7,-8}2.{4,-4}

According to the types of the nine octads, the nonads fall into 17 sets. This gives the following conclusion.

Theorem 3.5: On $PG(1,17)$ there are precisely 17 projectively distinct nonads, given in Table12.

Table -12: The distinct nonds

Type	The nonad	Type of octads	Stabilizer
S_1	$O_1 \cup \{3\}$	$O_1O_1O_2O_5O_2O_8O_5O_8O_2$	$\mathbf{Z_2} = \langle -x-1 \rangle$
S_2	$O_2 \cup \{6\}$	$O_2O_4O_8O_{12}O_4O_9O_{12}O_8O_9$	$\mathbf{Z_2} = \langle \frac{x+3}{-x-1} \rangle$
S_3	$O_3 \cup \{3\}$	$O_3O_1O_2O_{11}O_8O_{14}O_9O_{10}O_8$	$\mathbf{I} = \langle x \rangle$
S_4	$O_3 \cup \{6\}$	$O_3O_4O_4O_{14}O_{12}O_{14}O_{12}O_{16}O_{16}$	$\mathbf{Z_2} = \langle \frac{2}{x} \rangle$
S_5	$O_3 \cup \{-6\}$	$O_3O_3O_3O_3O_3O_3O_3O_3O_3$	$\mathbf{D_9} = \langle \frac{x-2}{x+2}, \frac{-x-1}{1} \rangle$
S_6	$O_4 \cup \{3\}$	$O_4O_1O_5O_7O_9O_8O_4O_{16}O_{12}$	$\mathbf{I} = \langle x \rangle$
S_7	$O_4 \cup \{4\}$	$O_4O_2O_{10}O_{12}O_3O_1O_{14}O_5O_6$	$\mathbf{I} = \langle x \rangle$
S_8	$O_4 \cup \{5\}$	$O_4O_3O_5O_6O_{11}O_{15}O_9O_8O_{14}$	$\mathbf{I} = \langle x \rangle$
S_9	$O_6 \cup \{4\}$	$O_6O_2O_7O_{12}O_2O_{11}O_{12}O_6O_7$	$\mathbf{Z_2} = \langle \frac{-3x-5}{x+3} \rangle$
S_{10}	$O_6 \cup \{-6\}$	$O_6O_3O_8O_4O_1O_{14}O_{14}O_{15}O_{16}$	$\mathbf{I} = \langle x \rangle$
S_{11}	$O_6 \cup \{-7\}$	$O_6O_4O_{10}O_{16}O_9O_{14}O_{17}O_{14}O_{12}$	$\mathbf{I} = \langle x \rangle$
S_{12}	$O_8 \cup \{-3\}$	$O_5O_8O_4O_{10}O_{13}O_8O_4O_5O_{10}$	$\mathbf{Z_2} = \langle \frac{-2x-5}{x+2} \rangle$
S_{13}	$O_{10} \cup \{6\}$	$O_{10}O_8O_{12}O_7O_8O_{12}O_{16}O_{16}O_{10}$	$\mathbf{Z_2} = \langle \frac{x-1}{3x-1} \rangle$
S_{14}	$O_{12} \cup \{-3\}$	$O_{12}O_4O_4O_{12}O_{12}O_4O_{12}O_4O_{17}$	$\mathbf{Z_4} = \langle \frac{4x-7}{1} \rangle$
S_{15}	$O_{12} \cup \{-8\}$	$O_{12}O_8O_8O_8O_{12}O_{12}O_{14}O_{14}O_{14}$	$\mathbf{Z_3} = \langle \frac{1}{-x+1} \rangle$
S_{16}	$O_{13} \cup \{6\}$	$O_{13}O_{12}O_{12}O_{12}O_{12}O_{12}O_{12}O_{12}O_{12}$	$\mathbf{Z_8} = \langle \frac{x+2}{x+1} \rangle$
S_{17}	$O_{15} \cup \{4\}$	$O_{15}O_{14}O_{14}O_{15}O_{14}O_{14}O_{14}O_{14}O_{15}$	$\mathbf{S_3} = \langle \frac{x+1}{-6x+7}, \frac{-x+2}{6x+1} \rangle$

The Partitions of $PG(1,17)$

The stabilizer G_{S_i} of S_i also fixed the complement ${S_i}^c$. The nonad S_i is projectively equivalent to its complement ${S_i}^c$, except that S_9 is not equivalent to ${S_9}^c$ and S_{12} is inequivalent to ${S_{12}}^c$.

This gives the following result on partitions into nonads.

Theorem 3.6: The projective line $PG(1,17)$ has 17 projectively distinct partitions into two equivalent nonads by Table 13.

Table-13: Partitions of $PG(1,17)$ into two nonads

No.	Symbol	Stabilizer of partition
1	$\{S_1; {S_1}^c\}$	$\mathbf{Z}_2 \times \mathbf{Z}_2 = \langle \frac{8x-6}{x-8}, \frac{-x-1}{1} \rangle$
2	$\{S_2; {S_2}^c\}$	$\mathbf{Z}_2 \times \mathbf{Z}_2 = \langle \frac{x-3}{4x-1}, \frac{x+3}{-x-1} \rangle$
3	$\{S_3; {S_3}^c\}$	$\mathbf{Z}_2 = \langle \frac{-x-8}{5x+1} \rangle$
4	$\{S_4; {S_4}^c\}$	$\mathbf{Z}_2 \times \mathbf{Z}_2 = \langle \frac{-x-4}{2x+1}, \frac{2}{x} \rangle$
5	$\{S_5; {S_5}^c\}$	$\mathbf{D}_{18} = \langle \frac{5x+2}{7x-5}, \frac{-x-1}{1} \rangle$
6	$\{S_6; {S_6}^c\}$	$\mathbf{Z}_2 = \langle \frac{-x-6}{2x+1} \rangle$
7	$\{S_7; {S_7}^c\}$	$\mathbf{Z}_2 = \langle \frac{x-3}{7x-1} \rangle$
8	$\{S_8; {S_8}^c\}$	$\mathbf{Z}_2 = \langle \frac{-x+3}{2x+1} \rangle$
9	$\{S_9; {S_{12}}^c\}$	$\mathbf{Z}_2 = \langle \frac{x-3}{4x-1} \rangle$
10	$\{S_{10}; {S_{10}}^c\}$	$\mathbf{Z}_2 = \langle \frac{-x-8}{5x+1} \rangle$
11	$\{S_{11}; {S_{11}}^c\}$	$\mathbf{Z}_2 = \langle \frac{3x+2}{x-3} \rangle$
12	$\{S_{12}; {S_9}^c\}$	$\mathbf{Z}_2 = \langle \frac{x-3}{4x-1} \rangle$
13	$\{S_{13}; {S_{13}}^c\}$	$\mathbf{Z}_2 \times \mathbf{Z}_2 = \langle \frac{-x+3}{7x+1}, \frac{x-1}{3x-1} \rangle$
14	$\{S_{14}; {S_{14}}^c\}$	$\mathbf{D}_4 = \langle \frac{8x-6}{x-8}, \frac{4x-7}{1} \rangle$
15	$\{S_{15}; {S_{15}}^c\}$	$\mathbf{S}_3 = \langle \frac{-x+3}{2x+1}, \frac{1}{-x+1} \rangle$
16	$\{S_{16}; {S_{16}}^c\}$	$\mathbf{D}_8 = \langle \frac{4x+2}{-x-4}, \frac{x+2}{x+1} \rangle$
17	$\{S_{17}; {S_{17}}^c\}$	$\mathbf{D}_6 = \langle \frac{4x+8}{3x+1}, \frac{-x+2}{6x+1} \rangle$

In above Table, we note that, for the stabilizer groups which are generated by two elements, the first generator transforms the nonad to its complement, while the second generator fixes the nonad and its complement.

The transformations between the nonads and their complements are given in Table 14.

Table -14: Classification of the complements of the nonads in $PG(1,17)$

No.	Equivalent nonads	Projective equation
1	$S_1 \rightarrow S_1{}^c$	$(\frac{8x-6}{x-8})$
2	$S_2 \rightarrow S_2{}^c$	$(\frac{x-3}{4x-1})$
3	$S_3 \rightarrow S_3{}^c$	$(\frac{-x-8}{5x+1})$
4	$S_4 \rightarrow S_4{}^c$	$(\frac{-x-4}{2x+1})$
5	$S_5 \rightarrow S_5{}^c$	$(\frac{3x+4}{-2x+1})$
6	$S_6 \rightarrow S_6{}^c$	$(\frac{-x-6}{2x+1})$
7	$S_7 \rightarrow S_7{}^c$	$(\frac{x-3}{7x-1})$
8	$S_8 \rightarrow S_8{}^c$	$(\frac{-x+3}{2x+1})$
9	$S_9 \rightarrow S_{12}{}^c$	$(\frac{x-3}{4x-1})$
10	$S_{10} \rightarrow S_{10}{}^c$	$(\frac{-x-8}{5x+1})$
11	$S_{11} \rightarrow S_{11}{}^c$	$(\frac{3x+2}{x-3})$
12	$S_{12} \rightarrow S_9{}^c$	$(\frac{x-3}{4x-1})$
13	$S_{13} \rightarrow S_{13}{}^c$	$(\frac{-x+3}{7x+1})$
14	$S_{14} \rightarrow S_{14}{}^c$	$(\frac{8x-6}{x-8})$
15	$S_{15} \rightarrow S_{15}{}^c$	$(\frac{-x+3}{2x+1})$
16	$S_{16} \rightarrow S_{16}{}^c$	$(\frac{4x+2}{-x-4})$
17	$S_{17} \rightarrow S_{17}{}^c$	$(\frac{4x+8}{3x+1})$

3.9 MDS Code of Dimension Two

As in Theorem 2.11, an $(n;n-d)$-arc in $PG(k-1,q)$ is equivalent to a projective $[n,k,d]_q$ −code. So, if $k=2$ and $n-d=1$, then there is a one-to-one correspondence between n-sets in $PG(1,17)$ and projective $[n,2,n-1]_{17}$ −code C. Since $d(C)$ of the code C is equal to $n-k+1$, thus the projective code C is MDS.

In Table 3.15, the MDS codes corresponding to the n-sets in $PG(1,17)$ and the parameter e of errors corrected are given.

Table -15: MDS code over $PG(1,17)$

n-set	MDS code	e
Triad	$[3,2,2]_{17}$	0
Tetrad	$[4,2,3]_{17}$	1
Pentad	$[5,2,4]_{17}$	1
Hexad	$[6,2,5]_{17}$	2
Heptad	$[7,2,6]_{17}$	2
Octad	$[8,2,7]_{17}$	3
Nonad	$[9,2,8]_{17}$	3

If C has minimum distance d, then it can detect $d-1$ errors and correct $e = \lfloor (d-1)/2 \rfloor$ errors, where $\lfloor m \rfloor$ denotes the integer part of m:

d	1	2	3	4	5	6	7	8
e	0	0	1	1	2	2	3	3

REFERENCES

1. Al-seraji N.A.M, " The Geometry Of The Plane Of Order Seventeen And Its Application To Error-Correcting Codes" Ph.D. Thesis, University of Sussex, UK, (2010).
2. Hirschfeld J.W.P, Korchmáros G and Torres F," *Algebraic Curves Over a Finite field"* Oxford University Press, Oxford, (2007).
3. Hirschfeld J.W.P," *Projective Geometries Over Finite Fields* " *econd Edition*, Oxford University Press, Oxford, (1998).
4. Al-seraji N.A.M, "Classification of The Projective Line Over Galois Field of Order Sixteen" to appear, 2013.
5. Al-zangana E.B, " The Geometry Of The Plane Of Order Nineteen And Its Application To Error-Correcting Codes" Ph.D. Thesis, University of Sussex, UK, (2011).
6. A.H. Ali, "Classification of Arcs in Galois Plane of Order Thirteen", Ph.D. Thesis, University of Sussex, 1993.

Controllability of Nonlinear System in Banach Spaces Using Schauder Fixed Point Theorem

Naseif J. Al-Jawari and Imad N. Ahmed
Al-Mustansiriya University/ College of Science / Department of Mathematics
Received 20/3/2013 – Accepted 15/9/2013

الخلاصة

في هذا البحث ، تم إثبات المبرهنة التي تتعامل مع الشروط الكافية للقابلية على السيطرة لنظام غير خطي في فضاءات بناخ وذلك باستخدام نظرية شبه الزمرة(شبه الزمرة المتراصة) وبعض الطرائق التقنية ضمن التحليل الدالي غير الخطي مثل نظرية النقطة الصامدة لشويدر كذلك، تم اعطاء مثال يوضح قيمة النظرية أعلاه .

ABSTRACT

In this paper, sufficient conditions for controllability of nonlinear system in Banach spaces are established. The results are obtained by using semigroup theory "compact semigroup"and some techniques of nonlinear functional analysis, such as, Schauder fixed point theorem. Moreover, example is provided to illustrate the theory.

1. INTRODUCTION

The theory of semigroup of linear operators lends a convenient setting and offers many advantages for applications. Control theory in infinite-dimensional spaces is a relatively new field and started blooming only after well-developed semigroup theory was at hand. Many scientific and engineering problems can be modeled by partial differential equations, integral equations, or coupled ordinary and partial differential equations that can be described as differential equations in infinite–dimensional spaces using semigroups. Nonlinear equations, with and without delays, serve as an abstract formulation for many partial equations which arise in problems connected with heat flow in materials with memory, viscoelasticity, and other physical phenomena. So, the study of controllability results for such systems in infinite–dimensional spaces is important. For the motivation of abstract system and controllability of linear system, one can refer to the [1, 2].

In this paper we discuss the controllability of mild solution of the following nonlinear control problem in arbitrary Banach spaces.

$$\left.\begin{aligned} &\dot{x}(t)+Ax(t)=(Bu)(t)+f(t,x(t))+Q(t,K(t,x(t))), \quad t\in J=[0,b] \\ &x(0)=x_0, \end{aligned}\right\} \tag{1}$$

where the state x (.) takes values in the Banach space X and the Control function u(.) is given in $L^2(J,U)$, a Banach space of admissible control functions, with U a Banach space. Here, the linear operator $-A$ generates a compact semigroup $T(t)$, $t>0$, on a Banach space X with norm $\|\cdot\|$, and B is a bounded linear operator from U into X. The nonlinear operators

$f \in C(J\times X, X)$, $K \in C(J\times X, X)$ and $Q \in C(J\times X, X)$ are all uniformly bounded continuous operators.

Controllability of the above system with different conditions has been studied by several authors. The case where $Q = 0$ and A generates an analytic semigroup is discussed in [3]. Where $Q = 0$ in (1), Yamamoto [4], studied the controllability for parabolic functions with uniformly bounded nonlinear terms. Al-Moosawy [5] discussed the controllability of the mild solution for the system (1) by using Banach fixed point theorem, where $f = 0$, A generates a strongly continuous semigroup (C_0-semigroup) on X and the operators K, Q are satisfying Lipschitz condition on the second argument. The work in [5] extended to study the controllability in quasi-Banach spaces of kind L^p, $0 < p < 1$, in [6] by using a quasi-Banach contraction principle theorem. The case where the operator Q in (1) is an integral operator is established in [7, 8] by using Schauder fixed point. From all the above we find a reasonable justification to accomplish the study of this paper. The purpose of this paper is to study the controllability of nonlinear system (1) in Banach spaces by using the Schauder fixed point theorem.

2. Definitions and Theorems

Before proceeding to main result, we shall set in this section some definitions and theorems that will be used in our subsequent discussion.

Definition 2.1 [9]: A family $T(t)$, $0 \le t < \infty$ of bounded linear operators on a Banach space X is called a (one-parameter) semigroup on X if it is satisfies the following conditions:

$T(t+s) = T(t)T(s), \forall t, s \ge 0$ *and* $T(0) = I$ (I is the identity operator on X).

Definition 2.2[9]: The infinitesimal generator A of the semigroup $T(t)$ on Banach
space X is defined by $Ax = \lim_{t\to 0^+}(1/t)(T(t)x - x)$,where the limit exists and the domain of A is $D(A) = \{x \in X: \lim_{t\to 0^+}(1/t)(T(t)x - x) \ exists\}$.

Definition 2.3[9]: A semigroup $T(t)$, $0 \le t < \infty$ of bounded linear operators on Banach space X is said to be strongly continuous semigroup (or C_0-semigroup) if:

$$\|T(t)x - x\|_X \to 0 \ as \ t \to 0^+ \text{ for all } x \in X.$$

Definition 2.4 [10]: A semigroup $T(t)$, $0 \le t \le \infty$ is called compact if $T(t)$ is a compact operator for each $t > 0$.

Definition 2.5 [11]: Let X be a Banach space, a subset E of X is said to be totally bounded (or precompact) iff for every $\epsilon > 0$, E may be covered by a finite collection of open balls of radius ϵ.

Definition 2.6 [11]: A subset E of C $[a, b]$ is said to be equicontinuous, if for each $\epsilon > 0$ there is a $\delta > 0$, depending only on ϵ, such that for all $f \in E$ and all $x, y \in [a,b]$ satisfying $|x - y| < \delta$ we have $|f(x) - f(y)| < \epsilon$. Note that δ does not depend on f.

Lemma 2.1 [11]: Let X and Y be normed spaces. Then;

(a) Every compact linear operator $T: X \to Y$ is bounded, hence continuous.

(b) If dim $X = \infty$, the identity operator $I: X \to X$ (which is continuous) is not compact.

Remark 2.1 [9]: A semigroup $T(t), 0 \leq t < \infty$ on X is called continuous in the uniform operator topology if:-

1. $\|T(t+\delta)x - T(t)x\|_{\mathscr{L}(X)} \to 0$, as $\delta \to 0, \forall x \in X$.
2. $\|T(t)x - T(t-\delta)x\|_{\mathscr{L}(X)} \to 0$, as $\delta \to 0, \forall x \in X$.

Theorem 2.1 [12]. (Banach Theorem): Every contraction mapping of a Banach space into itself has a unique fixed point.

Theorem 2.2 [12]. (Schauder Theorem): Every continuous operator that maps a closed convex subset of a Banach space into a compact subset of itself has at least one fixed point.

Theorem 2.3 [8]: (Arzela-Ascoli's Theorem) Suppose X is a Banach space and E is compact metric space. In order that a subset M of the Banach space $C(E, X)$ be relatively compact, iff M be equicontinuous and that for $x \in E$, the set $M(x) = \{f(x) = f \in M\}$ be relatively compact in X.

3. Controllability of Nonlinear System (1)

In this section we will study the controllability of the mild solution to the problem (1) in Banach spaces by using semigroup theory "compact semigrop", and Schauder fixed point theorem.

3.1. Preliminaries

Consider the linear system:-

$$\dot{x}(t) = Ax(t) + Bu(t), \quad x(0) = x_0, \tag{2}$$

where A generates a strongly continuous semigroup of bounded linear operators $T(t)$ on a Banach space X, and B is a bounded linear operator from a Banach space U into X. Now, if $x(.)$ is a classical solution of (2), then $x(t) \in D(A)$ (domain of A) for all $t \in [0,b]$[9]. So, in the general case when A is unbounded, $D(A) \neq X$, which means that the system cannot be steered to all of X. Therefore, only the mild solution [9],

$$x(t)=T(t)x_0+\int_0^t T(t-s)Bu(s)\,ds \qquad (3)$$

will be considered in this paper with the following definition of exact controllability.

Definition 3.1 [9]: The system (2) is said to be exactly controllable on $J = [0, b]$ if, for any two points $x_0, x_1 \in X$ there exists a control $u \in L^2(J, U)$ such that $x(b) = x_1$.

The following hypothesis is assumed throughout the paper:

(I) The linear operator W from $L^2(J, U)$ into X, defined by;

$$Wu=\int_0^b T(b-s)Bu(s)\,ds,$$

induces a bounded inverse operator $\tilde{W}^{-1}$ defined on $L^2(J, U)/ker(W)$.

Then by using the control $u(t) = \tilde{W}^{-1}[x_1 - T(b)x_0](t)$, in Eq. (3), hypothesis (I) yields $x(b) = x_1$, and so (2) is exactly controllable on J.

Remark 3.1. The construction of $\tilde{W}^{-1}$ is outlined as follows [13].

Let $Y = L^2[J,U]/\ker(W)$, since $ker(W)$ is closed, Y is a Banach space under the norm;

$\|[u]\|_Y = \inf_{u\in[u]}\|u\|_{L^2[J,U]} = \inf_{W\hat{u}=0}\left\|u+\hat{u}\right\|_{L^2[J,U]}$,Where $[u]$ are the equivalence classes of u.

Define $\tilde{W}: Y \to X$ by $\tilde{W}[u] = Wu,\ u\in[u]$.

Then, $\tilde{W}$ is one - to - one and $\|\tilde{W}[u]\|_X \le \|W\|\|[u]\|_Y$. Also, $V = \text{Range}(W)$ is a Banach space with the norm $\|v\|_v = \|\tilde{W}^{-1}v\|_Y$.

To see this, note that this norm is equivalent to the graph norm on $D(\tilde{W}^{-1})= \text{Range}\,\tilde{W}$. $\tilde{W}$ is bounded, and since $D(\tilde{W}) = Y$ is closed, $\tilde{W}^{-1}$ is closed. So, the above norm makes $\text{Range}(W) = V$, a Banach space. Moreover

$\|Wu\|_v = \|\tilde{W}^{-1}Wu\|_Y = \|\tilde{W}^{-1}\tilde{W}[u]\| = \|[u]\| = \inf_{u\in[u]}\|u\| \le \|u\|,$

so, $W \in \mathscr{L}(L^2[J, U], V)$. Since $L^2[J, U]$ is reflexive and $ker(W)$ is weakly closed, the infimum is actually attained. Therefore, for any $v \in V$, a control $u \in L^2[J, U]$ can be chosen such that $u = \tilde{W}^{-1}v$.

Remark 3.2. Triggiani [14] proved that, if X is infinite dimensional, then the system (2) is never exactly controllable when B is compact or when $T(t)$ is compact for all $t > 0$.

3.2. Controllability Result of the system (1)

We assume the following hypotheses for the system (1).

(i) The linear operator $-A$ generates a C_0 compact semigroup $T(.)$ such that $\max_{t>0}\|T(t)\| \le M_1$;

(ii) The linear operator W from U into X, defined by;

$$Wu = \int_0^b T(b-s)Bu(s)ds,$$

has an invertible operator W^{-1} defined on $L^2(J, U)$ /$kerW$, and there exists positive constants M_2, M_3 such that $\| B \| \le M_2$ & $\| W^{-1} \| \le M_3$.

(iii) The nonlinear operators $f(t, x(t))$ & $Q(t, K(t, x(t)))$, for $t \in J$ satisfy;

$\| f(t,x(t)) \| \le L_1$, $\| Q(t,K(t,x(t))) \| \le L_2$, where $L_1 > 0$ and $L_2 > 0$.

Now we want to define and find the mild solution of the problem (1).

By assumption (i), $T(t)$, $t > 0$ is a C_0 compact semigroup generated by the linear operator $-A$, let $x(.) \in X$ be the solution of (1), then we have $T(t)x$ is differentiable [9],that implies the X-valued function $H(s)=T(t-s)x(s)$ is differentiable for $0< s< t$, and

$$\frac{dH}{ds} = T(t-s)\frac{d}{ds}x(s) + x(s)\frac{d}{ds}T(t-s)$$

$$\frac{dH}{ds} = T(t-s)[-Ax(s)+(Bu)(s)+f(s,x(s))+Q(s,K(s,x(s)))]+x(s)[AT(t-s)]$$

$$\frac{dH}{ds} = T(t-s)\,(Bu)(s)+T(t-s)f(s,x(s))+T(t-s)\,Q(s,K(s,x(s))), \tag{4}$$

Integrating (4) from 0 to t, yields

$$H(t)-H(0) = \int_0^t T(t-s)(Bu)(s)ds + \int_0^t T(t-s)f(s,x(s))ds + \int_0^t T(t-s)\,Q(s,K(s,x(s)))\,ds$$

Since $H(s)=T(t-s)x(s)$; then

$$T(t-t)\,x(t)-T(t-0)\,x(0)=\int_0^t T(t-s)(Bu)(s)\,ds+\int_0^t T(t-s)\,f(s,x(s))\,ds+$$
$$\int_0^t T(t-s)\,Q(s,K(s,x(s)))ds,\ \text{then}$$

$$x(t)=T(t)x_0+\int_0^t T(t-s)(Bu)(s)ds+\int_0^t T(t-s)\,f(s,x(s))ds+$$
$$\int_0^t T(t-s)\,Q(s,K(s,x(s)))ds\,. \tag{5}$$

So according to the results above, the following definition has been presented.

Definition 3.2. A continuous function $x\in X$ given by (5) will be called a mild solution to the problem (1).

Definition 3.3. The system (1) is said to be controllable on the interval J if ,for every $x_0,\ x_1\in X$, there exists a control $u\in L^2(J,U)$ such that the solution x (.) of (1) satisfies $x(b)=x_1$.

Remark 3.3. The exact controllability result for the system (1) depends on the exact controllability of the linear system (2). It is assumed that the system (2) can be steered to the subspace V, then, Rang (W) contains V. It can be assumed without loss of generality that Rang $(W)=V$ and that an invertible operator $\tilde{W}^{-1}$ can be constructed.

Using hypothesis (ii), for an arbitrary function $x(.)$, define the control,

$$u(t)=\tilde{W}^{-1}[x_1-T(b)x_0-\int_0^b T(b-s)\,f(s,x(s))ds-\int_0^b T(b-s)\,Q(s,K(s,x(s)))ds](t).$$

It can be shown that (see, section 3.3 main result), by using this control, the operator $\Phi: C(J,X)\to C(J,X)$, defined by ,

$$(\Phi x)(t)=T(t)x_0+\int_0^t T(t-s)(Bu)(s)\,ds+\int_0^t T(t-s)f(s,x(s))\,ds+\int_0^t T(t-s)$$
$$Q(s,K(s,x(s)))\,ds,$$

has a fixed point, this fixed point is then a solution of the system (1) and satisfies the condition $x(b)=x_1$.

3.3 Main Result

In this section we will explain the ideas in remark 3.3, and prove the theorem that deals with the controllability of the problem (1).

Theorem 3.1. If the hypotheses (i)-(iii) are satisfied then the system (1) is controllable on J.

Proof:

Using the hypothesis (ii) for an arbitrary function x (.), define the control,

$$u(t)= W^{-1}[x_1 - T(b)x_0 - \int_0^b T(b-s)f(s,x(s))ds - \int_0^b T(b-s)\,Q(s,K(s,x(s)))ds](t)$$

Now, we shall show that when using this control the operator defined by,

$$(\Phi x)(t)=T(t)\,x_0+\int_0^t T(t-s)(Bu)(s)\,ds+\int_0^t T(t-s)f(s,x(s))\,ds + \int_0^t T(t-s)\,Q(s,K(s,x(s)))\,ds$$

has a fixed point. This fixed point is then a solution of (5).

Clearly , $(\Phi x)(b)=x_1$

which means that the control u steers the nonlinear control system from the initial state x_0 to x_1 in time b, provided we can obtain a fixed point of the nonlinear operator Φ .

Let $Y=C(J,X)$ *and* $Y_0=\{x : x\in Y,\ x(0)=x_0,\ \|x(t)\|\le r, \text{ for } t\in J\}$,

where r is a positive constant given by,

$$r=M_1\|x_0\|+M_1M_2M_3[\|x_1\|+M_1\|x_0\|+M_1b\ (L_1+L_2)]\,b+M_1b\ (L_1+L_2)$$

Then, Y_0 is clearly a bounded, closed, convex subset of Y [11]. Now we define a mapping,

$\Phi : Y\to Y_0$ *by*,

$$(\Phi x)(t)=T(t)x_0+\int_0^t T(t-s)f(s,x(s))\,ds+\int_0^t T(t-s)\,Q(s,K(s,x(s)))\,ds + \int_0^t T(t-\eta)BW^{-1}[x_1-T(b)x_0-\int_0^b T(b-s)f(s,x(s))\,ds - \int_0^b T(b-s)\,Q(s,K(s,x(s)))\,ds](\eta)\,d\eta \quad (6)$$

Taking the norm of both sides of (6)

$$\|(\Phi x)(t)\| = \|T(t)x_0 + \int_0^t T(t-s)f(s,x(s))ds + \int_0^t T(t-s)\,Q(s,K(s,x(s)))ds$$
$$+\int_0^t T(t-\eta)BW^{-1}[x_1 - T(b)x_0 - \int_0^b T(b-s)f(s,x(s))\,ds$$
$$-\int_0^b T(b-s)\,Q(s,K(s,x(s)))\,ds\,](\eta)d\eta\|$$

$$\|(\Phi x)(t)\| \le \|T(t)x_0\| + \left\|\int_0^t T(t-s)f(s,x(s))\,ds\right\| + \left\|\int_0^t T(t-s)\,Q(s,K(s,x(s)))\,ds\right\| +$$
$$\left\|\int_0^t T(t-\eta)BW^{-1}[x_1 - T(b)x_0 - \int_0^b T(b-s)f(s,x(s))ds - \int_0^b T(b-s)\,Q(s,K(s,x(s)))ds\,](\eta)d\eta\right\|$$

$$\|(\Phi x)(t)\| \le \|T(t)\|\,\|x_0\| + \int_0^t \|T(t-s)\|\,\|f(s,x(s))\|ds + \int_0^t \|T(t-s)\|\,\|Q(s,K(s,x(s)))\|ds$$
$$+\int_0^t \|T(t-\eta)\|\,\|B\|\,\|W^{-1}\|[\|x_1\| + \|T(b)\|\,\|x_0\| + \int_0^b \|T(b-s)\|\,\|f(s,x(s))\|ds$$
$$+\int_0^b \|T(b-s)\|\,\|Q(s,K(s,x(s)))\|ds\,](\eta)d\eta$$

$$\|(\Phi x)(t)\| \le M_1\|x_0\| + \int_0^t M_1L_1ds + \int_0^t M_1L_2ds + \int_0^t M_1M_2M_3[\|x_1\| + M_1\|x_0\|$$
$$+M_1L_1b + M_1L_2b\,](\eta)d\eta$$
$$\|(\Phi x)(t)\| \le M_1\|x_0\| + M_1M_2M_3[\|x_1\| + M_1\|x_0\| + M_1b(L_1+L_2)]\,b + M_1b\,(L_1+L_2)$$
$$\|(\Phi x)(t)\| \le r$$

Since f, Q are continuous and $\|(\Phi x)(t)\| \le r$, it follows that Φ is also continuous and maps Y_0 into itself.

Now, to prove that Φ is also maps Y_0 into a precompact subset of Y_0, we first show that for every fixed $t \in J$, the set $Y_0(t) = \{(\Phi x)(t) : x \in Y_0\}$ is precompact in X.
This is clear for $t = 0$ since $Y_0(0) = \{x_0\}$.
Let $t > 0$ be fixed and for $0 < \epsilon < t$, define,

$$(\Phi_\delta x)(t) = T(t)x_0 + T(\delta)\int_0^{t-\delta} T(t-s-\delta)f(s,x(s))ds +$$
$$T(\delta)\int_0^{t-\delta} T(t-s-\delta)\,Q(s,K(s,x(s)))ds + T(\delta)\int_0^{t-\delta} T(t-\eta-\delta)BW^{-1}[x_1 - T(b)x_0$$
$$-\int_0^b T(b-s)f(s,x(s))ds - \int_0^b T(b-s)\,Q(s,K(s,x(s)))ds\,](\eta)\,d\eta,$$

$$(\Phi\delta x)(t) = T(t)x_0 + \int_0^{t-\delta} T(t-s)f(s,x(s))ds + \int_0^{t-\delta} T(t-s)\,Q(s,K(s,x(s)))ds +$$
$$\int_0^{t-\delta} T(t-\eta)(B)(W^{-1})[x_1 - T(b)x_0 - \int_0^b T(b-s)f(s,x(s))ds -$$
$$\int_0^b T(b-s)\,Q(s,K(s,x(s)))ds\,](\eta)\,d\eta,$$

Since $T(t)$ is compact for every $t > 0$ (by (i)), B,W^{-1} & Q are all

bounded, the set $Y_{\delta}(t)=\{(\Phi_{\delta}x)(t):x\in Y_0\}$ is precompact in X for every δ, $0<\delta<t$.
Furthermore for $x\in Y_0$, we have ;

$$\|(\Phi x)(t)-(\Phi_{\delta}x)(t)\|\le$$

$$\left\|\int_{t-\delta}^{t}T(t-\eta)BW^{-1}[x_1-T(b)x_0-\int_0^b T(b-s)f(s,x(s))ds-\int_0^b T(b-s)\,Q(s,K(s,x(s)))ds](\eta)d\eta\right\|+$$

$$\left\|\int_{t-\delta}^{t}T(t-s)f(s,x(s))ds\right\|+\left\|\int_{t-\delta}^{t}T(t-s)\,Q(s,K(s,x(s)))ds\right\|$$

$$\|(\Phi x)(t)-(\Phi_{\delta}x)(t)\|\le\delta M_1M_2M_3[\|x_1\|+M_1\|x_0\|+M_1L_1b+M_1L_2b]+\delta M_1(L_1+L_2),$$

which implies that $Y_0(t)$ is totally bounded, i.e., precompact in X. Now, we want to show that
$\Phi(Y_0)=\{\Phi x:x\in Y_0\}$ is an equicontinuous family of functions.For that , let $t_2>t_1>0$.
Then we get that

$$\|(\Phi x)(t_1)-(\Phi x)(t_2)\|\le\|T(t_1)-T(t_2)\|\|x_0\|+\left\|\int_0^{t_1}[T(t_1-\eta)-T(t_2-\eta)]\,BW^{-1}[x_1-T(b)x_0-\right.$$

$$\int_0^b T(b-s)f(s,x(s))ds-\int_0^b T(b-s)Q(s,K(s,x(s)))ds](\eta)d\eta-\int_{t_1}^{t_2}T(t_2-\eta)BW^{-1}[x_1-T(b)x_0$$

$$-\int_0^b T(b-s)f(s,x(s))ds-\int_0^b T(b-s)\,Q(s,K(s,x(s)))ds](\eta)d\eta\|+\left\|\int_0^{t_1}[T(t_1-s)-T(t_2-s)]\,[f(s,x(s))\right.$$

$$+Q(s,k(s,x(s)))]ds-\int_{t_1}^{t_2}T(t_2-s)[f(s,x(s))+Q(s,K(s,x(s)))]ds\|$$

$$\|(\Phi x)(t_1)-(\Phi x)(t_2)\|\le\|T(t_1)-T(t_2)\|\|x_0\|+\int_0^{t_1}\|[T(t_1-s)-T(t_2-s)]\|M_2M_3[[\|x_1\|+M_1\|x_0\|+$$

$$M_1b(L_1+L_2)]ds+\int_{t_1}^{t_2}\|T(t_2-s)\|M_2M_3[\|x_1\|+M_1\|x_0\|+M_1b(L_1+L_2)]ds+$$

$$\int_0^{t_1}\|T(t_1-s)-T(t_2-s)\|(L_1+L_2)\,ds+\int_{t_1}^{t_2}\|T(t_2-s)\|(L_1+L_2)\,ds \tag{7}$$

Since $T(t),t>0$ is a compact, then $T(t)$ is continuous in the uniform operator topology for $t>0$.
Thus, the right – hand side of (7),which is independent of $x\in Y_0$, tends to zero as t_2-$t_1\to 0$. So, $\Phi(Y_0)$ is an equicontinuous family of function.

Also, $\Phi(Y_0)$ is bounded in Y, and so by the Arzela-Ascoli theorem $\Phi(Y_0)$ is precompact. Then by Schauder fixed point theorem, Φ has a fixed point in Y_0 [9].

Any fixed point of Φ is a mild solution of (1) on J, satisfying $(\Phi x)(t) = x(t) \in X$. Thus, the system (1) is controllable on J.

3.4. Example:

Consider the partial integrodifferential equation of the form

$$y_t(t,x)=y_{xx}(t,x)+(Bu)(t)+\sigma_1(t,y_{xx}(t,x)) + \int_0^t \sigma_3(t,s,y_{xx}(s,x),\int_0^s \sigma_2(s,\tau,y_{xx}(\tau,x))d\tau)\, ds, x \in I=(0,1), t \in J, \quad (8)$$

and given initial and boundary conditions

$$y(0,t)=y(1,t)=0, \quad (9a)$$

$$y(x,0)=y_0(x), \ x \in I, \quad (9b)$$

where $B:U \to X$, with $U \subset J$ and $X = L^2[I,R]$, is a linear operator such that there exists an invertibled operator W^{-1} on $L^2[J,U]/\ker W$, where W is defined by,

$$Wu=\int_0^b T(b-s)Bu(s)ds$$

$T(t)$ is a compact semigroup,and

$\sigma_1 : J \times X \to X$

$\sigma_2 : J \times J \times X \to X$

$\sigma_3 : J \times J \times X \times X \to X$

are all continuous and bounded by positive constants.

The problem (8)-(9) can be brought to the form (1), by making suitable choices of A, B, f, K, Q as follows,

Let $X = L^2[I,R]$, $Az = z_{xx}$, $B:U \to X$, and

$D(A)=\{z \in X, z_{xx} \in X; z(0)=z(1)=0\}$ be such that the condition in hypothsis (ii) is satisfied,and let $f(t,z)(x)=\sigma_1(t,z_{xx}(x)), (t,z) \in J \times X$, $K(t,z)(x)=\int_0^t \sigma_2(t,\tau,z_{xx}(x))d\tau$,

$$Q(t,z,\mu)(x)=\int_0^t \sigma_3(t,s,z_{xx}(x),\mu(x))dt, x \in I.$$

Then the system (8)-(9) becomes an abstract formulation of (1). Also by [15, theorem (3)], the solutions are all bounded.Further, all the conditions stated in the above theorem 3.1 are satisfied. Hence the system (8)-(9) is controllable on J.

Remark 3.4. If we assume that the nonlinear operators f, K, and Q in the problem (1) are satisfied Lipschitz condition on the second argument, we can prove that the system(1) controllable on J by using Banach fixed point theorem. The results are obtained by showing that the operator Φ in section 3.3, is an contraction mapping, i.e., for

$x_1(t), x_2(t) \in Y_0$, $\|\Phi x_1(t) - \Phi x_2(t)\| \le q \|x_1(t) - x_2(t)\|, 0 \le q < 1$.

4. Conclusion

1. Generalize nonlinear control problem by taking f,K,and Q in system (1) any nonlinear operators , and study the controllability of the problem (1) by using semigroup theory(compact semigroup) and Schauder fixed point theorem .
2. The idea of studying the controllability of problem (1) by using Banach fixed point theorem is introduced.

1. Future work

2. The observability and optimality for the problem (1) may be considered.

3. References

1. Curtain, R. E., and Zwart, H., An Introduction to Infinite-Dimensional Linear Systems Theory, Springer Verlag, New York, NY (1995).
2. Engel, K.J., and Nagel R., One-Parameter Semigroups of Linear Evolution Equations , Springer –Verlag , New York, Berlin,Inc.(2000).
3. Balachandran, K., and Dauer, J. P., Local Controllability of Semilinear Evolution Systems in Banach Spaces, Indian Journal of Pure and Applied Mathematics , Vol.29,pp.311-320 (1998).
4. Yamamoto, M., and Park, J.Y., Controllability for Parabolic Equations with Uniformly Bounded Nonlinear Terms, Journal of Optimization Theory and Applications, Vol.66 , PP.515-532 (1990).
5. AL-Moosawy, Atheer.G., The Controllability and Optimality of the Mild Solution for Some Control Problems in Infinite-Dimensional Spaces, Ph.D.Thesis, Department of Maths., College of Education, Al-Mustansiriyah Univ., Iraq (2007).
6. Al-Jawari, N.J., The Quasi-Controllability for Control Problems in Infinite Dimensional Spaces, Al-Mustansiriyah J.Sci., Vol.22 , No.3, pp.39-50 (2011).
7. Balachandran ,K., Dauer,J.P., and Balasubramaniam,P., Controllability of Nonlinear Integrodifferential System in Banach Space, Journal of Optimization Theory and Applications ,Vol.84, pp.83-91(1995).
8. Zboon,R. A., and Salah , M.A., Local Solvability and Controllability of Semilinear Initial Value Control Problems Via

Semigroup Approach, Journal of Al-Nahrain University,Vol.10(1), pp.101-110, Iraq, June (2007) .

9. Pazy, A., Semigroup of Linear Operator and Applications to Partial Differential Equations, Springer-Verlag, New-York, Inc. (1983).
10. Balakrishnan, A. V., Applied Functional Analysis, Springer-Verlag. New York, Inc. (1976).
11. Kreyszig, E., Introductory Functional Analysis with Applications, John Wiley and Sons, New York, Chichester (1978).
12. Siddiqi, A. H., Functional Analysis with Applications, by Tata McGraw-Hill Publishing Company Limited, India (1986).
13. Magnusson, K., Pritchard, A. J., and Quinn, M. D., The Application of Fixed –Point Theorems to Global Nonlinear Controllability Problems, Mathematical Control Theory, Banach Center Publications ,Vol.14, pp.319-344 (1985).
14. Triggiani, R., On the Lack of Exact Controllability for Mild Solutions in Banach Spaces, Journal of Mathematical Analysis and Applications, Vol. 50, pp.438-446 (1975) .
15. Hussain, M. A., On a Nonlinear Integrodifferential Equation in Banach Space, Indian Journal of Pure and Applied Mathematics, Vol.19, pp.516-529 (1988).

Solvable Special Cases for Flow Shop Scheduling Problem Involving Transportation Time

Niran Abbas Ali
Department of Mathematics, College of Science, Al-Mustansiriyah University
Received 17/3/2013 – Accepted 15/9/2013

الخلاصة

هذه الدراسة تبحث مشكلة جدولة n من النتاجات على m من المكائن مع زمن نقل بين المكائن للحد من وقت الاتمام الاقصى Makespan.
هذه المسألة، عندما لا يكون هناك وقت نقل، تعتبر NP- hard ، في حين ان المسألة مع وقت النقل تعتبر صعبة اكثر في حلها. اشتققنا واثبتنا نظريا ثلاثة عشر نتيجة بشأن الحل الامثل للمسألة، مع عشر خوارزميات.

ABSTRACT

This study considers the problem of scheduling n-jobs on m-machines with transportation time between machines to minimize the maximum completion time, Makespan.
This problem, when there is no transportation time, is considered NP-hard, while the problem with transportation time is considered more difficult to solve. Theoretically, we derive and prove 13 results concerning optimality of special cases for the problem with ten algorithms.

INTRODUCTION

There are many definitions for machine scheduling, but the simplest one for understanding is that, scheduling is the allocation of resources over time to perform a collection of tasks [1]. Resources and tasks are called machines and jobs respectively and both of them can take many forms. For example; we can consider a computer as a machine and the programs that are to be run on that computer as jobs.
Solving machine scheduling problem means finding the decision that makes us determine which job should we sequence first and on which machine. The aim is to find a good (near optimal) or if possible optimal schedule which gives an optimal solution and that enables to minimize the time spent on the problem which will minimize the cost for the problem.
In most manufacturing and distribution systems, semi-finished jobs are transferred from one processing facility to another by transporters such as automated guided vehicles (AGVs) and conveyors. Most machine scheduling models assume either that there are a finite number of transporters for delivering jobs or that jobs are delivered instantaneously from one location to another without transportation time involved. This study is studying machine scheduling problems with explicit transportation considerations.

Problem and Notation

The machine configuration inside a manufacturing facility can be flow shop, job shop, open shop, or other types. This study considers the transportation mainly in a flow shop environment.

Our problem can be described in general as follows: We are given a set of n jobs to be processed on m machines in a flow shop. Each job must first be processed on machine M_1, then machine M_2, etc., and finally on machine M_m. The processing time of job j on machine M_k is $P_{j,k}$. We assume that all of the jobs start at machine M_1. After a job is processed on machine M_k, it is transported to machine M_{k+1} by a transporter. There are total of n identical transporters initially located at machine M_1. Each transporter has a capacity of c=1, i.e. it can carry up to c=1 job in one shipment. The transportation time from machine M_k to machine M_{k+1} is denoted by $\ell_{k,k+1}$ which is assumed to be independent of the jobs being transported.

Let $C_{j,k}$ or $C_k(j)$ denote the completion time of job j, that is the time when job j is completed on the last machine M_k. We are concerned about minimizing makespan C_{max}.

We follow the commonly used three-field notation $\alpha/\beta/\gamma$ for machine scheduling problems.In the α field, the notation 'TF' will be used to denote a flow shop problem with transportation between machines. The problem considered by this study can be denoted as $TF_m\left|\ell_{i,1},\ldots,\ell_{i,m-1}\right|C_{\max}$, where $\ell_{i,k}$, $k=1,\ldots,m-1$ denote the n transporters time, each transporter with capacity 1 job from machine M_k to machine M_{k+1}.

The Calculation of Makespan

For any sequence $\sigma=(i_1,i_2,\ldots,i_n)$, let $C_K(i_q)$ be the completion time of job i_q on machine M_k, $q=1,2,\ldots,n$, $k=1,2,\ldots,m$. Then since the start time of the processing of job i_q on M_k is the same as the completion time of job i_{q-1} on M_k, $q=2,3,\ldots,n$ and the job i_q can be processed on M_k as soon as possible after both are completed on M_{k-1} and arrived to M_k and the job i_{q-1} is completed on $M_k, q=2,3,\ldots,n$; $k=2,3,\ldots,m$. The next relation would follow:

$$C_1(i_q)=C_1(i_{q-1})+P_{i_q,1}$$

$$C_K(i_q)=\max\ \{C_{k-1}(i_q)+\ell_{i_q,k-1}, C_k(i_{q-1})\}+P_{i_q,k}$$

where $(q=1,\ 2,\ \ldots,\ n;\ k=2,\ 3,\ \ldots,\ m), C_K(i_0)=0\ \ ,\ (k=1,2,\ldots,m)$

Hence, the Makespan of the sequence σ is equal to $C_m(i_n)$.

Machine Flow Shop Problem with Transportation Time

It is known that the classical m-machine flow shop makespan problem without transportation $F_m//C_{max}$ is strongly NP-hard for (m $\geq$3) [2], while the 2-machine problem $F_2//C_{max}$ is polynomially solvable by Johnson's rule. Thus, any m-machine problem with transportation must be strongly NP-hard. The transporter in a m-machine flow shop problem with transportation may be viewed as a "machine" (whose duty is to transport jobs) between each two real machines (whose duty is to process jobs).

Johnson's Rule for $F_2//C_{max}$ Problem

An optimal sequence for this problem was given by Johnson 1954. It is determined by the following theorem:

Theorem [3]:

An optimal sequence is determined by the next rule: If a criterion:

$\text{Min}(P_{i,1}, P_{j,2}) \le \text{Min}(P_{j,1}, P_{i,2})$ ...(1)

Hold with an inequality then job **i** it precedes job **J**. If equality holds in (1) either ordering is optimal.

This theorem can be stated in a different form as shown in the following theorem:

Theorem [4]:

Let the set of n jobs be decomposed into its two subset, $J_1 = \{ i | P_{i,1} \le P_{i,2} \}$, $J_2 = \{ i | P_{i,1} > P_{i,2} \}$ then an optimal se quence is determine by the next rule:

1. After the jobs in $\mathbf{J_1}$, arrange the jobs in $\mathbf{J_2}$.
2. In $\mathbf{J_1}$ arrange the jobs in increasing order of $P_{i,1}$. If a tie occurs either ordering is optimal.
3. In $\mathbf{J_2}$ arrange the jobs in decreasing order of $P_{i,2}$. If a tie occurs either ordering is optimal.

The Solvable Special Cases for m-machine:

Some special cases that are solvable in polymonially bounded computational effort can be identified. The following sufficient optimality conditions (SOC) will be stated for a given schedule to be optimal.

<u>First Case</u>

Theorem(1): In $TF_m | \ell_{i,1},\dots,\ell_{i,m-1} | C_{\max}$ problem, If $\max_{1\le i\le n}\{P_{i,k} + \ell_{i,k}\} \le \min_{1\le i\le n}\{P_{i,k+1}\}$ $k = 1,\dots,m-2$ and [$\ell_{i,m-1} \le \ell_{j,m-1} + P_{j,m-1}$ or $\ell_{i,m-1} \le \ell_{j,m-1} + P_{j,m}$ $\forall i,j$], then there exist an optimal sequence determined by the next rule which presented by algorithm (1).

Theorem(2): In $TF_m / \ell_{i,1},\dots,\ell_{i,m-1} / C_{\max}$ problem, if $P_{j,k} + \ell_{j,k} \le \ell_{i,k} + P_{i,k+1}$, $\forall i,j$, $\forall k, k = 1,\dots,m-2$, and [$\ell_{i,m-1} \le \ell_{j,m-1} + P_{j,m-1}$ or $\ell_{i,m-1} \le \ell_{j,m-1} + P_{j,m}$ $\forall i,j$], then there exist an optimal sequence determined by the next rule which presented by algorithm (1).

Algorithm (1)

1- Let $w_1 = (1,2,...,n)$ be a sequence on the last two machines M_{m-1} and M_m was obtained by applying Johnson's rule on the processing time $(P_{i,m-1} + \ell_{i,m-1}, \ell_{i,m-1} + P_{i,m})$. If $\sum_{r=1}^{m-2}(P_{1,r} + \ell_{1,r}) = \min_{1\le i\le n}\{\sum_{r=1}^{m-2}(P_{i,r} + \ell_{i,r})\}$, then w is optimal on M_1, to M_m. If not, read (2).

2- There exist at most (n-1) sequence $w_q = (q,1,...,q-1,q+1,...,n)$ obtained by moving the qth job $q\,(q \ne 1)$ which satisfy $\sum_{r=1}^{m-2}(P_{q,r} + \ell_{q,r}) \le \sum_{r=1}^{m-2}(P_{1,r} + \ell_{1,r})$ to the first of the sequence $w_1 = w_q$.

3- The sequence w which gives $\min_{1<q\le n} C_{max}(w_q)$ is the optimal sequence.

Proof (1) and(2) : for any permutation of the above problem, the C_{max} compute as follows:

$$C_{max}(w) = \max_{1\le h\le n}\{\sum_{r=1}^{m-2}(P_{1,r} + \ell_{1,r}) + \sum_{i=1}^{h} P_{i,m-1} + \ell_{h,m-1} + \sum_{i=h}^{n} P_{i,m}\}$$
$$= \sum_{r=1}^{m-2}(P_{1,r} + \ell_{1,r}) + \max_{1\le h\le n}\{\sum_{i=1}^{h} P_{i,m-1} + \ell_{h,m-1} + \sum_{i=h}^{n} P_{i,m}\}$$

The first term is as small as possible, and the second get the optimal value by using the following theorem and corollary (see [1]):

In the following theorem and corollary we will use the notations a_i, and b_i to denote, respectively, the processing time of job i on machine M_1 and M_2, and ℓ_i be transportation time for job i from M_1 to M_2.

Now we consider the following theorem and corollary to good use in the following special cases.

Theorem [1]:

In $TF_2|\ell_i|C_{max}$ problem, If we have $\ell_i \le a_j + \ell_j\ \forall i,j$. Then there exists an optimal schedule in which the two processing orders are identical. Furthermore the common processing order is obtained from the optimal processing order for the $F_2//C_{max}$ problem having processing time $(a_i + \ell_i, \ell_i + b_i)$.

Corollary [1]:

In $TF_2|\ell_i|C_{max}$ problem, If we have $\ell_i \le b_j + \ell_j\ \forall i,j$. Then there exists an optimal schedule in which the two processing orders are identical. Furthermore the common processing order is obtained from the optimal processing order for the $F_2//C_{max}$ problem having processing time $(a_i + \ell_i, \ell_i + b_i)$.

Second Case

Theorem(3): In $TF_m\left|\ell_{i,1},...,\ell_{i,m-1}\right|C_{\max}$ problem, If $\max_{1\le i\le n}\{P_{i,k+1}+\ell_{i,k}\}\le\min_{1\le i\le n}\{P_{i,k}\}$ $k=2,...,m-1$ and $[\ \ell_{i,1}\le\ell_{j,1}+P_{j,1}$ or $\ell_{i,1}\le\ell_{j,1}+P_{j,2}\ \forall i,j\ ]$, Then there exists an optimal sequence determined by the next rule which presented by algorithm (2).

Theorem(4): In $TF_m\left|\ell_{i,1},...,\ell_{i,m-1}\right|C_{\max}$ problem, If $\ell_{i,k}+P_{i,k+1}\le P_{j,k}+\ell_{j,k}$, $k=2,...,m-1$ and $[\ \ell_{i,1}\le\ell_{j,1}+P_{j,1}$ or $\ell_{i,1}\le\ell_{j,1}+P_{j,2}\ \forall i,j\ ]$, Then there exists an optimal sequence determined by the next rule which presented by algorithm (2).

Algorithm (2)

1- Let $w_n=1,2,...,n$ be a sequence on the first two machines M_1 and M_2 was obtained by applying Johnson's rule on the processing time $(P_{i,1}+\ell_{i,1},\ \ell_{i,1}+P_{i,2})$. If $\sum_{r=2}^{m-1}(\ell_{n,r}+P_{n,r+1})=\min_{1\le i\le n}\{\sum_{r=2}^{m-1}(\ell_{i,r}+P_{i,r+1})\}$, then w is optimal on M_1, to M_m. If not, read (2).

2- There exist at most (n-1) sequence $w_q=(1,...,q-1,q+1,...,n,q)$ obtained by moving the qth job $q\ (q\ne n)$ which satisfy $\sum_{r=2}^{m-1}(\ell_{q,r}+P_{q,r+1})\le\sum_{r=2}^{m-1}(\ell_{n,r}+P_{n,r+1})$ to the last of the sequence $w_n=w_q$.

3- The sequence w which gives $\min_{1\le q<n}C_{\max}(w_q)$ is the optimal sequence.

Proof (3) and (4) : For any permutation of the above problem, the $C_{\max}$ compute as follows:

$$C_{\max}(w)=\max_{1\le h\le n}\{\sum_{i=1}^{h}P_{i,1}+\ell_{h,1}+\sum_{i=h}^{n}P_{i,2}+\sum_{r=2}^{m-1}(\ell_{n,r}+P_{n,r+1})\}$$

$$=\max_{1\le h\le n}\{\sum_{i=1}^{h}P_{i,1}+\ell_{h,1}+\sum_{i=h}^{n}P_{i,2}\}+\sum_{r=2}^{m-1}(\ell_{n,r}+P_{n,r+1})$$

The first term get the optimal value by using the previous theorem and corollary, and the second is as small as possible.

Third Case

Theorem(5): In $TF_m\left|\ell_{i,1},...,\ell_{i,m-1}\right|C_{\max}$ problem, If $\max_{1\le i\le n}\{P_{i,k'}\}\le\min_{1\le i\le n}\{P_{i,k'+1}\}$ $\forall i$ for some $k',k'=2\,or...or\,m-1$, $P_{i,k}\le P_{i,k+1}$, and $P_{j,k}+\ell_{j,k}\le\ell_{i,k}+P_{i,k+1}$, $\forall k,k=1,...,m,\ k\ne k'$. Then there exists an optimal sequence determined by the next rule which presented by algorithm (3).

Algorithm (3)

1- Let $w_1 = (1,2,...,n)$ be a sequence was obtained by ordering jobs in non-increasing order of $\ell_{i,k'}$. If $\sum_{r=1}^{m-1}(P_{1,r}+\ell_{1,r}) = \min_{1\le i\le n}\{\sum_{r=1}^{m-1}(P_{i,r}+\ell_{i,r})\}$, then w is optimal on M_1, to M_m. If not, read (2).

2- There exist at most (n-1) sequence $w_q = (q,1,...,q-1,q+1,...,n)$ obtained by moving the qth job $q\ (q \ne 1)$ which satisfy $\sum_{r=1}^{m-1}(P_{q,r}+\ell_{q,r}) \le \sum_{r=1}^{m-1}(P_{1,r}+\ell_{1,r})$ to the first of the sequence $w_1 = w_q$.

3- The sequence w which gives $\min_{1<q\le n} C_{max}(w_q)$ is the optimal sequence.

Proof: for any permutation of the above problem, the C_{max} compute as follows:

$$C_{max} = \sum_{r=1}^{m-1}(P_{1,r}+\ell_{1,r}) + \sum_{i=1}^{n} P_{i,m}$$

The first term is small as possible, and the second is a constant.

Forth Case

Theorem(6): In $TF_m|\ell_{i,1},...,\ell_{i,m-1}|C_{max}$ problem, If $P_{j,k'-1} \le P_{j,k'} \le P_{i,k'+1}$, $\forall i,j$ for some $k', k' = 2 or ... or\, m-1$ and $P_{j,k} + \ell_{j,k} \le \ell_{i,k} + P_{i,k+1}$, $\forall k, k = 1,...,m-1, k \ne k'$. Then there exists an optimal sequence determined by the next rule which presented by algorithm (4).

Algorithm (4)

1- Let $w_1 = (1,2,...,n)$ be a sequence was obtained by ordering jobs in non-increasing order of $P_{i,k'} + \ell_{i,k'}$. If $\sum_{r=1}^{m-1}(P_{1,r}+\ell_{1,r}) = \min_{1\le i\le n}\{\sum_{r=1}^{m-1}(P_{i,r}+\ell_{i,r})\}$, then w is optimal on M_1, to M_m. If not, read (2).

2- There exist at most (n-1) sequence $w_q = (q,1,...,q-1,q+1,...,n)$ obtained by moving the qth job $q\ (q \ne 1)$ which satisfy $\sum_{r=1}^{m-1}(P_{q,r}+\ell_{q,r}) \le \sum_{r=1}^{m-1}(P_{1,r}+\ell_{1,r})$ to the first of the sequence $w_1 = w_q$.

3- The sequence w which gives $\min_{1<q\le n} C_{max}(w_q)$ is the optimal sequence.

Fifth Case

Theorem(7): In $TF_m\left|\ell_{i,1},\ldots,\ell_{i,m-1}\right|C_{\max}$ problem, If $\ell_{i,1}+P_{i,2}\le P_{j,1}$, $\ell_{j,1}+P_{j,1}\le P_{j,3}$, and $P_{j,k}+\ell_{j,k}\le \ell_{i,k}+P_{i,k+1}$, $\forall i,j$, $\forall k, k=3,\ldots,m-1$. Then there exists an optimal sequence determined by the next rule which presented by algorithm (5).

Algorithm (5)

1- Let $w_1=(1,2,\ldots,n)$ be a sequence was obtained by ordering jobs in non-increasing order of $P_{i,2}+\ell_{i,2}$. If $\sum_{r=1}^{m-1}(P_{1,r}+\ell_{1,r})=\min_{1\le i\le n}\{\sum_{r=1}^{m-1}(P_{i,r}+\ell_{i,r})\}$, then w is optimal on M_1, to M_m. If not, read (2).

2- There exist at most (n-1) sequence $w_q=(q,1,\ldots,q-1,q+1,\ldots,n)$ obtained by moving the qth job $q\ (q\ne 1)$ which satisfy $\sum_{r=1}^{m-1}(P_{q,r}+\ell_{q,r})\le\sum_{r=1}^{m-1}(P_{1,r}+\ell_{1,r})$ to the first of the sequence $w_1=w_q$.

3- The sequence w which gives $\min_{1<q\le n} C_{\max}(w_q)$ is the optimal sequence.

Sixth Case

Theorem(8): In $TF_m\left|\ell_{i,1},\ldots,\ell_{i,m-1}\right|C_{\max}$ problem, If $P_{j,k}+\ell_{j,k}\le\ell_{i,k}+P_{i,k+1}$, $\forall i,j$, $\forall k, k=1,\ldots,m-1$, Then there exists (n-1)! of an optimal sequence determined by the next rule which presented by algorithm (6).

Algorithm (6)

1- Let $w_1=(1,2,\ldots,n)$ be a sequence was obtained by ordering jobs in any order. If $\sum_{r=1}^{m-1}(P_{1,r}+\ell_{1,r})=\min_{1\le i\le n}\{\sum_{r=1}^{m-1}(P_{i,r}+\ell_{i,r})\}$, then w is optimal on M_1, to M_m. If not, read (2).

2- There exist one sequence $w_q=(q,1,\ldots,q-1,q+1,\ldots,n)$ obtained by moving the qth job $q\ (q\ne 1)$ which satisfy $\sum_{r=1}^{m-1}(P_{q,r}+\ell_{q,r})\le\sum_{r=1}^{m-1}(P_{1,r}+\ell_{1,r})$ to the first of the sequence $w_1=w_q$.

3- There exist (n-1)! such sequence w which gives $C_{\max}(w_q)$ is the optimal value with (n-1) job in a different order.

Proof (6-8) : It is clear, it is same as in theorem (5).

Seventh Case

Theorem(9): In $TF_m\left|\ell_{i,1},\ldots,\ell_{i,m-1}\right|C_{\max}$ problem, If $\max_{1\le i\le n}\{P_{i,k'+1}\}\le\min_{1\le i\le n}\{P_{i,k'}\}$ for some $k', k'=1 or \ldots or\ m-1$ and $\ell_{i,k}+P_{i,k+1}\le P_{j,k}+\ell_{j,k}$, $\forall i,j$,

$\forall k, k=1,...,m-1, k \neq k'$. Then there exists an optimal sequence determined by the next rule which presented by algorithm (7).

Algorithm (7)

1- Let $w_n = 1,2,...,n$ be a sequence was obtained by ordering jobs in non-decreasing order of $\ell_{i,k'}$. If $\sum_{r=1}^{m-1}(\ell_{n,r}+P_{n,r+1}) = \min_{1\le i\le n}\{\sum_{r=1}^{m-1}(\ell_{i,r}+P_{i,r+1})\}$, then w is optimal on M_1, to M_m. If not, read (2).

2- There exist at most (n-1) sequence $w_q = (1,...,q-1,q+1,...,n,q)$ obtained by moving the qth job $q\ (q \neq n)$ which satisfy $\sum_{r=1}^{m-1}(\ell_{q,r}+P_{q,r+1}) \le \sum_{r=1}^{m-1}(\ell_{n,r}+P_{n,r+1})$ to the last of the sequence $w_n = w_q$.

3- The sequence w which gives $\min_{1\le q<n} C_{\max}(w_q)$ is the optimal sequence.

***Proof*:** for any permutation of the above problem, the $C_{\max}$ compute as follows:

$$C_{\max} = \sum_{i=1}^{n} P_{i,1} + \sum_{r=1}^{m-1}(\ell_{n,r}+P_{n,r+1})$$

The first term is a constant, and the second is a small as possible.

Eighth Case

Theorem(10): In $TF_m|\ell_{i,1},...,\ell_{i,m-1}|C_{\max}$ problem, If $P_{i,k'+1} \le P_{i,k'}$, $\forall i$ and for some $k', k'=1 or ... or\ m-1$, and $\ell_{i,k}+P_{i,k+1} \le P_{j,k}+\ell_{j,k}$, $\forall i,j$, $,k=1,...,m-1, k\neq k'$. Then there exists an optimal sequence determined by the next rule which presented by algorithm (8).

Algorithm (8)

1- Let $w_n = 1,2,...,n$ be a sequence was obtained by ordering jobs in non- decreasing order of $P_{i,k'}+\ell_{i,k'}$. If $\sum_{r=1}^{m-1}(\ell_{n,r}+P_{n,r+1}) = \min_{1\le i\le n}\{\sum_{r=1}^{m-1}(\ell_{i,r}+P_{i,r+1})\}$, then w is optimal on M_1, to M_m. If not, read (2).

2- There exist at most (n-1) sequence $w_q = (1,...,q-1,q+1,...,n,q)$ obtained by moving the qth job $q\ (q \neq n)$ which satisfy $\sum_{r=1}^{m-1}(\ell_{q,r}+P_{q,r+1}) \le \sum_{r=1}^{m-1}(\ell_{n,r}+P_{n,r+1})$ to the last of the sequence $w_n = w_q$.

3- The sequence w which gives $\min_{1 \le q < n} C_{\max}(w_q)$ is the optimal sequence.

Ninth Case

Theorem(11): In $TF_m|\ell_{i,1},...,\ell_{i,m-1}|C_{\max}$ problem, If $\max_{1 \le i \le n}\{P_{i,2}\} \le \min_{1 \le i \le n}\{\ell_{i,1}\}$, $\max_{1 \le i \le n}\{\ell_{i,1}\} \le \min_{1 \le i \le n}\{P_{i,1}\}$, $\max_{1 \le i \le n}\{P_{i,3}\} \le \min_{1 \le i \le n}\{P_{i,2}\}, \forall i,j$ and $\ell_{i,k} + P_{i,k+1} \le P_{j,k} + \ell_{j,k}$, $\forall i,j$, $\forall k, k = 3,...,m-1$, . Then there exists an optimal sequence determined by the next rule which presented by algorithm (9).

Algorithm (9)

1- Let $w_n = 1,2,...,n$ be a sequence was obtained by ordering jobs in non- decreasing order of $P_{i,2} + \ell_{i,2}$. If $\sum_{r=1}^{m-1}(\ell_{n,r} + P_{n,r+1}) = \min_{1 \le i \le n}\{\sum_{r=1}^{m-1}(\ell_{i,r} + P_{i,r+1})\}$, then w is optimal on M_1, to M_m. If not, read (2).

2- There exist at most (n-1) sequence $w_q = (1,...,q-1,q+1,...,n,q)$ obtained by moving the qth job $q\ (q \ne n)$ which satisfy $\sum_{r=1}^{m-1}(\ell_{q,r} + P_{q,r+1}) \le \sum_{r=1}^{m-1}(\ell_{n,r} + P_{n,r+1})$ to the last of the sequence $w_n = w_q$.

3- The sequence w which gives $\min_{1 \le q < n} C_{\max}(w_q)$ is the optimal sequence.

Tenth Case

Theorem(12): In $TF_m|\ell_{i,1},...,\ell_{i,m-1}|C_{\max}$ problem, If $\ell_{i,k} + P_{i,k+1} \le P_{j,k} + \ell_{j,k}$, $\forall i,j$, $\forall k, k = 1,...,m-1$, Then there exists (n-1)! of an optimal sequence determined by the next rule which presented by algorithm (10).

Algorithm (10)

1- Let $w_n = 1,2,...,n$ be a sequence was obtained by ordering jobs in any order. If $\sum_{r=1}^{m-1}(\ell_{n,r} + P_{n,r+1}) = \min_{1 \le i \le n}\{\sum_{r=1}^{m-1}(\ell_{i,r} + P_{i,r+1})\}$, then w is optimal on M_1, to M_m. If not, read (2).

2- There exist one sequence $w_q = (1,...,q-1,q+1,...,n,q)$ obtained by moving the qth job $q\ (q \ne n)$ which satisfy $\sum_{r=1}^{m-1}(\ell_{q,r} + P_{q,r+1}) \le \sum_{r=1}^{m-1}(\ell_{n,r} + P_{n,r+1})$ to the last of the sequence $w_n = w_q$.

3- There exist (n-1)! such sequence w which gives $C_{\max}(w_q)$ is the optimal value with (n-1) jobs in a different order.

Proof(10-12) : is a same as in theorem (9).

Eleventh Case

Theorem(13): In $TF_m\left|\ell_{i,1},\ldots,\ell_{i,m-1}\right|C_{\max}$ problem, If $\max\limits_{1\le i\le n}\{\ell_{i,k}\}\le \ell_{j,k}+P_{j,k+1}$ and $\max\limits_{1\le i\le n}\{P_{i,k+1}\}+P_{j,k+1}\le P_{j,k}$, $\forall i,j$, $\forall k, k=1,\ldots,m-1$. Then ordering jobs by Johnson's rule on the processing time $(\sum_{k=1}^{m-1}(P_{i,k}+\ell_{i,k}), \sum_{k=2}^{m}(\ell_{i,k-1}+P_{i,k}))$ to get an optimal sequence.

***Proof*:** Makespan calculate as:

$$C_{\max}=\max_{1\le h\le n}\{\sum_{i=1}^{h}P_{i,1}+\sum_{k=2}^{m-1}(\ell_{h,k-1}+P_{h,k}+\ell_{h,k})+\sum_{i=h}^{n}P_{i,m})$$

$$=\max_{1\le h\le n}\{\sum_{i=1}^{h}(P_{i,1}+\sum_{k=2}^{m-1}(\ell_{i,k-1}+P_{i,k}+\ell_{i,k}))+\sum_{i=h}^{n}(\sum_{k=2}^{m-1}(\ell_{i,k-1}+P_{i,k}+\ell_{i,k})+P_{i,m})\}-\sum_{i=1}^{n}\sum_{k=2}^{m-1}(\ell_{i,k-1}+P_{i,k}+\ell_{i,k})$$

The term $\sum_{i=1}^{n}\sum_{k=2}^{m-1}(\ell_{i,k-1}+P_{i,k}+\ell_{i,k})$ is constant and the first term is an optimal value by theorem (3.4) in [5]

CONCLUSION

In this study, we discus the problem of scheduling m-machine with transportation time between machines where each machine can process one job at a time and each job i is transported from machine to another. This problem is considered NP-hard with out transportation times.

We have presented a discussion of ways to extend Johnson's two-machine result. This result has been extended to derive a special optimality conditions. The thirteen polynomial solvable special cases which discussion by this study are the first cases for the $TF_m/\ell_{i,1},\ldots,\ell_{i,m-1}/C_{\max}$ problem.

REFERENCES

1. Abdul Razaq, T. S., "Machine Scheduling Problem, a branch and bound approach", Ph.D. Thesis, University of keele (1987).
2. Fondrevelle, J. (Speaker), Oulamara, O., and Portmann, M-C., "Minimizing makespan in flowshop with time lags", arXiv:cs.DM/0507016 v1 6 Jul (2005).
3. Johnson S.M. "Optimal two and three stage production schedule with set-up times included", Naval res. Logist Quart 1, 61-68 (1954).1954).
4. Bellman R., A.O. Esogbue, Nabeshima I., "Mathematical Aspects of Scheduling and Applications", Perganon press, Great Britain, (1982).
5. Niran A. A. "Three machine flow shop problem with transportation time" M. sc. Thesis Mathematics department, College of Science University of Al-Mustansiriyah.(2006).

Using Entropy Loss Function To Estimate The Scale Parameter For Laplace Distribution

Huda Abdullah Rashed, Akbal Jabbar Sultan and Nadia Jaffer Fazah
Department of Mathematics , college of Science , AL – Mustansiriya University
Received 2/4/2013 – Accepted 15/9/2013

الخلاصة

يهدف هذا البحث الى ايجاد أفضل مقدر لمعلمة القياس لتوزيع لابلاس باستخدام دالة Entropy للخسارة مع دوال اسبقية معلوماتية وغير معلوماتية. لقد تمت المقارنة بين أداء هذه المقدرات مع أداء مقدرات بيز تحت دالة الخسارة التربيعية المعدلة مع نفس دالتي الأسبقية تبعاً لمتوسط مربعات الخطأ (MSE) . أظهرت النتائج أن مقدر بيز تحت دالة Entropy للخسارة مع دالة اسبقية معكوس كاما كان الأفضل عند احجام العينات المتوسطة والكبيرة بينما المقدر تحت التربيعية المعدلة مع دالة اسبقية كاما كان الأفضل مع احجام العينات الصغيرة في حالة كون معلمة القياس ذات قيمة صغيرة.

ABSTRACT

The object of the present paper is finding the best estimator for the scale parameter of Laplace distribution using Entropy loss function with informative and non-informative priors are presented and compared with bayes estimators under Modified quadratic loss function with the same two priors. The comparison was made on the performance of these estimators with respect to the mean square error (MSE). The results showed that the Bayes' estimator under Entropy loss function with Inverted Gamma is the best estimator with a moderate and large sample sizes while the estimator under Modified quadratic loss function was better with small sample sizes and when the scale parameter has a small value.

INTRODUCTION

In Bayesian analysis the unknown parameter is regarded as being the value of a random variable from a given probability distribution, with the knowledge of some information about the value of parameter prior to observing the data $x_1, x_2 \ldots x_n$.

The object of the present paper is to obtain Bayesian estimates of the scale parameter for Laplace distribution using Entropy loss function with informative and non-informative priors. The comparison was based on a Monte Carlo study. The efficiency for the estimators was compared according to the mean square error (MSE).

Bayes' Estimators

Let $x_1, x_2, \ldots, x_n$ be a random sample of size n, the n items have an independent and identically Laplace distribution, with probability density function given by[1] :

$$f(x|a,b) = \frac{1}{2b} exp\left[-\frac{|x-a|}{b}\right] \qquad -\infty < x < \infty \qquad (1)$$
$$-\infty < a < \infty , b > 0$$

Where a is the location parameter and b is the scale parameter.

Bayes' estimators for the scale parameter b was considered with Entropy loss function and Modified quadratic loss function with informative loss function represented by Inverted Gamma prior and non-Informative prior which represented by Jeffrey prior.

1. Bayes estimator under entropy loss function

Entropy loss function was first introduced by James and Stein for the estimation of the Variance-Covariance (i.e., Dispersion) matrix of the Multivariate normal distribution. Dey et al. [3],[7] considered this loss function for simultaneous estimation of scale parameters and their reciprocals, for p independent gamma distributions. Rukhin and Ananda considered the estimation problem of the variance of a Multivariate Normal vector under the Entropy loss and Quadratic loss.[7]

We consider the entropy loss function of the form:[6]

$$L(b,\hat{b}) = w\left[\left(\frac{\hat{b}}{b}\right) - \ln\left(\frac{\hat{b}}{b}\right) - 1\right] \quad , \quad w > o \qquad (2)$$

Then the Bayes estimator of b is:[6]

$$\hat{b} = \left[E\left(\frac{1}{b}\,\middle|\,\underline{X}\right)\right]^{-1} \qquad (3)$$

Where $E\left(\frac{1}{b}\,\middle|\,\underline{X}\right) = \int_0^\infty \frac{1}{b}\ h(b|\underline{X})db$

$h(b|\underline{X})$ is the posterior distribution.

Now, according to Entropy loss function we will estimate the scale parameter for Laplace distribution using informative and non informative priors as follows:

***(i)* Posterior distribution using Inverted Gamma prior (IG)**

Assuming that b has informative prior as Inverted Gamma prior which takes the following form [4]:

$$g_1(b) = \frac{\alpha^\beta}{\Gamma\beta} \cdot \frac{1}{b^{\beta+1}}\ e^{-(\alpha|b)}\ ,\ \alpha, \beta, b>0 \qquad (4)$$

So, the posterior distribution for the parameter b given the data $(x_1, x_2, \dots x_n)$ is:

$$h_1(b|\underline{X}) = \frac{\pi_{i=1}^n f(x_i|b) g_1(b)}{\int_0^\infty \pi_{i=1}^n f(x_i|b) g_1(b) db}$$

$$= \frac{\left(\frac{1}{b^{(n+\beta+1)}}\right) e^{-\frac{1}{b}\left\langle\sum_{i=1}^n |x_i - a| + \alpha\right\rangle}}{\int_0^\infty \left(\frac{1}{b^{(n+\beta+1)}}\right) e^{-\frac{1}{b}\left\langle\sum_{i=1}^n |x_i - a| + \alpha\right\rangle} db}$$

$$= \frac{\langle\sum|x_i - a| + \alpha\rangle^{n+\beta}\ .\ 1/b^{(n+\beta+1)}\ .\ e^{-\frac{1}{b}\left\langle\sum_{i=1}^n |x_i - a| + \alpha\right\rangle}}{\Gamma(n+t\beta)\ \int_0^\infty \frac{\langle\sum|x_i - a| + \alpha\rangle^{n+\beta}}{\lceil(n+\beta) b^{(n+\beta+1)}}\ e^{-\frac{1}{b}\left\langle\sum_{i=1}^n |x_i - a| + \alpha\right\rangle db}}$$

Then the posterior distribution became as follows:

$$h_1(b|\underline{X}) = \frac{(\sum|x_i - a| + \alpha)^{n+\beta} \cdot e^{-\frac{1}{b}(\sum_{i=1}^{n}|x_i - a| + \alpha)}}{b^{(n+\beta+1)}\Gamma(n+\beta)} \qquad (5)$$

Now, notice that $b \sim IG(n+\beta, (\sum|x_i - a|) + \alpha)$

Let $T = b^{-1}$

Thus $T \sim G(n+\beta, 1/(\sum|x_i - a|) + \alpha)$ and $E(T|\underline{X}) = \left[\frac{n+\beta}{(\sum_{i=1}^{n}|x_i - a|) + \alpha}\right]$

According to the Entropy loss function, the corresponding Bayes' estimator for b is such that:

$$\hat{b}_1 = \left[E(T|\underline{X})\right]^{-1} = \left[\frac{n+\beta}{(\sum_{i=1}^{n}|x_i - a|)}\right]^{-1} = \frac{\sum_{i=1}^{n}|x_i - a| + \propto}{n+\beta}$$

$$\hat{b}_1 = \frac{\sum_{i=1}^{n}|x_i - a| + \propto}{n+\beta} \qquad (6)$$

***(ii)* posterior distribution using Jeffery prior.**

Following the form of Jeffrey prior information [1]:

$$g_2(\theta) = k\frac{1}{\theta^c}, \text{ with k a constant, } c \in R^+ \qquad (7)$$

In the same way, the posterior distribution with Jeffrey prior information will be as follows:

$$h_2(b|\underline{X}) = \frac{\frac{1}{b^{n+c}}\ e^{-\frac{1}{b}(\sum_{i=1}^{n}|x_i - a|)}}{\int_0^\infty \frac{1}{b^{n+c}}\ e^{-\frac{1}{b}(\sum_{i=1}^{n}|x_i - a|)}db}$$

$$= \frac{(\sum_{i=1}^{n}|x_i - a|)^{n+c-1} \cdot \frac{1}{b^{n+c}}\ e^{-\frac{1}{b}(\sum_{i=1}^{n}|x_i - a|)}}{\Gamma(n+c-1)\int_0^\infty \frac{(\sum|x_i - a|)^{n+c-1}}{\Gamma(n+c-1)b^{n+c}} \cdot e^{-\frac{1}{b}(\sum_{i=1}^{n}|x_i - a|)}db}$$

$$h_2(b|\underline{X}) = \frac{(\sum_{i=1}^{n}|x_i - a|)^{n+c-1} \cdot \frac{1}{b^{n+c}}\ e^{-\frac{1}{b}(\sum_{i=1}^{n}|x_i - a|)}}{\Gamma(n+c-1)} \qquad (8)$$

$b \sim IG(n+c-1), (\sum_{i=1}^{n}|x_i - a|)$

Let $T = b^{-1}$

Thus, $T \sim G\left(n+c-1, \frac{1}{(\sum_{i=1}^{n}|x_i - a|)}\right)$

Hence, according to the Entropy Loss Function we get:

$$\hat{b}_2 = \frac{(\sum_{i=1}^{n}|x_i - a|)}{n+c-1} \qquad (9)$$

2. **Bayes estimator under Modified Quadratic Loss Function**

For the estimation of the scale parameter of Laplace distribution, a modified form of this loss function may be defined as follows:[1]

$$L(\theta, \hat{\theta}) = \left(\frac{\theta - \hat{\theta}}{\theta}\right)^2 \qquad (10)$$

$$\hat{b} = \frac{E\left(\frac{1}{b}\middle|\underline{X}\right)}{E\left(\frac{1}{b^2}\middle|\underline{X}\right)} \tag{11}$$

***(i)* Posterior distribution using Inverted Gamma prior (IG)**

To estimate the scale parameter for Laplace distribution using Inverted Gamma prior under modified quadratic loss function we use $h_1(b|\underline{X})$ where:

$b \sim IG(n+\beta, (\sum|x_i - a|) + \alpha)$

And we found that:

$$T \sim G\left(n+\beta, \frac{1}{\sum_{i=1}^{n}|x_i - a|}\right), where\ T = b^{-1}$$

$$E(T) = \frac{n+\beta}{(\sum|x_i - a|) + \propto} \tag{12}$$

$$var(T) = \frac{n+\beta}{(\sum_{i=1}^{n}|x_i - a| + \propto)^2}$$

Hence:

$$E(T^2) = \frac{n+\beta}{(\sum_{i=1}^{n}|x_i - a| + \propto)^2} + \frac{(n+\beta)^2}{(\sum_{i=1}^{n}|x_i - a| + \propto)^2} \tag{13}$$

$$E(T^2) = \frac{(n+\beta)(1+n+\beta)}{(\sum_{i=1}^{n}|x_i - a| + \propto)^2}$$

According to (11):

$$\hat{b}_3 = \frac{E(T)}{E(T^2)} \tag{14}$$

Substituting (12) and (13) in (14), we get:

$$\hat{b}_3 = \frac{\frac{n+\beta}{\sum_{i=1}^{n}|x_i - a| + \propto}}{\frac{(n+\beta)(1+n+\beta)}{(\sum_{i=1}^{n}|x_i - a| + \propto)^2}}$$

$$\hat{b}_3 = \frac{\sum_{i=1}^{n}|x_i - a| + \propto}{n+\beta+1} \tag{15}$$

***(ii)* Posterior distribution using Jeffery prior.**

The corresponding Bayes estimator for b with posterior distribution $h_2(b|x)$ comes out as:

$$T \sim G\left(n+c-1, \frac{1}{(\sum_{i=1}^{n}|x_i - a|)}\right), where\ T = b^{-1}$$

$$E(T) = \frac{n+c-1}{(\sum_{i=1}^{n}|x_i - a|)} \tag{16}$$

$$var(T) = \frac{n+c-1}{(\sum_{i=1}^{n}|x_i - a|)^2}$$

Thus: $E(T^2) = \frac{(n+c-1)(n+c)}{(\sum_{i=1}^{n}|x_i - a|)^2}$ (17)

Substituting (16) and (17) in (13), we find:

$$\hat{b}_4 = \frac{(\sum_{i=1}^{n} |x_i - a|)}{n + c} \qquad (18)$$

Simulation Results

In this section, Monte – Carlo simulation study is performed to compare the methods of estimation by using mean square Errors (MSE's) as follows:

$$MSE(\hat{b}) = \frac{\sum_{i=1}^{R} (\hat{b}_i - b)^2}{R}$$

Where R is the number of replications.

We generated R=3000 samples of size n = 10, 20, 50, and 300 to represent small, moderate and large sample sizes from Laplace distribution with the scale parameter $b = 1, 2$.

In order to compare the Bayes' estimators under two different loss functions and two priors, we chose the values of Jeffrey constants; ($c = 0.5, 2, 3$) and for the Inverted Gamma prior ($\alpha = 1.5, 3$) with $\beta = 2$.

The results were summarized and tabulated in the following tables for each estimator and for all sample sizes.

Table-1: Expected values and MSE of the different estimators for Laplace distribution when b=1 and β =2

n	criteria	$\hat{b}_1$		$\hat{b}_2$			$\hat{b}_3$		$\hat{b}_4$		
		$\alpha = 1.5$	$\alpha = 3$	c=0.5	c=2	c =3	$\alpha = 1.5$	$\alpha = 3$	c=0.5	c=2	c =3
10	EXP.	0.9608	1.0858	1.055	0.911	0.8358	0.8869	1.0027	0.955	0.8358	0.7715
	MSE	0.0717	0.0776	0.115	0.091	0.0972	0.0726	0.0598	0.093	0.0972	0.1120
20	EXP.	0.8901	1.0483	1.028	0.955	0.9119	0.9375	1.0027	0.978	0.9119	0.8723
	MSE	0.0432	0.0452	0.055	0.048	0.0506	0.0431	0.0392	0.049	0.0506	0.0555
50	EXP.	0.9905	1.0194	1.010	0.980	0.9617	0.9718	1.0001	0.990	0.9617	0.9435
	MSE	0.0187	0.0189	0.020	0.019	0.0201	0.0187	0.0179	0.019	0.0208	0.0211
300	EXP.	0.9989	1.0039	1.0022	0.9972	0.9939	0.9956	1.0005	0.9980	0.9939	0.9906
	MSE	0.0034	0.0033	0.003	0.003	0.0033	0.0033	0.0033	0.003	0.0033	0.00341

Table-2: Expected values and MSE of the different estimators for Laplace distribution when b=2 and β =2

n	Criteria	$\hat{b}_1$		$\hat{b}_2$			$\hat{b}_3$		$\hat{b}_4$		
		$\alpha = 1.5$	$\alpha = 3$	c=0.5	c=2	c =3	$\alpha = 1.5$	$\alpha = 3$	c=0.5	c=2	c =3
10	EXP.	1.7966	1.9216	2.1115	1.8235	1.6716	1.6584	1.7738	1.9104	1.6716	1.5430
	MSE	0.3222	0.2869	0.4604	0.3653	0.3886	0.3559	0.2904	0.3748	0.3886	0.4481
20	EXP.	1.8919	1.9602	2.0582	1.9107	1.8238	1.8097	1.8749	1.9573	1.8238	1.7455
	MSE	0.1829	0.1729	0.2215	0.1959	0.2023	0.1929	0.1724	0.1991	0.2023	0.2226
50	EXP.	1.9522	1.9810	2.0205	1.9611	1.9233	1.9154	1.9437	1.9805	1.9233	[illegible]
	MSE	0.0767	0.0748	0.0826	0.0789	0.0803	0.0788	0.0748	0.0793	0.08[illegible]	[illegible]
300	EXP.	1.9928	1.9978	2.0048	1.9944	1.9878	1.9862	1.9912	1.9978	1[illegible]	[illegible]
	MSE	0.0134	0.0134	0.0136	0.0135	0.0136	0.0135	0.0134	0.0135	[illegible]	[illegible]

RESULTS AND DISCUSSIONS

From table (1) It appears that in small samples (n = 10, 20) $\hat{b}_3$ is the best estimator which represented bayes estimator with inverted gamma prior under modified quadratic loss function when$\alpha = 3$, while $\hat{b}_3$ and $\hat{b}_1$ which represented bayes estimator with inverted gamma prior under Entropy loss function, are closed in MSE's with small value of α $(\alpha = 1.5)$ also we can say that the estimators under Entropy loss function with Inverted Gamma prior become the most efficient with the moderate and large sample sizes.

The results in table (2) showing that MSE's increases for all estimators when the scale parameter (b) increase. We can see clearly that the bayes estimator with inverted gamma prior under Entropy loss function $\hat{\boldsymbol{b}}_{\mathbf{1}}$ became the best with all sample sizes.

In general, we can say that, the Bayes' estimator under Entropy loss function with Inverted Gamma is the best estimator with a moderate and large sample sizes while the estimator under Modified quadratic loss function was better with small sample sizes and when the scale parameter has a small value.

REFERENCES

1. Al- Noor. N. H. and Rasheed, H. Abdullah(2012)," Minimax Estimation of the Scale Parameter of the Laplace Distribution under Quadratic Loss Function" ,International Journal for Sciences and Technology, Vol (7), No(3), pp. 100-107.
2. Abbasi, N. (2011),"Comparison of Bayes' estimator and Maximum Entropy estimator for discrete Laplace distribution" Int. J. Contemp. Math. Sciences: Vol.6, No. 9, pp 447- 452.
3. Dey, D.K.; Ghosh, M. and Srinivasan, C. (1987). Simultaneous estimation of parameters under entropy loss, J. Statist. Plann. Inference, 15, 347–363.
4. Esfahani, M. Nasr, Nematollahi, N.(2009), " Admissible and Minimax Estimators of a Lower Bounded Scale Parameter of a Gamma Distribution under the Entropy Loss Function", Journal of Mathematical Extension: Vol. 4, No. 1 (2009), 91-103.
5. Julia,O. and Vives-Rego, J. (2008), "A microbiology application of the skew-Laplace distribution". SORT Vol. 32, No. 2, pp.141 – 150.
6. Pandey, H., & Rao, A. K. (2009). Bayesian estimation of the shape parameter of a generalized Pareto distribution under asymmetric loss functions. Hacettepe Journal of Mathematics and Statistics. Vol, 38 (1), pp. 69-83.
7. Singh, S. Kumar, Singh, U. And Kumar, D. (2011)," BAYESIAN ESTIMATION OF THE EXPONENTIATED GAMMA PARAMETER AND RELIABILITY FUNCTION UNDER ASYMMETRIC LOSS FUNCTION", REVSTAT – Statistical Journal: Vol. 9, No. 3, pp247–260.

ON ONE-SIDED APPROXIMATION OF FUNCTION

Saheb AL – Saidy and Hamsa Ali Al – Saad
Department of Mathematics , college of Science , AL – Mustansiriya University
Received 10/3/2013 – Accepted 15/9/2013

الخلاصه

درسنا في هذا البحث موضوع (درجة التقريب الجانبي للداله غير المقيدة بواسطة المتعددات الجبرية في فضاءات الموزونه)

ABSTRACT

In this paper we studied the degree of one sided -approximation of unbounded functions by algebraic polynomials in the $L_{p,\alpha}$-weighted spaces in terms of weighted modules of continuity

1-INTROUDACTION

In 1997, the authors in [11],[12] and [13] introduced an interesting new concept of interwining approximation which is related to both copositive approximation and one sided -approximation .

Let X=[-1,1], then we denoted by $L_p$the space of all bounded measurable functions f on X such that :

$$\|f\|_p := \left(\int_{-1}^{1}|f(x)|^p dx\right)^{1/p} < \infty \ ,1 \le p \le \infty \qquad (1.1)$$

The degree of best approximation of $f \in L_p$ with respect to algebraic polynomials of degree r in $L_p - spaces$ is defined by:

$E_r(f)_p := inf_{p\in\pi_r}\|f - p\|_p, , 1 \le p \le \infty$

where π_r is the set of all algebraic polynomials of degree $\le r$

The best one-sided approximations of $f \in L_p$ with respect to algebraic polynomials from$L_p - spaces$ is given by:

$\tilde{E}_r(f)_p := \inf_{x\in[-1,1]}\{\|P - Q\|_p : P, Q \in \pi_r and\ P(x) \ge f(x) \ge Q(x)\}$

The k^{th} average modules of $f \in L_p$ with respect to algebraic polynomials from $L_p - spaces$ is given by

$\tau_k(f,\delta)_p := \|w_k(f,x,\delta)\|_p, \delta > 0$

where :

$w_k(f,x,\delta)_p :=$ $\sup\{\left|\Delta_h^k f(t)\right| : t\in \left[x - \frac{kh}{2}, x + \frac{kh}{2}\right], h \le \delta\}, \delta > 0$

Now Let β_α :={f:X→ IR: $|f(x)| \le Me^{\alpha x}$ },α> 1 such that

$$\|f\|_{p,\alpha} := \left(\int_{-1}^{1}|f(x)|^p e^{-\alpha p x}\, dx\right)^{1/p} < \infty \qquad (1.2)$$

The k^{th} symmetric difference [2] of $f \in \beta_\alpha$ is defined by:

$$\Delta_h^k f := \sum_{i=0}^{k}(-1)^i\binom{k}{i} f\left(x + k\left(\frac{h}{2}\right) - ik\right) \qquad (1.3)$$

The k^{th} $L_{p,\alpha}$-modules of continuity for $f \in \beta_\alpha$is defined by:

$$w_k(f,\delta)_\alpha := sup_{|h|<\delta}\left\{\left\|\Delta_h^k f\right\|_{p,\alpha}\right\}, \delta > 0 \qquad (1.4)$$

Let us define the $\emptyset k^{th}$ $L_{p,\alpha}$- weighted modules of continuity for f$\in \beta_\alpha$ by:

$w_k^{\emptyset}(f,\delta)_\alpha := sup\left\{\left|\Delta_h^{k\emptyset} f(t)e^{-\alpha t}\right| : t \in \left[x-\frac{kh}{2}, x+\frac{kh}{2}\right], h \leq \delta\right\}$ (1.5)

Where :

$\emptyset(x) = (1-x^2)^{1/2}$ for X=[-1,1] and where :

$\Delta_h^{\emptyset k} f(t) := \sum_{i=0}^{k}(-1)^i\binom{k}{i} f\left(x+\emptyset k\left(\frac{h}{2}\right)-i\emptyset k\right)$

Now ,we shall introduce the average modules of smoothness for f$\in \beta_\alpha$

The k^{th} average modules of smoothness for f$\in \beta_\alpha$ is defined by :

$\tau_k(f,\delta)_\alpha := \|w_k(f,x,\delta)\|_{p,\alpha}$ (1.6)

Where

$w_k(f,x,\delta)_\alpha$:=sup$\{\left|\Delta_h^k f(t)e^{-\alpha t}\right|$: t$\in \left[x-\frac{kh}{2}, x+\frac{kh}{2}\right]: h \leq \delta\}$

Then the best approximation of function s f$\in \beta_\alpha$ with polynomials from π_r in $L_{p,\alpha\_}$ weighted spaces is given by:

$E_r(f)_{p,\alpha} := inf_{p\in\pi_r}\|f-p\|_{p,\alpha}$ (1.7)

The best one-sided approximations of f$\in \beta_\alpha$ with polynomials from π_r in

$L_{p,\alpha\_}$ weighted spaces is given by:

$\widetilde{E_r}(f)_{p,\alpha} := \inf_{x\in[-1,1]}\{\|P-Q\|_{p,\alpha}: P,Q \in \pi_r \ and\ P(x) \geq f(x) \geq Q(x)\}$(1.8)

2-AUXILIARY LEMMAS

Here, we shall list some Lemmas which we need to prove our results.

Theorm (A) :(whitney's Inequality)[6]

Let f$\in L_p(X)$,0$< p \leq \infty$,then there exists a polynomial

$Q_n \in \pi_r$, $(n \leq r)$ of degree $\leq n$,such that :

$\|f-Q_n\|_{L(X)} \leq Cw_k(f,x,\delta)_p$,$\delta > 0$.

Here we want to prove the same result but for f$\in \beta_\alpha$:

Whitney's lemma (2.1): For f$\in \beta_\alpha$ there exists a polynomial Q$\in \pi_r$, such that:

$\|f-Q\|_{p,\alpha} \leq Cw_k(f,x,\delta)_{p,\alpha}$

Where C is an absolute constant.

Proof:

$\|f-Q\|_{p,\alpha}=(\int_{-1}^{1}|f(x)-Q(x)|^p e^{-\alpha px}dx)^{1/p}$

Since $|fe^{-\alpha x}| \leq M$ then $fe^{-\alpha x}$is a bounded function then by whitney's inequality $\exists\ Q \in \pi_r$ such that :

$\|f-Q\|_{p,\alpha}=(\int_{-1}^{1}|f(x)-Q(x)|^p e^{-\alpha px}dx)^{1/p}$

$\leq \|fe^{-\propto px} - Qe^{-\alpha px}\|_p \leq Cw_k(f,x,\delta)_{p,\alpha}$

Lemma (2.2):[3]

For f$\in L_p[-1,1]$,0< $p \leq \infty$,we have

$E_r(f)_p \leq Cw_k(f,n^{-1})_{L_{p[-1,1]}}$

Lemma(2.3) :For f$\in \beta_\alpha$ there is an absolute constant C such that:

$E_r(f)_\alpha \leq C\, w_k^{\emptyset}(f,\delta)_\alpha$

Proof:

Let P be the best approximation polynomial of f$\in \beta_\propto$ then

$E_r(f)_{p,\propto} = \|f - P\|_{p,\propto}$

$=(\int_{-1}^{1}|f(x) - P(x)|^p\, e^{-\propto px}dx)^{1/p}$

Since $|fe^{-\alpha x}| \leq M$then $fe^{-\alpha x}$is a bounded function by lemma(2.2)

$(E_r(f\, e^{-\alpha x}))_p \leq C(k)\, w_k^{\emptyset}(fe^{-\alpha x}, n^{-1})_p$

Hence $E_r(f)_\alpha \leq Cw_k^{\emptyset}(f,\delta)_\alpha$

Lemma(2.4): [4]

For f$\in L_p$ we get $\tau_k(f,\delta)_p \leq C\, \|f\|_p$

Lemma(2.5): For f$\in \beta_\alpha$we have

$\tau_k(f,\delta)_{p,\alpha} \leq C\, \|f\|_{p,\alpha}$where C is an absolute constant ?

Proof :

Let P be the best approximation polynomial of f$\in \beta_\propto$ then

$E_r(f)_{p,\propto} = \|f - P\|_{p,\propto}$

$=(\int_{-1}^{1}|f(x) - P(x)|^p\, e^{-\propto px}dx)^{1/p}$

Since $|fe^{-\alpha x}| \leq M$ then $fe^{-\alpha x}$ is a bounded function hence by lemma (2.4) we get

$\tau_k(fe^{-\alpha x},\delta)_p \leq C\, \|fe^{-\alpha x}\|_p$

Therefore

$\tau_k(f,\delta)_{p,\alpha} \leq C\, \|f\|_{p,\alpha}$

Lemma (2.6): for f$\in \beta_\alpha$then

$w_k(f,\delta)_\alpha \leq \delta w_{k-1}(f',\delta)_\alpha$

Proof:

By definition of$w_k(f,\delta)_\alpha$we get :

$$\left|\Delta_h^k f(t)e^{-\alpha t}\right| = \left|\Delta_h^{k-1}\left[f(t+x)e^{-\alpha(t+x)} - f(t)e^{-\alpha t}\right]\right|$$

$$= \left|\Delta_h^{k-1}\int_0^h (f'(t+x))dt\right|$$

$$=\left|\int_0^h \Delta_h^{k-1} f'(t+x)dt\right|$$

$$\leq \int_{\min(0,h)}^{\max(0,h)} \Delta_h^{k-1}\left|f'(t+x)\, dt\right|$$

$$\leq \int_{\min(0,h)}^{\max(0,h)} \Delta_h^{k-1}(f'(t),\delta)\text{where}f'=(f(t)e^{-\propto t})'$$

$$\leq \int_{\min(0,h)}^{\max(0,h)} w_{k-1}(f'(t),\delta)_{\alpha} dt$$
$$\leq \delta w_{k-1}(f',\delta)_{\alpha}$$

Lemma (2.7): For f $\in \beta_\alpha$ we get

$w_k^{\phi}(f,\delta)_\alpha \leq w_k(f,\delta)_\alpha \leq \tau_k(f,\delta)_\alpha$

Proof:

From (1.4) and (1.5)we get:

$w_k^{\phi}(f,\delta)_\alpha \leq w_k(f,\delta)_\alpha$

$$w_k(f,\delta)_\alpha = sup_{0\leq h\leq\delta}\{\int_{-1}^{1-kh}|\Delta_h^k f(t)e^{-\alpha t}|^p dt\}^{1/p}$$
$$\leq sup_{0\leq h\leq\delta}\{\int_{-1}^{1-kh}(w_k(fe^{-\alpha t},x+\frac{kh}{2},\delta))^p dt\}^{1/p}$$
$$= sup_{0\leq h\leq\delta}\{\int_{-1+\frac{kh}{2}}^{1+\frac{kh}{2}}(w_k(f,x,\delta)_\alpha)^p dt\}^{1/p}$$
$$= \tau_k(f,\delta)_\alpha$$

Thus $w_k^{\phi}(f,\delta)_\alpha \leq w_k(f,\delta)_\alpha \leq \tau_k(f,\delta)_\alpha$

Lemma(2.8) [3]: For f $\in L_p[-1,1]$,$0< p < \infty$ we have

$E_r(f)_p \leq \tilde{E}_r(f)_p \leq 2rE_r(f)_p$

Lemma(2.9):[7]

If f is a bounded measurable function on [-1,1] then :

$\int_{-1}^{1} f(x)dx \approx 2(n^{-1})\sum_{i=1}^{n} f(x_i)$ (2.1)

Where $x_i=1+\frac{2(2_i-1)}{2n}$

Lemma (2.10):

For $f \in \beta_\alpha$ we get:

$\int_{-1}^{1} f(x)e^{-\alpha x}dx \approx 2(n^{-1})\sum_{i=1}^{n} f(x_i)\, e^{-\alpha x_i}$

Where $x_i=1+\frac{2(2_i-1)}{2n}$

Proof:

Since $|fe^{-\alpha x}| \leq M$ then $fe^{-\alpha x}$ is a bounded measurable function then by equation (2.1)we get

$\int_{-1}^{1} f(x)e^{-\alpha x}dx \approx 2(n^{-1})\sum_{i=1}^{n} f(x_i)\, e^{-\alpha x_i}$, Where $x_i=1+\frac{2(2_i-1)}{2n}$

Lemma(2.11) [8]:

For any polynomial $Q_n \in \pi_r$, (n$\leq r$)$0< p \leq \infty$,we have

$|X|^{1/p}\|Q_n\|_{L_\infty(X)} \sim \|Q_n\|_{L_p(X)}$(2.2)

Also it is clear that $W_k(f,t)_p \leq W_k(f,t)_\infty$

Lemma (2.12)[9],[10]

For f$\in L_p$and k,$\mu \in N$, ($0< p \leq 1$) ,we get [9,10]

$\sum_{i=0}^{n-\mu-1} W_k(f,\cup_{i=j}^{\mu} X_i)_p^p \leq C(p,k,\mu)W_k^{\phi}(f,n^{-1})_p^p$(2.3)

Where C is an absolute constant

Lemma (2.13)[3]

For f$\in L_p$[-1,1] ,0< $p \leq \infty$, we have

$E_r(f)_\infty \leq \tilde{E}_r(f)_\infty \leq 2rE_r(f)_\infty$

Beatson Lemma [3]

Let k$\geq$ 2 be an integer and d=2(k-1)^2 ,let T=$\{t\}_{i=-\infty}^{\infty}$ be strictly increasing knote sequence with $t_0 = -1, t_d$=1 , let P,Q be two polynomials of degree less than r then there exists aspline polynomials such that :

i- s(x) is a number between P(x) and Q(x) $for\ x \in [-1,1]$

ii- s(x)=P(x) on (-∞, -1] and s(x) =Q(X) on [1,∞)

3.MAIN RESULTS:

In this paper , we shall find the following results about the best one-sided Approximation of f$\in \beta_\alpha$ with respect to algebraic polynomials in the $L_{p,\alpha}$-weighted spaces

Theorm(3.1): For f$\in \beta_\alpha$, we have

$\tilde{E}_r(f)_{p,\alpha} \cong w_k^{\emptyset}(f,|X|)_{p,\alpha}$

Proof :

Let P^*be the polynomial of best approximation of f$\in \beta_\alpha$ and let P and Q are polynomials of degree r such that (Q(x)$\leq f(x) \leq P(x)$)

$$\begin{aligned}
\tilde{E}_r(f)_{p,\alpha} &= \|P - Q\|_{p,\alpha} \\
&= \left(\int_{-1}^{1} |P(x) - Q(x)|^p e^{-\alpha x p}\, dx\right)^{1/p} \\
&\leq 2^{1/p} \sup\{|P(x) - Q(x)|e^{-\alpha x}\} \\
&= 2^{1/p}\|P - Q\|_{\infty,\alpha} \\
&= 2^{1/p}\tilde{E}_r(f)_{\infty,\alpha} \text{ (by lemma (2.13))} \\
&\leq 2E_r(f)_{\infty,\alpha}
\end{aligned}$$

By whitney's lemma we get

$$\begin{aligned}
C\, E_r(f)_{p,\alpha} &\leq C\|f - P^*\| \\
&\leq Cw_k(f,|X|)_{p,\alpha}
\end{aligned}$$

Therefore

$$\tilde{E}_r(f)_{p,\alpha} \leq Cw_k(f,|X|)_{p,\alpha}$$

By lemma (2.7) we get

$$\tilde{E}_r(f)_{p,\alpha} \leq Cw_k^{\emptyset}(f,|X|)_{p,\alpha}$$

Conversly let Q_i be the best approximation polynomial of f$\in \beta_\alpha$ on $X_{i=}[Z_i, Z_{i+1}], i = 1,2, \dots, r$ are points in[-1,1]

Now by lemmas (2.13),(2.11),(2.8), and (2.12) we get

$w_k^{\emptyset}(f,|X|)_{p,\alpha} \leq w_k(f,|X|)_{p,\alpha}$

By lemma(2.7) we get

$$\begin{aligned}
w_k(f,|X|)_{p,\alpha} &= sup_{x\in[-1,1]} \left\|\Delta_h^k f e^{-\alpha x}\right\|_p \\
&= \sum_{i=1}^{n} |X_i|\ sup\ \left\|\Delta_h^k f\, e^{-\alpha x}\right\|_{P(Xi)}
\end{aligned}$$

$$\leq \sum_{i=1}^{n} |Xi| \left\|\Delta_h^k (f - Qi)e^{-\alpha x}\right\|_{\infty,\alpha}$$

$\leq C\sum_{i-1}^{n} |X_i| \|(f - Q_i)e^{-\alpha}\|_{\infty,\alpha}$ by lemma (2.8) we get

$$= C\sum_{i-1}^{n} n^{-1}\ E_i\,(f)_{\infty,\alpha}$$

Since[Any two norms in afinite dimensional space are equivalent] we get

$\|Q - P\|_{\infty,\alpha} \leq C\|Q - P\|_{p,\propto}$

Thus

$w_k^{\emptyset}(f, |x|)_\alpha \leq C\sum_{i=1}^{n} n^{-1}\,E_i(f)_{p,\alpha}$ by lemma (2.8) we get

$\leq 2C\sum_{i=1}^{n} E_i(f)_{p,\alpha}$

$= 2C\sum_{i=1}^{n} \|f - Q_i\|_{p,\alpha}$

$\leq 2C\sum_{i=1}^{n} W_k(f, |X_i|)$by lemma (2.12) we get

$\leq C\, W_k^{\emptyset}(f, n^{-1})_{p,\propto}$

$\leq \tilde{E}_r(f)_{p,\alpha}$

Hence

$\tilde{E}_r(f)_{p,\alpha} \cong w_k^{\emptyset}\,(f, |X|)_{p,\alpha}$

Theorm(3.2)[Intertwining Spline Approximations ,0$< p \leq \infty$)]

Let $f \in \beta_\alpha$,let k≥ 2 be an integer and let s≥ 0,

$$Y_s = \{y_1, \dots, y_s \backslash y_0 = -1 < y_1 < y_2 < \cdots < y_s < 1\ = y_{s+1}\}.$$

Let T_n be a given knote sequence such that there are at least 4(k-1)^2 knote in each open intervals (y_i, y_{i+1}), j=1,2,…,s-1, then there exists an interwining pair of splines $\{\overline{S},\ S\}$ of order k on the knot sequence T_n,(i.e.$\overline{S},\ S \in C^{k-2}[-1,1]$ and $\overline{S} - f, S - f \in \Delta^0(Y_s)$) such that , for i=0,1,…,n-1

$$\|\bar{S} - S\|_{p,\alpha} \leq C|X_i|^2 W_{k-1}^{\emptyset}(f', |X_i|, X_i)_{p,\alpha}\ . \qquad (3.2.1)$$

Where C is a constant depending on k and on the maximum ratio

$p = max_{i=0}^{k-1} \frac{|X_{i\pm 1}|}{|X_i|}$.

And X_i is an interval such that $X_i \subseteq X_i \subseteq [z_{i-6(k-1)^2}, z_{i+6(k-1)^2}]$

Proof:

Let d=2$(r-1)^2$,m=[(n+d-1)d] and $\bar{Z}_i$:Z_{d_i}note that $\bar{Z}_i$=-1 for i≤ 0 and $\bar{Z}_i$=1 for i$\geq m$,we first construct over lapping polynomial pieces of degree less than r on the coarser partition $\bar{T}_n$:$\{\bar{Z}_i\}_{i=0}^{m}$We call the interval $\bar{X}_i$=[$\bar{Z}_i$,$\bar{Z}_{i+1}$] contaminated.

If $\bar{Z}_i < y_i < \bar{Z}_{i+1}$ for some $y_i \in Y_s$. By assumation there exists exactly one $y_i$in each of the contaminated interval $\bar{X}_{m_j}$,j=1,…,s and there is aleast one non-contaminated interval between

$\bar{X}_{m_j}$and$\bar{X}_{m_{j+1}}$ that is $X_{m_j} = [Z_j, Z_{j+1}]$ and $X_{m_{j+1}}$=$[Z_{j+1}, Z_{j+2}]$
$m_j < m_{j+2} \leq m_{j+1}$,j=1,...,s-1.
If $m_{j+1} = m_{j+2}$(i-e) if there is only one non-contaminatedinterval between ($\bar{X}_{m_j}$ and $\bar{X}_{m_{j+1}}$) then the following construction is not needed and the next two paragraphs can be skipped .
In case $m_{j+2} \leq m_{j+1}$ by whitneys inequality [6] for approximation on each of the interval $[\bar{Z}_i,\bar{Z}_{i+2}]$, i=$m_{j+1}, \dots, m_{j+1-2}$there exist two polynomials P_i and $Q_{i+1}$of degree less than r such that
P_i(x)≥ $f(x) \geq Q_i(x)$,$\forall x \in [\bar{Z}_i, \bar{Z}_{i+2}]$, by whitney's Lemma we get
$\|P_i - Q_i\|_{p,\propto} \leq \bar{E}(f) \leq CE_r(f) \leq Cw_k(f,\delta)_\alpha$
$$\leq C\tau_k(f,\delta)_\alpha . \qquad (3.2.2)$$
We defined p_i and $q_i$on$[\bar{Z}_i,\bar{Z}_{i+2}]$,, by p_i=P_i and q_i=Q_i if $(-1)^{s-j} > 0$.
And p_i=Q_i and q_i=P_i if $(-1)^{s-j} < 0$
hence $(-1)^{s-j}(P_i(x) - f(x)) \geq 0$,$(-1)^{s-j}(q_i(x) - f(x)) \leq 0$
and $\|p_i - q_i\|_{p,\propto} = \|P_i - Q_i\|_{p,\propto}$(by whitney's Lemma we get)
$$\leq Cw_k^{\emptyset}(f,x,\delta)_{p,\propto}\text{(by Lemma (2.6) we get)}$$
$$\leq Cw_{k-1}^{\emptyset}(f',\delta)_{p,\propto} . \qquad (3.2.3)$$
We should emphasize that when we speak of apolynomial on an interval we mean the restriction to the interval ,hence it is considered undefined outside near each point y_i,we construct local polynomials differently.more precisely ,we approximat f on $[\bar{Z}_{m_{j-1}},\bar{Z}_{m_j+2}]$, j=1,...,s from above and below by two polynomials.
$\breve{P}_{m_j}$ and$\breve{Q}_{m_j}$ of degree less than r-1 then P_{m_j} (x)≥ $f(x)Q_{m_j}$(x),
$\forall x \in [\bar{Z}_{m_{j-1}}, \bar{Z}_{m_j+2}]$,, and by whitneys Lemma we get
$\left\|\tilde{P}_{m_j} - \tilde{Q}_{m_j}\right\|_{p,\propto} \leq Cw_k^{\emptyset}(f,\delta)_{p,\propto}$by Lemma (2.6) we get
$$\leq Cw_{k-1}^{\emptyset}(f',\delta)_{p,\propto}$$
Define $\tilde{p}_{m_j}$=$\breve{P}_{m_j}$ and $\breve{q}_{m_j}$ =$\breve{Q}_{m_j}$ if $(-1)^{s-j} > 0$ and
$\tilde{p}_{m_j} = \breve{Q}_{m_j}and\breve{q}_{m_j}$=$\breve{P}_{m_j}$ if $(-1)^{s-j} < 0$

It is easy to check that
p_{m_j}(x)=$\int_{y_i}^{x}\int_{y_i}^{t_2} \tilde{P}_{m_j}(t_1)e^{-\propto pt_1}\, dt_1dt_2 + f(y_i)$
q_{m_j}(x) = $\int_{y_i}^{x}\int_{y_i}^{t_2} \tilde{Q}_{m_j}(t_1)e^{-\propto pt_1}\, dt_1dt_2 + f(y_i)$
Satisfy the inqualities :
$$\left\|p_{m_j} - q_{m_j}\right\|_{p,\propto} = \left\|\int_{y_i}^{x}\int_{y_i}^{t_2} \tilde{P}_{m_j}(t_1)e^{-\propto pt_1}\, dt_1dt_2 + \int_{y_i}^{x}\int_{y_i}^{t_2} \tilde{Q}_{m_j}(t_1)e^{-\propto pt_1}\, dt_1dt_2\right\|_{p,\propto}$$
$$= \left\|\int_{y_i}^{x}\int_{y_i}^{t_2} e^{-\propto pt_1}[\tilde{P}_{m_j}(t_1) - \tilde{Q}_{m_j}(t_1)]\, dt_1dt_2\right\|_{p,\propto}$$

$$\leq \left\| \int_{\bar{\bar{Z}}_{m_{j-1}}}^{\bar{Z}_{m_j+2}} \int_{\bar{\bar{Z}}_{m_{j-1}}}^{t_2} e^{-\propto pt_1}[\tilde{P}_{m_j}(t_1) - \tilde{Q}_{m_j}(t_1)]\, dt_1 dt_2 \right\|_{p,\propto}$$

$$\leq sup\left\{\left|\tilde{P}_{m_j} - \tilde{Q}_{m_j}\right|^p e^{-\propto pt_1} dt_1 dt_2\right\}^{1/p}$$

$$\leq \left(\int (\int_{\bar{\bar{Z}}_{m_{j-1}}}^{\bar{Z}_{m_j+2}} \int_{Z_{m_{j-1}}}^{t_2} e^{-\propto pt_1}[\tilde{P}_{m_j}(t_1) - \tilde{Q}_{m_j}(t_1)]\, dt_1 dt_2)^p\, dx \right)^{1/p}$$

$$\leq \left(\int (\int_{\bar{\bar{Z}}_{m_{j-1}}}^{\bar{Z}_{m_j+2}} c(m_j) \left|\bar{X}_{m_j}\right| e^{-\propto pt_1}(\tilde{P}_{m_j}(t_1) - \tilde{Q}_{m_j}(t_1) dt_1 dt_2)^p dx \right)^{1/p}$$

$$\leq c(m_j) \left|\bar{X}_{m_j}\right|^2 \left\|\tilde{P}_{m_j} - \tilde{Q}_{m_j}\right\|_{p,\propto}$$

$$\leq c(m_j) \left|\bar{X}_{m_j}\right|^2 w_{k-1}^{\emptyset}(f', \delta)_{p,\propto}$$

To constructed a local polynomials which are "interwning " with f and have the right approximation order ,we now let the two spline $\bar{S}$ and S on the orginal knote sequence T_n with the same properties . If both $\bar{X}_{i_{-1}}$ and $\bar{X}_i$are non- contaminated and i< m ,then $p_{i_{-1}}$ and p_i overlapping $\overline{X_i}$ on,which contain d-1 interior from T_n by beatosons Lemma [3] there exists aspline$\bar{S}_i$ of order r on$\bar{X}_i$on the knote connects with $p_{i_{-1}}$ and p_i in C^{r-2} manner $\bar{Z}_i$=Z_{d_i} $and \bar{Z}_{i_{+1}} = Z_{d_{(i+1)}}$respectively moreover,the graph of $\bar{S}_i$ lies between those of $p_{i_{-1}}$ and p_i hence

Sgn($p_{i_{-1}}$(x) - f(x)) = Sgn(p_i(x) - f(x))=sgn($\bar{S}_i$(x) - f(x)) , x∈ X_i

Similary ,considering the overlapping polynomials q_{i-1} and q_i we construct spline S_i satisfying :

Sgn(q_{i-1} (x) - f(x)) = Sgn(q_i (x) - f(x))=sgn(S_i(x) - f(x)) , x∈ X_i

Also

$$\int |\bar{S}_i - S_i|^p \leq 2^p (\int \left|p_{i_{-1}} - q_{i-1}\right|^p + \int |p_i - q_i|^p)$$

By (3.2.3) this given

$$\|\bar{S}_i - S_i\|_{p,\propto} \leq C w_k^{\emptyset}(f, \delta)_{p,\propto}$$
$$\leq c|\bar{X}_i|^2 w_k^{\emptyset}(f', \delta)_{p,\propto}$$

the blending of the overlapping polynomials pieces involving contaminated intervals can be done in the same way . The spline pieces $S_i$and $S_i$thus produced also satisfy the estimate above with a slighty larger interval in place of [$\bar{Z}_{i-1}$,$\bar{Z}_{i+2}$] on the righthand side ([$\bar{Z}_{i-2}$,$\bar{Z}_{i+3}$] as worst),which will make no difference in the rest of the proof . We define the final spline $\bar{S}$ on each $\bar{X}_i$as follows . If there is only one local polynomialp_i over $\bar{X}_i$set $\bar{S}$ to this polynomial . If there are two polynomials overlapping on $\bar{X}_i$ then there must be blending local $\bar{s}_i$ set S to s_i . It is clear from this construction that $\bar{S}$-f∈ $\Delta^{\circ}(Y_s)$ on the whole interval [-1,1] and $\bar{S} \in C^{k-2}$. Similary construct S$\in C^{k-2}$ such that

f-S$\in \Delta^{\circ}(Y_s)$. Now recall that all neighboring intervals X_i=[Z_i,Z_{i+1}] in the orginal partition $T_n$are comparable in size and each interval $\bar{X}_i$=[$Z_{d_{i-1}}$,$Z_{d_{(i+1)}}$] contains no more than d such that intervals . Therefore ,the inquality (3.2.1) follows directly from (3.2.2)and (3.2.3)

theorm(3.3) [3]: Let f$\in \beta_\alpha$, $0< p \leq \infty$ and let k≥ 2 be an integer then there exist splines polynomials $\bar{S}_r$ and S_r of order k on the knot sequence $T_n = \{z_i\}_{i=0}^{\infty}$ such that :

$\bar{S}_r$(x)$\geq f(x) \geq S_r(x)$,x$\in [-1,1]$

And for i=1,2,…,r-1

$$\|\bar{S}_{r-}S_r\|_{p,\propto} \leq CW_k^{\emptyset}(f,|X_i|,X_i)_{p,\propto}$$

Where C is aconstant depending on k and on the maximum ratio

$\rho = max_{i=0}^{k-1}\frac{|X_{i\pm 1}|}{|X_i|}$,

And X_i is an interval such that

$X_i \subseteq X_i \subseteq [z_{i-6(k-1)^2}, z_{i+6(k-1)^2}]$

Proof :

The proof of the above theorm follows directly from the proof of theorm (3.2) , by omitting the inequality (3.2.3).

Theorm (3.4)

For f$\in \beta_\propto$ we get

$\tilde{E}_r(f,\delta)_{p,\alpha} \leq C_k W_k^{\emptyset}$(f,$\delta)_{p,\alpha}$,Where C is an absolute constant

Proof:

Let P,Q be the best one –sided approximation polynomials of f$\in \beta_\propto$ then (Q(x)$\leq f(x) \leq P(x)$)

$$\tilde{E}_r(f,\delta)_{p,\alpha} = \|P-Q\|_{p,\alpha}$$

And by using theorms (3.2) and (3.3) we get

$$\tilde{E}_r(f,\delta)_{p,\alpha} \leq \|\bar{S}_{r-}S_r\|_{p,\propto}$$
$$\leq C_k W_k^{\emptyset}(f,\delta)_{p,\alpha}$$

CONCLUSIONS

By using a knote sequence T_n and obtaming the interwining pair of spline $\{\bar{S}, S\}$ of order k suchthat $\bar{S}-f, S-f \in \Delta^0(Y_s)$) and we prove that

$\|\bar{S}-S\|_{p,\alpha} \leq Cw_k^{\emptyset}(f',\delta)_{p,\propto}$

and find the degree of one sided -approximation of f$\in \beta_\propto$.

REFRENCES

1. E.S.Bhaya (1999),"a study on approximation of bounded measurable function with some discrete series in L_p_spaces; (0< $p \leq 1$) , M.SC.thesis, Baghdad university, college of. (Ibn Al-haitham)
2. A.H.AL_Abdulla (2000),"A constructive characteristic of the Best Approximation" ,college of (IbnAL_Haitham)
3. Hawraa A .Fadhil (2010),"on the consrained spline Approximation" ,M.SC.Thesis, submitted college of Babylon university.
4. S.K.Jassim ,E.S.Bhaya (2002),"Direct and inverse Theorms for best multi_ Approximation in, L_p .(1<P<∞) " , Mathematics and physics Journal ,17(3)1-8.
5. The Averaged moduli of smoothness "Applications in numerical methods and approximation" by BlagovestsenDov and vasilA.pov ,thesis , Bulgarian Academy of scienc
6. H.Burkill,1952:Cesaro_Perron almost periodic functions .J. approximation Theory,94;481_493.
7. B.sendov,V.A.Popove(1983)."Average modules of smoothness",Sofia
8. K.A.Kopotun,1997: Univariate Splines: Equivalence of Moduli of Smoothness and Approximations.Amarican Mathematical Society.
9. P.P.Petrusher,V.A.Popov,1987:Rational Approximation of Real Functions.Encyclopedia of Mathematics and its Applications,Vol 28.Combridge University Press,Combridge.
10. R.A.DeVore,D.Leviatan,X.N.Yu,1992 : Polynomial Approximation in L_p,0< $p < 1$. Constr.Approx.,8:187-201.
11. Y. K. Hu,1995 :Positive and Copositive Spline Approximation in $L_p[0,1]$. Computers Math. Applic . Elsevier Science Ltd.
12. L . Aleksandrov , D.Drynov , One- sided Multidimensional Approximation by Entire Functions and Trigonometric Polynomials in $L_p -$ metric 0< $p \leq \infty$. Mathematics Balkanica , New series ,3,fact 2, (1989),215-224.
13. D.Drynov , One- sided By Trigonometric Polynomials in $L_p - norm$,0< $p < 1$. Banach Center Publications ,Vol , 22 ,(1989) , 99-110.

Quasi Purely Baer Modules

Mehdi M.Abbas and Ali H. Al-Saadi
Department of Mathematics, College of Science, Mustansiriya University
Received 6/3/2013 – Accepted 15/9/2013

الخلاصة

في هذا البحث قدمنا مفهوم المقاسات شبة بير النقية كأعمام للمقاسات بير ، للمقاسات شبة بير وللمقاسات بير النقية .أعطينا العديد من الخواص والتوصيفات لهذا النوع من المقاسات . ناقشنا المركبات الجمع المباشر و كذلك الجموع المباشرة.أخيرا تأملنا الشروط التي تجعل المقاسات الشبة بير النقية ، مقاسات بير النقية.

ABSTRACT

In this article, we introduce the notion of quasi purely Baer modules as a general case of Baer modules, quasi Baer modules and purely Baer modules. A several properties and characterizations are given for such modules. We discuss this property on direct summands and direct sums. Further, we consider conditions under which quasi purely Baer modules versus purely Baer.

1. INTRODUCTION

All rings are assumed to be associative with non-zero unit, the modules are unital right modules. We usually denote the basic ring by R, the module by M, and its endomorphisms ring $End_R(M)$ by S.

The right annihilator of a subset X of M in R is denoted by $r_R(X)$, the right annihilator of a subset T of S in M is denoted by $r_M(T)$, and the left annihilator of a subset P of R in M is denoted by $\ell_M(P)$. Let M be an R-module. A submodule N of M is fully invariant, if N is S-submodule of M, that is $\alpha(N) \subseteq N$ for each $\alpha \; in \; S$. Cohn in [1] called a submodule N of an R-module M is pure if the sequence $0 \to N \otimes E \to M \otimes E$ is exact for every R-module E. This equivalent to saying that for each $n_j=\sum_{i=1}^{n} m_i r_{ji} \in N$, $m_i \in M$, $r_{ji} \in R$, $j = 1, 2, 3, \dots, k$, there exist $x_i \in N$, such that $n_j=\sum_{i=1}^{n} x_i r_{ji}$ for each j ([2], theorem4.89).

C.S . Roman in [3] introduced and studies Baer and quasi -Baer modules which are a generalization of Baer and quasi -Baer rings to a general module theoretic setting. In fact he studied the relation between the modules and their endomorphisms ring passing through the annihilator, an R-module M is (quasi-) Baer if the right annihilator in M of any left(two sided) ideal of S is a direct summand. It is well-known that every direct summand is pure. This lead to introduce Romans notion in purity. purely Baer modules were introduced in [4], an R-module M is called purely Baer, if $r_M(A)$ is a pure submodule of M for each left ideal A of S.

In this work, we introduce the concept of quasi purely Baer module which is a general case of Baer, quasi purely and purely Baer modules. We give a characterization of a quasi purely Baer modules in terms of endomorphisms family. As a consequence, in these module the intersection of arbitrary family of fully invariant direct summands is fully invariant pure. Examples are provided to show that quasi purely Baer modules is a proper generalization of quasi-Baer and purely Baer modules. We show that the property of quasi purely Baer is closed under direct sums. Finally we proved that quasi purely Baer property versus purely Baer property under semi commutative modules.

2.RESULTS

We start to introduce the concept of purely quasi Baer modules which is a proper generalization of that of quasi-Baer(and hence Baer) and purely Baer modules.

Definition(1): An R-module M is called quasi purely Baer, if for each two-sided ideal A of S=$End_R(M)$, $r_M(A)$ is pure in M. A ring R is quasi purely Baer, if it is quasi purely Baer R-module.

In the following we characterize purely quasi-Baer in terms of endomorphism family.

Theorem(1): An R-module M is called quasi purely Baer, if and only if for each family $\{ \alpha_\lambda \backslash \lambda \in \Lambda\}$ of endomorphisms of M , $\bigcap_{\lambda \in \Lambda} r_M(S\alpha_\lambda S)$ is fully invariant pure submodule in M.

Proof: Let A be a two sided ideal of S=$End_R(M)$. It is easy to see that A=$\sum_{a \in A} SaS$, so $r_M(\sum_{a \in A} SaS)= \bigcap_{a \in A} r_M(SaS)$, then by hypothesis $r_M(A)$ is a fully invariant pure submodule of M, and hence M is purely quasi-Baer. Conversely, let $\{ \alpha_\lambda \backslash \lambda \in \Lambda\}$ be a family of endomorphism of M. Put A=$\sum_{a \in A} SaS$, then Ais two-sided ideal in S, since M is purely quasi-Baer, $r_M(A)$ is a fully invariant pure submodule in M, but $\bigcap_{\lambda \in \Lambda} r_M(S\alpha_\lambda S)=r_M(A)$, then $\bigcap_{\lambda \in \Lambda} r_M(S\alpha_\lambda S)$ is a fully invariant pure submodule in M.

Corollary(1): A ring R is purely quasi-Baer if and only if for each subset A of R, $\bigcap_{a \in A} r_R(RaR)$ is two- sided pure ideal in R.

Corollary(2): M is purely quasi-Baer R-module and $\{A_\alpha\}_{\alpha \in \Lambda}$be a family of fully invariant direct summand of M, then $\bigcap_{\alpha \in \Lambda} A_\alpha$ is fully invariant pure in M.

Proof: For each $\alpha \in \Lambda$, there is a submodule B_α of M such that M= $A_\alpha \oplus B_\alpha$. Consider ρ_α: M→M be the projection mapping onto B_α, since Ker(ρ_α)= A_α is fully invariant in M, but M is purely quasi-Baer, then by theorem(1), $\bigcap_{\alpha \in \Lambda}$ ker(ρ_α)= $\bigcap_{\alpha \in \Lambda} A_\alpha$ is fully invariant pure in M.

Examples(1):

(a) All Baer, purely Baer and quasi-Baer modules are purely quasi-Baer.

(b) purely quasi-Baer property is a proper generalization of quasi-Baer property. By 7.54 in [2], there is a commutative von Neumann regular ring which is not Baer (=quasi-Baer), but each commutative von Neumann regular ring is purely Baer(=purely quasi-Baer) ring.

(c) purely quasi-Baer property is a proper generalization of quasi-Baer property. For example, let R=$\begin{pmatrix} Z & Z \\ 0 & Z \end{pmatrix}$ be the upper 2x2 triangular matrix over Z. Since Z is quasi-Baer, then R is quasi-Baer[5], then R is purely quasi-Baer. We claim that R is not purely Baer, if not, let $A = \begin{pmatrix} 2 & 1 \\ 0 & 0 \end{pmatrix} \in R$, then $r_R(A)=\{\begin{pmatrix} 0 & b \\ 0 & -2b \end{pmatrix} / b \in Z\}$ *is pure in* R_R, this implies that $r_R(A)x=R_x \cap r_R(A)$ for each $x \in R$, since $\begin{pmatrix} 0 & 1 \\ 0 & -2 \end{pmatrix} \in r_R(A)$, then there a non-zero element $\begin{pmatrix} 0 & c \\ 0 & -2c \end{pmatrix} \in r_R(A)$ such that $\begin{pmatrix} 0 & c \\ 0 & -2c \end{pmatrix}\begin{pmatrix} 0 & 1 \\ 0 & -2 \end{pmatrix}=\begin{pmatrix} 0 & 1 \\ 0 & -2 \end{pmatrix}$ implice that $\begin{pmatrix} 0 & -2c \\ 0 & 4c \end{pmatrix}=\begin{pmatrix} 0 & 1 \\ 0 & -2 \end{pmatrix}$ and hence $-2c=1$ which is a contradiction. Thus R is not purely Baer.

(d) Let F be any field and $R = \frac{F[x,y]}{<xy>}$ be the ring of polynomial in two commuting indeterminates x and y with coefficient in F modulo the ideal <x, y>. R is non singular and $r_R(\overline{x}R)=\overline{y}R$ which is not pure in R. As R is commutative, then R is not purely quasi-Baer. R is not self-injective, then E(R) is non-singular([6], proposition(1.22)), but E(R) is extending, so E(R) is Baer R-module([3], theorem2.2.2) and hence E(R) is purely quasi-Baer.

Theorem(2): Let R be a ring. If any one of R[x] R[[x]] is purely quasi-Baer then so is R.

Proof: Assume R[x] is purely quasi-Baer and let A be two sided ideal of R. Consider the following system $x_i=\sum_{j=1}^{k} m_j r_{ij}$ $\forall i = 1, 2, 3, \dots, n$ where $x_i \in r_R(A)$, m_j, $r_{ij} \in R$ for $i=1, 2, 3, \dots, n$, $j=1,2,3,\dots,k$. Let $J = \{\sum_{k=0}^{n} a_k x^k / a_k \in A, n \in N\}$, J is two sided ideal in R[x], then $r_{R[x]}(J)$ is pure in R[x]. It is easy to see that $r_R(A)$ is a subset of $r_{R[x]}(J)$(in fact $r_R(A)[x]=r_{R[x]}(J)$). Thus $x_i \in r_{R[x]}(J)$. By purity of $r_{R[x]}(J)$ in R[x], there are $a_j(x)=\sum_{r=0}^{nj} a_r^{(j)} r_{ij} x^r \in r_{R[x]}(J)$, $j=1,2,3,\dots,n$ such that $x_i=\sum_{j=1}^{k} a_j(x) r_{ij} = \sum_{j=1}^{k}(\sum_{r=0}^{nj} a_r^{(j)} x^r) r_{ij}$. Then we obtain $= x_i=\sum_{j=1}^{k}\sum_{r=0}^{nj} a_r^{(j)} r_{ij} x^r = \sum_{j=0}^{nj} a_0^{(j)} r_{ij} + \sum_{j=1}^{k}\sum_{r=1}^{nj} a_r^{(j)} r_{ij} x^r$ which implies that $x_i=\sum_{j=1}^{nj} a_0^{(i)} r_{ij}$. To show that $a_0^{(i)} \in r_R(A)$, let $f \in A$, then $f \in J$, but $a_j(x)=\sum_{r=1}^{nj} a_r^{(j)} x^r \in r_{R[x]}(J)$. Thus $fa_j(x)=\sum_{r=0}^{nj} a_r^{(j)} x^r=0$, so $fa_j(x)=0$ for each $j=1, 2, \dots, n$ and $k=0,\dots,n$, therefore $fa_0^{(i)}=0$ for each $j=1,\dots,n$. Then $a_0^{(i)} \in r_R(A)$ and hence $r_R(A)$ is pure in R. This shows that R is purely quasi-Baer.

Theorem(3): Direct summand of purely quasi-Baer module is purely quasi-Baer.

Proof: Let M be a purely quasi-Baer R-module and A a direct summand of $End_R(A)$. Let I be two-sided ideal of R. Consider the following system: $x_i=\sum_{j=1}^{k} m_j r_{ij}$ for $i=1,\dots,n$ where $x_i \in r_A(I)$, $m_j \in A$ and $r_{ij} \in R$, for each $i=1, 2, \dots, n$ and $j=0,\dots, k$. Since $r_A(I)$ is fully invariant submodule in A, then there is a fully invariant pure submodule of B such that $r_A(I) \oplus F$ is fully invariant in M where $M = A \oplus B$ ([3], Lemma

1.2.11), then $\ell_S(r_A(I)\oplus F)$ is ideal in S. Since M is purely quasi-Baer, then $r_M(\ \ell_S(r_R(A)\oplus F))$ is fully invariant submodule of M, but $r_A(I)\subseteq r_M(\ \ell_S(r_A(A)\oplus F))$, then there is m_j $r_M(\ \ell_S(r_A(I)\oplus F))$ such that $x_i=\sum_{j=1}^{k} m_j r_{ij}$ for i=1,…,n. Since $m_j'=a_j + b_j$ where $a_j\in A$ and $b_j\in B$ for j=1,…,k. We obtain $x_i=\sum_{j=1}^{k} a_j r_{ij}+\sum_{j=1}^{k} b_j r_{ij}$. Thus $x_i - \sum_{j=1}^{k} a_j r_{ij} = \sum_{j=1}^{k} b_j r_{ij} \in A\cap B=0$, so $x_i=\sum_{j=1}^{k} a_j r_{ij}$ for each i=1, 2, …,n. Now, to show $a_j\in r_A(I)$ for each j=1, 2, …,k. For each $\alpha\in I$, α can be extended trivially by putting $\alpha'(B)=0$, if $c \in r_A(I)\oplus F$, then c=a+b for some $a \in r_A(I)$ and $d\in f$, thus $\alpha'(c)= \alpha'(a+d)= \alpha(a)+0=0$ implies that $\alpha' \in (\ell_S(r_R(I)\oplus F)$. Since $m_j'=a_j+b_j\in r_M(\ell_S(r_A(I)\oplus F))$, then $0= \alpha'(m_j)= \alpha(a_j)$. Thus $a_j \in r_A(I)$ for j=1,…,k, then we have that $r_A(I)$ is pure in A.

Example (2): Finite direct sums of purely quasi-Baer modules may not be purely quasi-Baer. The Z-module $M = Z \oplus Z_2$ is not purely quasi-Baer, even though both of Z and Z_2 are purely quasi-Baer. $2Z\oplus 0$ is fully invariant submodule of M and $r_M(\ell_S(2Z\oplus 0)\ ) =2Z\oplus 0$ which is not pure in M.

Theorem(4): Let M_1 and M_2 be purely quasi-Baer modules. If for each $\psi \in Hom(M_i, M_j)$. $\psi(x)=0$ implies x=0 $(i \neq j, i, j = 1, 2)$. Then $M_1\oplus M_2$ is purely quasi-Baer.

Proof: Let $S=End_R(M_1\oplus M_2)$ and I a two sided ideal of S. Then $r_{M1\oplus M2}(I)= N_1\oplus N_2$ where N_i is submodule of M_i, $i = 1, 2$.

$$S=\begin{pmatrix} S_1 & Hom_R(M_2, M_1) \\ Hom_R(M_1, M_2) & S_2 \end{pmatrix}$$ where $S_i=End_R(M_i)$

i=1,2.

Now consider the following sets

$I_{11}=\{\phi\in S_1 \mid \phi=ƒ_{11} \text{ with } (ƒ_{ij})_{i,j=1,2}\in I\}$, $I_{22}=\{\phi\in S_2 \mid \phi=ƒ_{22} \text{ with } (ƒ_{ij})_{i,j=1,2}\in I\}$ $I_{12}=\{ \psi \in Hom_R(M_1, M_2) \mid \psi =ƒ_{21} \text{ with } (ƒ_{ij})_{i,j=1,2}\in I\}$, $I_{12}=\{ \psi \in Hom_R(M_2, M_1) \mid \psi =ƒ_{12} \text{ with } (ƒ_{ij})_{i,j=1,2}\in I\}$. As $I_{11}(I_{22})$ is two- sided ideal of $S_1(S_2)$ respectively, let $N'_1=r_{M1}(I_{11})$ and $N'_2=r_{M2}(I_{22})$, since M_1 and M_2 are purely quasi-Baer, then $N'_1(N'_2)$ is fully invariant pure in $M_1(M_2)$ respectively. By a similar way of ([3] theorem(3.3.2)), we can show that $N_1= N'_1\cap(\bigcap_{\psi\in I12} Ker(\psi))= N'_1= r_{M1}(I_{11})$ and $N_2= N'_2\cap(\bigcap_{\psi\in I21} Ker(\psi))= N'_2= r_{M2}(I_{22})$ then we have $r_{M1\oplus M2}(I)= N_1\oplus N_2$ which is fully invariant pure in $M_1\oplus M_2$. This shows that $M_1\oplus M_2$ is purely quasi-Baer.

Let M and N be two R-modules. Recall M is sub isomorphic to N, if M is isomorphic to a submodule of N.

Theorem(5): Let $M=\bigoplus_{i\in I}M_i$ be an arbitrary decomposition. If M_i is purely quasi-Baer R-module and sub isomorphic to M_i, for each $i\neq j \in I$ then M is purely quasi-Baer.

Proof : Let S_i be the endomorphism ring of M_i for each $i \in I$. Then the endomorphism ring S of M, is a ring of matrices with elements of S_i in the (i,i)–position and the maps
$M_j \rightarrow M_i$ in the (i,j)–position for each $i(\neq j) \in I$. Let J be a two sided ideal of S. Since $r_M(J)$ is fully invariant in M and $r_M(J)=\bigoplus_{i\in I}(r_M(J)\cap M_i)$, hence the column homomorphisms taking M_i into M for each $i \in M$. By a similar way used in the proof of theorem(4) we have that i th – column of J is two sided ideal of S has elements from a two sided ideal J_i of S_i in the i th-position, and certain elements from $Hom_R(M_i, M_j)$ in the other places, put A be the union of these sets. $r_M(J)\cap M_i= r_{Mi}(J)\cap(\bigcap_{\phi\in\wedge} Ker(\phi))$. But $M'_i = r_{Mi}(J)$ is fully invariant pure in M_i, since M_i is purely quasi-Baer for each $i \in I$. If $\phi\in A$, $\phi : Mi \rightarrow Mj$ (say) $i(\neq j) \in I$, then $\psi_{ji}\,\phi \in J_i$ where ψ_{ji}: $M_j \rightarrow M_i$ is the monomorphism taking M_j into M_i , we obtain this noting that if we multiply a homomorphism in J, having ϕ in the (j,i)–position with the homomorphism $(\alpha_{mn})_{mn\in I}$, where $\alpha_{mn}=0$ for $(m,n)\neq(i,j)$ and $\alpha_{ij}=\psi_{ji}$, then we get a homomorphism in J with $\psi_{ji}\,\phi$: $M_i\rightarrow M_i$ in the (i,i)–position. This mean that $\psi_{ji}\,\phi(M_i')=0$. As ψ_{ji} is a monomorphism, hence $\phi(M)=0$ thus $M_i'\subseteq Ker(\phi)$ since $\phi\in A$ was chosen arbitrary. $r_M(J)\cap M_i=$
$r_{Mi}(J_i)\cap(\bigcap_{\phi\in\wedge} Ker(\phi))= M_i'$ is fully invariant pure in M_i. Using this argument $\forall i\in I$ we obtain that $r_M(J)=\bigoplus_{i\in I} M_i'$ all hence $r_M(J)=\bigoplus_{i\in I} M_i$ which is fully invariant pure in M.
The following corollary follows from theorem(5) and theorem(3)

Corollary(3): A projective module over purely quasi-Baer ring is purely quasi-Baer.
Definition(2): Let M_2 and M_1 be two purely quasi-Baer R-modules. If $\cap Ker(\alpha)$ is pure in M_i, when $\alpha \in Hom_R(M_i, M_j)$, for $i(\neq j)=1, 2$, we say that M_2 and M_1 are relative purely quasi-Baer.

If M_2 and M_1 are regular in the sense of Field house (hence semi simple), then M_2 and M_1 are relative purely quasi-Baer. While the Z-modules Z and Z_2 are not relative purely quasi-Baer, since $\cap Ker(\alpha)=2Z$, where $\alpha \in Hom_Z(Z, Z_2)$ which is not pure in Z.
Theorem(6): If $M=\bigoplus_{i\in I}M_i$ is purely quasi-Baer R-module, then M_i, M_j are relative purely quasi-Baer for $i(\neq j)\in I$.
Proof: M_i is purely quasi-Baer for $i\in I$, Theorem(3). For sake of simplifying notation assume we concentrate on $M= M_1\bigoplus M_2$. Let

$K_i=\cap Ker(\alpha)$ when $\alpha \in Hom_R(M_i, M_j)$, $i(\neq j)=1, 2$. First, we claim that $K_1 \oplus K_2$ is fully invariant in $M_1 \oplus M_2$. Let $\alpha=\begin{pmatrix} \alpha 11 & \alpha 12 \\ \alpha 21 & \alpha 22 \end{pmatrix} \in End_R(M_1 \oplus M_2)$ where $\alpha_{ij}: M_j \rightarrow M_i$, for $i,j \in \{1, 2\}$. It's clear, by the definition of K_1 *and* K_2, that $\alpha_{12}(K_2)=0$ *and* $\alpha_{21}(K_1)=0$. Consider $\alpha_{11}(K_1)$. Taking any $\psi \in Hom_R(M_1, M_2)$, $\psi(\alpha_{11}(K_1))=\psi\, \alpha_{11}(K_1)=0$ as $\psi\, \alpha_{11}: M_1 \rightarrow M_2$ and by the definition of K_1. Hence $\alpha_{11}(K_1) \subseteq K_1$. Similarity $\alpha_{22}(K_2) \subseteq K_2$. Putting the above together, we obtain that $\alpha(K_1 \oplus K_2) \subseteq K_1 \oplus K_2$. But α was chosen arbitrary we get that $K_1 \oplus K_2$ is fully invariant in $M_1 \oplus M_2$. This implies that K_i is fully invariant in M_i for $i=1, 2$. We are complete by claim that $K_1 \oplus K_2$ is pure in $M_1 \oplus M_2$. Let $\alpha \in \ell_{S12}(K_1 \oplus K_2)$ where $S_{12}= End_R(M_1 \oplus M_2)$. α is matrix(as above), we note the following $\alpha_{21}(k_1)+ \alpha_{12}(k_2)= \alpha_{11}(k_1)=0 \rightarrow \alpha_{11} \in \ell_{S1}(K_1)$ and $\alpha_{21}(k_1)+ \alpha_{22}(k_2)= \alpha_{22}(k_2)=0 \rightarrow \alpha_{22} \in \ell_{S2}(K_2)$ where $k_1 \in K_1$ and $k_2 \in K_2$, $S_1= End_R(M_1)$ and $S_2= End_R(M_2)$. At the same time $\alpha \in S_{12}$ so that $\alpha_{11} \in \ell_{S1}(M_1)$, $\alpha_{22} \in \ell_{S2}(M_2)$ and α_{12}, α_{21} are arbitrary in their respective $Hom_R(M_2, M_1)$, $Hom_R(M_1, M_2)$. Thus for $\alpha \in \ell_{S1}(K_1 \oplus K_2)$,

$$\ell_{S1}(K_1 \oplus K_2)=\begin{pmatrix} \ell_{S1}(K_1) & Hom_R(M_2, M_1) \\ Hom_R(M_1, M_2) & \ell_{S2}(K_2) \end{pmatrix}$$

Now consider $r_{M1 \oplus M2}(\ell_{S1}(K_1 \oplus K_2))$. Since $\ell_{S1}(K_1 \oplus K_2)$ is two sided ideal of S_{12}, then $r_{M1 \oplus M2}(\ell_{S1}(K_1 \oplus K_2))$ is fully invariant in $M_1 \oplus M_2$, hence it decomposes on to the two components $r_{M1 \oplus M2}(\ell_{S1}(K_1 \oplus K_2))= K'_1 \oplus K'_2$ where $K'_i= r_{M1 \oplus M2}(\ell_{S1}(K_1 \oplus K_2) \cap M_i$ for $i=1, 2$. Now we can analyze the two components separately. Consider $\alpha \in \ell_{S1}(K_1 \oplus K_2)$(as a matrix above); $\alpha(k'_1)=0$ implies $\alpha_{11}(k'_1)=0$ and $\alpha_{21}(k'_1)=0$, for $k'_1 \in K'_1$, thus
$K'_1= r_{M1 \oplus M2}(\ell_{S1}(K_1) \cap (\cap Ker(\psi))$ when $\psi \in Hom_R(M_1, M_2)$. Since $K_1 \subseteq r_{M1}(\ell_{S1}(K_1))$ and $\cap Ker(\psi)= K_1$ when $\psi \in Hom_R(M_1, M_2)$, thus $K'_1= K_1$. Similarly $K'_2= K_2$. Then $r_{M1 \oplus M2}(\ell_{S12}(K_1 \oplus K_2))= K_1 \oplus K_2$. Since $M_1 \oplus M_2$ is purely quasi-Baer and $\ell_{S12}(K_1 \oplus K_2)$ is two sided ideal of S_{12}, then $r_{M1 \oplus M2}(\ell_{S12}(K_1 \oplus K_2))$ is fully invariant pure in $M_1 \oplus M_2$. Then we have K_1 and K_2 are pure in M_1 and M_2 respectively . This shows that M_1, M_2 are relative purely quasi-Baer.
Proposition(1) : Let $\{R_\lambda \backslash \lambda \in \wedge\}$ be a family of rings. Then $R=\oplus_{i \in I} R_\lambda$ is purely quasi-Baer if and only if R_λ is purely quasi-Baer for each $\lambda \in \wedge$.
Proof : for each $\lambda \in \wedge$, R_λ is purely quasi-Baer, theorem(3). Conversely , let A be two sided ideal of R. Consider $\rho_\lambda: R \rightarrow R_\lambda$ be the projection mapping onto R_λ for each $\lambda \in \wedge$. Then $\rho_\lambda(A)$ is two sided ideal of R_λ. Since R_λ is purely quasi-Baer, then $r_{R\lambda}(\rho_\lambda(A))$ is a pure ideal of R_λ. We claim that $r_R(A)= \oplus\, r_{R\lambda}(\rho_\lambda(A))$. For this , let $a=(a_\lambda)_{\lambda \in \wedge} \in$

$r_R(A)$, then $Aa=0$ implies that $\rho_\lambda(A)\ a_\lambda=0$ for each $\lambda\in\wedge$,thus $a_\lambda\in r_{R\lambda}(\rho_\lambda(A))$, so

$a\in\bigoplus_{\lambda\in\wedge}r_{R\lambda}(\rho_\lambda(A))$. Now let $b=(b_\lambda)_{\lambda\in\wedge}\in\bigoplus_{\lambda\in\wedge}r_{R\lambda}(\rho_\lambda(A))$, then we have $\rho_\lambda(A)\ b_\lambda=0$ for each $\lambda\in\wedge$. But $I_R=\sum_{\lambda\in\wedge}\rho_\lambda$, then $Ab= I_R(Ab)=\sum_{\lambda\in\wedge}\rho_\lambda(Ab)=\sum_{\lambda\in\wedge}\rho_\lambda(A)b_\lambda=0$, thus $b\in r_R(A)$. Thus $r_R(A)=\bigoplus_{\lambda\in\wedge}r_{R\lambda}(\rho_\lambda(A))$. But $r_{R\lambda}(\rho_\lambda(A))$ is a pure ideal of R_λ for each $\lambda\in\wedge$, so $r_R(A)$ is a pure ideal of R.

Recall that a ring R is semi commutative if $r_R(x)$ is two sided ideal of R for each $x\in R$, [5]. Recall also that a ring R is reduced if R has non- zero nilpotent elements. Equivalently, if $x\in R$, $x^2=0$ implies $x=0$. Now we give a generalization of these concepts for modules.

Definition(2): Let M be an R-module and $S=End_R(M)$ is endomorphism ring. Then

1. M is called semi commutative if $r_M(\alpha)=Ker(\alpha)$ is fully invariant pure in M (that is for any $\theta\in S$ and $m\in M$, $\alpha(m)=0$ implies $\alpha\ \theta\ (m)=0$)
2. M is called reduced if for any $\alpha\in S$ and $m\in M$, $\alpha(m)=0$ implies that $S_m\cap\ \alpha(m)=0$.

Examples(3)

a. It is clear that a ring R is semi commutative if and only if R is semi commutative R-module.

b. A ring R is reduced if and only if R is reduced R-module.

Proof: Frist observe that $S=End_R(R)=R^{(e)}\simeq R$ where $R^{(e)}$ is the ring of all left multiplication by some induced element of R. Let $x\in R$ and $\alpha\in S$ with $\alpha(x)=0$. We can assume that α is non-zero, then there is a non-zero element $a\in R$ such that $\alpha=\alpha_a$, that is $\alpha(y)=\alpha_a(y)=ay$, for $y\in R$. Let $m\in S_x\cap\ \alpha(R)= S_x\cap\ aR$, then $m=\beta_b(x)=ar$, so $m=bx=ar$ for some $r\in R$. Thus $m^2=(bx)(ar)=b(xa)r=0$, but R is reduced ring, then $m=0$ and so $S_x\cap\ \alpha R=\ 0$. Conversely , let $x\in R$ with $x^2=0$. Defined $\alpha:R\to R$ by $\alpha(r)=xr$ for $r\in R$, then $\alpha(x)=x^2=0$, but R is reduced R-module, then $S_x\cap\ \alpha(R)=S_x\cap xR=0$. Now $I_R\in S$, so $x=I_R(x)\in S_x\cap\ xR$ and hence $x=0$. This shows that R is a reduced ring.

c. The Z-module Q is semi commutative, in general every quasi-Dedekind module (each non zero endomorphism is a monomorphism) is semi commutative.

d. $Z\oplus Z$ as Z-module is not semi commutative, consider the Z-homomorphism α: $Z\oplus Z\to Z\oplus Z$ defined by $\alpha(a, b)=(a, 0)$, then $\ker(\alpha)=0\oplus Z$. Now consider β defined by $\beta(a, b)=(b, a)$, thus $\beta(\ker(\alpha))=Z\oplus 0\nsubseteq 0\oplus Z$. Then $\ker(\alpha)$ is not fully invariant.

e. For each prime number p, the Z-module Zp^2 is not reduced. Let $\alpha\in End_Z(Zp^2)$ defined by $\alpha(\overline{x})=\overline{px}$, then $\alpha(\overline{p})=0$, but $o\neq\overline{p}\in S(\overline{p})\cap\alpha(Zp^2)$, so $S\ \overline{p}\cap\alpha(Zp^2)\neq 0$.

f. Every reduced module M is semi commutative.

Proof: Let $\alpha \in S=End_R(M)$ and $m \in \ker(\alpha)$, then $\alpha(m)=0$. Since $S(m)\cap \alpha(m)=0$, that is for each $\theta \in S$ implies $\alpha\theta(m) \in S(m)\cap\alpha(m)=0$ and $\alpha\,\theta(m)=0$. Thus $Ker(\alpha)$ is fully invariant in M.

Proposition(2): Let M be a semi commutative(reduced) R-module. Then M is purely Baer if and only if M is purely quasi-Baer.

Proof: Let A is a left ideal of $S=End_R(M)$, then $r_M(A)=\bigcap_{\alpha\in\Lambda} Ker(\alpha)$. Since M is semi commutative, then $Ker(\alpha)$ is fully invariant in M for each $\alpha \in A$, thus $Ker(\alpha)= r_M(S\alpha_\lambda S)$. Therefore $r_M(A) = \bigcap_{a\in A} r_M(SaS)$ $=r_M(\sum_{a\epsilon A} SaS)$, it's clear that $\sum_{a\epsilon A} SaS$ is two sided ideal of S, but M is purely quasi-Baer, then $r_M(A) = r_M(\sum_{a\epsilon A} SaS)$ is pure in M. Thus M is purely Baer.

REFERENCES

1. P. M. Cohn: on the free product of associative rings, Math .Z. 71, 380-398, 1959.
2. T. Y. Lam, Lectures on Modules and Rings, Springer-Verlag, 1999.
3. C. S. Roman: Baer and quasi-Baer modules, ph. D. Thesis , The Ohio state university, 2004.
4. M.S. Abbas and A. H. Al-saadi. Purely Baer modules.
5. P. Pollingher and A. Zake : On Baer and quasi-Baer rings,. Duke Math. J, 37, 127-138, 1970.
6. K. R. Goodeal. Ring Theory, non-singular ring and modules, Mercel Dekker, INC. New York, 1976.
7. T. K. Lee and Y. Zhou, Reduced modules, Rings, Modules, Algebras and A belian groups, Lecture Note in pure and Appl. Math., 236, Mercel Dekker. New York. 365-377, 2004.

Aspect of pseudo-injectivity

Mehdi S. Abbas[1] and Samer Mohammed Saeed Abdul Alameer[2]
[1]Department of Mathematics, College of Science, Mustansiriya University
[2]The Ministry of Education Directorate General for Education in Wasit
Received 6/3/2013 – Accepted 15/9/2013

الخلاصة

في هذا العمل، قدمنا مفهوم الاغمارية الكاذبة بالنسبة لصنف مقاسات جزئية المغلقة(المقاسات المغلقة الكاذبة الاغمارية) عرضت و درست، وهذا أعمام فعلي لمفهومي المقاسات التوسيع و المقاسات الاغمارية الكاذبة من النمط-(أي سي). بينا أن هذا المفهوم يكون مغلقا بالنسبة لمركبات الجمع المباشر . أعطينا كثير من الخواص و التوصيفات . برهنا كل مقاس طليق على الحلقات -(بري) الوراثية تكون مقاسا توسيعا. ناقشنا متى تكون المقاسات المغلقة الاغمارية الكاذبة مقاسات اغمارية كاذبة من النمط-(أي سي) ، المقاسات التوسيع.

ABSTRACT

In this work, the notion of pseudo-injectivity relative to a class of submodules (namely, closed pseudo-injectivity) has been introduced and studied, which is a proper generalization of (IC-)pseudo-injective and extending module. This notion is closed under direct summands. Several properties and characterizations have been given. We show that over a hereditary pri-ring, every free module is extending. We discuss the question of when an closed-pseudo-injective module is IC-pseudo-injective, extending module.

1.INTRODUCTION

Throughout, R represents an associative ring with identity and R-modules are unitary right R-modules. A submodule N of an R-module M is essential(or M is essential extension of N), if N has non-zero intersection with every non-zero submodule of M. In case N has no proper essential extension in M, then N is called closed. A non-zero R-module U is said to be uniform, if every non-zero submodule of U is essential in U([1], P. 85). Let M and N be two R-modules, N is called (pseudo)-M-injective, if for every submodule A of M, any R-homomorphism (R-monomorphism) from A to N can be extended to an R-homomorphism from M to N. An R-module is injective , if it is M-injective for all R-module M. An R-module M is called quasi(pseudo)-injective, if it is (pseudo)-M-injective[2]([3]). An R-module M is called IC-pseudo-injective if each R-monomorphism of a submodule of M which is isomorphic to a closed submodule of M into M can be extended to a endomorphism of M [4]. A submodule N of R-module M is said to be a direct summand of R-module M, if $M = N \oplus L$, for some submodule L of M. An R-module M is said to be semi simple, if every submodule of M is direct summand([1], P. 27). An R-module M is called CS-module(extending), if every submodule of M is essential in a direct summand of M, this is equivalent to saying that every closed submodule of M is a direct summand [5]. M which satisfies condition (C_2), if every submodule of M which is isomorphic to a direct summand of M is itself direct summand[5]. An R-module M is projective, if every epimorphism $\alpha: A \rightarrow B$ and any R-homomorphism $\beta: M \rightarrow B$, where A, B are two R-modules, there exists an R-homomorphism $\gamma: M \rightarrow A$ such that $\alpha o \gamma = \beta$ [6]. Let R be a ring and I any index set. For each $i \in I$, let $R_i \cong R$. Denote by $R^{(I)}$ the direct sum $\oplus_{i \in I} R_i$. If $I = \{1, 2, \ldots, n\}$, then write $R^{(n)}$ for $R^{(I)}$ If M is an R-module, then we say M is free, if M is isomorphic to $R^{(I)}$ for some index I [6]. In this paper, we introduce a proper generalization of IC-pseudo-injective modules(namely closed pseudo-injective modules). Several properties of these modules are given. We characterize extending modules in terms of closed pseudo-injectivity and we characterize right hereditary rings in terms of closed pseudo-injective modules.

2. CLOSED PSEUDO-INJECTIVE MODULES

the concept of pri-ring R (every right ideal of R is principal) has been generalized to modules. An R-module M is called epi-retractable if every submodule of M is a homomorphic image of M [7]. A ring R is called right hereditary if every right ideal is projective ([8], P.20). In the following, we show that over a hereditary pri-ring every free module is extending.

Proposition(2.1): Let R be a right hereditary pri-ring. Then every free R-module is a extending. In particular, every right hereditary pri-ring R is a extending as R-module.

Proof : Let M be a free R-module and X a (closed) submodule of M. Since R is hereditary, then X is projective. By ([7], proposition(2.5)), M is epi-retractable and hence there is an R-epimorphism $\alpha : M \rightarrow X$. Projectivity of X, implies that there is an R-homomorphism $\beta : X \rightarrow M$ such that $\alpha o \beta = I_X$. Then X is a direct summand of M by ([9], Proposition(4.2.1)). This shows that M is extending.

In the following, we give a decomposition of projective modules over right hereditary pri- rings. Recall that an R-module M is hereditary if every submodule of M is a projective, [10].

Theorem(2.2): Let R be a right hereditary pri-ring. Then every projective R-module is a direct sum of noetherian uniform submodules, each with a division endomorphism ring.

Proof: Let M be a projective R-module. there is a free R-module $F = V \oplus U$ such that V is R-isomorphic to M [6]. Proposition (2.1) implies that F (hence V and M) is extending. Since R is right hereditary then M is hereditary extending. Then $M = \oplus_{i \in I} N_i$ where N_i is a Noetherian uniform with $End_R(N_i)$ is a division ring, for each I, by ([10], proposition(9)).

Definition(2.3): Let M and N be two R-modules . M is said to be closed (pseudo)-N-injective, if for each closed submodule A of N, every R-homomorphism (R-monomorphism) from A to M can be extended to an R-homomorphism from N into M [11]. An R-module M is called closed quasi-injective, if M is closed-M-injective [12]. The R-module M is called closed pseudo-injective, if it is closed pseudo-M-injective .

In [13] studied modules in which isomorphic copies of complements are again complements. These are called SICC-modules.

Remarks(2.4):

1- In [11] proved every uniform closed pseudo-injective module is closed quasi-injective. While every extending (uniform) module is closed pseudo-injective and closed quasi-injective, this follows from the fact that in extending module , every closed submodule is direct summand .

2- Every pseudo-injective module is closed pseudo-injective, but the converse may not be true in general. In fact by (1) , for example any extending module is closed pseudo-injective, but there is extending modules which are not pseudo-injective , Z as Z-module.

3- Every IC-pseudo-injective module is closed pseudo-injective, but the converse may not be true in general. for example Z as Z-module. (of course, these notions coincide for SICC-modules).

4. Every closed quasi-injective (extending) module is closed pseudo-injective . But the converse is not true, in general. For example ([14], Lemma (2)), let M be an R-module whose lattice of submodules is

$$\begin{tikzcd} & N_1 \arrow[dr, dash] & & \\ 0 \arrow[ur, dash] \arrow[dr, dash] & & N_1\oplus N_2 \arrow[r, dash] & M \\ & N_2 \arrow[ur, dash] & & \end{tikzcd}$$

where N_1 is not isomorphic to N_2, and the endomorphism rings of N_i are isomorphic to $Z/2Z$. the existence of such modules was shown by Hallett and Teply. It was shown in [14] , that M is pseudo-injective (and hence closed pseudo-injective) which is not closed quasi-injective, since $N_1 \oplus N_2$ is closed submodule of M and the natural projection of $N_1 \oplus N_2$ onto N_i $(i = 1,2)$ can not be extended to an endomorphism of M.

5. An R-isomorphic module to closed pseudo-M-injective is closed pseudo-M-injective.

The proof of the following follows from ([1], P.18) and Definition(2.3).

Proposition(2.5): Let M and N_i be R-modules where $i \in I$ and I is finite index set, If $\oplus_{i\in I} N_i$ is closed pseudo-M-injective, then $\forall\, i \in I$, N_i is closed pseudo-M-injective. In particular, every direct summand of closed pseudo-injective R-module is closed pseudo-injective.

Proposition(2.6): Let N be an closed submodule of an R-module M and N be a closed pseudo-M-injective. Then every R-monomorphism α from N into M(where Imα is closed submodule of M) splits. In particular, if M is an R-module whose closed submodules are closed pseudo-M-injective, then M is CS-module.

Proof. Let $\alpha: N \to M$ be an R-monomorphism. Consider the isomorphism $\alpha^{-1}: \alpha(N) \to N$. As N is closed pseudo-M-injective module, there exists an R-homomorphism g: $M \to N$, such that $g \circ \alpha = I_N$. For m$\in$M then $g(m) \in N$, there exists $\alpha(n) \in \alpha(N)$ such that $\alpha^{-1}(\alpha(n)) = g(m) = g(\alpha(n))$ and hence $m - \alpha(n) \in \ker g$. It follows that $m = \alpha(n) + (m - \alpha(n)) \in \alpha(N) + \ker g$. Moreover, $\alpha(N) \cap \ker g = \ker(\alpha^{-1}) = 0$. Thus $M = \alpha(N) \oplus \ker g$.

An R-module M satisfies CC_2, if every closed submodule which isomorphic to a direct summand of M is direct summand of M [11]. Every C_2-condition is CC_2-condition. But converse is not true, for example Z *as* Z-module. An R-module M is said to be co-Hopfian, if every injective endomorphism f: $M \to M$ is an automorphism [15]. An R-module M is directly finite, if M which is not isomorphic to a proper direct summand ([1], p.165). In [11] proved that every closed pseudo-injective module satisfies C_2, also every closed pseudo-injective module M is a directly finite if and only if it is co-Hopfian. However their proofs are incorrect, since Z as Z-module is directly finite and closed pseudo-injective, but it has not C_2 and not co-Hopfian.

Definition(2.7): An R-module N satisfies $M - CC_2$-condition if every closed submodule of M is isomorphic to a direct summand of N is itself a direct summand of M.

In the following, we shall show that $M - CC_2$-condition can be characterized by lifting monomorphisms from certain submodules of M to N.

Lemma (2.8): Let M and N be R-module and K be a closed submodule of M such that K is isomorphic to a direct summand of N. Then K is a direct summand of M if and only if every R-monomorphism $\varphi: K \to N$ can be lifted to An R- homomorphism $\theta: M \to N$.

Proof. The necessity is immediate. Conversely, let L be a direct summand of N and, an R-isomorphism f: $K \to L$. Then there exists an R-monomorphism $i_L of: K \to N$ such that $f(K)$ is a direct summand of N, since f(K)=L and L is direct summand of N. By hypothesis, f can be lifted to an R-homomorphism g: $M \to N$. Let $\pi: N \to f(K)$ denote the canonical projection. Then $\beta = \pi o g: M \to f(K)$ is an R-homomorphism. Note that $\beta(k) = \pi g(k) = \pi f(k) = f(k)$, each $k \in K$, and hence prove $M = K \oplus \ker(\beta)$.

Corollary(2.9): Let M and N be two R-modules. N satisfies ($M - CC_2$)-condition if and only if, for every closed submodule K of M which is isomorphic to a direct summand of N, every monomorphism $\varphi: K \to N$ can be lifted to a homomorphism $\theta: M \to N$.

It is well-known a submodule N is a direct summand of M if and only if $N = e(M)$ for some idempotent $e \in End_R(M)$ [5].

Proposition(2.10): The following statements are equivalent for an R-module M.

(1) N satisfies ($M - CC_2$)-condition,

(2) For any direct summand A of N, every R- monomorphism $f: A \to M$ where Imf is closed submodule of M, there is an R-homomorphism $g: M \to N$ such that $gof = i_A$, where $i_A: A \to N$ is a injection mapping.

(3) For every closed submodule K of M which is R-isomorphic to a direct summand of N, every R-monomorphism $f: K \to N$ can be lifted to an R-homomorphism $g: M \to N$.

Proof : (1) $\to$ (2). Let A be a direct summand of N, an injection $i_A: A \to M$ and every R-monomorphism $f: A \to M$. Then $\alpha: A \to f(A)$ is R-isomorphism, since A be a direct summand of N, by (1) implies f(A) is a direct summand of M. Then $f = i_{f(A)} o\alpha: A \to M$, there exists an R-monomorphism $i_A o\alpha^{-1}: f(A) \to N$. By direct summand f(A) of M, there exists an R-homomorphism $g = i_A o\alpha^{-1} o\pi_{f(A)}: M \to N$ such that $i_A o\alpha^{-1} = g \, o \, i_{f(A)}$, and hence, $g \, o \, i_{f(A)} o\alpha = i_A$ then $gof = i_A$,

(2) $\to$ (1). Let A be a closed submodule of M and an R-isomorphism $f: K \to A$ where K is a direct summand of N. Then $i_A of: K \to M$, by (2), there exists an R-homomorphism $g: M \to N$ such that $goi_A of = i_K$ where $i_K: K \to N$ is the injection mapping. We can use the same manner in the proof of Lemma (2.8). (1) $\leftrightarrow$ (3). Immediate by Corollary(2.9).

Proposition(2.11): Every closed pseudo-M-injective R-module satisfies $M - CC_2$.

Proof. Let N be a closed pseudo-M-injective R-module, A a direct summand of N and $A \cong B$ where B is closed submodule of M. Let f be an R-isomorphism $B \to A$. By N is closed pseudo-M-injective, Proposition(2.5) and Remark (2.4) then B is closed pseudo-M-injective. Therefore, by Proposition(2.6), i_B splits, that is; B is direct summand of M.

Corollary(2.12): Let M be a closed pseudo-injective R-module. Then every closed submodule of M which is isomorphic to M is a direct summand in M .

Proof. Let $\alpha : K \to M$ be an isomorphism. There exists a homomorphism $\beta : M \to M$ that extends α , since M is closed pseudo - injective. $\forall\ x \in M$, there exists $y \in K$ such that $\beta(x) = \alpha(y) = \beta(y)$ and hence $x - y \in ker\beta$. It follows that $x = y + (x - y) \in K + ker\beta$. Moreover , $K \cap ker\beta = 0$. Thus $M = K \oplus ker\beta$ and K is a direct summand of M .

In the following, we characterize extending modules in terms of closed pseudo-injectivity, the proof of the proposition(2.13) follows from Proposition(2.6) and Remarks(2.4).

<u>Proposition (2.13):</u> The following statements are equivalent for an R-module M:

(1) M is extending module .

(2) Every R-module is closed pseudo -M-injective .

(3) Every closed submodule of R-module M is closed pseudo-M-injective .

A submodule N of an R-module M is said to be pseudo stable, if $\alpha(N) \subseteq N$, for each R-monomorphism $\alpha : N \to M$. In case each (closed)submodule of M is pseudo-stable, the R-module M is called fully (closed) pseudo stable [16]. Every fully pseudo-stable R-module is fully closed pseudo stable, but converse is not true , for example $Z\ as\ Z$ −module.

<u>Proposition(2.14):</u> Let M be a extending R-module. If $S = End_R(M)$ is commutative, then M is a fully closed pseudo stable.

Proof: Let N be any closed submodule of M and $f: N \to M$ any R-monomorphism. There exists a submodule K of M such that $M = N \oplus K$. f can be extended to an R-homomorphism $g: M \to M$ by putting $g(k) = 0$ for each $k \in K$. Define $h: M \to M$ by $h(x, y) = x$ for each x $\in$N and $y \in$K. Let f(x) = y + l for some y $\in$ N and l$\in$K. Now hog(w) = hog (x + k) = y, on the other hand goh(w) = y + l, since hog=goh, then l = 0, thus f(x) $\in$ N. Therefore f(N) $\subseteq$ N, hence, M is an fully closed pseudo stable R-module.

An R-module M is multiplication if each submodule is of the form MA for some right ideal A of R [17].

<u>Proposition(2.15):</u> Let M be a multiplication R-module. If M is a closed Pseudo-injective then M is a fully closed pseudo-stable.

Proof: Let N be a closed submodule of M and an R-monomorphism $g: N \to M$. Since M is multiplication, then N = M I for some right ideal I of R. Then g can be extended to an R-homomorphism $h: M \to M$ Now $g(N) = h(N) = h(MI) = h(M)I \subseteq MI = N$.

<u>Remark(2.16):</u> Let M be a fully closed pseudo-stable R-module. Then every two distinct closed submodules of M are not isomorphic.

Proof. Assume that M is fully closed pseudo stable R-module and M has two distinct closed submodules N_1 and N_2 such that $N_1 \cong N_2$. No loss of generality if it is assumed that $N_1 \not\subset N_2$. Then there exists a non-zero element x in N_1 not in N_2. Let $\theta : N_1 \to N_2$ be an R-isomorphism, consider the following two R-monomorphisms, $i_{N_2} o\theta : N_1 \to M$ and $i_{N_1} o\theta^{-1} : N_2 \to M$, by fully closed pseudo-stability of M, then $i_{N_1} o\theta^{-1}(N_2) \subseteq N_2, i_{N2} o\theta\ (N_1) \subseteq N_1$. Now let $\theta(x) = y \in N_2$, so $i_{N_1} o\theta^{-1}(y) = x \in N_2$ which is a contradiction.

The proof of the proposition(2.17) follows from Remark(2.16)

Proposition (2.17): If M is a fully closed pseudo-stable then M has CC_2 –condition .

Proposition(2.18): Every closed submodule of multiplication closed pseudo-injective is closed pseudo-injective.

Proof: Let N be a closed submodule of M and an R-monomorphism $g : N \to M$. Since M is multiplication, then M = NI for some right ideal I of R. Then g can be extended to an R-homomorphism $h : M \to M$, since M is closed pseudo-injective. Now $g(N) = h(N) = h(MI) = h(M)I \subseteq MI = N$.

An R-module M is self-similar, if every submodule of M is isomorphic to M [18]. In the following, we show that the distinction between closed pseudo-injectivity and extending module vanishes for self-similar R-modules, and the proof of the following follows from proposition(2.13) and corollary(2.12).

Proposition(2.19): Let M be self-similar R-module. Then M is closed pseudo-injective if and only if M is extending module.

Recall that a ring R is said to be a quasi-Frobenius, if it is a right self injective Noetherian ring [6]. In the following, we characterize right hereditary rings in terms of closed pseudo-injective modules.

Theorem(2.20): The following statements are equivalent for a quasi-Frobenius ring.

(1) Every closed pseudo-injective R-module is semi simple.

(2) Every injective R-module is semi simple.

(3) R is a hereditary ring.

Proof : (1)→ (2). trivial. (2)→(1). Let M be a closed pseudo-injective R-module, E(M) injective hull of M. By (2), E(M) is semi simple. By proposition(1.9), we have M is semi simple.(2)↔(3). By([19], proposition(3.2)).

REFERENCES

1. Goodearl, K.R, Ring Theory, Nonsingular Rings and Modules, Marcel Dekker. Inc. New York, 1976.

2. R. E. Johnson and E. T. Wong: Quasi-injective modules and irreducible rings, J. London Math. Soc. 260-268, 39 (1961).
3. H. Q. Dinh, A note on pseudo-injective modules, comm. Algebra , 33 , ,361-369, 2005.
4. M. S. Abbas and S. M. Saied(Saeed), IC-Pseudo-Injective Modules, International Journal of Algebra, Vol. 6, no. 6, 255 – 264, 2012.
5. S .Mohamed and Thanaa, Continuous modules ,Arabian J. for science and Engineering 2,107 – 112, (1976).
6. Kasch, F, Modules and Rings. Academic Press Inc. London (English Translation), 1982.
7. A. Ghorbani, M. R. Vedadi, epi-retractable modules and some application , Bull. Iranian Math. Soc, vol.35, No.1, 155-166, 2009.
8. N.V. Dung, D.V. Huynh, P.F. Smith and R. Wisbauer, Extending Modules, Pitman, 1996.
9. M. Hazewinkel, N. Gubareni, V.V. Kirichenko, Algebras, Rings and Modules.Vol.1. Kluwer Academic Publishers. 2004.
10. P .F. Smith , N. V. Dung ,Hereditary CS-modules, Math. Scand. Vol.71, 173-180, 1992.
11. T. Sitthiwirattham, S. Baupradist and S. Asawasamrit, On Generalizations of Pseudo-Injectivity, Int. Journal of Math. Analysis, Vol. 6, no. 12, 555 – 562, 2012.
12. C. Clara- Gomes, Some generalizations of Injectivity . Ph.D. Thesis. University of Glasgow, 1998.
13. A. Al-Ahmadi, N. Er, S. K. Jain, Modules which are invariant under monomorphisms of their injective hulls, J. Aust. Math. Soc. 79, 349-360, 2005 .
14. S. K. Jain, and S. Singh, Quasi-injective and pseudo-injective modules. Canad. Math. Bull. 18, 359-366, 1975 .
15. K. Varadarajan, Hopfian and co-Hopfian objects, publicacions Mathematiques, Vol 36, 293-317, (1992).
16. M. S. Abbas, On fully stable modules, Ph.D. Thesis, College of Science, University of Baghdad, 1991.
17. Barnard, A, Multiplication modules, Journal of Algebra 71, 174-178, 1981.
18. V. S. Rodrigues, A. A. Sant'Ana, A note on a problem due to Zelmanowitz, Algebra and Discrete Mathematics, Number 3. pp. [85 – 93], 2009.
19. M. K. Patel, B. M. Pandeya, A. J. Gupta and V. Kumar, Applications of epi-retractable modules, Bulletin of the Iranian Mathematical Society Vol. XX No. X, pp XX-XX, 201X .

Kernel–Injective Module

Mehdi S. Abbas[1] and Samer Mohammed Saeed Abdul Alameer[2]
[1]Department of Mathematics, College of Science, Mustansiriya University
[2]The Ministry of Education Directorate General for Education in Wasit
Received 6/3/2013 – Accepted 15/9/2013

الخلاصة

في هذا العمل، مفهوم الاغمارية بالنسبة إلى التشاكل المغلق النواة المعممة عرضت و درست، وهذا أعمام لمفهوم المقاسات شبة الاغمارية. بينا أن هذا المفهوم يكون مغلقا بالنسبة لمركبات الجمع المباشر . أعطينا كثير من الخواص و التوصيفات . وصفنا بعض الحلقات مثل الحلقات شبة البسيط الارتينية ، الحلقات النوثيرية، الساحات الديدكايندية و الحلقات من نمط –(أس أي) بدلالة هذا المفهوم.

ABSTRACT

In this work, the notion of injectivity relative to a class of closed kernel sub modules (namely, kernel-injectivity) has been introduced and studied, which is a generalization quasi-injective module. This notion is closed under direct summands. Several properties and characterizations have been given. we provide a characterization of semi simple Artinian ring , SI-ring and Dedekind domain in terms of Ker-quasi-injective R-module

INTRODUCTION

Throughout, R represents an associative ring with identity and R-modules are unitary left R-modules. For an R-modules M and N, $Hom_R(M,N)$will denote the set of R-module homomorphisms from M to N. The kernel of any $\beta \in Hom_R(M,N)$ is denoted by ker(β) and its image by $\beta(M)$. S=$End_R(M)$ will denote the ring of R-endomorphisms of M [1]. A sub module N of R-module M is said to be an essential sub module of an R-module M, if N has nonzero intersection with every nonzero sub module of M [2]. A sub module K of R-module M is said to be a closed in M ,if K has no proper essential extensions in M ([3], P.5). We shall use $\vartheta(R)$ to stand for the set of all essential right ideals of the ring R . Given any R-module M, we set Z(M)={ x$\in M$| x I $= 0$, for some I$\in\vartheta(R)$} ([2], P. 30). An R-module M, is singular provided Z(M)=M. At the other extreme, we say M is a nonsingular provided Z(M)=0 ([2], P.31). A sub module N of R-module M is said to be a direct summand of R-module M, if M = N$\oplus$L, for some sub module L of M [2]. An R-module M is said to be semi simple, if every sub module of M is direct summand ([2], P.27). An R-module M is called CS-module (or extending ((C_1)-condition)), if M satisfies any one of the following equivalent conditions (1) for every sub module N of M, there is a decomposition M =A$\oplus$B such that N is essential in A, (2) every closed sub module of M is a direct summand [4]. A CS-module M which satisfies (C_2)-condition: every sub module of M which is isomorphic to a direct summand of M is itself direct summand, is called continuous[4]. Let M and N be two R-modules, N is called M-injective, if for every submodule A of M, any R-homomorphism from A to N can be extended to an R-homomorphism from M to N([5], P.28). An R-module N is called injective, if it is M-injective for all R-module M. A right R-module M is (minimal) quasi-injective, if every homomorphism from a (simple) submodule of M to M can be extended to an endomorphism of M[6]([7]). Let M and N be two R-modules, N is called pseudo-M-injective, if for every submodule A of M, any R-monomorphism from A to N can be extended to an R-homomorphism from M to N. An R-module M is pseudo-injective, if it is pseudo-M-injective [8].

Ker-quasi-injective module

Definition(2.1): Let M and N be two R-modules. M is said to be Ker-N-injective, if for each sub module A of N, every R-homomorphism α from A to M (where Ker(α) is closed of N) can be extended to an R-homomorphism from N into M. The R-module M is called Ker-quasi-injective, if it is Ker-M-injective.

Examples and remarks (2.2)

(1) Every quasi-injective R-module is Ker-quasi-injective.

(2) every direct summand of Ker-quasi-injective R-module is Ker-quasi-injective.

(3) Every Ker-quasi-injective R-module is pseudo-injective.

But the converse is not true, in general. For example ([9], Lemma (2)), let M be an R-module whose lattice of sub modules is

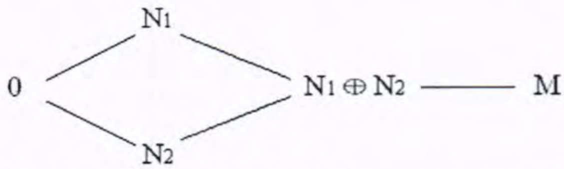

where N_1 is not isomorphic to N_2, and the endomorphism rings of N_i are R-isomorphic to $Z/2Z$ where i=1,2. The existence of such R-modules was shown by [9]. It was shown [9], that M is pseudo-injective which is not Ker-quasi-injective, since $N_1 \oplus N_2$ is sub module of M and the natural projection $\rho : N_1 \oplus N_2$ onto N_i (i=1,2) (so Ker(ρ) is closed in M) cannot be extended to an R-endomorphism of M [9].

(4) isomorphic to Ker -M-injectivity is Ker -M-injectivity.

(5) Every Ker- quasi-injective over Noetherian rings is quasi-injective.

Proof (5) : it follows by([10], theorem 3.6), over Noetherian ring R , module M is quasi-injective if and only if M is pseudo-injective and CS.

In Goldie [11] and Johnson, Wong [6] they have defined an R-sub module in M for sub module N as follows: cl N = {m ∈ M \ (N; m) is an essential left ideal in R}. If cl N = N, then N is called closed. We call cl(0) the singular sub module of M. Let N be a sub module of M and B a complement of N. Then M is an essential extension of B⊕N. Hence, cl (B⊕N) = M ([12], Lemma 1.4).

Proposition(2.3): Every Ker-quasi-injective R-module is continuous.

Proof: Let M be a Ker-quasi-injective R-module, A and B two sub modules of M with A is a direct summand in M and B is R-isomorphic to A. Let f: B → A be an R-isomorphism. Then A is Ker -M-injective, Examples and remarks (2.2), B is Ker-quasi -M-injective. The inclusion mapping i_B: B → M, there exists an R-homomorphism g: M→B such that $goi_B = I_B$. Then M = B⊕ker(g). That is; B is a direct summand in M, then M has C_2-condition.

Now to prove M is extending . Let N be a closed sub module and B a complement of N in M. Put M_0= B⊕N. Let p be a projection of M_0 to N and Ker p =B is closed in M , since N a complement of B in M. Then there exists an element g ∈ Hom $_R$(M, M) such that $g\backslash_{M0}$=p. Since B⊆$g^{-1}(0)$ and $g^{-1}(0) \cap N = (0), B = g^{-1}(0)$. Furthermore, since cl$M_0$= M by([12] , Lemma 1.4), there exists an essential left ideal L for any element m ∈ M such that Lm ⊆ M_0. Therefore, L g(m) = g(Lm) ⊆ N. Since cl N = N, g(m) ∈ N Hence, g(M) = N. Therefore, M = $g^{-1}(0)$+ g(M) = B⊕N. Then M is continuous R-module.

Theorem(2.4): Let M be a nonsingular module such that all sub modules of M are Ker-quasi-injective. Then M is quasi-injective.

Proof: Let A be sub module of M and let $\phi: A \to M$ be a R-homomorphism . By Proposition(2.3), A is CS, A = B⊕C where C contain Ker(ϕ) as an essential sub module. Since $\frac{A}{Ker(\phi)}$ embeds in M, $\frac{A}{Ker(\phi)}$ is nonsingular, and so Ker(ϕ) is a closed sub module of A, A=B⊕Ker(ϕ). It is then clear that $\phi|_B$ is a monomorphism. As M is CS, M=B^*⊕D, where B is essential in B^*. Since B^* is pseudo-injective, $\phi|_B$ is extended to monomorphism g: $B^* \to B^*$. ∀ x ∈ M. We have x = b + d , (b ∈ B^* , d ∈ D). Using this we define a map ϕ^*:M → M by setting $\phi^*(x) = g(b)$. Then it is obvious that ϕ^*:M → M that extends ϕ. This shows that M is quasi-injective.

Proposition(2.5): Let M be a Ker-quasi-injective R-module. Then every sub module of M which is isomorphic to closed sub module in M is closed in M.

Proof : Let M be a Ker-quasi-injective R-module, K a closed in M and A a sub module of M with An R-isomorphism f: A → K. Consider the following diagram where $i_A: A \to M$, $i_K: K \to M$ are two inclusion homomorphism. Then f extends to some g in End(M) such that $i_K of = go\, i_A$, by Ker-quasi-M-injectivity of M. Now let Ω be collection of the set of all essential extension of A in M. $\Omega \neq \phi$, since A∈Ω. By Zorn's lemma, there exists maximal essential member A'. that is; A' is maximal essential extension sub module in M, which is evidently, it is closed sub module of M. thus $g|_{A'}$ is an R-monomorphism. Since $g(A) = f(A)$, hence K = g(A) is essential in g(A'), by A is essential sub module in A'. Since K is a closed in M. This implies K = g(A), whence $A = A'$. The conclusion follows.

An R-module M is multiplication, if each submodule is of the form M A for some right ideal A of R [13].

Proposition(2.6): Every closed sub module of a multiplication a Ker-quasi -injective is a Ker-quasi-injective.

Proof: Let L be a sub module of a closed sub module N of M and let α :L→N be an R-homomorphism with Ker(α) is closed of N . Since N is closed sub module of R-module M, then Ker(α) is closed of M. By hypothesis, there exists $g: M \to M$, by multiplication property of M , then N = MI for some right ideal I of R, $g|_N = g(N) = g(MI) = g(M)I \subseteq MI = N$.

Proposition(2.7): The following statements are equivalent for an R-module M:

(1) M is semi simple.

(2) Every R-module is Ker-M-injective.

(3) Every sub module of M is Ker -M-injective.

Proof. (1) →(2) → (3). It is clear.

(4)→(1). K be sub module of M. By (3) K is Ker-M-injective, by The identity mapping i_K: K → K, there exists an R-homomorphism g: M → K such that $goi_K = I_K$. Then $M = K \oplus \ker(g)$. That is; L is a direct summand in M.

An R-module M is said to be co-Hopfian if every injective endomorphism $f: M \to M$ is an automorphism [14]. An R-module M is directly finite, if $fog = I_M$ implies that $gof = I_M$ for all f; g ∈ End(M) ([2], Lemma (6.9)). An R-module M is called weakly co-Hopfian, if any injective R-endomorphism f: M → M is essential, that is; f(M) is an essential submodule of M [15]. In the following proposition, a sufficient condition for Ker-quasi-injective modules to be co-Hopfian is given.

Proposition (2.8): A Ker-quasi-injective R-module M is directly finite if and only if it is co-Hopfian.

Proof. Let f be injective R-endomorphism of M and I_M: M → M the identity map. Since M is a Ker-quasi-injective, there exists a map g: M → M such that, $gof = I_M$. By directly finite of M , we have $fog = I_M$ which shows that f is an automorphism. Hence M is co-Hopfian. The converse is clear.

In the following proposition, we give a condition for weakly co-Hopfian modules to be co-Hopfian.

Proposition (2.9): The following conditions are equivalent for a Ker-quasi -injective R-module M:

(1) M is weakly co-Hopfian .

(2) M is co-Hopfian.

Proof. (1) $\rightarrow$(2) Let f: M $\rightarrow$ M be an R-monomorphism. By(1) we have f(M)is essential in M. f splits and hence f(M) is a direct summand of M, since M is a Ker-quasi-injective. Therefore f(M) = M. This shows that M is co-Hopfian. (2)$\rightarrow$(1) is obvious.

It is well-known that an R-module M is injective if and only if M is N-injective for each R-module N.

Proposition(2.10): The following statements are equivalent for an R-module M :

(1) M is injective.

(2) M is Ker -N-injective, for each R-module N.

Proof: (1)$\rightarrow$(2): Obvious, (2)$\rightarrow$ (1): Let $E = E(M)$ be the injective hull of M. Let $\iota: M \rightarrow E$ be the inclusion mapping and $j: E \rightarrow M \oplus E$ the natural injection. Ker -M$\oplus$E-injectivity of M , implies that the identity mapping I_M of M can be extended to an R-homomorphism $f: M\oplus E \rightarrow M$ such that $go\iota = I_M$ where $g = foj$. Then $E = M \oplus \ker(g)$, then M=E, hence M is injective.

An R- module M is called polyform (or non-M-singular) if, for any sub module K of M and f : K $\rightarrow$ M, Ker(f) is closed in M [16].

Proposition(2.11): Every polyform Ker-quasi-injective R-module is quasi-injective.

It is well-known that if R is a semi simple Artinian ring , then every R-module is injective ([2], Theorem(1.18)). Also, Osofsky in [17] a proved that ring R is semi simple Artinian if and only if every cyclic R-module is injective. Recall that R is a right V-ring, if every simple R-module is injective [18].We now provide a characterization of semi simple Artinian rings in terms of Ker-quasi-injective modules.

Theorem (2.12) : The following conditions are equivalent for a ring R.

(1) R is semi simple Artinian,

(2) R is a right V-ring and every minimal quasi-injective right R-module is Ker-quasi-injective,

(3) Every R-module is Ker-quasi -injective,

(4) The direct sum of every two Ker-quasi -injective modules is Ker-quasi - injective. And every cyclic R-module is Ker-quasi -injective,

Proof. (1) $\rightarrow$ (2). It follows from([2], Theorem(1.18)).

(2) $\rightarrow$ (3). Since R is a right V-ring, every simple R-module is injective and hence every simple right R-module is a direct summand of

each module containing it. So every R-module is minimal quasi-injective, hence is Ker-quasi-injective R-module. (3) → (4). It is clear.

(4)→(1). Let M be Ker-quasi -injective module and E the injective hull of M. By(4) M⊕E is Ker-quasi -injective. Then Examples and remarks (2.2), M is Ker-M⊕E-injective and Proposition(2.10), hence M is injective. By every cyclic R-module is Ker-quasi-injective, then every cyclic R-module is injective , that is; R is semi simple Artinian , by Osofsky's theorem in [17].

Recall that an *R*-module *M* is direct injective, if given any direct summand *A* of *M*, an injection i_A: *A*→*M* and every *R*-monomorphism $f : A \to M$, there is an R-endomorphism g of *M* such that $gof = i_A$ [19].

Nicholson in([20], Theorem(7.13)) proved that direct injective *R*-module is equivalent to C_2-condition. Proposition(2.3) shows that every Ker-quasi injective R-module is a direct injectiveand every direct injective R-module is divisible [19]. Then we have the following:

Proposition (2.13): Every Ker-quasi -injective R-module is divisible.

The converse of Proposition(2.13) may not be true.

Ker-quasi - injectivity is not closed under direct sums in general, as we see in the following

R=$\begin{pmatrix} F & F \\ 0 & F \end{pmatrix}$, A= $\begin{pmatrix} 0 & 0 \\ 0 & F \end{pmatrix}$, B= $\begin{pmatrix} F & F \\ 0 & 0 \end{pmatrix}$, C= $\begin{pmatrix} 0 & F \\ 0 & 0 \end{pmatrix}$

Where $= Z/2Z$. It Is easy to see that the R-modules A and B are quasi-injective. And hence by Examples and remarks (2.2), they are Ker-quasi -injective. However R=A⊕B is not Ker-quasi -injective, since otherwise R satisfies (C2)-condition, by Proposition(2.3). But A is isomorphic to C and C is not a direct summand in R, contradiction.

Since A and B are two divisible R-modules. And every direct sum of divisible R-modules is divisible. That is; A⊕B is divisible. But it is not Ker-quasi -injective.

In the following, we show that the distinction between Ker-quasi -injectivity and divisibility vanishes over Dedekind domain. A domain R is called Dedekind ring, if every divisible R-module is injective ([21], Theorem(4.24)). We now provide a characterization of domain R is Dedekind rings in terms of Ker-quasi -injective R-modules.

Theorem(2.14): The following conditions are equivalent for a ring R.

(1) R is Dedekind domain,

(2) Every divisible R-module is Ker-quasi -injective.

Proof: (1)→(2). By ([21], Theorem(4.24)).

(2)→(1). Let M be a divisible R-module and E(M) an injective hull of M. By ([5], proposition (2.6)), E(M) is divisible and by ([5], Lemma(2.5)), then M⊕E(M) is divisible. By(2) M⊕E is Ker-quasi -

injective. Then Examples and remarks (2.2) , M is Ker- M⊕E-injective and Proposition(2.10). That is; M is injective, implies R is Dedekind domain [21].

Recall that a ring R is SI-ring, if every singular R-module is injective ([3], below Corollary (7.16)). Over non singular ring; we provide a characterization of SI-ring in terms of Ker-quasi -injective R-modules.

Proposition(2.15): The following statements are equivalent for non singular ring R :

(1) R is SI-ring.

(2) Every singular R-module is Ker-quasi -injective,

Proof: (1) → (2) is clear.(2) →(1). Let M be a singular R-module and E(M) the injective hull of M. ([2], Proposition(1.23) and (1.22)), then M⊕E(M) is singular. By(2) M⊕E is Ker-quasi -injective. Then Examples and remarks (2.2), M is Ker-M⊕E-injective and Proposition(2.10), hence M is injective. That is; R is SI-ring .

In the next part we characterize some rings by Ker-quasi-injectivity. In the following, Noetherian rings are characterize as in terms of Ker-quasi-injective. Recall that a R-module M is F-injective, if for any finitely generated ideal L of R, every R-homomorphism of L into M, can be extended to an R-homomorphism R into M [22].

Proposition (2.16) : The following conditions are equivalent:

(1) R is Noetherian ring ;

(2) Every F-injective R-modules are injective;

(3) Every F-injective R-module is Ker-quasi -injective.

Proof. (1) implies (2) and (2) implies (3) are evidently.

Assume (3) . Let M be a F-injective R-module, E the injective hull of M. Write Q=M⊕E is F-injective R-module. By(3) M⊕E is Ker-quasi -injective. Then Examples and remarks (2.2) , M is Ker- M⊕E-injective and Proposition(2.10), hence M is injective. We have shown that every F-injective R-module is injective. Since any direct sum of F-injective R-modules is F-injective, then every direct sum of injective modules is injective which implies that R is Noetherian, by ([21], P.82). Thus (3) implies (2) and (2) implies (1).

REFERENCES

1. Kasch, F, Modules and Rings. Academic Press Inc. London (English Translation) (1982).
2. Good earl, K.R, Ring Theory, Nonsingular Rings and Modules, Marcel Dekker. Inc. New York, (1976).
3. N.V. Dung, D.V. Huynh, P.F. Smith and R. Wisbauer, Extending Modules, Pitman, (1996).

4. S .Mohamed and Thanaa, Continuous modules ,Arabian J. for science and Engineering 2,107 – 112, (1976).
5. ND. W. Sharpe, P. Vamos, Injective Modules, Cambridge University Press, Cam-bridge, (1972).
6. R. E. Johnson and E. T. Wong: Quasi-injective modules and irreducible rings, J. London Math. Soc. 260-268, 39 (1961).
7. Zhu Z. and Tan, Z. S., Minimal quasi-injective modules. Sci. Math. Jpn. 62, 465-469, (2005).
8. H. Q. Dinh, A note on pseudo-injective modules, comm. Algebra , 33,361-369,(2005).
9. S. Singh and S. K. Jain, Quasi-injective and pseudo-injective modules. Canad. Math. Bull, 359-366, 18, (1975).
10. A. Al- Ahmadi, N. Er, S. K. Jain, Modules which are invariant under
1. monomorphisms of their injective hulls, J. Aust. Math. Soc. 349-360, 79, (2005).
11. A. W. Goldie : Torsion-free modules and rings, J. Algebra, 268-287, 1, (1964).
12. M. Harada, Note on quasi-injective modules, Osaka J. Math. 351-356, 2, (1965).
13. Barnard, A, Multiplication modules, Journal of Algebra 71, 174-178, (1981).
14. K. Varadarajan, Hopfian and co-Hopfian objects, publicacions Mathematiques, Vol 36 293-317, (1992).
15. M. R. Vedadi and A. Haghany, Modules whose injective endomorphisms are essential, Journal of Algebra 243, 765-779,(2001).
16. C. S. Roman: Baer and quasi-Baer modules, ph. D. Thesis , The Ohio state university, (2004).
17. B. L. Osofsky, Rings all of whose finitely generated modules are injective, Pacific J. 645-650, Math. 14, (1964).
18. O. E. Villamayor and G. O. Michler, On rings whose simple modules are injective, Algebra 25, 185-201,(1973).
19. Chang -woo Han and Su-Jeong Chol, Generalizations of the quasi-injective modules, comm. Korean Math. Soc. 10, No.4, pp. 811-813, (1995).
20. W. K. Nicholson, M. F. Yousif: Quasi-Frobenius Rings, Cambridge
2. University Press, 2003.
21. J. J. Rotman, An Introduction to Homological Algebra, New York: Academic Press, (2000).
22. R.Y. C. Ming. On regular rings and self-injective rings, IV, Publications De l'institut Mathematique, Nouvelle serie tome 45(59), pp. 65-72, (1989).

FI-HOLLOW-LIFTING MODULES

Saad A. Alsaadi and Nedal Q. Saaduon
Department of mathematics, College of science, University of AL-Mustansiriya [1 2].
Received 28/3/2013 – Accepted 15/9/2013

الخلاصة

في هذا البحث، تم تقديم مفهوم مقاسات الرفع المجوف من النمط FI كتعميم فعلي لمقاسات الرفع المجوف . نقول عن M انه مقاس رفع مجوّف من النمط FI إذا كان لكُلّ مقاس جزئي ثابت N من M بحيث ان $\frac{M}{N}$ مقاس مجوف، يوجد مقاس جزئي K من N بحيث ان $M=K\oplus K^*$ و $K \subseteq_{ce} N$ في M . تم أعطاء عدد من التشخيصات و الخواص للمقاسات الرفع المجوف من النمط FI . على العكس من مقاسات الرفع و مقاسات الرفع المجوف، برهنا الجمع المباشر المنتهي لمقاسات رفع المجوف من النمط FI تكون مقاس رفع المجوف من النمط FI.

ABSTRACT

In this paper, we introduce and study the concept of FI-hollow-lifting modules which is a proper generalization of hollow-lifting modules. We say M called a fully invariant hollow-lifting module (or briefly FI-hollow lifting) if every fully invariant submodule N of M with M/N is hollow has coessential submodule that is a direct summand of M . Many characterizations and properties of FI-hollow-lifting modules are given. Unlike lifting modules and hollow –lifting modules, we prove a finite direct sum of FI-hollow lifting modules is FI-hollow-lifting.

1.Introduction

N.Orhan, D.keskin and R.Tribak introduced the concept hollow-lifting modules as a generalization of lifting modules. An R-module M is called Hollow –lifting if every submodule N of M such that M/N is hollow has coessential submodule that is a direct summand of M [1]. On other direction, Y.T.alebi and T.Amoozegar are introduced FI-lifting modules as a generalization of lifting module. An R-module M is called FI-Lifting if every fully invariant submodule N of M contains a direct summand such that K coessential submodule N in M [2].

In this paper, we introduce and study the concept of FI-hollow-lifting modules which is a generalization of both hollow-lifting modules and FI-lifting modules. We say that M called a fully invariant hollow-lifting module (or briefly FI-hollow lifting) if every fully invariant submodule N of M with M/N is hollow has coessential submodule that is a direct summand of M . Many characterizations and properties of FI-hollow-lifting modules are given. Also we call an R-module M is FI- hollow module if every proper fully invariant submodule is small. We assert that a FI-hollow module is a proper generalization of hollow modules. We give the relationship between FI- lifting modules and FI-hollow modules.

Throughout this paper R will denote arbitrary associative ring with identity and all R-modules are unitary left R-module, $N \subseteq M$ will mean N is a submodule of an R-module M. Let M be a module and N be a submodule of M. N is called a small submodule of M (denoted by

$N \ll M$) if for any $X \subseteq M$, $M=N+X$ implies $X=M$. An R- module M is called hollow if every proper submodule is small in M. The module M is called local if has a unique maximal submodule N which contains all proper submodules of M. Let K, N be submodules of M such that $K \subseteq N \subseteq M$. Recall that K is called coessential submodule of N in M (briefly $K \subseteq_{ce} N$ in M) if $N/K \ll M/K$. A submodule N of M is called a coclosed submodule of M if N has no proper coessential submodule in M. If N and L are submodules of M, then N is called a supplement of L, if $N + L = M$ and $N \cap L \ll N$. A module M is called lifting if every submodule N of M contains a direct summand K of M such that $K \subseteq_{ce} N$ in M. Recall that a submodule K of M is fully invariant if $g(K) \subseteq K$ for all $g \in End(M)$. An R-module M is called duo if every submodule of M is fully invariant [3]. Moreover, a submodule of an R-module M is a called a stable if $f(N) \subseteq N$ for each homomorphism $f:N \to M$. An R-module is called fully stable if every submodule of M is stable[4].

2. FI-Hollow Modules

Recall that a non-zero R-module is uniform if every non-zero submodule of M is essential. Dully, a non-zero R-module M is called hollow if every proper submodule of M is small. As a generalization of hollow module, we introduce the following concept:

Definition (2.1): An non-zero R-module M is a called FI-Hollow if every proper fully invariant submodule of M is small.

Example and Remark(2.2):

1-Every hollow module is FI-hollow, while the converse is not true in general. For example $Z_2 \oplus Z_8$ as Z-module is FI-hollow which is not hollow.

2-Z as Z-module is not FI-hollow. Since 2Z is fully invariant of Z_2 and $Z_2 + Z_3 = Z$ but $Z_3 \neq Z$.

3-We call an non-zero R- module M is called FI-simple if (0) and M are the only fully invariant of M. It is clear that every FI-simple is FI-hollow.

The next result gives the relationship between FI-lifting module and FI-hollow

Compare this result with [5, corollary (4.9)]

Proposition (2.3): An indecomposable module is FI-hollow if and only if FI-lifting.

Proof: Suppose that M is FI-hollow and let A be fully invariant submodule of M. thus A is small and hence $A=(0)+A$ with (0) is a direct summand of M and $A \ll M$ .So by ([2],pro.(2.5)) then M is FI-Lifting.

Conversely, suppose that M is FI-lifting and let A be a fully invariant proper submodule of M [2, pro.(2.5)].$A=N \oplus D$ where N is a direct summand of M and D<< M. Now, since M is indecomposable then either N=(0) or N=M if N=M then M=N⊆A which implies that A=M which is a contradiction .so N=(0) thus A=D << M is FI-hollow.

In following Proposition, we give some of the basic properties of FI-Hollow module.

Proposition (2.4): If an R-module M is a FI-hollow module, then M/N is a FI- hollow module for every proper fully invariant submodule N of M.

Proof: Assume that M is FI-hollow and let N be a proper fully invariant submodule of a FI- hollow module M. Let K/N be a proper fully invariant submmodule of M/N then M/N=K/N+H/N $=\frac{K+H}{M}$ and so it is implies that M=K+H. Since K/N proper fully invariant of M/N and N proper fully invariant submodule of M thus K is proper fully invariant submodule of M [6, Lemma(2.2)]. Since M is FI-hollow then K is small submodule of M thus H=M, so H/N=M/N hence K/N<<M/N therefore, M/N is FI-hollow.

We do not know whether a fully invariant submodule of FI-hollow module is FI-hollow.

Proposition(2.5): Every non-zero coclosed fully invariant submodule of a FI- hollow module is FI-hollow.

Proof: Let M be a FI-hollow module and let N be a non-zero fully invariant coclosed submodule of M. Suppose L is a proper fully invariant submodule of N, then L is a Proper fully invariant submodule of M. Therefore L << M and hence L << N by [7, pro.(1.2.1)].Thus N is a FI- hollow module. □

Recall that the Jacobson Radical of a module M (notation Rad M) is the intersection of all maximal submodules of M and Rad(M)=M, in case M has not max. submodule [10].

It is well- Known that, if an R-module hollow which has maximal submodule K, then RadM=K [8].

In the next result, we generalize this result to FI-hollow module.

Lemma (2.6): If M is FI-hollow module which has maximal submodule K, then RadM =K.

Proof: Let K be a maximal submodule in M. Suppose that RadM≠K.Since K is maximal submodule of M, then Rad(M) ≠M (i.e) Rad(M) is a proper submodule of M. hence Rad(M)+K=M. But Rad(M) is fully invariant submodule of M, so by FI-hollow property of M, RadM≪M. So, we have K=M which is a contradiction. Hence RadM = K.

□

Corollary (2.7): Let M be hollow which has a maximal submodule K.Then RadM=K.

Proposition(2.8): Let M be a FI-hollow module and RadM $\neq$ M if and only if M is a FI-hollow and cyclic module.

Proof: Let M be a FI- hollow module with RadM $\neq$ M, since RadM is fully invariant of M and M is FI-hollow. Then RadM $<<$ M. Also by lemma(2.6) RadM is the unique maximal submodule of M and thus M / RadM is a simple module so RadM is cyclic. Let M / RadM $= <x + \text{RadM}>$ for some x $\in$ M. We claim that M = Rx. Let m $\in$ M then m + RadM $\in$ M / RadM, and therefore there is r $\in$ R such that m + RadM = r (x + RadM)= rx + RadM. Thus m – rx $\in$ RadM which implies that m – rx = y for some y $\in$RadM. Thus m = rx + y$\in$ Rx + RadM, hence M =Rx +RadM. But RadM $\ll$ M implies M = Rx. Conversely, since M is cyclic, then M is finitely generated and hence RadM $\neq$ M.

Recall that an R- module M is called SS-module if every direct summand is stable [9].

Proposition (2.9): Let M is be a FI-hollow module and SS-module, then every direct summand of M is FI-hollow.

Proof: Let $M=M_1 \oplus M_2$ be a FI-hollow module .Then $M/M_2 \cong M_1$ and hence, M/M_2 is a FI-hollow by proposition (2.4), thus M_1 is FI-hollow.

It is well-known that a direct sum of hollow module need not be true. For example, Z-module Z_p and Z_{p3} are both hollow (where p is a prime number). But $Z_p \oplus Z_{p3}$ is not hollow Z-module [5].

Proposition(2.10) : If M_1 and M_2 are FI-hollow modules, then $M=M_1 \oplus M_2$ is
FI-hollow.

Proof: Let N be proper fully invariant submodule of M. Then $N=N\cap M_1 \oplus N\cap M_2$ and both $N\cap M_1$ and $N\cap M_2$ are both fully invariant submodule of M_1 and M_2 respectively [3]. Now $N\cap M_i$ is proper submodule of M_i (i=1,2) since otherwise $N\cap M_i = M_i$ .So $M_i \subset N$ which implies that $M= M_1+ M_2 \subset N$ which is contradiction. Since M_1 and M_2 are FI-hollow then we have $N\cap M_1$ is small submodule of M_1 in M and $N\cap M_2$ is small submodule of M_2 in M. Then $N = N\cap M_1 \oplus N\cap M_2 \ll M_1 \oplus M_2=M$ [5] Therefore, $M =M_1 \oplus M_2$ is FI-hollow. □

Corollary (2.11): A finite direct sum of FI-hollow module is FI-hollow.

Corollary (2.12): A finite direct sum of hollow module is FI-hollow.

3. FI-Hollow-lifting Modules

Hollow-lifting modules introduced by N. orhan, D. Keskin and R. Tribak [1] as a generalization of lifting modules. An R-module M is called Hollow –lifting if every submodule N of M such that M/N is hollow has coessential submodule which is a direct summand of M. Recall that an R-module M is called FI-Lifting if every fully invariant submodule N of M contains a direct summand such that K coessential submodule N in M . Here, we introduce and study the concept FI-hollow-lifting mosules which is a generalization of both hollow –lifting modules and FI-Lifting modules.

Definition (3.1): An R-module M is called FI-hollow-lifting if for every fully invariant submodule N of M with $\frac{M}{N}$ is hollow, there exists a direct summand K of M such that $K \subseteq_{ce} N$ in M.

Examples and Remarks (3.2):

1- Every hollow –lifting module (resp. Lifting module) is FI-Hollow-lifting. But the converse is not true in general. For example , consider $M= Z_p \oplus Z_{p^3}$ as Z-module is FI-hollow-lifting but not hollow-lifting where p is a prime number [1].

2- Z as Z-module is not FI-Hollow-lifting .To see that , assume that Z as Z-module is FI-hollow-lifting. since 2Z is fully invariant submodule of Z_z such that $Z/2Z \cong Z_2$ is hollow so by FI- hollow –lifting property Z_2, there is a direct summand k of Z_z such that $k \subseteq_{ce} 2Z$ in Z .But Z is indecomposable Z-module So k=0.Hence $2Z \ll Z$ which is a contradiction. since $2Z+3Z=Z$ but $3Z \neq Z$.

3-If M is Duo then M is hollow -lifting module if and only if M is FI-hollow-lifting module in particular, a commutative ring R is hollow -lifting if and only if R is FI-hollow-lifting .

4-Every FI-hollow module is FI-hollow-lifting.

The following result gives a characterization of FI-Hollow lifting modules.

Theorem (3.3): An R-module M is FI- hollow-lifting if and only if for every fully invariant submodule N of M with $\frac{M}{N}$ hollow, there exists a submodule K of N such that $M = K \oplus K^*$ and $N \cap K^* << K^*$.

Proof: Let N be a fully invariant submodule of M with $\frac{M}{N}$ hollow.Since M is FI-hollow-lifting then there is a submodule K of M such that $K \subseteq_{ce} N$ in M and $M = K \oplus K^*$, where $K^* \subseteq M$. Let $(N \cap K^*) + X = K^*$, where X submodule K^*. So $M=K + K^*=K + (N \cap K^*)+X$. Now, $\frac{M}{K} = \frac{K+(N\cap K^*)}{K} + \frac{X+K}{K}$. But $K \subseteq_{ce} N$ in M and $K + (N \cap K^*) \subseteq N$. Therefore by proposition [8,p.20], $K \subseteq_{ce} (K + (N \cap K^*))$ in M and so $M = X + K$. Since $M = K \oplus K^*$ and $X \subseteq K^*$ then $X = K^*$ Thus $N \cap K^* << K^*$.

Conversely, let N be a fully invariant submodule of M such that $\frac{M}{N}$ is hollow, then by our assumption, there exists a submodule K of N such that $M = K \oplus K^*$ and $N \cap K^* << K.^*$ Now, we want to show that

$K \subseteq_{ce} N$ in M. Let $\frac{N}{K} + \frac{X}{K} = \frac{M}{K}$ where X is a submodule of M containing K, then $M = N + X$. By modular law, $N = N \cap M = N \cap (K \oplus K^*) = K \oplus (N \cap K^*)$, hence $M = N + X = K + (N \cap K^*) + X$. But $N \cap K^* << K^*$, therefore $N \cap K^* << M$. So $M = K + X = X$ and hence $K \subseteq_{ce} N$ in M. Thus M is FI- hollow-lifting.

By the same manner of the proof of Theorem (3.3), we can give another characterization of FI-hollow -lifting module.

Proposition(3.4): An R-module M is FI-hollow-lifting if and only if for every fully invariant submodule N of M with $\frac{M}{N}$ hollow, there exists a submodule K of N such that $M = K \oplus K^*$ and $N \cap K^* << M$.

Let U and V be two submodule of an R-module M. Recall that V is a supplement of U in M. If V is a minimal element in the set of submodule $L \subseteq M$ with N+L=M. Unlike a complement submodul, ther is a submodule which has no supplement [7]. For example, consider Z as Z-module 2Z has no supplement in Z as Z-module. An R -module M is called supplemented if every submodule of M has a supplement in M. Recall that V of an R-module M is strong supplement of U in M if V is a supplement of U and $V \cap U$ is a direct summand of U [5].

By using strong supplement property, we have another characterization of FI-hollow –lifting modules.

Theorem (3.5): An R-module M is FI- hollow-lifting if and only if for every fully invariant submodule N of M with $\frac{M}{N}$ hollow has a strong supplement in M.

Proof : Suppose that M is a FI- hollow-lifting module and N is a fully invariant submodule of M such that $\frac{M}{N}$ is hollow. Then there is a submodule K of N such that $K \subseteq_{ce} N$ in M and $M = K \oplus K^*$, for some $K^* \subseteq M$. By modular law, $N = N \cap (K \oplus K^*) = K \oplus (N \cap K^*)$. One can easily show that $M = N + K^*$. We want to show that $N \cap K^* << K^*$. Let $(N \cap K^*) + X = K^*$, where $X \subseteq K^*$ So $M = K + K^* = K + (N \cap K^*) + X$. This implies that $M = N + X$ and $\frac{M}{K} = \frac{N+X}{K} = \frac{N}{K} + \frac{X+K}{K}$. Since $K \subseteq_{ce} N$ in M, then $M = X + K$. But $M = K \oplus K^*$ and $X \subseteq K^*$, therefore $X = K^*$ and hence $N \cap K^* << K^*$. Thus N has a strong supplement K^* in M.

Conversely, let N be a fully invariant submodule of M such that $\frac{M}{N}$ is hollow. Then by our assumption there is a strong supplement K of N in M, then $M = N + K, N \cap K << K$ and $N = (N \cap K) \oplus L$, where $L \subseteq M$. Now, $M = N + K = (N \cap K) + L + K = L + K. L \cap K = 0$, so $M = L \oplus K$. We want to show that $L \subseteq_{ce} N$ in M. Let $\frac{N}{L} + \frac{X}{L} = \frac{M}{L}$, where

$X \subseteq M$ containing L, then $N + X = M$. Hence $M = (N \cap K) + L + X$. But $N \cap K << M$, therefore $M = L + X$. Since $L \subseteq X$, then $M = X$. Thus M is FI- hollow-lifting module.

By [2] an R-module M is lifting if and only if every submodule N of M can written in the form N=A $\oplus$ S where A is a direct summand of M and S $<<$ M .We have analogous result for FI-hollow –lifting modules.

Theorem (3.6): The following statmenet are equivalent for an R-module M:

1- M is FI- hollow-lifting .

2-Every fully invariant submodule N of M such that M/N is hollow, can be written as N=K $\oplus$ L with K is a direct summand of M and L$<< M$.

3-Every fully invariant submodule N of M such that M/N hollow , there exists a direct summand K of M such that N=K +L and L $<< M$.

Proof: (1⇒2) Let N be a fully invariant submodule of M such that $\frac{M}{N}$ hollow. Since M is FI- hollow-lifting, there exists a submodule K of M such that $K \subseteq_{ce} N$ in M and $= K \oplus K^*$, where $K^* \subseteq M$. By modular law, $N = N \cap M = N \cap (K \oplus K^*) = K \oplus (N \cap K^*)$. We want to show that $N \cap K^* << K^*$. Let $X \subseteq K^*$ with $(N \cap K^*) + X = K,^*$ then $N + X = M$. Now, $\frac{M}{K} = \frac{N+K}{K} = \frac{N}{K} + \frac{X+K}{K}$. Since $K \subseteq_{ce} N$ in M, then $M = X + K$. But $M = K \oplus K^*$ and $X \subseteq K^*$, therefore $X = K^*$. Let $L = N \cap K^*$. Thus N=K$\oplus$L with K is a direct summand of M and L<<M.

(2⇒3): It is obvious

(3⇒1): let N be a fully invariant submodule of M with $\frac{M}{N}$ hollow. Then by our assumption $N = K + L$, where K is a direct summand of M and $L << M$ such that $M = K \oplus K^*$, for some $K^* \subseteq M$. Since K^* is a supplement of K in M, and since $L << M$, then by [11, p.348] K^* is a supplement of $K + L = N$ in M. So $N \cap K^* << K.^*$Thus by Theorem (3.3),M is FI- hollow-lifting. □

Proposition (3.7): Let M be an indecomposable module .If M is a FI-hollow-lifting module, then either M is hollow or else M has no fully invariant submodule N such that M/N is hollow .

Proof: Suppose that M has fully invariant submodule N such that $\frac{M}{N}$ is hollow. Since M is FI-hollow-lifting, then there is a direct summand K of M such that $K \subseteq_{ce} N$ in M. But M is indecomposable module, therefore $K = 0$, henceN $<<$ M. Thus by [7,p.5] M is hollow.

It is well known that if M is hollow module then M/N is hollow for each submodule N of M. On other direction if M is hollow-lifting then M/N is hollow-lifting for every fully invariant submodule N of M.

Proposition(3.8)_Let M be an R-module. If M is FI-hollow-lifting module, then $\frac{M}{N}$ is FI-hollow-lifting module for every fully invariant submodule N of M.

Proof: Let N be a fully invariant submodule of M. Let $\frac{A}{N}$ be a fully invariant submodule of $\frac{M}{N}$ such that $\frac{\frac{M}{N}}{\frac{A}{N}}$ is hollow. Then by the (third isomorphism theorem) $\frac{\frac{M}{N}}{\frac{A}{N}} \cong \frac{M}{A}$ and hence $\frac{M}{A}$ is hollow. Since $\frac{A}{N}$ and N are fully invariant , then we get A is fully invariant by [6,Lemma(2.2)]. But M is FI-hollow-lifting module, so there exists a submodule K of M such that $K \subseteq_{ce} A$ in M and $M = K \oplus K^*$, for some $K^* \subseteq M$. Now, $N+K \subseteq$ A hence $\frac{N+K}{N} \subseteq \frac{A}{N}$ .We can define a map f: $\frac{M}{K} \rightarrow \frac{M}{N+K}$ as follows $f(m + K) = m + (N + K)$, for all $m \in M$. It is clear that f is an epimorphism. Since $K \subseteq_{ce} A$ in M, then by[8],f $(\frac{A}{K}) << \frac{M}{N+K}$ and hence $(N+K) \subseteq_{ce} A$ in M. By (third isomorphism theorem) we get, $\frac{N+K}{N} \subseteq_{ce} \frac{A}{N}$ in $\frac{M}{N}$. Now, thus by [1,Lemma (5.4)]. $\frac{M}{N} = \frac{K \oplus K^*}{N} = \frac{K+N}{N} \oplus \frac{K^*+N}{N}$ and hence $\frac{N+K}{N}$ is a direct summand of $\frac{M}{N}$ .Thus $\frac{M}{N}$ is FI-hollow-lifting.

Corollary (3.9): Let be R-module .If M is FI-hollow-lifting module, then $\frac{M}{N}$ is FI-hollow-lifting module for every stable submodule N of M.

Corollary (3.10): If R is FI- hollow –lifting module then R/I is FI-hollow-lifting for each two sided ideal I of R.

We do not know in general whether FI-hollow-lifting property is inherited by direct summand .The following results are partial answering the question. When is the FI-hollow-lifting property inherited by direct summand s?

Proposition (3.11): Let M be a FI-hollow-lifting SS-module, then every direct summand of M is FI-hollow-lifting.

Proof: Suppose that M is a FI-hollow-lifting module. Let N be a direct summand of M, then $M = N \oplus N^*$, for some $N^* \subseteq M$.since M is ss-module then N and N^* are fully invariant submodules of M. By the (second isomorphism theorem), $\frac{M}{N^*} \cong N$. Thus by proposition (3.8), N is FI-hollow-lifting. □

Remark: The concepts of FI-hollow-lifting modules and ss-modules are different. For example, Z as Z-module is ss-module which is not FI-hollow-lifting. In other hand M= $Z_{p^\infty} \oplus Z_{p^\infty}$ is FI- hollow-lifting which is not ss-module [9, remark and example (2.2.9)].

Corollary (3.12) : A direct summand of FI-hollow-lifting fully stable module is FI-hollow-lifting.

Corollary(3.13) : A direct summand of FI-hollow-lifting Duo module is FI-hollow-lifting.

Corollary(3.14): An ideal which direct summand of a commutative FI-hollow-lifting ring is FI-hollow-lifting.

Proposition (3.15): Let M be FI-hollow-lifting module. Then every fully invariant coclosed submodule K of M with $\frac{M}{K}$ hollow is a direct summand of M.

Proof: Let K be a fully invariant coclosed submodule of M such that Thus $\frac{M}{K}$ is hollow. Since M is FI-hollow-lifting, then there is a direct summand N of M such that N $\subseteq_{ce} K$ in M Since K is a coclosed submodule of M, then N=K , thus K is a direct summand of M

It is well known that a finite direct sum of (lifting) Hollow – lifting module need not be (lifting)Hollow lifting module. In fact, Z/3Z and Z/27Z are hollow Z-modules and so there are lifting (resp. hollow-lifting) but Z/3Z⊕Z/27Z is not lifting (resp. hollow-lifting) [1].In the following result we assert that a finite direct sum of FI-Hollow – lifting module is FI-hollow-lifting.

Theorem (3.16): If M1 and M_2 are FI-hollow-lifting modules . Then M $=M_1 \oplus M_2$ is FI-hollow-lifting.

Proof: Let N be fully invariant submodule of M such that $\frac{M}{N}$ hollow. Then M= $M_1 \oplus N$ or M= $M_2 \oplus N$. Suppose that M= $M_1 \oplus N$ (the case M= $M_2 \oplus N$ being analogous). Where N$\subseteq M_1$, M= $M_1 \oplus N$ then $\frac{M}{N} = \frac{M1\oplus N}{N} \cong \frac{M1}{M1\cap N}$ is hollow .Then N$\cap$ M_1 and N$\cap M_1$ are fully invariant submodule of M. Since M_1 is FI-hollow-lifting we have N$\cap$ $M_1 = L_1 \oplus S_1$ where L_1 is a direct summand of M_1 and $S_1 \ll M_1$. In similar method, we have N$\cap$ $M_2 = L_2 \oplus S_2$ where L_2 is a direct summand of M_2 and $S_2 \ll M_2$. Then N=L⊕S , where $L = L_1 \oplus L_2$ is a direct summand of M and $S = S_1 \oplus S_2 \ll M$. Therefore, M = $M_1 \oplus M_2$ is FI-lifting module (by Theorem (3.6)).

Corollary (3.17): A finite direct sum of FI-hollow-lifting modules is FI-hollow-lifting.

Corollary (3.18): A finite direct sum of hollow-lifting (lifting) modules is FI-hollow-lifting.

In the following theorem we give another characterization of hollow-lifting modules.

Theorem (3.19): Let M be an R-module. Then M is FI-hollow-lifting if and only if for every fully invariant submodule N of M with $\frac{M}{N}$ hollow, there exists an idempotent e $\in$ End(M) with $e(M) \subseteq N$ and $(I-e)(N) << (I-e)(M)$.

Proof: Let N be a fully invariant submodule of M such that $\frac{M}{N}$ hollow. Since M is FI-hollow-lifting, then by Theorem (3.4), there exists a strong supplement K of N in M. Hence $M=N+K$, $N \cap K << K$ and $N = (N \cap K) \oplus X$ for some $X \subseteq M$. Then $M = N + K = (N \cap K) + X + K = X + K$ and $X \cap K = 0$ and hence $M = X \oplus K$. Let $e : M \to X$ be the natural projection map.One can easily show

that e is an idempotent and $e(M) \subseteq X$.Since $X \subseteq N$, then $e(M) \subseteq N$. Now, $(I-e)(M) = \{(I-e)(m),\ m \in M\} = \{(I-e)(a+b)$, where $a \in X, b \in K\} =$

$\{(I-e)(a+b) = a+b-a = b\} = K$. We want show that $(I-e)(N) = N \cap (I-e)(M)$. Let $x \in (I-e)(N)$, then there is $n \in N$ such that $x=(I-e)(n)=n-e(n)$. Thus $x \in N$ and $x \in (I-e)(M)$. So $x \in N \cap (I-e)(M)$. Hence, $(I-e)(N) \subseteq N \cap (I-e)(M)$. Let $d \in N \cap (I-e)(M)$, then $d \in N$ and $d \in (I-e)(M)$. There is $y \in M$ such that $d = (I-e)(y) = y-e(y)$. Thus $d+e(y)=y \in N$, then $d \in (I-e)(N)$. So $(I-e)(N)=N \cap (I-e)(M)= N \cap K << K$. Hence, $(I-e)(N) << (I-e)(M)$.

Conversely, let N be a fully invariant submodule of M such that $\frac{M}{N}$ is hollow. By our assumption there exists an idempotent $e \in End(M)$ with $e(M) \subseteq N$ and $(I-e)(N) << (I-e)(M)$. We Claim that $M=e(M) \oplus (I-e)(M)$. To show that, let $m \in M$ then $m = m+e(m)-e(m)=e(m)+m-e(m)=e(m)+ (I-e)(m)$. Thus $M=e(M) + (I-e)(M)$. Now, let $w \in e(M) \cap (I-e)(M)$, then $w = e(m_1)$ and $w=(I-e)(m_2)$, for some $m_1, m_2 \in M$. So $e(w)=e(m_1)=e((I-e)(m_2))=e(m_2)-e(m_2) = 0$, then $e(e(m_1)) = e(m_1) = 0$, hence $w = 0$. Thus $M=e(M) \oplus (I-e)(M)$. Clearly, $N \cap (I-e)(M)=(I-e)(N)$.Since $(I-e)(N) << (I-e)(M)$, then $N \cap (I-e)(M) << (I-e)(M)$, thus M is FI-hollow-lifting.

Proposition (3.20): Let M be an indecomposable FI- hollow-lifting module, If M has a maximal fully invariant submodule then it is unique.

Proof: Let N be a maximal fully invariant submodule of M . Assume that M has another maximal fully invariant submodule say K which is different from N, then N+K=M . By [11, p.41], $\frac{M}{N}$ a simple module and hence hollow. Since M is FI-hollow-lifting module, then there is a direct summand A of M such that $A \subseteq_{ce} N$ in M. But M is indecomposable module then A=0, hence $N << M$, this implies that $M = K$ that is a contradiction, thus M has a unique maximal fully invariant submodule. □

Proposition (3.21): If M is FI-hollow-lifting module a local ring R then for each fully invariant submodule Ra ($a \in M$) with $\frac{M}{Ra}$ hollow, either Ra is a direct summand of M or $Ra << M$.

Proof: Let $a \in M$ such that $\frac{M}{Ra}$ is hollow. Since M is FI-hollow-lifting module, then by Theorem (3.6), Ra=K⊕L, where K is a direct summand of M and $L << M$. Since R is local ring, then by the [10, corollary 7.1.3, p.171], we have Ra is local. Thus we get either Ra=K or Ra=L. This implies that either Ra is a direct summand of M or $Ra << M$.

It is well-known the Jacobson radical Rad(M) =The sum of all small submodules of M [8].

Proposition (3.22): Every fully invariant N of FI-hollow-lifting module M with $\frac{M}{N}$ hollow and Rad(M)=0 is a direct summand of M.

Proof: Let N be a fully invariant submodule of M such that $\frac{M}{N}$ is hollow. Since M is FI-hollow-lifting, then by Theorem (3.6), N can be written as N=K⊕ L , where K is a direct summand of M and $L << M$. But $Rad(M)$=0, so $L = 0$ and hence N=K. Thus N is a direct summand of M. □

Proposition (3.23): Let M be FI-hollow-lifting module having a fully invariant maximal submodule N of M. Then M has a local submodule which is a direct summand.

Proof: Suppose that M is FI-hollow-lifting module and let N be a fully invariant maximal submodule of M. So by [5, p.41], $\frac{M}{N}$ is simple. Hence $\frac{M}{N}$ is hollow. By Theorem (3.4), M=N+K, $N \cap K$<<K and N=($N \cap K$) ⊕ L, where $L \subseteq M$.Then M= ($N \cap K$) ⊕ L +K. But N ∩ K<<M (since $N \cap K$<<K), thus M=L ⊕ K. Since K is a supplement of a maximal submodule, then by [12, p.348], K is local. □

Let M be an R-module. Recall that an R-module P is called Projective if for any epimorphism φ : M→ N and for any homomorphism f: P→N there is homomorphism h: $P \to M$ such that f= φh. Also an R-module P is called projective cover of M if, P is projective and there exists an epimorphism $\varphi : P \to M$ with $ker\varphi << P$.

Proposition(3.24): Let M be a projective module. Then the following statements are equivalent:

1-M is FI-hollow-lifting module.

2-For every fully invariant submodule N of M such that $\frac{M}{N}$ is hollow, $\frac{M}{N}$ has a projective cover.

Proof: 1⇒2 Let N be a fully invariant submodule N of M such that $\frac{M}{N}$ is hollow. Since M is FI-hollow-lifting module, then by Theorem (3.3), there exists a submodule K of N such that $M=K\oplus K^*$, for some $K^*\subseteq M$ and $N \cap K^* << K^*$.

Now, consider the following two short exact sequences:

$$0 \to N \overset{i_1}{\to} N+K^* \overset{T_1}{\to} \frac{N+K^*}{N} \to 0$$
$$0 \to N \cap K^* \overset{i_2}{\to} K^* \overset{T_2}{\to} \frac{K^*}{N\cap K^*} \to 0$$

Where i_1 , i_2 are the inclusion maps and T_1 , T_2 are the natural epimorphisms. By the (second isomorphism theorem), $\frac{M}{N} = \frac{N+K^*}{N} \cong \frac{K^*}{N\cap K^*}$. Since M is a projective and K^* is a direct summand of M, then K^* is a projective. But $ker\, T_2 = N \cap K^* << K^*$, therefore K^* is a projective cover of $\frac{K^*}{N\cap K^*}$. Since $\frac{M}{N} \cong \frac{K^*}{N\cap K^*}$, thus $\frac{M}{N}$ has a projective cover.

(2⇒1). Let N be a fully invariant submodule of M such that $\frac{M}{N}$ is hollow and let $\varphi : M \to \frac{M}{N} \to 0$ be the natural epimorphism. By (2), $\frac{M}{N}$ has a projective cover. Thus by Lemma [12, 17.17], there exists a decomposition $M = M_1 \oplus M_2$ such that $\varphi|M_2 : M_2 \to \frac{M}{N} \to 0$ is a projective cover and $M_1 \subseteq Ker\varphi$. This implies that $M_1 \subseteq N$ and $ker(\varphi|\, M2) = N \cap M_2 << M_2$. Thus M is FI-hollow-lifting module. By proposition (3.3)

Corollary (3.25): A ring R is a FI-hollow-lifting if and only if R/I has a projective cover for every two sided ideal of R.

Proposition (3.26): Let R be an indecomposable ring and M be a projective R-module. If M is FI--hollow-lifting module, then for each cyclic fully invariant submodule Ra ($a \in M$) with $\frac{M}{Ra}$ hollow, either Ra is projective summand of M or $Ra << M$.

Proof: Let N be a cyclic fully invariant submodule of M with M/N is hollow. Let N =Ra Suppose that M is a projective FI-hollow-lifting module and $a \in M$. Then by Theorem (3.5), N can be written as $N= K \oplus L$, where K is a direct summand of M and $L << M$. Now, let $\varphi: R \rightarrow N$ be a map defined by $\varphi(r)=ra$, for all $r \in R$. It is clear that φ is an epimorphism. Let $\rho: N \rightarrow K$ be a projection map. Clearly $\rho \circ \varphi : R \rightarrow K$ is an epimorphism. Consider the following short exact sequence:

$$0 \rightarrow ker(\rho \circ \varphi) \xrightarrow{i} R \xrightarrow{\rho \circ \varphi} K \rightarrow 0$$

where i is the inclusion map. Since M is projection K is a projective then by [11, p. 150], this sequence is splits. Thus $ker(\rho \circ \varphi)$ is a summand of R. Now, $ker(\rho \circ \varphi)= \{r \in R, \rho \circ \varphi(r)=0\}=\{r \in R, \rho \circ (\varphi(r))=0\}=\{r \in R, \varphi(r) \in L\}=\varphi^{-1}(L)$.Thus $\varphi^{-1}(L)$ is a direct summand of R. But R is an indecomposable ring, therefore either $\varphi^{-1}(L)=0$, then $L=0$ and hence $N=K$. Then N is a projective direct summand of R or $\varphi^{-1}(L)=R$, then $\varphi\ \varphi^{-1}(L)= \varphi(R)$ and hence $L=N$. This implies that $N << M$.

REFRENCES

1. Orhan, N. D. K. Tutuncu and R. Tribak, *On hollow-lifting modules*, Taiwanese J. Math., 11 (2), (2007), 545-568
2. TaLeBi Y. and T.AmoozeGar, strong FI-Lifting module.International Electronic J.of Algebra 3(2008), 75-82.
3. Ozcan A. C. Duo Modules,Glasgow Math. J. Trust 48(2006)533-545.
4. Abbas M. S. On fully stable modules, Ph.D. Thesis, Univ. of Baghdad, 1991.
5. Clark, J. C. Lomp, N. Vanaja and R. Wisbauer, *Lifting modules*, Frontiers in Mathematics, Birkhäuser, 2006.
6. TALEBI Y. AND T. AMOOZEGAR fully invariant TM-Lifting Modules, Albanian J. of Math. V. 3, 19-53, 1930-1235: (2009) .
7. Lomp, C. *On dual Goldie dimension, Diploma Thesis*, University of Dusseldorf (1996)..
8. Payman M. H., Hollow modules and semihollow modules, M.Sc., Thesis, University of Baghdad 2005.
9. ALsaadi Saad A. Abdulkadhim, S-extending modules and Related Concepts. Ph.D. thesis, AL-Mustinsiriya Univ. 2007
10. Kasch, F. Modules and rings, Academic Press., London, 1982.

11. Wisbauer, R. Foundations of module and ring theory, Gordon and Breach, Philadelphia, 1991.

12. Anderson F. W. and K. R. Fuller, Rings and categories of modules, Springer- Verlag, New York, 1974.

On Fuzzy Setting of Complex Version of the Malceski's Extension Theorem of N-Bounded N-Linear Functional in N-Normed Space

Faria Ali C.
Department of Mathematics, College of Science, Al-Mustansiriyah University
Received 17/3/2013 – Accepted 15/9/2013

الخلاصة

ان الغرض الرئيسي من هذا البحث يقسم الى سمتين رئيسيتين:-
الهدف الاول هو دراسة مبرهنة هان- بناخ الموسعة للدالي n- الخطي n- المقيد في الفضاءات n- المعياريه والتي تعود الى سريفاستافا واخرون والتي تعتبر النسخة العقدية لمبرهنة توسع لملساسكي للدالي n- الخطي n- المقيد في الفضاء n- المعيار كما تم اعطاء بعض الحقائق المتعلقة بها.
الهدف الثاني هو تقديم مبرهنة هان- بناخ الموسعة للدالي n- الخطي n- المقيد الضبابي في الفضاء n- المعياري الضبابي ، للدالي n- الخطي n- المضاد المقيد في الفضاء n- المضاد المعياري الضبابي وللدالي n- الخطي n- المقيد الضبابي الحدسي في الفضاء n- المعياري الضبابي الحدسي كما تم اعطاء بعض تطبيقات المتعلقة بها.

ABSTRACT

The main purpose of this paper is divided into two main aspects:-
First, we study Hahn–Banach extension theorem for n-bounded n-linear functional in n-normed spaces due to Srivastava and et. al. which is complex verision of the malceski's extension theorem of n-bounded n-linear functionals in n-normed space and give some results that are related with it.

Second, we introduce Hahn-Banach extension theorem for fuzzy n-bounded n-linear functional in fuzzy n-normed space, fuzzy n-antibounded n-linear functional in fuzzy n-antinormed space and intuitionistic fuzzy n-bounded n-linear functional in intuitionistic fuzzy n-normed space then we give some applications that are related with it.

INTRODUCTION

The theory of real n-normed linear space has been introduced by Gahler in [1]. In [2], Narayanan and Vijayabalaji introduced fuzzy n-normed space. Also the definitions of fuzzy n-antinormed linear space and intuitionistic fuzzy n-normed linear space was introduced in [3]. Malceski in [4] gave the required Hahn-Banach type extension theorem for real n-normed linear spaces. The new Hahn–Banach extension theorem for n-bounded n-linear functionals in complex n-normed linear spaces which generalize all the known results has been established in [5]. The Hahn–Banach theorem in fuzzy normed space and fuzzy antinormed space were given in [6] and [7] respectively. In this paper some results related to applications of the Hahn–Banach theorem extension in n-normed space are established and then the Hahn-Banach extension theorem due to Srivastava and et.al. in fuzzy n-normed linear space, fuzzy n-antinormed linear space and intuitionistic fuzzy n-normed linear space are discussed then some results related to applications of the Hahn–Banach theorem extension in fuzzy setting are proved. Some facts that appeared in [6], [7] and [8] are generalized in this work.

Hahn-Banach Extension Theorem in N-Normed Spaces

In this section, some theorem of Hahn-Banach extension in n-normed space due to Srivastava and et.al. are presented. Also, some results related to it are discussed.

Definition 1, [5]:-

Let X be a linear space over F (where F is the field of real or complex numbers) of dimension $d \geq n$. A function

$\|.,...,\|: X \times X \times ... \times X = X^n \longrightarrow R$ satisfy the following axioms:

(N_1)

$\|x_1, x_2,...,x_n\| = 0$ if and only if $x_1, x_2,...,x_n$ are linearly dependent.

(N_2) $\|x_1, x_2,...,x_n\|$ is an invariant under any permutation of $x_1, x_2,...,x_n$

(N_3) $\|x_1, x_2,...,cx_n\| = |c| \, \|x_1, x_2,...,x_n\|$ for any $c \in F$. (N_4) $\|x_1, x_2,...,x_{n-1}, x+y\| \leq \|x_1, x_2,..x_{n-1}, x\| + \|x_1, x_2,...,x_{n-1}, y\|$; where $x_1,...,x_n, x, y \in X$.

is said to be an n-norm on X and the pair $(X, \|.,...,\|)$ is called an n-normed space.

Definition 2, [5]:-

Let $W_{i,i=1,2,...,n}$ be a n-linear subspaces of the linear space X. A mapping $T: W_1 \times W_2 \times ... \times W_n \to F$ is said to be a n-linear functional in case satisfies the following conditions: for all $x_i, y_i \in W_i, i = 1,2,..n$.

$$(1) T(x_1 + y_1, x_2 + y_2,...,x_n + y_n) = \sum_{\substack{z_i \in \{x_i, y_i\} \\ i=1,2,...,n}} T(z_1, z_2,...,z_n)$$

$$(2) T(\alpha_1 x_1, \alpha_2 x_2,...,\alpha_n x_n) = \alpha_1 \alpha_2 .. \alpha_n T(x_1, x_2,...,x_n) \text{ for all } \alpha_i \in F,$$

$i = 1,2,...,n$.

Definition 3, [5]:-

Let $W_{i,i=1,2,...,n}$ be a n-linear subspaces of the n-normed space X. The n-linear functional T on $W_1 \times W_2 \times ... \times W_n$ is said to be n-bounded on $W_1 \times W_2 \times ... \times W_n$ in case there exists K>0 such that for each $(x_1, x_2,...,x_n) \in W_1 \times W_2 \times ... \times W_n$, $|T(x_1, x_2,...,x_n)| \leq K \|x_1, x_2,...,x_n\|$

Proposition 4, [5]:-

Let $W_{i,i=1,2,...,n}$ be a n-linear subspaces of the n-normed space X and T be n-bounded n-linear functional on $W_1 \times W_2 \times ... \times W_n$ then

$$\|T\| = \operatorname{Sup}\left\{\frac{|T(x_1, x_2, \ldots, x_n)|}{\|x_1, x_2, \ldots, x_n\|} : (x_1, x_2, \ldots x_n) \in \overset{n}{\underset{i=1}{X}} W_i \text{ and } \|x_1, x_2, \ldots, x_n\| \neq 0\right\}$$

Is a norm on linear space of all n-bounded n-linear functional.

Note 5 :-

Let $W_{i,i=1,2,\ldots,n.}$ be a n-linear subspaces of the n-normed space X . We denote by $(W_1 \times W_2 \times \ldots \times W_n, F)^*$ the set of all n-bounded n-linear functionals on $W_1 \times W_2 \times \ldots \times W_n$ and we call $(W_1 \times W_2 \times \ldots \times W_n, F)^*$ the conjugate space of $W_1 \times W_2 \times \ldots \times W_n$.

Theorem 6, [5]:-

Let W be a linear subspace of an n-normed linear space X over F and let $x_1, x_2, \ldots, x_{n-1} \in X$. If T is an n-bounded n-linear functional on $W \times [x_1] \times \ldots \times [x_{n-1}]$ then there exists an n-bounded n-linear functional $\widetilde{T}$ on $X \times [x_1] \times \ldots \times [x_{n-1}]$ satisfying

1- $\|\widetilde{T}\| = \|T\|$

2- $\widetilde{T}(x, \lambda_1 x_1, \ldots, \lambda_{n-1} x_{n-1}) = T(x, \lambda_1 x_1, \ldots, \lambda_{n-1} x_{n-1})$

Theorem 7:-

Let $(X, \|.,\ldots,\|)$ be n-normed space and $x, x_1, x_2, \ldots, x_{n-1} \in X$ are linearly independent elements of X. Then there exist a n-bounded n-linear functional $\widetilde{T}$ on $X \times [x_1] \times [x_2] \times \ldots \times [x_{n-1}]$ such that

$\|\widetilde{T}\| = 1, \quad \widetilde{T}(x, x_1, \ldots, x_{n-1}) = \|x, x_1, \ldots, x_{n-1}\|$

Proof:-

We consider the subspace

$Z = \{(t\ x\ , t_2 x_1, \ldots, t_n x_{n-1}) : t_i \in F, i = 1,2,\ldots,n\}$ of X^n and defined a n-linear functional T on Z by $T(t_1 x\ , t_2 x_1, \ldots, t_n x_{n-1}) = \|t_1 x\ , t_2 x_1, \ldots, t_n x_{n-1}\| = |t_1||t_2|..|t_n|\|x\ , x_1, \ldots, x_{n-1}\|$

Then T is n-bounded n-linear and has norm $\|T\| = 1$. Then by theorem 6 implies that T has n-bounded n-linear functional of norm $\|\widetilde{T}\| = \|T\| = 1$ and $\widetilde{T}(x, x_2, \ldots, x_n) = T(x, x_1, \ldots, x_{n-1}) = \|x, x_1, \ldots, x_{n-1}\|$

Theorem 8:-

For every linearly independent elements $x, x_1, x_2, \ldots, x_{n-1} \in X$ we have

$$\|x, x_1, \ldots, x_{n-1}\| = \sup_{\substack{T \in (X \times [x_1] \times \ldots \times [x_{n-1}], F)^* \\ T \neq 0}} \frac{|T(x, x_1, \ldots, x_{n-1})|}{\|T\|}$$

Proof:-

$$\sup_{\substack{T\in(X\times[x_1]\times\ldots[x_{n-1}],F)^* \\ T\neq 0}} \frac{|T(x,x_1,\ldots,x_{n-1})|}{\|T\|} \geq \frac{|\tilde{T}(x,x_1,\ldots,x_{n-1})|}{\|\tilde{T}\|}$$

$$= \frac{\|x,x_1,\ldots,x_{n-1}\|}{1}$$

$$= \|x,x_1,\ldots,x_{n-1}\|$$

And from $|T(x,x_1,\ldots,x_{n-1})| \leq \|T\|\|x,x_1,\ldots,x_{n-1}\|$ we obtain

$$\sup_{\substack{T\in(X\times[x_1]\times\ldots\times[x_{n-1}],F)^* \\ T\neq 0}} \frac{|T(x,x_1,\ldots,x_{n-1})|}{\|T\|} \leq \|x,x_1,\ldots,x_{n-1}\|$$

Hence

$$\|x,x_1,\ldots,x_{n-1}\| = \sup_{\substack{T\in(X\times[x_1]\times\ldots\times[x_{n-1}],F)^* \\ T\neq 0}} \frac{|T(x,x_1,\ldots,x_{n-1})|}{\|T\|}$$

Fuzzy n-Normed Linear Space, Fuzzy n-Antinormed Linear Space and Intuitionistic Fuzzy n-Normed Linear Space

In this section, we give some definitions and theorems which will be needed in the work.

Definition 9, [6]:-

A fuzzy subset N of $X\times R$ is said to be a fuzzy norm on a linear space X in case for each $x,y\in X$ and $c\in F$, the following conditions hold:-

(FN_1) $N(x,t)=0$ for each $t\leq 0$;

(FN_2) $N(x,t)=1$ for each $t>0$ if and only if $x=0$

(FN_3) If $0\neq c\in F$ then $N(cx,t)=N(x,\frac{t}{|c|})$ for each $t>0$.

(FN_4) $N(x+y,s+t)\geq \min\{N(x,s),N(y,t)\}$ for each $s,t\in R$.

(FN_5) $N(x,.)$ is a non-decreasing function of R and $\lim_{t\to\infty} N(x,t)=1$

The pair (X,N) will be referred to as a fuzzy normed space

Example 10, [6]:-

Let $(X,\|.\|)$ be a normed linear space. Define

$$N^*(x,t)=\begin{cases}0 & \text{if } t\leq\|x\|, t\in R, x\in X\\ 1 & \text{if } t>\|x\|, t\in R, x\in X\end{cases} \quad \ldots\ldots\ldots\ldots(1)$$

Then (X,N^*) is a fuzzy normed linear space.

Theorem 11, [6]:-

Let (X,N) be a fuzzy normed space satisfying the following two conditions:

(FN_6) For each $t > 0$, $N(x,t) > 0$ implies $x = 0$

(FN_7) For $x \neq 0$, $N(x,.)$ is a continuous function of R and strictly increasing on the subset $\{t : 0 < N(x,t) < 1\}$ of R.

Let $\|x\|_\alpha = \text{Inf}\{t > 0 : N(x,t) \geq \alpha\}, \alpha \in (0,1)$ and $N_1 : X \times R \longrightarrow [0,1]$ be a function defined by

$$N_1(x,t) = \begin{cases} \text{Sup}\{\alpha \in (0,1) : \|x\|_\alpha \leq t\} & \text{for } (x,t) \neq (0,0) \\ 0 & \text{for } (x,t) = (0,0) \end{cases}$$

Then,

(a) $\{\|.\|_\alpha : \alpha \in (0,1)\}$ is a family of $\alpha - 2-$norms corresponding to the fuzzy normed space (X,N).

(b) (X, N_1) is a fuzzy normed space.

(c) $N_1 = N$

Definition 12, [2]:-

A fuzzy subset N of $X^n \times R$ into [0,1] is said to be a fuzzy n-norm on the linear space X in case the following axioms hold:

(FN_1) $N(x_1, x_2, ..., x_n, t) = 0$ for each $t \leq 0$.

(FN_2) $N(x_1, x_2, ..., x_n, t) = 1$ for each $t > 0$ if and only if $x_1, x_2, ..., x_n$ are linearly dependent.

(FN_3) $N(x_1, x_2, ..., x_n, t)$ is an invariant under any permutation of $x_1, x_2, ..., x_n$.

(FN_4) If $0 \neq c \in R$ then $N(x_1, x_2, ..., cx_n, t) = N(x_1, x_2, ..., x_n, \frac{t}{|c|})$ for each $t > 0$.

(FN_5) for each $s, t \in R$

$N(x_1, x_2, .. x_{n-1}, x + y, s + t) \geq \min\{N(x_1, x_2, ..., x_{n-1}, x, s), N(x_1, x_2, ..., x_{n-1}, y, t)\}$

(FN_6) $N(x_1, x_2, ... x_n, .)$ is a non-decreasing function of R and $\lim_{t \to \infty} N(x_1, x_2, ..., x_n, t) = 1$

The pair (X,N) will be referred to a fuzzy n-normed space.

Theorem 13, [9]:-

Let (X,N) be a fuzzy n-normed space satisfying the following conditions:

(FN_7) For each $t > 0, N(x_1, x_2, ..., x_n, t) > 0$ implies $x_1, x_2, ..., x_n$ are linearly dependent.

(FN_8) For $x_1, x_2, ..., x_n$ are linearly independent $N(x_1, x_2, ..., x_n, t)$ is a continuous of $t \in R$ and strictly increasing in the subset $\{t : 0 < N(x_1, x_2, ..., x_n, t) < 1\}$ of R.

Let $\|x_1,x_2,\ldots,x_n\|_\alpha = \mathrm{Inf}\{t : N(x_1,x_2,\ldots,x_n,t) \geq \alpha\}$, $\alpha \in (0,1)$ and $N_1 : X^n \times R \longrightarrow [0,1]$ is defined by

$$N_1(x_1,x_2,\ldots,x_n,t) = \begin{cases} \mathrm{Sup}\{\alpha \in (0,1) : \|x_1,x_2,\ldots,x_n\|_\alpha \leq t\} & \text{when } x_1,x_2,\ldots,x_n \text{ are linearly independent}, t \neq 0 \\ 0 & \text{otherwise} \end{cases}$$

Then

(a) $\{\|.,\ldots,\|_\alpha : \alpha \in (0,1)\}$ is an ascending family of $\alpha - n -$ norms corresponding to the fuzzy n-normed space (X,N).

(b) (X, N_1) is a fuzzy $n -$ normed space.

(c) $N_1 = N$

Definition 14, [10]:-

A fuzzy subset M of $X \times R$ is said to be a fuzzy antinorm on a linear space X in case for each $x, y \in X$ and $c \in F$, the following conditions hold:-

(FM_1) $M(x,t) = 1$ for each $t \leq 0$;

(FM_2) $M(x,t) = 0$ for each $t > 0$ if and only if $x = 0$

(FM_3) If $0 \neq c \in F$ then $M(cx,t) = M(x, \frac{t}{|c|})$ for each $t > 0$.

(FM_4) $M(x+y, s+t) \leq \max\{M(x,s), M(y,t)\}$ for each $s,t \in R$.

(FM_5) $M(x,.)$ is a non-increasing function of R and $\lim\limits_{t\to\infty} M(x,t) = 0$

The pair (X,M) will be referred to as a fuzzy antinormed linear space.

Example 15, [10]:-

Let $(X, \|.\|)$ be a normed linear space. Define

$$M^*(x,t) = \begin{cases} 0 & \text{if } t > \|x\|, t \in R, x \in X \\ 1 & \text{if } t \leq \|x\|, t \in R, x \in X \end{cases} \qquad \ldots\ldots\ldots\ldots\ldots(2)$$

Then (X, M^*) is a fuzzy antinormed linear space.

Theorem 16, [7]:-

Let (X,M) be a fuzzy antinormed space satisfying the following two conditions:

(FM_6) For each $t > 0$, $M(x,t) < 1$ implies $x = 0$

(FM_7) For $x \neq 0$, $M(x,.)$ is a continuous function of R and strictly decreasing on the subset $\{t : 0 < M(x,t) < 1\}$ of R.

Let $\|x\|_\alpha = \mathrm{Inf}\{t : M(x,t) \leq 1 - \alpha\}, \alpha \in (0,1)$ and $M_1 : X \times R \longrightarrow [0,1]$ be a function defined by

$$M_1(x,t)=\begin{cases}\operatorname{Inf}\{1-\alpha\in(0,1):\|x\|_\alpha\le t\} & \text{for } (x,t)\neq(0,0)\\ 1 & \text{for } (x,t)=(0,0)\end{cases}$$

Then,

(a) $\{\|\cdot\|_\alpha:\alpha\in(0,1)\}$ is a family of $\alpha-$norms corresponding to the fuzzy antinormed space (X,M).

(b) (X, M_1) is a fuzzy antinormed linear space.

(c) $M_1=M$

Definition 17, [3]:-

A fuzzy subset M of $X^n\times R$ into [0,1] is said to be a fuzzy n-antinorm on the linear space X in case the following axioms hold:

(FM_1) $M(x_1,x_2,\dots,x_n,t)=1$ for each $t\le 0$.

(FM_2) $M(x_1,x_2,\dots,x_n,t)=0$ for each $t>0$ if and only if $x_1,x_2,\dots,x_n$ are linearly dependent.

(FM_3) $M(x_1,x_2,\dots,x_n,t)$ is an invariant under any permutation of $x_1,x_2,\dots,x_n$.

(FM_4) If $0\neq c\in R$ then $M(x_1,x_2,\dots,cx_n,t)=M(x_1,x_2,\dots x_n,\frac{t}{|c|})$ for each $t>0$.

(FM_5) for each $s,t\in R$

$M(x_1,x_2,\dots,x_{n-1},x+y,s+t)\le\max\{M(x_1,x_2,\dots,x_{n-1},x,s),M(x_1,x_2,\dots,x_{n-1},y,t)\}$

(FM_6) $M(x_1,x_2,\dots,x_n,.)$ is a non-increasing function of R and $\lim_{t\to\infty}M(x_1,x_2,\dots,x_n,t)=0$

The pair (X,M) will be referred to as a fuzzy n-antinormed space.

Theorem 18, [11]:-

Let (X,M) be a fuzzy n-antinormed space satisfying the following conditions:

(FM_7) For each $t>0, M(x_1,x_2,\dots,x_n,t)<1$ implies $x_1,x_2,\dots,x_n$ are linearly dependent.

(FM_8) For $x_1,x_2,\dots,x_n$ are linearly independent $M(x_1,x_2,\dots,x_n,t)$ is a continuous of $t\in R$ and strictly decreasing in the subset $\{t:0<M(x_1,x_2,\dots,x_n,t)<1\}$ of R.

Let $\|x_1,x_2,\dots,x_n\|_\alpha=\operatorname{Inf}\{t:M(x_1,x_2,\dots,x_n,t)\le 1-\alpha\}$, $\alpha\in(0,1)$ and $M_1:X^n\times R\longrightarrow[0,1]$ is defined by

$$M_1(x_1,x_2,\dots,x_n,t)=\begin{cases}\operatorname{Inf}\{1-\alpha\in(0,1):\|x_1,x_2,\dots,x_n\|_\alpha\le t\} & \text{when } x_1,x_2,\dots,x_n \text{ are linearly independent}, t\neq 0\\ 1 & \text{otherwise}\end{cases}$$

Then

(a) $\{\|.,...,\|_\alpha : \alpha \in (0,1)\}$ is a family of $\alpha - n -$ norms corresponding to the fuzzy n-antinormed linear space (X, M).

(b) (X, M_1) is a fuzzy $n -$ antinormed linear space.

(c) $M_1 = M$

Definition 19, [8]:-

An intuitionistic fuzzy norm on X is a set of the form $A = \{((x,t), N(x,t), M(x,t)) \,|\, (x,t) \in X \times R^+\}$, where N, M are fuzzy subsets of $X \times R^+$, where the functions N and M denote the degree of membership and non-membership of the element $(x,t) \in X \times R^+$, satisfying the following conditions:

$(IF\,N_1)$ N is a fuzzy norm on a linear space X.

$(IF\,N_2)$ M is a fuzzy antinorm on a linear space X.

$(IF\,N_3)$ $N(x,t) + M(x,t) \le 1,\ \forall (x,t) \in X \times R^+$.

Remark 20:-

It is obvious that the fuzzy subset $A^* = \{((x,t), N^*(x,t), M^*(x,t)) \,|\, (x,t) \in X \times R^+\}$ ....(3)

is an intuitionistic fuzzy norm where N^* and M^* are defined in eq.(1) and eq. (2) respectively.

Theorem 21, [11]:-

Let A be an intuitionistic fuzzy norm on a linear space X satisfying the following conditions:

(IFN_4) For each $t > 0$, $N(x,t) > 0$ and $M(x,t) < 1$ implies $x = 0$

(IFN_5) For $x \ne 0$, $N(x,.)$ is a continuous function of R^+ and strictly increasing on the subset $\{t : 0 < N(x,t) < 1\}$ of R^+ and $M(x,.)$ is a continuous function of R^+ and strictly decreasing on the subset $\{t : 0 < M(x,t) < 1\}$ of R^+.

Let

$\|x\|_\alpha = \mathrm{Inf}\{t : N(x,t) \ge \alpha, M(x,t) \le 1 - \alpha\}, \alpha \in (0,1)$ and $N_1 : X \times R^+ \longrightarrow [0,1]$

$M_1 : X \times R^+ \to [0,1]$

be a functions defined by

$N_1(x,t) = \mathrm{Sup}\{\alpha \in (0,1) \,|\, \|x\|_\alpha \le t\}$ and

$M_1(x,t) = \mathrm{Inf}\{1 - \alpha \in (0,1) \,|\, \|x\|_\alpha \le t\}$

$A_1 = \{((x,t), N_1(x,t), M_1(x,t)) \,|\, (x,t) \in X \times R^+\}$

Then

(a) $\{\|\cdot\|_\alpha : \alpha \in (0,1)\}$ is a family of α – norms corresponding to the intuitionistic fuzzy norm A.

(b) A_1 intuitionistic fuzzy norm.

(c) $A_1 = A$

Definition 22, [11]:-

An intuitionistic fuzzy n-norm on X is a set of the form $A = \{((x_1,...,x_n,t), N(x_1,...,x_n,t), M(x_1,...,x_n,t)) \,|\, (x_1,...,x_n,t) \in X \times ... \times R^+\}$, where N, M are fuzzy subsets of $X \times X \times R^+$, where the functions N and M denotes the degree of membership and non-membership of the element $(x_1, x_2, .. x_n, t) \in X \times X \times ... \times R^+$, satisfying the following conditions:

(IFN_1) N is a fuzzy n-norm on a linear space X.

(IFN_2) M is a fuzzy n-antinorm on a linear space X.

(IFN_3) $N(x_1,x_2,...,x_n,t) + M(x_1,x_2,...,x_n,t) \le 1$

Theorem 23, [11]:-

Let A be an intuitionistic fuzzy n-norm satisfying the following conditions:

(IFN_4)For each $t > 0$, $N(x_1,x_2,...,x_n,t) > 0$ and $M(x_1,x_2,...,x_n,t) < 1$ implies $x_1, x_2,...,x_n$ are linearly dependent

(IFN_5) For $x_1, x_2,...,x_n$ are linearly independent, $N(x_1,x_2,...,x_n,.)$ is a continuous function of R^+ and strictly increasing on the subset $\{t : 0 < N(x_1,x_2,...,x_n,t) < 1\}$ of R^+ also $M(x_1,x_2,...,x_n,.)$ and is a continuous function of R^+ and strictly decreasing on the subset $\{t : 0 < M(x_1,x_2,...,x_n,t) < 1\}$ of R^+.

Let

$\|x_1,x_2,...,x_n\|_\alpha = \text{Inf}\{t : N(x_1,x_2,...,x_n,t) \ge \alpha, M(x_1,x_2,...,x_n,t) \le 1-\alpha\}$, $\alpha \in (0,1)$

be a $N_1 : X \times X \times ... R^+ \longrightarrow [0,1]$, $M_1 : X \times X \times ... \times R^+ \to [0,1]$ functions defined by

$N_1(x_1,x_2,...,x_n,t) = \text{Sup}\{\alpha \in (0,1) \,|\, \|x_1,x_2,...,x_n\|_\alpha \le t\}$

and

$M_1(x_1,x_2,...,x_n,t) = \text{Inf}\{1-\alpha \in (0,1) \,|\, \|x_1,x_2,...,x_n\|_\alpha \le t\}$

$A_1 = \{((x_1,x_2,...,x_n,t), N_1(x_1,x_2,...,x_n,t), M_1(x_1,x_2,...,x_n,t))$
$|(x_1,x_2,...,x_n,t) \in X \times X \times ... \times R^+\}$

Then

(a) $\{\|.,...,\|_{\alpha} : \alpha \in (0,1)\}$ is a family of $\alpha - n -$ norms corresponding to the intuitionistic fuzzy n-norm A.

(b) A_1 intuitionistic fuzzy n-norm.

(c) $A_1 = A$

Hahn–Banach Extension Theorem in Fuzzy n-Normed Linear Space, Fuzzy n-Antinormed Linear Space and Intuitionistic Fuzzy n-Normed Linear Space

In this section, we discuss and present complex versions of the Makeski's Hahn-Banach theorem in fuzzy n-bounded n-linear functional in fuzzy n-normed linear space, fuzzy n-antibounded n-linear functional in fuzzy n-antinormed linear space and intuitionistic fuzzy n-bounded n-linear functional in intuitionistic fuzzy n-normed linear space.

We start this section by giving the definition of fuzzy n-bounded n-linear functional which based on the idea that appeared in [8].

Definition 24:-

Let $T:(X,N) \longrightarrow (F,N^*)$ be a n-linear functional where (X,N) be a fuzzy n-normed linear space and N^* be a fuzzy norm defined in eq.(1). T is said to be fuzzy n-bounded on X in case there exists a positive number K such that ,for each $(x_1, x_2,...,x_n) \in X$ and $s > 0$,

$$N^*(T(x_1, x_2,...,x_n,),s) \geq N(x_1, x_2,...,x_n, \frac{s}{K}).$$

Note 25:-

Let (X,N) be a fuzzy n-normed linear space. The set of all fuzzy n-bounded n-linear functionals on X^n will be denote by $B^*(X^n,F)$ and call B^* the fuzzy conjugate space of X^n. On the other hand the proof that B^* is linear space is easy to check.

Next, the definition of the uniformly fuzzy bounded of linear operator with respect to fuzzy normed space due to cheng and Mordeson appeared in [6]. With the aid of this definition we give the definition of uniformly fuzzy n-bounded of n-linear functional with respect to fuzzy n-normed space due to Narayauan and Vijayabalaji [2].

Definition 26:-

Let $T:(X,N) \longrightarrow (F,N^*)$ be a n-linear functional where (X,N) be a fuzzy n-normed linear space satisfying (FN_7) and (F,N^*) be a fuzzy normed space where N^* defined in eq.(1). T is said to be uniformly n-bounded in case there exists K>0 such that

$|T(x_1, x_2,...,x_n)| \leq K\|x_1, x_2,,...,x_n\|_{\alpha}$ for each $\alpha \in (0,1)$.

The relation between fuzzy bounded linear functional and uniformly fuzzy bounded linear functional appeared in [6], here we modify this relation to be valid between fuzzy n-bounded n-linear functional and uniformly n-bounded n-linear functional.

Theorem 27:-

Let (X,N) be a fuzzy n-normed linear space satisfying (FN_7) and $T:(X,N)\longrightarrow(F,N^*)$ be a n-linear functional. If T is fuzzy n-bounded n-linear functional then T is uniformly n-bounded.

Proof:

Suppose that T is fuzzy n-bounded n-linear functional, thus there exists K>0 such that $N^*(T(x_1,x_2,\dots,x_n),s)\geq N(x_1,x_2,\dots,x_n,\frac{s}{K})$

Then $N^*(T(x_1,x_2,\dots,x_n),s)\geq N(x_1,x_2,\dots,Kx_n,s)$

Now $\|x_1,x_2,\dots,Kx_n\|_\alpha<t$ then $\operatorname{Inf}\{s:N(x_1,x_2,\dots,Kx_n,s)\geq\alpha\}<t$

Thus there exists $s_0<t$ such that $N(x_1,x_2,\dots,Kx_n,s_0)\geq\alpha$.

Then there exists $s_0<t$ such that $N^*(T(x_1,x_2,\dots,x_n),s_0)\geq\alpha$.

Hence $|T(x_1,x_2,\dots,x_n)|\leq s_0<t$. Then

$|T(x_1,x_2,\dots,x_n)|\leq K\|x_1,x_2,\dots,x_n\|_\alpha$. This implies that T is uniformly n-bounded with respect to $\alpha-n-\text{norm}$, $\alpha\in(0,1)$.

The norm and the fuzzy norm of fuzzy bounded linear functional that appeared in [6], here we generalized that facts to fuzzy n-bounded n-linear functional.

Definition 28:-

Let (X,N) be a fuzzy n-normed linear space satisfying (FN_7) and (FN_8) and T is a fuzzy n-bounded n-linear functional, we define

$$\|T\|_\alpha^*=\operatorname{Sup}\left\{\frac{|T(x_1,x_2,\dots,x_n)|}{\|x_1,x_2,\dots,x_n\|_{1-\alpha}}:\|x_1,x_2,\dots,x_n\|_{1-\alpha}\neq0\right\}$$

$\forall\alpha\in(0,1)$

we define

$$N_2(T,s)=\begin{cases}\operatorname{Sup}\{\alpha\in(0,1):\|T\|_\alpha^*\leq s\} & \text{for } (T,s)\neq(0,0)\\ 0 & \text{for } (T,s)=(0,0)\end{cases}$$

It is clear that N_2 is fuzzy norm on B^*.

Definition 29:-

Let (X,N) be a fuzzy n-normed linear space satisfying (FN_7), (FN_8) and (F,N^*) be the fuzzy normed linear space defined in Example 10 and $x_1,x_2,\dots,x_{n-1}\in X$. We defined $(X\times[x_1]\times\dots\times[x_{n-1}],F)_\alpha^*$ be the set of all n-linear functionals defined from $X \times [x_1] \times \ldots \times [x_{n-1}]$ to (F, N^*) which are n-bounded with respect to $\|.,\ldots,\|_\alpha$ and $\|.\|_\alpha$ where $\|.,\ldots,\|_\alpha$ and $\|.\|_\alpha$ denote the $\alpha-n-$norm of N and $\alpha-$normof N^* respectively, for each $\alpha \in (0,1)$.

The theorem of fuzzy Hahn–Banach appeared for fuzzy bounded linear functional for fuzzy normed space in [6], here we modify complex verision of the malceski's extension theorem to be valid for fuzzy n-bounded n-linear functional in fuzzy n-normed space,

Theorem 30:-

Let (X,N) be a fuzzy n-normed linear space satisfying (FN_7), (FN_8) and $x_1, x_2, \ldots, x_{n-1} \in X$. Let W be a linear subspace of X and T is a fuzzy n-bounded n-linear functional on $W \times [x_1] \times \ldots \times [x_{n-1}]$. Then for each $\alpha \in (0,1)$, $\exists T_\alpha \in (X \times [x_1] \times \ldots \times [x_{n-1}], F)^*_{1-\alpha}$ which is an extension of T and if $T \neq 0$ then N^{**} $(T, \|T_\alpha\|_{1-\alpha}) \geq \alpha$ where N^{**} is the fuzzy norm on $B^*(W \times [x_1] \times \ldots \times [x_{n-1}], F)$.

Proof:-

Since T: $(W \times [x_1] \times \ldots \times [x_{n-1}], N) \to (F, N^*)$ is a fuzzy n-bounded n-linear functional thus

$$\|T\|^*_\alpha = \sup_{\substack{(x,\lambda_1 x_1,\ldots\lambda_{n-1}x_{n-1}) \\ \|x,\lambda_1 x_1,\ldots\lambda_{n-1}x_{n-1}\|_{1-\alpha} \neq 0}} \left\{ \frac{|T(x,\lambda_1 x_1,\ldots,\lambda_{n-1}x_{n-1})|}{\|x,\lambda_1 x_1,\ldots\lambda_{n-1}x_{n-1}\|_{1-\alpha}} \right\} \text{ and}$$

$$N^{**}(T,s) = \begin{cases} \sup\{\beta \in (0,1) : \|T\|^*_\beta \leq s\} & \text{for}(T,s) \neq (0,0) \\ 0 & \text{for}(T,s) = (0,0) \end{cases}$$

where

N^{**} is the fuzzy norm on $B^*(W \times [x_1] \times \ldots \times [x_{n-1}], F)$. Also,

T: $(W \times [x_1] \times \ldots \times [x_{n-1}], \|.,\ldots,\|_{1-\alpha}) \to (F, \|.\|)$ is uniformly n-bounded $\forall \alpha \in (0,1)$. Then by the theorem 6 we have for each $\alpha \in (0,1), \exists$ n-linear functional say $T_\alpha \in (X \times [x_1] \times \ldots \times [x_{n-1}], F)^*_{1-\alpha}$ which is an extension of T such that $\|T_\alpha\|_{1-\alpha} = \|T\|^*_\alpha$

Hance, $N^{**}(T, \|T_\alpha\|_{1-\alpha}) = \sup\{\beta \in (0,1) : \|T\|^*_\beta \leq \|T_\alpha\|_{1-\alpha}\}, T \neq 0$

Therefore, $N^{**}(T, \|T_\alpha\|_{1-\alpha}) \geq \alpha$.

The following theorems appeared in [6] for fuzzy bounded linear functional, here we modify these theorems to fuzzy n-bounded n-linear functional

Theorem 31:-

Let (X,N) be a fuzzy n-normed linear space satisfying (FN_7), (FN_8) and $x ,x_1,...,x_{n-1} \in X$ are linearly independent elements in X. Then for each $\alpha \in (0,1)$, $\exists\, T_\alpha \in (X\times[x_1]\times...\times[x_{n-1}],F)^*_{1-\alpha}$ such that $\|T_\alpha\|_{1-\alpha} = 1$ and $T_\alpha(x,x_1,...,x_{n-1}) = \|x,x_1,...,x_{n-1}\|_{1-\alpha}$

Proof:-

Since (X,N) be a fuzzy n-normed linear space satisfying (FN_7) then for each $\alpha \in (0,1)$, $(X ,\|.,...,\|_{1-\alpha})$ is a n-normed linear space. Hence by theorem 7, $\exists\, T_\alpha \in (X\times[x_1]\times...\times[x_{n-1}],F)^*_{1-\alpha}$ such that $\|T_\alpha\|_{1-\alpha} = 1$ and $T_\alpha(x,x_1,...,x_{n-1}) = \|x,x_1,...,x_{n-1}\|_{1-\alpha}$

Theorem 32:-

Let (X,N) be a fuzzy n-normed linear space satisfying (FN_7), (FN_8) and $x,x_1,...,x_{n-1} \in X$ are linearly independent elements in X. Then $N(x,x_1,...,x_{n-1}, \sup\limits_{\substack{T\in(X\times[x_1]\times...[x_{n-1}],F)^*_{1-\alpha}\\ T\neq 0}} \dfrac{|T(x,x_1,...,x_{n-1})|}{\|T\|_{1-\alpha}}) \geq 1-\alpha$ $\forall \alpha \in (0,1)$.

Proof:-

Let $\|.,...,\|_{1-\alpha}$ be the corresponding $(1-\alpha)$-n-norm of N. Thus $(X ,\|.,...,\|_{1-\alpha})$ is a n-normed linear space for each $\alpha \in (0,1)$. By theorem 8 we have

$$\|x,x_1,...,x_{n-1}\|_{1-\alpha} = \sup_{\substack{T\in(X\times[x_1]\times..\times[x_{n-1}],F)^*_{1-\alpha}\\ T\neq 0}} \frac{|T(x,x_1,...,x_{n-1})|}{\|T\|_{1-\alpha}} = s_\alpha,$$

$\forall \alpha \in (0,1)$, hence

$N(x,x_1,...,x_{n-1},s_\alpha) = \sup\{\beta \in (0,1) : \|x,x_1,...,x_{n-1}\|_\beta \leq s_\alpha\}$

$N(x,x_1,...,x_{n-1},s_\alpha) \geq 1-\alpha, \forall \alpha \in (0,1)$

Next, complex version of the Makeski's Hahn-Banach theorem of fuzzy n-antibounded n-linear functional in fuzzy n-antinormed linear space is discussed and presented.

Based on the idea that appeared in [8], the definition of fuzzy n-antibounded n-linear functional will given.

Definition 33:-

Let $T:(X,M)\longrightarrow(F,M^*)$ be a n-linear functional where (X,M) be a fuzzy n-antinormed linear space and M^* be a fuzzy antinorm defined in eq.(2). T is said to be fuzzy n-antibounded on X in case there exists $K>0$ such that, for each $(x_1,x_2,...,x_n)\in X^n$ and $s>0$,

$$M^*(T(x_1,x_2,...,x_n),s)\le M(x_1,x_2,...,x_n,\frac{s}{K}).$$

Note 34:-

Let (X,M) be a fuzzy n-antinormed linear space. We denote by $B'(X^n,F)$ the set of all fuzzy n-antibounded n-linear functionals on X^n and we call B' the fuzzy anticonjugate space of X^n. On the other hand the proof that B' is linear space is easy to check.

Next, the definition of the uniformly fuzzy antibounded of linear operator with respect to fuzzy antinormed linear space due to Jebril and Samanta appeared in [7]. With the aid of this definition we give the definition of uniformly fuzzy n-antibounded of n-linear functional with respect to fuzzy n-antinormed space due to Vijayabalaji and Thillaigovindan [3].

Definition 35:-

Let $T:(X,M)\longrightarrow(F,M^*)$ be a 2-linear functional where (X,M) be a fuzzy n-antinormed linear space satisfying (FM_7) and (F,M^*) be a fuzzy antinormed space where M^* defined in eq.(2). T is said to be uniformly fuzzy n-antibounded in case there exists K>0 such that $|T(x_1,x_2,...,x_n)|\ge K\|x_1,x_2,...,x_n\|_\alpha$ for each $\alpha\in(0,1)$.

The relation between fuzzy antibounded linear functional and uniformly fuzzy antibounded linear functional appeared in [7], here we modify this relation to be valid between fuzzy n-antibounded n-linear functional and uniformly fuzzy n-antibounded n-linear functional.

Theorem 36:-

Let (X,M) be a fuzzy n-antinormed linear space satisfying (FM_7) and $T:(X,M)\longrightarrow(F,M^*)$ be a n-linear functional. If T is fuzzy n-antibounded n-linear functional then T is uniformly fuzzy n-antibounded.

Proof:

Suppose that T is fuzzy n-antibounded n-linear functional. Thus there exists K>0 such that $M^*(T(x_1,x_2,...,x_n),s)\le M(x_1,x_2,...,x_n,\frac{s}{K})$

Then $M^*(T(x_1,x_2,...,x_n),s)\le M(x_1,x_2,...,Kx_n,s)$

Now $\|x_1,x_2,...,Kx_n\|_\alpha>t$ then $\mathrm{Inf}\{s:M(x_1,x_2,...,Kx_n,s)\le 1-\alpha\}>t$

Thus there exists $s_0 > t$ such that $M(x_1, x_2, ..., Kx_n, s_0) \le 1 - \alpha$.
Then there exists $s_0 > t$ such that $M^*(T(x_1, x_2, ..., x_n), s_0) \le 1 - \alpha$.
Hence $|T(x_1, x_2, ..., x_n)| \ge s_0 > t$. Then
$|T(x_1, x_2, ..., x_n)| \ge K\|x_1, x_2, ..., x_n\|_\alpha$. This implies that T is uniformly fuzzy n-antibounded with respect to $\alpha - n -$ norm, $\alpha \in (0,1)$

The norm and the fuzzy antinorm of fuzzy antibounded linear functional that appeared in [7], here we generalize that facts to fuzzy n-antibounded n-linear functional.

Definition 37:-

Let (X, M) be a fuzzy n-antinormed linear space satisfying (FM_7) and (FM_8) and T is a fuzzy n-antibounded n-linear functional, we define

$$\|T\|_\alpha' = \operatorname{Inf}\left\{\frac{|T(x_1, x_2, ..., x_n)|}{\|x_1, x_2, ..., x_n\|_{1-\alpha}} : \|x_1, x_2, ..., x_n\|_{1-\alpha} \ne 0\right\}$$

$\forall \alpha \in (0,1)$

we define

$$M_2(T, s) = \begin{cases} \operatorname{Inf}\{1 - \alpha \in (0,1) : \|T\|_\alpha' \le s\} & \text{for } (T, s) \ne (0,0) \\ 1 & \text{for } (T, s) = (0,0) \end{cases}$$

It is clear that M_2 is fuzzy antinorm on B'.

Definition 38:-

Let (X, M) be a fuzzy n-antinormed linear space satisfying $(FM_7), (FM_8)$ and (F, M^*) be the fuzzy antinormed defined in Example 15 and $x_1, x_2, ..., x_{n-1} \in X$. We defined $(X \times [x_1] \times ... \times [x_{n-1}], F)_\alpha'$ be the set of all n-linear functionals defined from $X \times [x_1] \times ... \times [x_{n-1}]$ to (F, M^*) which are n-bounded with respect to $\|.,...,.\|_\alpha$ and $\|.\|_\alpha$ where $\|.,...,.\|_\alpha$ and $\|.\|_\alpha$ denote the $\alpha - n -$ antinorm of M and $\alpha -$ antinorm of M^* respectively, for $\alpha \in (0,1)$.

The theorem of fuzzy Hahn–Banach appeared for fuzzy antibounded linear functional fuzzy antinormed space in [7], here we modify Hahn-Banach theorem due to Srivastava and et.al. to be valid for fuzzy n-antibounded n-linear functional in fuzzy n-antinormed space.

Theorem 39:-

Let (X, M) be a fuzzy n-antinormed linear space satisfying (FM_7), (FM_8) and $x_1, x_2, ..., x_{n-1} \in X$. Let W be a linear subspace of

X and T is a fuzzy n-antibounded n-linear functional on $W\times[x_1]\times\ldots\times[x_{n-1}]$. Then for each $\alpha\in(0,1)$, there exists $T_\alpha\in(X\times[x_1]\times\ldots\times[x_{n-1}],F)'_{1-\alpha}$ which is an extension of T and if $T\neq 0$ then $M^{**}(T,\|T_\alpha\|'_{1-\alpha})\leq 1-\alpha$ where M^{**} is the fuzzy antinorm on $(W\times[x_1]\times\ldots\times[x_{n-1}],F)'$.

Proof:-

Since T: $(W\times[x_1]\times\ldots\times[x_{n-1}],M)\to(F,M^*)$ is a fuzzy n-antibounded n-linear functional thus

$$\|T\|'_\alpha=\operatorname{Inf}\left\{\frac{|T(x,\lambda_1x_1,\ldots,\lambda_{n-1}x_{n-1})|}{\|x,\lambda_1x_1,\ldots,\lambda_{n-1}x_{n-1}\|_{1-\alpha}}:\|x,\lambda_1x_1,\ldots,\lambda_{n-1}x_{n-1}\|_{1-\alpha}\neq 0\right\}$$ and

$$M^{**}(T,s)=\begin{cases}\operatorname{Inf}\{1-\beta\in(0,1):\|T\|'_\beta\leq s\} & \text{for}(T,s)\neq(0,0)\\ 1 & \text{for}(T,s)=(0,0)\end{cases}$$

Also,

T: $(W\times[x_1]\times\ldots\times[x_{n-1}],\|.,\ldots,\|_{1-\alpha})\to(F,\|\,\|)$ is uniformly fuzzy n-antibounded $\forall\alpha\in(0,1)$. Then by theorem 6 we have for each $\alpha\in(0,1),\exists$ n-linear functional say $T_\alpha\in(X\times[x_1]\times\ldots\times[x_{n-1}],F)'_{1-\alpha}$ which is an extension of T such that $\|T_\alpha\|_{1-\alpha}=\|T\|'_\alpha$

Hance, $M^{**}(T,\|T_\alpha\|_{1-\alpha})=\operatorname{Inf}\{1-\beta\in(0,1):\|T\|'_\beta\leq\|T_\alpha\|_{1-\alpha}\}$, $T\neq 0$

Therefore, $M^{**}(T,\|T_\alpha\|_{1-\alpha})\leq 1-\alpha$.

The following theorems appeared in [7] for fuzzy antibounded linear functional, here we modify these theorems to fuzzy n-antibounded n-linear functional

Theorem 40:-

Let (X,M) be a fuzzy n-antinormed linear space satisfying (FM_7), (FM_8) and $x,x_1,\ldots,x_{n-1}\in X$ are linearly independent elements in X. Then for each $\alpha\in(0,1)$, $\exists\, T_\alpha\in(X\times[x_1]\times\ldots\times[x_{n-1}],F)'_{1-\alpha}$ such that $\|T_\alpha\|_{1-\alpha}=1$ and $T_\alpha(x,x_1,\ldots,x_{n-1})=\|x,x_1,\ldots,x_{n-1}\|_{1-\alpha}$

Proof:-

Since (X,M) be a fuzzy n-antinormed linear space satisfying (FM_7) then $(X,\|.,\ldots,\|_{1-\alpha})$ is a n-normed linear space for each $\alpha\in(0,1)$

Hence for each $\alpha \in (0,1)$, $\exists\, T_\alpha \in (X \times [x_1] \times \ldots \times [x_{n-1}], F)'_{1-\alpha}$ such that $\|T_\alpha\|_{1-\alpha} = 1$ and $T_\alpha(x\ ,x_1) = \|x\ ,x_1,\ldots,x_{n-1}\|_{1-\alpha}$

Theorem 41:-

Let (X,M) be a fuzzy n-antinormed linear space satisfying (FM_7), (FM_8) and $x\ ,x_1,\ldots,x_{n-1} \in X$ are linearly independent elements in X. Then sow also $M(x,x_1,..x_{n-1}, \inf_{\substack{T\in(X\times[x_1]\times..\times[x_{n-1}],F)_{1-\alpha}' \\ T\neq 0}} \frac{|T(x,x_1,\ldots,x_{n-1})|}{\|T\|_{1-\alpha}}) \le \alpha\ \forall \alpha \in (0,1)$.

Proof:-

Let $\|.,\ldots,\|_{1-\alpha}$ be the corresponding $(1-\alpha)$-n-norm of M. Thus $(X,\|.,\ldots,\|_{1-\alpha})$ is a n-normed linear space for each $\alpha \in (0,1)$, therefore

$$\|x,x_1,\ldots,x_{n-1}\|_{1-\alpha} = \inf_{\substack{T\in(X\times[x_1]\times..\times[x_{n-1}],F)' \\ T\neq 0}} \frac{|T(x,x_1,\ldots,x_{n-1})|}{\|T\|_{1-\alpha}} = t_\alpha,$$

$\forall \alpha \in (0,1)$, hence

$M(x,x_1,\ldots,x_{n-1},s_\alpha) = \operatorname{Inf}\{1-\beta \in (0,1) : \|x,x_1,\ldots,x_{n-1}\|_\beta \le s_\alpha\}$

Then

$M(x,x_1,\ldots,x_{n-1},t_\alpha) \le \alpha$

We start by giving the definition of intuitionistic fuzzy n-bounded n-linear functional in intuitionistic fuzzy n-normed linear space which based on the idea that appeared in [8].

Definition 42:-

Let $T : A \longrightarrow A^*$ be a n-linear functional where A be a intuitionistic fuzzy n-normed linear space and A^* be a intuitionistic fuzzy norm defined in remark 20. T is said to be intuitionistic fuzzy n-bounded on X in case there exists a positive number K such that, for each $(x_1,x_2,\ldots,x_n) \in X^n$ and $s > 0$,

$$N^*(T(x_1,x_2,\ldots,x_n,),s) \ge N(x_1,x_2,\ldots,x_n,\frac{s}{K})$$

and

$$M^*(T(x_1,x_2,\ldots,x_n),s) \le M(x_1,x_2,\ldots,x_n,\frac{s}{K})$$

Note 43:-

Let A be a intuitionistic fuzzy n-normed linear space. We denote by $IB(X^n,F)$ the set of all intuitionistic fuzzy n-bounded n-linear functionals on X^n and we call $IB(X^n,F)$ the intuitionistic fuzzy conjugate space of X^n. On the other hand the proof that $IB(X^n,F)$ is linear space is easy to check.

Next, we give the definition of intuitionistic uniformly fuzzy n-bounded of n-linear functional with respect to intuitionistic fuzzy n-normed space.

Definition 44:-

Let $T:A \to A^*$ be a n-linear functional where A be a intuitionistic fuzzy n-norm satisfying (IFN_4) and A^* be a intuitionistic fuzzy normed space where A^* defined in remark 20. T is said to be intuitionistic uniformly fuzzy n-bounded in case there exists $K > 0$ such that $|T(x_1,x_2,...,x_n)| = K\|x_1,x_2,...,x_n\|_\alpha$ for each $\alpha \in (0,1)$

Theorem 45:-

Let A be a intuitionistic fuzzy n-norm satisfying (IFN_4) and $T:A \to A^*$ be a n-linear functional. If T is intuitionistic fuzzy n-bounded n-linear functional then T is intuitionistic uniformly fuzzy n-bounded.

Proof:-

Suppose that T is intuitionistic fuzzy n-bounded n-linear functional thus there exists K>0 such that

Now $\|x_1,x_2,...,Kx_n\|_\alpha < t$ then

$\text{Inf}\{s: N(x_1,x_2,...,Kx_n,s) \geq \alpha, \text{ and } M(x_1,x_2,...,Kx_n,s) \leq 1-\alpha\} < t$

Thus there exists $s_0 < t$ such that $N(x_1,x_2,...,Kx_n,s_0) \geq \alpha$ and $M(x_1,x_2,...,Kx_n,s_0) \leq 1-\alpha$.

Then there exists $s_0 < t$ such that $N^*(T(x_1,x_2,...,x_n),s_0) \geq \alpha$ $M^*(T(x_1,x_2,...,x_n),s_0) \leq 1-\alpha$.

Hence, $|T(x_1,x_2,...,x_n)| \leq s_0 < t$. Then

$|T(x_1,x_2,...,x_n)| \leq K\|x_1,x_2,...,x_n\|_\alpha$. On the other hand

Now $\|x_1,x_2,...,Kx_n\|_\alpha > t$ then

$\text{Inf}\{s: N(x_1,x_2,...Kx_n,s) \geq \alpha \text{ and } M(x_1,x_2,...,Kx_n,s) \leq 1-\alpha\} > t$

Thus there exists $s_0 > t$ such that $N(x_1,x_2,...,Kx_n,s_0) \geq \alpha$ and $M(x_1,x_2,...,Kx_n,s_0) \leq 1-\alpha$.

Then there exists $s_0 > t$ such that $N^*(T(x_1,x_2,...,x_n),s_0) \geq \alpha$ $M^*(T(x_1,x_2,...,x_n),s_0) \leq 1-\alpha$.

Hence, $|T(x_1,x_2,...,x_n)| \geq s_0 > t$.

Then $|T(x_1,x_2,...,x_n)| \geq K\|x_1,x_2,...,x_n\|_\alpha$.

Then T is intuitionistic uniformly fuzzy n-bounded n-linear functional.

Definition 46:-

Let A be a intuitionistic fuzzy n-norm satisfying (IFN_4) and (IFN_5) and T is a intuitionistic fuzzy n-bounded n-linear functional, we define

$$\|T\|_\alpha^{**} = \mathrm{Sup}\left\{ \frac{|T(x_1,x_2,\ldots,x_n)|}{\|x_1,x_2,\ldots,x_n\|_{1-\alpha}} : \|x_1,x_2,\ldots,x_n\|_{1-\alpha} \neq 0 \right\}$$

$\forall \alpha \in (0,1)$

we define

$$N_2(T,t) = \mathrm{Sup}\{\alpha \in (0,1) \mid \|T\|_\alpha^{**} \leq t\}$$

$$M_2(T,t) = \mathrm{Inf}\{1-\alpha \in (0,1) \mid \|T\|_\alpha^{**} \leq t\}$$

$$A_2 = \{((T,t), N_2(T,t), M_2(T,t)) \mid (T,t) \in IB(X^n,F) \times R^+\}$$

It is clear that A_2 is intuitionistic fuzzy norm on $IB(X^n,F)$.

Definition 47:-

Let A be a intuitionistic fuzzy n-norm satisfying $(IFN_4),(IFN_5)$ and A^* be the intuitionistic fuzzy norm defined in remark 20 and $x,x_1,\ldots,x_{n-1} \in X$. We defined $IB(X\times[x_1]\times\ldots\times[x_{n-1}],F)_\alpha^*$ be the set of all n-linear functionals defined from $X\times[x_1]\times\ldots[x_{n-1}]$ to (F,M^*) which are n-bounded with respect to $\|.,\ldots,\|_\alpha$ and $\|.\|_\alpha$ where $\|.,\ldots,\|_\alpha$ and $\|.\|_\alpha$ denote the $\alpha-n-$norm of A and $\alpha-$norm of A^* respectively, for $\alpha \in (0,1)$.

Next, here we modify Hahn-Banach theorem due to Srivastava and et.al. to be valid for intuitionistic fuzzy n-bounded n-linear functional in intuitionistic fuzzy n-normed space.

Theorem 48:-

Let A be a intuitionistic fuzzy n-norm on X satisfying (IFN_4), (IFN_5) and $x,x_1,\ldots,x_{n-1} \in X$. Let W be a linear subspace of X and T is a intuitionistic fuzzy n-bounded n-linear functional on $W\times[x_1]\times\ldots\times[x_{n-1}]$. Then for each $\alpha \in (0,1)$,

$\exists T_\alpha \in IB(X\times[x_1]\times\ldots\times[x_{n-1}],F)_{1-\alpha}^*$ which is an extension of T and if $T\neq 0$ then $N^{**}(T,\|T_\alpha\|_{1-\alpha}) \geq \alpha$ and $M^{**}(T,\|T_\alpha\|_{1-\alpha}) \leq 1-\alpha$ where N^{**} and M^{**} is the fuzzy norm and fuzzy antinorm on $IB(W\times[x_1]\times\ldots\times[x_{n-1}],F)^*$.

Proof:-

Since T: $A \rightarrow A^*$ is a intuitionistic fuzzy n-bounded n-linear functional thus

$$\|T\|_{\alpha}^{**} = \operatorname{Sup}\left\{ \frac{|T(x, \lambda_1 x_1, \ldots, \lambda_{n-1} x_{n-1})|}{\|x, \lambda_1 x_1, \ldots, \lambda_{n-1} x_{n-1}\|_{1-\alpha}} : \|x, \lambda_1 x_1, \ldots, \lambda_{n-1} x_{n-1}\|_{1-\alpha} \neq 0 \right\} \text{ and}$$

we define

$N^{**}(T,t) = \operatorname{Sup}\{\alpha \in (0,1) | \|T\|_{\alpha}^{**} \leq t\}$

and

$M^{**}(T,t) = \operatorname{Inf}\{1-\alpha \in (0,1) | \|T\|_{\alpha}^{**} \leq t\}$ where N^{**} and M^{**} are fuzzy norm, fuzzy antinorm on $IB(W \times [x_1] \times \ldots \times [x_{n-1}], F)^*$ respectively . Also

T: $(W \times [x_1] \times \ldots \times [x_{n-1}], \|\cdot, \ldots, \|_{1-\alpha}) \rightarrow (F, \|\cdot\|)$ is intuitionistic uniformly n-bounded $\forall \alpha \in (0,1)$. Then by the Hahn –Banach extension theorem in n-normed linear space we have for each $\alpha \in (0,1), \exists$ n-linear functional say $T_\alpha \in IB(X \times [x_1] \times \ldots \times [x_{n-1}], F)_{1-\alpha}^*$ which is an extension of T such than $\|T_\alpha\|_{1-\alpha} = \|T\|_{\alpha}^{**}$

Hence, $N^{**}(T, \|T_\alpha\|_{1-\alpha}) = \operatorname{Sup}\{\beta \in (0,1) : \|T\|_{\beta}^{**} \leq \|T_\alpha\|_{1-\alpha}\}, T \neq 0$

Therefore, $N^{**}(T, \|T_\alpha\|_{1-\alpha}) \geq \alpha$.

and

Hence, $M^{**}(T, \|T_\alpha\|_{1-\alpha}) = \operatorname{Inf}\{1-\beta \in (0,1) : \|T\|_{\beta}^{**} \leq \|T_\alpha\|_{1-\alpha}\}, T \neq 0$

Therefore, $M^{**}(T, \|T_\alpha\|_{1-\alpha}) \leq 1-\alpha$

Theorem 49:-

Let A be a intuitionistic fuzzy n-norm satisfying $(IFN_4), (IFN_5)$ and $x, x_1, \ldots, x_{n-1} \in X$ are linearly independent elements in X. Then for each $\alpha \in (0,1)$, $\exists\, T_\alpha \in IB(X \times [x_1] \times \ldots \times [x_{n-1}], F)_{1-\alpha}^*$ such that $\|T_\alpha\|_{1-\alpha} = 1$ and $T_\alpha(x, x_1, \ldots, x_{n-1}) = \|x, x_1, \ldots, x_{n-1}\|_{1-\alpha}$

Proof:-

Since A be a intuitionistic fuzzy n-norm satisfying (IFN_4) then $(X, \|\cdot, \ldots, \|_{1-\alpha})$ is a n-normed linear space for each $\alpha \in (0,1)$. Hence, by theorem (7), for each $\alpha \in (0,1)$, $\exists\, T_\alpha \in IB(X \times [x_1] \times \ldots \times [x_{n-1}], F)_{1-\alpha}^*$ such that $\|T_\alpha\|_{1-\alpha} = 1$ and $T_\alpha(x, x_1, \ldots, x_{n-1}) = \|x, x_1, \ldots, x_{n-1}\|_{1-\alpha}$

Theorem 50:-

Let A be a intuitionistic fuzzy n-norm satisfying (IFN_4), (IFN_5) and $x, x_1, \ldots, x_{n-1} \in X$ are linearly independent elements in X. Then

$$N(x, x_1, \ldots, x_{n-1}, \sup_{\substack{T \in IB(X \times [x_1] \times .. \times [x_{n-1}], F)^*_{1-\alpha} \\ T \neq 0}} \frac{|T(x, x_1, \ldots, x_{n-1})|}{\|T\|_{1-\alpha}}) \leq \alpha$$

$\forall \alpha \in (0,1)$.

And

$$M(x, x_1, \ldots, x_{n-1}, \sup_{\substack{T \in IB(X \times [x_1] \times .. \times [x_{n-1}], F)^*_{1-\alpha} \\ T \neq 0}} \frac{|T(x, x_1, \ldots, x_{n-1})|}{\|T\|_{1-\alpha}}) \geq 1 - \alpha$$

Proof:-

Let $\|.,\ldots,\|_{1-\alpha}$ be the corresponding $(1-\alpha)$-n-norm of A. Thus $(X, \|.,\ldots,\|_{1-\alpha})$ is a n-normed linear space for each $\alpha \in (0,1)$, therefore

$$\|x, x_1, \ldots, x_{n-1}\|_{1-\alpha} = \sup_{\substack{T \in (X \times [x_1] \times .. \times [x_{n-1}], F)^* \\ T \neq 0}} \frac{|T(x, x_1, \ldots, x_{n-1})|}{\|T\|_{1-\alpha}} = t_\alpha,$$

$\forall \alpha \in (0,1)$, hence

$$N(x, x_1, \ldots, x_{n-1}, t_\alpha) = \sup\{1 - \beta \in (0,1) : \|x, x_1, \ldots, x_{n-1}\|_\beta \leq t_\alpha\}$$

$$M(x, x_1, \ldots, x_{n-1}, t_\alpha) = \inf\{1 - \beta \in (0,1) : \|x, x_1, \ldots, x_{n-1}\|_\beta \leq t_\alpha\}$$

and

$$N(x, x_1, \ldots, x_{n-1}, t_\alpha) \geq 1 - \alpha$$

$$M(x, x_1, \ldots, x_{n-1}, t_\alpha) \leq \alpha$$

REFERENCES

1. Gahler S., "Untersuchugen Uber Verallgemeinerte m-metrische Raume I", Mathematische Nachrichten, Vol.40, PP. 165-169, 1969.
2. Narayanan A. and Vijayabalaji S., "Fuzzy n-normed linear space, "International Journal of Mathematics and Mathematical Sciences,Vol.24,PP.3963-3977,2005.
3. Vijayabalaji S., Thillaigovindan N. and Jun Y., "Intuitionistic Fuzzy n-normed linear space", Bull. Kerean Math. Soc., Vol. 44, PP. 291-308, 2007.
4. Malceski R., "The Hahn-Banach theorem for bounded n-linear functionals", Mat. Bilt. Vol. 23, PP.47-58, 1999.
5. Srivastava N., Bhattacharya S. and LAL S. "On Hahn-Banach extension of linear N-Functionals in N-Normed spaces ", Math .Maced. Vol.4,PP.25-32,2006.
6. Bag T. and Samanta S., " Fuzzy bounded linear operator", Fuzzy sets and systems, Vol.151, PP. 513-547, 2005.

7. Dinda B., Samanta T. and Jebril I., "Fuzzy anti-bounded linear functionals" Global J. of science frontier research, Vol. 10,PP.36-45,2010.
8. Narayanan N.Vijayabalaji S. and Thillalgovindan, "Intuitionistic fuzzy bounded linear operators", Iranian journal of fuzzy systems Vol.4,PP.89-101,2007.
9. Vijayabalaji S. and Thillaigovindan N., "Fuzzy n-inner product space", Bull. Kerean Math. Soc., Vol. 43, PP. 447-459, 2007.
10. Jebril I. and Samanta T." Fuzzy anti-normed linear space", J. of math. And Tech. ISSN, PP.2078-0257, 2010.
11. Thillaigovindan N., Anita S. and Vijayabalaji S., "Normalsize some fixed point theorems intuitionistic fuzzy n-normed linear spaces", Int. J. open problems compt. Math.,Vol.2,PP.1998-6262,2009.

Comparative Study of Multi-Scale Retinex with Adaptive and Integrated Neighborhood-Dependent Enhancement Methods for Captured Images at Different Camera Aperture

Eqbal Shemal Mussaa[1], Athraa Juhi Jani[2], Ali A.D. Al-Zuky[3], Anwar H.M. Al-Saleh[4]
[1,2,4]Department of Computer Science, College of Science, Al- Mustansariya University
[3]Department of Physics, College of Sciences, Al- Mustansariya University
Received 26/3/2013 – Accepted 15/9/2013

الخلاصة

في هذا البحث تم التركيز على دراسة تأثير تغير قطر فتحةالكاميرا على جودة الصورة من خلال التقاط صورلثلاثة بالونات بألوان مختلفة ، ثم تم تحسين هذه الصور الملتقطة باستخدام خوارزمية Retinex متعددة النطاقات، بالاضافة الى ذلك تم تحسين الصور الاصلية باستخدام طريقة التحسين AINDANE.
الاطار الرئيسي الذي تم اخذه بنظر الاعتبار هو مقارنة و تقييم كل طريقة للتحسين من خلال دراسة و تحليل النتائج للخصائص الاحصائية للصورة المحسنة و من خلال حساب التباين لهذه الصور.
من خلال تقييم الخصائص الاحصائية و تحليل النتائج للصور المحسنة باستخدام طريقة AINDANE وجدنا بان هناك زيادة تدريجية في اضائة كل لون و سهولة التمييز بين الحزم اللونية على عكس الصور التي تم تحسينها بطريقة Retinex.

ABSTRACT

This paper has focused on studying the effects of changing camera aperture diameter on image quality through capturing images of three balloons with different colors. Then these captured images have been enhanced using Multi-Scale Retinex algorithm. Besides, the original images were enhanced using AINDANE method.
The main scopes are to compare and evaluate each enhancement method through examining and analyzing the results of image's statistic properties and computing its contrast.
We conclude form the results of the statistical properties of the enhanced images using AINDANE method that there was gradual increment in the lightness of each color and it's easy to distinguish between the color bands on contrary with the enhanced images using Retinex method.

1. INTRODUCTION

Image Enhancement is one of the important aspects of image processing to improve the interpretability of the information present in images for human viewers [1]. The main purpose of image enhancement is to bring out detail that is hidden in an image or to increase contrast in a low contrast image. Image enhancement algorithms provide a multitude of choices for improving the visual quality of images [2]. The choice of such techniques is a function of the specific task, image content, observer characteristics, and viewing conditions [3].
The performance of image enhancement is generally judged subjectively, and there are currently no automated methods to verify the optimal parameters for these algorithms. If an algorithm was introduced that could be used to automatically select parameters for an enhancement algorithm, then more complex enhancement algorithms could become more practical [4]. Most of image enhancement

techniques require interactive procedures to obtain satisfactory results, and therefore are not suitable for routine applications [5]. Observer-specific factors, such as the human visual system and the observer's experience, will introduce a great deal of subjectivity into the choice of image enhancement methods [3].

A great deal of study on Image Contrast Enhancement had been done, which would be useful to analyze the existing method for both the grayscale and color images; here will be discussed briefly as the following.

In [6] Rahman, Jobson and Woodell focused on multi-scale retinex based approach for color image enhancement. Main goals were to achieve an image rendering close to the original scene, and to increase the local contrast in dark regions of high dynamic range scenes. A color restoration method was proposed to compensate for the de-saturation effect inherent in retinex-based methods due to non-conformity to gray world assumption both globally and locally. However, color restoration was found to be inadequate for preserving the saturation of the lighter colors, and thus a white balance process was introduced to address this issue.

In [7] Unaldia, Asari and Rahman, proposed a wavelet-based dynamic range compression algorithm to improve the visual quality of digital images captured from high dynamic range scenes with non-uniform lighting conditions. Although the colors of the enhanced images produced by the proposed algorithm are consistent with the colors of the original image, the proposed algorithm fails to produce color constant results for some "pathological" scenes that have very strong spectral characteristics in a single band. The linear color restoration process is the main reason for this drawback.

In [8] Tao and Asari proposed INDANE which is an algorithm to improve the visual quality of digital images captured under extremely low or uniform lightening conditions. It consists of two main parts: Luminance enhancement and contrast enhancement.

In [9] also Tao and Asari proposed AINDANE algorithm which is an adaptive version of INDANE algorithm. As INDANE, AINDANE algorithm consists of two main parts: Adaptive luminance enhancement and adaptive contrast enhancement. During intensity transformation, the luminance of the dark pixels is increased and the image is compressed dynamic range at the same time.

In this paper the main ideas we focused on are: first the effects of changing camera aperture diameter on image quality. Second enhance the original images using modified retinex algorithm, and then enhance the original images using AINDANE. Finally compare the resulted images of both algorithms through computing the contrast of each image and evaluating its statistical properties to analyze the power of enhancement process of each algorithm.

2. Retinex Enhancement Method

Retinex theory aims to explain how the visual system extracts consistent information from the world despite changes of illumination. Retinex determines the perceived color by spatial comparisons of color surfaces across the whole image. This processing takes place independently in each waveband [10].

For any color enhancement method based on retinex theory, the main weakness lies in the fact that no direct interdependence is assumed between the luminance and chrominance data. Algorithms based on retinex theory are in many ways simply lightness adjustment and/or local contrast enhancement algorithms. Further, retinex based methods are computationally expensive, making them difficult to implement in commercial imaging devices [11].

3. Adaptive and Integrated Neighborhood-Dependent Approach for Nonlinear Enhancement Method

AINDANE (adaptive and integrated neighborhood dependent approach for nonlinear enhancement) is a quite original image enhancement algorithm for improving the visual quality of digital images captured under extremely low or nonuniform lighting conditions [12].

The main idea of this method for color images in RGB color space are converted to intensity (grayscale) images $I(x, y)$ and normalized.

AINDANE method suffers from a major technical flaw in the final stage. The assumption that the relationship between the RGB channel values will be maintained even after several nonlinear processing is fundamentally wrong. This also requires a manual adjustment of the color correction results compared to other published methods [11].

4. Image Contrast

Contrast can be defined as the fractional difference in some measurable quantity in two regions of an image. Contrast measures the relative decrease in the luminance in an image. It is highly correlated to the intensity gradient. Contrast can be defined locally or globally. The local contrast can be estimated depending on the local differences in gray levels of picture elements. Here one can directly define a contrast as a function of image edges. The contrast globally or locally can be given by [12]:

$$Cont = \frac{I_{Max} - I_{Min}}{I_{Max} + I_{Min}} \qquad \dots\dots\dots\dots (1)$$

5. Sobel Edge Detection Operator

Edge detection is one of the fundamental operations in image processing. The edges of items in an image hold much of the information in the image. The edges tell us where items are, their size, shape, and something about their texture [13].

An edge is where the gray level of the image moves from an area of low values to high values or vice versa. The edge itself is at the center of this transition. The detected edge gives a bright spot at the edge and dark areas everywhere else. Convolution of the image with masks is the most often used technique of doing this. The idea is to take a 3 × 3 array of numbers and multiply it point by point with a 3 × 3 section of the image, then sum the products and place the result in the center point of the image [14].

There are many edge detection techniques; in this work Sobel Operator will be used with different thresholds, where *Sobel edge detection operator* consists of two masks to determine the edge in vector form. The Sobel operator was the most popular edge detection operator. It proved popular because it gave a better performance than other edge detection operators. The coefficients of smoothing within the Sobel operator, Figure **1**, are those for a window size of 3×3 [13].

1	0	-1
2	0	-2
1	0	-1

1	2	1
0	0	0
-1	-2	-1

Figure-1: Templates for Sobel operator

Edge values above a threshold value were set to 255 and all others were set to zero. This gives a clear picture of edges and no edges [15].

6. Statistical Digital Image Properties

The analysis of statistical properties of images is dictated by the concern of adapting secondary treatments such as filtering, restoring, coding, and shape recognition to the image signal . There are several image properties can be calculated from image data, the most imported properties (mean μ, standard deviation σ, and single to noise ratio SNR) of the image or image regions. The basic techniques implemented to suppress a noise or increase a weak signal all rely on hypotheses regarding what is the signal and what is noise, i.e. on signal and noise models [16].

6.1 The Mean (μ)

Image mean brightness is known as the mean brightness for the image elements (or sub image) and it determined from the following relationship [17]:

$$\mu = \frac{1}{MN}\sum_{X=1}^{M}\sum_{Y=1}^{N} I(X,Y) \ldots\ldots\ldots (2)$$

Where M and N denotes the high and the width of the image (or sub image), the multiplication of them equals the number of image elements.

6.2 Standard Deviation (STD)

The standard deviation represents the mean of variations of the element values with respect to its mean and it determined from the following relationship [18]:

$$\sigma = \frac{1}{MN}\sqrt{\sum_{X=1}^{M}\sum_{Y=1}^{N}(I(x,y)-\mu)^2} \;\ldots\ldots\; (3)$$

6.3 ignal - to- Noise Ratio (SNR)

Signal-to-Noise Ratio is a measure used in science and engineering that compares the level of a desired signal to the level of background noise. The definition of SNR is as the reciprocal of the coefficient of variation, i.e., the ratio of mean to standard deviation of a signal or measurement [19]:

$$SNR = \frac{\mu}{\sigma} \qquad \ldots\ldots\ldots\ldots\; (4)$$

7. Experimental Design

Figure 2 represent the System block diagram. It is shown that system architecture which consists of two steps: first is to enhance the input image using Retinex method and AINDANE methods, second is to compete the following: statistical properties, contrast1 and contrast2 for the enhanced images in each method, and comparing the results to evaluate each method.

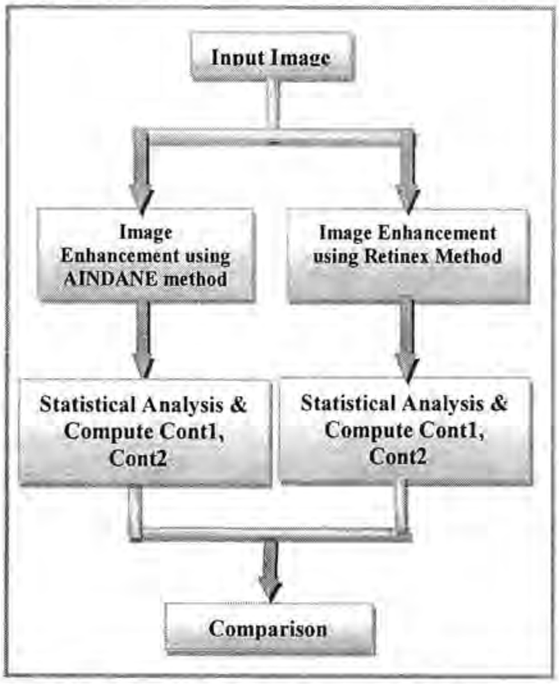

Figure-2: Block diagram of basic steps which been done in this research

Figure (3) shows lighting system, which consists of two light sources (one from the right and another from the left). All images in this study are captured by (Canon 8 Mp Camera), the lens's diameter equals to (D=23.3 mm), these captured images are of the (JPEG) format. On the other side the object is placed to be captured. The object is three balloons with different colors (red, green and blue) and white background, the distance between the camera and the object equals to (1 meter). In this paper it have been studied the effect of changing the diameter of the camera's lens on the image contrast and lightness, through studying the statistic properties of the image (the mean, the standard deviation, and SNR). The changes of the lens diameter were vary from $\Delta D= -2$ mm to $\Delta D =+2$ mm.

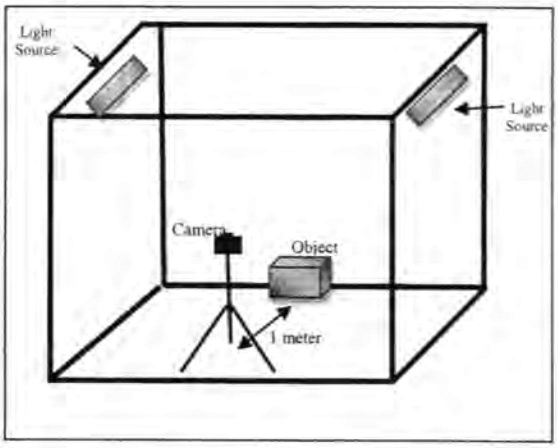

Figure-3: The Lighting System

After capturing the images of the three balloons with different lens diameter, its statistic properties (μ and SNR) have been computed in order to verify and analyze the effects of changing aperture diameter on the images. After that the original images have been enhanced by Multi Scale Retinex method, through applying Algorithm (1) on it. Then using AINDANE method, the original images have been enhanced through applying Algorithm (2).

The main scopes which been taken in account is to compare and evaluate each enhancement method through examining and analyzing the results of image's statistic properties and computing its contrast through applying Algorithm (3), (4) and (5) on the enhanced images in each method.

Algorithm (1): Multi Scale Retinex Algorithm

Input: The input of the algorithm is the color image $Ii(x,y)$, i= r,g,b.

Output: The output is enhanced image $Ipi(x,y)$.

Step 1: Calculate Gaussian surrounds function $F(x,y,c_n)=(k)\exp(\frac{-(x^2-y^2)}{c_n^2})$ where k is normalization constant, the constant values are offset values intrinsically depend upon the implementation of the algorithm in software. *cn* represent a list of the constants used to produce all the outputs in this paper which been selected from a standardized offset table, *cn*, n=3, {c1=*250, c2=120, c3=80*}.

Step 2: Compute SSR from $R_i(x,y,c)=\log[I_i(x,y)]-\log[F(x,y,c_n)\otimes I_i(x,y)]$

Step 3: Compute MSR from $R_{MSR}(x,y,w,c)=\sum_{n=1}^{N}W_n R_i(x,y,c_n)$, where *N=3* and *{w1=w2=w3=1/3}*.

Step 4: Calculate MSR with color restoration by: $I_i'(x,y,a,b)=b\log[1+a\frac{I_i(x,y)}{\sum_{i=1}^{3}I_i(x,y)}]$, where b=100, a=125.

Step 5: Output image obtaine from gain offset by *Ipi(x,y)=0.35(* $I_i'(x,y,a,b)$ *+0.56)*.

Step 6: end.

Algorithm (2): AINDANE Method Algorithm

Input: The input of the algorithm is the color image *Ci(n,m),* i=r,g,b.

Output: The output of the algorithm is enhanced image

$r'=\frac{R}{I}r$, $g'=\frac{R'}{I}g$, $b'=\frac{R}{I}b$

Step 1: Transform color image *C(n,m)* from *RGB* space to *YIQ* space and estimated lightness component *Y(n,m).*

Step 2: Normalize lightness component I *(m,n)= Y(n,m)/255* .

Step 3: Calculate Gaussian surrounds function

$F(x,y,c_n)=(k)\exp(\frac{-(x^2-y^2)}{c_n^2})$ where k is normalization constant, as mentioned in Algorithm (1) the values of c represent selected offset values , c_n, n=3, {c1=*5, c2=20, c3=240*}.

Step 4: Compute convolution image to normalize the illumination from

$I_c(x,y)=\sum_{m=0}^{M-1}\sum_{n=0}^{N-1}I(m,n)\,F(m+x,n+y,c_n)$

Step 5: The intensity images are treated by a nonlinear transfer function that enhances the dark region of the image and compresses the dynamic range. This transfer function is calculated through:

$I'_n=\frac{I_n^{(0.75z+0.25)}+0.4(1-I_n)(1-z)+I_n^{(2-z)}}{2}$, where

$$z = \begin{cases} 0, & L \leq 50 \\ \dfrac{L-50}{100}, & 50 < L \leq 150 \\ 1, & L > 50 \end{cases}$$

Step 6: Compute reflectance image from $R(x,y) = 255 I_n^{'}(x,y)^{E(x,y)}$, $E(x,y) = (\frac{I_c(x,y)}{I(x,y)})^P$,P=1, P is calculated from this relation , $P = \begin{cases} 3, & \sigma \leq 3 \\ \frac{27-2\sigma}{7}, & 3 < \sigma \leq 10 \\ 1, & \sigma > 10 \end{cases}$

, where I_c is the convolution image which had been calculated in step4.

Step 7: Output image result from components

$r' = \frac{R}{I} r$, $g' = \frac{R'}{I} g$, $b' = \frac{R}{I} b$.

Step: END.

Algorithm (3): Sobel Edge Detection Algorithm

Input: the input of the algorithm is a color image $Img(\mathrm{i,j})$ RGB of sized (r×c) with color pixel values between 0 and 255.

Output: the output of the algorithm is an edge image *eImg* (i,j) of sized (r×c) with pixel values either 0 or 255.

Step 1: Two square windows each of size (3×3) as in figure 1 are used to scan across the entire image, the first from left to right and the second from top to bottom. In each scan the filter output associated with center of the window is denoted as y (which is representing the output of the algorithm).

Step 2: Calculates the weighted inputs sum_1, sum_2 as follow:-

$$sum_1 = \sum_{i=1}^{3}\sum_{j=1}^{3} W_1(i,j) * \mathrm{Im}\,g(i,j)$$

$$sum_2 = \sum_{i=1}^{3}\sum_{j=1}^{3} W_2(i,j) * \mathrm{Im}\,g(i,j)$$

where *Img*(i,j) denote the input image, and $W_1(i,j)$, $W_2(i,j)$ as shown in figure 1.

Step 3: $sum_1 = abs\ (sum_1)\ /4$

$sum_2 = abs\ (sum_2)\ /4$

Step 4: Evaluate the value of y:

$y = max\ (sum_1,\ sum_2)$

Step 5: The output y (which represents edge point in the output edge image eImg (i,j)), can be determined using the following condition:-

If $y > th$ *then* $y = 255$

Else y=0

Where (th) is represent the threshold value, and different values of threshold were used. (th = 30 , 70 , 130 , 170 , 210).

Step 6: End.

Algorithm (4): Evaluating μ, σ, SNR, Cont1, Cont2 Algorithm

The Inputs: The input of the algorithm are the color image *Img*(i,j), enhanced image using Retinex method *Ipi(x,y)*, and enhanced image using AINDANE method $r'=\frac{R}{I}r$, $g'=\frac{R'}{I}g$, $b'=\frac{R}{I}b$, where the values of *Img* are between 0 and 255.

The outputs: are the mean μ, σ, SNR the standard deviation, for each of the input images.

Step 1: Extract 4 blocks from the input image; the size of each block is equal to 20×20 pixels.

Step 2: Calculate μ, σ, and SNR as follow: -

count = 20×20=400 (compute number of count in each extracted block)

$$sum = sum+Img\ (i,j)$$

$$\mu = sum\ /\ count$$

$$\sigma = \sqrt{(\mathrm{Im}\,g(x,y)-\mu)^{\wedge}2\ /\ count}$$

$$SNR = \frac{\mu}{\sigma}$$

Step3: End.

Algorithm (5): Evaluating Cont1, Cont2 Algorithm

The Inputs: The input of the algorithm are the color image *Img*(i,j), enhanced image using Retinex method *Ipi(x,y)*, and enhanced image using AINDANE method , where the values of *Img* are between 0 and 255, and the values of edge image *eImg* are either 0 or 255.

The outputs: are Cont1 and Cont2 for each of the input images.

Step1: Calculate the μ_e, σ_e for the input images after performing Algorithm (3) to detect the edges of the input images as follow:-

If eImg (i,j) =255 then
ne = ne+1
se = se+Img (i,j)
sse = sse+Img(i,j)^2
end if

$$\mu_e = s_e/ne$$

$$\mu_{se} = ss_e/ne$$

$$\sigma_e = \sqrt{\mu_{se} - {\mu_e}^2}$$

$$Cont1 = \sigma_e/\mu_e$$

Where ne = number of edge points.

se = summation for edge image values (*Img(i,j)*).

sse = summation for square edge image values ($Img(i,j)^{\wedge 2}$).

μ_e = mean of edge image values.

μ_{se} = mean of square edge image values.

std_e = standard deviation of values.

Step 2: To compute Cont2 for the original image and the enhanced images but we still need the edge image *eImg (i,j)* to compute the Cont2 for the rest images.

(a) Start a loop:

Loop x←2 to x← r-1

y←2 to x←c-1

(b) Determine the maximum (max) image pixel value and minimum (min) pixel value in each edges in the input images

(c) Compute Cont2

$$Cont2 = \frac{I_{Max} - I_{Min}}{I_{Max} + I_{Min}}$$

(d) End loop

Step 3: End.

8. RESULTS AND DISCUSSION

In this research three colored balloons red, green, and blue, placed on a white background, under two fluorescent lighting and the distance between the camera and the object to be photographed is 1m, we have been capture 5 images, using different aperture diameter (ΔD = -2 mm) to (ΔD = 2mm), by increment 1mm each time. Figure 4 shows the results of original captured images.

ΔD = -2 ΔD = -1 ΔD = 0 ΔD = 1 ΔD = 2

Figure- 4: The Original Images

Then we calculate the statistical properties of images the mean (μ) and the Single-to-Noise Ratio (SNR) for each image, where the statistical properties were drawn as a function of camera aperture diameter and the results were shown in figurer (5).

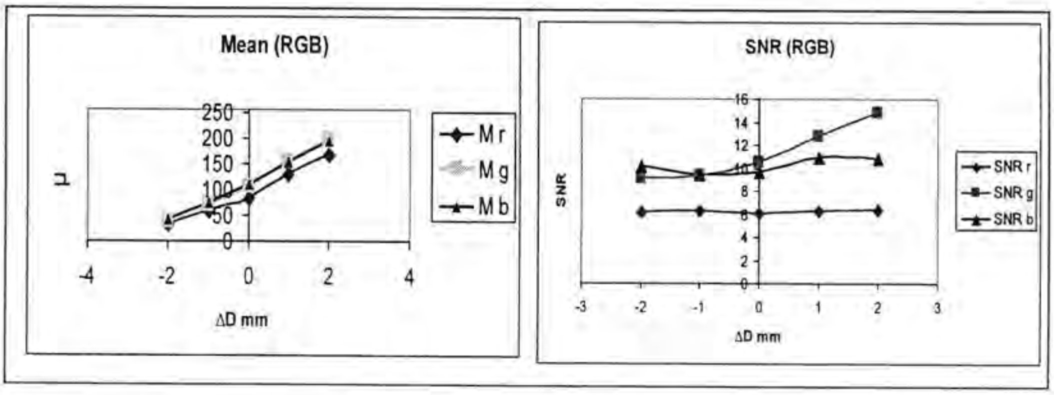

Figure-5: The (μ) and the (SNR) of the color compound (RGB) for the images as a function of different camera diameter.

Then we calculate the contrast (Cont1) and (Cont2) (as been explain in Algorithm5) for each image, where the Cont1 and Cont2 are drawn as a function of camera aperture diameter, and the results were shown in figurer (6)

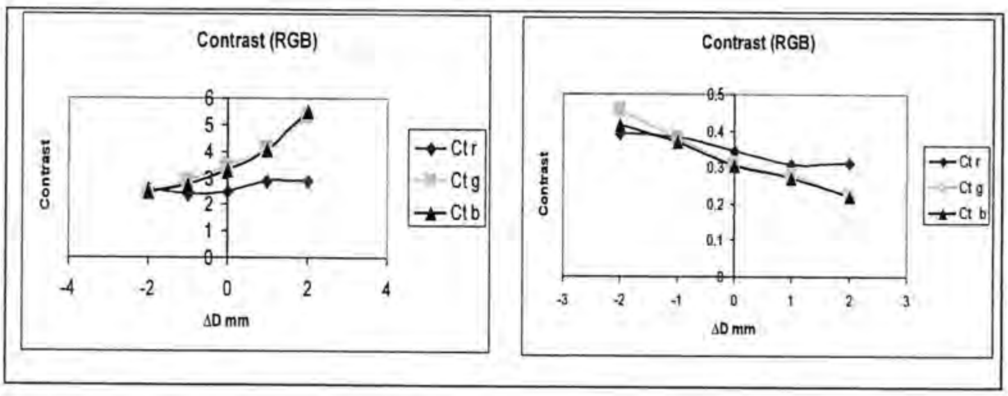

Cont1 **Cont2**

Figure-6: The (Cont1) and the (Cont2) of the color compound (RGB) for the images as a function of different camera diameter

Figures 7 show the resulted images after applying Multi-Scale Retinex enhancement method on the original images.

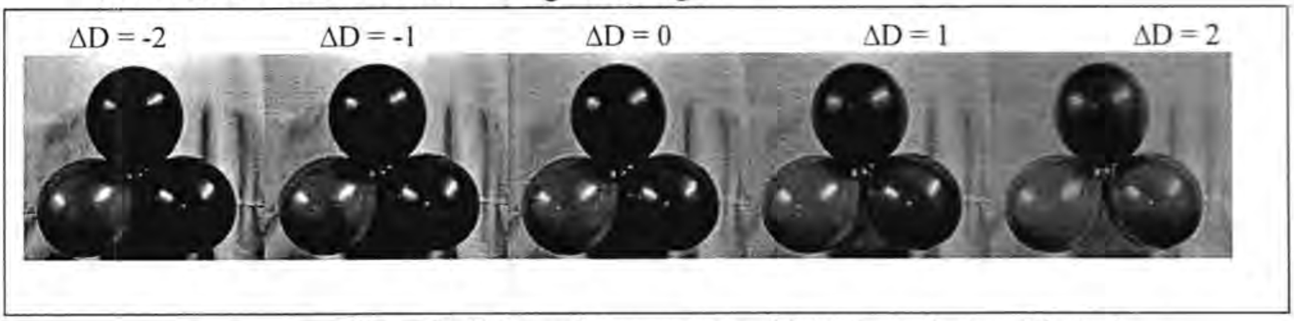

Figure-7: Enhanced Images Using Multi-Scale Retinex Method

The statistical properties of enhanced images using Multi-Scale Retinex method, the mean (μ) and Single-to-Noise Ratio (SNR) were calculated, and drawn as a function of different camera aperture diameter. The results were shown in figurer (8).

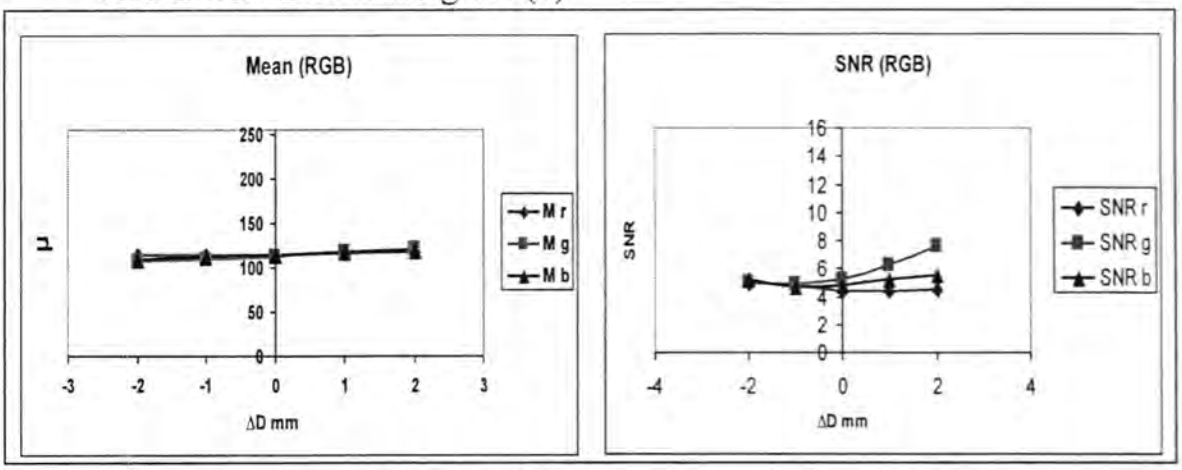

Figure-8: The (μ) and (SNR) of the color compound (RGB) for the enhanced images using Multi-Scale Retinex method as a function of different camera aperture diameter.

Then we calculate the contrast (Cont1) and (Cont2) (as been explain in Algorithm5) for each enhanced image, where the Cont1 and Cont2 were drawn as a function of camera aperture diameter, and the results were shown in figurer (9).

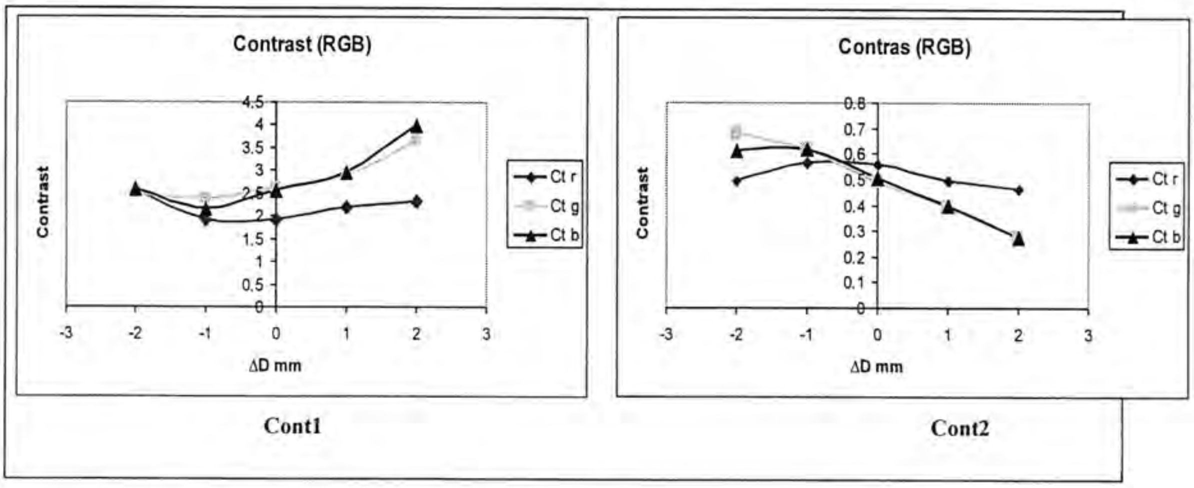

Figure-9: The (Cont1) and the (Cont2) of the color compound (RGB) for the enhanced images using Multi-Scale Retinex method as a function of different camera aperture diameter.

Figures 10 show the resulted images after applying AINDANE enhancement method on the original images.

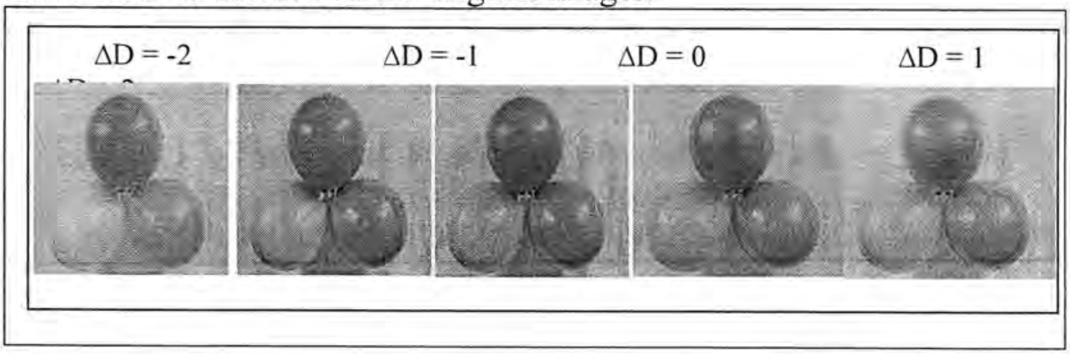

Figure-10: Enhanced Images Using AINDANE Method

The statistical properties of enhanced images using AINDANE method, the mean (μ) and the standard deviation (SNR) were calculated, and drawn as a function of different camera aperture diameter. The results were shown in figurer (11).

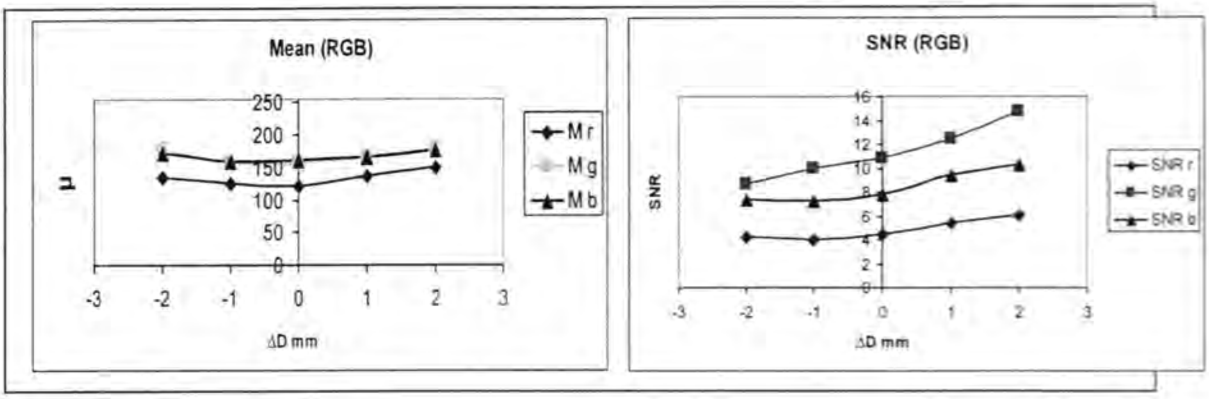

Figure-11: The (μ) and (SNR) of the color compound (RGB) for the enhanced images using AINDANE method as a function of different camera aperture diameter.

Then we calculate the contrast (Cont1) and (Cont2) (as been explain in Algorithm5) for each enhanced image, where the Cont1 and Cont2 are drawn as a function of camera aperture diameter, and the results were shown in figurer (12).

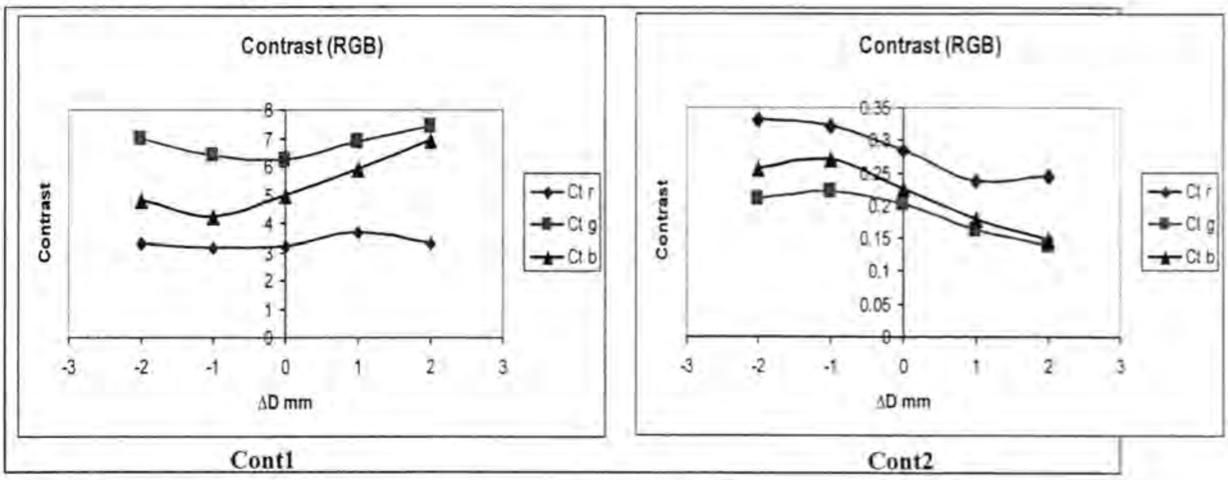

Figure-12: The (Cont1) and the (Cont2) of the color compound (RGB) for the enhanced images using AINDANE method as a function of different camera aperture diameter.

9. CONCLUSIONS

1. It's obvious to notice the effects of ΔD (the variations in camera aperture diameter) on the original images, the image lightening increase by expanding the aperture diameter, but this does not represent indication for good quality images production, as the effects caused by the raise in the entered light.

2. Enhancing the images help us to improve the resulted images, we noticed from the figure of μ and SNR of the enhanced images using Retinex method that there was consistency in the lightness of each color, and it was difficult to distinguish between each color band, on the other hand there was gradual increment in the lightness of each color

and the color bands was distinguishable in the enhanced images using AINDANE method.

10. REFERENCE

1. SANJAY SINGH, CHAUHAN R.P.S., DEVENDRA SINGH, "Comparative Study of Image Enhancement using Median and High Pass Filtering Methods," Journal of Information and Operations Management, ISSN: 0976–7754 & E-ISSN: 0976–7762, Volume 3, Issue 1, 2012, pp-96-98.
2. Saruchi, Madan Lal, "COMPARATIVE STUDY OF DIFFERENT IMAGE ENHANCEMENT TECHNIQUES," International Journal of Computers & Technology, Volume 2 No. 3, June, 2012.
3. Raman Maini, Himanshu Aggarwal, "A Comprehensive Review of Image Enhancement Techniques," JOURNAL OF COMPUTING, VOLUME 2, ISSUE 3, MARCH 2010, ISSN 2151-9617.
4. Eric Wharton, Sos Agaian, Karen Panetta,"A Logarithmic Measure of Image Enhancement,"Tufts University, 161 College Avenue, Medford, MA USA 02155, 2006.
5. Komal Vij, "Comparative Study of Different Techniques of Image Enhancement for Grayscale and Colour Images," Master Thesis, Thapar University, Department of Electrical and Instrumentation Engineering, July 2011.
6. Zia-ur Rahman, Daniel J. Jobson, Glenn A. Woodell,"Retinex Processing for Automatic Image Enhancement," *Journal of Electronic Imaging,* January 2004.
7. Numan Unaldia, Vijayan K. Asari , Zia-ur Rahman, "Fast and Robust Wavelet-Based Dynamic Range Compression and Contrast Enhancement Model with Color Restoration", SPIE Proceedings Vol. 6978, April 2008.
8. Li Tao and K. Vijayan Asari, "An integrated neighborhood dependent approach for nonlinear enhancement of color images," Proceedings of the IEEE Computer Society International Conference on Information Technology: Coding and Computing – ITCC 2004, vol. 2, pp. 138-139, April 2004.
9. Li Tao and K. Vijayan Asari, "An adaptive and integrated neighborhood dependent approach for nonlinear enhancement of color images," SPIE Journal of Electronic Imaging, vol. 14, no. 4, pp. 1.1-1.14, October 2005.
10. Laurence Meylan , Sabine Süsstrunk, "Color image enhancement using a Retinex-based adaptive filter,"LCAV, EPFL, Ecole Polytechnique Fédérale de Lausanne CH-1015 Switzerland, 2004.

11.Prem Kalra, Shmuel Peleg, "Computer Vision, Graphics and Image Processing", 5th Indian Conference, ICVGIP 2006, Madurai, India, December 13-16, 2006, Proceedings

12.Ayten Noori Hussian Al-Bayati, "ADAPTIVE ALGORITHM FOR IMAGE CONTRAS ESTIMATION", Institute of Medical Technology\ Almansour, 14/4/2005.

13.William B.and Shirly P.and Ferwerda J.,"A spatial Post Processing algorithm for Images of Night Scenes" Author Address: University of Utah and Cornell University (2003).

14.Peli E . , Arend L. , Labiance T. , " Contrast Perception a Cross Changes in Luminance and Spatial Frequency " , Opt.Soc.Am.A , vol.13, no.10/October 1996/J.Opt.Soc.Am.A (1996) .

15.Statistical Properties of Images, Digital Book Chapter, (online) www.iste.co.uk/data/doc_noyoaiyjtdiw.pdf, February 2013 (last access).

16.Osmun nuri and Capt Ender 2007, "A non-linear Technique for the Enhancement of Extremely Non-Uniform Lighting Images," Journal of aeronautics and space technologies June V.3 No.2.

17.M. C. Hanumantharaju, M. Ravishankar, D. R. Rameshbabu and S. Ramachandran 2011," Color Image Enhancement Using Multiscale Retinex with Modified Color Restoration Technique." Proceedings of the Second International Conference on Emerging Applications of Information Technology, Pages 93-97 IEEE Computer Society Washington, DC, USA.

18.Mark S. Nixon, Alberto S. Aguado, "Feature Extraction and Image Processing", Typeset at Replika Press Pvt Ltd, Delhi 110 040, India Printed and bound in Great Britain, pages(1-111), First edition (2002).

Contrast Enhancement of Object based on Top-Hat Transformation

Amel Hussain[1] and Jamila Harbi[2]
[1]Al-Mustensiriyh University, College of Science, dept. Physics.
[2]Al-Mustensiriyh University, College of Science, dept.Comp.Sci.
Received 24/3/2013 – Accepted 15/9/2013

الخلاصة

التشكل الرياضي هو نظرية تجهز عدد من الادوات المفيدة لتحليل الصور. تحسين التباين في الصور يأتي كخطوة ما قبل المعالجة التي تحتاج في تطبيقات مختلفة. في بحثنا المقترح تم استخدام تحويل Top-Hat . يعمل تحويل Top-Hat في علم التشكل و الذي يستخدم في تحسين التباين في الصور لاستخراج التفاصيل الصغيرة او الضيقة، المضيئة او المظلمة في الصورة. في هذا البحث تم اقتراح طريقة لتحسين التباين باستخدام تحويل Top-Hat على صورة رمادية حجم (512*512) وممثلة ب 8 bit/pixel و صورةx-ray بحجم (370*370) ملونة مع اطوال مختلفة SE و بزوايا مختلفة (0،45،90). و السبب باستخدام اطوال و زوايا مختلفة لل SEلكي يتم الوصول الى كل متجاورات عناصر الصورة. اظهرت النتائج التجريبية كيف ان الاطوال و الزوايا المختلفة اثرت على اضاءة الصورة. لذلك تم استخدام مرشح لعمل تحسين على الصور الناتجة من تطبيق تحويل Top-Hat.

ABSTRACT

Mathematical Morphology is a theory which provides a number of useful tools for image analysis. Correction of non-uniform illumination in images is needed as a preprocessing step in various applications. In our proposed approach the Top-Hat transform is used. Top-Hat transformation operated in morphology which is used in image contrast enhancement, for extracting small or narrow, bright or dark features in an image. In this paper we proposed an approach to contrast enhancement by using Top-Hat filtering with different structuring element lengths and orientations (0, 45, and 90) of gray-scale of size (512x512) represented by 8 bit/pixel and x-ray color of size (370x370) images. We used different orientation to reach all the entire pixels in neighbor. The experimental results show how the different lengths and orientations are affected on the illuminate of images. Therefore we applied some post-processing after top-hat filtering by using an adaptive mask to enhance the resultant images.

INTRODUCTION

Morphology is a broad set of image processing operations that can process images based on the shape. Morphological operations applied a structuring element to an input image then creating an output image of the same size. The mechanism of morphological operation is the value of each pixel in the output image based on a comparison of the corresponding pixel in the input image (original) image with its neighbors. By choosing the size and shape of the neighborhood, a morphological operation can be constructed to specific shapes in the input image [1].

The principle two morphological operations are dilation and erosion. Dilation allows objects to expands, thus potentially filling in small holes and connecting disjoint objects. Erosion shrinks objects by etching away (eroding) their boundaries. These operations can be customized for an application by the proper selection of the structuring element, which determines exactly how the objects will be dilated or eroded [2].

Mathematical morphology (MM) is a theory devised for the shape analysis of objects and functions. MM operators treat the processed image as the set and are made of two parts: a reference shape called the structuring element (SE) or function that is translated and compared to the original function all over the plane and a mechanism that details how to carry out the comparison [3]. In this paper we can use top-hat transformation to correct uneven illumination of image when the background is dark. Susanta and Bhabatosh[4] extracted the intensity values of the scale-specific features of the image using multi-scale top-hat transformation are modified for achieving local contrast enhancement. In [5] theyusemulti-scale image decomposition, obtained witha series of morphological top-hat transformations wherethe scale of enhancement corresponds to expected objectsize. In [6] they implemented six efficient digitalmammogram enhancement algorithms based on wavelet transformand top-hat filtering. Ritikaand Sandeep [7] performed morphological contrast enhancement by using the white and black top-hat transformation and they used structuring element of various shapes and sizes.

Erosion and Dilation

In image processing, usually used mathematical morphologyas a tool for extracting image components thatare useful in the representation and description of regionshape[8]. Erosion and dilation are fundamental operationsof morphological processing. Before we discuss the erosionand dilation processing, we briefly introduce the definitionsof them.

1. Erosion

To perform erosion of a binary image, the center pixel of thestructuring element successively placed on each foreground pixel (value 1). If any of the neighborhood pixels arebackground pixels (value 0), then the foreground pixel is switched to background. Formally, the erosion of image A by structuring element B is denoted [8]:

$$Erosion = A \ominus B \ldots (1)$$

One of the simplest uses of erosion is to eliminateirrelevant detail (in terms of size) from a binary image[9].

In order to eliminate the white areas as many aspossible except the large one, the object, eroded the imagewith a structuring element of a size somewhat smallerthan the objects wished to keep.

2. Dilation

To perform dilation of a binary image,successively placed the center pixel of the structuring element on each background pixel. If any of the neighborhood pixels areforeground pixels (value 1), then the background pixel is switched to foreground. Formally,the dilation of image A by structuring element B is denoted [1]:

$$Dilation = A \oplus B \ldots (2)$$

One of the simplest applications of dilation is for bridginggaps. Clearly that the erosion operationcan eliminate the irrelevant detail from the binary image, and the dilation operation is good to retrieve the original image [1].

Morphological Operations

On initial consideration of the morphological operations, it is not easy to see how the opening and closing can be useful orindeed why they differ from one another in their effect on an image. After all, erosion anddilation are logical opposites and superficial consideration would tempt to conclude thatit will make little practical difference which one is used first? However, their different effectsstems from two simple facts.Grey-scale opening and closing are defined in exactly the same way as for binary images andtheir effect on images is also complementary. Grey-scale opening (erosion followed bydilation) tends to suppress small bright regions in the image whilst leaving the rest of theimage relatively unchanged, whereas closing (dilation followed by erosion) tends to suppresssmall dark regions [10].

1. **Opening Morphology**

Opening is the name given to the morphological operation of erosion followed by dilationwith the same structuring element. The opening operation of A by structuring element B can be written as [2]:

$$A \circ B = (A \ominus B) \oplus B \ldots (3)$$

The general effect of opening is to remove small, isolated objects from the foreground ofan image, placing them in the background. It tends to smooth the contour of a binary objectand breaks narrow joining regions in an object.

2. **Closing Morphology**

Closing is the name given to the morphological operation of dilation followed by erosionwith the same structuring element. The closing operation of A by structuring element B as [2]:

$$A \cdot B = (A \oplus B) \ominus B \ldots (4)$$

Closing tends to remove small holes in the foreground, changing small regions ofbackground into foreground. It tends to join narrow isthmuses between objects.

The Top-Hat Transformation

The Top-Hat transform is a very useful tool for extracting features less the structuringelement chosen from the processed image.The top-hat transformation is defined as the difference between the image and the imageafter opening with structuring element B, namely [11]:

$$Top - Hat\ Trans. = I - I \ominus B \ldots (5)$$

Opening has the general effect ofremoving small light details in the image whilst leaving darker regions undisturbed. Thedifference of the original and the opened image thus tends to lift out the local details ofthe image independently of the intensity variation of the image as a whole. For this reason, thetop-hat transformation is useful for uncovering detail which is rendered invisible by illumination or shading variation over the image as a whole [12].

Error Metrics

Two of the error metrics used to compare the various image compression techniques are the Mean Square Error (MSE) and the Peak Signal to Noise Ratio (PSNR). The MSE is the cumulative squared error between the compressed and the original image, whereas PSNR is a measure of the peak error. The mathematical formulas for the two are [13]:

$$MSE = \frac{1}{MN} \sum_{y=0}^{M-1} \sum_{x=0}^{N-1} [I(x,y) - I^{\sim}(x,y)]^2 \dots (6)$$

$$PSNR = 10log_{10} \frac{(l-1)^2}{\sqrt{MSE}} \dots (7)$$

Where: I(x, y) is the original image, I'(x, y) is the approximatedversion (which is actually the decompressed image) and MN are the dimensions of the images.

Our Suggested Approach

In this paper we proposed an approach based on Top- Hat transformation applied on gray scale and color images.One principal application of these transforms is in removingobjects from an image by using a structuring element in the opening andclosing that does not fit the objects to be removed. Thedifference then yields an image with only the removedobjects. The Top-Hatis used for light objects on a darkbackground and the bottom-hat – for dark objects on alight background.The white top-hat transform of input image "I" is given by:

$$T_1 = I - (I \circ B) \dots (6)$$

The bottom-hat transform of input image "I" is given by:

$$T_2 = (I \cdot B) - I \dots (7)$$

Where "I" means the input image and "B" is the structure element. "T_1" Shows the top-hattransform output and "T_2" shows bottom-hat transform output. Also, "$\circ$" denotes theopening operation and "$\cdot$" denotes closing operation.

An important use of top-hat transformation is in correctingthe effects of non-uniform illumination.In our suggested approach we use top hat transformation using line-shaped structuring element to remove the non-uniform background illumination from an image.

The suggested approach algorithm steps are:

1- First step is to take the gray-scale or color image.
2- Then apply the line structuring element with different lengths and orientations.
3- Perform the top hat transforming and display the image.
4- Use image adjust to improve the visibility of the result.

RESULTS AND DISCUSSIONS

The performance of the proposed method was evaluated use of the MATLABsoftware. In this work the line SE with different lengths was calculated, and the illumination non-uniform corrected by means of an open top-hat gray scale morphological operation. At the end there were available the original image, the image with resulted illumination unbalance and the result of the correction process.The effectiveness of the proposed algorithm was evaluated by comparing the original image with the recovered image after correcting the illumination unbalance. These evaluations depend on PSNR and MSE criteria between these two images, for each connected component in the segmentation mask, and with a pixel-wise comparison of intensities. Other important parameters that were considered are the SE length obtained, the number of objects and the number of pixels that entered in the calculations.Other variables shown in the Table1 are the length and the orientation of the SE. Figure1 illustrated the Top-Hat filtering to increase the local image detail with increase the length of SE. Also we can see from Figure1 a, and c the output of Top-Hat filtering need to make some post-processing to increase and enhance the brightness, therefore we used the adaptive mask called contrast mask (see Figure1b and d). The coefficient of this mask is $\begin{bmatrix} 0.1 & 0.3 \\ 0.1 & 0.3 \end{bmatrix}$.If we increase the length of SE with keep the orientation constant (i.e., in 0 angle), we obtained the high details resolution. Figure2 and table 1 are shown these effects.

Now we examined the effect of the SE orientation with the same values of length which are shown in Table1. We can see from Figure3 and Figure4removing all features smaller than the structuring element length (i.e., 50 and 60) and rotating SE by $45^{\circ}$and 90°it means the entire pixels neighborhood can be reached. More fine detail in x-ray image can't affected with small length of SE therefore, we examined all length ranging (3-60) the obvious affected can be seen when we applied SE of length ranging (30-60) with different orientations.

Also we applied Top-Hat transform to another image, Table2 showing the results of Lena imageof size (512x 512) with different SE lengths and orientations. From Table2 slightly affected of details with SE length ranging (3-60). Also, we conclude LENA image has more fine detail therefore when we applied top-hat transformation with small length (see Figure5) only the edge affected, but when used length of SE 50 and 60 the fine detail affected (see Figure6). If we want to reach all entire pixels in the neighborhood with different orientation of SE such as45° *and* 90°(see Figs.7 and 8).

CONCLUSIONS

In our suggested approach we calculated the size of the structuring element used to correct the non-uniform illumination in a class of images. Calculating the SE size automatically applied with different kind of images to be processed. Further development of the method will demand obtaining more exact criteria PSNR and RMEas well as a thorough evaluation of the possible effects of noise. PSNR values proportional with SE length when the SE length increase PSNR values are increased too.Also, the effects of parameters like lengths of SE and orientations different from image to another. Our suggested method need to post processing therefore we suggest an adaptive mask to enhance the results after applied top-hat transformation.Experimental results show thatthe suggested method is simple and effective, whichmakes the non-uniform illumination image correctionreached a satisfactory result.

Table-1: Structuring element line shape with different orientations for x-ray image.

SE length	Identical		45°		90°	
	PSNR (dB)E+03	MSE E+03	PSNR (dB)E+03	MSE E+03	PSNR (dB)E+03	MSE E+03
6	0.0083	9.6448	0.0082	9.7798	0.0083	9.5930
9	0.0089	8.4153	0.0085	9.1581	0.0089	8.3500
12	0.0092	7.7376	0.0098	6.8511	0.0092	7.7938
15	0.0094	7.4736	0.0101	6.3714	0.0093	7.5974
18	0.0097	6.9996	0.0103	6.0830	0.0096	7.2099
21	0.0098	6.7869	0.0105	5.7962	0.0097	7.0167
30	0.0104	5.93748	0.0111	5.0476	0.0103	6.0261
40	0.0108	5.3748	0.0119	4.2459	0.0108	5.3483
50	0.0113	4.8602	0.0124	3.7092	0.0112	4.9113
60	0.0117	4.4342	0.0130	3.2858	0.0114	4.6661

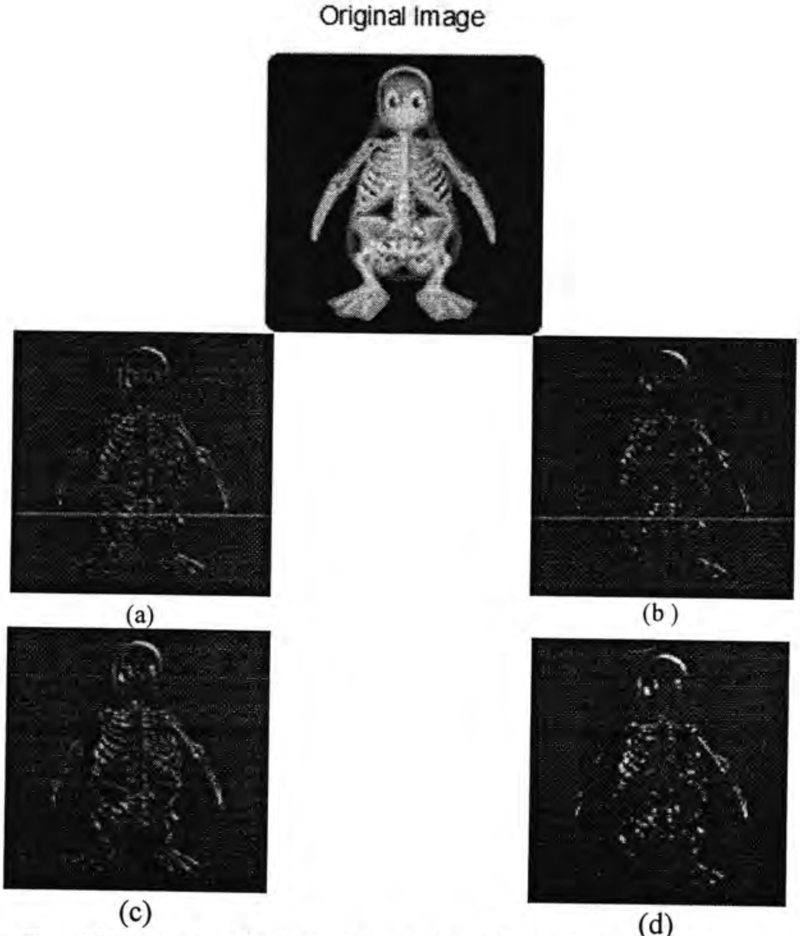

Figure-1: Top-Hat filtering from Left to right: original image; (a) and (c):Top-Hat filter of SE length are 6 and 9 (b) and (d): Top-Hat transformation after enhancement

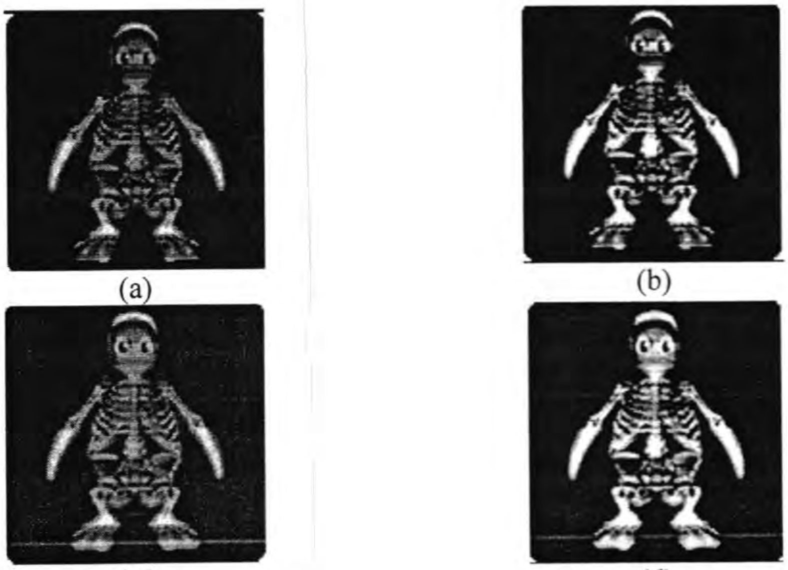

(a) (b)

(c) (d)

Figure-2: Top-Hat filtering with increases the length and keeping the orientation unchanged. ; (a) And(c): Top-Hat filter of SE length are 50 and 60; (b) and (d): Top-Hat transformation after enhancement

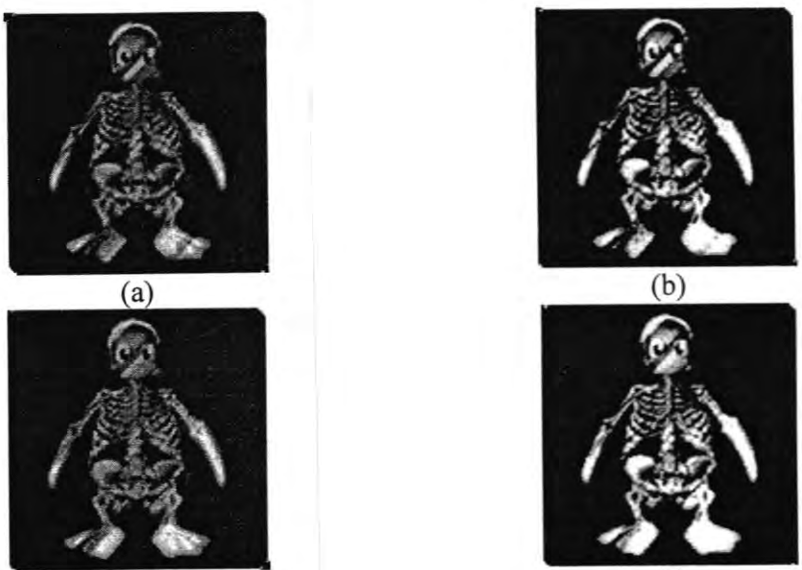

(a) (b)

(c) (d)

Figure-3: Top-Hat filtering when the SE rotated by45°; (a) and (c) Top-Hat of SE length (50 and 60); (b) and (d) after contrast enhancement applied.

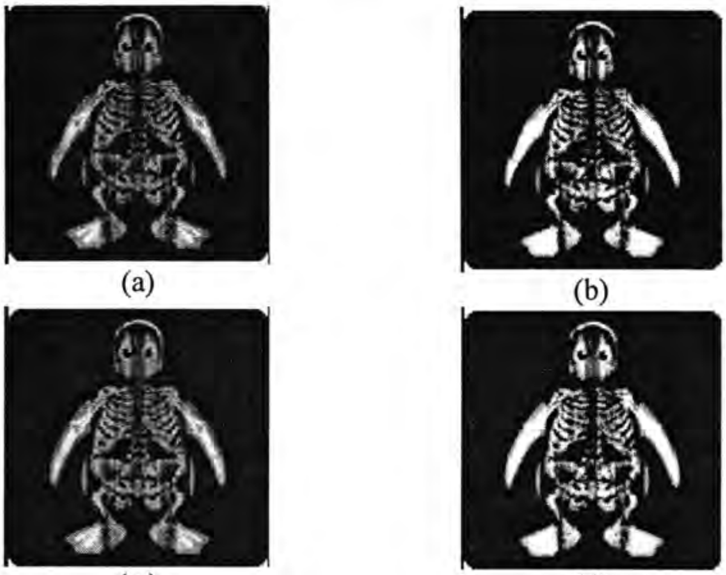

Figure-4: Top-Hat filtering when the SE rotated by90° ; (a) and (c) Top-Hat of SE length (50 and 60); (b) and (d) after contrast enhancement applied.

Table-2: Structuring element line shape with different orientations for LENA image.

SE length	Identical		45°		90°	
	PSNR (dB)E+04	MSE E+04	PSNR (dB)E+04	MSE E+04	PSNR (dB)E+04	MSE E+04
6	0.0006	1.6563	0.0006	1.6828	0.0006	1.6745
9	0.0006	1.6308	0.0006	1.6560	0.0006	1.6565
12	0.0006	1.5860	0.0006	1.6310	0.0006	1.6245
15	0.0006	1.5648	0.0006	1.6064	0.0006	1.6114
18	0.0006	1.5194	0.0006	1.5813	0.0006	1.5833
21	0.006	1.4973	0.0006	1.5588	0.0006	1.5699
30	0.0007	1.3826	0.0006	1.4987	0.0006	1.5139
40	0.0007	1.2604	0.0007	1.4071	0.0006	1.4589
50	0.0007	1.1899	0.0007	1.3286	0.0007	1.4030
60	0.0008	1.1368	0.0007	1.2378	0.0007	1.3521

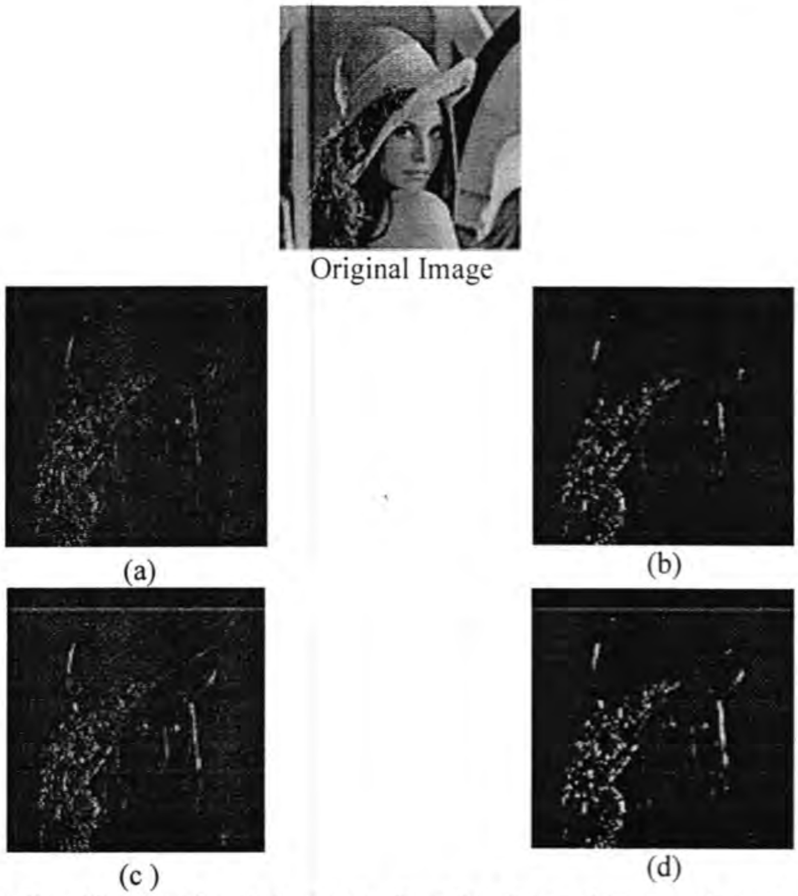

Figure-5: Top-Hat filtering; (a) and (c): Top-Hat filter of SE length are 6 and 9 (b) and (d): Top-Hat transformation after enhancement:

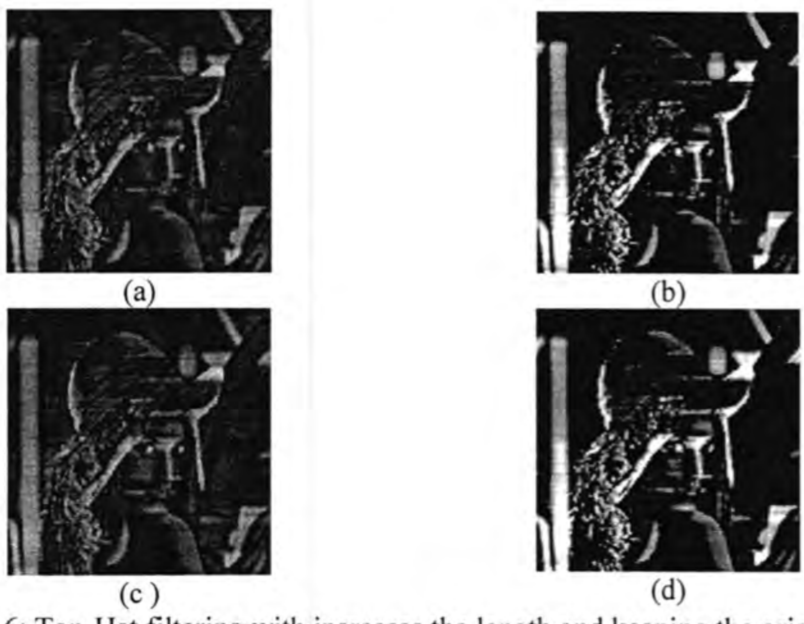

Figure-6: Top-Hat filtering with increases the length and keeping the orientation unchanged. ; (a) And (c): Top-Hat filter of SE length are 50 and 60; (b) and (d): Top-Hat transformation after enhancement

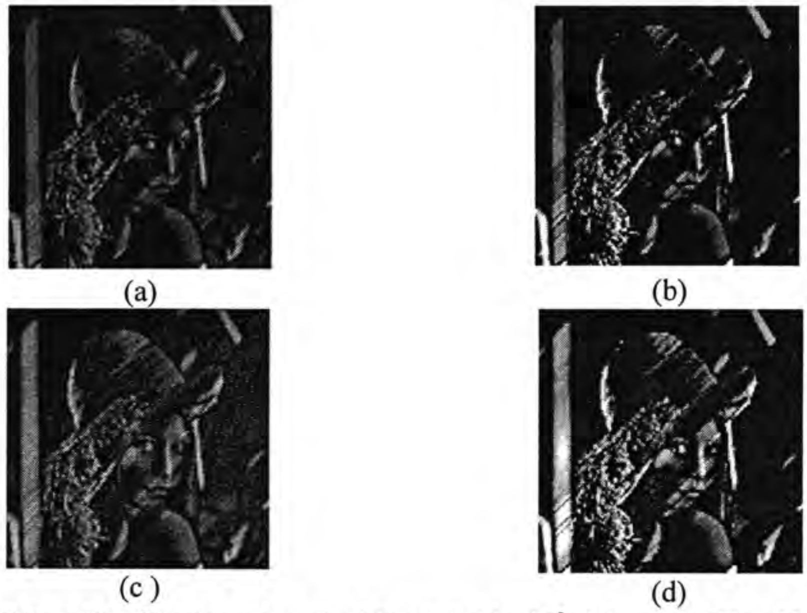

(a) (b) (c) (d)

Figure-7:Top-Hat filtering when the SE rotated by45°; (a) and (c) Top-Hat of SE length (50 and 60); (b) and (d) after contrast enhancement applied.

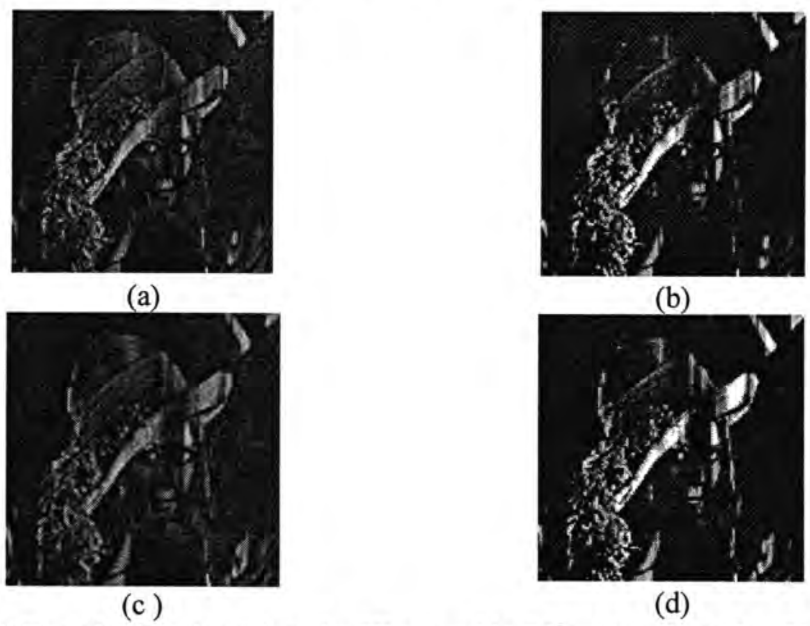

(a) (b) (c) (d)

Figure-8:Top-Hat filtering when the SE rotated by90° ; (a) and (c) Top-Hat of SE length (50 and 60); (b) and (d) after contrast enhancement applied.

REFERENCES

1. A.Zadorozny and H.Zhang," Contrast Enhancement using Morphological Scale Space", pp. 804-807,2009.
2. E.ScottUmbaugh," Digital Image Processing and Analysis: Human and Computer Vision Applications with CVIP Tools", Taylor & Francis Group, 2^{nd} edition, 2011.
3. Gasteratos A., Andreadis I., " Non-linear image processing in

hardware", Pattern Recognition Vol. 33, pp. 1013-1021, 2000.

4. Susant M., and Bhabatosh Ch., "A Multi-Scale Morphological Approach to Local Contrast Enhancement", Signal Processing 80, pp.685-696, 2000.
5. Andrzej Z. and Hong Zh., "Contrast Enhancement Using Morphological Scale Space" Proceedings of the IEEE, International Conference on Automation and Logistics Shenyang, China, 2009.
6. Rajkumar K. K., et al., "Enhancement of Mammograms Using Top-Hat Filteringand Wavelet Decomposition", Journal of Computer and Mathematical Sciences Vol. 2, Issue 6, pp.780-898, 2011.
7. Ritika and Sandeep K., "Contrast Enhancement Techniques for Images :A Visual Analysis", International Journal of Computer Applications (0975 – 8887) Vol. 64, No.17, 2013.
8. R. C. Gonzalez, R. E. Woods, "*Digital Image Processing*", 2nd d., Prentice Hall, USA, pp. 423-425, 2003.
9. Ch.Solomon and T.Breckon, "Fundamentals of Digital Image Processing:A Practical Approach", John Wiley & Sons, Ltd., 2011.
10. AlperPahsa,"Morphological Image Processing With Fuzzy Logic", HavacilikVcUzayTeknolojileri Der GisiOcak,CICK2SAY13(27-34), 2006.
11. T. Chen, and Q.H. Wu,"A Pseudo Top-Hat Mathematical Morphological Approach to Edge Detection in Dark Regions", Pattern Recognition, 35, pp. 199-210, 2002.
12. J.Tang,E.Peli,and S.Acton. "Image enhancement using a contrast measure in the compressed domain" IEEE Signal Processing Letters, 10(110):289-292, October 2003.
13. Beant K. and Anil G., "Comparative Study of Different edge Detection Techniques", International Journal of Engineering Science and Technology (IJEST), Vol. 3 No. 3 March 2011.

A Speech Scrambler Algorithm Based on chaotic system

Saad N.Al-saad and Eman H.Hashim
Al-Mustansiriyah University/ College of Science/ Computer Science Dept.
Received 3/4/2013 – Accepted 15/9/2013

الخلاصة

يقدم البحث خوارزمية آمنة لبعثرة أشارة الكلام. تتكون الخوارزمية من جزئين من عمليات الابدال. يتم في الجزء الاول توليد مفتاح ابدال باستخدام خرائط (logistic) لابدال المعاملات الناتجة من التحويل المويجي المتقطع. عمليه الابدال الثانية تتولد من تطبيق خريطة (chaotic) ذات البعدين نوع (Arnold cat map). نتائج المحاكاة التي قدمت في هذا البحث تشير الى أن الخوارزمية تقدم كلام مبعثر غير مفهوم وكلام مسترجع بعد التشفير ذو نوعية جيدة.

ABSTRACT

This paper presents a secure scramble speech signal algorithm. The algorithm composed of two types of permutations. The first permutation key is generated from two logistic maps to permute the coefficients resulting from Discrete Wavelet Transform (DWT). The second permutation is generated from performing two dimensional chaotic map using Arnold cat map. Simulation results presented in the paper indicate that the algorithm provides scrambled speech of low residual intelligibility and good quality recovered speech.

1. INTRODUCTION

Speech encryption techniques are used to encrypt clear speech into an unintelligible signal in order to avoid eavesdropping. Speech has more redundancy as compared with written text or digital data and contains two types of information, the content of the speech and the personality of the speaker. This makes encryption of speech signal with low residual intelligibility and high cryptanalytic strength is very difficult task [1, 2].

In general there are two basic speech encryption modes: digital and analog [1]. Digital encryption is cryptanalytic strength and retains a lower residual intelligibility, but it needs complex implementation and produce low quality recovered speech. On other hand, analog speech encryption, also called speech scrambling, acts on the speech samples themselves. Analog encryption schemes are relatively less secure compared to digital encryption schemes, but have an advantage of less complexity and provide good quality of recovered speech [1].

In general, there are five main categories domains in analog speech encryption: frequency-domain, time-domain, amplitude, two-dimensional scrambling that combines the frequency-domain scrambling with the time-domain scrambling and transform domain [1]. Regarding other types of scramblers which can attain a high degree of security, the transform domain scrambler has advantage in that the number of effective permutations is much larger than the number of permutations available in other domain scrambling algorithms.

Many analog speech encryption methods in the transform domain are proposed, e.g., Fast Fourier Transform, a Prolate Spheroidal Transform (PST), Hadamard Transform domain, circulant transform domains, discrete wavelet transform domain (DWT) and discrete cosine transform (DCT). Among the transform-domain techniques, DCT and DWT have proved to be the best for speech encryption[2].

One interesting new speech encryption methods is connected to chaos theory. That theory focuses primarily on the description of these systems that are often very simple to define, but whose dynamics appears to be very confused. Indeed, chaotic systems are characterized by their high sensitivity to initial conditions and pseudo-random behavior. The extreme sensitivity to the initial conditions (i.e. a small deviation in the input can cause a large variation in the output) makes chaotic system very attractive for pseudo-random number generators [3]. It is impossible to predict the behavior of the chaotic system even if we have partial knowledge of its organization that made chaotic system [4].

In this paper chaotic map is used to produce the chaotic sequence by logistic map and samples are permutated using Arnold cat map.

2. Wavelet Transform Scrambling Process

Transform of a signal is just another form of representation to the signal. It does not change the information content present in a signal. The Wavelet Transform provides a time – frequency representation of the signal. It was developed to overcome the short coming of the Short Time Fourier Transform (STFT), which can also be used to analyze non-stationary signals. STFT gives a constant resolution at all frequencies while the Wavelet Transform uses multi-resolution technique by which different frequency is analyzed with different resolutions [5].

The analog scrambling process which employs a transformation of the input speech to facilitate encryption can best be described using matrix algebra. Let us consider the vector x which contains N speech time samples obtained from analog to digital conversion process, representing a frame of the original speech signal. Let this speech sample vector x be subject to an orthogonal transformation matrix F such that [5, 6, 7]:

$$u = F\,x \qquad (1)$$

This transformation results in a new vector u made up of N transform coefficients (N is the number of coefficient produce from the transform in frequency domain). A permutation matrix P is applied to u, such that each transform coefficient is moved to a new position within the vector given by [5, 6, 7]:

$$v = P\,u \qquad (2)$$

A scrambled speech vector y is obtained by returning vector v to the time domain using the inverse transformation F^{-1} where [5, 6, 7]:

$$y = F^{-1}\,v \qquad (3)$$

Descrambling, or recovery of the original speech vector x' is achieved by first transforming y back to the transform domain .The inverse permutation matrix P^{-1} is then used to return the transform coefficients to their original position. Finally, the resulting transform vector is returned to the time domain by multiplying by F^{-1} [5, 6, 7]:

$$\acute{x} = F^{-1}\,P^{-1}F\,y \qquad (4)$$

The transform domain scrambling process outlined above requires the transform matrix F to have an inverse. One attempts to insure that the scrambling transformation $T=F^{-1}PF$ is orthogonal since orthogonal transformations are norm preserving. The inverse transformation T^{-1} will also be orthogonal .This property is useful since any noise added to the scrambling signal during transmission will not be enhanced by the descrambling process [5, 6, 7].

3. Generation of Permutation Key Scheme

The prime requirement of any permutation key is that the Residual Intelligibility should be minimized after permutation. So the problem of key generation is therefore an important issue in the design of a scrambling system. High key sensitivity is required by secure cryptosystems, which means that the cipher cannot be decrypted correctly although there is only a slight difference between encryption or decryption keys.

Logistic map is one-dimensional linear chaotic map has the advantages of high-level efficiency and simplicity is defined as:

$$x_{n+1} = r.x_n.(1-x) \qquad (5)$$

Where x_n is an initial condition variable which lies in the interval (0, 1) and r is called control parameter which lies in the interval (1, 4) [8]. The parameter $\boldsymbol{r}$ can be divided into three segments, when $\boldsymbol{r}$ (0, 3) the calculation results come to the same value after several iterations without any chaotic behavior. When r in the interval [3, 3.6), the phase space concludes several points only, while $\boldsymbol{r}$ [3.6, 4), it becomes a chaotic system [8].

The resulting plot that depicts the possible output values for different parameter conditions is called the Bifurcation Diagram, as shown in Figure (1)

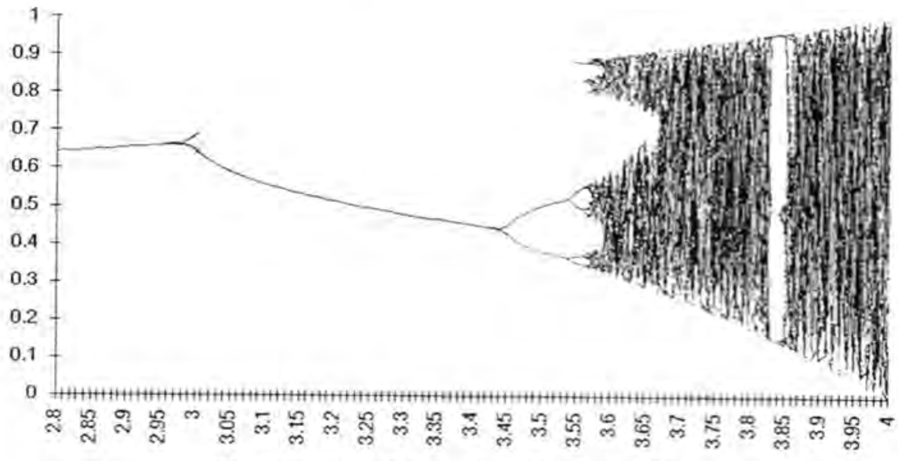
Figure-1:The Bifurcation Diagram [9].

4. Arnold Cat Map Scrambling

Arnold Cat Map is used to reduce the autocorrelation samples of speech signal. Arnold cat map is given by:

$$\begin{bmatrix} x_{n+1} \\ y_{n+1} \end{bmatrix} = \begin{bmatrix} 1 & a \\ b & ab+1 \end{bmatrix} \cdot \begin{bmatrix} x_n \\ y_n \end{bmatrix} mod\ (N) \qquad (6)$$

Where x_n ,y_n are the position of samples in the *NxN* matrix, and $x_n, y_n \in \{0,1,2,\ldots,N-1\}$ and x_{n+1}, y_{n+1} are the transformed position after cat map, taking mod in order to bring x, y in unit matrix, *a* and *b* are two control parameters and are positive Integers[10].

For applying Arnold cat map, the signal must convert from 1-D vector to 2-D. Matrix resizing operations for both 1-D vector to 2-D matrix and 2-D matrix to 1-D vector is shown in Figure (2).

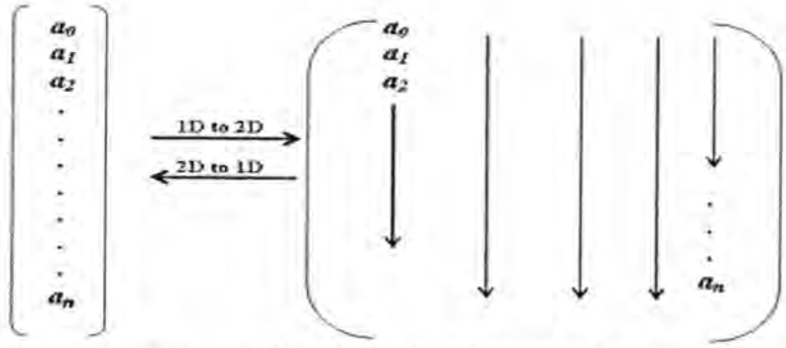

Figure-2:Matrix converter operations for both 1D vector to 2D matrix and 2D matrix to 1D vector [2]. vector to 2D matrix & 2D matrix to 1D vector [].

5. Measurements Criteria

Generally speech quality assessment falls in two categories: subjective and objective quality measures. Subjective quality measures are based on comparison of original and processed speech data by a listener or a panel of listeners. Objective speech quality measures are based on some physical measurement.

Objective speech quality measures can be classified to time domain measures and spectral domain measures. Time domain measures take up speech waveforms directly in time domain(*Signal-to-Noise Ratio (SNR), Segmental Signal-to-Noise Ratio (SEGSNR))* while spectral domain measures are computed using speech segment, they are more reliable than the time-domain measures(*Log-Likelihood Ratio (LLR) , Cepstrum Distance (CD)*)

Signal-to-Noise Ratio (SNR)

This common measure is given as

$$\mathrm{SNR} = 10\log_{10}\frac{\sum_{n=\infty}^{\infty} x^2\ (n)}{\sum_{n=\infty}^{\infty}[x(n)-y(n)]^2}\,(\mathrm{dB}) \qquad (7)$$

Where *n* is the number of samples, *x(n)* is the input speech signal and *y(n)* is the reconstructed speech signal.

A high SNR (SNR >> 1) indicates high precision data, while a low SNR indicates noise contaminated data [11, 12].

Segmental Signal-to-Noise Ratio (SEGSNR)

It is an improved version measure that can be obtained if SNR is measured over short frames. It is given as:

$$\mathrm{SEGSNR} = \frac{10}{M}\sum_{m=0}^{M-1}\log_{10}\sum_{n=Nm}^{Nm+N-1}\frac{\sum_{n=\infty}^{\infty} x^2\ (n)}{\sum_{n=\infty}^{\infty}[x(n)-y(n)]^2}\,(\mathrm{dB}) \ (8)$$

Where M is the number of segments in the output signal, and K is the length of each segment. It is a good estimator for speech signal quality [12]. As depicted in Figure (3), high intelligibility and low intelligibility correspond to high and low number respectively.

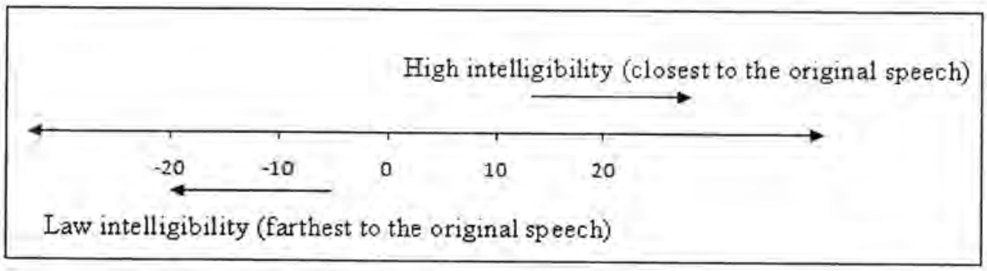

Figure-3:Segmental signal-to-noise ratio measure.

Log-Likelihood Ratio (LLR)

The Log-Likelihood Ratio (LLR) measure is a distance measure that can be directly calculated from the LPC vector of the clean and distorted speech. LLR measure can be calculated as follows:

$$d_{llR}(a_d, a_c) = log \frac{a_d R_c a_d^T}{a_c R_c a_c^T} \qquad (9)$$

Where a_c is the LPC vector for the clean speech, a_d is the LPC vector for the distorted speech, a^T is the transpose of a, and R_c is the auto-correlation matrix for the clean speech [13].

Cepstrum Distance (CD)

The Cepstrum Distance (CD) is an estimate of the log-spectrum distance between clean and distorted speech. Cepstrum can also be calculated from LPC parameters with a recursion formula.CD can be calculated as follows:

$$d_{CEP} = \frac{10}{log_{10}} \sqrt{2 \sum_{k=1}^{p} \{c_c(k) - c_d(k)\}^2} \qquad (10)$$

Where c_c and c_d are Cepstrum vectors for clean and distorted speech, and P is the order (number of LPC coefficient). Cepstrum distance is also a very efficient computation method of log-spectrum distance [13]. As the value of LLR and CD are increasing the low residual intelligibility for scrambled signal (the scrambled signal is farthest to the original speech signal).

6. A Proposed Speech Scrambling algorithm

The proposed algorithm can be treated as two major parts: speech scrambling and speech descrambling. Figure (4) shows the steps for each part.

The proposed scrambling algorithm steps can be summarized as follows:

1. Segmentation (frames of length N=256 samples per frame)
2. First part
    - Generation of key permutation (two logistic maps used)
    - Application of the DWT (Haar DWT).
    - Permutation the coefficient of DWT with the key permutation.
    - Application of the Inverse DWT.
3. Second part
    - convert into 2-D format.
    - Application Arnold cat map on the samples in time domain.
    - convert into 1-D format.

4. Synthesis segments and saves to the wave file.

The descrambling steps of the proposed algorithm can be summarized as follows:

1. Segmentation (frames of length N=256 samples per frame)
2. First part
   - convert into 2-D format.
   - Application inverse Arnold cat map on the samples in time domain
   - convert into 1-D format.
3. Second part
   - Generation of key permutation (using same initial condition and control parameters value that used in sender).
   - Application of the DWT (Haar DWT).
   - Inverse permutation of the coefficient of DWT with the key permutation.
   - Application of the Inverse DWT
4. Synthesis segments and saves to the wave file.

These steps are taken to be illustrated separately in more details

6.1 ***Speech Scrambling***

It is composed of main steps: segmentation, transformation and two types of permutation applied in transform domain and in time domain.

Segment and Framing

The sampled speech is segmented into frames of length N=256 samples per frame that means a time frame of (32 msec), with sampling frequency of 8 KHz, Mono, 16 bit resolution. The speech files used for scrambling purposes are taken from the web page http://www.1speechsoft.com/voices.html as wave files [14].

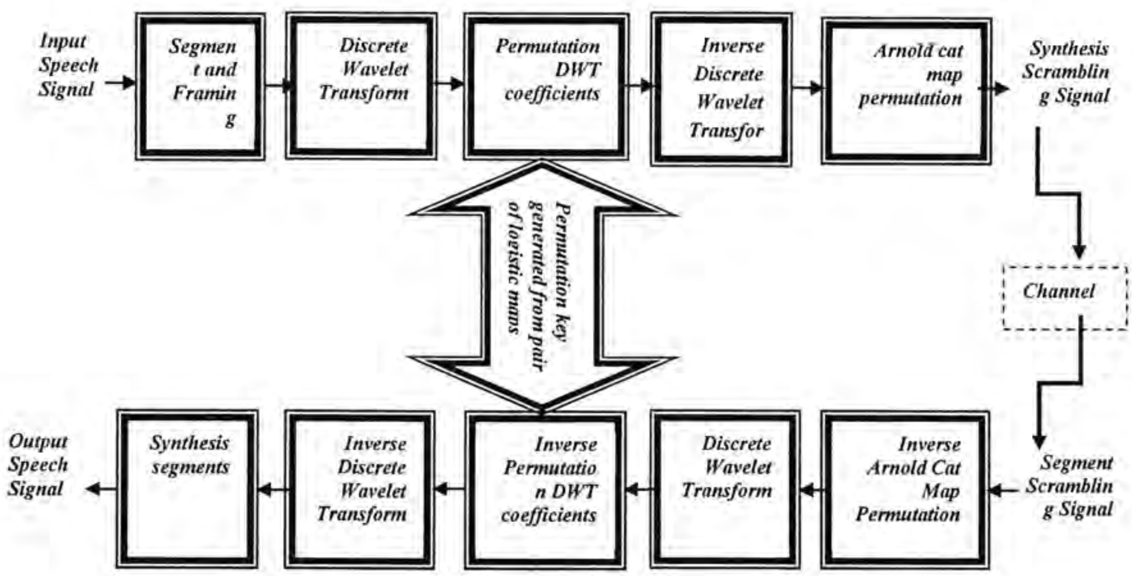

Figure-4:A Proposed Speech Scrambling algorithm.

Discrete Wavelet Transform

A wavelet transform of type (Haar) is chosen and performed on each frame with specified level (two levels of decomposition). The result is transforming coefficients.

The Permutation Key

The wavelet coefficients are permuted using the following procedure: Choosing two logistic maps and cross-coupled as shown in the Figure (5). The output generated by the first logistic map is fed to the second logistic map as the input (initial condition) and vice versa. The output is two rows of sequence. The first one contains real value representing the chaos sequence. The second row represents the positions of chaos sequence. Finally the chaos sequence is sorted in ascending order. The resultant position row is used as permutation key.

Generating permutation key sequence can be summarized as follows:

Step1. Generate the chaotic sequence of length n by using two logistic maps and store it in a one dimensional matrix $\{a1, a2, a3, a4, \ldots \ldots, an\}$.

Step2. Find the index of the smallest number from the sequence of n number and then store it in $b\ (1)$. Next find the index of the 2^{nd} smallest number and store it in $b\ (2)$. Repeat this process until nth smallest number is stored in $b\ (n)$.

Step3. The array b contains sequence of n random number generated from the chaos sequence.

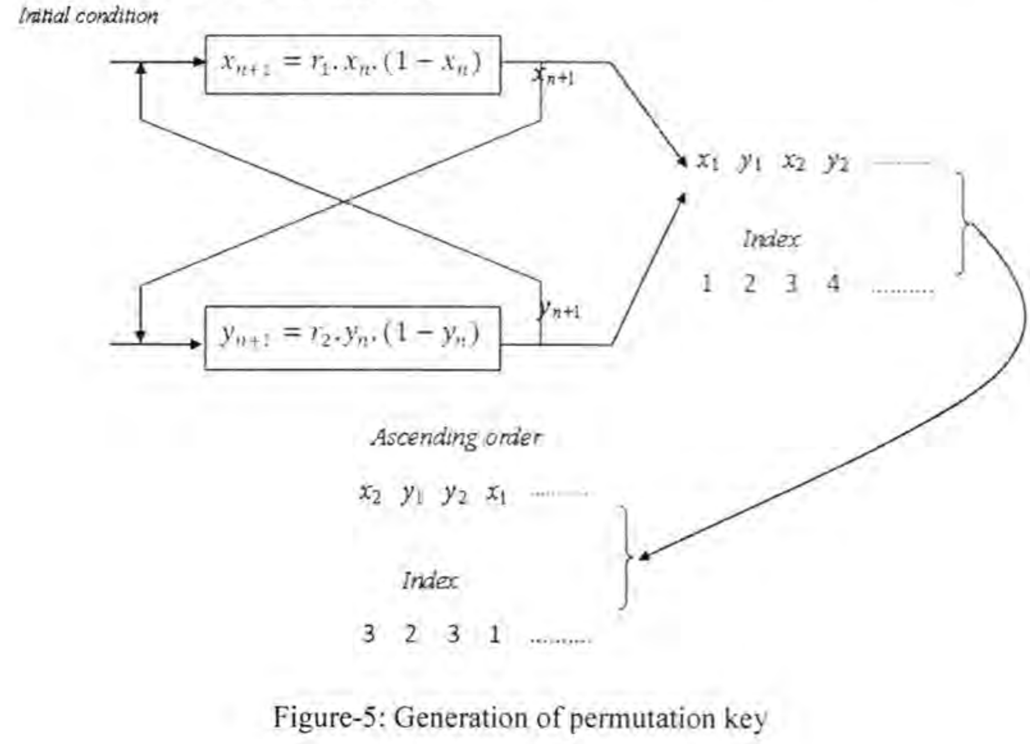

Figure-5: Generation of permutation key

Permutation using Arnold Cat Map

The sample in time domain are converted in to 2-D matrix of samples, and then permuted by multiplying by Arnold cat map matrix, the output is resized to 1-D vector again. Synthesize the scrambling frames produced from Arnold cat map permutation part and the resulting scrambled speech signal was saved as a wave file.

6-2 *Speech Descrambling*

After transmission through the channel, the receiver receives the scrambled speech. The receiver segment the received signal to be ready to descramble it.

Inverse Permutation using Arnold Cat Map

First the matrix of sample is resized to 2-D and multiplied by the inverse Arnold cat map matrix, the output is then resized to 1-D vector to be the input to the DWT step.

Descrambling using DWT

Applying the DWT used to generate wavelet coefficients. These coefficients are rearranged using inverse permutations (that means recovering of the original order of every frame), then the inverse wavelet transform is applied to transform the signal in to time domain. Synthesize the frames to present the recovered speech (descrambled speech signal) and save in wave file.

7. Simulation Results

Subjective Test is considered by playing the scrambled speech files back to a number of listeners to measure the residual intelligibility. The judge is that; the listened files contain noise only, which means that the residual intelligibility is low. The analog recovered speech files have been tested in a similar way to measure the quality of the recovered speech files; the judge is that the files are the same as the original copies.

The key permutation is computed using pair of logistic maps with initial conditions ($x1=0.41$) and control parameters ($r1=3.94$ and $r2=3.98$). That key is used to permute the DWT coefficient.

As the chaotic system are dynamic systems, which are very much sensitive to the initial condition and control parameter, thus, a small variation to the control parameters(seed) creates a major impact on the scrambled signal. This effect can be viewed in the simulation example (key length =25) by changing the r1 and r2 value from 3.992 and 3.882 to 3.991 and 3.881 respectively. Table (1) and (2) show the result.

Table-1: Generation key permutation with (x1=0.65, r1=3.992, r2=3.882)

Chaotic sequence control parameter r1=3.992 r2=3.882	Index	Ascending order of chaotic sequence	Key permutation
0.406189350901439	1	0.0100887719665914	6
0.962868651965901	2	0.0124404457790751	11
0.142724423220861	3	0.0398680586780157	7
0.488437815650636	4	0.0490444389028686	12
0.997466333045141	5	0.097210470535722	19
0.0100887719665914	6	0.142724423220861	3
0.0398680586780157	7	0.152808157528446	8
0.152808157528446	8	0.174814511298517	16
0.51679563548866	9	0.186183215006961	13
0.9968738832611	10	0.331561955484688	22
0.0124404457790751	11	0.350340295056151	20
0.0490444389028686	12	0.40618935090143	1
0.186183215006961	13	0.407080208006824	24
0.604863949622878	14	0.488437815650636	4
0.954102179861406	15	0.51679563548866	9
0.174814511298517	16	0.575863556568406	17
0.575863556568406	17	0.604863949622878	14
0.975024925372891	18	0.884741471638152	23
0.097210470535722	19	0.908587075082751	21
0.350340295056151	20	0.954102179861406	15
0.908587075082751	21	0.962868651965901	2
0.331561955484688	22	0.963532721725732	25
0.884741471638152	23	0.975024925372891	18
0.407080208006824	24	0.9968738832611	10
0.963532721725732	25	0.997466333045141	5

Table-2: Generation key permutation with (x1=0.65, r1=3.991, r2=3.881)

Chaotic sequence control parameter r1=3.991 r2=3.881	Index	Ascending order of chaotic sequence	Key permutation
0.892720158268834	1	0.0188734642187522	18
0.382221571261605	2	0.0563252995375079	9
0.942387812720144	3	0.0739023709594386	19
0.216683455418336	4	0.155841640655474	15
0.677399356645127	5	0.212132665836546	10
0.872151107833224	6	0.216683455418336	4
0.44501067977757	7	0.273147274809314	20
0.98568191307394	8	0.359629161171157	24
0.0563252995375079	9	0.382221571261605	2
0.212132665836546	10	0.401839544925735	13
0.667025400105211	11	0.44501067977757	7
0.8864111402373	12	0.525036099559897	16
0.401839544925735	13	0.656611234201804	22
0.959294819512916	14	0.667025400105211	11
0.155841640655474	15	0.677399356645127	5
0.525036099559897	16	0.792364523724575	21
0.995248416131838	17	0.872151107833224	6
0.0188734642187522	18	0.8864111402373	12
0.0739023709594386	19	0.8927201582688	1
0.27314727480931	20	0.899862428995255	23
0.792364523724575	21	0.91911144617749	25
0.656611234201804	22	0.942387812720144	3
0.899862428995255	23	0.959294819512916	14
0.359629161171157	24	0.985681913073947	8
0.91911144617749	25	0.995248416131838	17

From above example, we can conclude that the permutation key that used in proposed algorithm is very sensitive to the initial seed that means the scrambled signal cannot be descrambled correctly, if there is tiny change in initial seed. key sensitivity indicate high security and suitability of the proposed algorithm.
Objective Test is another valuable measure to the residual intelligibility of the scrambled speech and the quality of the recovered speech. In this paper (SNR), (SEGSNR), (LLR), (CD) measures are calculated for speech signal for two male and two female persons on sentences in English language. The sentence is "*This is an example of the AT and T natural voice speech engine, it is the most human sounding text to speech engine in the world*". Table (3) and (4) explains the result.

Table-3:Result for comparison of original and scrambled speech signal.

File name	*SNR*	*SEGSNR*	*LLR*	*CD*
Mike8(male)	-2.62555	-2.56744	4.18696	7.7533
Claire8(female)	-2.58369	-2.52513	1.148503	4.63589
charles8 (male)	-2.61635	-2.45871	3.78171	8.21462
lauren8(female)	-2.58401	-2.54969	2.13405	5.74775

Table-4:Result for comparison of original and descrambled speech signal.

File name	***SNR***	***SEGSNR***	***LLR***	***CD***
Mike8(male)	13.67320	62.84561	0.002382	0.30001
Claire8(female)	14.79295	61.20851	0.010630	0.61856
charles8 (male)	16.52925	62.022102	0.00393	0.34891
lauren8(female)	13.88546	62.34254	0.00100	0.17526

From table (3) the LLR (also called LPC distance) and CD measures for all the scrambled speech files are high while SNR and SEGSNR measures are low (negative value) which means that the residual intelligibility is very low, when compared with [6] that used LLR,CD, and SEGSNR measures for scrambling algorithm using different transform.
From table (4) the LLR and CD measures for all the descrambled speech files are low while SNR and SEGSNR measures are high. As the values of the LLR and CD are decreased, and the value of SND and SEGSR are increased that indicates high precision data and good quality of the descrambled speech signals.
The Figure (6) shows the waveform for original speech signal, scrambling signal and descrambling signal.

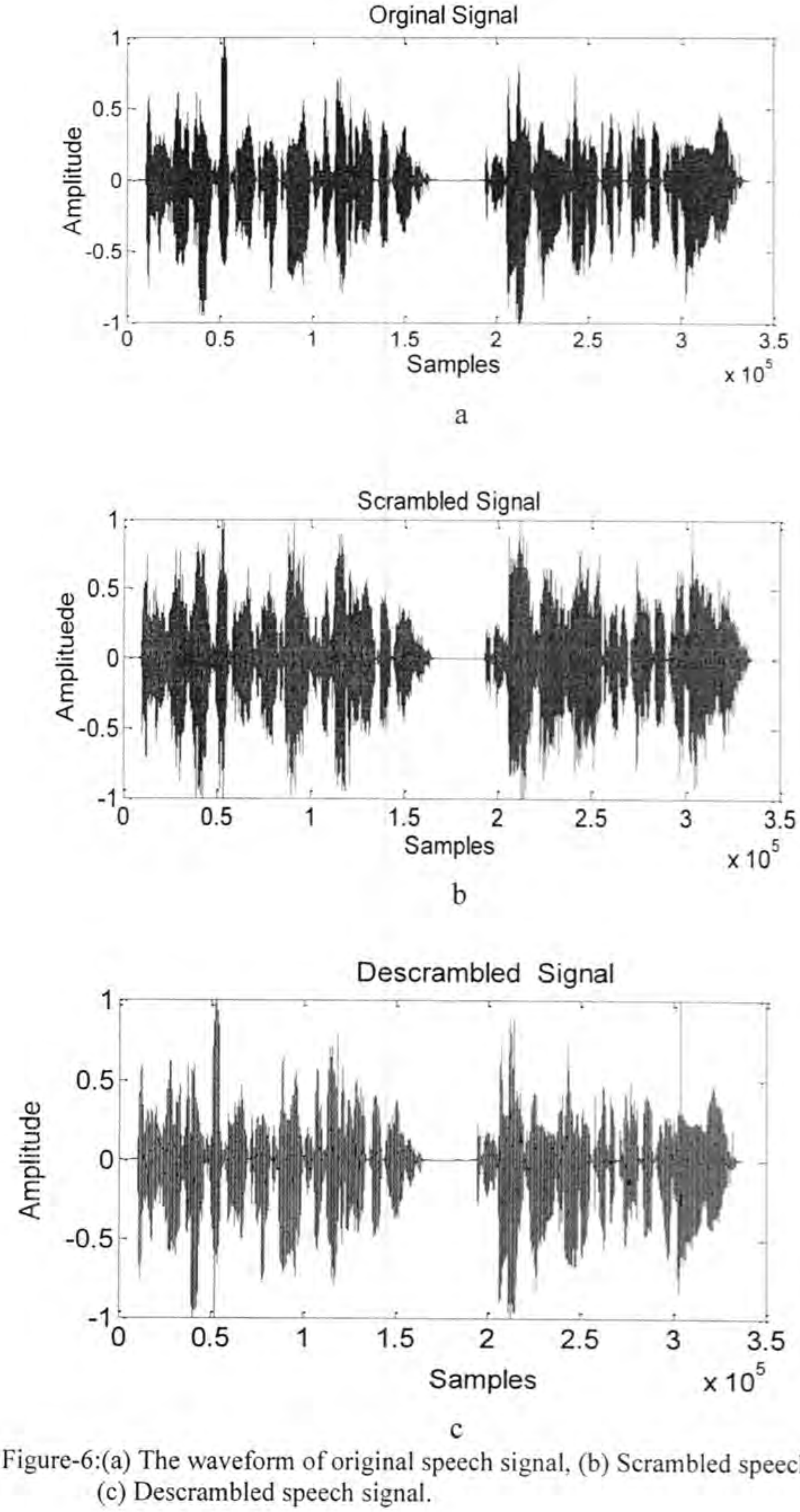

Figure-6:(a) The waveform of original speech signal, (b) Scrambled speech signal, (c) Descrambled speech signal.

The spectrum and spectrogram plotting is used because it is a powerful tool that allowed to see the different in the frequency and time domains. Note that on the scrambled plot it is observed that the order of the frequencies has changed. And, as expected the descrambled version has been decoded to its original form.
The Figures (7) and (8) show spectrum and spectrogram for original speech signal, scrambling signal and descrambling signal.

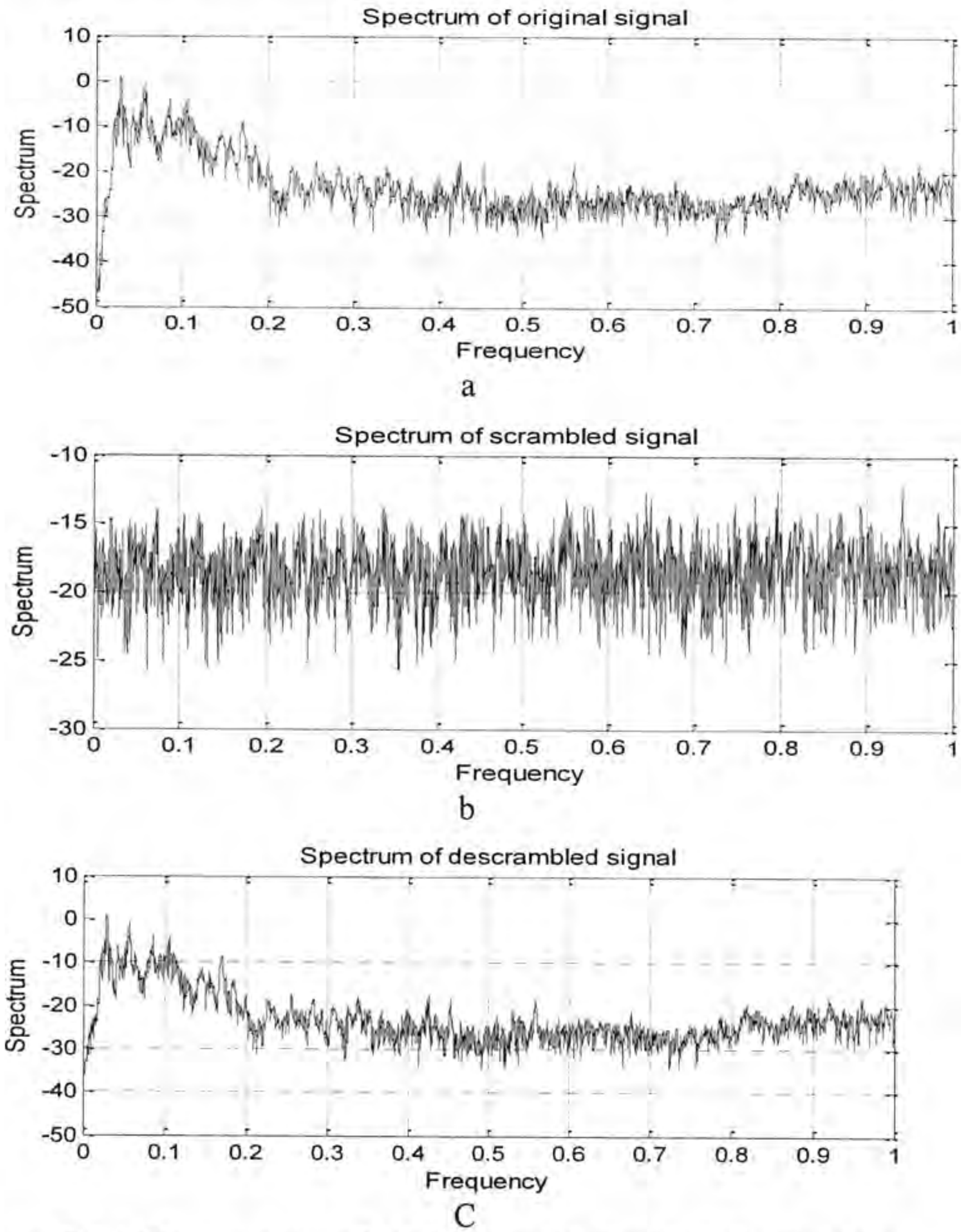

Figure-7:(a) The spectrum of original speech signal, (b) Scrambled speech signal, (c) Descrambled speech signal.

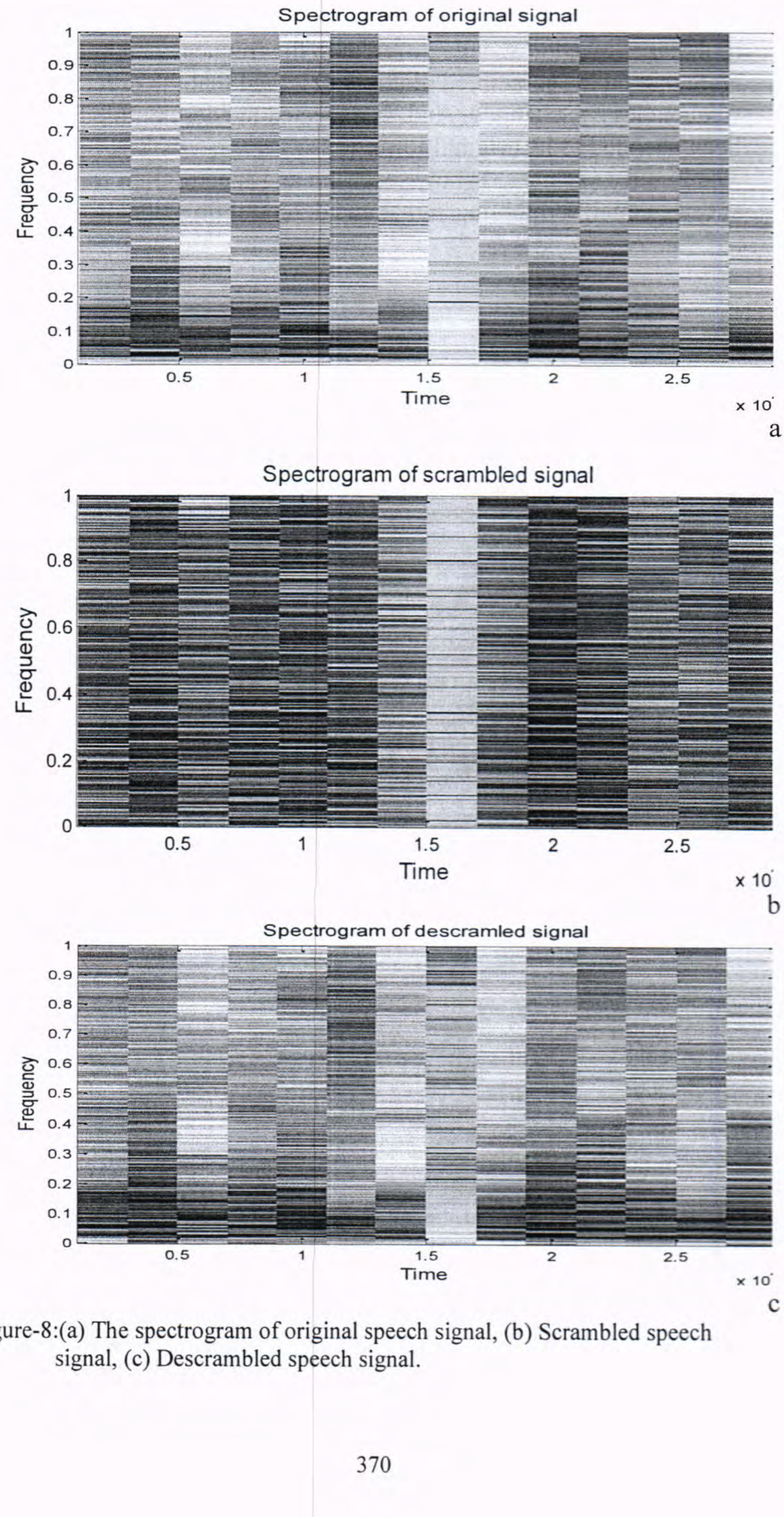

Figure-8:(a) The spectrogram of original speech signal, (b) Scrambled speech signal, (c) Descrambled speech signal.

8. CONCLUSIONS

This paper presents new idea for speech scrambling algorithm based on wavelet transforms domain and chaotic system. The performance of proposed algorithm is examined on actual English Speech Signals, and the results showed that there is low residual intelligibility in the scrambled speech signal while preserving the quality of the reconstructed speech signal.

Using two parts to scramble the speech signal; the first part works with time–frequency features and the second part works on time features with advantage of chaotic system (Sensitivity to initial conditions, Topological transitivity with iterative process) make the system difficult to decrypt that means it is crypt analytically strong and secure.

9. REFERENCES

1. A.Srinivasan1 P.Arul Selvan, "A Review of Analog Audio Scrambling Methods for Residual Intelligibility", Innovative Systems Design and Engineering, Vol 3, No 7, 2012.
2. L. A. Abdul-Rahaim, "Proposed Realization of modified Scrambling using 2D-DWT Based OFDM Transceivers ",MASAUM Journal of Computing, Volume 1 Issue 2, September 2009.
3. M. Francois and D. Defour, "A Pseudo-Random Bit Generator Using Three Chaotic Logistic Maps ", hal-00785380, version 1 - 6 Feb 2013.
4. M. N. Elsherbeny, M. Rahal, "Pseudo Random Number Generator Using Deterministic Chaotic System ", International Journal of scientific& technology research, Vol 1, Issue 9, October 2012.
5. S. B. Sadkhan, N. H. Kaghed, L. M. AlSaidi, "Design and Evaluation of Transform Based Speech Scramblers using different Wavelet Transformations", (CSNDSP, Greece, 2006).
6. S.Sridharan, E.Dawson, B.Goldburg, "Design and cryptanalysis of transformbased analog speech scramblers", IEEE Journal on selected areas in communications , (735744), (June 1993) .
7. D. B.Sadkhan, D. Abdulmuhsen, N. F.Al-Tahan, "A proposed analog speech scrambler based on parallel structure of wavelet transforms", 24th National Radio Science Conference (NRSC) (C13/1C13/12), (2007).
8. I. Q. Abduljaleel, "Speech Encryption Technique Based on Bio-Chaotic Algorithm", AL-Mansour Journal, Basra University, No.17/ Special Issue, 2012.
9. A.V. Prabu S. Srinivasarao, Tholada Apparao, M. Jaganmohan Rao and K. Babu Rao, "Audio Encryption in Handsets", International Journal of Computer Applications, Vol. 40 No.6 (0975 – 8887) (2012).

10.M. Ashtiyani , P. Moradi Birgani, S. S. Karimi Madahi, "Speech Signal Encryption Using Chaotic Symmetric Cryptography", J. Basic. Appl. Sci. Res., 2(2) (1678-1684) (2012).
11.S. Sadkhan and N. Abbas, "Performance evaluation of speech scrambling methods based on statistical approach", Attidella "Fodazione Giorgio Ronchi" Anno LXVI, N. 5, (2011).
12. E. Mosa, N. W. Messiha, O. Zahran, F. E. Abd El-Samie, "Chaotic encryption of speech signals", Springer US, Vol. 14, Issue4,(285-296), December (2011).
13.K. Kondo, "Subjective Quality Measurement of Speech its Evaluation, Estimation and Applications", Signals and Communication Technology, Springer US (2012)
14. http://www.1speechsoft.com/voices.html.

No-reference Quality Assessment of Gaussian Blurred Images

Radhi Sh.Hamoudi[1], Hana' H. kareem[2] , Hazim G. Dway[3]
[1,2] AL – Mustansiriyah University Physics Department, College of Education.
[2] AL – Mustansiriyah University Physics Department, College of Science
Received 25/3/2013 – Accepted 15/9/2013

ABSTRACT

No-reference measurement of blurring artifacts in images is a difficult problem in image quality assessment field. In this paper, we present a no-reference blur metric to measure the quality of the images. These images are degraded using Gaussian blurring. Suggestion method depends on developing the Mean of Locally Standard deviation and Mean of the image (MLSD) model, this method is called Blur Quality Metric (BQM) and it calculates from numerical integral of the function in this model. And the BQM is compared with the No-reference Perceptual Blur Metric (PBM), the BQM is a simple metric and gives good accuracy in metrics the quality for the Gaussian blurred image if it compared with the PBM.

1. INTRODUCTION

Measurement of image quality is very important for many image processing algorithms, such as acquisition, compression, restoration, enhancement and other applications. Image quality assessment is a very important activity for many image applications. The image quality metrics can be broadly classified into two categories, subjective and objective. A large numbers of objective image quality metrics have been developed during the last decade. Objective metrics can be divided [1], [2], [3] in three categories: Full Reference, Reduced Reference and No Reference. For the existing no-reference image quality metrics that existed in the literature, most of these are developed for measuring image blockiness [4]. In [5],[6] A blur metric relies on measuring the spread of edges in an image. And [7] suggested the no reference perceptual blur metric using the image gradients along local image structures. In this paper, we are focusing on the no reference image quality assessment for measuring the Gaussian blurring. The Blur Quality Metric (BQM) was inspired from the Mean of Locally Standard deviation and Mean of the image (MLSD) model by calculated the area under the curve form this relation. This paper is organized as follows. Gaussian Blurring is presented in section 2.Section 3 introduces No reference Quality of blurring image, in this section includes the adaptive BQM. Section 4 presents the experimental results acquired with of quality assessment using many blurred image. Finally the paper concludes in Section 5.

2. Gaussian Blurring

Blurring is unsharp image was generated from a variety of sources, like atmospheric scatter, lens defocus, optical aberration, and spatial and temporal sensor integration [1]. In digital image there are three common types of Blur effects: average blurs, Gaussian blur and motion blur [2]. The Gaussian blur is a type of image-blurring filter that uses a Gaussian function (which also expresses the normal distribution in statistics) for calculating the transformation to apply to each pixel in the image. The equation of a Gaussian function in one dimension is:

$$G(x) = \frac{1}{\sqrt{2\pi s^2}} e - \frac{x^2}{2s^2} \tag{1}$$

In two dimension

$$G(x, y) = \frac{1}{\sqrt{2\pi s^2}} e - \frac{x^2+y^2}{2s^2} \tag{2}$$

Where x is the distance from the origin in the horizontal axis, y is the distance from the origin in the vertical axis, and S is the standard deviation of the Gaussian distribution. When applied in two dimensions, this formula produces a surface whose contours are concentric circles with a Gaussian distribution from the center point. Values from this distribution are used to build a convolution matrix which is applied to the original image. Each pixel is approximately equal the new value is set to a weighted average of that pixel's neighborhood. The original value of the pixel receives the heaviest weight (having the highest Gaussian value) and neighboring pixels receive smaller weights as their distance to the original pixel increases. This results in a blur that preserves boundaries and edges better than other, more uniform blurring filters. The blurring image is given by:

$$Ib = I * G \tag{3}$$

Where Ib being the blurring image and G is the Gaussian function Figure(1) shows the different burring image with deferent values of S.

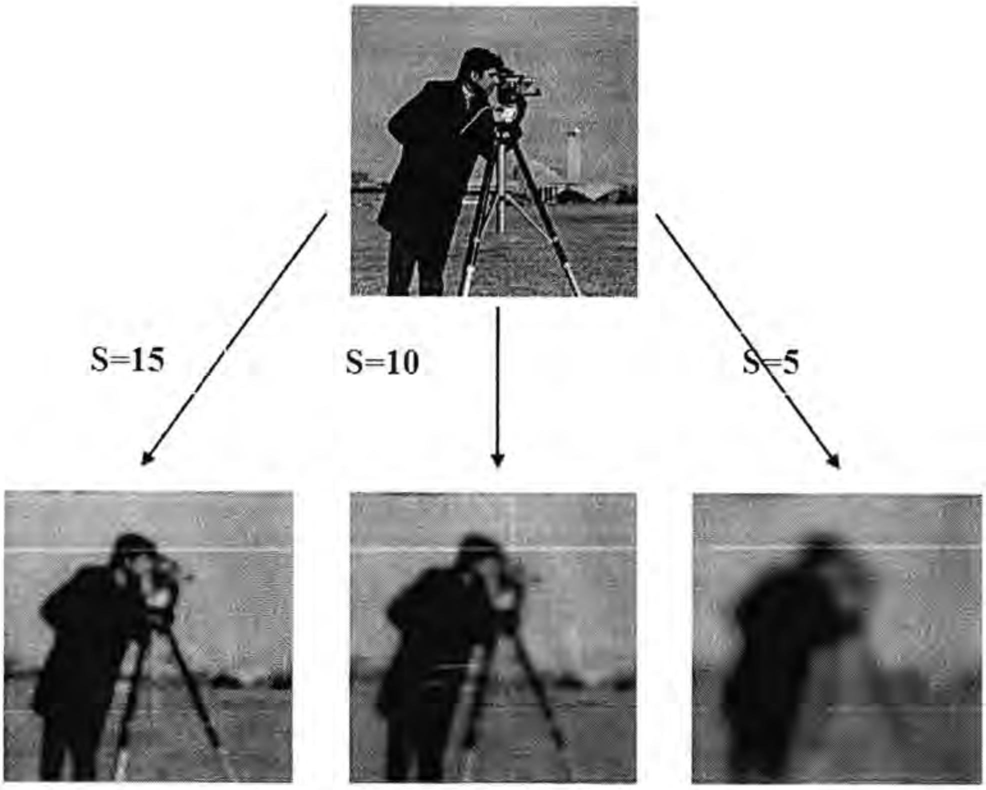

Figure-1: Original image is degraded with Gaussian blurring at different value of sigma (S).

2.No-Reference Perceptual Blur metric

In this method the original image blurred with a low-pass filter and the blurred image re-blurred with the same low-pass filter. There is a high difference in term of loss of details between the first and the second image and a slight difference between the second and the third image. And consider only the neighboring pixels variations which have decreased after the blurring step. This method takes advantage of the possibility to access to specific local variations representatives of the blur effect. The flow chart in Figure 2 describes the steps of the algorithm description and refers to the following equations of No-reference perceptual blur metric [8],To estimate the blur annoyance of gray image the first step consists in blurred it in order to obtain a blurred image B. We choose an horizontal and a vertical strong low-pass filter to model the blur effect and to create B_{ver} and B_{Hor} ,where the average low bass kernel in the vertical direction is :

$$h_v = \frac{1}{9} \times [111111111] \qquad (4)$$

And in the horizontal direction :

$$h_h = transpose(h_v) = h'_v \qquad (5)$$

And image filters are :

$$B_{ver} = h_v * F \quad , \quad B_{Hor} = h_h * F \qquad (6)$$

Then, in order to study the variations of the neighboring pixels, we compute the absolute difference images D_F_{ver}, D_F_{Hor}, D_B_{ver} and D_B_{Hor}

$$D\_F_{ver}(i,j) = Abs\big(F(i,j) - F(i-1,j)\big)$$
$$for\ i = 1\ to\ m-1, j = 0\ to\ n-1 \qquad (7)$$
$$D\_F_{Hor}(i,j) = Abs\big(F(i,j) - F(i,j-1)\big)$$
$$for\ j = 1\ to\ n-1, i = 0\ to\ m-1 \qquad (8)$$
$$D\_B_{ver}(i,j) = Abs\big(B_{ver}(i,j) - B_{ver}(i-1,j)\big)$$
$$for\ i = 1\ to\ m-1, j = 0\ to\ n-1 \qquad (9)$$
$$D\_B_{Hor}(i,j) = Abs\big(B_{Hor}(i,j) - B_{Hor}(i,j-1)\big)$$
$$for\ j = 1\ to\ n-1, i = 0\ to\ m-1 \qquad (10)$$

if we need to analyze the variation of the neighboring pixels after the blurring step. If this variation is high, the initial image or frame was sharp whereas if the variation is slight, the initial image or frame was already blur. This variation is evaluated only on the absolute differences which have decreased where

$$V_{Ver} = Max\big(0, D\_F_{ver}(i,j) - D\_B_{ver}(i,j)\big)$$
$$for\ i = 1\ to\ m-1, j = 0\ to\ n-1 \qquad (11)$$
$$V_{Hor} = Max(0, D\_F_{Hor}(i,j) - D\_B_{Hor}(i,j)$$
$$for\ i = 1\ to\ m-1, j = 0\ to\ n-1 \qquad (12)$$

Then, in order to compare the variations from the initial image, we compute the sum of the coefficients are:

$$S\_F_{Ver} = \sum_{i,j=1}^{m-1,n-1} D\_F_{ver}(i,j) \qquad (13)$$
$$S\_F_{Hor} = \sum_{i,j=1}^{m-1,n-1} D\_F_{Hor}(i,j) \qquad (14)$$
$$S\_V_{Ver} = \sum_{i,j=1}^{m-1,n-1} D\_V_{ver}(i,j) \qquad (15)$$
$$S\_V_{Hor} = \sum_{i,j=1}^{m-1,n-1} D\_V_{Hor}(i,j) \qquad (16)$$

And the Normalize Perceptual Blur Metric (PBM) in a defined range from 0 to 1 is given by:

$$PBM = Max\big|(b_{F_{ver}}, b_{F_{Hor}})\big| \qquad (17)$$

where

$$\left.\begin{aligned} b\_F_{Ver} &= \frac{S\_F_{Ver} - S\_V_{Ver}}{S\_F_{Ver}} \\ b\_F_{Hor} &= \frac{S\_F_{Hor} - S\_V_{Hor}}{S\_F_{Hor}} \end{aligned}\right\} \qquad (18)$$

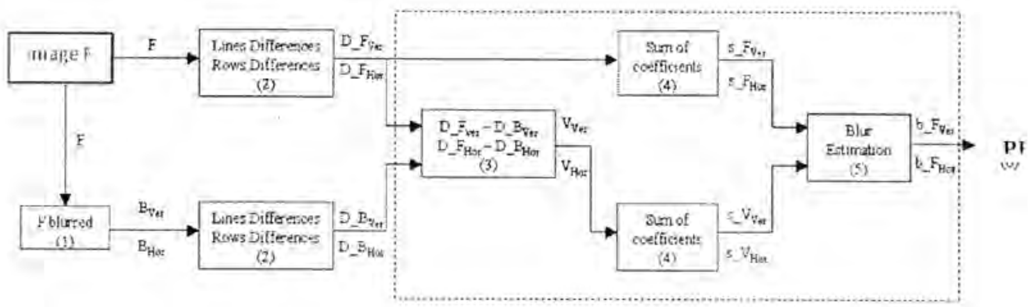

Figure-2: Flow chart of the PBM algorithm [8].

3. No reference Quality of Blurring Image

The Mean of locally (standard deviation, mean) or MLSD model , proposed the idea that good visual representations seem to be based upon some combinations of high regional visual lightness and contrast[9]. To compute the regional parameters, we divided the image into non overlapping blocks that are 50×50 pixels or less. For each block, the mean (m) and a standard deviation (g) are computed, and then taking the mean of them (m) and (g) as shown in figure (3). If the points tend to visual optimal region the image has higher quality of lightness and contrast, whereas if g (without m) is increased, it makes image having insufficient lightness, but if m (without g) is increased it makes insufficient contrast in the image.

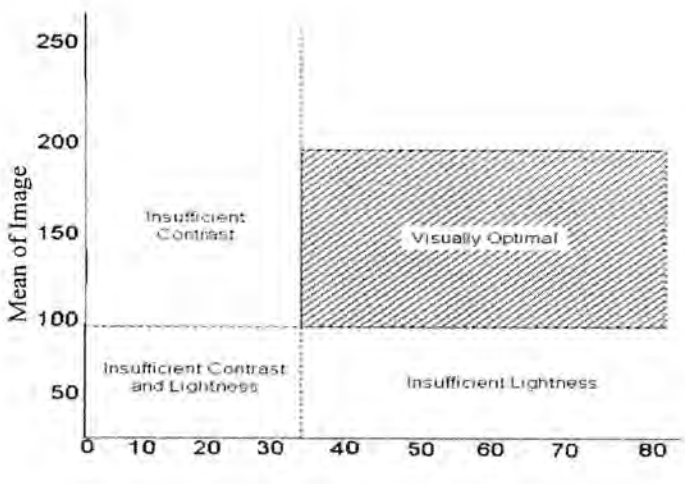

Figure -3:Image quality description according to MLSD model [9].

if Gaussian blurring has been applied on the original image with different value of S (from 1 to 15) and then applied this model as demonstrated in the figure (4,a) we can see the quality of these image are increased if S have a maximum value and it near with the optimal region(due to increasing contrast), whereas decreasing value in S makes images in the visual optimal. From this relation we can see:

$$g = f(m) \tag{19}$$

figure (4,b) shows the MLSD model for (7 database images) after it degraded by the Gaussian from this figure we can defined the general faction is :

$$g = ce^{(a+\frac{b}{m})} \tag{20}$$

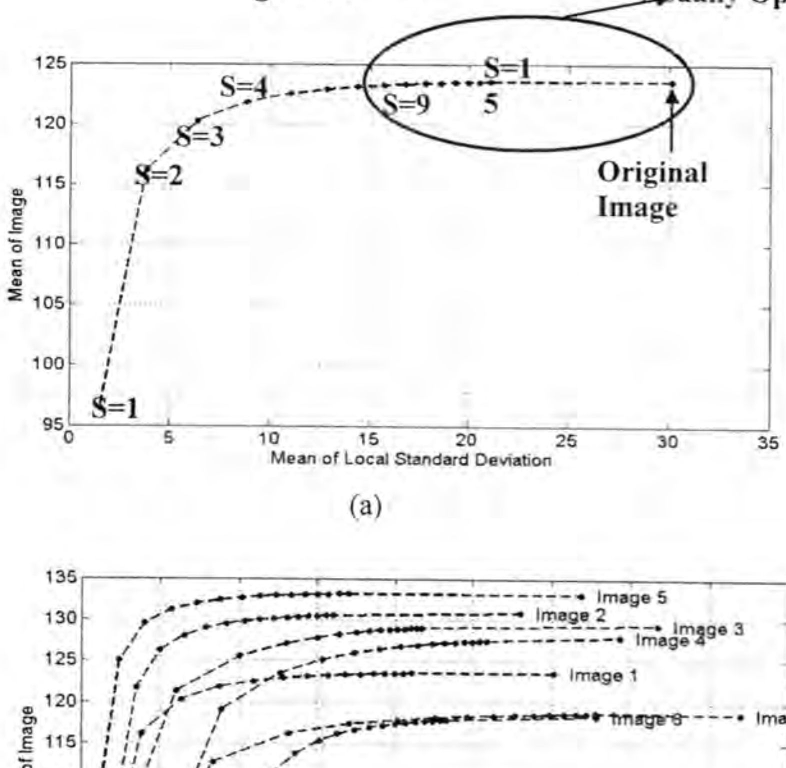

(a)

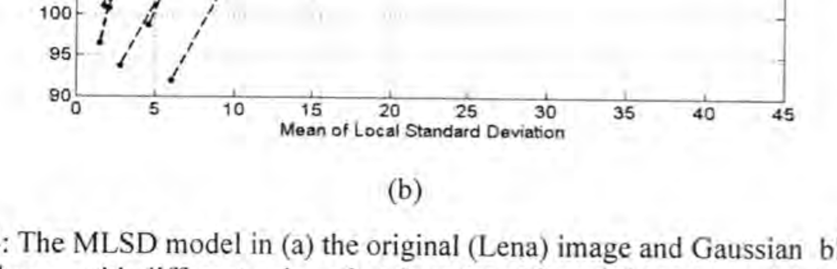

(b)

Figure-4: The MLSD model in (a) the original (Lena) image and Gaussian blurring of this image with different value of s (from 1 to 15) and (b)same model for data images.

Where a, b and c are general constants ,depending on the contrast and mean in the images. And this function is the best fit of these curves.

From the curves in the figure (4-b), the area under the curve represent the Blur Quality Metric (BQM), and this value has been simply numerically circulated without find a ,b and c constant by using trapezoidal method where:

$$BQM = \int_{m-m1}^{m=m2} f(m)\, dm \tag{21}$$

$m1$ and $m2$ are the minimum and maximum mean value. In this metric the area under the curve preoperational directed with the BQM, figure (5) is show increasing the quality of the image according to incising the S value and this value is depending on the area under the curve of the shadow region. In figure(5-b) the blurring image is represented the point in the curve is staring of the shadow region then the images is increasing in blurring at five value of (S=5,4,3,2,1) ,this mean that the shadow region limited between $m1$ at S=1 (very blurring image) and $m2$ is the mean of the blurring image (image need to know your quality). And the total curves have the same behavior in the figure (5) .

BQM has been circulated from the following steps:

1. Input degradation blurring image Io(x,y).

2. Increasing blurring in image Io(x,x) in five value of sigma by using Gaussian blurring (S=5,4,3,2,1) getting five image(I_5, I_4, I_3, I_2, I_1).

3. Calculate Mean of locally (m ,g) for all image in the step 1,2

4. Find BQM using numerical integration.

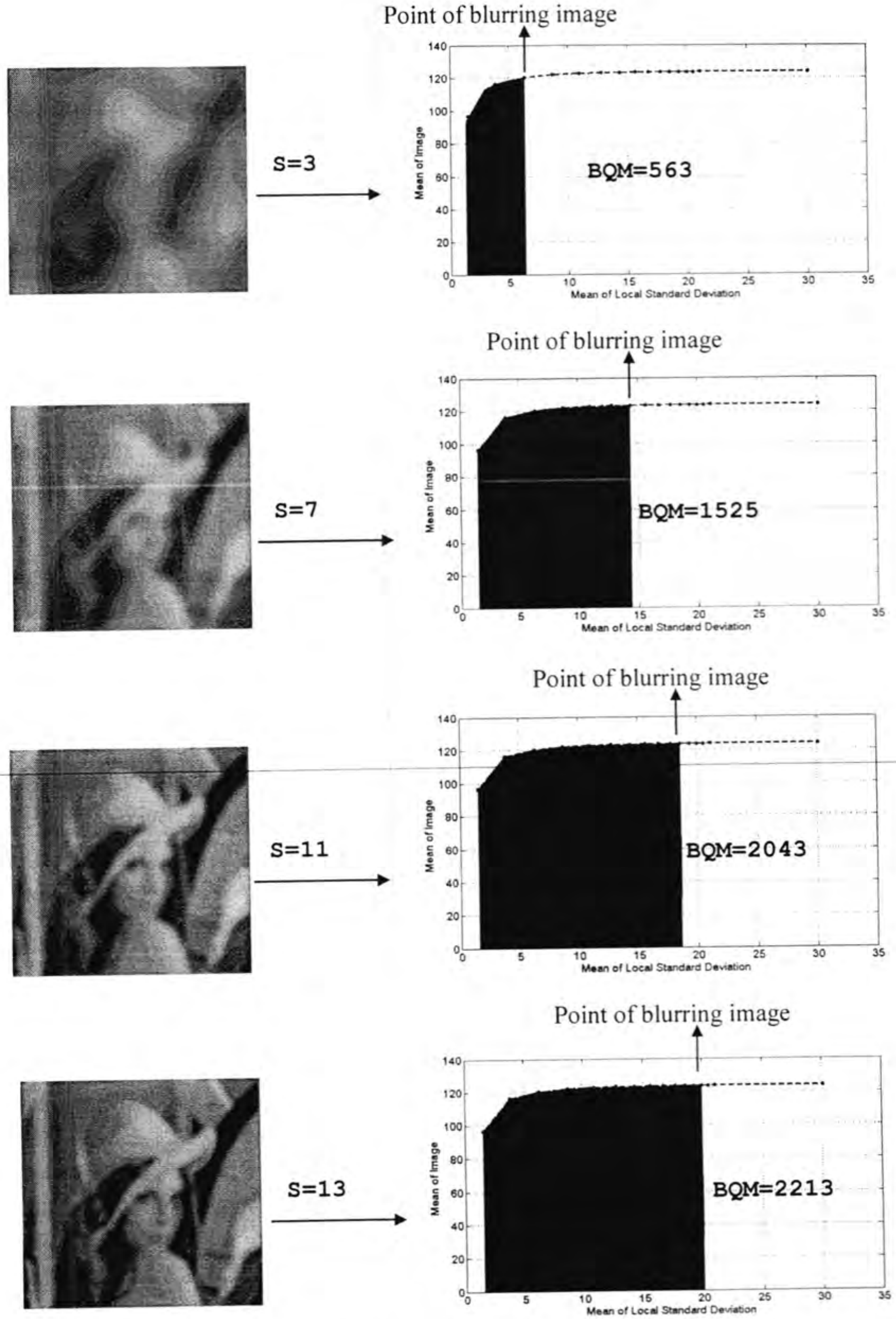

Figure-5: The BQM for blurring lena images at different values of sigma, these value direct proportional with the area under the curve in the (m, g) mode after they reblurring at (S=3,7,11,13).

4. RESULTS DISCUSSIONS

In our approach, several images were used as a data to test our metrics (all gray images with size 512×512), see figure 6, the Gaussian blurring are added for each image form (S=15) of the low blurring to (S=1) the highest blurring. Figure 7 illustrated the($NMSE^{-1}$, BQM,PBM) in normalization (0-1) state as function of blurring factor (Sigma).the normalization had been done by $Qn = \frac{Q-\min(Q)}{\max(Q)-\min(Q)}$, Where Q is the matching ($NMSE^{-1}$, BQM,PBM) .from this figure we can see the BQM curve (no reference quality) nearest from $NMSE^{-1}$ (reference quality) curve if it is compared with PBM method. There is direct proportion between the blurring factor S and the metrics and this behavior can be generalized for all distorted images, this is demonstrated in the figure 8. If we compare this figure with the figure (4-b) can see the in the moderate and low blurring image the points in the curves(for each image) in this figure are more distinct form the point in the curves in the figure (4-b) .

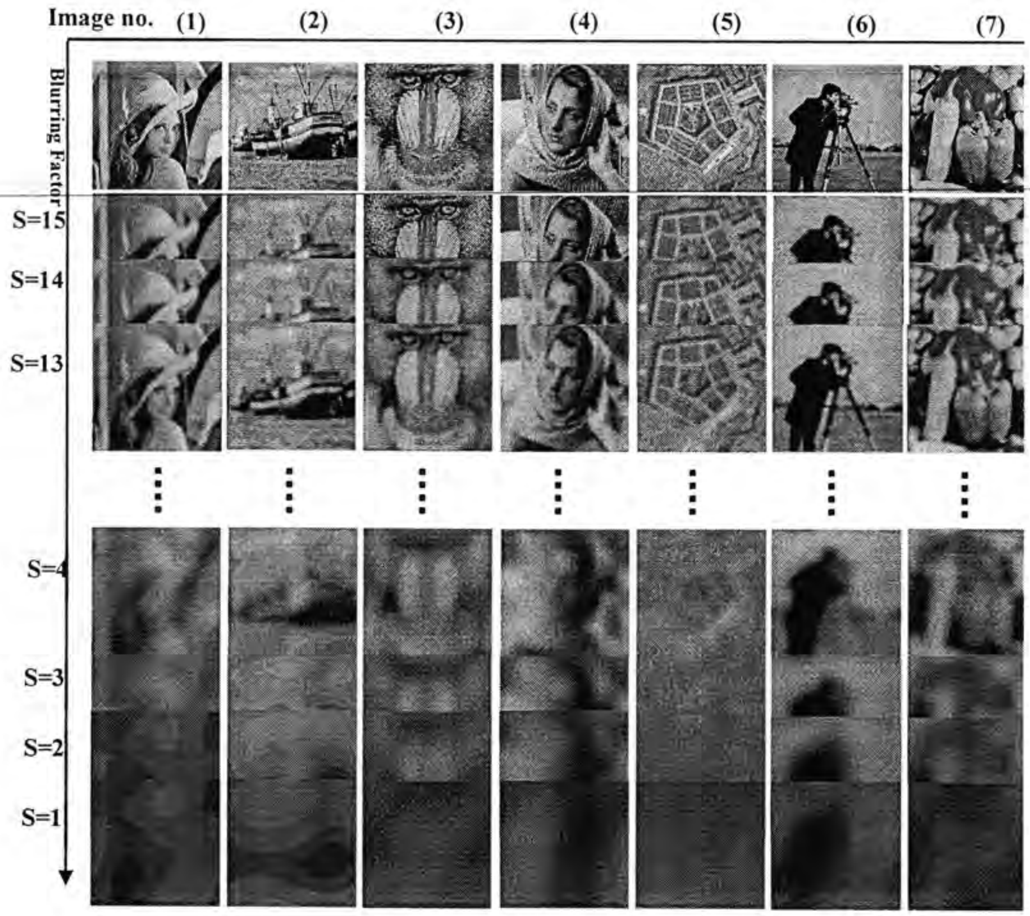

Figure-6: The test images are blurred from S=15 to S=1.

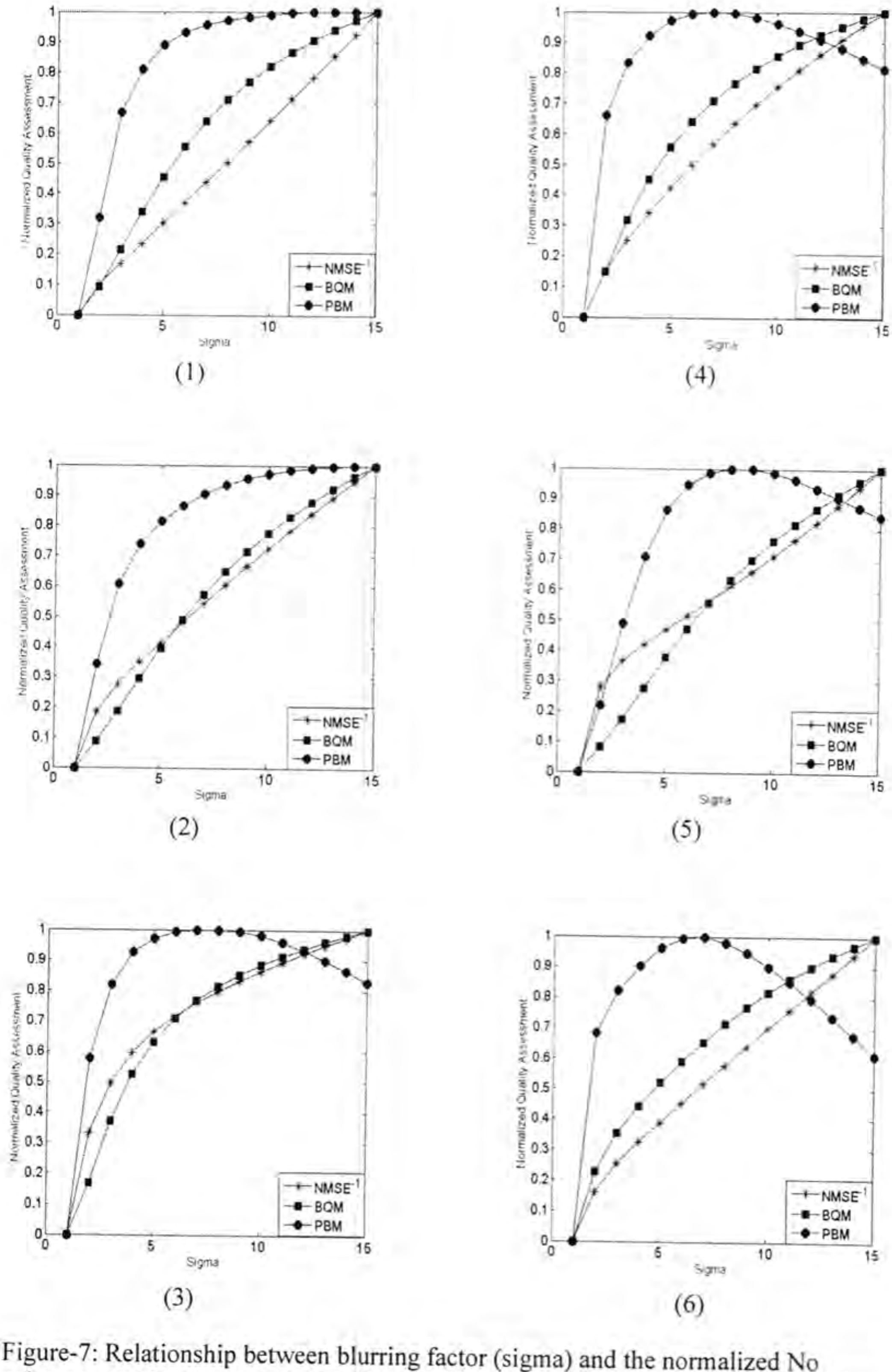

Figure-7: Relationship between blurring factor (sigma) and the normalized No reference quality assessment (BQM and PBM) and (1/NMSE) as a reference quality assessment for all tested data images.

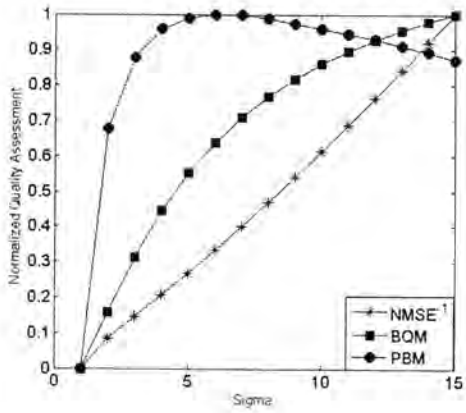

(7

Figure (7) : Continued.

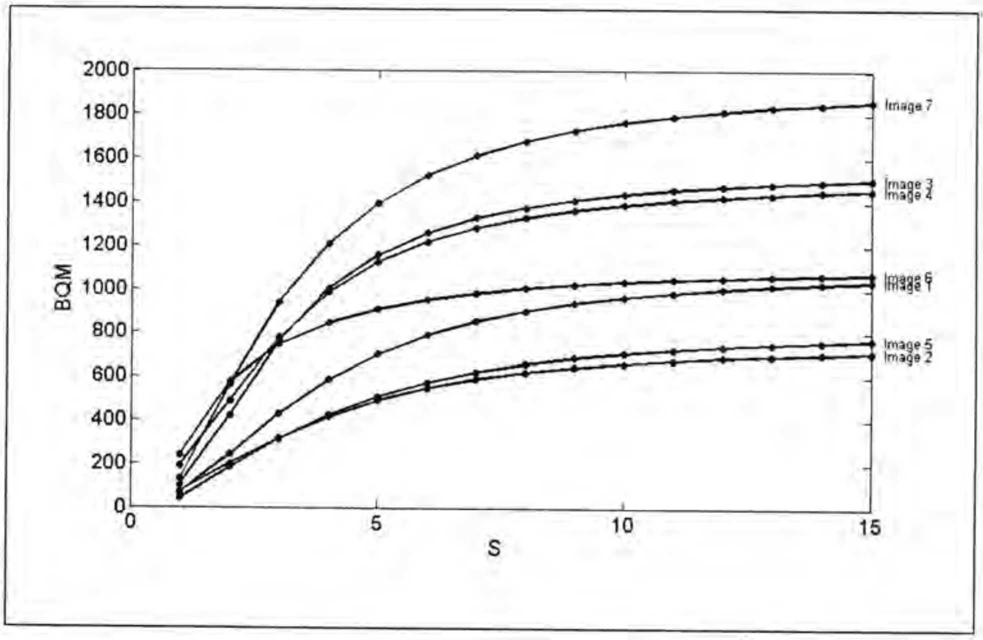

Figure-8: The BQM as a function of blurring factor S for the data images test.

5. CONCLUSION

In This paper we suggested a no reference quality assessment for measuring Gaussian blurring in the various gray-scale images. This method is developed form MLSD model. From the result we can say the BQM method is simple method, gives numerical value and more accurate from MLSD model. And the suggestion method is belter then PBM.

REFERENCE

1. A. M. Eskicioglu and P. S. Fisher, "Image quality measures and their performance," IEEE Trans. Communication. , vol. 43, pp. 2959–2965, Dec. 1995.
2. Z. Wang and A. C. Bovik, "A universal image quality index," IEEE Signal Processing Letters , vol. 9, pp. 81–84, Mar. 2002.
3. D. A. Silverstein and J. E. Farrell, "The relationship between image fidelity and image quality," in Proc. IEEE Int. Conf. Image Processing, pp. 881–884, 1996.
4. Zhou Wang, Alan C.Bovik, and Brian L.Evans,"Blind measurement of blocking artifacts in images",IEEE Proc.ICIP, Vol.3, pp.981-984,2000.
5. P. Marziliano, F. Dufaux, S. Winkler and T. Ebrahimi ،A no-reference perceptual blur metric," in Proc. IEEE ICIP , pp. 57-60, 2002 .
6. L. Liang, J. Chen, S. Ma, D. Zhao, W. Gao, "A no-reference perceptual blur metric using histogram of gradient profile sharpness," in Proc. IEEE ICIP, pp . 4369-4372, 2009.
7. Luhong Liang, Jianhua Chen, Siwei Ma, Debin Zhao, Wen Gao: A no-reference perceptual blur metric using histogram of gradient profile sharpness. ICIP: 4369-4372, 2009.
8. F. C. Roffet, T. Dolmiere, P. Ladret, and M. Nicolas, "The Blur Effect:Perception and Estimation with a New No-Reference Perceptual Blur Metric," inSPIE proceedings SPIE Electronic Imaging Symposium ConfHuman Vision and Electronic Imaging, n Jose United States,vol. XII, pp. EI 6492–16, 2007.
9. D. J. Jabson, Z. Rahman, G. A. Woodell, "Retinex processing for automatic image enhancement," Journal of Electronic Imaging, Vol. 13(1), PP.100–110, January 2004.

Monitoring Wetlands Using Satellite Image Processing Techniques

Hussain Zaydan Ali
Expert / Ministry of science and technology
Received 14/3/2013 – Accepted 15/9/2013

الخلاصة

تعد الاراضي الرطبة من المصادر الطبيعية الاكثر اهمية على الارض . ان ألاراضي الرطبة تجهز الحياة لملايين الناس، ويعتبر انعاش الارض الرطبة ضرورة ملحة بسبب حاجة الحياة البرية الى بيئة بنوعية عالية اذا اريد لها ان تتكيف للتغير المناخي .تعتبر ادارة البيئة تحدي مهم بالدول النامية. ان الهدف العام من هذا البحث هو لكشف التغيرات بالمسطحات المائية باستخدام بيانات متعددة الاطياف.ان هدف البحث هو حساب مساحة المسطحات المائية (الاهوار ،البحيرات ،الخزانات) باستخدام برنامج أيرداس النسخة 9.2 والمطبق على صور لاندسات بتواريخ مختلفة لبعض المناطق المنتخبة في العراق .تم تطبيق التصنيف على الصور الفضائية لاستخلاص طبقات المسطحات المائية. الكلمات المفتاحية: الاستشعار عن بعد ، التصنيف الموجه ، الاهوار ، الاراضي الرطبة.

ABSTRACT

Wetlands are one of the most important natural resources on Earth. They provide livelihoods for millions of people. Restoring wetlands is urgent, because wildlife will need more high-quality habitat if it is to adapt to climate change. Environment management is a significant challenge in developing Countries. The general objective of this study is to reveal water body's changes using multi resolution data. The aim of this research is to calculate the area of water bodies(Marshes, lakes, reservoir) using ERDAS program Ver. 9.2 applied on ETM+ images at different dates for some selected regions in Iraq. Classification of satellite images was applied to extract water bodies' layers.
Key Words: Remote Sensing, Supervised Classification, Marshes, Wetlands.

INTRODUCTION

Wetlands are one of the most important natural resources on Earth. They provide livelihoods for millions of people, support a stunning variety of wildlife, and form part of a healthy and functional landscape. Sadly, this natural wealth is being eroded. Wetlands have been drained, rivers straightened and the quality and quantity of water in the environment compromised by pollution and abstraction. The term wetland covers a wide variety of wildlife habitats including those dominated by standing open water such as lakes, ponds and seasonally flooded areas, as well as those where ground is waterlogged to varying degrees such as reed beds, marshes, and wet headland. The unifying feature of wetlands is the dominant role of water which profoundly influences the ecological functioning of these habitats[1],[2]. Wetlands are vital to life - they provide water for our basic needs and our economic prosperity. In the developing world millions of people rely entirely on wetlands for their livelihoods and food security. Wetlands are also important for biodiversity and play a key role by affording habitat to many rare and endangered species. Wetlands are the most threatened of all the earth's ecosystems. Yet despite their importance the world's wetlands are frequently mismanaged, and many are now so degraded that the people who rely directly on them for their livelihoods have become more vulnerable to or have fallen deeper into poverty[1],[2].

MATERIALS AND METHODS

The general objective of this study is to reveal water bodies changes using multi resolution data. Satellite image classification involves designing and developing efficient image classifiers. A particularly important application of remote sensing is the generation of land-use/ land-cover maps from satellite imagery[3]. Compared to more traditional mapping approaches such as terrestrial survey and basic aerial photo interpretation, land-cover mapping using satellite imagery has the advantages of low cost, large area coverage, repetitively, and competitively[4]. In this study, we presented an approach for the extraction and representation of land-cover information based on high-resolution Landsat imagery data. Figure(1) present the flowchart of data processing of Landsat image. Several regions around the word are currently undergoing rapid, wide-ranging changes in land cover. These changes in land cover, have attracted attention.

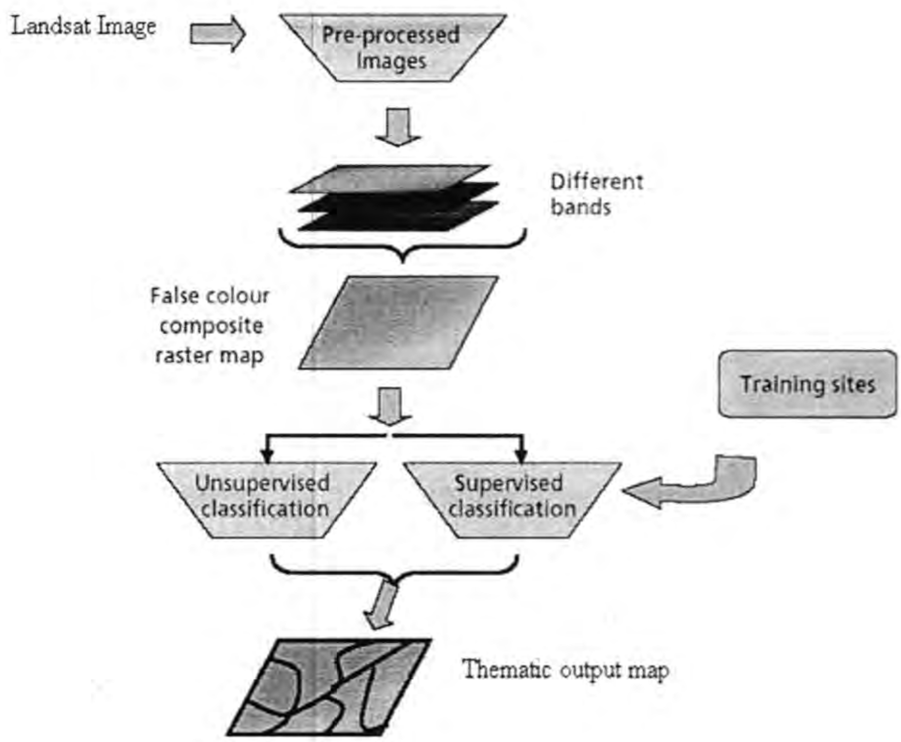

Figure-1: Flowchart of data processing.

Remote sensing provides a viable source of data from which updated land-cover information can be extracted efficiently and cheaply in order to inventory and monitor these changes effectively. Digital image processing is the technique of manipulating and interpreting digital images with the aid of a computer [5],[6]. It starts with one image and produces such information products as segmented images, data, and maps. Digital image processing permits rapid and repeatable analysis, allows for statistical treatment of multivariate data and produces quantitative results. The ultimate goal of digital image processing is to identify and interpret patterns in an image, i.e. pattern recognition[7]. Pattern recognition is the science and art of finding meaningful patterns in data [8]. A pattern is simply any well-defined set of measurements. The pattern recognition process consists of three phases, i.e., 1) image segmentation, 2) feature extraction, and 3) classification. Multi spectral satellite image classification is an application of pattern recognition in the geo science. In a satellite image the natural pattern is one ground resolution element or pixel. The receptor may be an airborne or space borne multi spectral scanner. The feature of a natural pattern is a set of n radiance measurements obtained in the various wavelength bands for each pixel. This set of measurements is referred to as a measurement vector in the measurement space. Classifier or the decision maker assigns the measurement vector to one of a set of classes according to an appropriate decision rule [7],[4]. The fundamental basis for multi spectral satellite image classification is the electromagnetic reflectance properties of earth surface features. Because ground objects have their own characteristic spectral response in different spectral bands of the electromagnetic spectrum, they can be identified and delineated in a multi spectral image[9]. The often-used decision rules in supervised classification are Parallelepiped, Minimum Distance, Mahalanobis Distance, and Maximum Likelihood/ Bayesian[10].

RESULTS AND DISCUSSION

Two regions are considered in this paper; Al Dalmaj marsh located south-east of capital Baghdad with Wasit Governorate, and Al Razzaza lake located in Karbala Governorate. Land cover within these areas is divided principally among water body, sand dunes and agriculture. The water layer represent our concern in this paper. A key issue relating to wetlands and watercourses is that they are extremely sensitive and man easily affects their wildlife interest. This includes modifications such as deliberate drainage of wetlands and changes in water levels. They are particularly prone to pollution, including nutrient enrichment, and the effects can be very wide ranging. Wetlands are places where land and water meets. Classifying wetlands is difficult . Such places are highly dynamic, changing with the seasons and over time. Their precise boundaries are hard to define. Image classification is a process of assigning pixels in an image to one of a number of classes or labels. Classification is based solely on the feature vector. The spectral reflectance characteristics of ground objects are described by spectral reflectance curves. A spectral reflectance curve is a graph of the spectral reflectance of an object as a function of wavelength as shown in figure(2). Because spectral responses measured by remote sensors over various features often permit an assessment of the type and/or condition of the features, these responses are also referred to as spectral signatures. The configuration of these spectral reflectance curves gives us insight into the spectral characteristics of the objects.

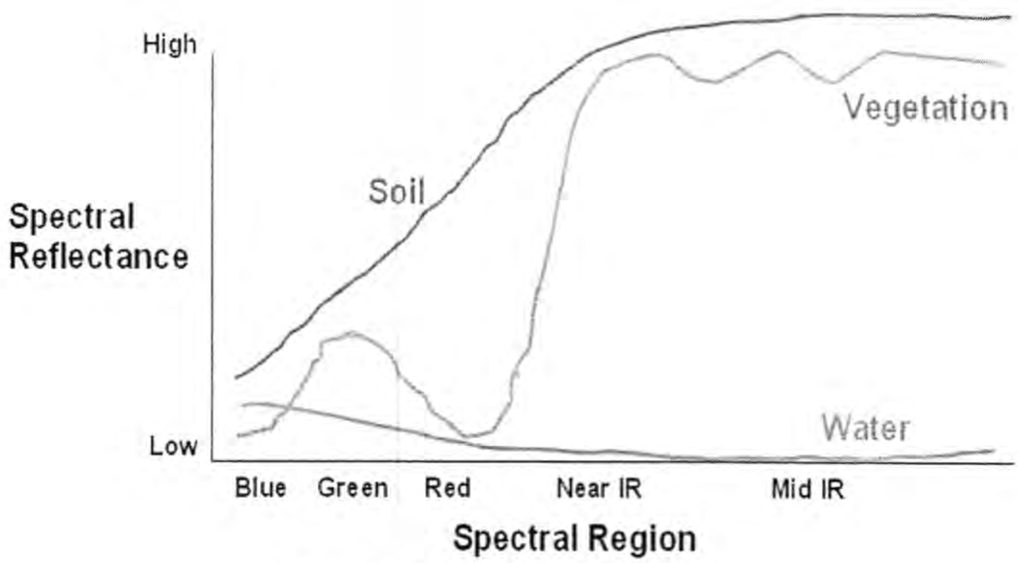

Figure-2: Spectral reflectance curve.

The multi spectral approach forms the heart of the application of remote sensing in discrimination of land-cover types and conditions. By analyzing a scene in several spectral bands, we can improve our ability to distinguish the identity and condition of terrain features. For example, water and vegetation might reflect nearly equally in visible wavelengths, yet these features are almost always separable in near-infrared wavelengths. Satellite images comprise of several bands linked together to give an output that is most suitable for the requirement of the user. Each of these bands consists of separate pixels recording the reflectance value from an object. The reflectance varies from object to object as well as from band to band. Satellite land cover map is made usually by supervised or unsupervised classification method. The first approach requires interactive training area selection and knowledge on the study area. This method cannot be automated by any way. The second approach is carried out mainly by clustering technique. This is done automatically based on a number of chosen classes and seperability measure among them. The monitoring task can be accomplished by supervised classification techniques. The aim of this study is to generate a thematic map of Al Dalmaj marsh; Al Razzaza lake and its surrounding area using supervised classification method based on calculating the classes profiles shown above for the purposes of land cover mapping. A primary goal of using multi spectral remote sensing image data is to discriminate, classify, identify as well as quantify materials present in the image. A thorough knowledge and understanding of spectral characteristics of various earth surface objects is required for identifying the classes and collecting region of interest. The results of classification of Landsat images acquired at 1972 , 1990 and 2002 of Al Dalmaj Marsh are shown in figures (1), (2) and (3).

Figure-3: Classified image(1972).

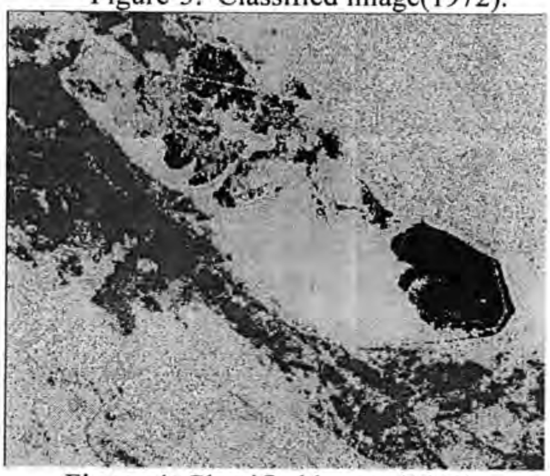

Figure-4: Classified image (1990).

Figure-5: Classified image(2002).

Shown in table(1) the changes of the areas of Al Dalmaj Marsh during 1972 to 2002.

Table-1: Areas of the study region.

Year	1972	1990	2002
Area(Hectares)	6566	18080	10872

The results of classification of Landsat images acquired at 1990 , 2002 and 2005 of Al Razzaza Lake are shown in figures (4), (5) and (6).

Figure-6:Classified Image 1990

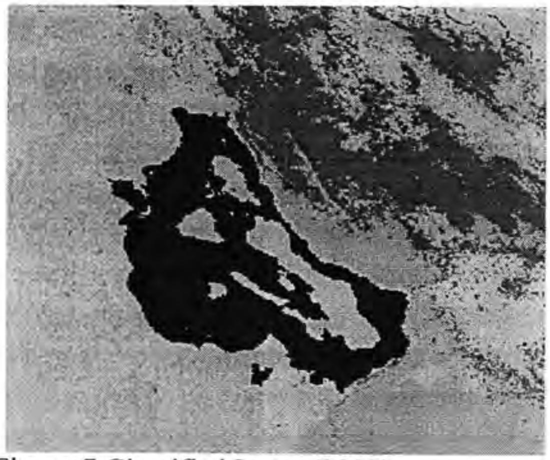

Figure-7:Classified Image(2002)

Figure-8: Classified Image(2005).

Shown in table(2) the changes of the areas of Al Razzaza Lake during 1990 to 2005.

Table-2: Areas of the Al Razzaza Lake.

Year	1990	2002	2005
Area (Hectare)	154,000	95,50	87,50

CONCLUSION

Compared to more traditional mapping approaches such as basic aerial photo interpretation, land-use mapping using satellite imagery has four advantages. First, land-use types can be mapped from digital satellite imagery faster and often with lower costs. Second, fast and inexpensive updating of land-use map products is possible. This is because satellite images are captured for the same geographic area at a high revisit rate. Third, satellite imagery data are captured in digital forms. They can therefore easily be integrated with other types of ground object information through such techniques as GIS. Fourth, satellite images cover large geographic areas. The great economies of scale provided by digital image processing make it relatively inexpensive to map large expanses of land, making it easier and more cost effective to generate large amounts of map products. The multispectral approach forms the heart of the application of remote sensing in discrimination of land-cover types and conditions. By analyzing a scene in several spectral bands, we can improve our ability to distinguish the identity and condition of terrain features. For example, water and vegetation might reflect nearly equally in visible wavelengths, yet these features are almost always separable in near-infrared wavelengths.

REFERENCES

1. Barbier, E. B., M. Acreman and D. Knowler. 1997. Economic valuation of wetlands. Ramsar Convention Bureau, Gland, Switzerland.
2. Mitsch, W.J. and Gosselink, J.G. (2000). Wetlands.3rd ed, . Wiley, New York.
3. Ban F.,Y , Namir K.S. ,and Hussain Z. Ali, (2004), " The use of remote sensing techniques in the classification of Al- Najaf soil", M.Sc. thesis in Remote Sensing Engineering, Building and Construction Engineering Department, University of technology.
4. Lillesand TM AND Kiefer R.,W., 1999, Remote Sensing and Image Interpretation. John Wiley & Sons, Inc. New Jersey.
5. Castleman, K.R., 1996. Digital Image Processing, Prentice-Hall, New Jersey.
6. Swain, P.H., and S.M. Davis (editors.), 1978. Remote Sensing: The Quantitative Approach, McGraw-Hill, New York.
7. Hall, E.L., 1979. Computer Image Processing and Recognition, Academic Press, New York.
8. Bhanu, B., P. Symosek, and S. Das, 1997. Analysis of Terrain Using Multispectral Images, Pattern Recognition, 30(2):197-215.
9. Mather P.M., Computer Processing of Remotely Sensed Images: An introduction, 3rd ed., Chichester, UK: John wiley and sons, 2004.
10. ERDAS Field Guide, 1997.

Video Compression for Communication and Storage Using Wavelet Transform and Adaptive Rood Pattern Search Matching Algorithm

Hameed Abdul-Kareem Younis and Marwa Kamel Hussein
Dept. of Computer Science, College of Science, University of Basrah
Received 1/3/2013 – Accepted 15/9/2013

الخلاصة

تستخدم تكنولوجيا الوسائط المتعددة في الوقت الحاضر بشكل واسع، لذلك تساعد عملية ضغط الفيديو كثيرا في التقليل من المساحة الخز نية المطلوبة، وكذلك تساعد في عملية التراسل عبر شبكات الاتصالات.

في هذا البحث، يضغط زوج من إطارات الفيديو بضغط الإطار الأول كما في عملية ضغط الصورة الواحدة ، ثم يضغط الإطار الثاني بتخمين عدم التكافؤ (الاختلاف) بين الإطارين.

لغرض تقدير الحركة (الاختلاف) تم استخدام خوارزمية تطابق الكتلة باستخدام خوارزمية بحث نمط الصليب التكيفي (Adaptive Rood Pattern Search (ARPS تم استخدام ترميز هوفمان لترميز متجه الحركة الناتج أما الجزء المتبقي فتتم عملية ضغطه كما في طريقة الصورة الواحدة. النتائج التجريبية بينت نتائج جيدة عند حسب نسبة قمة الإشارة إلى الضوضاء (PSNR) ونسبة الضغط (CR) ووقت المعالجة.

ABSTRACT

Currently, multimedia technology is widely used. Using the video encoding compression technology can save storage space, and also can improve the transmission efficiency of network communications. In video compression systems, the first frame of video is independently compressed as a still image, this is called ***intra coded frame***. The remaining successive frames are compressed by estimating the disparity between two adjacent frames, which is called ***inter coded frames***. In this paper, intra frame was transformed using Discrete Wavelet Transform (DWT).

The disparity between each two frames was estimated by Adaptive Rood Pattern Search (ARPS) algorithm. The result of the Motion Vector (MV) was encoded into a bit stream by Huffman encoding while the remaining part is compressed like the compression was used in intra frame. Experimental results showed good results in terms of Peak Signal-to-Noise Ratio (PSNR), Compression Ratio (CR), and processing time.

1. INTRODUCTION

An images sequence (or video) can be acquired by video or motion picture cameras, or generated by sequentially ordering two-dimension (2D) still images as in computer graphics and animation. As shown in Fig.1.

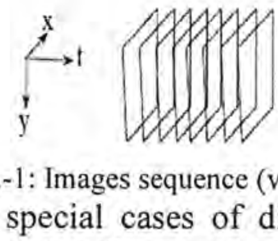

Fig.-1: Images sequence (video).

Video processing is special cases of digital processing in which signals are processed are video files or video streams. It is extensively used in television sets, Digital Versatile Disks (DVD), video players, ..., etc. Although digital video signals can be transferred over the long distances with a low probability of bit error rate, the raw material of digital video requires high bandwidth for transmission and high storage capacities when compared to its analog equivalent. Therefore, compression basically is necessary to reduce data, a digitized analog video sequence can comprise of up to 165 Mbps of data. To reduce the media overheads for distributing these sequences, the following techniques are commonly employed to achieve desirable reductions in image data [1]:

i . Reduce color nuances within the image.

ii . Reduce the resolution with respect to the prevailing light intensity.

iii . Remove spatial redundancy or correlation between neighboring pixels values.

iv .Compare adjacent images and removes details that are unchanged between adjacent frames in sequence of images.

The first three of above points are image based compression techniques that is called ***intra frame***, where only one frame is evaluated and compressed at a time. The last one is called ***inter frame,*** where different adjacent frames are compared as a way to further reduced image data. All of these techniques are based on the term of motion. Motion is an essential aspect of video sequences. The ability to estimate, analyzes, and compensate for relative motion is a common requirement of many video processing, analysis and compression algorithms and techniques. Fig.2 shows flowchart of video compression.

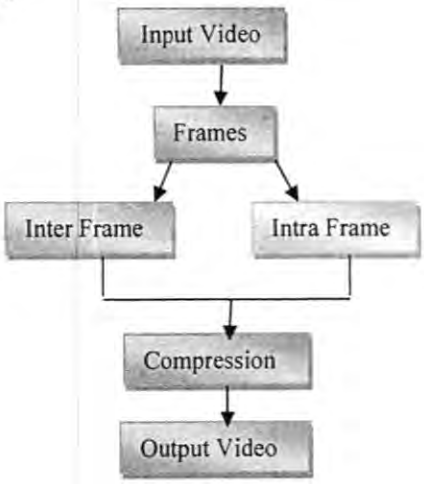

Fig.-2: Flowchart of video compression.

Hassan B. and Malik K. in 2006 [2] have proposed a method for video compression based on skipping some frames which have little information from the fames sequence. They have designed an algorithm to compare two frames on sub frame level and decides which one is more important for the overall video quality as perceived by eye of the user and skipping the frame which have little information.

Bjorn B. in 2005 [3] Developed a video codec. This codec consist of three parts, transformation, quantization and encoding. These three fundamental parts are used for the purpose of compressing the data. Through the transform, the energy in a picture is concentrated to a small region. These regions are then rounded off through quantization to compress the data. Author has also proposed a method to cope the problem of error that can be introduced through transmitted it over channels by sent side information over another channel to describes the information in yet another way. Consequently, a coding scheme called *Multiple* has been presented.

The work aims to propose an efficient technique for video compression by wavelet transform by using two systems, intra and inter coded frames. In this present work, video compression system is developed using wavelet transform, and ARPS. The rest of this paper is organized as follows. Some of basic principles has been explained in Section 2. We show our proposed video compression system in Section 3. Section 4 give the experimental results. Finally, the paper has been concluded in Section 5.

2. Basic Principles

2.1 Intra and Inter Coded Frames

The motion estimation and the motion compensation blocks work, only if there is a past frame that is stored. So, question is how do we encode the first frame in a video sequence, for which there is no past frame reference? The answer to this question is fairly straight forward. We treat the first frame of a video sequence like a still image, where only the spatial, i.e., the intra frame redundancy can be exploited [4].

The frames that use only intra frame redundancy for coding are referred to as the ***intra coded frame***. The first frame of every video sequence is always an *intra-coded frame*. From the second frame onwards, both temporal as well as spatial redundancy can be exploited. Since these frames use inter frame redundancy for data compression, these are referred to as ***inter coded frame.*** However, it is wring to think that only the first frame of a video sequence would be intra-coded and the rest inter-coded. In some of the multimedia standards, intra-coded frames are periodically introduced at regular intervals to prevent accumulation of prediction error over frames. It is obvious that intra-coded frames would require more bits to encode as compared to inter-coded frames since the temporal redundancy is not exploited in the form. As shown in Fig.3 and Fig.4.

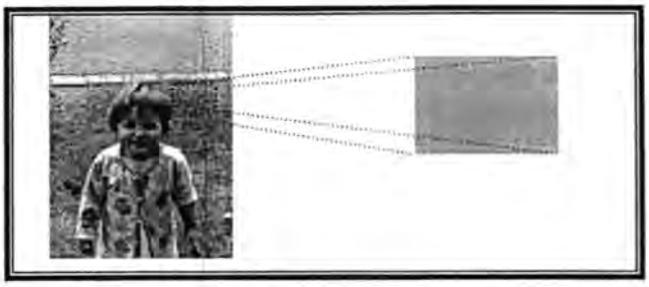

Fig.-3: Intra frame.

Fig.-4: Inter frames.

2.2 Discrete Wavelet Transform (DWT)

The basic operation in wavelet transform is to filter an image with a low pass filter (L) and a high pass filter (H) and down-sample the output by a factor of 2. Both operations on the x direction, two new images are obtained L and H. They are filtered and down sampled again but this time in the y direction. Four sub bands images are obtained which can be combined to recover the original one. The same amount of information is present, but this new configuration is more suitable for efficient coding [5].
The inverse wavelet transform is performed by enlarging the wavelet transform data to it is original size. Insert zeros between each of four sub images, and sum the results to obtain the original image [6]. The Haar wavelet is one of the most common used wavelets. It resembles a stepfunction and is defined by:

$$\text{Lowpass} = \frac{1}{\sqrt{2}}[\,1 \quad 1\,]$$

$$\text{Highpass} = \frac{1}{\sqrt{2}}[\,1 \quad -1\,]$$

2.3 The Embedded Zero Tree Wavelet (EZW) Quantization

An EZW encoder was especially designed by Shapiro to be used with wavelet transform. In fact, EZW coding is a quantization method. The EZW encoder is based on progressive encoding to compress an image into a bit stream with increasing accuracy. This means that when more bits are added to the stream, the decoded image will contain more detail. A zero tree is a tree of which all nodes are equal to or smaller than the root. The tree is coded with a single symbol and reconstructed by the decoder as a tree filled with zeroes [6].

2.4 Arithmetic Encoding

Arithmetic encoding, and its derivative technique, Q-coding, is used to overcome some of the limitations of Huffman codes. It is a non-block code, in that a single codeword is used to represent an entire sequence of input symbols, in contrast to Huffman coding where a source symbol block corresponds to a codeword block. Instead, it uses the real numbers to represent a sequence of symbols by recursively subdividing the interval between 0 and 1 to specify each successive symbol. The limitation of this technique is the precision required in performing the calculations and arriving at the code word which will represent the entire sequence correctly [7].

2.5 Huffman Encoding

A Huffman encoding developed by D.A. Huffman, a Huffman encoder takes a block of input characters with fixed length and produces a block of output bits of variable length. It is a fixed-to-variable length code. Huffman encoding uses a variable length code for each of the elements within the information. This normally involves analyzing the information to determine the probability of elements within the information. The most probable elements are coded with a few bits and the least probable coded with a greater number of bits [8].

2.6 PSNR and CR

Evaluation criteria that usually used in digital image and video compression are in two directions. First direction is to evaluate quality of the reconstructed image. Second direction is Compression Ratio (CR). In terms of quality evaluation, two mathematical metrics are used. First one is Mean Square Error (MSE), which measures the cumulative square error between the original and the reconstructed image. Second meter is Peak Signal-to-Noise Ratio (PSNR). The formula for MSE is giving as [9]:

PSNR is the standard method for quantitatively comparing a compressed image with the original. For an 8-bit grayscale image, the peak signal value is 255. Hence, the PSNR of an M×N 8-bit grayscale image *C* and its reconstruction *R* is calculated as [9]:

$$PSNR = 10\log_{10}\frac{255^2}{MSE} \qquad \dots (1)$$

where the MSE is defined as:

$$MSE = \frac{1}{N^2}\sum_{i=0}^{N-1}\sum_{j=0}^{N-1}\left[C_{ij}(m,n) - R_{ij}(m,n)\right]^2 \quad \ldots (2)$$

PSNR is measured in decibels (dB), M: height of the image, N: width of the image.

The second direction of comparing the compressed and the original images is the compression ratio. It is defined as [10]:

$$\text{Compression Ratio} = \frac{\text{Compressed File Size}}{\text{Uncompressed File Size}} = \frac{\text{Size}_c}{\text{Size}_u} \quad \ldots (3)$$

In addition to measuring the quality of image, we also measure the compression ratio. Compression ratio is the ratio of the compressed file size to the original file size. In general, the higher the compression ratio, the smaller is the size of the compressed file. Compression speed, on the other hand, is the amount of time required to compress and decompress the image. This value depends on a number of factors, such as the complexity of the algorithm, the efficient of the implementation, and the speed of the processor [10].

2.7 Motion Estimation

Motion Estimation (ME) is the process of analyzing successive frames in a video sequence to identify objects motion. The motion of an object is usually described by a two-dimensional motion vector, which is the placement of the co-ordinate of the best similar block in previous frame for the block in current frame. This placement is represented by the length and direction of motion [11].

2.8 Motion Compensation

Motion Compensation (MC) predication has been used as a main tool to remove temporal redundancy that comes from little change in the content of the image from one video sequence to another. It provides coding system with a high compression ratio. This technique is adopted by all of the existing international video coding standards, such as Picture Expert Group (MPEG) series and H.26x series.

Motion compensation prediction assumes that the current frame can be locally modeled as a translation of the frames in the previous (or reference and next) time. Fig.5 shows motion compensation between two frames [12].

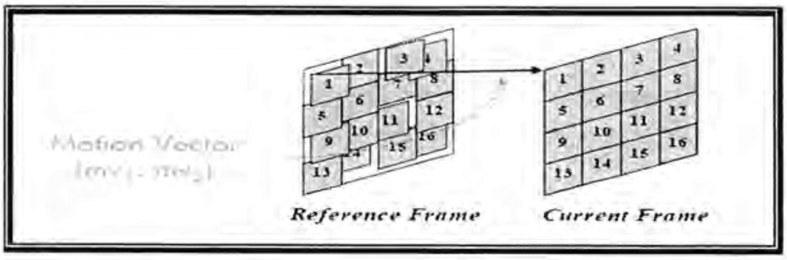

Fig.-5: Motion compensation between two frames.

2.9 Motion Estimation Algorithms

These algorithms assume that a frame has been divided into M non-overlapping blocks that together cover the entire frame. Moreover, the motion in each block is assumed to be constant, that is, it is assumed that entire block undergoes a translation that can be encoded in the associated motion vector. The problem of block-based ME algorithms is to find the best MV for each block, as shown in Fig.6 these algorithms are also called ***Block Matching Algorithms (BMA)*** [13].

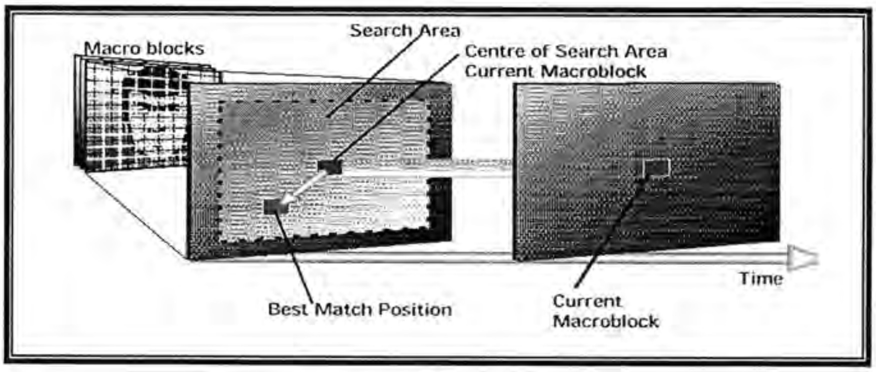

Fig.-6: Block Matching Algorithms.

2.9.1 Block Matching Algorithms

Block Matching Algorithm (BMA) is the most popular technique used for motion estimation in which the current luminance frame is divided into non-overlapped macro blocks (MBs) of size NxN that are then compared with corresponding macro block (MB) and its adjacent neighbors in the reference frame to create a vector that stipulates the movement of a macro block from one location to another in the reference frame [14], i.e., finding matching macro block of the same size NxN in the search area in the reference frame.

The position of motion vector has two parts, horizontal and a vertical. These parts can be positive or negative. A positive value means motion was to the right or motion downward while a negative value means motion was to the left or motion upward. This Motion Vector

(MV) will be used to predict new frame from the reference which is called ***motion compensation***. The matching measurement is usually determined using one of Block Distortion Measure (BDM) like Mean Absolute Difference (MAD) given by Equation1 or MSE given by Equation2. The macro block with the least cost is considered the matching to the current frame macro block [15].

$$MAD = \frac{1}{N^2}\sum_{i=0}^{N-1}\sum_{j=0}^{N-1}\left|C_{ij} - R_{ij}\right| \qquad ...(4)$$

$$MSE = \frac{1}{N^2}\sum_{i=0}^{N-1}\sum_{j=0}^{N-1}\left(C_{ij} - R_{ij}\right)^2 \qquad ...(5).$$

Where:

N^2: Block size N x N.
C_{ij}: Pixel in position (i, j) in current block.
R_{ij}: Pixel in position (i, j) in reference block.

2.9.2 Adaptive Rood Pattern Search (ARPS)

algorithm makes use of the fact that the general motion in a frame is usually coherent, i.e., if the macro blocks around the current macro block moved in a particular direction, then there is a high probability that the current macro block will also have a similar motion vector. This algorithm uses the motion vector of the macro block to its immediate left to predict its own motion vector. An example is shown in Fig.4. In addition to checking the location pointed by the predicted motion vector, it also checks at a rood pattern distributed points, where they are at a step size of S = Max (|X|, |Y|). The X and Y are the x-coordinate and y-coordinate of the predicted motion vector.

This rood pattern search is always the first step. It directly puts the search in an area where there is a high probability of finding a good matching block. The point that has the least weight becomes the origin for subsequent search steps, and the search pattern is changed to SDSP. The procedure keeps on doing Small Diamond Search Pattern (SDSP) until least weighted point is found to be at the center of the SDSP. A further small improvement in the algorithm can be to check for Zero Motion Prejudgment, using which the search is stopped half way if the least weighted point is already at the center of the rood pattern.

The main advantage of this algorithm over DS is if the predicted motion vector is (0, 0), it does not waste computational time in doing

Large Diamond Search Pattern (LDSP), it rather directly starts using SDSP. Furthermore, if the predicted motion vector is far away from the center, then again ARPS save on computations by directly jumping to that vicinity and using SDSP, whereas DS takes its time doing LDSP. Care has to be taken to not repeat the computations at points that were checked earlier.

Care also needs to be taken when the predicted motion vector turns out to match one of the rood pattern location. We have to avoid double computation at that point. For macro blocks in the first column of the frame, rood pattern step size is fixed at 2 pixels [16], as shown in Fig. (7).

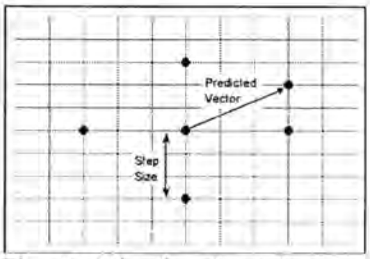

Fig.-7: Adaptive Root Pattern.

3. Proposed Compression Video System

3.1 Intra Coded Frame

The proposed compression system in this system includes three stages, the first stage is the wavelet transform, here we use Haar filter with 1-level. The output from the transform will be different sub bands with different important information. After that, EZW will quantize these sub bands in efficient manner then the output will be stream of zeros and ones, this stream will be compressed by arithmetic encoding.

Algorithm of Intra Coded Frame.

Input: Digital video clip.
Output: Compressed frame.

Step 1: Partition video into frames.
Step 2: Read first frame in video.
Step 3: Transform first frame using DWT.
Step 4: Quantization of first frame using EZW.
Step 5: Encoding of first frame using arithmetic method.
Step 6: Save the compressed frame.

3.2 Inter Coded Frame

The proposed compression system applies DWT on video frames, then Adaptive Rood Pattern Search algorithm is used in order to find MV using forward motion estimation. Motion vector was coded by Huffman encoding. On the other hand, the remaining part (the similar blocks of frames) will be compressed as the compression system that was used in intra frame coded.

Algorithm of Inter Coded Frames.

Input: Digital video clip.
Output: Compressed video.

Step 1: Partition video into frames.
Step 2: Transform these frames by DWT.
Step 3: Divide these frames into 16x16 macro block.
Step 4: Estimate the motion between each two frames using ARPS algorithm.
Step 5: Encoding the result from Step 4 (MV) by Huffman encoding.
Step 6: Compress the remaining part of frames after find the motion as intra coded frame.
Step 7: Save the compressed video.

4. RESULTS AND DISCUSSIONS

This section explains the experiments which have been implemented on two video clips. Clip1 and clip2 as test clips, each one of them is in size of 256*256 and of JPG format. MATLAB version 7.4.0.287 (R2007a) was used as a work environment to carry out these experiments. The first frame in these clips is compressed as intra and the remaining frames as inter through wavelet Haar filter (1 level). This approach was tested by using AVI files format with 5 frames for each clip.

4.1 Results of Intra Coded Frame

In this experiment, the first frame of video has been compressed using the first system, namely; intra coded frame. In this system, this frame is compressed as a still image. Two gray scale clips were used in this experiment. Fig.8 and Fig.9 show the result of applying this system on these clips. Table1 and Table 2 illustrate the PSNR and CR which are resulted from applying of this system on clip1 and clip2, respectively.

(a) (b)

Fig.-8: Reconstructed frame resulted from applying of the first system on clip1.
(a) Original frame. (b) Reconstructed frame.

Table-1: PSNR and CR of intra coded system on clip1.

	PSNR (dB)	CR
Frame1	61.697	0.1447

(a) (b)

Fig.-9: Reconstructed frame resulted from applying of the first system on clip2.
(a) Original frame. (b) Reconstructed frame.

Table-2: PSNR and CR of intra coded system on clip2.

	PSNR(dB)	CR
Frame1	59.389	0.1493

4.2 Results of Inter Coded Frame

In this experiment, frames starting from the second frame have been compressed using inter coded frame system. In this system, these frames are compressed using DWT followed by motion estimation using ARPS algorithm. Two gray scale clips were used in this experiment. Fig.10 and Fig.11 show the result of applying this system on these clips. Table3 and Table4 illustrate the PSNR, CR, and processing time which are resulted from applying of this system on clip1 and clip2, respectively.

(a) (b)

Fig.-10: Reconstructed frame resulted from applying of the second system on clip1. (a) Original frame. (b) Reconstructed frame.

Table-3: PSNR, CR, and time of inter coded system on clip1.

	PSNR (dB)	CR	Time (Sec.)
Without DWT	55.214	0.125	4.544
With DWT	58.122	0.135	2.508

(a) (b)

Fig.-11: Reconstructed frame resulted from applying of the second system on clip2. (a) Original frame. (b) Reconstructed frame.

Table-4: PSNR, CR, and time of Inter coded system on clip2.

	PSNR (dB)	CR	Time (Sec.)
Without DWT	55.484	0.135	1.813
With DWT	60.344	0.145	0.213

5. Discussion and Conclusions

In this paper, a system for video compression has been proposed. This system based on discrete wavelet transform and Adaptive Rood Pattern Search algorithm as a block matching algorithm to find the motion vector which will be used at the stage of motion compensation to finally estimate the current frame depending on reference frame. Use of this system on two clips (one is considered as a standard clip and the another is non standard) has shown good results in terms of PSNR, CR, and processing time. ***PSNR*** value in ARPS algorithm is better with

DWT proposed approach than this algorithm without ***PSNR***, as shown in Tables 3, and 4 in clip1, and clip 2, respectively. But in CR, the first proposed approach (without DWT) is better than the second proposed approach (with DWT). It is clearly noticed that the use of DWT minimize the processing time, almost, up to 40% - 50%.

REFERENCES

1. Sayood K., "Introduction to Data Compression", Morgan Kaufmann Publishers, 2006.
2. Hassan B. and Malik K. , "Quality-Aware Frame Skipping for MPEG-2 Video Based on Inter Frame Similarity", The Department of Computer Science and Electronics, Malardalen University, Vasteras, Sweden, 2006.
3. Bjorn B., Sweden, " Image and Video Compression Using Wavelet Transform and Error Robust Transform", M.Sc. Thesis, Stockholm, Sweden KTH Electrical Engineering, September 2005.
4. Niehsen W., "Fast Full Search Block Matching", In IEEE Transactions on Circuits and Systems for Video Technology, pp. 241-247, 2001.
5. Keinert F., "Wavelets and Multiwavelets", USA, 2004.
6. Erick S., "Compression of Medical Image Stacks Using Wavelet and Zero-tree Coding ", M.Sc. Thesis, Department of Electrical Engineering, Linkoping University, 'Lith-ISY-Ex-3201', 2002.
7. Saif B., "Wavelet Compression Using Tree and Adaptive Arithmetic Codes", M.Sc Thesis, Baghdad University, College of Science, 2004.
8. Fast Huffman Code Processing", UCI-ICS Technical Report No. 99-43, Department of Information and Computer Science, University of California, Irvine, October 1999.
9. John M., "Compressed Image File Formats", ACM Press, A Division of The Association of Computing Machinery, Inc. (ACM), 1999.
10. Panrong X., "Image Compression by Wavelet Transform", M.Sc. Thesis, East Tennessee State University, Department of Computer and Information Sciences, 2001.
11. Shi Q. and Sun H., "Image and Video Compression for Multimedia Engineering", 2000.
12. Aydin B., " Motion Compensated Three Dimensional Wavelet Transform Based Video Compression and Coding ", M.Sc. Thesis, University of Middle East Technical University, Electrical and Electronics Engineering Science , January 2005.
13. Djordje M., "Video Compression", University of Edinburgh,2008. http://homepage.inf.ed.ac.uk/rbf/CVonline/LOCALCOPIES/AVo506/s0561282.pdf.

14. Koga T., Iinuma K., Hirano A., Iijima Y. and Ishiguro T., "Motion Compensated Inter Frame Coding for Video- conferencing", Proc. NTC81, Nov. 1981.
15. Jain J. and Jain A., "Displacement Measurement and Its Applications", IEEE Transactions on Communications, Dec. 1981.
16. Yao Nie, and Kai-Kuang Ma, "Adaptive Rood Pattern Search for Fast Block-Matching Motion Estimation", *IEEE Trans. Image Processing*, Vol 11, No. 12, pp. 1442-1448, December 2002.

Encrypting a Text by Using Affine Cipher and Hiding it in the Colored Image by Using the Quantization stage

Salah Taha Alawi[1] and Nada Abdulazeez Mustafa[2]
[1]Computer Science Department, College of Science Al- Mustansiriyah University
[2]College of Languages, Baghdad University
Received 22/3/2013 – Accepted 15/9/2013

الخلاصة

هذا البحث يركز على اهمية الجمع بين التشفير والأخفاء واستخدام الصورة المضغوطة بطريقة JPEG لنقل المعلومات كونها واحدة من اكثر الانواع المستخدمة في الانترنت. هذا العمل يبدأ بتشفير النص باستخدام طريقة (Affine) وهي أحدى طرق التشفير التقليدية ، ثم تحويل نتيجة النص المشفر الى سلسلة من ارقام النظام الثنائي (0,1). عملية اخفاء النص تجري اثناء مراحل تحويل الصورة المدخلة نوع BMP الى صورة مضغوطة نوع JPEG حاملة للنص المشفر من خلال أحداث تغيير في البيانات الاصلية لعدد محدد من النقاط وحسب الحاجة وذلك بأضافة أو طرح (1) الى / من البيانات الاصلية لهذه النقاط.

ABSTRACT

This paper focuses on the strength of combining cryptography and steganography methods and using an image compression (JPEG) to transfer the text being one of the most kinds that used through internet. This work begins by encrypting the text using one of the classical cryptography methods (Affine method), then converting the result of the encryption text to sequence of binary numbers (0,1). The operation of text hiding happens during steps of converting the entered image BMP to compression image JPEG holding the encryption text through making a change in the original data for some pixels when needed by adding or subtracting to/from the data of these pixels.

1. INTRODUCTION

Cryptography and Steganography are well known and widely used techniques that manipulate information in order to cipher or hide their existence respectively [1].

Steganography is the art and science of communicating in a way which hides the existence of the communication. A steganographic system thus embeds hidden content in unremarkable cover media so as not to arouse an eavesdropper's suspicion. As an example, it is possible to embed a text inside an image or an audio file. On the other hand, cryptography is the study of mathematical techniques related to aspects of information security such as confidentiality, data integrity, entity authentication, and data origin authentication [2].

To make a steganographic communication even more secure the message can be compressed and encrypted before being hidden in the carrier. Cryptography and steganography can be used together. If compressed the message will take up far less space in the carrier and will minimize the information to be sent. The random looking message which would result from encryption and compression would also be easier to hide than a message with a high degree of regularity. Therefore encryption and compression are recommended in conjunction with steganography [3].

2. Affine Cipher

The affine cipher is a type of monoalphabetic substitution cipher, wherein each letter in an alphabet is mapped to its numeric equivalent, encrypted using a simple mathematical function, and converted back to a letter. The formula used means that each letter encrypts to one other letter, and back again, meaning the cipher is essentially a standard substitution cipher with a rule governing which letter goes to which. As such, it has the weaknesses of all substitution cipher [4].

In the affine cipher the letters of an alphabet of size m are first mapped to the integers in range $0,\ldots,m-1$. It then uses modular arithmetic to transform the integer that each plaintext letter corresponds to into another integer that corresponds to a ciphertext letter. The encryption function a single letter is [4][5].

$$E(x) = (ax + b) \bmod m \quad \ldots\ldots\ldots\ 1$$

Where modulus (m) is the size of the alphabet and (a and b) are the key of the cipher. The value (a) must be chosen such that (a and m) are coprime. The decryption function is.

$$D(x) = a^{-1}(x - b) \bmod m \quad \ldots\ldots\ldots\ 2$$

Where a^{-1} is the modular multiplicative inverse of a modulo m. i.e., it satisfies the equation.

$$1 = aa^{-1} \bmod m \quad \ldots\ldots\ldots\ 3$$

The multiplication inverse of (a) only exists if (a and m) are coprime. Hence without the restriction on (a) decryption might not be possible [4][5].

3. JPEG Algorithm

The general progression of the JPEG technique can be seen in fig.(1). The steps must be performed in a sequential manner because the operations in each block depend on the output from the previous block. Where the parallelism can be extracted is limited to the operations within each block [6].

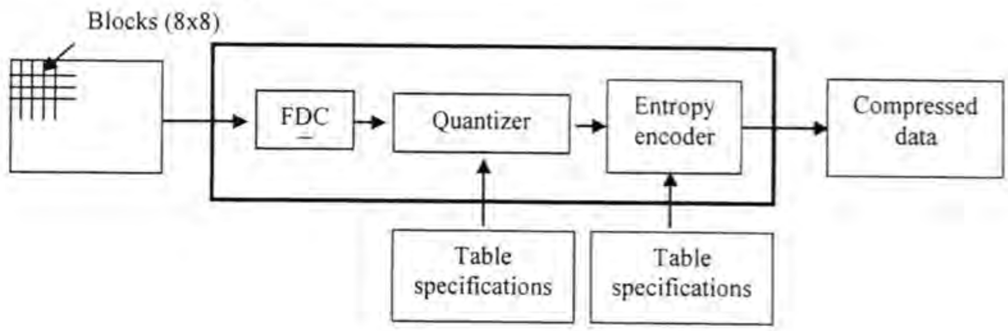

Fig.-1: DCT-based encoder simplified diagram

The image is loaded into the main memory and the image is segmented into block of size (8x8) pixels called macro blocks. A 2D discrete cosine transform (DCT) is performed on each (8x8) macro block to separate it into its frequency components [6]. The forward 2D_DCT transformation is given by equation 4 [7].

$$C(u,v) = D(u)C(v)\sum_{x=0}^{n-1}\sum_{y=0}^{n-1} f(x,y)\cos\left(\frac{(2x+1)u\pi}{2n}\right)\cos\left(\frac{(2y+1)v\pi}{2n}\right) \quad \text{...........4}$$

Where u,v= 0,1,2,3,…,n-1

The result at the top left corner (u=0, v=0) is the DC coefficient and the other 63 results of the macro blocks are the AC coefficients. The purpose of the DCT is to remove the higher frequency information since the eye is less sensitive to it [6].

Quantization is achieved by dividing each element in the transformed image block by corresponding element in the quantization table, and then rounding to the nearest integer value. The scaled quantization table is then rounded and clipped to have positive integer values ranging from 1 to 255. For rounded off use equation 5.

$$T(u,v) = round\left(\frac{C(u,v)}{Q(u,v)}\right) \text{...........5}$$

After that a new block produce where the coefficients situated near the upper-left corner correspond to the lower frequencies to which the human eye is most sensitive of the image block. Whereas, zeros represent less important, higher frequencies that have been discarded, giving rise to the lossy part of compression. Thus, only nonzero coefficients will be used to reconstruct the image [8].

At this point, all the lossy compression has occurred, meaning that high frequency components have been removed. The final step is to encode the data in a lossless fashion to conserve the most space. This involves two steps. First, zig-zag reordering reorders each macro blocks from the top left to the bottom right in a zig-zag fashion so that the 0's end up at the end of the stream. This way, all the repeated zeros can be cut. The final step is to use Huffman encoding to encode the whole picture by replacing the statistically higher occurring bits with the smallest symbols. This can be done with a standard Huffman table or can be generated based on the image statistics [6].

4. Proposed System

This paper focuses on using cryptography, steganography and image compression as a base in work. The input color image (BMP) and a text will be encrypted. The output is a compression image (JPEG) holding the encryption text and the key of decryption text. Figure (2) shows the steps of hiding the text and then extracting it.

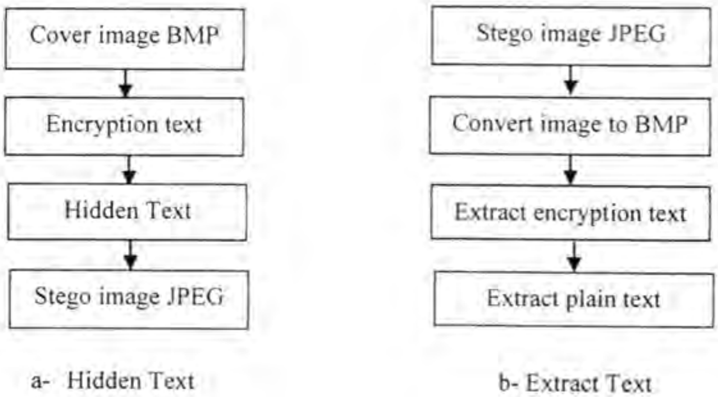

Fig.-2: a) Hidden text steps b) Extract text steps

4.1 Hiding Stage

In this stage a color image (BMP) and a text are entered. The entered text is encrypted by using affine method. The number of the symbols that used in this work is (28) symbols, which are divided into two groups; the first of them is (26) characters the English alphabet (A..Z). Secondly (2) symbols (' ', '.') which represent the space between the words and the dot that shows the end of text. After the encryption text, the keys of decryption and the encryption text are converted to a sequence of numbers of binary system (0,1).

This work uses the DC coefficient in every block to hide one bit from the encryption text in the quantization stage. To hide a bit (1) the value of DC coefficient should be even, but to hide a bit (0) the value of DC coefficient should be odd.

The mechanism of our proposed technique; to hide one bit (1) the value of the DC coefficient should be even. If the value of DC coefficient is even there will be no change on the data of the pixels, but if it is odd, the original data of some pixels should be changed before DCT stage performed to make the needed changed in order to convert the value of DC coefficient from odd to even in the quantization stage. To count the number of pixels that will be changed we shall do the following:

1. Counting the value of DC coefficient in the quantization stage with or without rounding.

$$DC1 = 11.3$$
$$DC2 = round\ (11.3) = 11$$

2. Counting the additional value that should be added to the DC coefficient to convert it from odd to even after rounding. The additional value (0.5) is at maximum.
$$D3 = 11.3 - 11 = 0.3$$
$$D4 = 0.5 - 0.3 = 0.2$$
3. Adding the additional value to the DC coefficient without rounding.
$$DC = 11.3 + 0.2$$
$$= 11.5$$
4. Counting the DC coefficient after rounding.
$$DC = round\ (11.5)$$
$$= 12$$
5. Counting the effect value that happened by adding (1) to the original data for one pixel in the block (8x8), through dividing the maximum of the additional value to the number of the block pixels (64).
$$efct = 0.5 / 64 = 0.0078$$
6. Counting the number of pixels that will be changed in its value by add (1) to its original data, through dividing the additional value to the effect value.
$$No.p = int\ (0.2 / 0.0078) + 1$$
$$= int\ (25.64) + 1 = 26$$
7. After changing the original data of these pixels, the DCT and quantization stage will be performed and then the DC coefficient will be an even number.

This operation is repeated until finishing the hiding text completely.

4.2 Extracting Stage

The operation of extracting text will be done through making some operations on the stego image which is JPEG. The input image will be converting into BMP image, then image compression stages done on it. Getting the value of DC coefficient from every block in order to know the value of the hidden bit. If the DC value is an even value this represents hidden bit with value (1), and if it represents an odd number this represents hidden bit with value (0). After getting a group consisted of 6 bits this group will be converted to decimal number. The first two groups represent the decryption key. Work is stopped when getting a group represents the dot which stands for the end of hidden text.

5. RESULTS AND DISCUSSIONS

The JPEG compression image is considered one of the most kinds that used in the internet because of the small size compared with BMP image. The output of this work is JPEG image containing the encryption text and the key of the text decryption, therefore the receiver will not find any difficulty to extract the plain text. Sending the key in side the stego image will decrease the number of connecting between the receiver and the sender so it lessens the doubt about this image. The stego image keeps the text and the key inside it even though decompression and compression repeation happens to it.

In this method, the cover image is BMP type with size 352*288. Figure (3) shows the steps of entering cover image and the text in additional to selecting the encryption key. The length of text depends on the size of image.

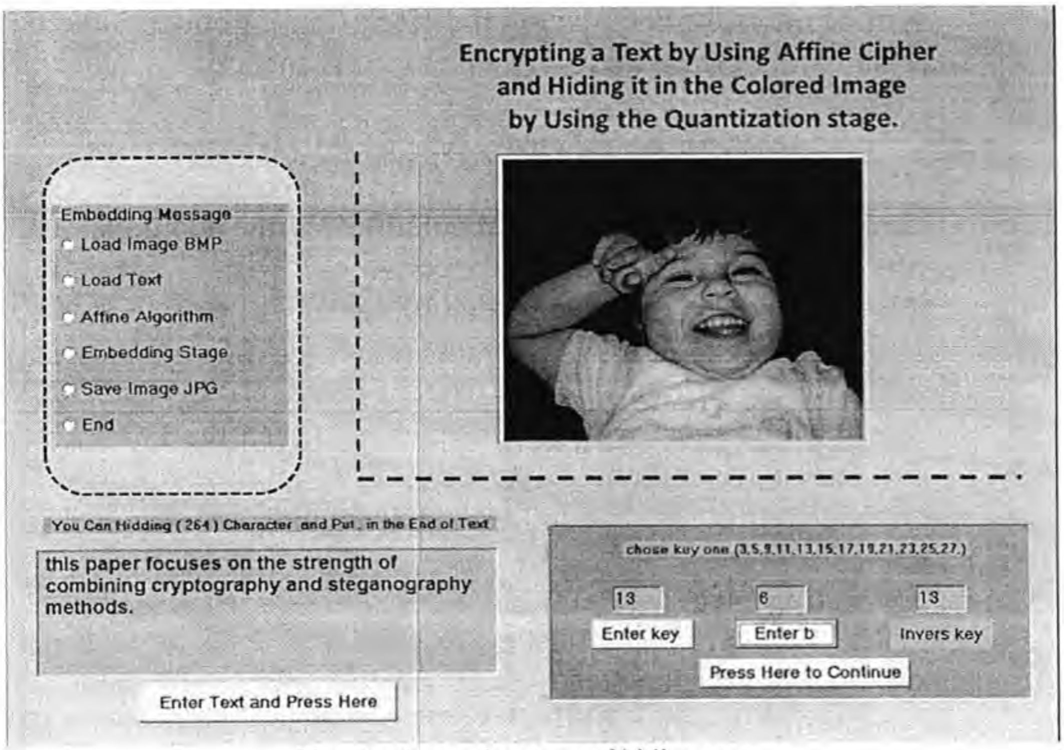

Fig.-3: shows the steps of hiding text

Figure (4) shows how to recall the stego image and extract the plain text.

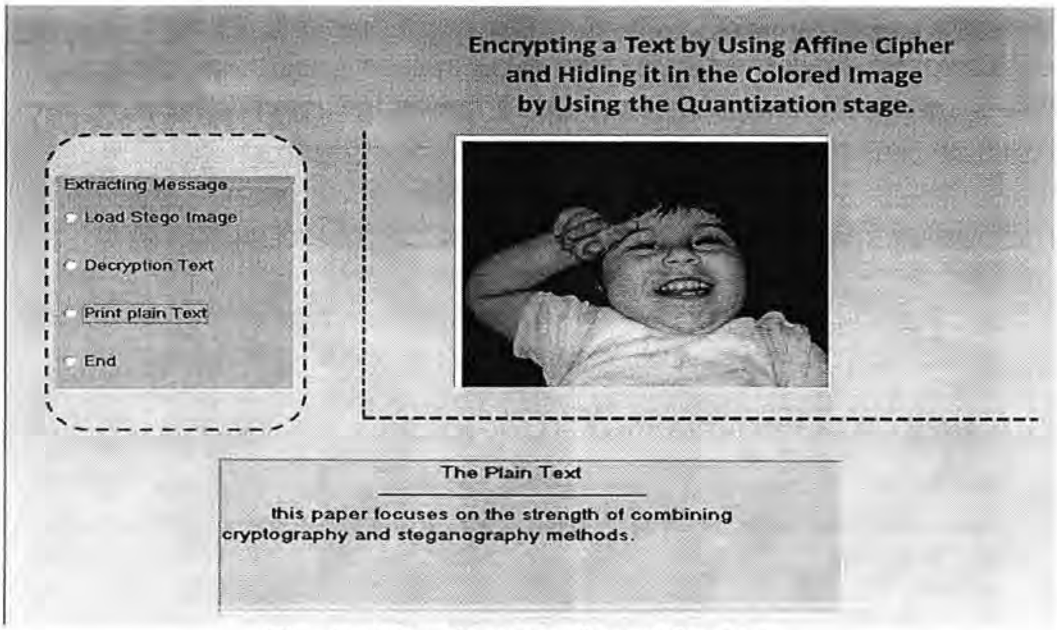

Fig.-4: shows the steps of extracting text

The quality evaluation results of proposed method by using PSNR and MSE measures are shown in table 1.

Table-1: evaluation the proposed method

Test	Red color	Green color	Blue color
PSNR	35.08	36.14	35.35
MSE	4.49	3.97	4.35

REFERENCE

1- A. Joseph Raphael, V. Sundaram "Cryptography and Steganography – A Survey", Int. J. Comp. Tech. Appl., Vol 2 (3), 626-630, 2011.

2- Domenico Bloisi, Luca Iocchi " Image Based Steganography and Cryptography", Dipartimento di Informatica e Sistemistica, Sapieniza University, Italy. 2004.

3- Keven Curran "An Evaluation of Image Based Steganography Methods", International Journal of Digital Evidence. Volume 2, Issue 2. Fall 2003.

4- William Stallings "Cryptography and Network Security Principles and practice", Prentice Hell, 5th edition, 2010.

5- Dennis Luciano, Gordon Prichett "Cryptology: From Caesar Ciphers to Public-Key Cryptosystems", The College Mathematics Journal, January, Volume 18, Number 1, pp. 2–17, 1987.

6- Pranit Patel, Jeff Wong, Manisha Tatikonda, and Jarek Marczewski, "JPEG Compression Algorithm Using CUDA", Department of Computer Engineering, University of Toronto, 2005.

7- "Image Compression Using Discrete Cosine Transform & Discrete Wavelet Transform", International Journal of Scientific & Engineering Research Volume 2, Issue 8, August-2011.

8- Pravin B. Pokle, N. G. Bawane " Lossy Image Compression using Discrete Cosine Transform "National Conference on Innovative Paradigms in Engineering & Technology (NCIPET-2012)

Audio Compression Method Based on Slantlet Transform

Dhia Alzubaydi and Zinah Sadeq Abdul Jabbar
University of Al-Mustansiriyah, College of Science, Computer Science Department, Baghdad-Iraq
Received 16/3/2013 – Accepted 15/9/2013

الخلاصه

ان التقدم السريع في مجال الانترنيت وتكنلوجيا الوسائط المتعدده ادى الى زيادة البيانات ولان الصوت احد اهم الوسائط المنتقله لذا هناك حاجه ضروريه لاستخدام عمليات الضغط لزيادة كفاءة الانتقال .ان التقنيه المقترحه " طريقة ضغط البيانات السمعيه باستخدام تحويل الموِيل" يهدف الى تطوير عملية الضغط القابله للضياع لبيانات ملفات الصوت من نوع (Stereo Wave Files) وتعتمد على التشابه الكبير مابين قناتي ملف الصوت باستخدام تحويل الموِيل لغرض التحويل وباستخدام التشفير الحسابي في مرحلة التشفير. تبعاً للنتائج التجريبيه تراوحت نسبة الضغط مابين (12 – 24) وتراوحت ذروة نسبة الاشاره الى الضوضاء ما بين(51 – 58 دسبل).
لقد تم تحسين (12 – 14) من زمن الترميز والزمن المستغرق في عملية فتح الترميز باستخدام الترميز الحسابي من نوع (Adaptive) .

ABSTRACT

The development of internet and multimedia technologies that grow rapidly, resulting in amount of information managed by computer is necessary. Audio is the most important medium be transmitted and for successfully transmission, there is a need for compression.
A proposed Audio compression method based on Slantlet transform is a lossy audio compression. It exploits the high similarity between the channels of stereo audio Wave file, using Slantlet transform for transformation and Arithmetic coding in coding step. The experimental results show that compression ratio ranges (12-24) and *PSNR* results ranges (51 - 58 dB), encoding and decoding time improved (12 - 14) times by using programmed Adaptive Arithmetic coding.

1. INTRODUCTION

Data compression is one of the most important fields and tools in modern computing; it provides a comprehensive reference for the many different types and methods of compression [1]. Compression is the process of re-encoding digital data to reduce file size; a specialized program called a *codec*, for *CO*mpressor/*DEC*ompressor, changes the original file to the smaller version and then decompresses it to again present the data in a usable form [2].

Audio is used in multimedia, and especially when it is delivered over the internet, there is a need for compression [3]. Audio compression is the technology of converting human speech into an efficiently encode representation that can later be decoded to produce a close approximation of the original signal [4]. To manipulate with audio, first it must be convert to a digital format, the samples can be processed, transmitted, and converted back to analog format. Any compression technique belongs to either lossy compression or lossless compression; the goal of lossless compression is to encode the data in a way such that the matching decoder is able to reconstruct an exact copy of the original signals that are input to the encoder [5].Lossless compression is used when it is important that the original and the decompressed data be identical, for example, it is used in popular ZIP file format, other examples are executable programs and source code. Lossy compression technique involve some loss of information, and data that have been compressed using lossy techniques generally cannot be reconstructed exactly [6]. In digital audio coding, a lossy codec is also called a perceptual codec because the design principle of a lossy audio codec is to remove the perceptually irrelevant or unimportant information as much as possible [5].

Coding was done by using arithmetic coding. In static arithmetic coding, the model may assign a predetermined probability to each symbol in the alphabet. Alternatively, in adaptive models the probabilities are updated whenever a symbol is encoded.

2. Slantlet Transform

The discrete wavelet transform (DWT) is usually carried out by filter bank iteration, for a fixed number of zero moments; this does not yield a discrete time basis that is optimal with respect to time localization [7].Slantlet transform (SLT) is an orthogonal DWT, with two zero moments and with improved time localization. The basis is not based on filter bank iteration; instead, different filters are used for each scale [7].

In general the algorithm to obtain l -scales Slantlet filter banks is as follows:

- The L scale filter bank has $2l$ channels. The low pass filter is to be called $h_l(n)$. The adjacent to the low pass filter is to be called $f_l(n)$. Both $h_l(n)$ and $f_l(n)$ are to be followed by down sampling $2l$.
- The remaining $2l$ -2 channels are filtered by $g_i(n)$ and its shifted time-reverse $g_i((2i+1-1)-n)$ for $i=1,\ldots\ l-1$, each is to be followed by down sampling 2i+1 [7].

In the Slantlet filter bank, each filter $g_i(n)$ appears together with its time reverse. While $h_i(n)$ does not appear with its time reverse, it always appears paired with the filter $f_i(n)$. Fig (1) illustrates a three-scale Slantlet filter bank.

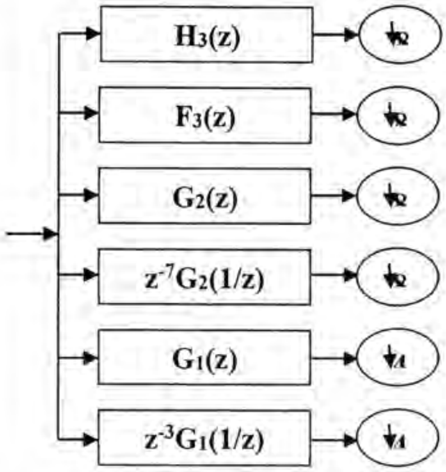

Figure -1: Three-scale Slantlet filter bank [7]

The transfer functions $g_i(n)$, $h_i(n)$ and $f_i(n)$ for l-scale Slantlet are calculated using the following expressions and the parameters [7][8]:

$$g_i(n) = \begin{cases} a_{0,0} + a_{0,1} n, & for \quad n = 0, \ldots 2^i - 1 \\ a_{1,0} + a_{1,1}(n - 2^i), & for \quad n = 2^i, \ldots, 2^{i+1} - 1 \end{cases} \quad \ldots (1)$$

Where

$m=2^i$

$s_1 = 6\sqrt{m/((m^2-1)(4m^2-1))}$ $\qquad s_0 = -s_1.(m-1)/2$

$t_1 = 2\sqrt{3/(m.(m^2-1))}$ $\qquad t_0 = \left((m+1).s_1/3 - mt_1\right)(m-1)\,/\,(2m)$

$a_{0,0} = (s_0 + t_0)\,/\,2$ $\qquad a_{0,1} = (s_1 + t_1)\,/\,2$

$a_{1,0} = (s_0 - t_0)\,/\,2$ $\qquad a_{1,1} = (s_1 - t_1)\,/\,2$

Note that the parameters $a_{0,0}$,$a_{0,1}$,$a_{1,0}$ and $a_{1,1}$ depend on $\boldsymbol{i}$,The same approach works for $f_i(n)$ and $h_i(n)$. Using, again, a piecewise linear form $\boldsymbol{f_i(n)}$ and $\boldsymbol{h_i(n)}$ can be written in terms of eight unknown parameters $b_{0,0}$,$b_{0,1}$,$b_{1,0}$ $b_{1,1}$, $c_{0,0}$,$c_{0,1}$,$c_{1,0}$ and $c_{1,1}$

$$h_i(n) = \begin{cases} b_{0,0} + b_{0,1} n, & for \quad n = 0, \ldots 2^i - 1 \\ b_{1,0} + b_{1,1}(n - 2^i), & for \quad n = 2^i, \ldots, 2^{i+1} - 1 \end{cases} \quad \ldots (2)$$

$$f_i(n)=\begin{cases} c_{0,0}+c_{0,1}n, & for \quad n=0,...2^i-1 \\ c_{1,0}+c_{1,1}(n-2^i), for & n=2^i,...,2^{i+1}-1 \end{cases} \quad ...(3)$$

Where

$m=2^i$

$u = 1 / \sqrt{m}$

$v = \sqrt{(2m^2+1)/3}$

$q = \sqrt{3/(m(m^2-1))} / m$

$b_{0,0} = u.(v+1)/(2m)$

$b_{1,0} = u - b_{0,0}$

$b_{0,1} = u / m$

$b_{1,1} = -b_{0,1}$

$c_{0,1} = q.(v-m)$

$c_{1,1} = -q.(v+m)$

$c_{1,0} = c_{1,1}.(v+1-2m)/2$

$c_{0,0} = c_{0,1}.(v+1)/2$

3. Proposed System

A demonstration for suggest system "audio compression using Slantlet transform" used for compression stereo audio file will be presented using the following steps:

1. Loading audio file in buffer.
2. Split left from right channel.
3. (Blocking)
   Each channel is divided into small blocks and padding with zero if required.
4. (Transformation)
   Each block is transformed separately using Slantlet transform to transform it from time domain into frequency domain.
5. (Filtering)
   Find adaptive threshold for filtering coefficients and to isolate the important from less important coefficients, and save only the important coefficients with their locations. In this step for each channel we have two arrays, one for coefficients and the other for location.
6. (Choose only one channel)
   Graphical representation of audio raw data, left channel and right channel are shown in figures (2), (3.a) and (3.b) respectively.
   Due to the high similarity of the two channels, which is the property of all stereo audio wave file, can be exploited by choosing only one channel for processing and duplicated this channel in decoding unit. The choosing process is done by finding the channel with higher energy, the compression ratio will be increased by this step as well as the encoding and decoding times will be decreased. This step does not affect the quality of reconstructed file.
7. (Quantization and Differencing)

Slantlet transform coefficients Quantized to appropriate step, this process sharply increases the compression ratio.
Differencing process will be performed to location array; this step will decrease the number of symbols before the coding step and thus increase the compression ratio.

8. (Coding)
Coding was done using arithmetic coding; two arrays will be input into arithmetic coding and storing the output in the compression file.

The steps for implementation encoding algorithm are shown in figure (4).

Decoding unit is an inverse steps of encoding unit.

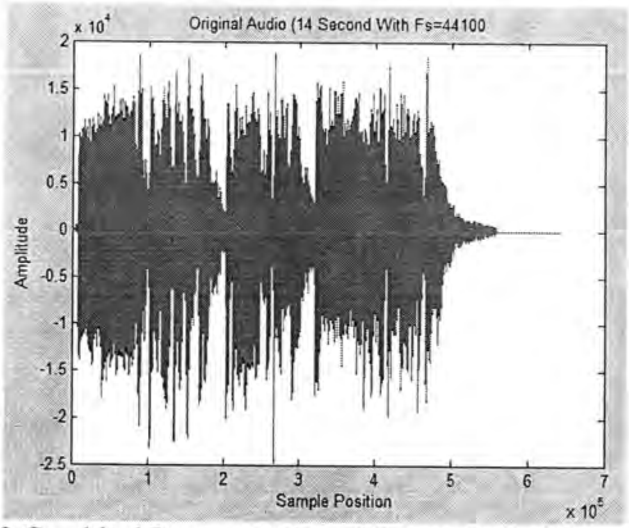

Figure-2:Graphical Representation of Stereo Audio Wave File

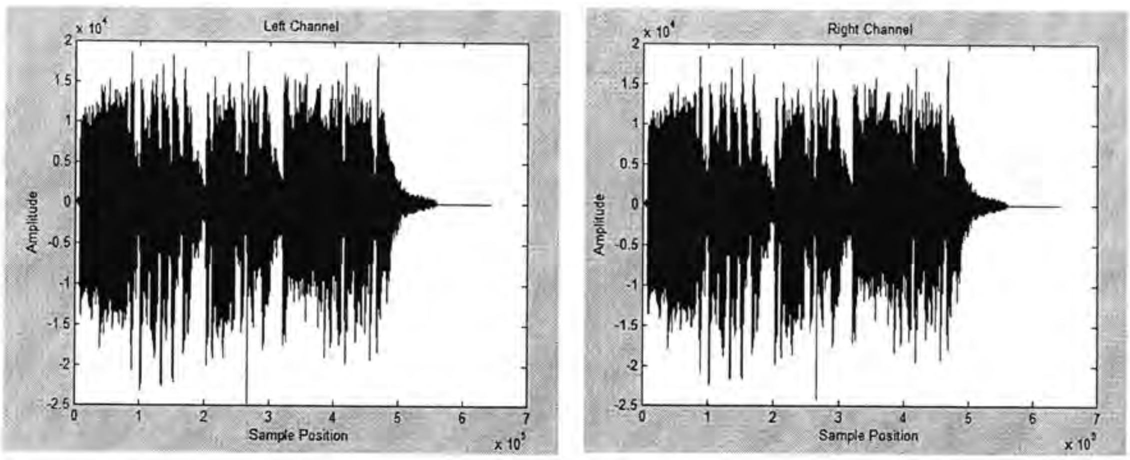

Figure-3:a) Left Channel b) Right Channel

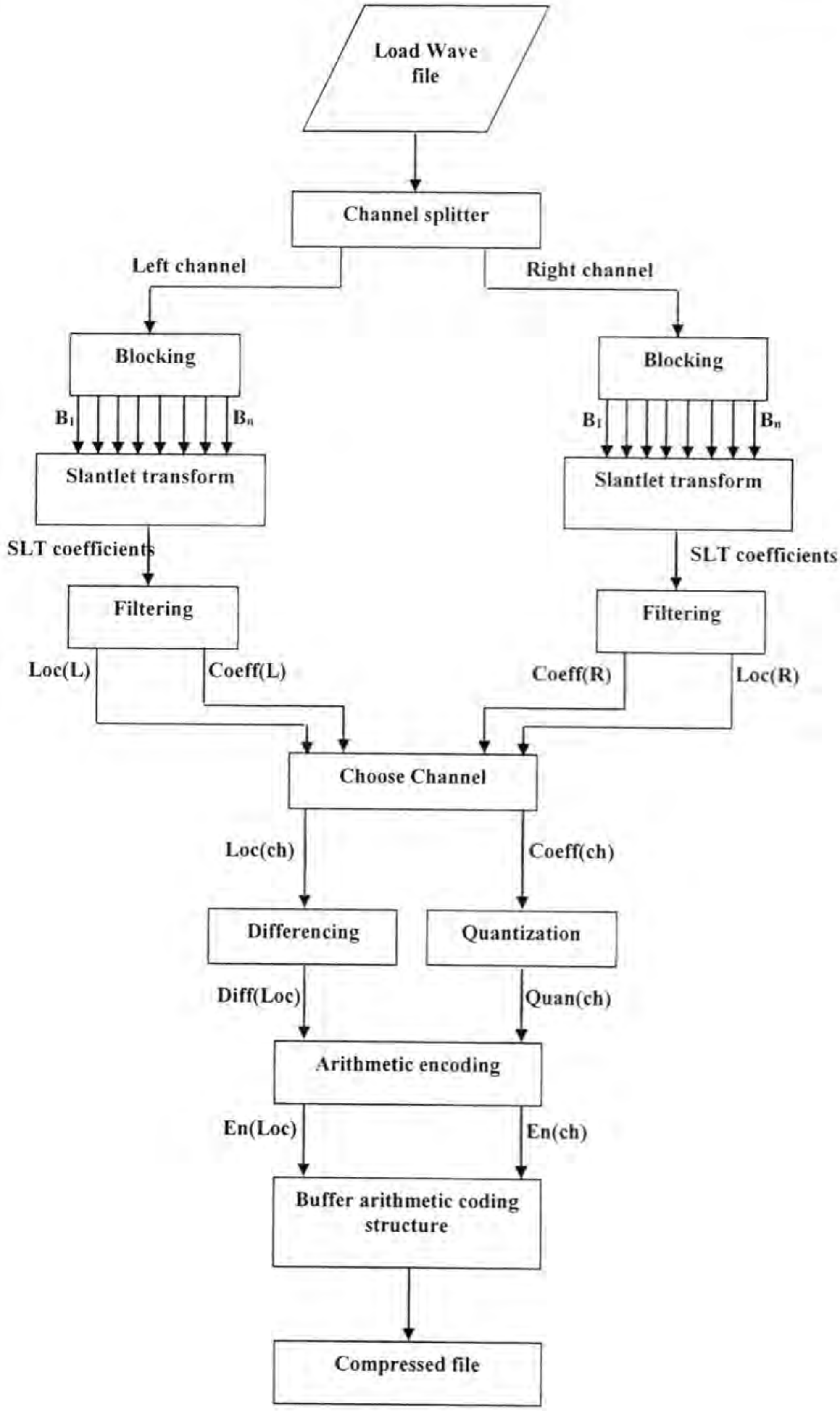

Figure-4: Block Diagram of Encoding Unit

4. RESULTS AND DISCUSSIONS

To test the performance of our proposed coder, a test set including five files with different size (stereo and 16 bit per sample) with different sampling rate. For evaluation the objective quality measures (such as the Mean Square Error (MSE) and the Peak Signal to Noise Ratio (PSNR) were utilized. Several parameters were taken to study the performance of the suggested audio compression system, these parameters are: Block size and quantization step. The adopted parameters are the compression ratio (CR), encoding time (ET), decoding time (DT) and fidelity criteria (MSE and PSNR).Table (1) describes the data files used.

Table-1: Data File Description

File name	Duration (Sec)	Sampling rate(FS)	Thr(L)	Thr(R)
File(1)	40	48000	265	265
File(2)	14	44100	705	686
File(3)	24	44100	1314	1318
File(4)	14	48000	733	771
File(5)	60	48000	501	600

Where (FS) denoting the number of samples per second and Thr(L), Thr(R) are the adaptive thresholds for left and right channel respectively.

Each channel in audio file is further divided into a number of blocks with appropriate size (2^n); the length of channel is made to accommodate a number of blocks, by padding it with zero if required. Table (2) presents the effect of different block size.

Table-2: Use of Different Block Size

Block Size=512					
File name	CR	MSE	PSNR dB	ET (Sec)	DT (Sec)
File(1)	24.0269	8812.37	56.8773	16.0057	7.3632
File(2)	16.8756	18646.83	53.8976	5.8321	2.3554
File(3)	13.2079	28294.84	51.8123	13.3225	6.0060
File(4)	16.6368	25470.84	52.2689	6.8952	2.9796
File(5)	17.3578	23088.53	52.6952	27.8930	12.7921
Block Size=1024					
File(1)	24.1571	8815.43	56.8770	14.7421	7.4412
File(2)	16.9748	18647.47	53.6233	5.1012	2.3760
File(3)	13.2298	28293.92	51.8125	13.0729	6.1464
File(4)	16.6878	25472.45	52.2688	6.0060	2.6520
File(5)	17.4233	23089.5	52.6953	27.0458	14.6485

Two types of quantization: uniform quantization and non-uniform quantization, in a proposed system uniform quantization will be used. The coefficients are uniformly quantizes using the general equation:

$$\text{Quantized output} = \text{Round}\left(\frac{\text{Slantlet}}{\text{QS}}\right)$$

Where QS is step size parameter and can be adjusted to give the required results.

Table-3: Use of Different Quantization Step

File name	CR	MSE	PSNR dB	ET(Sec)	DT(Sec)
Quantization Step=300					
File(1)	20.8758	6619.53	58.1212	16.4269	8.0029
File(2)	15.3266	18262.15	53.7131	6.1308	2.6052
File(3)	11.9936	28159.62	51.8332	16.0837	7.1292
File(4)	15.0292	25250.28	52.3068	7.0980	3.1044
File(5)	15.9390	22564.21	52.7950	33.8366	16.6297
Quantization Step=400					
File(1)	22.6132	7450.13	57.6078	14.7421	7.4256
File(2)	16.2819	18375.01	53.6863	5.2728	2.3244
File(3)	12.3899	28230.37	51.8223	13.9465	6.3336
File(4)	15.7205	25344.59	52.2906	6.0372	2.7924
File(5)	16.6178	22895.67	52.7317	31.9334	15.7093
Quantization Step=500					
File(1)	24.1571	8815.43	56.8770	14.7421	7.4412
File(2)	16.9748	18647.47	53.6233	5.1012	2.3760
File(3)	13.2298	28293.92	51.8125	13.0729	6.1464
File(4)	16.6878	25472.45	52.2688	6.0060	2.6520
File(5)	17.4233	23089.5	52.6953	30.0458	14.6485

Tables (4), (5) and (6) present the effects of different types of Arithmetic coding on encoding and decoding time.

Table -4:Programmed Adaptive Arithmetic coding

File Name	CR	MSE	PSNR dB	ET (Sec)	DT (sec)
File(1)	24.1571	8815.43	56.8770	14.7421	7.4412
File(2)	16.9748	18647.47	53.6233	5.1012	2.1684
File(3)	13.2298	28293.92	51.8125	13.0729	6.1464
File(4)	16.6878	25472.45	52.2688	6.0060	2.6520
File(5)	17.4233	23089.5	52.6953	30.0458	14.6485

Table-5: Programmed Static Arithmetic coding

File Name	CR	MSE	PSNR dB	ET (Sec)	DT(Sec)
File(1)	24.1571	8815.43	56.8770	30.9194	12.0901
File(2)	16.9748	18647.47	53.6233	12.2617	4.1964
File(3)	13.2298	28293.92	51.8125	28.9382	10.8889
File(4)	16.6878	25472.45	52.2688	14.4925	4.8516
File(5)	17.4233	23089.5	52.6953	60.7936	23.9930

Table-6:MATLAB Arithmetic coding

File Name	CR	MSE	PSNR dB	ET (Sec)	DT (Sec)
File(1)	24.0854	8815.43	56.8770	54.2727	75.5513
File(2)	16.8965	18647.47	53.6233	25.3658	34.6010
File(3)	13.1822	28293.92	51.8125	53.1651	74.2721
File(4)	16.6122	25472.45	52.2688	28.4234	38.9066
File(5)	17.3935	23089.5	52.6953	111.7747	156.2662

5. CONCLUSIONS

From the above results which were done on some selected samples, a number of conclusion remarks were drawn:

1. Compression ratio is proportional with Block Size and Quantization Step as shown in figures (5) and (6) respectively.

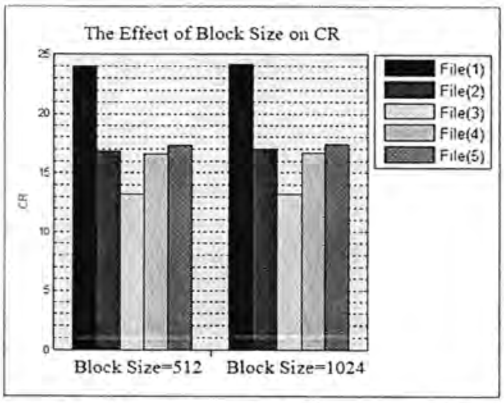

Figure-5:The Effect of Block Size on CR

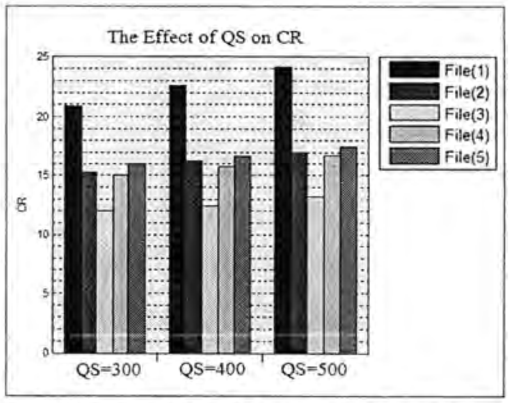

Figure-6:The Effect of QS on CR

PSNR is inversely proportional with Block Size and Quantization Step as shown in figures (7) and (8) respectively.

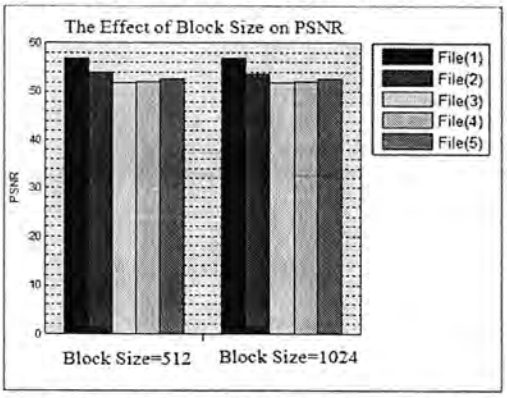

Figure-7:The Effect of Block Size on PSNR

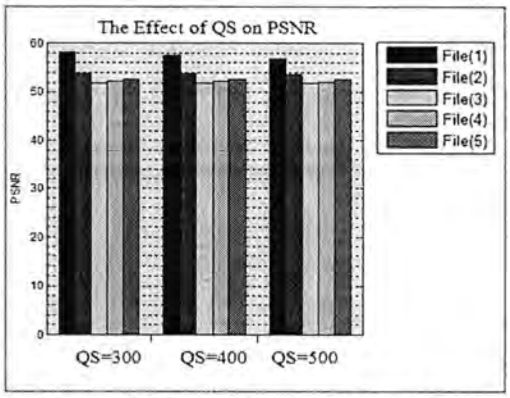

Figure-8:The Effect of QS on PSNR

2. MSE is proportional with Block size and Quantization Step as shown in figures (9) and (10) respectively.

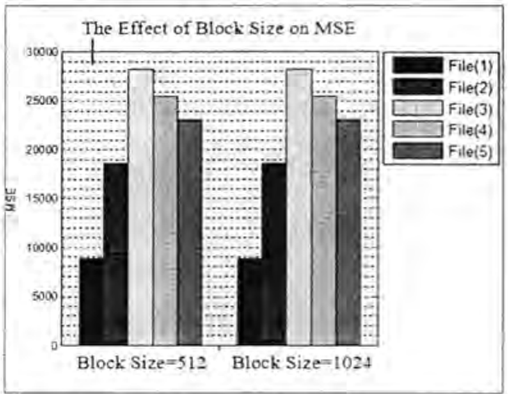

Figure-9:The Effect of Block Size on MSE

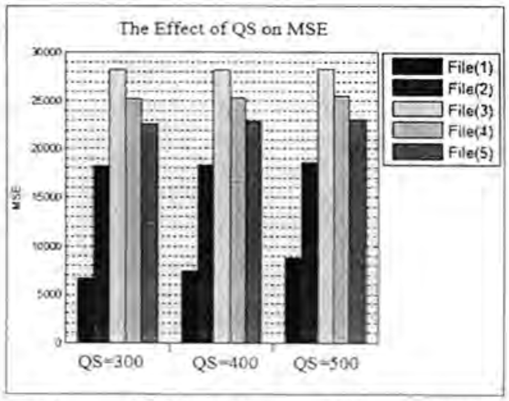

Figure-10:The Effect of QS on MSE

3. Encoding and decoding time affected by the type of Arithmetic coding, best results in encoding and decoding time when using a programmed Adaptive arithmetic coding, where in adaptive models the probabilities are updated whenever a symbol is encoded. Programmed Static Arithmetic coding, the model may assign a predetermined probability to each symbol in the alphabet, present result better than MATLAB Arithmetic coding.

REFERENCES

1. D.Salomon,"Data Compression the Complete Referance", Springer-Verlag London Limited, 2007.
2. T.M.SAVAGE, K.E.VOGEL, "An Introduction To Digital Multimedia", by Jones and Bartlett Publishers, LLc, 2008.
3. Nigel Chapman and Jenny Chapman, "Digital Multimedia", John Wiley & Sons Ltd, England, 2009.
4. D.Naveen, "Implementation of Psychoacoustic model in Audio Compression using Munich and Gammachirp Wavelets", International Journal of Engineering Science and Technology, Vol.2 (5), 2010
5. Dai Tracy Yang, Chris Kyriakakis, and C.-C. Jay Kuo , "High Fidelity Multichannel Audio coding",Hindawi Publishing Corporation, 2006.
6. Khalid Sayood, "Introduction to Data Compression", Elsevier Inc, 2006.
7. Selesnick I. W., "*The Slantlet Transform*", IEEE Transactions on Signal Processing, Vol. 47, No. 5, pp. 1304-1313, May 1999.
8. Hikmat N. Abdullah, Safa'a A. Ali, "*Implementation of 8-Point Slantlet Transform Based Polynomial Cancellation Coding-OFDM System Using FPGA*", IEEE System Signals and Devices (SSD), 7th International Multi-Conference on Systems, June 2010.

Simulation of Inverse Kinetic Solution for Artificial Human Arm using Hybrid Algorithm in Virtual Reality

Abbas Hussien Miry, Mohammed Zeki Al-Faiz, MIEEE and Abduladhem Ali
Electrical Engineering Dept, AL-Mustansiriyah University
Computer Engineering Dept., Nahrain University
Computer Engineering Dept., Basrah University
Received 14/2/2013 – Accepted 15/9/2013

الخلاصة

هذا العمل يقدم محاكاة لذراع الإنسان. انها تهدف للسماح لهذا الذراع لتنفيذ الحركة الفعلية للذراع الإنسان في الواقع الافتراضي من خلال حل معكوس لذراع الإنسان الحركية باستخدام خوارزمية هجينة. مشكلة الحل الحركي المعكوس ليست خطية. هذا يعني أن الحلول التحليلية لا تتوفر إلا في حالات محدودة. يعرض هذا البحث استراتيجية تقوم على الحلول التحليلية جنبا إلى جنب مع خوارزمية التحسين غير الخطية لحل المشكلة الحركية العكسي. يستخدم الحل التحليلي للحد من حجم المشكلة من 7 متغيرات الى متغير واحد لإيجاد الحل التقريبي الذي يجعل الوقت اللازم للحساب صغير جدا. وضعت هذه المحاكاة من خلال استخدام أدوات الواقع الافتراضي و Simulink في MATLAB .

ABSTRACT

This work simulate an artificial human arm. It aims to allow this arm to implement the actual movement of the human arm in virtual reality by solving the inverse kinematic of human arm using a hybrid algorithm. Inverse kinematics problem is not linear; this means that the analytical solutions are available only in limited cases. This paper presents a strategy based on analytical solutions along with non-linear optimization algorithm solutions to solve the Inverse Kinematic Problem (IKP). The analytical solution is used to reduce the size of the problem of variables from 7 angles to one variable. Nonlinear optimization is used to find the approximate solution that makes computation time is very small. Virtual reality in the MATLAB environment provides communications and controls that have been developed on the basis of Virtual Reality Modeling Language (VRML).

1. INTRODUCTION

Robotics is one of the most important disciplines in the industry which can be used in the development of new technologies. Synergies of robots with different applications, such as submarine mission, vehicle assembly process, vision systems and artificial intelligence allows innovation and reduces manufacturing costs. For this purpose, it is important that programmers robot able to visualize and test the behavior of robots in different circumstances and different parameters [1].

Kinematics is the study of motion without regard to the forces that create it. the representation of the position of the robot end effecter through the Robotics Engineering (common parameters and link) forward kinematics [2]. Forward kinematics is a set of equations that calculate the position and orientation of the end effectors in terms of certain common angles. This group is created from the equations using the (Denavit Hartenberg) DH parameters obtained from the bottom frame. Inverse kinematics problem (IKP) robotic manipulator involves obtaining the required values manipulator joint position given the desired end point and direction. What is usually complicated because

there is no unique solution and close the form of direct expression of inverse kinematics mapping [3]. Optimal solution for IKP is linear, and there is another approach to deal with inverse kinematics using Tomo by [4] is to use the Levenberg-Marquardt method with strong damping with n variable depends on the problem, which can take a long time.
Some other works only make a 3D virtual that deal with the use of Matlab for systems simulations , M.Z. Al-Faiz [5] presents architecture for posture learning of an anthropomorphic robotic arm using matlab/simulink with virtual reality. The approach was aimed to allow the robotic system to perform complex movement operations of human arm; in this paper only forward kinematic is used in the simulation. B.Lee et al [6] presents the simulation of humanoid walking pattern using 3D simulator with Virtual Reality Toolbox. By using the Virtual Reality Toolbox
incorporated with MATLAB, The simulator was composed of three modules, namely, waking pattern code, kinematics code and display code. V.Sanchez et al [1] simulated methodology of the 5-DOF includes mathematical modeling of the direct, inverse and differential kinematics as well as the dynamics of the manipulator. This method was applied to test the robot CATALYST 5 by using a project in Simulink and Matlab .The method implements the path following in the 3D space and uses the Matlab- Simulink approach.
The main objective of this work is to show a complete simulation of a human arm, where it is proposed analytical solutions with non-linear optimization algorithm to solve the truth and the virtual IKP. Method allows manipulating the human arm system and visualizing the behavior of the robot from different points of view.

2. Structure and Kinematics of Human Arm [7]

Kinetic mode, high Degrees Of Freedom (DOF) and discusses human model that can be used to predict realistic human arm Positions. One can deal with by anthropomorphic arm the 7-DOF and carry origin in the shoulder joint. The first joint is the shoulder joint with 3 DOF. This means the kinetic chain 3 spherical joints with the shoulder joint, wrist and single joint of the elbow joint.

Table -1:Numeric Value for D-H Parameters

Frame (joint)	q_i(rad)	d_i(cm)	a_i(cm)	α_i(rad)
1	q_1	0	0	$\pi/2$
2	q_2	0	0	$\pi/2$
3	q_3	0	0	$-\pi/2$
4	q_4	0	l_4	$\pi/2$
5	q_5	0	l_5	$-\pi/2$
6	q_6	0	0	$-\pi/2$
7	q_7	0	0	$-\pi/2$

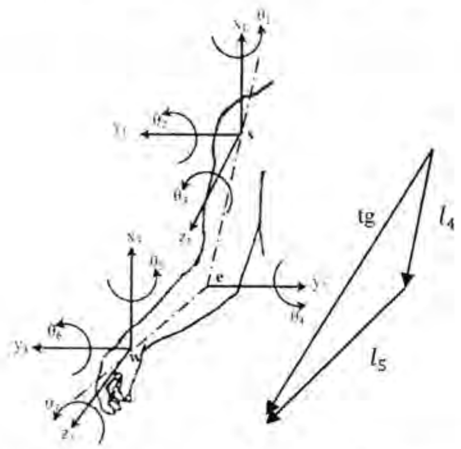

Figure 1. Kinematic chain of human arm [5]

The spherical joints have 3 DOFS while the hinge joint has only one DOF, giving a total of 7 DOFs for this kinematic chain, see Fig.1.

The homogeneous transformation matrices for the frame transitions are set up with D-H parameters.

$$A_1 = \begin{bmatrix} c_1 & -s_1 & 0 & 0 \\ 0 & 0 & -1 & 0 \\ s_1 & c_1 & 0 & 0 \\ 0 & 0 & 0 & 1 \end{bmatrix}, A_2 = \begin{bmatrix} c_2 & -s_2 & 0 & 0 \\ 0 & 0 & -1 & 0 \\ s_2 & c_2 & 0 & 0 \\ 0 & 0 & 0 & 1 \end{bmatrix} A_3 = \begin{bmatrix} c_3 & -s_3 & 0 & 0 \\ 0 & 0 & 1 & 0 \\ -s_3 & -c_3 & 0 & 0 \\ 0 & 0 & 0 & 1 \end{bmatrix}, A_4 = \begin{bmatrix} c_4 & -s_4 & 0 & l_4 \\ 0 & 0 & -1 & 0 \\ s_4 & c_4 & 0 & 0 \\ 0 & 0 & 0 & 1 \end{bmatrix}$$

$$A_5 = \begin{bmatrix} c_5 & -s_5 & 0 & l_5 \\ 0 & 0 & 1 & 0 \\ -s_5 & -c_5 & 0 & 0 \\ 0 & 0 & 0 & 1 \end{bmatrix}, A_6 = \begin{bmatrix} c_6 & -s_6 & 0 & 0 \\ 0 & 0 & -1 & 0 \\ s_6 & c_6 & 0 & 0 \\ 0 & 0 & 0 & 1 \end{bmatrix} A_7 = \begin{bmatrix} c_7 & -s_7 & 0 & 0 \\ 0 & 0 & 1 & 0 \\ -s_7 & -c_7 & 0 & 0 \\ 0 & 0 & 0 & 1 \end{bmatrix}$$

It has following transformation matrices where 'c' is cosine of theta and 's' is sin of theta, The forward kinematic represents by T

$$\mathrm{T} = \mathrm{A}_1 * \mathrm{A}_2 * \mathrm{A}_3 * \mathrm{A}_4 * \mathrm{A}_5 * \mathrm{A}_6 * \mathrm{A}_7$$

$$\mathrm{T} = \begin{bmatrix} nx & ox & ax & dx \\ ny & oy & ay & dy \\ nz & oz & az & dz \\ 0 & 0 & 0 & 1 \end{bmatrix} \qquad (1)$$

3. Proposed Method of Inverse Kinematics

A) Analytical part

The proposed algorithm can be explained in the following (see Fig.2):

Step one: In first we find θ_4 because it depend on posture of arm , tg represent the distance between start point and target point as shown in fig .1 , according to kinematics equation

Then $$\theta_4 = cos^{-1}\frac{tg^2-l_4{}^2-l_5{}^2}{2l_4l_5} \quad (2)$$

$$\theta_1 = \begin{cases} tan^{-1}\left(\frac{-dx}{dz}\right) - \varphi & if\ dz \neq 0 \\ \frac{\pi}{2} - \varphi & if\ dz = 0 \end{cases} \quad (3)$$

$$\theta_3 = sin^{-1}\frac{rcos\varphi}{l_5cos\theta_4 + l_4} \quad (4)$$

Step 4: In this step find θ_2: By compare dy with k_2

$$dy = l_5(s_2s_4 - c_2c_3c_4) - l_4c_2c_3 \quad (5)$$

Rearrangement k_2 and dy

$$s_2(l_5c_4c_3 + l_4c_3) + c_2(l_5s_4) = k_2 \quad (6)$$

$$-c_2(l_5c_4c_3 + l_4c_3) + s_2(l_5s_4) = dy \quad (7)$$

Let

$$k_3 = l_5c_4c_3 + l_4c_3 \quad (8)$$

$$k_4 = l_5s_4 \quad (9)$$

Let

$$\begin{bmatrix} k_5 \\ k_6 \end{bmatrix} = \begin{bmatrix} k_3 & k_4 \\ k_4 & -k_3 \end{bmatrix}^{-1} \begin{bmatrix} k_2 \\ dy \end{bmatrix} \quad (10)$$

From latest equations we get

$$\theta_2 = \begin{cases} tan^{-1}\frac{k_5}{k_6}\ if\ k_6 \neq 0 \\ \frac{\pi}{2}\ if\ k_6 = 0 \end{cases} \quad (11)$$

After these procedure $\theta_1, \theta_2, \theta_3\ and\ \theta_4$ are found

In next steps we find $\theta_5, \theta_6\ and\ \theta_7$

$A_1 * A_2 * A_3 * A_4$ is specified ,to find $A_5 * A_6 * A_7$ apply

$$A_5 * A_6 * A_7 = [A_1 * A_2 * A_3 * A_4\ ]^{-1} * T \quad (12)$$

$$A_5 * A_6 * A_7 =$$
$$\begin{bmatrix} c_5 * c_7 * s_6 - s_5 * s_7 & -c_7 * s_5 - c_5 * s_6 * s_7 & c_5 * c_6 \\ -c_6 * c_7 & c_6 * s_7 & s_6 \\ -c_5 * s_7 - c_7 * s_5 * s_6 & s_5 * s_6 * s_7 - c_5 * c_7 & -c_6 * s_5 \end{bmatrix} \quad (13)$$

$$\theta_6 = \sin^{-1} r_{23} \quad (14)$$

$$\theta_5 = \begin{cases} \tan^{-1} - \frac{r_{33}}{r_{13}}\ if\ r_{13} \neq 0 \\ \frac{\pi}{2}\ \text{if}\ r_{13} = 0 \end{cases} \quad (15)$$

$$\theta_7 = \begin{cases} \tan^{-1} - \frac{r_{22}}{r_{21}} \ if \ \ r_{21} \neq 0 \\ \quad \frac{\pi}{2} \ if \ r_{21} = 0 \end{cases} \tag{16}$$

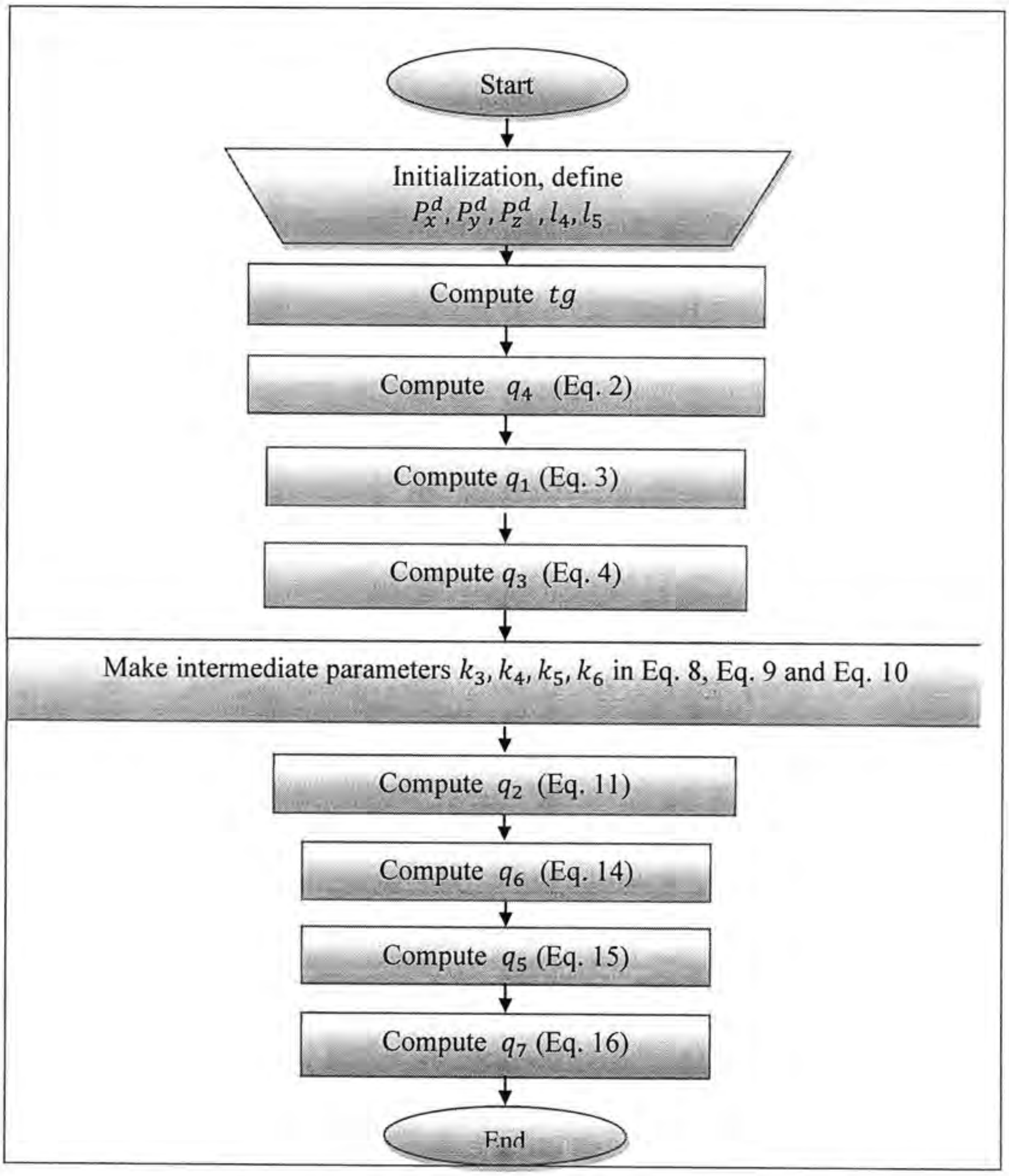

Figure-2:Flowchart for the simplification of human arm inverse kinematic producer

From previous derivative all angle ($\theta_1, \theta_2, \theta_3, \theta_5, \theta_6$ and θ_7) are made in term single angle φ therefore the our problem convert from multivariable to one variable which reduce the time required to find the solution .until last step analytical solution is performed.

B) Optimization part

Now the non linear optimization solution is performed depend on seven angle which depend on single angle φ therfor the next problem has single varaible .The robot kinematics is mathematically represented by a set of constraints on the joint displacement vector $\theta = [\theta_1 \ \theta_2 \cdots \theta_7]^T$,where 7 is the degree of freedom. A positional constraint is represented as

$$p(\theta) = p^d \tag{17}$$

Where

The vector θ depended on the value of φ from provieus procdure

p^d Target position in the space.

$p(\theta)$ Calculated position as function of joint space

For an orientation constraint,

$$R(\theta) = R^d \tag{18}$$

R^d Target orientation in the space.

$R(\theta)$ Calculated orientation as function of joint space

In both cases, the residual vector $e(q)$ can be defined as

$$e(\theta) = \begin{cases} P^d - P(\theta) \text{ (for a positional constraint)} \\ a(R^d * R(\theta)^T \text{)(for an orientational constraint)} \end{cases} \tag{19}$$

$$\text{Where } a(RT) = \left[\frac{1}{\|l\|} tan^{-1} \frac{\|l\|}{r_{11}+r_{22}+r_{33-1}}\right] l \tag{20}$$

$$RT = R^d * R^T(q) = \begin{bmatrix} r_{11} & r_{12} & r_{13} \\ r_{21} & r_{22} & r_{23} \\ r_{31} & r_{32} & r_{33} \end{bmatrix} \tag{21}$$

$$l = \begin{bmatrix} r_{32} - r_{23} \\ r_{13} - r_{31} \\ r_{12} - r_{12} \end{bmatrix} \tag{22}$$

Our interest starts from solving the following nonlinear Equation [4]:

$$e(\theta)=0 \tag{23}$$

The conventional IK based on NR tries to find $\theta = \theta^*$ which satisfies Eq.(23) by the following update rule

$$q^{k+1} = q^k - J^{-1} e(\theta^k) \tag{24}$$

Where

$$J = \nabla e(\theta^k) \tag{25}$$

After introduce both analytic and non linear optimization the IK solution will be considered now. The explanation of solution for the kinematic chain introduced in the previous section is present. It required

minimizing the error between the target transformation matrix and calculated transformation matrix ,the problem can be formularizing as optimization problem as following:
Minimize

$$e(\theta_1,\theta_2,\theta_3,\theta_4,\theta_5,\theta_6,\theta_7)=\begin{bmatrix}|P_x^d-dx|\\|P_y^d-dy|\\|P_z^d-dz|\\a\end{bmatrix} \quad (26)$$

Subject to
$\theta_i{}^l \le \theta_i \le \theta^u{}_i$ i=1… 7
θ^l=[$-\frac{\pi}{2}$ $-\frac{11\pi}{2}$ $-\frac{\pi}{2}$ $\frac{\pi}{12}$ $-\frac{\pi}{3}$ $-\frac{\pi}{9}$ $-\pi$],θ^u=[$\frac{\pi}{2}$ $\frac{2\pi}{3}$ $\frac{\pi}{2}$ $\frac{5\pi}{6}$ $\frac{\pi}{3}$ $\frac{\pi}{9}$ 0]

4. Optimization Problem

For optimization of the composition of a common reference angle regarding the similarity measure, one can use the Levenberg-Marquardt algorithm. The algorithm provides a standard way to solve problems non-linear least squares before they meet again to the minimum of the function also expressed the sum of the squares. Combinating Gauss, Newton's method most ratios, the algorithm unites the advantages of both methods. And then, using the method of LM, and achieved more robust convergence behavior at points far from the local minimum, while the faster close to the minimum. Become because of numerical stability, and the way LM also a popular tool to solve inverse kinematics [8].

5. Levenberg-Marquardt Algorithm

The Levenberg–Marquardt (LM) method uses the second-order derivatives of the mean squared error, so that better convergence behavior is observed. It is assumed that function f (θ) and its Jacobean J are known at point $[\theta]$. The aim of the Levenberg–Marquardt algorithm is to compute the variable vector$[\theta]$ such that

$$e(\theta)=d_t-F(\theta) \quad (27)$$

is minimum[9].

6. Virtual Reality

Virtual reality is a technology that is often as a natural extension of the 3D computer graphics with advanced input and output devices. This technology has only recently matured enough to justify serious engineering applications. Many companies and government agencies investigating the application of virtual reality techniques to design and manufacturing processes. . The state technology for the implementation of projects designed to demonstrate the feasibility and usefulness of VR in facilitating the design of the product. In very simple terms, VR can be defined as a synthetic environment that gives a person a sense of reality. This definition includes any artificial environment that gives the feeling of "being there. VR generally refers to computer environments that are created, though there are many environments in which immersive not manufactured entirely by computer. Examples of these include the use of a video camera for environments attendance for after or use embedded devices immersive. more people exposure to the concept of VR through reports in the media and scientific journals, and science fiction, but researchers who participated in the actual knowledge of VR, and applications are more mundane, and the problems are much more real [10].

7. Proposed Model and VR Simulation for a Human Arm

The simulation was built using MATLAB with virtual reality tools. MATLAB provides a powerful tool including geometry functions that are used frequently. It is easy to implement control algorithm including the visualization of the data used in the algorithm. In addition, using the tools of virtual reality, and it is convenient for the treatment of 3D objects defined with VRML (virtual reality modeling language). Thus, it is possible to build a simulator within a relatively short period. Virtual reality (VR) is a system that allows one or more users to move and interact in a computer environment that was created. Basic VR systems allow the user to use visual information from computer screens. Simulation contains two parts, the first, building a model of the human arm in VRML, second, simulink model constitution in MATLAB and then call and run the sample using tools virtual reality human arm.

To achieve a model of human arm VRML save your file as All.wrl, which is the file format for virtual reality programs, VRML model is designed for the human arm in the world 2.0 V-Albany. Fig.3 shows VRML model of the human arm.

And can be seen by the manipulation simply VRML Simulink model in Fig.4, where a human arm several blocks: the first goal career one name that represents the desired goal, and is calculated second block kinematics inverse desired goal required for the production of angle Part and Part III is to simulate using VR. Fig.5 shows the proposed method of drawing block.

8. RESULTS AND DISCUSSIONS

Simulate human arm and built in VR technology, and achieved a solution of inverse kinetic equations MATLAB Ver.R2009a. Fig.4 represents the relationship between MATLAB \ Simulink, which solves the equations of kinetic, and VR model of the human arm. Calculated orders are executed to transfer this model in MATLAB and then in the VR. As input sources to block sites that are part kinematics target, and a joint account human arm angle using the hybrid method. Using VRML editor to build a V-MATLAB, is allocated form. Then followed by planning programming box in Simulink so that the user can control the human arm structure appears in a VRML browser through MATLAB controls.

Being simulated to validate the algorithm derived inverse kinematics. The experiment was carried out to verify the validity of the proposed method derived in Section 4, with the positions and orientations unreachable.

In the experiment Y = 14 cm and z = 6 cm, while X vary from 35 cm to 40 cm. Table 2 shows the error-norm and CPU time in the proposed method and the method of LM. The trial results indicate that the inverse kinematics derived to provide the minimum error with the minimum of time with respect to the other way, because the optimization problem with a single variable that provides the minimum error, as shown in this experiment. In addition, human arm movement appears in Figure 6.

Figure-3: The VRML model of the Human arm

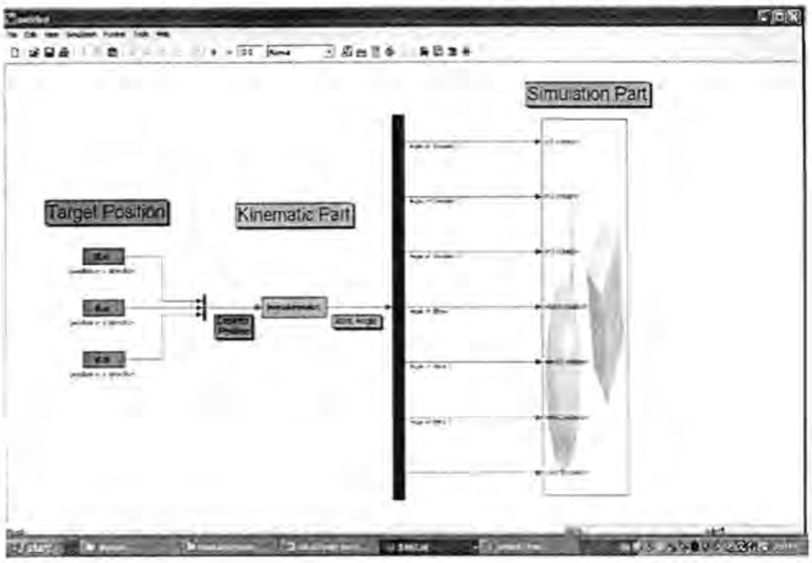

Figure-4: The Simulink model for A Human Arm

Table-2: CPU time and norm error of experiment result with x vary from 35 to 40

x	CPU Time(sec) of proposed	CPU Time(sec) of LM	$\|\|e\|\|$ in (cm) of proposed	$\|\|e\|\|$ in (cm) of LM
35	0.0250	1.0698	$0.285x10^{-3}$	0.1181
36	0.0168	1.1378	$0.179 x10^{-3}$	0.1192
37	0.0153	1.2134	$0.179 x10^{-3}$	0.1200
38	0.0157	1.2289	$0.176 x10^{-3}$	0.1217
39	0.0139	1.2176	$0.171 x10^{-3}$	0.1247
40	0.0192	1.0510	$0.174 x10^{-3}$	0.1309

9. Conclusion

This paper describes the feasibility of simulation and animation of a human arm in order to assess the performance of robot design to meet some of the rules of the contest. The first interest for the use of virtual reality is to enable students to assess quickly and clearly visualize the movement of the human arm, second benefit is the interaction between the robot and its environment before spending a lot of time in building the robot. Strategy based on combining the solution with analytical solutions of nonlinear optimization algorithm that will be proposed to the IKP solution. combine these methods address the weakness each other, through the use of analytical solutions, which provides angles manipulating common effectors end of the arm to a certain position, and can be accessed any direction with the best method which is linear solution approximation when the solution is to provide flour. With the use of MATLAB Ver.R2009a, and results are obtained satisfied with reducing both the error and CPU time from the way that provides the ability of the proposed algorithm to solve the inverse problem of the human arm real engine for several DOF.

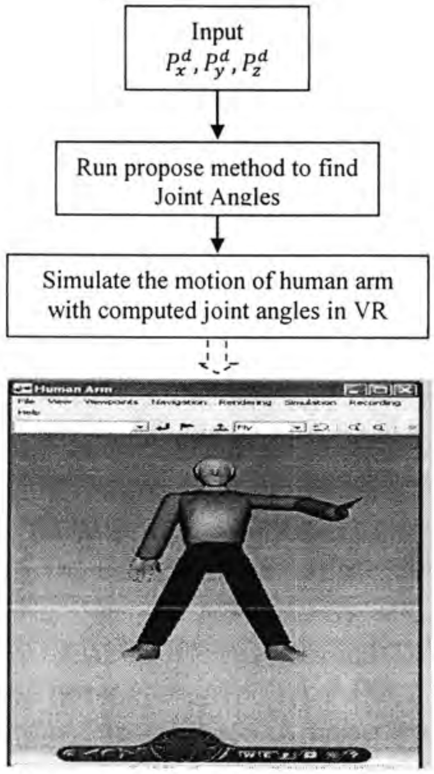

Figure-5: Block diagram for Human Arm Movement based Kinematic

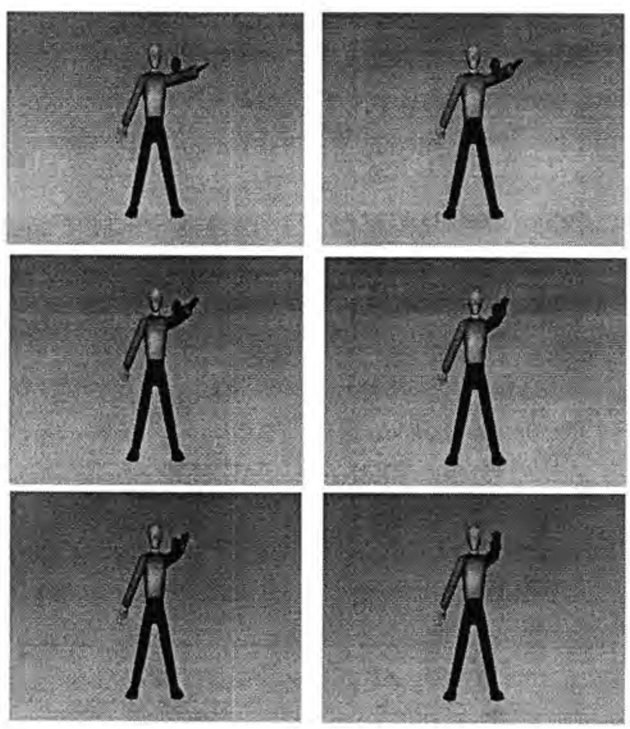

Figure-6:Human arm movements

REFERENCE

1. V.Sanchez,R.Gutierrez, G.Valdovinos and P.Ortega, "5-DOF manipulator simulation based on MATLAB-Simulink methodology ",2010 20th International Conference on Electronics, Communications and Computer (CONIELECOMP), 2010 , pp: 295 – 300
2. V. Grecu, N. Dumitru, and L. Grecu," Analysis of Human Arm Joints and Extension of the Study to Robot Manipulator", Proceedings of the nternational MultiConference of Engineers and Computer Scientists, Vol 2, March 18 - 20, 2009 pp:1348-1351.
3. C. Hua, C. and Wei-shan, "Wavelet network solution for the inverse kinematics problem in robotic manipulator",Chen Zhejiang Univ Science , Vol. 7 ,No. 4 ,2006 PP: 525-529.
4. T. Sugihara," Solvability-unconcerned Inverse Kinematics based on Levenberg-Marquardt Method", 2009 IEEE-RAS International Conference on Humanoid Robots, , Paris, Dec, 2009 ,pp:555-560
5. Al-Faiz ,M.Z., 2009," A Posture Human Robotic Arm by Inverse Kinematic With Virtual Environment", MASAUM Journal of Basic and Applied Sciences,Vol.1, No. 4,
6. Lee .B, Kim .Y, Yoo .J, Park .I and Kim .J, 2008,"Walking Pattern Simulation based on Virtual Reality Toolbox",.
7. M. Z. Al-Faiz, Y. I. Al-Mashhadany, "Analytical Solution for Anthropomorphic Limbs Model (IK of Human Arm)", IEEE Symposium on Industrial Electronics and Applications (ISIEA 2009), Malaysia ,October 2009 pp: 684-689
8. Do, M.; Azad, P.; Asfour, T.," Imitation of human motion on a humanoid robot using non-linear optimization", Humanoid Robots, 2008. 8th IEEE-RAS International Conference pp : 545 – 552 .
9. E.Derya," Detecting variabilities of ECG signals by Lyapunov exponents",Neural Computing & Applications, Springer Vol.18 ,No.7, 2009 pp: 653-662 .
10. B. Ma . Z. Guo . H. Zhou and D. Li, "Virtual plastic injection molding based on virtual reality technique", Springer-Verlag , Int J Adv Manuf Technol Vol.31 , pp: 1092–1100 , 2007

A Text Steganography Algorithm Without Changing Cover Image

Saad Najim Al Saad, Ahmed A. Bader, Ali T. Razak
Al-Mustansiryia University, College of Science
Al-Mustansiryia University, College of Science,
Received 15/3/2013 – Accepted 15/9/2013

الخلاصة

البحث يقدم خوارزمية مقترحة لأخفاء نص بدون تغيير ملامح صورة الغلاف المستخدمة. صورة الغلاف قبل وبعد أخفاء النص لم يطرأ عليها تغيير. أن صورة الغلاف لم تستخدم لأخفاء النص وأنما أستخدمت لأستخراج المفاتيح التي تستخدم لترميز الرسالة. الخوارزمية تمتلك مرونه في أختيار طول المفتاح كما انها لا تعطي أمكانية للتغير بصورة الغلاف التي تكون غير مرئية.

ABSTRACT

The paper presents a proposed steganography algorithm to hide text message without changing cover image. The stegao image and the cover image are same. The cover image is not used for hiding but it is used to extract the keys for translating the message. The algorithm has flexibility to choose the length of key and not give the ability to make change on the cover image because of invisibility.

1. INTRODUCTION

Online facilities are closely tied with securing the information exchanging over communication media. To make this information out of used of the intruders, many techniques have been used. One of these techniques is Steganography. The idea of Steganography, which dates back to the time of ancient Greeks, focuses to

1- hide the secret message from being seen or discovered.
2- avoid draw the suspicion to existence of hidden message.

Steganography "in Greek means covered writing" is the science of hiding information by embedding message within other one [1]. Unlike cryptography, which simply conceals the content or meaning of the message, Steganography's goal is to hide a message while Steganalysis is's goal is to detect the presence of hidden message. [2,3].

The generic description of image stenographic process has two important functions, embedding part and extracting part. The embedding function $\boldsymbol{E}$ is a function that maps the cover-object c, message $\boldsymbol{m}$ to a stego-object s.

$$E(c, m) = s.$$

The extracting function $\boldsymbol{D}$ is a mapping from s to m.

$$D(s) = m$$

The major goal of image steganography is to enhance communication security by embedding a secret message into digital cover_image, modifying the nonessential pixels of the image [4]. Stego_iamge, is the resultant of encapsulate or embed secret message in cover_iamge, is sent to the receiver through a public channel. The opponent may attack the stego_image if he/she doubts it carries any secret message.

For this reason, an ideal steganography scheme is to keep the stego from drawing the opponent attention; the message should be hidden inside cover without changing its visible properties. It should look higher similarities between cover and stego. The dissimilarities should not be discovered by humanin such a way that the visual system can recognize the different colors or the human Auditory System (HAS) can recognize the different audios.

Any steganography technique has to satisfy three basic requirements [5,6,7]. The first requirement is perceptual transparency or Stego-image quality, i.e. cover and stego must be perceptually indiscernible. Transparency between cover-images and stego-images is often computed using the peak signal-to-noise ratio (PSNR). The second constraint is capacity of the embedded data (message) that can be hidden with an acceptable resultant stego-image quality. Capacity is measured in bits per pixel (bpp) in images and in bits per second (bps) in audio. Lastly, robustness can be explained as the amount of modification the stego-image can withstand before an adversary can destroy hidden information.

It can say that a scheme does have its contribution to this field of research if it proves to either increase the payload while maintaining an acceptable stego-image quality or improve the stego-image quality while keeping the hiding capacity at the same level, or better if it can get both promoted.

There are many steganographic schemes have been proposed for still image. A simple and well-known approach is directly hiding secret data into the least-significant bit (LSB) of each pixel in an image. Based on LSB substitutions many algorithms are presented for improving the stego-image quality[8,9,10]. All these algorithm focuses to shorten the dissimilarities between cover_image and stego_imageas much as can.

In 2003 an algorithm is published that proposed an algorithm to hide information without changing cover image **[11].** The idea is interested since no differences between the actual image and the cover image but actually it suffers from the following weaknesses:

1- Unnecessary additional operations which cause increasing in complexity
2- There is a big chance that the algorithm may not find all possibilities from zeros to ones with of length n-1.
3- Large size of key.

The algorithm in that paper studied well and some developments has been made for improvement.

2. Proposed System

This algorithm is designed for concealing text inside digital image, by using (XOR) operation, without any changing in the cover image to prevent as much as possible any suspicion lead to finding the hidden text. As it is known the algorithm composes of two stages: Embedding and extracting. Below is the algorithm of each stage.

2.1 Embedding Algorithm

Input: Cover image and secret data.

Output: Key

Step1: Divide the cover image into blocks, each of size n × n.

i=0;

Step2: Repeat

i=i+1

Obtain all possible combinations for the $(block)_i$ by:

a) For each row, exclusive-or all bits. Append the result to get binary sequence r1r2...r(n).
b) For each column, exclusive-or all bits. Append the result to get binary sequence c1c2...c(n).
c) Save: the block number and (row) or (column) obtained from (a) and (b).

Until all required combinations of (n) bits are obtained.

Step3: Divide the binary bits of secret message into blocks of n bits length

Replace each block with block number that has the same value.

Example:

Input: Consider the bit representation of cover image is depicted in figure (1-a), the bit representation of secret image is: **010100011001.**

Step1: The first step is to divide the cover image into blocks each of size (n x n). Suppose that the block size is 3. Figures 1-b and 1-c represents first and second block respectively.

1	0	0	0	1	1	0	1
1	1	0	1	0	0	1	1
1	1	1	0	1	0	1	1
0	0	0	1	0	1	0	1
1	0	1	0	0	0	1	1
0	0	0	0	1	0	1	0
1	0	1	1	1	1	0	0
0	1	0	1	0	1	1	1

a

Binary cover image

1	0	0
1	1	0
1	1	1

b

block 1

0	0	0
1	0	1
1	1	0

c

block2

Figure-1:

<u>**Step2(a)**</u>: Exclusive-or all bits in each row to get **r1r2r3.**

$r1 = 1 \oplus 0 \oplus 0 = 1$

$r2 = 1 \oplus 1 \oplus 0 = 0$

$r3 = 1 \oplus 1 \oplus 1 = 1$

The result is 101

<u>**Step2(b)**</u>:Exclusive-or all bits in each column to get **c1c2c3**.

$c1 = 1 \oplus 1 \oplus 1 = 1$

$c2 = 0 \oplus 1 \oplus 1 = 0$

$c3 = 0 \oplus 0 \oplus 1 = 1$

The result is 101

The result of block1

[101,1,row] and
[101,1,column] ignored because of the same result

Performing the same operation on block 2 gives:
[000, 2, row]
[011, 2, column]

Continuing with step2 until all required combinations are obtained(Table 1).
From Table 1, all combinations of n bits are extracted with block number and row or column and considered to be the reference keys (Table 2).

S3:

The secret binary message is divided into blocks of length 3. Each block is replaced with its key. (Table 3)

Table-1:The output of step 2

Block no.	Test	Result	Status
• **1**	**Row**	**101**	**saved**
1	Col	101	Ignored
• **2**	**Row**	**000**	**saved**
• **2**	**Col**	**011**	**saved**
• **3**	**Row**	**110**	**saved**
3	Col	100	Ignored
4	Row	011	Ignored
4	Col	101	Ignored
• **5**	**Row**	**010**	**saved**
5	Col	010	Ignored
6	Row	000	Ignored
6	Col	101	Ignored
7	Row	010	Ignored
• **7**	**Col**	**001**	**saved**
8	Row	001	Ignored
8	Col	010	Ignored
9	Row	101	Ignored
9	Col	101	Ignored
10	Row	110	Ignored
10	Col	011	Ignored
11	Row	101	Ignored
11	Col	110	Ignored
12	Row	000	Ignored
12	Col	101	Ignored
13	**Row**	**100**	**saved**
13	Col	010	Ignored
14	Row	011	Ignored
14	Col	101	Ignored
15	Row	011	Ignored
15	Col	011	Ignored
16	Row	100	Ignored
16	Col	111	Ignored
17	Row	011	Ignored
17	Col	111	Ignored
18	Row	000	Ignored
18	Col	101	Ignored
19	Row	000	Ignored
19	Col	101	Ignored
20	Row	110	Ignored
20	Col	011	Ignored
21	**Row**	**111**	**saved**

Table-2: Reference keys

Reference keys
[000, 2, row]
[001, 7, column]
[010, 5, row]
[011, 2, column]
[100, 13, row]
[101, 1, row]
[110, 3, row]
[111, 21, column]

Table-3: secret message

Secret message.	key
010	**[5,row]**
100	**[13,row]**
011	**[2,column]**
001	**[7,column]**

2.2 Extracting Algorithm

Input: key and cover image

Output: Secret message

for i:= 1 to number of keys

Obtain the block(nxn) from $(\text{key})_i$

if key is row then for each row, call step2 (a) and save the result. r1r2...r(n)
else call step2 (b) and save the result c1c2...c(n).
end.

Example:
The first key is [5, row]. Step2(a) is performed on block 5. The result is **010**
The first key is [13, row]. Step2(a) is performed on block 13. The result is **100**
The first key is [2, column]. Step2(b) is performed on block 2. The result is **011**
The first key is [7, column]. Step2(b) is performed on block 7. The result is **001**

3. RESULTS AND DISCUSSIONS

The algorithm is written in visual basic. The cover image is JPG type with 256*256 size. Figure (2) shows the user interface to select cover image and plain text to be sent. The figure also shows the keys that extracted with 8 bits length. The experimental result points to the following

1. The length of key depends on the block size mentioned in step1. Figure 11 shows the key of length 8 and the block size is 8*8. (advantage)
2. Mostly the number of keys extracted to send to the receiver is more than the length of plaintext. (disadvantage)
3. The cover image is used to extract keys not to hide information. This is considered as strength of the algorithm but on the account of the key length.
4. As a future work it is important to address the drawbacks by reducing the the number of keys. Below some suggestions
   A:- A database of images is stored in both receiver and sender, so the cover image is not necessary sent, only the image index number. So the cover image is not visible to the intruder.
   B:- Replace row and column with 0 and 1.
   C:- Give flexibility to the sender to choose the suitable block size.

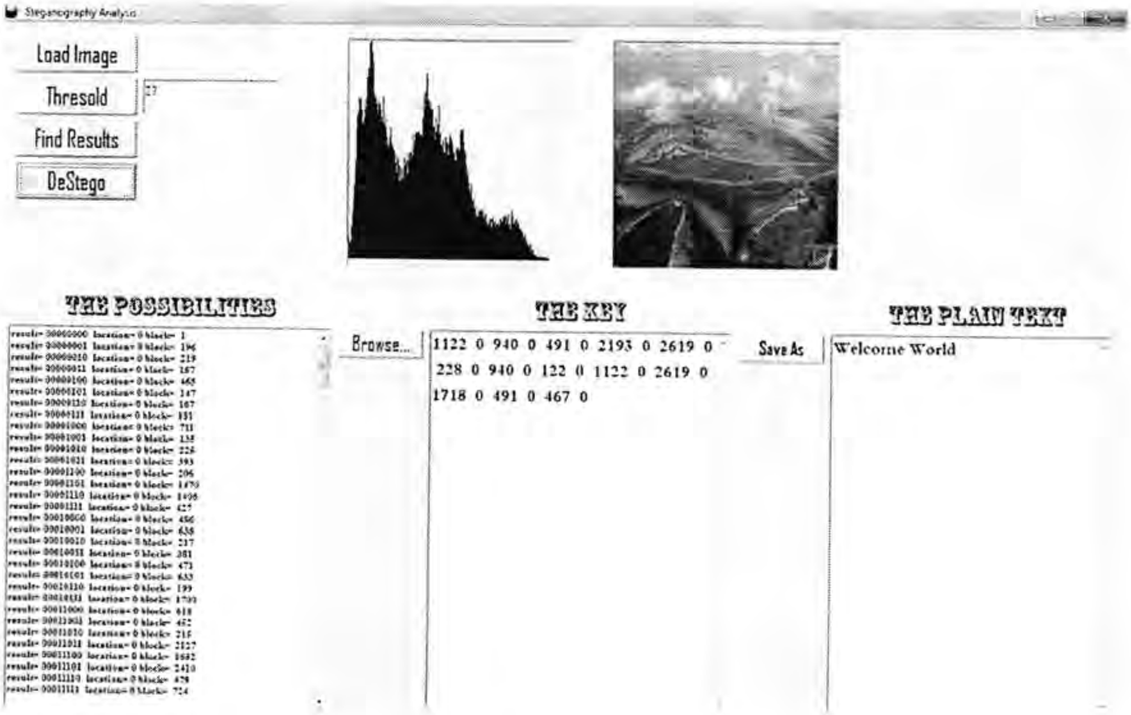

Figure-2: user interface for algorithm implementation

REFERENCES

1. Henk C. A. van Tilborg (Ed.), Encyclopedia of cryptography and security,pp.159, Springer 2005.
2. Dr.H.B.Kekre and A.A.Archana, "Information hiding usingLSB technique with increased capacity", International Journalof Cryptography and Security, vol. 1, No.2, October 2008.
3. W. Zeng, H. Yu, C. Lin, "Mutimedia Security Technologies for DigitalRights Management". Academic Press.Elsevier,2006.
4. Feng, J.B., Lin, I.C., Tsai, C.S., Chu, Y.P.. Reversible watermarking:current status and key issues. International Journal of NetworkSecurity 2 (May), 161–170, 2006
5. C. Parthasarathy and Dr. S.K.Srivatsa, "IncreasedRobustness OfLsb Audio Steganography By ReducedDistortion Lsb Coding" ,2005 *www.jatit.org/volumes/research-papers/Vol7No1/9Vol7No1.pdf*
6. Wu, N.I., Hwang, M.S.,. Data hiding: current status and key issues.International Journal of Network Security 4 (January), 1–9, 2007
7. Dittmann, D. Meg´ıas, A. Lang, Jordi Herrera-Joancomart´ı, "Theoretical framework for a practical evaluation and comparison of audio watermarking schemes in the triangle of robustness, transparency and capacity", Transactions on Data Hiding and Multimedia Security I, pp. 1-40, Springer-Verlag (2006).

8. Chang, C.C., Tseng, H.W.,. A steganographic method for digitalimages using side match. Pattern Recognition Letter 25 (September),1431–1437, 2004
9. Thien, C.C., Lin, J.C., . A simple and high-hiding capacity methodfor hiding digit-by-digit data in images based on modulus function, 2003
10. Wu, H.C., Wu, N.I., Tsai, C.S., Hwang, M.S., Image steganographicscheme based on pixel-value differencing and LSB replacementmethods. IEE Proceedings – Vision Image and Signal Processing 152(October), 611–615, 2005.
11. Ahmed Al-Jaber, Khair Eddin Sabri," Information Hiding Without Changing the Cover Image, ICITNS International Conference on Information Technology and Natural Sciences, 2003.

Diurnal Variation of Some Statistical Estimators with Time

Fatin E. M. Al-Obaidi, Ali A. D. Al-Zuky, Amal M. Al-Hillou
Department of Physics, College of Science, Al-Mustansiriyah University
Received 17/3/2013 – Accepted 15/9/2013

الخلاصة

ان التغاير في اضائية السماء الناجمة عن الطقس، فصل السنة والوقت من الصعب تقديره. ولبيان هذا التأثير فقد صمم نظام بصري مائل مواجه لخط الأستواء لدراسة التغاير اليومي لبعض العوامل والمقاييس الأحصائية مع الزمن. هذه العوامل هي التباين المستند على الخواص الأحصائية(C_t)، تباين مايكلسن(C_M) ونسبة الأشارة الى الضوضاء(SNR). اجريت عملية التحليل لخطين مستقطعين على صور تم التقاطها لمشهد داخل هذا النظام البصري؛ خط يمر خلال منطقة بيضاء متجانسة والأخر يمر خلال مناطق لونية مختلفة. وفقا" لموقع الخط ومن بين العوامل الأحصائية المستخدمة يمكن للمرء ان يلاحظ السلوك المحسن لحالة التشوه في حالة الخط الذي يمر بالمنطقة البيضاء المتجانسة لعلاقات تغايرSNR مع الزمن. الى جانب ذلك فلايوجد اي تأثير يذكر للخط الأخر والذي يمر بمناطق لونية مختلفة.

ABSTRACT

The variation in sky luminance caused by weather, season and time of the day are difficult to codify. To meet this, a tilted system facing the equator has been optically designed for studying the diurnal variation of some statistical estimators with time. These estimators are; contrast based on statistical properties (C_t), Mickelson contrast (C_M) and Signal to Noise Ratio (SNR). The analysis process has been performed for two selected lines upon the captured images for the scene inside the optical system; one passes through homogeneous white region and the other line passes through different color regions. According to line's position and among the different used estimators, one can noticed the enhancement behavior to the distortion effect in the case of line that passes through homogeneous white region for SNR relationship with time. Besides, there is no effect can be seen in the case of that passes through different color regions.

1-INTRODUCTION

The sunlight is absorbed when light passes through the atmosphere, and sky light consists of light scattered by particles in the air. On the way, passing through the atmosphere the light is attenuated, and its spectrum changes [1]. The atmosphere is transparent for the visible solar radiations; this property defines the so-called atmospheric window. This is a key point since it makes it possible to heat and to light the Earth's surface [2]. The management of data obtained from a scene with a large range of luminance is an important issue in image acquisition, analysis and display [3]. Image analysis combines techniques that compute statistics and measurements based on the gray-level intensities of the image pixels. One can use the image analysis functions to determine whether the image quality is good enough for the inspection task, understand its content and to decide which type of inspection tools to use to handle the application. Image analysis functions also provide measurements that one can be used to perform basic inspection tasks such as presence or absence verification [4][5].

2-Image Data Analysis Methods

Computer image analysis largely contains the field of computer or machine vision, medical imaging, make a heavy use of pattern recognition, digital geometry and signal processing. The applications of digital image analysis are continuously expanding through all areas of science and industry. Computers are indispensable for the analysis of image amounts of data for tasks that require complex computation or for the extraction of quantitative information [6].

Image analysis combines techniques that compute statistics and measurements based on the *RGB* intensity levels of the image pixels. In this process, the information content of the improved images is examined for specific features such as intensity, contrast, edges, contours, areas and dimensions. The result of analysis algorithms are feature vectors that give quantified statements about the feature concerned [7].

3-Contrast Computing Technique

Among the most widely used statistical estimators to analyze images and according to Zuheri [8], the results of contrast computing technique based on statistical properties are efficient in determining contrast values.

The estimates of the mean value of a random variable x_i whose probability density function is $p(x_i)$ is:

$$\mu = \bar{x}_i = \sum_{i=0}^{K=1} x_i p(x_i) \quad \text{......(1)}$$

Where

$$p(x_i) = \frac{M(x_i)}{K} \quad \text{......(2)}$$

Here $M(x_i)$ is the number of times that can obtain the value x_i in data set and K is the total number of random variable in the set, while the estimates of the standard deviation is given by the following equation [8][9]:

$$\sigma = \sqrt{\sum_{i=0}^{K=1} (x_i - \bar{x}_i)^2 . p(x_i)} \quad \text{......(3)}$$

Contrast computing technique (C_T) defined as the standard deviation over the mean value given by [8][9]:

$$C_T = \frac{\sigma}{\mu} \quad \text{......(4)}$$

While the ratio of the mean gray level to its standard deviation is denoted as *SNR* which is defined as [8][10]:

$$SNR = \frac{\mu}{\sigma} \qquad (5)$$

The contrast can also be specified by the contrast modulation (or Michelson contrast), C_M. Michelson contrast measure is used to measure the contrast of a periodic pattern such as a sinusoidal grating defined as[8][11]:

$$C_M = \frac{L_H - L_L}{L_H + L_L} \quad with \quad 0 \le C_M \le 1 \qquad (6)$$

4-The Optical Builted System

The designed system shown in Fig.(1) is a tilted wooden box with a square apertures (40x40, 30x30, 25x25, 20x20, 15x15, & 10x10cm^2) facing the equator. The wooden box was painted by a grey paint.

The scene is located at the end of the wooden box facing window's aperture such that the center of aperture window is optically in line with that of the scene.

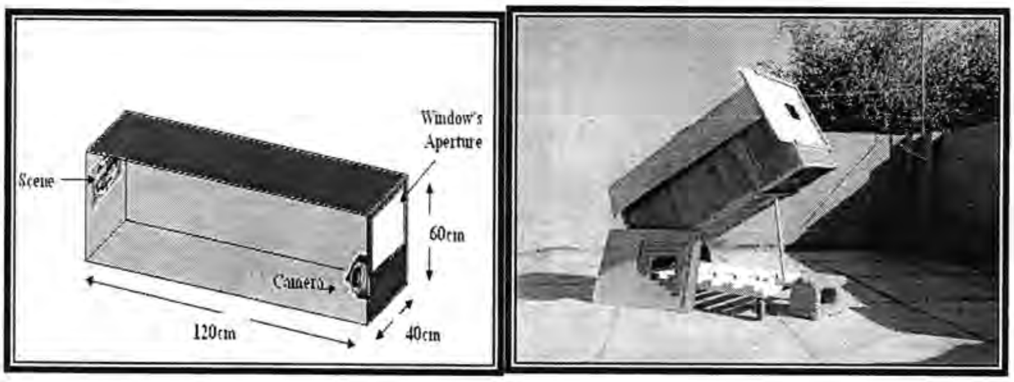

Figure-1:Schematic diagram of experimental setup

5-Data Acquisition Site

Baghdad (Latitude 33.2° N, Longitude 44.2° E) is the capital and biggest city of Iraq. The climate of Baghdad region (which is part of the plain area at the central of Iraq) may be defined as a semi arid, subtropical and continental, dry, hot and long summer cool winters and short springs.

6-Acquisition Data

By using the optical builted system shown in Fig.(1), images of the scene have been captured with size of (323x229) pixels. The capturing operation has been done at regular intervals from sunrise to sunset at two clear days (May 27 and December 22 in 2010) and two other haze days (October 22 and November 27 in 2010) as shown in Fig.(2). The analysis process has been performed for two selected lines upon the captured images. One of them passes through homogeneous white region (no.224) and the other line passes through different color pigments (no.165). The previous lines' locations were shown in Fig.(3).

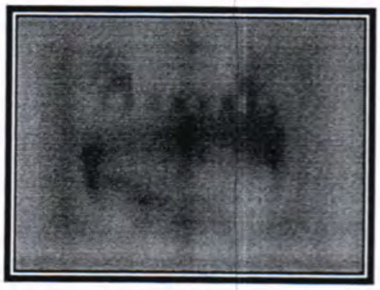

BNON1
27-5-2010
22.16°-Clear

(a)

RNON1
22-10-2010
38.2°-Haze

(b)

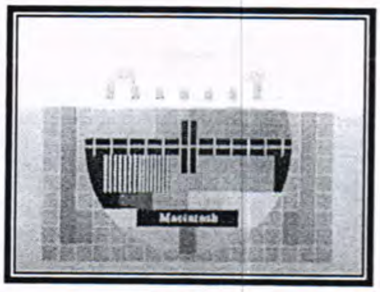

BNON1
22-12-2010
48.2°-Clear

(c)

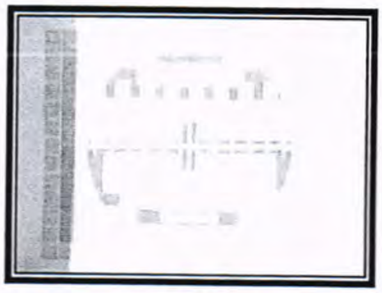

BNON1
27-11-2010
44.19°-Haze

(d)

Figure -2:Captured images under different tilted angles and weather conditions for:
(a) Before Noon (BNON1) using 40x40 cm^2
(b) At Noon (RNON1) using 40x40 cm^2
(c) Before Noon (BNON1) using 40x40 cm^2
(d) Before Noon (BNON1) using 40x40 cm^2

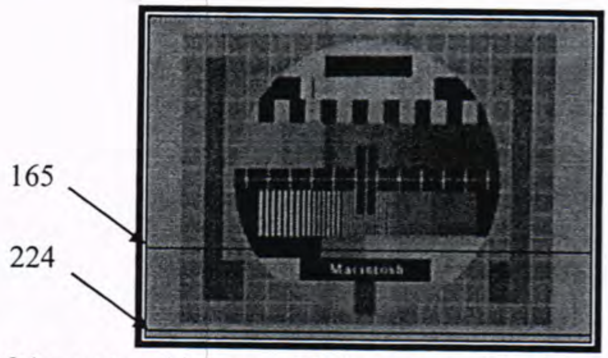

Figure-3:One of the captured images with the extracted horizontal lines upon it

7- RESULTS AND DISCUSSIONS

According to the fact that most sensitivity of human eyes is to the yellow-green light, the G-band will be handled in the next results discussions.

7.a The Horizontal Extracted Line That Passes Through Different Color Regions (no. \165)

The distortion and high interior illuminance effects distinguished significantly upon the captured images. That role can be seen obviously by noting Fig.(4) for diurnal variation of Michelson's contrast with time. Based on statistical properties, the resulted contrast (i.e. statistical contrast) as in Fig.(5) seems to be best than that for Michelson. The role of window's aperture area takes place in contradiction to that for Michelson contrast where no significant role can be noticed for the different areas of window's aperture. Fig.(6) represents the diurnal variation of $1/C_t$ with time for the horizontal extracted line number 165 for all dates.

7.b The Extracted Line That Passes Through Homogeneous White Region (no. 224)

Due to line's passage through homogenous white region, a different behavior for each contrast with time was noticed. This can be noticed in Figs.(7) and (8).

According to the previous result, one cannot use the contrast in its two types in the case of line number 224 to represent the diurnal intensity variation with time because of its incorrect representation for an intensity variations with time.

Regions in which lines were extracted are affected strongly. The effectiveness appeared upon the statistical estimator that best described the variations of intensity with time. A significant role for statistical contrast takes place in the case of line number 165 to no role in the case of line number 224.

Figure(9) shows the diurnal variations of *SNR* with time for the horizontal extracted line number 224 for all dates. No role for the area of window's aperture area can be noticed in such relationships except for the case of higher interior illuminance presented in Fig.(9c). The distortion effect doesn't appear in such relationship shown in Fig.(9a). This presents a good enhanced estimator for such situation without any processing in contradiction to that for line number 165.

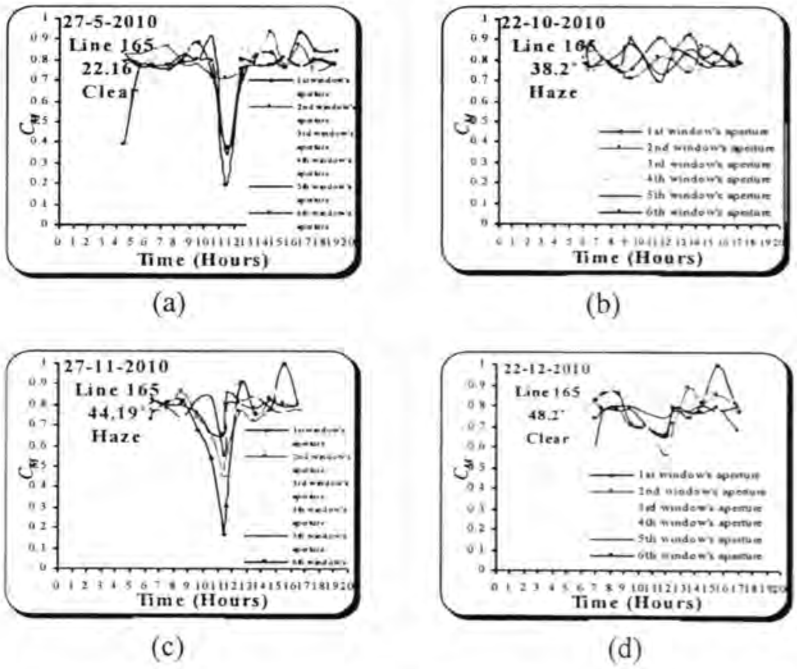

Figure-4: Diurnal variation of Michelson's contrast with time for the horizontal extracted line number 165 for all dates

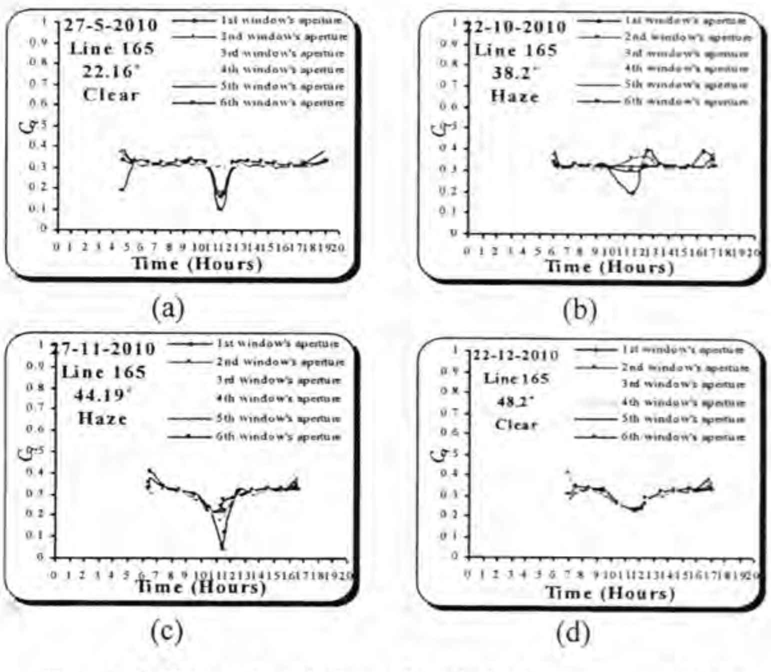

Figure-5: Diurnal variation of statistical contrast with time for the horizontal extracted line no.165 for all dates

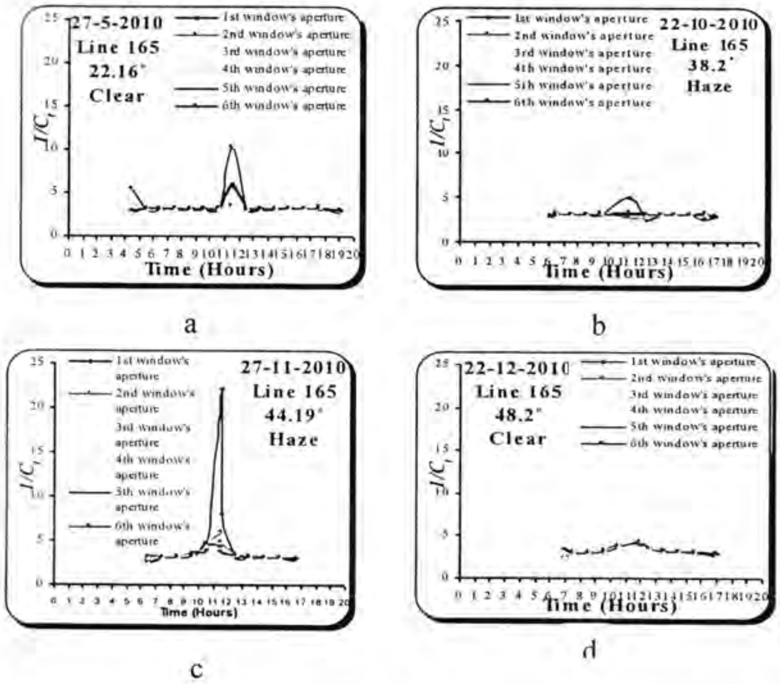

Figure-6: Diurnal variation of $1/C_t$ with time for the horizontal extracted line number 165 for all dates

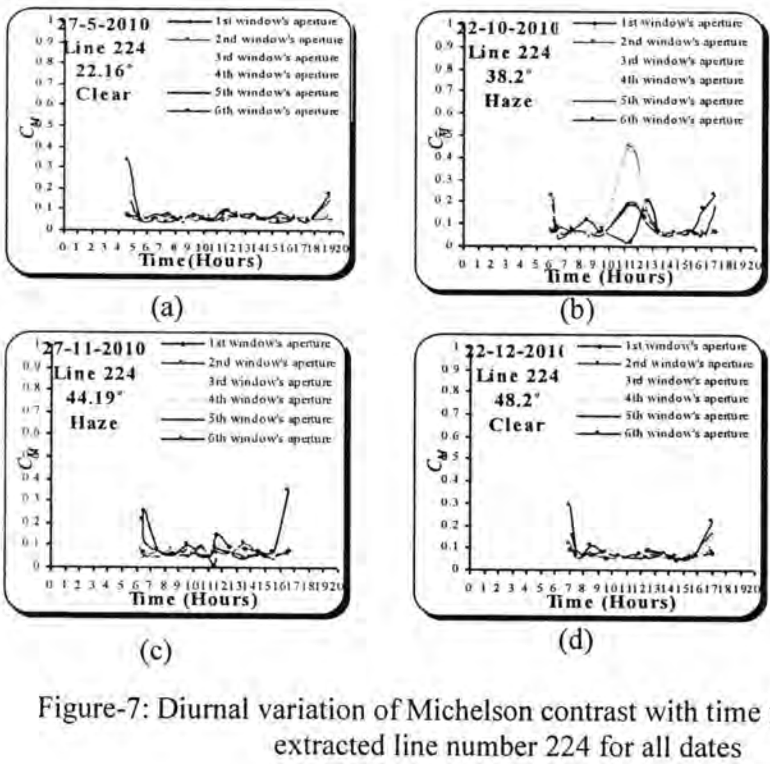

Figure-7: Diurnal variation of Michelson contrast with time for the horizontal extracted line number 224 for all dates

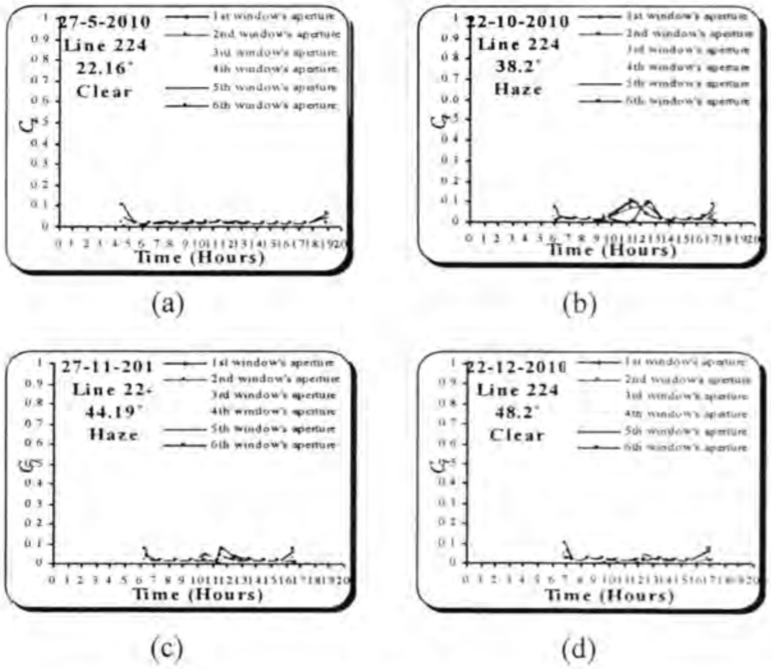

Figure-8: Diurnal variation of statistical contrast with time for the horizontal extracted line number 224 for all dates

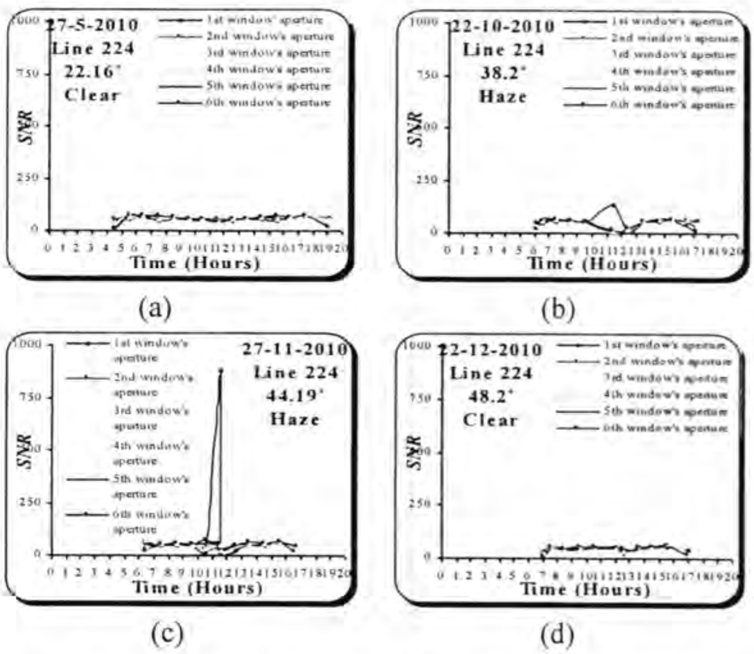

Figure-9: Diurnal variation of *SNR* with time for the horizontal extracted line number 224 for all dates

8-CONCLUSIONS

Regions in which lines were extracted are affected strongly. The effectiveness appeared upon the statistical estimator that best described the variations of intensity with time. Thus, a significant role for statistical contrast takes place in the case of line number 165 to no role in the case of line number 224.

In *SNR* relationships with time and according to line's location, different behaviors for the distortion case have been noticed. An enhancement for distortion occurred in the case of line passing through homogeneous white region in its relationship with time. Besides, there is no effect seen in the case of line passes through different color regions.

REFERENCES

1. T. Nishita, T. Sirai, K. Tadamura, E. Nakamae, "Display of the earth taking into account atmospheric scattering", Intern. Conf. on Computer Graphics and InteractiveTechniques, Proc. of the 20th Annual Conference on Computer Graphics and Interactive Techniques, 1993.
2. B. Sportisse, "Fundamentals in air pollution from process to modelling", Springer Science+Business Media B. V., 2010.
3. F. Xiao, J. M. Dicarlo, P. B. Catrysse, B. A. Wandell, "High dynamic range imaging of natural scenes", Tenth Color Imaging Conf. Color Science and Engineering Systems, Technologies and Applications, 2003.
4. A. M. Al-Hillou, A. A. D. Al-Zuky and F. E. M. Al-Obaidi, "Effects of intensity analysis of a colored test image under cleas sky daylight", Atti Della "Fondazione Giorgio Ronchi", ANNO LXVI, N. 1, 2011.
5. W. K. Pratt, "Developing visual applications XIL: An imaging foundation library, Sun Microsystems, Inc., 1997.
6. A. M. Al-Hillou, A. A. D. Al-Zuky and F. E. M. Al-Obaidi, "Digital image testing and analysis of solar radiation variation with time in Baghdad city", Atti Della "Fondazione Giorgio Ronchi", ANNO LXV, No. 2, pp. 223-233, 2010.
7. W. Osten, "Optical inspection of Microsystems", Taylor & Francis Gropu LLC., Boca Raton, 2007.
8. S. S. S. Zuheri, "A study lighting effect in determining of test image resolution", M. Sc. thesis, College of Science, Al-Mustansiriayah University, 2009.
9. E. Miles, A. Roberts, "Non-destructive speckle imaging of subsurface detail in paper-based cultural materials", Optics Express 12309, 17 (15), 2009.

10.F. E. M. Al-Obaidi, "Segmentation of coherent objects", M.Sc. thesis, College of Science, Al-Mustansiriyah University, 2001.
11.P. Dickinson and S. T. Lau, "Contrast formula for use with contrast measuring devices", Spectrum Technologies PLC, 1999.

3D Image Reconstruction for Wooden Object Based on Laser Triangulation Technique

Mohammed Y. Kamil[1], Mazin Ali A. Ali [2], Muayyed J. Zory[3], Israa F. Alsharuee[4]
Department of Physics, College of Sciences, AL–Mustansiriyah University.
Received 15/3/2013 – Accepted 15/9/2013

الخلاصة

تُقدّم الورقة طريقة لبناء نظام قادر على تحديد وقياس ابعاد الجسم وإعادة بناء الشكل ثلاثي الابعاد لجسم خشبي منتظم بالأستناد على تقنية التثليث الليزرية لأيجاد عمق الجسم. أظهرت النتائج أن الخوارزمية المقترحة لأعاد بناء سطح ثلاثي الأبعاد كانت لها دقة عالية وتم التغلب على الصعوبات في اعاد تشكيل صورة الجسم الخشبي باستخدام صورة مأخوذة من كاشف ضوئي، كذلك تبين ان كفاءة جودة الصور تقل كلما كانت الزاوية بين الكاشف الضوئي ومصدر الأضاءة صغيرة جدا.

ABSTRACT

This paper presents a way of constructing a system capable of determine the dimensions and reconstructs a 3D shape for symmetric wooden object based on laser triangulation technique to find the depth of object. The results show that the proposed algorithm for reconstruct 3D surface of object is accurate and get rid of the difficulties in reconstruction symmetric wooden object using captured images by photo detect. Also, the images efficiency is less when the angle between the photo detector and the illumination source is very small.

1. INTRODUCTION

To understand the complexity of laser triangulation scanning process we have to understand its working principles first. A laser scanner is a well-known non-contact measuring and scanning device, widely applied in reverse engineering process used for acquisition of surface forms of 3D objects as well as in other fields of science, especially in medicine [1, 2, 3]. Their main components are illuminant and a sensor, which is usually CCD camera. The illuminant can be either coherent or incoherent. However, coherent illuminants such as lasers offer several distinct advantages over incoherent light sources [4]. The scanner design is very straight forward, involving simple trigonometry. The image captured by the webcam is 2D. The depth of the object cannot be determined from the image. In order to find the depth, laser scanning is done. In laser triangulation, the laser is projected over an object and the image is captured by a camera. Since the price of components used also affect the accuracy of the laser scanner, higher price and branded components will produce better result than low price components. Hence, higher the accuracy to cost ratio, higher will be the optimization. The line joining the laser, object and the camera makes a triangle; hence the term triangulation is coined [5]. The purpose of a 3D scanner is usually to create a point cloud of geometric samples on the surface of the subject. These points can then be used to extrapolate the shape of the subject (a process called reconstruction). If color information is collected at each point, then the colors on the surface of the subject can also be determined. 3D scanners share several traits with cameras. Like cameras, they have a cone-like field of view, and like cameras, they can only collect information about surfaces that are not obscured. While a camera collects color information about surfaces within its field of view, a 3D scanner collects distance information about surfaces within its field of view. The "picture" produced by a 3D scanner describes the distance to a surface at each point in the picture. This allows the three dimensional position of each point in the picture to be identified [6].

2. Laser Scanner Triangulation

3D Models can be used in a large range of exciting applications areas: Animation, Architecture, Dentistry, Education, Fashion and Textiles, Forensics, Games, Industrial Design, Manufacturing, Medical, Movies, Multimedia, Museums, As-built Plants Rapid Prototyping, Toys, and Web Design [7].

The basic geometrical principle of optical triangulation is shown in Fig. (1). The collection of the scattered laser light from the surface is done from a vantage point distinct from the projected light beam [8].

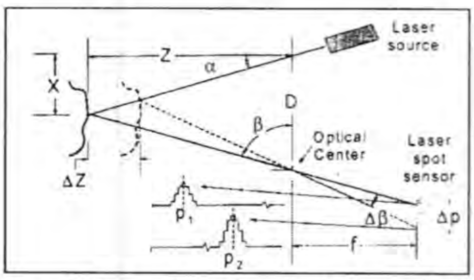

Figure-1: Laser based optical triangulation.

The light source and focusing optics generate a collimated or focused beam of light that is projected onto a target surface. An imaging lens captures the scattered light and focuses it onto a photo detector. The photo detector may be either a lateral-effect detector for high-speed measurement, or a CCD for environments with high background light. As the target surface distance changes, the imaged spot shifts due to parallax. Knowing the angle (θ) of a triangle relative to its base (baseline b) determines the dimensions of this triangle. To generate a three-dimensional image of the part surface, the sensor is scanned in two dimensions, thus generating a set of distance data that represents the surface topography of the part [9].

3. Experimental Setup

The system consists of: illumination source, photo detector, rotary table and processing unit as shown in fig.(2). The illumination source is the gas laser (He-Ne, ML800, power=1mw, wavelength is 600-700nm, divergence 1.7mrad). The photo detector is a CCD camera 16 Mpixel from Nikon Coolpix (4300), image size (1280x720). A camera placed parallel to the laser source which captures the image of the object while it is scanned. A rotary table (rotate 360 degree with clockwise) to place the object on during the test and scanned it horizontally. Finally is the controlling, operating and image processing unit. In this work, the object is symmetric wood has dimensions (4x3x2) cm. We have chosen a wood body, where the previous attempt failed because a complex logarithmic computation was needed and also required a high resolution camera [10]. To select suitable sites for equipment tried several distances between the source, body and camera at different angles, Best results obtained when the distance between the source and the body is 20 cm, also the camera and the source is 30cm. the angle of the camera corner can be determined which is (33.69°). Also we capture 72 images for the different faces of the object which angle of object rotate was 5 degree. The first face includes 21 images and the second face is 15 images, similarity with the other faces of the shape.

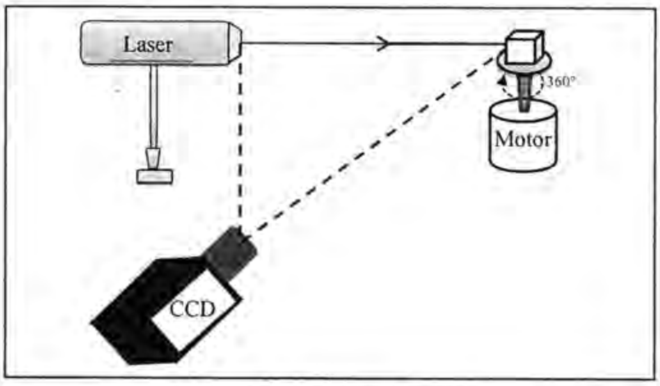

Figure-2: System diagram.

4. Images Processing Algorithm

The image preprocessing algorithm consists of edge detection, noise removing and extract the dimensions of object done automatically in the same program. Algorithm written by MATLAB software (version R2012a), the algorithm steps can be given as follow:

1. Read image as bmp format from CCD camera recorder.
2. Convert color image to grayscale intensity image.
3. Convert image to binary image, based on threshold. Another word for object detection is segmentation. The object to be segmented differs greatly in contrast from the background image.
4. Invert the image representation, the (black) background pixels become (white) foreground.
5. Smoothen the Object, in order to make the detect object without noise, we smoothen the object by eroding the image with a rectangle structuring element. We create the rectangle structuring element using the "strel" function.

6. Find initial point (x_i, y_j) on each boundary for object using "min" and "find" function (smallest elements in array and find indices and values of nonzero elements) and calculate the distance for object polygon in order to extract the dimensions.
7. Compute standard statistical computations; include median, mean, standard deviation and coefficient of variation to compare among dimensions.
8. Write image to graphics file as bmp format (save image).
9. Finally, display graphically the object using "fill3" function creates flat-shaded polygons (filled 3-D polygons).

5. RESULTS AND DISCUSSION

After apply of the laser triangulation method we can display the results that we have obtained in the above-mentioned distances in experimental setup paragraph. Fig. (3) show raw data for some first face of the object has dimension 1280 in rows and 720 in columns at BNP format. Fig. (4) illustrate raw data for second face after rotating the object at angle 90 which image take same dimensions and format. Also the third and fourth faces of the object which gives us similar results of the first two-faces when rotate the object to angle 360°, with the presence of some of the differences that have been occurred because of the statistical calculations to determine the dimensions of object. Therefore, Results will show the first and second faces only.

Figure-3: Raw images for first face.

Figure-4: Raw images for second face.

After using image processing algorithm on the raw image data to all faces, we get different shape dimensions of each frame (image capture) in pixel unit. Fig. (5) and (6) shows the first and second face for object shape after the implementation of a processing algorithm to extract the three dimensions. Also, table (1) and (2) illustrates the statistical operations on images which include median, mean, standard deviation (std) and coefficient of variation (CV) for object dimensions in x-axis and y-axis of the captured image. Table (1) the values of the x-axis have changed to the rotation of the object at angle of 90° around the vertical axis. Thus, the x values for first face in table (1) is the first dimension (object length), and in second face values represent the second dimension (object width), and the y-axis values represent the values of the third dimension (object height). Finally, after finding the dimensions of the object, the program will draw three-dimensional shape within the limits of the original images captured by the camera. The difference y-axis values in the tables due to the presence of some of the obstacles that lead to do not accuracy in measurement. Including the use of metal rotary table are reflect light falling on them, as well as the loss of high-accuracy components parts of the measurement system through distance and inclination, etc. That needs high calibration by the designer. There are some losses in hardware components, such as resolution of the photo detector (CCD) and illumination source (laser).

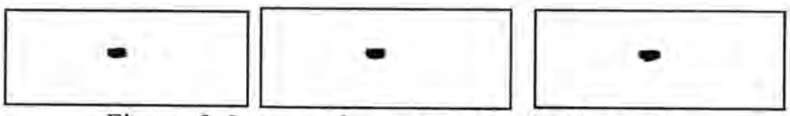

Figure-5: Images after processing the first face.

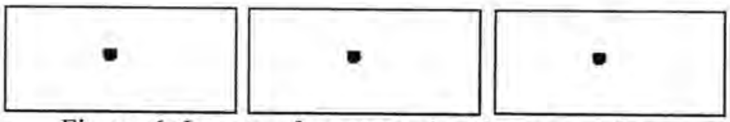

Figure-6: Images after processing the second face.

Table-1: Statistics of selected images.

face	value	Im.1	Im.2	Im.3	median	mean	std	CV
1'st	X	118	119	121	119	119	1.527	0.0128
	y	79	84	85	84	83	3.214	0.0389
2'nd	X	89	90	91	90	90	1.527	0.0169
	y	80	83	86	83	83	3.000	0.0361

Fig. (7) Illustrate the comparison between the image of the final result (3D image reconstruction) obtained after the implementation of the program with the original image of the object before to processing. When the image size is the same, the results showed a match between the original image and the image that was built in this program.

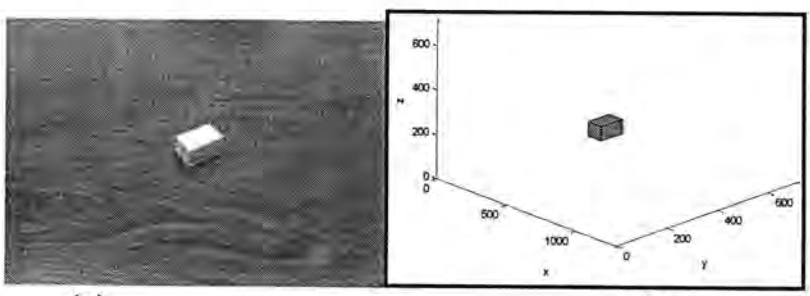

(a) (b)

Figure-7: Compare between: (a) original object. (b) final result.

6. CONCLUSIONS

Laser triangulation method provides a rapid and simple way for obtaining distance measurements in the laser scanner system which is used in the 3D image reconstruction because of its simplicity and robustness gives more accurate results as compared with other technique. The reconstruction investigation was at different distances between parts of the system, the results showed that the quality of the images less whenever the angle between the photo detector and the illumination source are very small. In this research, we get rid of the difficulties in reconstruction symmetric wooden object image through the use of appropriate algorithms based on morphological processing. The proposed algorithm has been tested on different sizes of wooden object and gave results very approach of reality through the graphical drawing of the object within the software automatically and without the use of other programs.

7. REFERENCES

1. Bračun, D., Jezeršek, M., Diaci, J. Triangulation model taking into account light sheet curvature, Measurement Science and Technology, 2006, vol. 17, pp. 2191-2196.
2. Vukašinović, N., Kolšek, T., Duhovnik, J., "Case study - surface reconstruction from point clouds for prosthesis production", Journal of eng. design., vol. 18, no. 5, p. 475-488, 2007.
3. Jezeršek, M., Fležar, M., Možina, J. "Laser Multiple Line Triangulation System for Real-time 3-D Monitoring of Chest Wall During Breathing", Strojniški vestnik – Journal of Mechanical Engineering, vol. 54, no. 7-8, p. 503-506, 2008.
4. Curles, B.L. "New methods for surface reconstruction from range images", Department of Electrical Engineering of Stanford University, 1997.
5. A. Malhorta, K. Gupta, K. Kant, "Laser Triangulation for 3D Profiling of Target ", International Journal of Computer Applications, vol.35, no. 8, 2011.
6. Fausto Bernardini, Holly E. Rushmeier, "The 3D model acquisition pipeline", Comput. Graph. Forum 21 (2): 149–172, 2002.
7. Stephen. J. Marshall and John .H. Gilby, "New Opportunities in Non-ontact 3D Measurement", Imaging Hagerston Partnership, Maryland, 2000.
8. J. Beraldin, "Integration of laser scanning and close-range photogrammetry - the last decade and beyond," in XXth Congress. International Society for Photogrammetry and Remote Sensing, Istanbul, Turkey, pp. 972-983, 2004.
9. M. Buzinski, A. Levine, W. H. Stevenson, "Performance characteristics of range sensors utilizing optical triangulation". In: IEEE, National Aerospace and Electronics Conference, pp. 1230-1236, 1992.
10. Nuha. J. Mohammed, "Image Reconstruction of 3D Shape Object Using Non-Contact Optical Sensing Technique", M. Sc, thesis, Institute of Laser for Postgraduate Studies, University of Baghdad, 2005.

Studying Satellite Image Fusion Analysis Based On Edge And Homogenious Image Quality Measuers

Heba K.Abbas[1], Ali A. Al-Zuky[2] and Anwar H.Mahdy[3]
[1]Dept. of Physics, College of Science for women, Baghdad University
[2]Dept. of Physics, College of Science Dept. Mustansiriyah University
[3]Dept. of Computer, College of Science Dept. Mustansiriyah University
Received 17/3/2013 – Accepted 15/9/2013

الخلاصة

في التحسس عن بعد ،تعد تقنية انشطار الصور اداة مفيدة تستخدم لدمج الصور ذات الوضوحية المكانية العالية (صورة PAN) مع صور ذات وضوحية مكانية واطئة (صورة MS) لأنشاء صورة مفردة عالية الوضوحية المكانية مع الاحتفاظ بالوضوحية الطيفية لصور (MS) نحصل على صورة الانشطار (المدمجةF).هنالك العديد من التقنيات المستخدمة لأنشطار الصورة بعضها معتمد على عنصر الصورة حيث طورت هذه التقنيات لتحسين الوضوحية المكانية وحفظ الخصائص الطيفية لصورة(MS).في هذا البحث نحاول فهم دراسة انشطار الصورة بأستخدام تقنيات مختلفة الاولى معتمدة على عنصر الصورة مثل المجموعة الحسابية المتمثلة بطرق (BT,CNT and MLT).والثانية المعتمدة على تنقية التردد المتمثلة بطرق (HPFA and HFA). والثالثة معتمدة على الطرق الاحصائية المتمثلة (LMM and RVS).في هذا ابحث ركزنا على تحديد جودة تفاصيل الصورة وخصوصاً التفاصيل الدقيقة والحافات حسب المعايير المتمثلة (AMSE,PSNR,MSE). وكذلك الاعتماد على معايير تخمين التجانس لتحديد التجانس في مناطق الصورة المختلفة باستخدام (µ ,SD,SNR) بالأضافة الى معياري (MI,SF). كانت عملية التقييم من التجارب عملية جيدة وكفوءة لأنها اخذت بنظر الاعتبار قياس جودة الحافات وقياس جودة المناطق المتجانسة .

ABSTRACT

This paper attempts to undertake the study of image fusion ,by using pixel –based image fusion techniques i.e. arithmetic combination ,frequency filtering methods of pixel –based image fusion techniques and different statistical techniques of image fusion. The first type includes Brovey Transform (BT), Color Normalize Transformation (CNT) and Multiplicative Method (MLT). The second type includes High-Pass Filter Additive Method (HPFA and HFA). The third type includes Local Mean Matching (LMM), Regression Variable Substitution (RVS). This paper also devotes to concentrate on the analytical techniques for evaluating the quality of image fusion (F) , in this study will concentrate on determination image details quality specially tiny detail and edges by uses two criterion edge detection then quality measurements determine and estimation homogenous to determine homogenous in different regions image using Mean (µ) and Standard Deviation (SD), Signal –to Noise Ratio (SNR) ,and compute Absolute Mean Square Error (AMSE),Mean Square Error (MSE), Peak- Signal- To –Noise Ratio(PSNR) , Mutual Information(MI) and Spatial Frequency(SF) ,therefore will be evaluation active and good because to take into consideration homogenous and edge quality measurements .

1. INTRODUCTION

Satellite remote sensing offer offers a wide variety of image data with different characteristics in terms of temporal, spatial, radiometric and spectral resolutions. Although the information content of these images might be partially overlapping [1], imaging systems somehow offer a tradeoff between high spatial and high spectral resolution, whereas no single system offers both. Hence, in the remote sensing community, an image with 'greater quality 'often means higher spatial or higher spectral resolution, which can only be obtained by more advanced sensor[2]. However, many applications of satellite images require both spatial and spectral resolution to be high. In order to automate the processing of these satellite images new concepts for sensor fusion are needed. It is, therefore, necessary and very useful to be able to merge images with higher spectral information and higher spatial information [3]. Image fusion is a sub area of the more general topic of data fusion. So, satellite remote sensing image fusion has been a hot research topic of remote sensing image processing [4]. This obvious from a mount of conferences and workshops focusing and data fusion, as well as the spatial issue of scientific journals dedicated to the topic. Previously, data fusion, and in particular image fusion belonged to the world of research and development. In meantime, it has become a valuable technique for data enhancement in many applications. The term "fusion" get several words to appear, such as merging, combination, synergy, integration, and several others the express more or less the same concept have since appeared in literature. A general definition of data fusion can be adopted as follows "Data fusion is a formal frame work which expresses means and tools for the alliance of data originating from different sources. It aims at obtaining information of greater quality; the exact definition of "greater quality" will depend upon application. Many image fusion or pan sharpening techniques have been developed to produce high – resolution multispectral images. Most of these methods seem to work well with images that were acquired at the same time by one sensor (single – sensor, single – data fusion).It becomes, therefore increasing important to fuse image data from different sensors which are usually recorded at different dates. Thus, there is a need investigate techniques that allow multi –sensor, multi- data image fusion Generally, image fusion techniques can divided into three levels, namely: pixel level, feature level and decision level of representation. This paper was focused on using previous dependable merge methods to do simulation process by use camera to make satellite images merge [5]. At suggestions by use contrast and homogenous to purpose evaluated results image quality, In this study will concentrate on determination image details quality specially tiny details and edges by uses criterion Edge detection then contrast determine.

2. Arithmetic Combination Techniques

This category includes simple arithmetic techniques. Different arithmetic combinations have been employed for fusing MS and PAN images. They directly perform some type of arithmetic operation on the MS and PAN bands such as addition, multiplication, normalized division, ratios and subtraction which have been combined in different ways to achieve a better fusion effect. These models assume that there is high correlation between the PAN and each the MS bands [6], some of the popular AC methods for PAN sharpening are BT, CNT and MLT. The algorithms are described in the following sections.

2.1 Brovey Transform (BT)

The Brovey transform is a ratio method where the data values of each band of the MS data set are divided by the sum of the MS data set and the multiplied by the PAN data set .The Brovey transform attempts to maintain the spectral integrity of each band, by incorporating the proportionate value of each band as related to the MS data set before merging it with the PAN data set. By adjusting the effects of the PAN data set's spectral properties when combining the data sets, the spectral quality of the MS data set is mainly preserved [7].

$$BT_{i,j,k} = \frac{MS_{i,j,k}}{\sum_u MS_{i,j,u}} \times PAN_{i,j} \qquad ,............(1)$$

Where $BT_{i,j,k}$ is the output image and i and j are pixel coordinates, k is the band index. The Brovey transform was developed to increasing the contrast visually at the low and high ends of an images histogram. Consequently, the Brovey transform should not be use if the condition of preserving the original scene radiometry in necessary. However, it is good for producing RGB images with a higher degree of contrast in the low and high ends of the image histogram, and for producing visually data taking from different sensors [8].

2.2 Color Normalized Transform (CNT)

The color normalized transformation fuses the two spectral and spatial data sets assuming there is a certain spectral overlap between the MS bands and the more highly resolved PAN band. This constrains is violated for the near infrared band, and leads to poor fusion results. Equation 2 shows the merging process whereby the additive constants avoid division by zero [8]:

$$CNT_{i,j,k} = \frac{3*\left(MS_{i,j,k}^{low}+1\right)(PAN^{high}+1)}{\sum_{s,t}(MS_{s,t,k}^{low}+3)} \qquad ,.............. (2)$$

2.3 Multiplicative Model (MLT)

The multiplicative algorithm is derived by using the four possible arithmetic methods to incorporate an intensity image into a chromatic image (addition, subtraction, division and multiplication). Only multiplication is unlikely to distort the color. The multiplicative model companies the two data sets by multiplying each pixel in each band by the corresponding pixel of the PAN data. To compensate the increased BV'S the square root of the mixed data set is taking. The square root of the multiplicative data set reduces the data to combination reflecting the mixed spectral properties of both data sets [7]:

$$MLT_{i,j,k} = \sqrt{PAN_{i,j} x MS_{i,j,k}} \qquad ,................ (3)$$

Where MLT is the output image, (i,j) are pixels coordinates, and k is the band index.

3. Frequancy Filtering Methods (FFM)

Many outhers have found fusion methods in the spatial domain (high frequency inserting procedures) superior over the other approaches, which are known to deliver fusion results that are spectrally distorted to some degree. Fusion techniques in this group use high pass filters to model the frequency components between the PAN and MS images by injecting spatial details in the PAN and introducing them into the MS image. Therefore, the original spectral information of the MS channels is not or only minimally affected [9].Such algorithms make use of classical filter technique in the spatial domain. One of the popular FFM for PAN sharpening is the HPFA based methods.

3.1 High-Pass Filter Additive Method (HPFA)

The High Pass Filter Additive (HPFA) technique was first introduced by Schowengerdt (1980) as a method to reduce data quantity and increase spatial resolution for Landsat MSS data [10]. HPF basically consists of an addition of spatial details, taken from a high- resolution pan observation, into the low resolution MS image. The high frequencies information is computed by filtering the PAN with a high – pass filter through a simple local pixel averaging, i.e. box filters. It is performed by emphasize the detailed high frequency components of an image and deemphasize the more general low frequency information. The HPF method uses standard square box HP filters .For example, a 3*3 pixel kernel, which is used in this study given by [10]:

$$P_{HPF} = \frac{1}{9}\begin{bmatrix} -1-1-1 \\ -1\ 8\ -1 \\ -1-1-1 \end{bmatrix}, \ldots\ldots\ldots\ldots\ldots\ldots(4)$$

In its simplest form, the HP filter matrix is occupied by "-1" at all but at the center location. The center value is derived by c=n*n-1, where c is the center value and (n*n) is the size of the filter box. The HP is filters that compute a local average around each pixel in the PAN image. The extracted high frequency components of P_{HPF} was superimposed on the MS image by simple addition and the result divided by two to offset the increase in brightness values. This technique can improve spatial resolution for either color composites or an individual band .This is given by [11]:

$$F_K = \frac{(M_K + P_{HPH})}{2} \quad , \ldots\ldots\ldots\ldots(5)$$

The high frequency is introduced equally without taking into account the relationship between the MS and PAN images. So the HPF alone will accentuate edges in the result but loses a large portion of the information by filtering out the low spatial frequency components [11].

4. Statistical Fusion Methods: In this study work two statistical fusion methods had been used, they are: **4.1 Local Mean Matching**

The general local mean matching (LMM) algorithm to integrate two images, PAN into MS resampled to the same size as P, as follow is given by [12]:

$$F_{K(i,j)} = PAN_{(i,j)} \times \frac{\bar{M}_{K(i,j)(w,h)}}{\overline{PAN}_{(i,j)(w,h)}}, \ldots\ldots\ldots\ldots\ldots\ldots\ldots\ldots(6)$$

Where $F_{k(I,j)}$ is the fused image ,$PAN_{(I,j)}$ and $M_{K(I,j)}$ are respectively the high and low spatial resolution images at pixel coordinates (I,j);$\bar{M}_{K(i,j)(w,h)}$ and $\overline{PAN}_{(i,j)(w,h)}$ are the local means calculated inside the window of size (w,h),which used in this study a 3*3 pixel window .

4.2 Regression Variable Substitution

This technique is based on inter-band relations, due to the multiple regressions derives a variable, as a linear function of multi-variable data that will have maximum correlation with unvaried data .In image fusion, the regression procedure is used to determine a linear combination (replacement vector) of an image channel that can be replaced by another image channel [13]. This method is called regression variable substation (RVS) [14] called it a statistics based fusion ,which currently implemented in the PCI& Geometric a software as special module , pans harp shows significant promise as an automated technique. The fusion can be expressed by the simple regression shown in the following eq.

$$F_k = a_k + b_k . PAN, \ldots\ldots\ldots\ldots\ldots\ldots\ldots (7)$$

The bias parameter a_k and the scaling parameter b_k can be calculated by a least squares approach between the resembled band MS and PAN images. The bias parameter a_k and the scaling parameter b_k can be calculated by using eq.(8&9) between the resample bands multispectral M_k and PAN band P (see appendix)

$$b_k = \frac{S_{PM_k}}{S_{PP}} \quad , \ldots\ldots\ldots\ldots\ldots\ldots\ldots\ldots (8)$$

Where S_{PM_k} and S_{PP} are the covariance between P with M_k of band K and the variance P respectively .

$$a_k = \bar{M}_k - b_k . \bar{P} , \ldots\ldots\ldots\ldots\ldots\ldots\ldots (9)$$

Where $\bar{M}_K$ and $\bar{P}$ are the mean of M_K and P. Instead of computing global regression parameters a_k and b_k in this study, the parameter are determine in a sliding window a 3*3 pixel window was applied.

5. STUDYING CASES

In order to validate the theoretical analysis ,the performance of the methods discussed above was further evaluated by experiments, data sets used for this study were collected by the Panchromatic SPOT image (recording data 16 March 2003) with 5 m pixel size which is the size(893×893)pixels this image explained in the fig.1(a) and multispectral Land sat ETM image (band 1-5 and 7)with 30m ground pixel size which is the size(895×893)pixels and both possess bit depth (24bits), showing a region east of the city of Aachen (Germany) was registered to ground coordinates (German Gauß-Krügery system)and served as the master image .The Land sat image form fig.1(b) was registered to the SPOT image. Fig.2 shows the fused images of the BT, CNT, MLT, HFA, HPFA, LMM and RVS methods are employed to fuse (a) and (b) images in fig.1. To evaluate the ability of enhancing spatial details and preserving spectral information, some for excite quality measurement including Mean (μ), Standard Deviation (SD), Signal- To –Noise Ratio(SNR), Absolute Mean Square Error (AMSE),Mean Square Error (MSE), Peak- Signal- To –Noise Ratio(PSNR) , Mutual Information(MI) and Spatial Frequency(SF)of the image were used (Table 1a,b) are shown the results.

Figure-1: (a) Land sat Image, (b): Spot Image

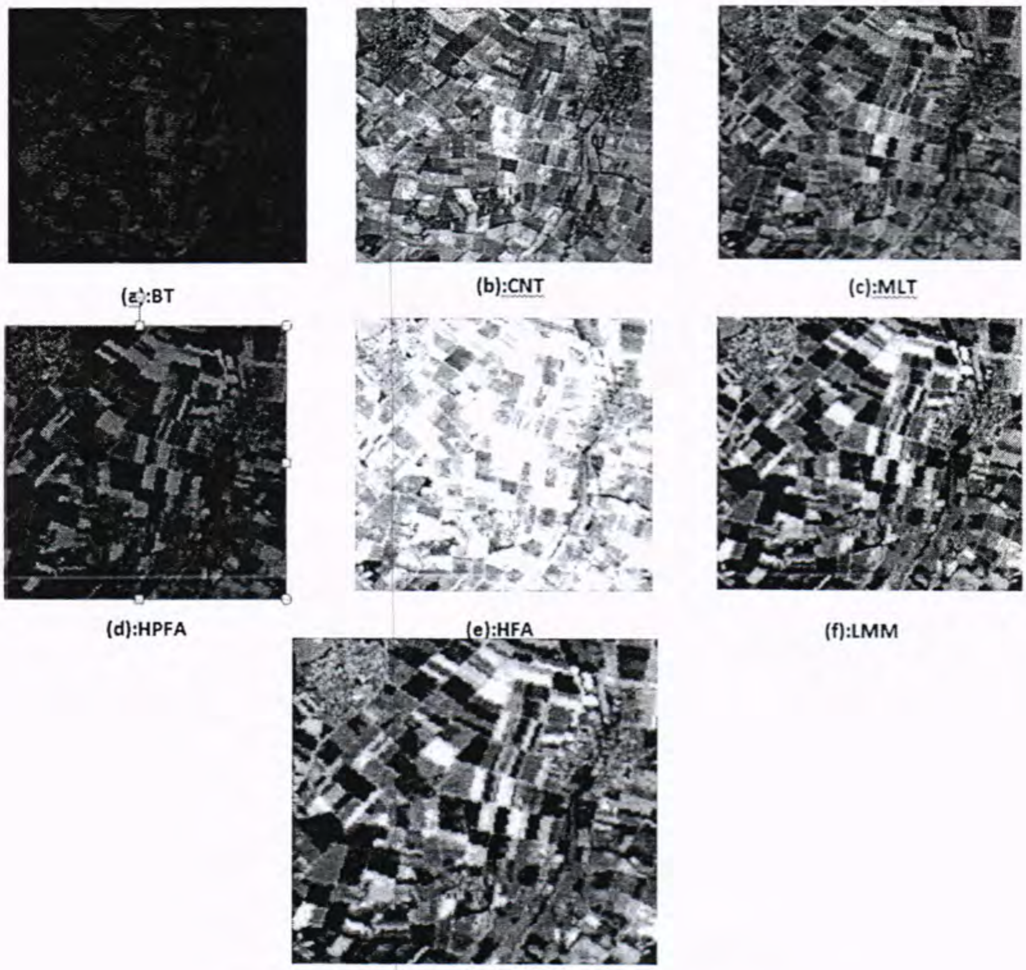

(g):RVS

Figure-2: The representation of Fused Images

Table1a,b: Quantitative analysis of original MS and fused image results through the different methods

a

Methods	AMSE	AMSE-e	AMSE-h	MSE	MSE-e	MSE-h	PSNR	PSNR-e	PSNR-h	MI	SF
BT	81.65	99.73	80.91	9.99×10^3	1.30×10^4	9.86×10^3	6.89	5.73	6.94	1.29	9.24
CNT	69.33	59.37	69.74	7.56×10^3	5.39×10^3	7.65×10^3	9.34	10.81	9.29	1.33	25.43
MLT	29.13	31.14	29.01	$1.32\text{x }10^3$	$1.50\text{x }10^3$	$1.31\text{x }10^3$	16.87	16.32	16.90	2.08	15.74
HPFA	58.75	30.53	58.88	$4.34\text{x }10^3$	$1.39\text{x }10^3$	$4.35\text{x }10^3$	10.51	15.42	10.51	1.86	10.39
HFA	94.72	85.74	95.09	1.09×10^4	9.13×10^3	1.09×10^4	7.76	8.52	7.73	1.66	19.13
LMM	11.13	23.78	10.61	315.83	$1.04\text{x }10^3$	286.18	23.13	17.95	23.56	1.97	24.14
RVS	7.67	9.76	7.59	168.9	226.42	166.57	25.85	24.58	25.91	1.97	13.15

b

Methods	Bands	μ	SD	SNR
ORG.1	R	130	47	2.76
	G	161	49	3.3
	B	100	49	2.04
ORG.2	R,G,B	151	38	3
BT	R	62	16	1.97
	G	59	23	2.5
	B	42	32	2.7
CNT	R	172	73	2.3
	G	170	55	3.08
	B	136	48	2.82
MLT	R	130	49	2.6
	G	137	50	2.7
	B	118	52	2.2
HPFA	R	67	31	2.17
	G	78	34	2.27
	B	65	37	1.73
HFA	R	208	37	5.6
	G	222	36	6
	B	204	52	3.9
LMM	R	114	50	2.30
	G	137	66	2.06
	B	103	62	1.66
RVS	R	111	43	2.56
	G	128	60	2.12
	B	94	52	1.77

6. Algorithm Correlation and Evaluations μ, σ, SNR,PSNR$_{t,e,h}$,AMSE$_{t,e,h}$,MSE$_{t,e,h}$,MI, and SF

Input: The input of the algorithm is the color image (x, y), where the values of Img are between 0 and 255 for each bands, of size M×N×3 ,and gray image (x,y),where the values of Img are between 0 and 255,of size M×N .

Output : The outputs of the algorithm are the μ, σ, SNR,AMSE$_{t,e,h}$,AIA$_{t,e,h}$, PSNR$_{t,e,h}$,MI, and SF for the input image.

Step 1: Extract 5 blocks from the input image; the size of each block is equal to 5×5 pixels.

Step2: calculate μ, σ and SNR as follow:-

count =5×5=25 (compute number of count in each extracted block) :

sum = sum+Img (i,j)

$$\mu = sum / \ count$$

$$\sigma = \sqrt{(\operatorname{Im} g(x,y)-\mu)^{\wedge}2} \, / \, count$$

$$SNR = \frac{\mu}{\sigma}$$

Step 3: calculate AMSE$_{t,e,h}$,MSE$_{t,e,h}$, PSNR$_{t,e,h}$ as follows:-

• Compute size of image N×M then calculate AMSE$_t$ as follows:

$$AMSE_t = \frac{1}{m \times n}\left|\sum_{i=1}^{m}\sum_{j=1}^{n} F_K(i,j) - M_K(i,j)\right|$$

• Compute no. of edges then calculate AMSE$_e$ as follows:

$$AMSE_e = \frac{1}{m \times n} \left| \sum_{i=1}^{m} \sum_{j=1}^{n} F_K(i,j) - M_K(i,j) \right|$$

•Compute no. of homogenous regions in images during $TT = N \times M - no.of\ edges$ Then calculate

$$AMSE_h = \frac{1}{m \times n} \left| \sum_{i=1}^{m} \sum_{j=1}^{n} F_K(i,j) - M_K(i,j) \right|$$

Whereon F_K to express color image,M_K to express fused image in different methods.

•Compute $MSE_{t,e,h}$ as follows :-

$$MSE_{t,e,h} = (sqrt(\frac{1}{M \times N} \sum_{i=1}^{M} \sum_{j=1}^{N} (F_K(i,j) - M_K(i,j))^2)$$

•Compute $PSNR_{t,e,h}$ as follows:-

$$PSNR_{t,e,h} = 10 \log \left[\frac{M_K(i,j)}{MSE_{t,e,h}}\right]$$

Step 4: Calculate SF and MI creation of the image

$$SF = \sqrt{(RF)^2 + (CF)^2} \qquad MI_F^{AB} = I_{FA}(f;a) + I_{FB}(f;b)$$

Step 5: End

7. RESULTS AND DISCUSSIONS

A. The original image are shown in (Fig. 1(a),(b). From the results, it is observed that BT,HPFA,LMM and RVS based image fusion algorithms would provide good fused image and these could be suitable for real time applications. One way to obtain best fused image is, compute the performance of the fusion for different quality measurement for image to evaluate quality image and then select the fused image corresponding to best performance metrics. Since very high computational facility is available, it could be possible to implement this idea for real time applications.

B. One criteria was applied to test image quality particular homogeneity and edges to be results observed to assume the following figures .Seven different types of image fusion algorithms based on BT-CNT-MLT-HPFA-HFA-LMM and RVS and fused image quality was evaluated using performance evaluation metrics .From figure (3) show those parameters for the fused images using various methods .It can be seen that from fig.3a the μ of the fused images approximate remains constant for MLT,LMM and RVS except BT,HPFA to be lower value but CNT to come to pass on the higher value. It can be seen that from fig.3b the SD of the fused images remains constant except CNT and LMM wherein it is known that standard deviation is composed of the signal and noise part and this is metrics would be more efficient in the absence of noise. It measures the contrast in the fused image. Images with high contrast would have a high standard deviation. According to the computation results SNR. The results of SNR appear changing significantly. It can be observed, from the fig.3c,show that the CNT and MLT methods give the best results with respect to other methods indicating that these methods maintain most of information spectral content of the original multispectral image which get the same values presented the lowest value of the other methods as well as the higher of the SNR. In contrast, by combining the visual inspection results, it can be seen that the experimental results overall method are the CNT, MLT and LMM results which are the best results. As to with respect to fig.3d and fig.3e to express amount of information added to the original image wherein that it can be seen changing significantly except MLT, LMM and RVS wherein $AMSE_{t,h}$ approximating similar values but $AMSE_e$ to different value and it has higher value in BT and CNT while it can be seen that from fig.3f to be express about $PSNR_{t,h}$ that obtained on higher values in MLT,LMM and RVS except BT,CNT and HPFA obtained the lower values but $PSNR_e$ that obtained on the higher value in MLT and RVS except the other methods obtained the lower values. As to with respect to fig.3g to express about MI approximate remains constant implies better image quality that can be observed in all these methods except BT and CNT and it can be seen in the same figure that SF appears larger value in LMM and CNT methods.

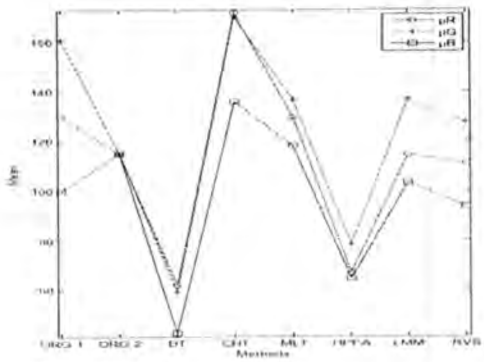

(a) :chart representation of μ of fused image

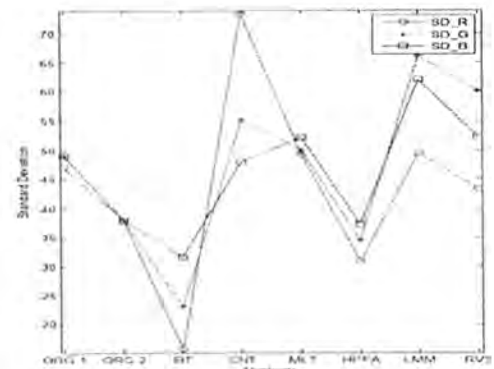

(b) :chart representation of SD of fused image

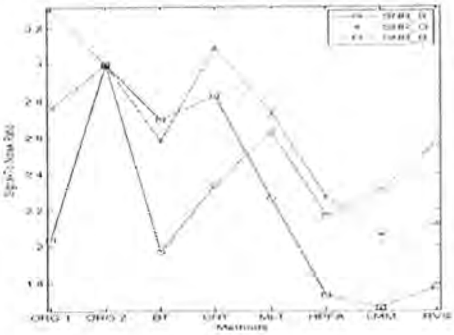

(c) :chart representation of SNR of fused image

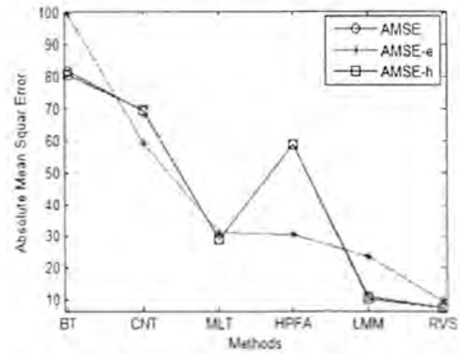

(d) :chart representation of AMSE of fused image

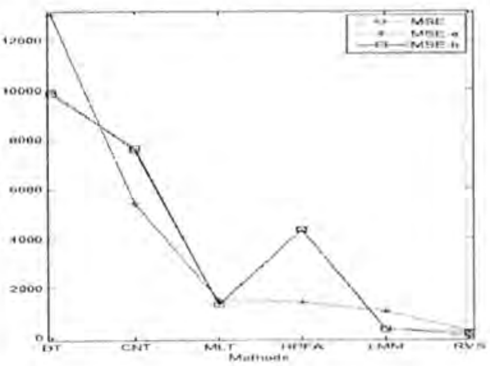

(e) :chart representation of MSE of fused image

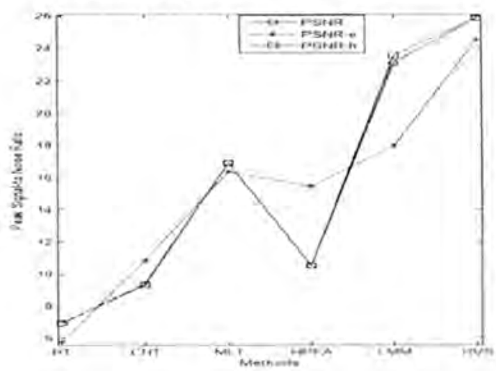

(f) :chart representation of PSNR of fused image

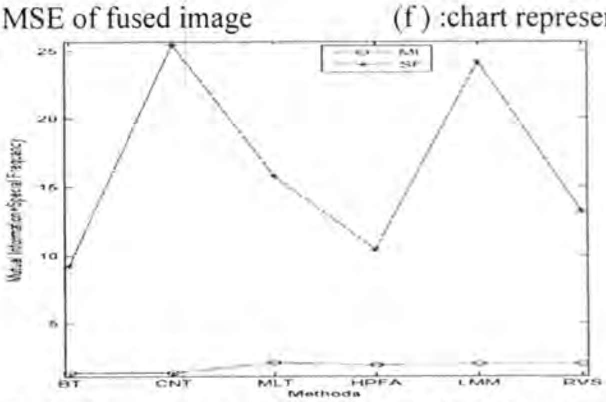

(g) :chart representation of MI &SF of fused image

Figure-3: chart representation of μ, SD, SNR,AMSE,MSE,PSNR,MI and SF of fused images

CONCLOSION

After the following apply two criteria quality image particular homogeneity and edges to be results observed to assume the following figures and tables. Seven different types of image fusion algorithms based on BT,CNT,MLT,HFA,HPFA,LMM and RVS and fused image quality was evaluated using performance evaluation metrics.

- We found that the fusion procedures of the first type, which includes (BT; CN; MLT) by using all PAN bands, produce more distortion of spectral characteristics because such methods depend on the degree of global correlation between the PAN and multispectral bands to be enhanced. Therefore, these fusion techniques are not adequate to preserve the spectral characteristics of original multispectral. But those methods enhance the spatial quality of the imagery except BT.
- The fusion procedures of the second type include HPFA based fusion method by using selected (or Filtering) PAN band frequencies including HPFA algorithms and the third types include LMM and RVS. The preceding analysis shows that the CNT, MLT, LMM and RVS methods maintain the spectral integrity and enhance the spatial quality of the imagery. The HPF A method does not maintain the spectral integrity and does not enhance the spatial quality of the imagery
- In general types of the data fusion techniques, the use of these techniques to evaluated quality details image based on criterions quality images based edge and homogenous to be results evaluation process active and good because to take into consideration homogenous and edge quality measurements.
- We found the importance of quality measurements or evaluation of its importance in determining the quality of the details of the image and especially the accurate details and edges.

REFERENCES

1. Wenbo W.,Y.Jing, K. Tingjun , "Study Of Remote Sensing Image Fusion And Its Application In Image Classification" The International Archives of the Photogrammetry, Remote Sensing and Spatial Information Sciences. Vol. XXXVII. Part B7, Beijing, pp.1141-1146, 2008.
2. Pohl C., H. Touron, "Operational Applications of Multi-Sensor Image Fusion". International Archives of Photogrammetry and Remote Sensing, Vol. 32, Part 7-4-3-w6, Valladolid, Spain,1999 .
3. Steinnocher K.,"Adaptive Fusion Of Multisource Raster Data Applying Filter Techniques." International Archives of Photogrammetry and Remote Sensing, Vol. 32, Part 7-4-3 W6, Valladolid, Spain, 3-4 June, pp.108-115. 1999.

4. Zhang Y.,"Understanding Image Fusion ."Photogrammetric Engineering & Remote Sensing", pp .661657. 2004.
5. Pohl C. and Van Genderen J. L., "Multisensor Image Fusion In Remote Sensing: Concepts, Methods And Applications".(Review Article), International Journal Of Remote Sensing, Vol. 19, No.5, pp. 823 -845,1998.
6. Dong J.,Zhuang D., Huang Y.,Jingying Fu,"Advances In Multi-Sensor Data Fusion: Algorithms And Applications ". Review, ISSN 1424-8220 Sensors, 9, pp.7771-7784, 2009.
7. Carter D.B, 'The use of intensity –hue-saturation –transformations fo merging SPOT panchromatic and multispectral image data ', published M.Sc. Thesis, Virginia, 1998.
8. Saroglu E,Bektas F,Musaoglu N ,Gokesl C ,'Fusion of multisensor remote sensing data: assessing the quality of resulting images', ISPRS congress , Istanbul ,Turkey,2004.
9. Gangkofner U. G., P. S. Pradhan, and D. W. Holcomb, "Optimizing the High-Pass Filter Addition Technique for Image Fusion". Photogrammetric Engineering & Remote Sensing, Vol. 74, No. 9, pp. 1107–1118, 2008.
10. Lillesand T., and Kiefer R. "Remote Sensing And Image Interpretation". 3rd Edition, John Wiley And Sons Inc, 1994.
11. Vijayaraj V., O'Hara C. G. And Younan N. H.,"Quality Analysis Of Pansharpened Images". 0-7803-8742-2/04/(C) IEEE,pp.85-88,2004
12. ŠVab A.and Oštir K., "High-Resolution Image Fusion: Methods To Preserve Spectral And Spatial Resolution". Photogrammetric Engineering & Remote Sensing, Vol. 72, No. 5, May 2006, pp. 565–572, 2006.
13. L. Chen,J.Tain, " **Adaptive multi-focus image fusion using a wavelet-based statistical sharpness measure". Journal,Volume** 92 Issue 9,Pages 2137-2146. September, 2012.
14. Q. Miao1, C. Shi1, P. Xu1, M. Yang1, Y. Shi2," **Multi-focus image fusion algorithm based on shearlets"**,Chin. Opt. Lett., 09(04): pp.041001. 2011.

Compute the Covered Area by the Dust Particles Deposited, of the Aerosol in the Baghdad City, as a function of time during the day Using Digital Image Processing Techniques

Huda A. Abood, Ali A. Al-Zuky and Anwar H. Mahdy
Dep. of Physics , College of Science, AL-Mustansiriyah University
Received 1/4/2013 – Accepted 10/9/2013

الخلاصة

مصطلح الهباء الجوي يعني مجموعة المواد الصلبة والسائلة غير الدائمة الموجودة في الغلاف الجوي وتسمى الجزيئات الصلبة منها بالغبار، ولها تأثير مهم على مناخ الارض وصحة الانسان وعلى نوعية الغلاف الجوي. ان الاهتمام بقياسات جسيمات الهباء الجوي يرجع لكونها في كل مكان وانها متغيرة ومعقدة التركيب وتتفاعل مع محيطها في الغلاف الجوي. في هذه الدراسة تطرقنا الى وضع خوارزمية لقياس المساحة التي يغطيها الغبار ونصف قطر ذرات الغبار المترسبة لساعات زمنية مختلفة خلال اليوم، حيث استخدمنا شرائح الزجاج الشفاف لجمع عينات من ذرات الغبار المترسبة لأوقات مختلفة من اليوم في جهة الرصافة لمدينة بغداد، وتم التقاط صور رقمية للعينات بواسطة المجهر الضوئي (بقوة تكبير x 1000) وما تم ملاحظته هو الاختلاف في انصاف اقطار ومساحة ذرات الغبار المترسبة وكذلك الاختلاف في كثافتها لكل شريحة حسب المدة التي وضعت فيه الشريحة.

ABSTRACT

Term of aerosol mean's set of solid and liquid material non-permanent in the atmosphere, and the solid particle called dust. its have impact on public health, the climate, and the quality of the atmospheric environment. The attention to measurements aerosol because Its presence everywhere, changeable, Complex installation, and interaction with ambient of atmosphere. In this study, We developed an algorithm to measure the covered area by the dust particles, and the radius of dust particle deposited for different time hours of the day. We used slices transparent glass to collect samples of dust particle deposited for different time of the day in Rusafa area of Baghdad city, were taken digital image of the samples through a optical microscope (zoom more than X 1000). What has been noticeable is the difference in radii and areas of dust particles deposited as well as the difference in the density of dust particles for each slice according to time that put the slice to deposition.

INTRODUCTION

Air pollution is one of the features of the modern age, with increasing use of fuels from oil and natural gas in various fields of life, spread in the environment in which we live many air pollutants such as gases resulting from industrial activities or different modes of transport[1]. Aerosol light-absorption measurements are important for health, climate, and visibility applications[2]. Previous studies, (C.J. Wong et al. (2007))[3]. Developed an algorithm to convert multispectral image pixel values was acquired by an Internet Video Surveillance camera into quantitative values of concentrations of particulate matter with diameter less than 10 micrometers (PM10). This algorithm was based on the regression analysis of relationship between the measured reflectance components from a surface material and the atmosphere. The newly developed algorithm can be applied to compute the PM10 values. These computed PM10 values were compared to other standard values measured by a Distract meter. The correlation results showed that this newly develop algorithm produced a high degree of accuracy as indicated by high correlation coefficient (R2) of 0.7566 and low root-mean-square-error (RMS) values of ±3.8306 μg/m3. This study indicates that the technique of using Internet

Video Surveillance camera images can be a useful tool for monitoring temporal development of air quality.[4]. In This study presents a description of the basics of the proposed atmospheric correction procedure, which combines the darkest object subtraction principle and the radiative transfer equations. The method considers the true reflectance values of the selected dark targets acquired in situ and the atmospheric parameters such as the aerosol single scattering phase function, single scattering albedo and water vapour absorption, which are also found from ground measurements. The proposed procedure is applicable to short wavelengths such as Landsat TM band 1, 2 and ASTER band 1 in which water vapour absorption is negligible. [1] The proposed algorithm has been developed to allow the quantification of the aerosol optical thickness (AOT) over land .The algorithm compares multitemporal satellite data sets and evaluates radiometric alterations due to the optical atmospheric effects of aerosols. Novel features of this algorithm which is based on the application of radiative transfer calculations are the inclusion of applying iteration procedures for selecting the suitable object for determining the aerosol optical thickness and the automatic division into working grid cells. [5]Developed quantify the concentration of aerosol black carbon (BC). In this method, a measured volume of ambient air passed through an aerosol sampler, and the aerosol particles were collected onto a quartz fiber filter. Digital pictures of the filter were taken, and then analyzed to determine the optical attenuation (ATN) of the particle layer on the filter. The ATN was related to the mass loading of BC, in mg BC per cm2 of filter area, by performing calibration against thermal optical analysis (TOA). The average aerosol BC concentration was then calculated with known BC loading, sampling time, and filter area.

Atmospheric Aerosols

Aerosols are minute particles suspended in the atmosphere. When these particles are sufficiently large, can be observedtheir presence as they scatter and absorb sunlight. Their scattering of sunlight can reduce visibility (haze) and redden sunrises andsunsets[6].Measured by unit size micrometer largest minutes of 50 micrometers can be seen by the naked eye but smaller (0.005) micrometers see only electronic microscope. Minutes of extreme importance in the study of air pollution ranging from (0.01 -100) micrometers size and minutes younger than 10 micrometers tend not to sedimentation quickly remain in the atmosphere for a long time either fumes and smoke and metal dust cement and fly ash carbon black spray sulfuric acid are all located within the range (10 -100) micrometers which are larger and heavier than the outstanding and deposited near sources and physical deposition of these minutes are the most important natural process of self-cleaning to remove the minutes from the air[6].Particles are typically classified as total suspended particulate (TSP: comprising all particle sizes), medium to fine particulate (PM10: particles less than 10 mm in diameter), fine particulate (PM2.5: particles less than 2.5 mm in diameter), and ultra fine particulate (PM1.0 and smaller).Fine particles, or PM2.5, are the most significant contaminant influencing visibility conditions because their specific size allows them to scatter or absorb visible light. It also allows them to remain airborne for long periods of time, and under favorable climatic conditions they may be transported over long distances. This is one reason why locations distant from the main pollution sources.Secondary reactions are influenced by a wide range of factors, such as temperature, sunlight, the mixture of gases present, and time. Secondary formation of particles from gaseous pollutants can take some time to occur and will be exacerbated under conditions of low wind speed and poor dispersion. The major component comes in the form of sulfate aerosols created by the burning of coal and oil. The concentration of human-made sulfate aerosols in the atmosphere has grown rapidly since the start of the industrial revolution. At current production levels, human-made sulfate aerosols are thought to outweigh the naturally produced sulfate aerosols. The sulfate aerosols absorb no sunlight but they reflect it, thereby reducing the amount of sunlight reaching the Earth's surface. Sulfate aerosols are believed to survive in the atmosphere for about 3-5 days[6].

Total Optical Depth (TOD)

To clarify the amount of scattering and absorption of radiation occurring in the atmosphere and the higher this value the atmosphere was worse and lamp vision toughest (TOD) Mainly consists of two components First:aerosol optical depth (AOD) second: Rayleigh optical depth(ROD) Add other components are not have the effect dispersion and absorption is happening among layer and the other because of other rare gases scientific researches suggests that most of the pollution is at an altitude of less than 1500 _2000 meters. (ROD) dispersion and absorption happening because of the same components of the atmosphere (nitrogen / oxygen) value generally small and do not change in one place they fixed rate so it was interesting all global campaigns the value (AOD) is the value that cannot be calculated accurately or even expected in the future as change dramatically (AOD) dispersion and absorption happening in the atmosphere due to hanging from dust, fumes and ashes and other large plankton[8].

Study Area

Baghdad city is located in central of Iraq within the sector of flat sedimentary plain. It is consider center of economical and administrative, instructive for states. were studied the amount of dust deposited on the slice precisely in Rusafa at Palestine street, it is classified a commercial residential area, at day (16-3-2013) the weather was between cloudy and sime-cloudy with gradually rising dust during the day and the wind was southeasterly mild to moderate (10-20)km/h, and the visibility (6-8) km, according to what has been obtained from the Public Authority for meteorological Iraqi

Dusty image capturing

In this research have beenstudying the aerosol deposited in the cited region of Baghdad city by used the glass slice of thickness (1mm). We put the slice exposed to the air on height (3m) on the earth's surface, and (32m)on level of sea surface. Four slices placing in the same time, then dragging one slice each (4) hours and saving it in the customized portfolio. Taking picture to slices by used optical microscope, in greateningfour timestheregularimage (4/0.1_160/-) of lens. We have obtained 4 images for different slices and different times. These images of the type (bmp) and dimensions (1280×1024), size (3.75 MB) these parameters fixed and shown in figure (1).

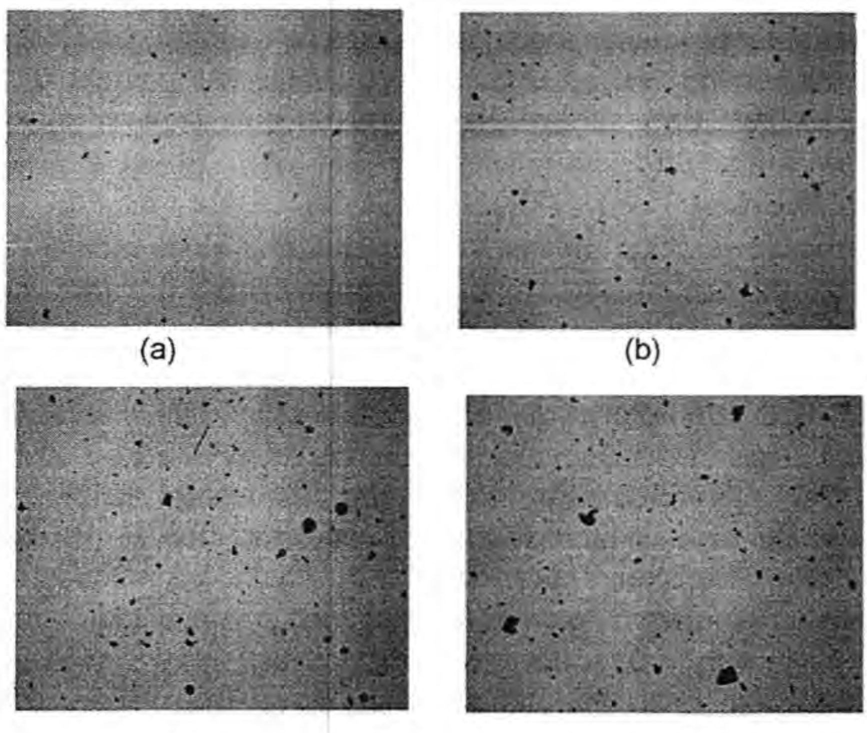
(a) (b) (c) (d)

Figure-1: Image Microscope slide for (9 am, 1pm, 5pm, 9pm) to image a, b, c, and d respectively.

Application Algorithms

After capture the images for the four slices, we extract n (i)blocks (i=1, 2, 3, 4), from each target such that most dust particles were taken, and the size of blocks are different. Next we calculated the area and radius of dust particles thatfallingon the slices. Figure (2) shows the blocks of each image.

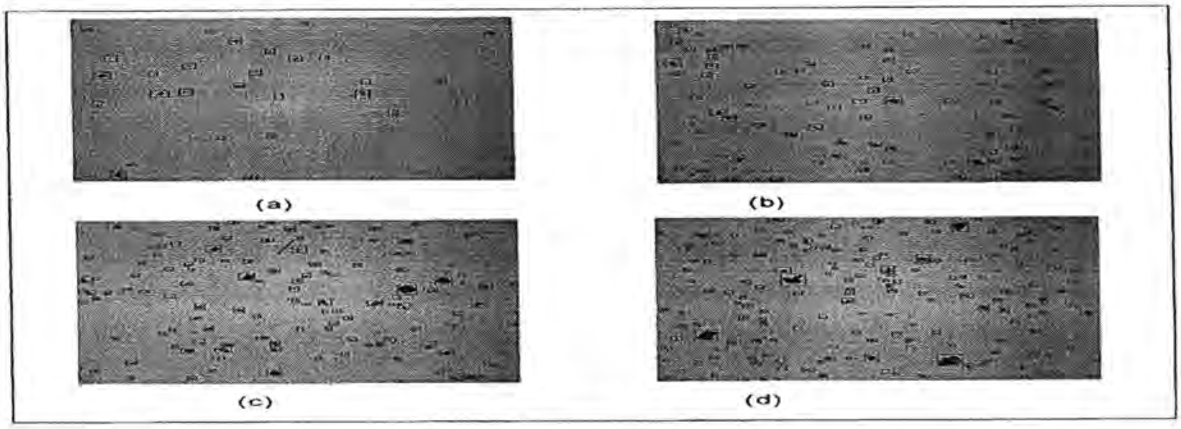

Figure -2: The Blocks of each dust particle in the 4-images

For each block we calculated the center ofthe dust particle in the block, firstwe found the distance between the center and each point in the edge of the dust particle, and then taking the average, which represents the radius of the object (R_1).

$$R_1 = \text{mean(rad)} \;\ldots\ldots\ldots \;(1)$$

Calculate R_1 as follow:-ne=0 ; rad=[]

```
for i=1:r
for j=1:c
If  imge(i,j) ==1
        d=round (sqrt(i - cx)^2 + (j - cy)^2))
        ne=ne+1
        rad=[rad;d]
end
end
end
        R1=mean(rad)
```

Where (r,c)= is the size of block.

d=distance from points the center to point edge of the dust particle.

ne=sum of points the edge.

rad=totaldistance between the center and each point in the edge of the dust particle

R_1=first radius of dust particle.

Then calculate the covered area of dust particle (A_1) by law of the area of the circle as follow: $A_1=\pi R_1^2$ .... (2)

Second calculate The number of pixels of the dust particle (nb), which represent the second covered area of dust particle (A_2).

A_2=nb ....(3)

then we evaluate (R_2) using the following equation:

$$\mathbf{R_2}= \sqrt{\frac{A_2}{\pi}} \ldots\ldots\ldots\ldots\ldots\ldots(4)$$

histogram for(A_2), (R_1)were evaluated. Figure 3 shows the block, the center of object, the histogram of the distances and the histogram of radius.

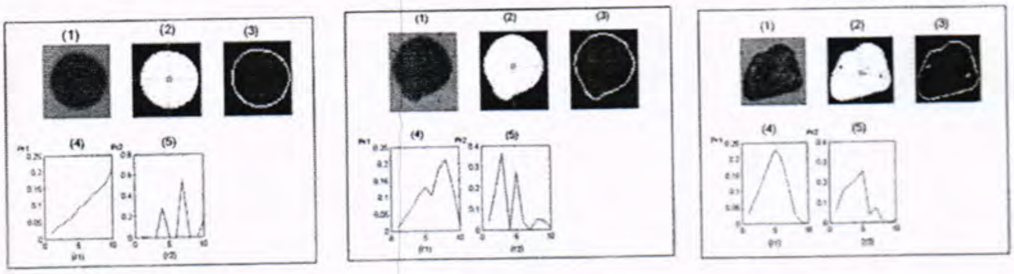

(a) dust particle (area=0.002688mm²). (b)dust particle(area=0.001793mm²) (c) dust particle (area=0.004595mm²).

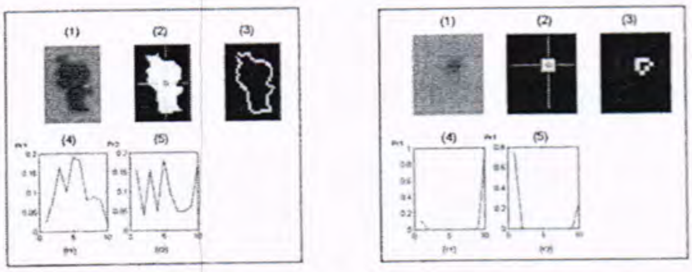

(d) dust particle (area=0.000527mm²). (e) dust particle (area=0.000013mm²).

Figure-3: Samples of blocks to dust particles and its histograms.

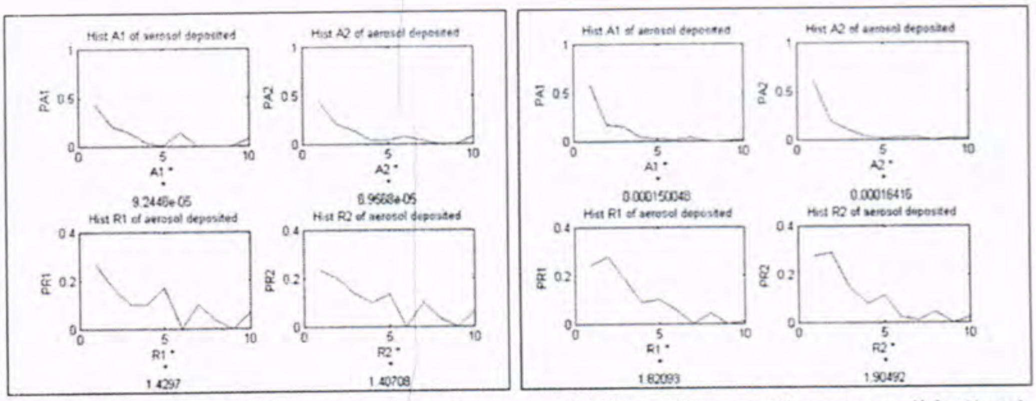

(a) hist.of Image Microscope slide (9am). (b) hist. of Image Microscope slide (1pm).

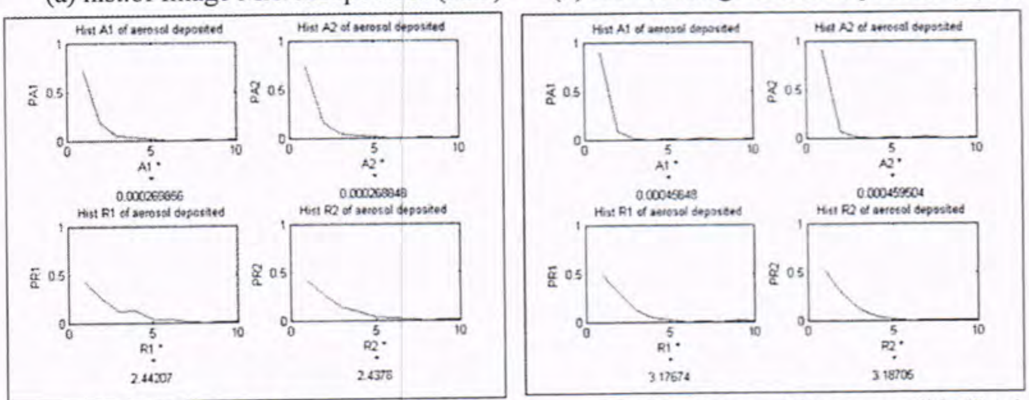

(c) hist. of Image Microscope slide (5pm). (d) hist. of Image Microscope slide (9pm).

Figure-4:the histogram for the dust particle radii(R_1 and R_2), and the histogram of the area that covered by the dust (A_1 and A_2). For images captured in (9am, 1pm, 5pm, 9pm).

Then calculate the scale factor to chart bar of optical microscopy its equal (0.0012 mm/pixel), and multiply the results by the scale factor to get the results in unit (mm).
To compute the ratio of black points to white points we clipped dense block of dust particle from each image, then obtain the area for each image as show in the following table(1):

Table-1: of the total covered area of dust particle in the image.

Captured image at day time	Size of block	The covered area of dust particle mm^2
Image Microscope slide (9pm).	632x790	$5.9005x10^{-6}$
Image Microscope slide (1am).	614x778	$1.4924x10^{-5}$
Image Microscope slide (5am).	774x772	$3.6092x10^{-5}$
Image Microscope slide (9am).	602x962	$3.3250x10^{-5}$

CONCLUSIONS

In this research studied the aerosol in Baghdad city of dust particles. We captured four images by optical microscope to four slides. These slides were put at (5am), and then one slide was dragging each four hours.Through our study and observe by the optical microscopy, showing that the most dust particle are the spherical or semi-spherical, as show in figure 3,and addition to easiness calculate the area, we suppose that all dust particle spherical, and has the area circular section. After processing these image the following results were obtained:

1-The density of dust particle deposited on the first slide was few compares with other slides, and the covered area to each dust particle is mediummeasurement.

2- There is significantly increased density of dust particle on the second slice and different kinds of shapes and sizes of dust particle, that can be observed from the histogram of the second slice the peaks is reduced for curve to areas (A_1, A_2) that means increased in kinds the covered area of dust particle gradually from very small to large.

3-On the third slide there was increased density but difference less the first cases.

4-In the last case was observed that the small particle of the dust is the most increased, this is due to her nature of slow deposition, and that clear in histogram, the Curved rise because the dust proportion increased due to increased hours of the deposition, and the start of the curve is rise at the low values of covered area to dust particle, and the peaks non-existent Almost at the high values. was obtain the results different of shapes and areas, there symmetric, semi-symmetric and asymmetric and asymmetric is majority.

REFERENCES

1. Bassim et al."Using remote sensing data and GIS to evaluate air pollution and their relationship with land cover and land use to Baghdad city"(2010), AL Mustansiriyah University, Baghdad, Iraq.
2. W. Patrick Arnott et al."Towards Aerosol Light-Absorption Measurements with a 7-Wavelength Aethalometer: Evaluation with aPhotoacoustic Instrument and 3-Wavelength Nephelometer" (2005).Aerosol Science and Technology, 39:17–29, 2005 Copyright _c American Association for Aerosol Research.
3. C.J. Wong et al."Using Image Processing Technique for the Studies on Temporal Development of Air Quality"(2007) School of Physics, UniversitiSains Malaysia, 11800 USM, Penang, Malaysia.
4. Diofantos G. et al. "Determination of aerosol optical thickness through the derivation of an atmospheric correction for short-wavelength Landsat TM and ASTER image data: an application to areas located in the vicinity of airports at UK and Cyprus"(2009)ApplGeomat (2009) 1:31–40.
5. K. Du et al."Digital photographic method to quantify black carbon in ambient aerosols".(2011) Atmospheric Environment 45 (2011).
6. Internet (http://www.nasa.gov).
7. Faiza Ali et al."Evaluation and statistical analysis of the measurements of the total outstanding minutes and bullets in the air of the city of Baghdad for the year (2008)"Iraqi Ministry of the Environment (http://www.moen.gov.iq/lastest-stadies.html).
8. internet (http://blog.icoproject.org).

Automatic Test Data Generation Based On Fuzzy Logic

Amir S. Almallah and Ismael Abdulsattar
Dep. of computer science,Collage of science, University of Mustansiriya
Received 26/3/2013 – Accepted 15/9/2013

الخلاصة

اختبار البرمجيات واحدة من اعقد المهام في دورة تطوير البرمجيات. إنها المعالجة الأكثر إحباط واستهلاكا للوقت. حيث إن تعقيد أنظمة البرمجيات ازداد بصورة كبيرة في العقد الأخير وان اختبار تلك البرمجيات أصبح أكثر فأكثر كلفة مع زيادة تعقيد تلك البرمجيات. هكذا مع التوليد التلقائي للبيانات فان كلفة اختبار البرمجيات تنخفض بصورة كبيرة. في هذه الورقة البحثية سوف نستخدم مفاهيم المنطق المضبب لتوليد بيانات الاختبار بصورة تلقائية حيث يتم استخدام تلك البيانات في تغذية برمجيات التي تستخدم في تطبيقات المنطق المضبب.

ABSTRACT

The complexity of software systems has been increasing dramatically in the past decade, and software testing as a labor-intensive component is becoming more and more expensive. With the complexity of the software, the cost of testing software is also increased. Thus with automatic test data generation the cost of testing will dramatically be reduced. This paper uses fuzzy logic concepts to generate test data automatically and this data will be used for the future to feed software which used in fuzzy logic applications like(industrial automation, decision making process , such as signal processing or data analysis...etc). Software testing is probably the most complex task in the software development cycle. It is one of the most time-consuming, costing and frustrating process.

1. INTRODUCTION

Software testing is a process, which is used to identify the correctness, completeness and quality of a software. [1]. The effective generation of test data is one of the most difficult and expensive problems in software testing. Test data generation is the process of creating program inputs that satisfy some testing criterion [2]. Obviously, manually developing a large test data set to satisfy a testing criterion is usually expensive, laborious, difficult and error-prone. If test data could be automatically generated, the cost of software testing would be significantly reduced. It is usually observed that the input data near the boundary of a domain are more sensitive to program faults and should be carefully checked. A domain testing strategy is very effective in verifying the correctness of the boundary of a path domain; however, such a domain strategy is hard to implement since the strategy requires test data generated on and near the boundary, and the test generation is more difficult when some of the constraints are nonlinear or in a discrete space [3]. In general automatic test data generator are contain big challenges especially in the huge software that could make any decision based on fuzzy data here the challenges will be more[4][5] .Test Data Generation (TDG) is crucial for software testing because test data is one of the key factors for determining the quality of any software test during its execution [7]

In the fuzzy logic concept if there is no interference among the generated data intervals that means no fuzziness to solve and it would be useless data generated to participate as input for fuzzy applications programs.[6]

But the huge mathematics problem will rise in this case which is "what are the thresholds values to stop generating" as we know all the close intervals contains two boundaries start number and end number. let have close intervals a, b

Symbols: $\boldsymbol{a \leq x \leq b \; or \; [a, b]}$

how many numbers between $\boldsymbol{a}$ and $\boldsymbol{b}$ need to be generated to find the intersection with other closed intervals to decide this two intervals useful to feed fuzzy program or useless then we could eliminate it from the test data generator. This mechanism will play good threshold condition for filtering our generated data, for instance if we have the following two intervals α *and* β as

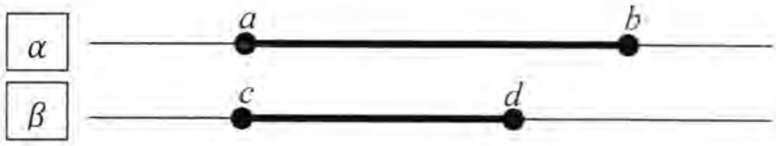

In the above figure we see that the whole interval β[c, d] intersect with α [a, b] in such case the generated interval will be useful but in the following case will show how it is useless input that we should eliminate it

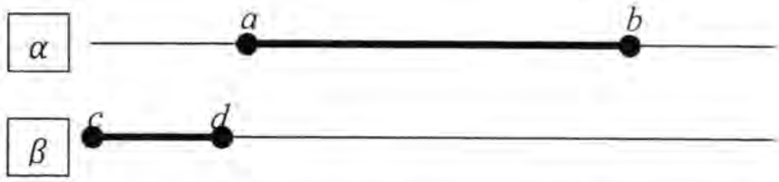

In the above cases we show how the intersection will work in the close intervals but the intersection is only one of basic concept in fuzzy logic due to the fuzzy set has intersection with each other with degree of membership for each element in the fuzzy set.

2. Fuzzy logic and fuzzy set

In figure (1) showing below we have the following sets A [-4, 4] and B [0, 8] and they are intersect in the interval [0, 4] these two intervals will be useful as input for fuzzy program

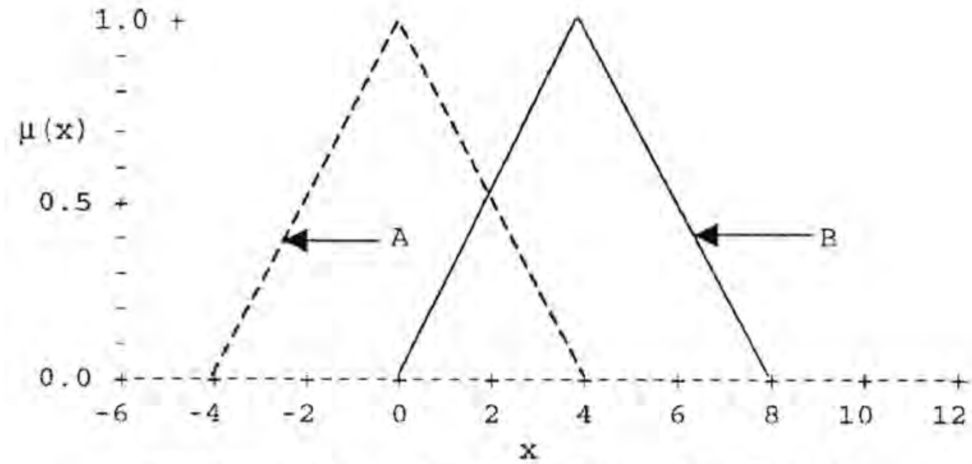

Figure:1- two fuzzy set A and B with degree of membership

Fuzzy set can have different mechanisms to implement but they are all have the same concept, on the other hand if there is no intersection it will be useless pair to consider as input for fuzzy program.

3. Proposed Mechanism

Here we create three factors ($\alpha, \varepsilon, \beta$) for filtering test data generated form random data generator that generate random intervals the rule of the first factor α will decide which two or more interval useful or not by found if there is an intersection among them or not, the rule of the second factor ε is to determine the value of intersection that will decide based on user demand or program requirements, and the third one is to decide the maximum number (capacity) that the intervals could take which also can be determined based on user demand that can fulfill user requirement. As show in the figure (2) :

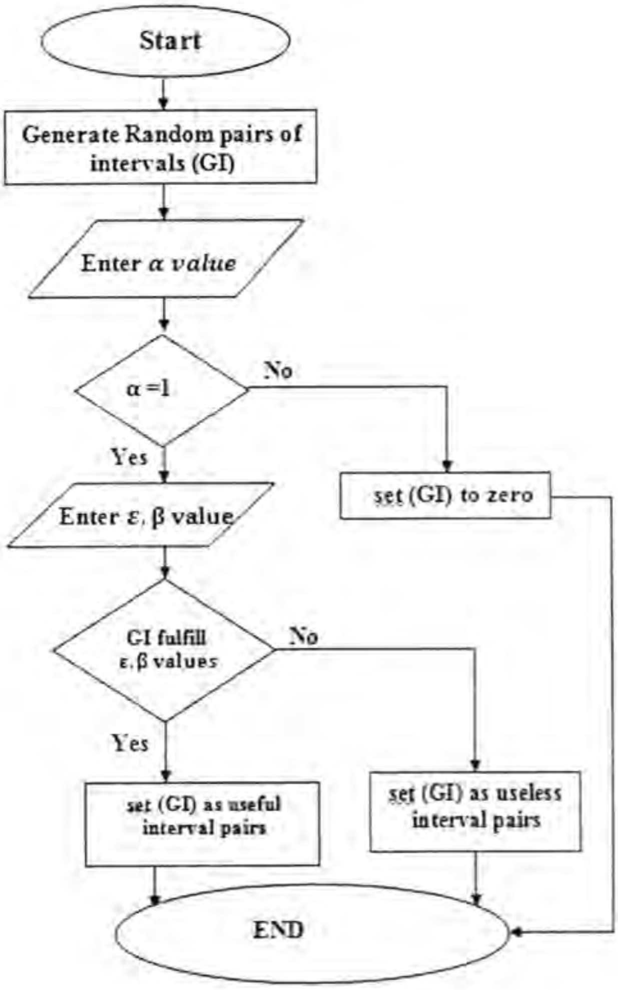

Figure:2- propsed mechanism

4. Experimental Result

As the random generator generate random pairs of intervals we run the program several times with different possible values of our factors α, ε *and* β and show the effect of that factors over generated intervals. we can see clearly here if the value of α equal to zero that is mean there is no intersection among the generated interval, and we can take crisp decision that will be useless interval pair and if it is one that means there is an intersection values then move to the next factor ε to test how much the minimum ratio required to take in our account and third factor is β use to determine how much possible degree you divide the intersection intervals. Thus we can see the big effect of that three factors to filterize random gnerated intervals and eliminate the useless interval pairs as shown in the following table.

Table-1:

# generated intervals	α value	ε value	β value	# useful intervals
10582	1	0.2	27	7010
10110	1	0.15	52	7301
12001	0	0.4	42	0
15040	1	0.5	20	1560
17080	1	0.13	48	8120
18090	1	0.029	41	8601
20100	1	0.02	49	9092
21988	1	0.015	50	10906
22078	0	0.0011	0.0023	0

Table-1:and figure(3) showing the affection of α, ε, and β factors on the generated intervals

We can see the big filtering process done over the random generated intervals.

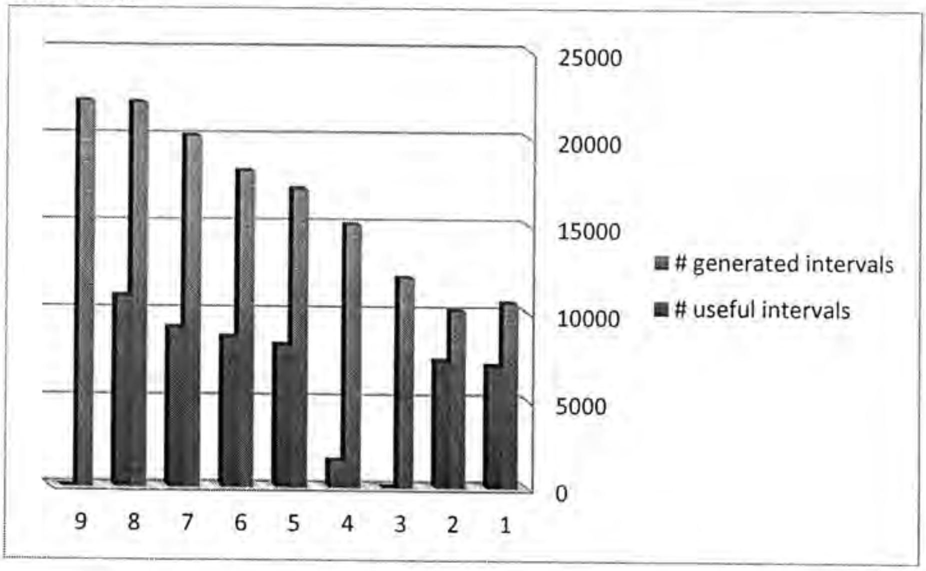

Figure-3: shows the automatic test data generator and useful one of it

5. Suggestions and Conclusion

The automatic test data generation is huge concept to deal with and our invent mechanism to use not normal data but fuzzy data that would use to test fuzzy software in all its applications and we can see how three filters did significant reduction over the automatic random generated data. This approach also can fit the crisp decision software by manipulating the second and third factor. We suggest as future work to take adaptive factor that will select based on program that we want to test it that will be great factor can we use to determine the useful path will take to have good test data generator.

REFERENCES

1. H. Tahbildar and B. Kalita "Automated Test Data Generation For Programs Having Array Of Variable Length And Loops With Variable Number Of Iteration" , IMECS, March 17-19, 2010.
2. Shahid Mahmood, "A Systematic Review of Automated Test Data Generation Techniques" ,Master Thesis Software Engineering Thesis no: MSE-2007:26 October 2007.
3. Gautam Kumar Saha, "Understanding Software Testing Concepts", ACM Ubiquity Vol 9,Issue 6, February12-18, 2008.
4. M. Prasanna, S.N. Sivanandam, R. Venkatesan, R. Sundarrajan, "A survey on automatic test case generation", Academic Open Internet Journal, www.acadjournal.com , Vol 15, 2005.
5. Mark Utting,Alexander Pretschner, Bruno Legeard, "A Taxonomy of Model-based testing",April 2006.
6. Hung Tran, "Test generation using Model Checking", 2007.
7. Ashif Ali, Jana Shafi," Automated Test Data Generation via Path Table"December 2012.

Using Swarm Intelligence Algorithms to Solve n-Queens Problem

Ahmed Tariq Sadiq[1] and Muhanad Tahrir Younis[2]
[1]Dep. Of Computer Sciences, University of Technology
[2]Dep. Of Computer Sciences, College of Sciences AlMustansiria University
Received 8/3/2013 – Accepted 15/9/2013

الخلاصة

تعتبر مشكلة n-Queens واحدة من المشاكل الصعبة الحل. هنالك عدة بحوث مهتمة بحل هذه المشكلة بأستخدام طرق ذكية مختلفة. هذا البحث يقوم بحل مشكلة n-Queens بأستخدام خوارزميات ذكاء الحشود وهي: خوارزمية النحل، خوارزميات امثلية حشود الجسيمات و بحث طائر الوقواق. النتائج العملية لتطبيق هذه الخوارزميات اعطت افضل الحلول النسبية. بمقارنة النتائج يتبين ان خوارزمية النحل افضل من خوارزميات امثلية حشود الجسيمات و خوارزميات امثلية حشود الجسيمات افضل من بحث طائر الوقواق في حل هذه المشكلة.

ABSTRACT

The N-Queens problem is considered as one of the hard problem to be solved. Many researches have been interested to solve it with different intelligent methods. This paper solves the N-queens problem using three swarm intelligence algorithms: Bees algorithm, Particle Swarm Optimization (PSO) and Cuckoo search. The experimental results with these algorithms method give the best results relatively. By comparing, Bees algorithm is better than the PSO, PSO is better than Cuckoo search to handle n-queens problem.

1. INTRODUCTION

The eight queens is a well known NP-complete problem proposed by C. F. Gaus in 1850. The Problem was investigated by several 19^{th} century mathematicians. The characteristic property of this problem is that it requires large amount of computations. The general N-Queen problem was explored in 1950's by Yaglom and Yaglom. A general N-Queen problem is defined by the following constraints on an $N*N$ grid **[1]**:

1. Only one queen can be placed in any row.
2. Only one queen can be placed in any column.
3. Only one queen can be placed on any diagonal.
4. Exactly N queens must be placed on the grid.

Because queens can move any number of squares vertically in a single turn, such placement is not cost efficient. Rather than viewing the board as consisting of n x n squares, it can be seen as comprised of n columns, each with n rows. Because we are placing n queens in n columns, there has to be one and only one queen in each column that can be determined. Applying this knowledge to the recursive algorithm makes placing the queens more efficient. This is also true for the horizontal direction, as the board can be rotated. As for the last, the diagonal direction must be accounted for as well **[2].**

There have been several approaches taken in the study of this problem (as diverse as algorithmic design, program development, parallel and distributed computing, and artificial intelligence). This widespread interest in the N-Queen problem is in part due to the property that characterizes difficult problems, viz., satisfying a set of global constraints **[1]**.

Swarm-based algorithms mimic nature's methods to drive a research towards the optimal solution. A key difference between Swarm-based algorithms and direct search algorithms such as hill climbing and random walk is that Swarm-based algorithms use a population of solutions for every iteration instead of a single solution. As a population of solutions is processed in an iteration, the outcome of each iteration is also a population of solutions. If an problem has a single optimum solution, Swarm-based algorithm population members can be expected to converge to that optimum solution [3]. There are several swarm algorithms such as Bees Algorithm (BA), Ant Colony Optimization (ACO), Particle Swarm Optimization (PSO), Cuckoo Search (CS), Fish Swarm Algorithm (FSA).

This paper solves N-queens using three types of swarm intelligent algorithms: Bees, PSO and Cuckoo Search. Section 2 includes the principle of PSO and parameters. Bees Algorithm will be explained in Section 3. Section 4 contains Cuckoo Search Algorithm with Levy flight. The solving of N-queens problem using swarm intelligent algorithms will be illustrated in section 5. The experimental results will be shown in section 6. Finally, section 7 includes the conclusion.

2- **Particle Swarm Optimization (PSO)**

Particle swarm optimization (PSO) is a population based stochastic optimization technique developed by Dr. Eberhart and Dr. Kennedy in 1995 [4], inspired by social behavior of bird flocking or fish schooling and swarm theory.

2.1 The Principle

PSO shares many similarities with evolutionary computation techniques such as Genetic Algorithms (GA). The system is initialized with a population of random solutions and searches for optima by updating generations. However, unlike GA, PSO has no evolution operators such as crossover and mutation. In PSO, the potential solutions, called particles, fly through the problem space by following the current optimum particles. Compared to GA, the advantages of PSO are that PSO is easy to implement and there are few parameters to adjust. PSO has been successfully applied in many areas; function optimization, artificial neural network training and fuzzy system control. PSO simulates the behavior of bird flocking, suppose a group of birds are randomly searching food in an area. Not all the birds know where the food is. The effective strategy is to follow the bird that is nearest to the food. In PSO, each single solution is a "bird" in the search space. We call it "particle". All particles have fitness values that are

evaluated by the fitness function to be optimized, and have velocities, which direct the flying of the particles [4].
PSO is initialized with a group of random particles (solutions) and then searches for optima by updating generation. In each generation, each particle is updated by following two "best" values. The first one is the best solution (fitness) it has achieved so far. This value is called pbest. Another "best" value that is tracked by the particle swarm optimizer is the best value, obtained so far by any particle in the population. This best value is a global best and is called gbest. When a particle takes part of the population as its topological neighbors, the best value is a local best and is called *l*best. After finding the two best values, the particle updates its velocity and position with the following equations [4]:

$$V_i[t+1] = w\, V_i[t] + C_1 * r1 * (pbest_i[t] - present_i[t]) + C_2 * r2 * (gbest_i[t] - present_i[t]) \quad \ldots(1\text{-a})$$

$$present_i[t] = present_i[t] + V_i[t] \quad \ldots\ldots\ldots\ldots(1\text{-b})$$

where, $i = 1,2,\ldots,N$; w is the inertia weight, V[t] is the particle's velocity, present[t] is the current particle (solution), pbest and gbest are defined as stated before, r1 and r2 are two random numbers between (0,1), C_1 and C_2 are learning factors. However these values of C_1, C_2 are problem dependent. These are very essential parameters in PSO [4]. Particles' velocities on each dimension are clamped to a maximum velocity Vmax.

2.2 Discrete PSO

Several adaptations of the method to discrete problems, known as Discrete Particle Swarm Optimization (DPSO). Since, in words of the inventors of PSO, it is not possible to "throw to fly" particles in a discrete space [4], several Discrete Particle Swarm Optimization (DPSO) methods have been proposed.

A DPSO whose particles at each iteration are affected alternatively by its best position and the best position among its neighbors was proposed by Al-Kazemi and Mohan [6]. Pampara et al. [7] solved binary problems by combining continuous PSO and Angle Modulation with only four parameters. Furthermore, several PSO variants applied to problems where the solutions are permutations were considered in [8, 9]. The multi-valued PSO (MVPSO) proposed by Pugh and Martinoli [10] deals with variables with multiple discrete values.

Another DPSO was proposed in [11] for feature selection problems, which are problems whose solutions are sets of items. A new DPSO proposed in [12, 13] does not consider any velocity since, from the lack of continuity of the movement in a discrete space, the notion of velocity loses sense; however they kept the attraction of the best positions.

2.4 Parameters of PSO

The convergence and performance of PSO are largely dependent upon parameters chosen *w* is termed as inertia weight [17] and is incorporated in the algorithm to control the effect of the previous velocity vector of the swarm on the new one. It facilitates the trade-off between the local and the global exploration abilities of the swarm and may result in less number of iterations of the algorithm while searching for an optimal solution. It is experimentally found that inertia weight *w* in the range [0.8, 1.2] yields a better performance [14]. The velocity lies in the range [-Vmax , Vmax] where, - Vmax denotes the lower range and Vmax is the upper range of the motion of the particle. The roles of C_1 and C_2 are not so critical in the convergence of PSO, however, a suitably chosen and fine tuned value can lead to a faster convergence of the algorithm. A default value of $C_1 = C_2 = 2$ is suggested for general purpose, but somewhat better results are found with $C_1 = C_2 = 0.5$ [15]. However, the values of cognitive parameter, C_1 larger than the social parameter C_2 are preferred from the performance point of view with the constraint $C_1 + C_2 \leq 4$ [16]. The parameters r1 and r2 used to maintain the diversity of the population in equation (1a).

3. The Bees Algorithm

3.1. Bees in nature

A colony of honey bees can extend itself over long distances to exploit a large number of food sources [20, 21]. A colony prospers by deploying its foragers to good fields [18, 22, 23].

The foraging process begins in a colony by scout bees being sent to search for promising flower patches. Scout bees move randomly from one patch to another [18, 21].

When those scout bees found a patch which is rated above a certain quality threshold (measured as a combination of some constituents, such as sugar content) deposit their nectar or pollen and go to the "dance floor" to perform a dance known as the "waggle dance" [20].

This mysterious dance is essential for colony communication, and contains three pieces of information regarding a flower patch: the direction in which it will be found, its distance from the hive and its quality rating (or fitness) [18, 20, 23]. This information helps the colony to send its bees to flower patches precisely, without using guides or maps [23]. After waggle dancing on the dance floor, the dancer (i.e. the scout bee) goes back to the flower patch with follower bees that were waiting inside the hive. More follower bees are sent to more promising patches. This allows the colony to gather food quickly and efficiently [18, 23].

3.2. *Bees Algorithm*[18]

As mentioned, the Bees Algorithm is an optimization algorithm inspired by the natural foraging behaviour of honey bees to find the optimal solution [19]. Figure 1 shows the pseudo code for the algorithm in its simplest form. The algorithm requires a number of parameters to be set, namely: number of scout bees (*n*), number of sites selected out of n visited sites (*m*), number of best sites out of m selected sites (*e*), number of bees recruited for best e sites (*nep*), number of bees recruited for the other (*m-e*) selected sites (*nsp*), initial size of patches (*ngh*) which includes site and its neighborhood and stopping criterion. The algorithm starts with the n scout bees being placed randomly in the search space. The fitnesses of the sites visited by the scout bees are evaluated in step 2.

In step 4, bees that have the highest fitnesses are chosen as "selected bees" and sites visited by them are chosen for neighborhood search. Then, in steps 5 and 6, the algorithm conducts searches in the neighborhood of the selected sites, assigning more bees to search near to the best (e) sites. The bees can be chosen directly according to the fitnesses associated with the sites they are visiting. Alternatively, the fitness values are used to determine the probability of the bees being selected. Together with scouting, this differential recruitment is a key operation of the Bees Algorithm.

However, in step 6, for each patch only the bee with the highest fitness will be selected to form the next bee population. In step 7, the remaining bees in the population are assigned randomly around the search space scouting for new potential solutions. These steps are repeated until a stopping criterion is met. At the end of each iteration, the colony will have two parts to its new population– representatives from each selected patch and other scout bees assigned to conduct random searches.

```
Bees Algorithm
  1. Initialize population with random solutions.
  2. Evaluate fitness of the population.
  3. While (stopping criterion not met)
       //Forming new population.
  4. Select sites for neighborhood search.
  5. Recruit bees for selected sites (more bees for best e sites) and evaluate
  fitnesses.
  6. Select the fittest bee from each patch.
  7. Assign remaining bees to search randomly and evaluate their fitnesses.
  8. End While.
```

Figure -1: Pseudo code of the basic bees algorithm

4- Cuckoo Search Algorithm

CS is a heuristic search algorithm which has been proposed recently by Yang and Deb [24]. The algorithm is inspired by the reproduction strategy of cuckoos. At the most basic level, cuckoos lay their eggs in the nests of other host birds, which may be of different species. The host bird may discover that the eggs are not its own and either destroy the egg or abandon the nest all together. This has resulted in the evolution of cuckoo eggs which mimic the eggs of local host birds. To apply this as an optimization tool, Yang and Deb used three ideal rules [24, 25]:

(1) Each cuckoo lays one egg, which represents a set of solution co-ordinates, at a time and dumps it in a random nest;

(2) A fraction of the nests containing the best eggs, or solutions, will carry over to the next generation;

(3) The number of nests is fixed and there is a probability that a host can discover an alien egg. If this happens, the host can either discard the egg or the nest and this result in building a new nest in a new location. Based on these three rules, the basic steps of the Cuckoo Search (CS) can be summarized as the pseudo code shown as in Fig. 2.

```
Algorithm of Cuckoo Search via Levy Flight
Input: Population of the problem;
Output: The best of solutions;
 Begin
  Objective function f(x), x = (x1, x2, ...xd)^T
    Generate initial population of n host nests xi
                                    (i = 1, 2, ..., n)
    While (t <Max Generation) or (stop criterion)
        Get a cuckoo randomly by Levy flight
        Evaluate its quality/fitness Fi
        Choose a nest among n(say,j)randomly
        If (Fi > Fj) replace j by the new solution;
        A fraction(pa) of worse nests are abandoned and new ones are
         built;
        Keep the best solutions (or nests with quality solutions);
        Rank the solutions and find the current best;
        Pass the current best solutions to the next generation;
    End While
 End.
```

Figure- 2: Basic Cuckoo Search Algorithm

When generating new solution $x^{(t+1)}$ for, say cuckoo i, a Levy flight is performed

$$x^{(t+1)}_i = x(t)_i + \alpha \oplus Levy(\beta) \ .... \ (2)$$

where $\alpha > 0$ is the step size which should be related to the scales of the problem of interests. In most cases, $\alpha = 1$ can be used. The product $\oplus$ means entry-wise walk while multiplications. Levy flights essentially provide a random walk while their random steps are drawn from a Levy Distribution for large steps

$$Levy \sim u = t^{1-\beta} \quad (0 < \beta \leq 2) \ldots\ldots\ldots (3)$$

This has an infinite variance with an infinite mean. Here the consecutive jumps/steps of a cuckoo essentially form a random walk process which obeys a power-law step-length distribution with a heavy tail. In addition, a fraction *pa* of the worst nests can be abandoned so that new nests can be built at new locations by random walks and mixing. The mixing of the eggs/solutions can be performed by random permutation according to the similarity/difference to the host eggs.

5. Swarm Intelligence for N-Queens Problem

In Bees algorithm each bee represents a solution of N-queens problem using integer numbers style. The mutation operator will be used to update these solutions. Figure (3-a) illustrates how it appears in the population, the particle for N=6 problems may be the following: 3 6 2 4 1 5. The first number means the first queen is at the third position in the first row, the second number means the second queen is at the sixth position in the second row, and so on. Figure (3-b) shows a translation from the permutation to the chessboard positions [26].

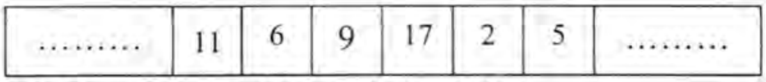

(a) N-queen permutation random solution

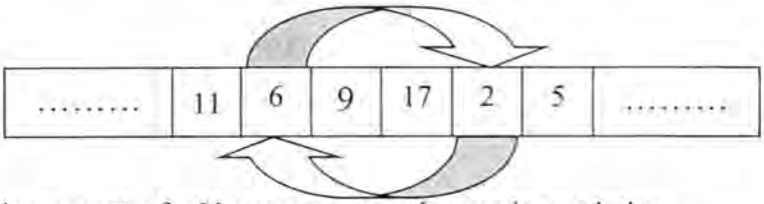

(b) Mutation operator for N-queen permutation random solution

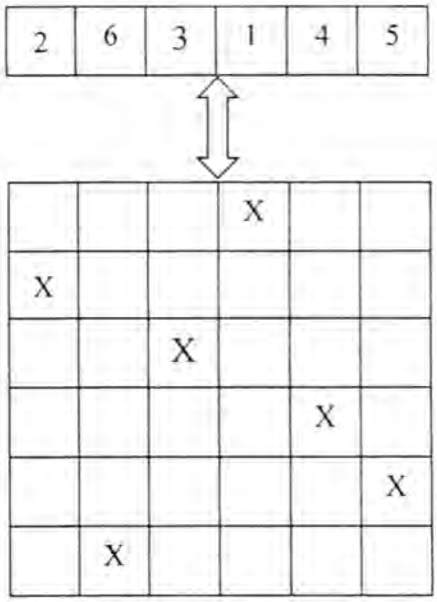

(c) N-queen permutation random solution representation as 2-dimension matrix

Figure-3: Permutation representation of n-queens problem with mutation operator

By using permutations, the horizontal and vertical conflicts of the queens are eliminated [27]. Thus to find a solution, the objective is to eliminate the diagonal conflicts. The fitness function is defined as the number of conflicts or collisions along the diagonals of the hoard. The objective is changed to minimize the number of conflicts or collisions. The fitness value of an ideal final solution should be zero.

In Cuckoo search algorithm each cuckoo's egg represents a solution of N-queens problem using integer numbers style. The mutation operator will be used to update these solutions. The Bees algorithm, the same representation of N-queens problem in Cuckoo search will be used.

In PSO, each particle represents a solution in the parameter space. The particle is encoded as a string of positions, which represent a multidimensional space. All the dimensions typically are independent of each other, thus the updates of the velocity and the particle are performed independently in each dimension. This is one of merits of PSO. However, it is not applicable for permutation problems since the elements are not independent of each other. It is possible that two or more positions can get the same value after the update, which breaks the permutation rule. Thus the conflicts must be eliminated. Here a new particle update strategy is proposed. In traditional PSO, the velocity is added to the particle on each dimension to update the particle, thus it is a distance measure. If the velocity is larger, the particle may explore more distant areas. Similarly, the new velocity in the permutation scenario represents the possibility that the particle changes. If the velocity is larger, the particle is more likely to change to a new permutation sequence. The velocity update formula remains the same. However the velocity is limited to absolute values since it only represents the difference between particles. The particle update process is changed as follows: the velocity is normalized to the range of 0 to 1 by dividing it by the maximum range of the particle. Then each position randomly determines if there is a swap with a probability determined by the velocity. If a swap is required, the position will set to the value of same position in nBest by swapping values. This process is shown in Figure 4 [26].

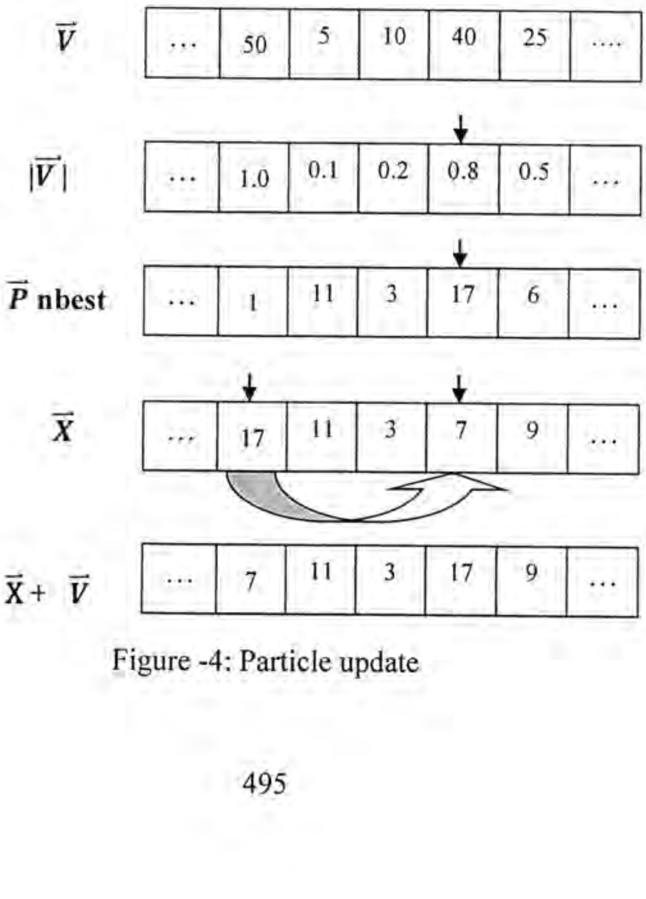

Figure -4: Particle update

6-RESULTS AND DISCUSSIONS

In Bees algorithm, experiment with several numbers of parameters has been done. Table (1) shows the best value for each parameter in Bees algorithm to solve N-queens problem.

Table-1: Best Value for Bees Algorithm Parameters to Solve N-Queens Problem

Parameter	Best Value
Population size	100
Number of selected sites	60
Number of elite sites	25
Number of recruited bees for best m sites	15
Number of recruited bees for best e sites	8
Number of iterations	150

Cuckoo search algorithm has two important parameters in addition to the classical others, these are P_a, α and β. experiment with several numbers of parameters. Table (2) shows the best value for each parameter to solve N-queens problem.

Table-2: Best Value for Cuckoo Search Algorithm Parameters to Solve N-Queens Problem

Parameter	Best Value
Population size	100
Fraction(P_a)	0.25
α	1.2
β	1.5
Number of iterations	250

Table (3) shows the best value parameters to solve N-queens problem using PSO. These values represent the best in average, therefore some time there are other values are succeeded to find the solutions of N-queens problem.

Table-3: Best Value for PSO Parameters to Solve N-Queens Problem

Parameter	Best Value
Number of Particle in the Swarm	80
The Maximum of Velocity	1.5N
Self-Confidence (C1)	2
Swarm-Confidence (C2)	3
Inertia Weight	1.4
Number of iterations	230

Figure (5) shows the results for the problems of 10 to 150 queens. Each parameter combination was run 25 times and the results represent the mean number of function evaluations to reach a solution. From the results, it can be seen that all these swarm intelligence algorithms successfully find a solution of the n-queens problems in a good time.

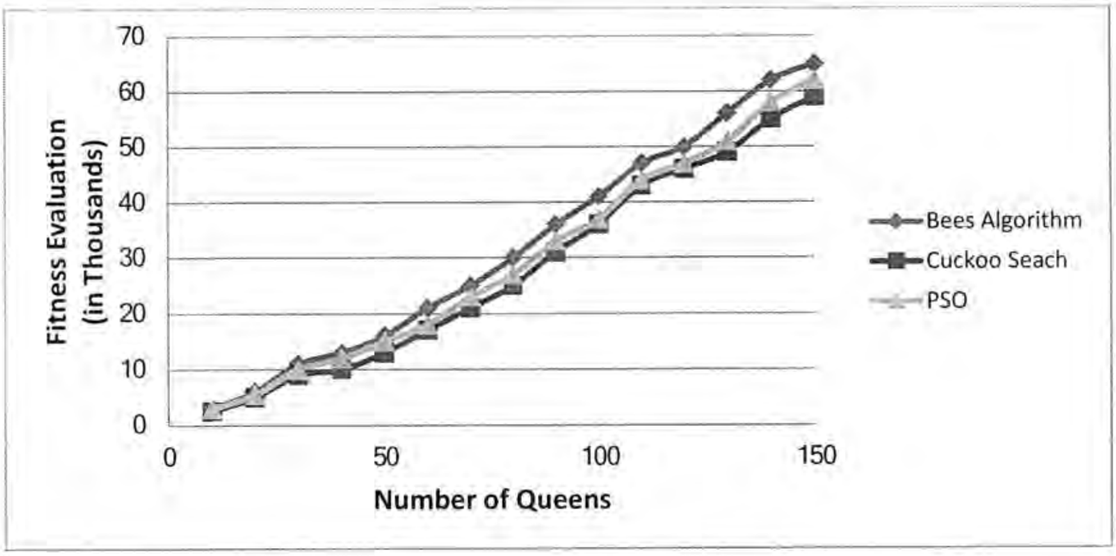

Figure-5: Fitness Evaluations Chart for the 3 Swarm Intelligence Algorithms (Bees, Cuckoo Search and PSO)

7- CONCLUSIONS

The objective of this paper was to determine how well some intelligence algorithms can handle permutation parameter sets by solving the n-queens problem. The performance of these algorithms gives a good and near results. It shown that Bees algorithm is better than the PSO, PSO is better than Cuckoo search to handle n-queens problem. The run time of these algorithms depend on the parameters of each one but in almost it is depend on maximum generation.

REFERENCES

1. H. Ahrabian, A. Merzaei and A. Nowzari-Dalini, "A DNA Sticker Algorithm for Solving N-Queen Problem", International Journal for Computer Science and Applications, vol. 5, No. 2, pp 12-22, 2008.
2. Jesper Goos, "Using Genetic Programming to Solve the n Queens Problem", Datalogi Roskilde Universitetscenter, November 2005.
3. Pham D.T., Ghanbarzadeh A., Koc E., Otri S., Rahim S., and Zaidi M. "The Bees Algorithm - A Novel Tool for Complex Optimization Problems", Proceeding of the 2nd Virtual International conference On Intelligent Production Machines and Systems, D.T. Pham, E. E.

Eldukhri and A. J. Soroka (eds), Elsevier (Oxford) (2006), ISBN-10:08-045157-8.

4. Kennedy J. and Eberhart R., "Particle Swarm Optimization", in Proceedings of the IEEE International Conference on Neural Networks, pp. 1942-1948, 1995.
5. Eberhart R.C. and Kennedy J., "A New Optimizer Using Particle Swarm Theory", Proc. 6th Symposium on Micro Machine and Human Science, pp. 39–43, 1995.
6. Al-Kazemi, B and Mohan C., "Multi-phase Discrete Particle Swarm Optimization". In: Fourth International Workshop on Frontiers in Evolutionary Algorithms, Kinsale, Ireland, 2002.
7. Pampara G., Franken N. and Engelbrecht A., "Combining Particle Swarm Optimization with Angle Modulation to Solve Binary Problems". In: Proceedings of the IEEE Congress on Evolutionary Computing, vol 1, pp 89-96, 2005.
8. Onwubolu G. and Clerc M., "Optimal Operating Path for Automated Drilling Operations by a New Heuristic Approach Using Particle Swarm Optimization". International Journal of Production Research 42(3):pp.473-491, 2004.
9. Pang W., Wang K., Zhou C. and Dong L., "Fuzzy Discrete Particle Swarm Optimization for Solving Traveling Salesman Problem". In: Proceedings of the 4th International Conference on Computer and Information Technology (CIT04), IEEE Computer Society, vol 1, pp 89-96, 2004.
10. Pugh J. and Martinoli A., "Discrete Multi-Valued Particle Swarm Optimization". In: Proceedings of IEEE Swarm Intelligence Symposium, vol 1, pp 103-110, 2006.
11. Correa E., Freitas A. and Johnson C., "A New Discrete Particle Swarm Algorithm Applied to Attribute Selection in a Bio-informatic data set". In: Proceedings of GECCO 2006, pp35-42, 2006.
12. Martinez-Garcia F., Moreno-Perez J., "Jumping Frogs Optimization: A New Swarm Method for Discrete Optimization". Tech. Rep. DEIOC 3/2008, Dep. of Statistics, O.R. and Computing, University of La Laguna, Tenerife, Spain, 2008.
13. Moreno-Perez J., Castro-Gutierrez J., Martinez-Garcia F., Melian B, Moreno-Vega J. and Ramos J., "Discrete Particle Swarm

Optimization for the p-median Problem". In: Proceedings of the 7th Metaheuristics International Conference, Montreal, Canada, 2007.

14. Shi Y. and Eberhart R., "A Modified Particle Swarm Optimizer", Proc. IEEE Conference on Evolutionary Computation, 1998.
15. Kumar A., and Zhang D., "Palm Print Authentication Using Multiple Representation", Pattern Recognition Journal, vol. 38, pp.1695-1704, 2005.
16. Carlisle A. and Dozier G., "An off-the-Shelf PSO", Proc .Particle Swarm Optimization Workshop, pp. 1–6, 2001.
17. Khanesar M., Teshnehlab M., and Shoorehdeli M., "A Novel Binary Particle Swarm Optimization", Proc. 15th Mediterranean Conference on Control and Automation, 2007.
18. Pham D.T., Ghanbarzadeh A., Koç E., Otri S., Rahim S., and Zaidi M, "The Bees Algorithm, A Novel Tool for Complex Optimization Problems". Proc 2nd Virtual International Conference on Intelligent Production Machines and Systems. 2006, Elsevier (Oxford), pp. 454-459.
19. Eberhart, R., Y. Shi, and J. Kennedy, "Swarm Intelligence", Morgan Kaufmann, San Francisco, 2001.
20. Von Frisch K. "Bees: Their Vision, Chemical Senses and Language", Cornell University Press, N.Y., Ithaca, 1976.
21. Seeley T.D., "The Wisdom of the Hive: The Social Physiology of Honey Bee Colonies", Massachusetts: Harvard University Press, Cambridge, 1996.
22. Bonabeau E, Dorigo M, and Theraulaz G., "Swarm Intelligence: from Natural to Artificial Systems", Oxford University Press, New York, 1999.
23. Camazine S, Deneubourg J, Franks NR, Sneyd J, Theraula G and Bonabeau E., "Self-Organization in Biological Systems", Princeton: Princeton University Press, 2003.
24. X. S. Yang and S. Deb, "Cuckoo search via Lévy flights", World Congress on Nature & Biologically Inspired Computing (NaBIC 2009), IEEE Publications, pp. 210–214, December, 2009.
25. H. Zheng and Y. Zhou, "A Novel Cuckoo Search Optimization Algorithm Base on Gauss Distribution", Journal of Computational Information Systems 8: 10, 4193–4200, 2012.

26. Xiaohui Hu, Russell C. Eberhart, and Yuhui Shi, "Swarm Intelligence for Permutation Optimization:A Case Study of n-Queens Problem", Proceedings of the IEEE on Swarm Intelligence Symposium, p. 243 – 246, 2003.
27. Homaifar. A. A., Tumer, I., and Ali. S., "The n-queens Problem and Genetic Algorithm", Proceedings of the IEEE Southeast Conference, pp. 262-261, 1992.

Authentication of Fingerprint Image Based on Digital Watermarking

Methaq T. Gaata
Computer Science Department, University of Mustansiriyah, Baghdad, Iraq
Received 21/3/2013 – Accepted 15/9/2013

الخلاصة

هذه المقالة تقدم طريقة لاثبات صحة صور طبعة الاصابع باستخدام تقنية اخفاء العلامة المائية في صور طبعات الاصابع. هذه الطريقة تعتمد على ملف التنحيف لتحديد المواقع المناسبة التي سيتم خزن بيانات العلامة المائية فيها دون التأثير على ميزات صور طبعة الاصابع، وبهذا فأن الطريقة المقترحة لاتأثر على اداء أنضمة تصنيف و تمييز صور طبعة الاصابع. لقد أضهرت النتائج التجريبية ان الطريقة المقترحة تمتلك درجة عالية من الشفافية اعتمادا على خصائص نظام الرويا البشري وكذالك اثبتت فعاليتها لانها لا تتطلب عمليات حسابية معقدة.

ABSTRACT

This paper presents an authentication method to establish the authenticity of fingerprint images by embedding the watermark data into fingerprint image. The method depends on the thinning file of fingerprint image in determining the appropriate locations in which the watermark bits will be stored in the original fingerprint image to preserve feature regions without any change, therefore the proposed method inserts watermark data in locations which not use in feature extraction operation thus prevents watermarking of regions used for fingerprint classification and recognition. The experimental results show the high visibility of the proposed method depending on the properties of human visual system. Our method is also efficient as it only uses simple operations.

1. INTRODUCTION

A biometric is defined as a unique, measurable, biological characteristic or trait for automatically recognizing or verifying the identity of a human being. Statistically analyzing these biological characteristics has become known as the science of biometrics. These days, biometric technologies are typically used to analyze human characteristics for security purposes. Five of the most common physical biometric patterns analyzed for security purposes are the fingerprint, hand, eye, face, and voice [1].

With the wide spread utilization of biometric identification systems, establishing the authenticity of biometric data itself has emerged as an important research issue. The fact that biometric data is not replaceable and is not secret, combined with the existence of many types of attacks that are possible in a biometric data, makes the issue of security/integrity of biometric data extremely critical [2].

The fingerprints are digitized, stored, and transmitted over a network; they become susceptible to malicious as well as accidental attacks. Therefore, it becomes necessary to protect the originality of fingerprint images that stored in databases or transmitted through transmitter channels against intentional and unintentional attacks. In order to preserve the authenticity of this information and prevent alterations from being made at will, a protective scheme must be used [3].

Digital watermarking of fingerprint images can be used in some applications like: (a) protecting the originality of fingerprint images stored in databases against intentional and unintentional attacks, (b) fraud detection in fingerprint images by means of fragile watermarks (which do not resist to any operations on the data and get lost, thus indicating possible tampering of the data), and (c) guaranteeing secure transmission of acquired fingerprint images from intelligence agencies to a central image database, by watermarking data prior to transmission and checking the watermark at the receiver site [4].

In recent years, a number of adaptive watermarking methods for digital image have been proposed. Bilge and et al [4] introduce spatial method in order to embed watermark data into fingerprint images, without corrupting their features. Anil and et al. [5] introduce an application of steganography and watermarking to enable secure biometric data (e.g., fingerprints) exchange. In [6], Chouhan and et al. blind watermarking scheme based on wavelet domain has been proposed as a means to provide protection against false matching of a possibly tampered fingerprint by embedding watermark data in the fingerprint itself.

In this paper, we propose method to hide watermark into fingerprint image to guarantee the image source is authentic and the information content in the image has not been modified in transit to its destination or that stored in database.

This paper is organized in the following manner.The watermark inserting and detecting method is proposed in Section 2. Experimental results are shown in Section 3. Section 4 concludes this paper.

2. Proposed Watermarking Method

In this section, we describe the main steps of the proposed watermark embedding and extraction procedures. The block diagram of the proposed watermarking method is presented in Fig.1.

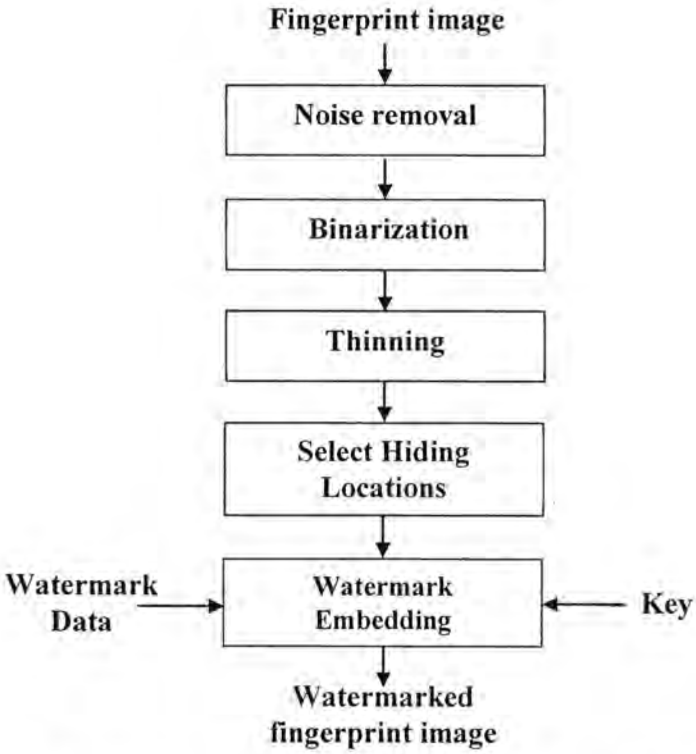

Figure-1: The Block diagram of proposed watermarking method.

2.1 Noise Removal

Fingerprint image may not always be well defined due to elements of noise that corrupt the clarity of the ridge structures. This corruption may occur due to variations in skin and conditions of capturing such as humidity, dirt, and non-uniform contact with the fingerprint capture device. Thus, this step is employed to reduce noise, to improve the clarity of ridge structures of fingerprint images, and to prepare fingerprint image to determine the hiding locations. In this step, the median filter is used for the noise removal from fingerprint image.

2.2 Binarization Process

Binarization is the process that converts a fingerprint image into a binary image.One ways of accomplishing this process is by using the edge detection operation and optimal thresholding technique.

As described in literature a number of different gradient filters to edge detection are available. Since the Sobel operator is the most popular one used for edge detection purposes and it yields the best results and very quick to computer and rather simple to implement, it will be used in the proposed method to detected edges in fingerprint image [7].

The Sobel operator is followed by a global thresholding operation in which each pixel in the image is assigned a value representing either white or black depending on the magnitude of the gradient at that point as follow:

$$B(x,y) = \begin{cases} 1 \text{ if } EM(x,y) > T_n \\ 0 \text{ if } EM(x,y) \leq T_n \end{cases} \quad \ldots (1)$$

where $EM(x, y)$ is the edge magnitude value which results from convolution a Sobel operator.The threshold (T_n) isrepresents mean value for pixels values in neighborhood of pixel at index (x,y). The optimal thresholding technique is effective in separating the ridges (white pixels) from the valleys (black pixels). Somehow the fingerprint image is converted to binary image $\{1, 0\}$ where the value 1corresponds to object (ridges) and 0 to background (valleys).

2.3 Thinning Operation

Thinning is normally only applied to binary images, and produces another binary image as output. After the fingerprint image is converted to binary form, it is then submitted to the thinning algorithm which reduces the ridge thickness to one pixel wide. The thinning must be performed without modifying the original ridge.

The purposes of thin image which produced from the thinning algorithm are and play very important role to determine the hiding locations in which the watermark bits will be stored in the original fingerprint images.

The standard thinning operation is described in [8] [9], which perform the thinning algorithm using two sub-iterations.The thinning algorithm is described as follows:

Thinning Algorithm

```
Begin
Step1: Create the two Buffers that equal to the binary file (BUF1, BUF2).
Step2: Step=0.
Step3: Repeat
          Flag=0.
           For i= 1 to Image Hight-1
            For j= 1 to Image Width-1
              Begin
               ▪ If BUF2 [i, j] =1 Then compute N (P1). {Equation (2.3)}
                  Else go to Step4.
               ▪ If (2<= N (P1)<=6) Then compute T (P1).
                  Else go to Step4.
               ▪ If T (P1)=1 Then test the condition (C) as:
                                    If Step=0 then C = P2·P4· P6.
                     Else C=P2 ·P4· P8.
                 Else go to Step4.
               ▪ If condition (C) is True Then test the condition (D) as:
                                    If Step=0 then D = P4 ·P6· P8.
                     Else D =P2 ·P6· P8.
                 Else go to Step4.
               ▪ If condition (D) is True Then BUF1 [i, j] =0, Flag =1.
Next j, Next i.
Step4: If Flag =1 Then BUF2=BUF1.
Step5: If Step =0 Then Step =1 Else Step =0.
Step6: If Flag ≠0 Then go to Step3.
End.
```

2.4 Select Hiding Locations

After getting the resulted thin image file from the thinning operations as shown in section before, this file consists two values are 0 or 1only these values will be used to determine the places in which the watermark bits will be stored in the original fingerprint image.And this is done by checking pixel of the edgeimage file and thin imagefile as follow:

$$\alpha\,(i,j) = \begin{cases} 1 \text{ if } B(i,j)=1 \text{ and } Thin(i,j)=0 \\ 0 \quad \text{otherwise} \end{cases} \qquad \dots (2)$$

To obtain α *(i, j)*, it is got the resulted binary image file from the binarization process section as described before, and get the resulted thin image file from thinning operation section as described before, if binary pixel *(i, j)* =1and thinning pixel *(i, j)* =0 then α *(i, j)* =1 otherwise α *(i, j)* =0. The *B(i, j)*and *Thin (i,j)*represent the values of binary and thinning files, respectively. For example:

0	1	1	0	0
0	1	1	0	0
0	0	1	1	0
0	0	0	1	1
0	0	0	0	1

B (i, j)

0	1	0	0	0
0	0	1	0	0
0	0	0	1	0
0	0	0	0	1
0	0	0	0	0

Thin (i, j)

0	0	1	0	0
0	1	0	0	0
0	0	1	0	0
0	0	0	1	0
0	0	0	0	1

α *(i, j)*

2.5 Watermark Embedding

In this method, Watermark data are embedded onto pixels of fingerprint image according to the embedding condition given below:

***If α (i, j) =1Then insert watermark bit (W) in I (i, j)*...(3)**

where*I (i, j)* are pixel values referring to original pixels at watermark embedding location *(i, j)*. The value of watermark bit is denoted as *W*, where $W \in [0, 1]$. The α *(i, j)* term guarantees the pixels (called marked pixels) which will store watermark bit are not belonging to region which used in the recognition and classification processesof fingerprint images, therefore the performance of a method which will using the watermarked image (e.g., fingerprint verification in the case of watermarked fingerprint images) is unchanging; α *(i, j)*, takes the value 0 if the pixel (i; j) under consideration belongs to a fingerprint feature region; it has value 1 otherwise.In other words, the watermark bit will be embedded in edge pixels or busy regions only which are not belonging to features areas.The algorithm of this method is as shown below:

Input: Original Fingerprint Image, Binary File, Thin File, and Watermark Data.
Output: Watermarked Image.

Begin
Step1: Load original fingerprint image.
Step2:Get the binary fingerprint image file, this file resulted from binarization process.
Step3: Get the thinning file this file resulted from thinning operation.
Step4: Read the watermark data.
Step5: Convert the watermark data into a bits stream.
Step6: Compute α *(i, j)* from binary file and thin file.
Step7: Insert watermark data to original fingerprint image, the fingerprint pixel values are changed according to the following condition:
If α (i, j) =1Then Insert watermark bit (W) in I (i, j)
Step8:Save and display fingerprint watermarked image.
End.

2.6 Watermark Extraction

Watermark extraction is the inverse process of watermark embedding. We need to compute the *α (i, j)* values and the secret key. The algorithm of watermark extraction is as shown below:

Input: Fingerprint Image.
Output: The Image Authentic or Unauthentic.

Step1: Compute α *(i, j)* from binary file and thin file.
Step2: Extract the watermark bit from the hiding locations in the loaded fingerprint image depending on α *(i, j)*.
Step3: If watermark bits are found in fingerprint image then
- Collect the extracted bits and convert them to values.
- Display the extracted watermark data on screen; this means the loaded fingerprint image is authentic.

Else
- Display message" the loaded fingerprint image is unauthentic "; this means the fingerprint image is either replaced or modified".

End.

---

3. RESULTS AND DISCUSSIONS

In this method, the watermark bits are embedded in locations selected based on the *α (i, j)* values that is built by using thinning operation. This experiment has been implemented using twofingerprint images of size 512×512. The Fig.2 shows the original fingerprint image with the corresponding binary image, thin image, and watermarked image for each one.

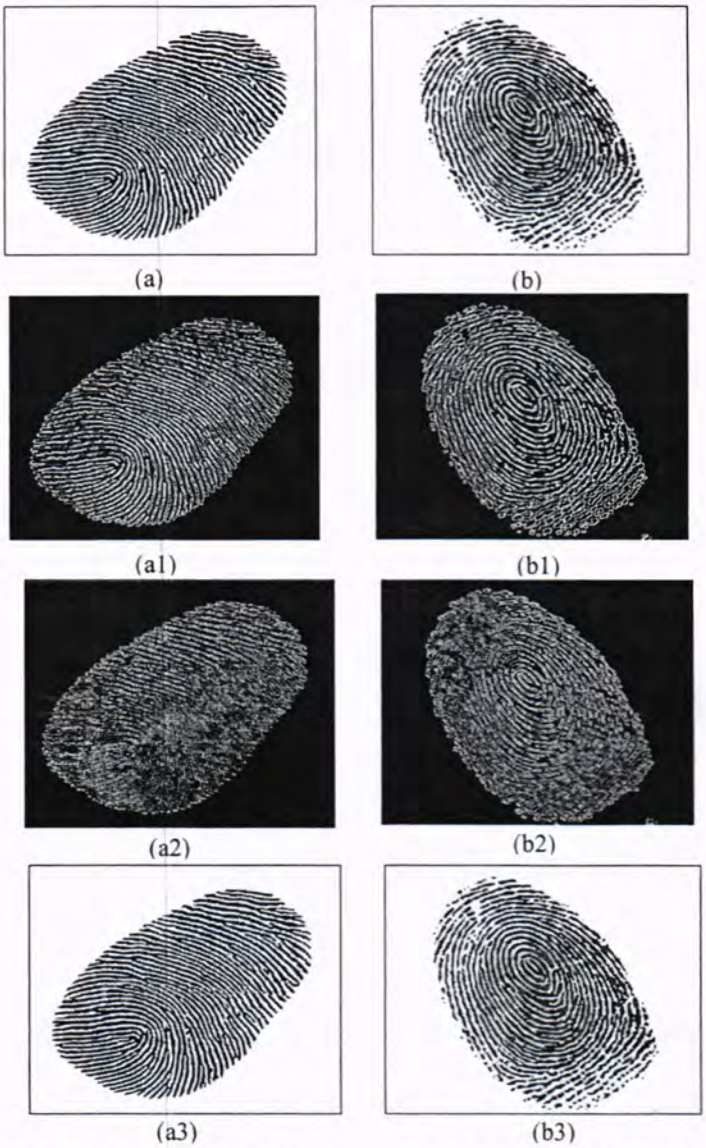

Figure-2: (a&b) Original images, (a1&b1) binary image, (a2&b2) thin image, (a3&b3) watermarked image.

As seen in Fig.2, the proposed method is providing high degree of transparencybetween original fingerprint image and its watermarked image, because the hiding locations are the edge pixels regions only. Due to the fact that human visual system is relatively less sensitive to changing pixel value in busy image regions and edge image regions, the visibility of the watermark does not increase significantly. Therefore, watermarked fingerprint image is similar to original fingerprint image.

To determine the amount of distortion ofproposed watermarking method introduced into the host image. Thetwo of image quality measures are used. These measures are PSNR [10] and SSIM [11] measures. The results of quality evaluation are shown in Table 1.

Table-1. Quality evaluation for proposed method

Image	PSNR	SSIM
Image A	42.13	9.72
Image B	39.77	9.53

As noted results of PSNR and SSIM in Table 1, the proposed method has the highest quality degree. The reasons for that, the proposed method embedded the watermark bits in the edge regions which are not belong to the main structure of fingerprint image. In this case, the watermark bit will not effect on the feature regions.

It is taken another example of test to fingerprint image watermark which attacked by attacker (unauthorized) as shown in Fig.3 thus the watermark not extract that means this image is unauthentic.

Figure-3: Attacked Watermarked Image.

In Fig.3, the all images are unauthentic, because the some type of attacks aredone on the fingerprint watermarked image. In this case, the synchronization of watermark is lost in extraction side.

4. Conclusions

In this paper, we have proposed a watermarking method based on thinning operation which can be used for authentication of fingerprint image. Experimental results show that the degradation by embeddingthe watermark is too small to be visualized. Also, the proposed method can enhance the security of a fingerprint-based personal authentication system.

REFERENCES

1. Davide M., Dario M. and Anil k., "Fingerprint Image Recognition", Hand Book, 2002.
2. S. Jain, "Digital Watermarking Techniques: a Case Study in Fingerprints & Faces", Proc. ICVGIP 2000, Bangalore, India, PP. 139-144, Dec. 2000.

3. Jessica .F,Miroslav .G and Rui .D, "Lossless Data Embedding – New Paradigm in Digital Watermarking", SUNY Binghamton, Binghamton, NY 13902, 2001.
4. Uludag Umut, Gunsel Bilge and Ballan Meltem, "A Spatial Method for Watermarking of Fingerprint Images", TUBITAK Marmara Research Center, Information Tech. Research Institute, Turkey, 2002.
5. Jain A. K. and Uludag Umut, "Hiding Fingerprint Minutiae in Images", Computer Science and Engineering Department, Michigan State University, 2002.
6. Rajlaxmi Chouhan, Agya Mishra, Pritee Khanna, "Fingerprint Authentication by Wavelet-based Digital Watermarking," International Journal of Electrical and Computer Engineering (IJECE), vol.2, No.3, 2012.
7. Scharr, Hanno, "Optimal Filters for Extended Optical Flow," IWCM 2004. LNCS, vol. 3417, pp. 14–29. Springer, Heidelberg, 2007.
8. Rafael C. Gonzalez , Richard E. Woods, "Digital Image Processing," (3rd Edition), 2007.
9. T. Acharya and A. K. Ray, Image Processing Principles and Applications, Published by John Wiley & Sons, Inc., Hoboken, New Jersey, 2005.
10. S. Radharani and M.L. Valarmathi, "A Study on Watermarking Schemes for Image Authentication," International Journal of Computer Applications, vol. 2, no.4, pp. 24-32, June 2010.
11. Z. Wang, A. C. Bovik, H. R. Sheikh and E. P. Simoncelli, "Image quality assessment: From error visibility to structural similarity," IEEE Trans. Image Processing, Vol. 13, No. 4, pp. 600–612, 2004.

Enhancement of the Underwater Images Using Modified Retinex Algorithm

Nabeel Mubarak Mirza[1], Ali Abid Dawood Al – Zuky[2] and Hazim Gati' Dway[3]
[1]Department of Physics, College of Education, AL-Mustansiriyah University, Baghdad, Iraq.
[2,3]Department of Physics, College of Science, AL-Mustansiriyah University, Baghdad, Iraq.
Received 16/3/2013 – Accepted 15/9/2013

الخلاصة

صور الأجسام تحت الماء غير واضحة للعيان بسبب التباين المنخفض نتيجة التشتت الكبير للضوء ووجود ضوضاء في البيئة المائية مما يؤدي إلى فقدان تفاصيل الصورة كذلك لونها الأصلي. خوارزمية (Retinex) تعمل على تحسين مستوى السطوع، التباين والشدة من الصورة. في هذه الدراسة، أقترحنا خوارزمية جديدة لتحسين الصورة تعتمد على تعديل متعدد النطاق مع أستعادة اللون (MMSRCR). هذه التقنية تستخدم عنصر الإضاءة في الفضاء اللوني (YIQ) حيث تستخدم (Sigmoid Function) كتحويل لها. العلاقة بين المعدل ومعدل الأنحراف المعياري تم حسابها لمعرفة كفاءة هذه الطريقة حيث قورنت مع خوارزمية AINDANE وكذلك مع خوارزمية تسوية الهستوغرام الاعتيادية (HE)، جميع هذه الخوارزميات انجزت باستخدام برنامج Matlab.

ABSTRACT

The objects in the underwater images are not clearly visible due to low contrast and scattering of light and the large noise present in the environment which leads to lose its original color and details. The Retinex is an image enhancement algorithm that improves the brightness, contrast and sharpness of an image. In this study, we proposed a new image enhancement algorithm dependent on the Modified Multi Scale Retinex Algorithm with Color Restoration (MMSRCR). This technique is using the lightness component in YIQ color space that is transformed by the Sigmoid Function and then it is applied in the traditional multi scale retinex algorithm MSRCR image after reveres transformation. Relationship between the mean and the average of standard deviation for image has been done to examine the efficiency of the method. All algorithms has implemented using program (Matlab).

1. INTRODUCTION

Underwater image enhancement techniques provide a way to improving the object identification in underwater environment. There is lot of research started for the improvement of image quality, but limited work has been done in the area of underwater images, because in underwater environment image get blurred due to poor visibility conditions and effects like absorption of light, reflection of light, bending of light, denser medium (800 times denser than air) and scattering of light. These are the important factor which causes the degradation of underwater images [1]. The researchers have reviewed several techniques related to images enhancement viz "Contrast Stretching" "Histogram Equalization" "Contrast Limited Adaptive Histogram Equalization (CLAHE)". The (MSRCR) is a non-linear spatial and spectral transform that produces images that have a high degree of visual fidelity to the observed scene [2]. Here we are going to the process of testing, developing and extensively using the Histogram Equalization (HE), Adaptive Integrated Neighborhood Dependent

Approach (AINDANE), Multiscale Retinex with Color Restoration (MSRCR) and Modify Multi scale Retinex with Color Restoration (MMSRCR) algorithms for image enhancement.

2. Related Works

A number of researches have been conducted to study the contrast and lightness color image enhancement in different ways, in the following some of these studies:

• Foster [3] (2011) identified fundamental problems with defining color constancy in complex natural visual environments and in the same year they proposed an adaptive multi-scale retinex that determines the size of the Gaussian filters and corresponding weights according to the intensity distribution of the input image [4].

• Hana H. [5] (2012) enhanced the color images with dim regions by using modify histogram equalization (MHE) algorithm. This technique uses the lightness component in YIQ color space is transformed using sigmoid function.

3. MATERIALS AND METHODS

For the results in this study, we have selected test color which is consisting of (red, green, blue, magenta, cyan, yellow, white and black). After that we spraying paint on the metallic plate by using the sprayer dyes, the metallic plate (13.5×15 cm) connected with wood pole of length (4.5 m) to controlling of the distance between the object and camera at different depths as showing in Figure 1. The video clips have been done by using underwater camera (Sony DSC-TX10), we used "Ulead Video Studio program version 11" to obtain images of BMP format with size (243×243 pixel); note of that these images were taken from the swimming pool (clean water), after that these images are processed in Matlab.

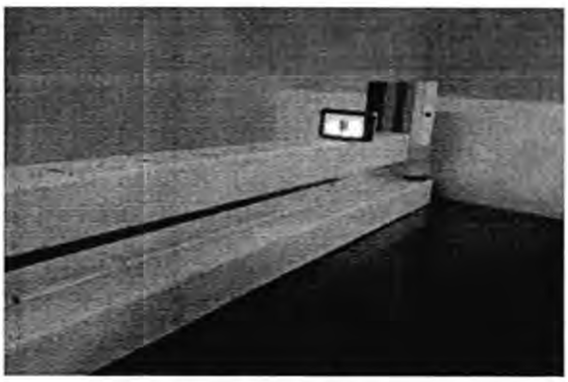

Figure-1: Experimental Setup.

3.1 Histogram Equalization (HE)

A global technique which works well for a variety of images is histogram equalization If lightness levels are continuous quantities normalized to the range (0, 1) and pr(r) refers to the Probability

Density Function (PDF) of the lightness levels in a given image, where the subscript is used for differentiating between the PDFs of the input and output images. Suppose that the following transformation perform on the input levels get output (processed) intensity levels [6].

3.2 AINDANE Algorithm

Adaptive Integrated Neighborhood Dependent Approach for Nonlinear Enhancement of Color Images (AINDANE) is an algorithm to improve the visual quality of digital images captured under extremely low or uniform lightening conditions. It is composed of three main parts: Adaptive Luminance enhancement, contrast enhancement and color restoration [5].

3.3 MSRCR Algorithm

The Multi-Scale Retinex (MSR) is explained from Single-Scale Retinex (SSR) that is a combination of weighted different scale of SSR, which given by [7]:

$$R_i(x,y,c) = \log\left[I_i(x,y)\right] - \log\left[F(x,y,c) \otimes I_i(x,y)\right] \quad (1)$$

where, R_i (x, y, c) the output of channel i (i ϵ R,G,B) at position x, y, c is the Gaussian shaped surrounding space constant, Ii (x, y) is the image value for channel i and symbol ⊗ denoted convolution. F (x, y, c) Gaussian surrounds function that is calculated by Eq. 2.

$$F(x,y,c) = k \; e^{-[\frac{(x^2-y^2)}{c^2}]} \quad (2)$$

$$\iint F(x,y,c)\,dx\,dy = 1 \quad (3)$$

The MSR output is then simply a weighted sum of the outputs of several different SSR output where [8]:

$$R_{MSR}(x,y,w,c) = \sum_{n=1}^{N} W_n R_i(x,y,c_n) \quad (4)$$

where, N is the number of scales, R_i (x, y, cn) the I'th component of the n'th scale, RMSR (x, y, w, c) the I'th spectral component of the MSR output and Wn the weight associated with the n'th scale. We insist that ($\sum Wn=1$). The result of the above processing will have both negative and positive RGB values and the histogram will typically have large tails. Thus a final gain-offset is applied as mentioned in [8] and discussed in more detail below. This processing can cause image colors to go towards gray and thus an additional processing step is proposed in [7] to calculate MSR with color restoration by Esqs. (5&6):

$$R' = R_{MSR} * I_i'(x,y,c) \quad (5)$$

where, I' given by [8]:

$$I_i'(x,y,a,b) = b \log\left[1 + a\frac{I_i(x,y)}{\sum_{i=1}^{3} I_i(x,y)}\right] \tag{6}$$

where, we have taken the liberty to use log (1 + x) in place of log (x) to ensure a positive result. In [8] a value of 125 is suggested for (a); we empirically settled on a value of (b = 100) for a specific test image. The difference between using these two values is small. In eq. (4) a second constant is used which is simply a multiplier of the result. And the final step is gain-offset by 0.35 and 0.56 respectively. The present research uses: ($w_1 = w_2 = w_3 = 1/3$) and ($c_1 = 250$, $c_2 = 120$, $c_3 = 80$) [9].

3.4 MMSRCR Algorithm

First step in this algorithm is transform color image from basic RGB color space to YIQ color space, the forward transform is given by Eq. 7 [8]:

$$\left.\begin{array}{l} y = I \\ i = 0.596r - 0.27g + 0.322b \\ q = 0.211r - 0.253g + 0.312b \end{array}\right\} \tag{7}$$

where, y is lightness component, i,q are chromatic components. In second step is transformed normalized lightness value by using sigmoid function that is given by Eq.8 [9]:

$$S_n = 1/\left(1 + \sqrt{\frac{1 - I_n}{I_n}}\right) \tag{8}$$

where, I_n is the normalized lightness value that is equal (I/255). Figure2 shows the relationship between input lightness in versus output lightness S_n.

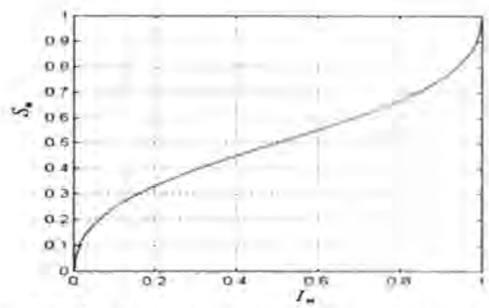

Figure-2:Relationship between input lightness versus output lightness.

Then used the inverse transformation from YIQ to RGB color space calculated in YpIQ that is given by [8]:

$$\left.\begin{array}{l} r_p = y_p + 0.956i + 0.621q \\ g_p = y_p - 0.272i - 0.647q \\ b_p = y_p - 1.106i + 1.703q \end{array}\right\} \tag{9}$$

Finally the MSRCR had been applied on new component in Eq.9.

4. Image Quality Assessment

Some researchers in NASA Langley research center studied regional means (visual lightness) and standard deviations (visual contrast) and found that they tend to converge on consistent global aggregates [10]. This implies that a good visual representation can be associated with well-defined statistical measures for visual quality. In scientific terms, this implies the existence of a canonical visual image as a statistical practical ideal. Such a defined ideal can then serve as the basis for the automatic assessment of visual quality.

To compute the regional parameters, we divide the image into non overlapping 25×25 pixel blocks. For each block, a mean I_b and a standard deviation σ_b are computed. This regional scale is sufficiently granular to capture the visual sense of regional brightness and contrast. Both the global contrast and lightness can then be measured in terms of the regional parameters. The overall lightness is measured by the image mean $\mu=\overline{I_b}$, which is also the ensemble measure for regional lightness. The overall contrast is measured by taking the mean of regional standard deviations $\overline{\sigma_b}$ as shown in Figure 3 and it provides a gross measure of the regional contrast variations. A classification of excellent, good, or poor is then based on how many of these regional blocks exceed a given contrast and brightness threshold.

5. RESULTS DISSCUSSIONS

We study new ways to control intensity of light and color for the purpose of capturing better quality data in poor visibility environments. The images which used in the present study have been illustrated in Figure 4. These images were enhanced by using different algorithms as shown in Figs. (5-8), the relationship between mean of local standard deviation and mean for image it is illustrated in Figure 9 a-g the points of MMSRCR tend to visual optimal region. In fact, this algorithm was enabled to increase both lightness and contrast in image which compared with other points. We can conclude that the MMSRCR is robust method to enhance color-image with degraded lightness levels.

6. Conclutions

A computation like the MMSRCR appears to have two very useful properties simultaneously: a diminishment in the dependence of the appearance of the image on poor visibility environments and extraneous variables, such as spatial spectral and lighting. The former is inherently useful because it can lead to better image classifications and the latter because it shows very clearly that the appearance of a color is dependent not only on the spectral characteristics of a pixel, but also its surround. Together these properties may be able to provide a basis for bringing more advanced levels of visual intelligence into computing.

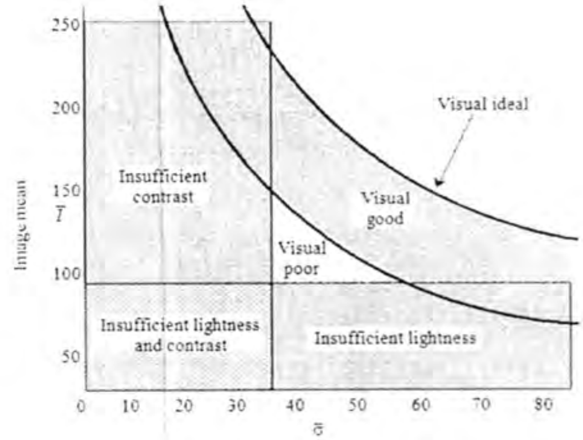

Figure-3: Image quality description [10].

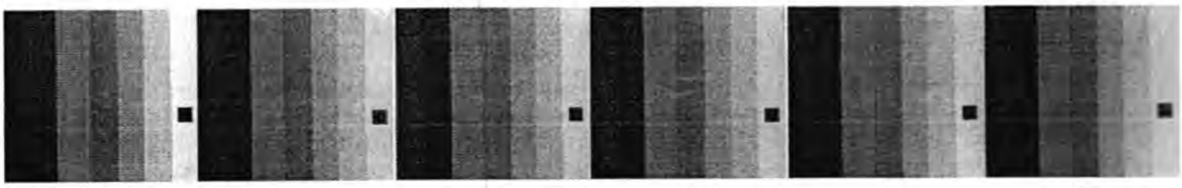

A B C D E F

Figure-4: Original images (a) in air, (b) in depth 50 cm underwater, (c) in depth 100 cm underwater, (d) in depth 150 cm underwater, (e) in depth 200 cm underwater, (f) in depth 250 cm underwater.

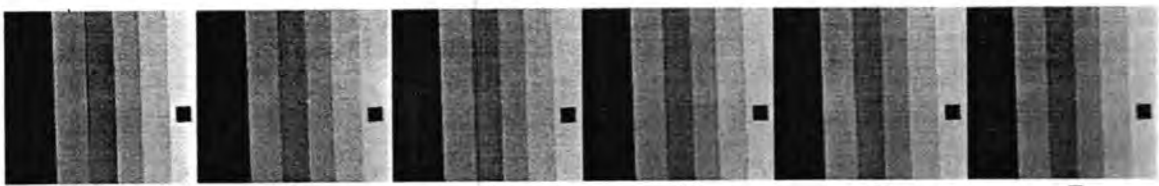

A B C D E F

Figure-5: Enhanced images by using MMSRCR algorithm (a) in air, (b) in depth 50 cm underwater, (c) in depth 100 cm underwater, (d) in depth 150 cm underwater, (e) in depth 200 cm underwater, (f) in depth 250 cm underwater.

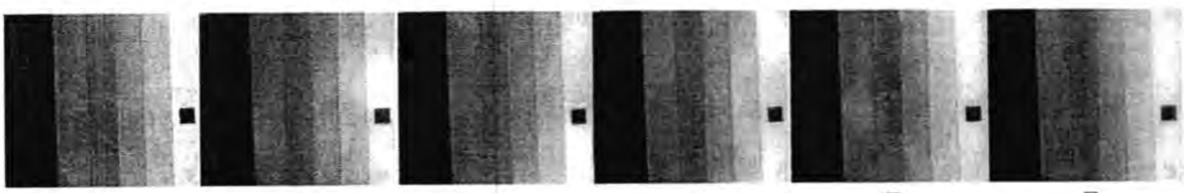

A B C D E F

Figure- 6: Enhanced images by using HE (a) in air, (b) in depth 50 cm underwater, (c) in depth 100 cm underwater, (d) in depth 150 cm underwater, (e) in depth 200 cm underwater, (f) in depth 250 cm underwater.

A B C D E F

Figure-7: Enhanced images by using MSRCR algorithm (a) in air, (b) in depth 50 cm underwater, (c) in depth 100 cm underwater, (d) in depth 150 cm underwater, (e) in depth 200 cm underwater, (f) in depth 250 cm underwater.

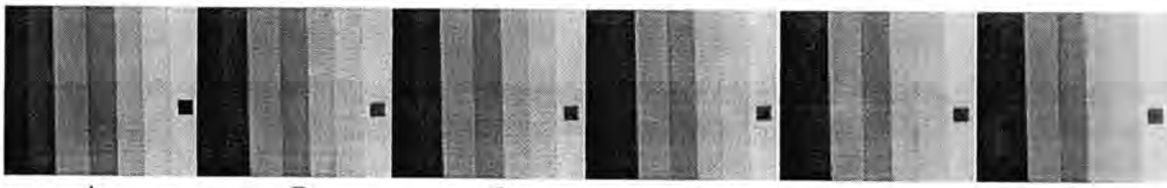

A B C D E F

Figure-8: Enhanced images by using AINDANE algorithm (a) in air, (b) in depth 50 cm underwater, (c) in depth 100 cm underwater, (d) in depth 150 cm underwater, (e) in depth 200 cm underwater, (f) in depth 250 cm underwater.

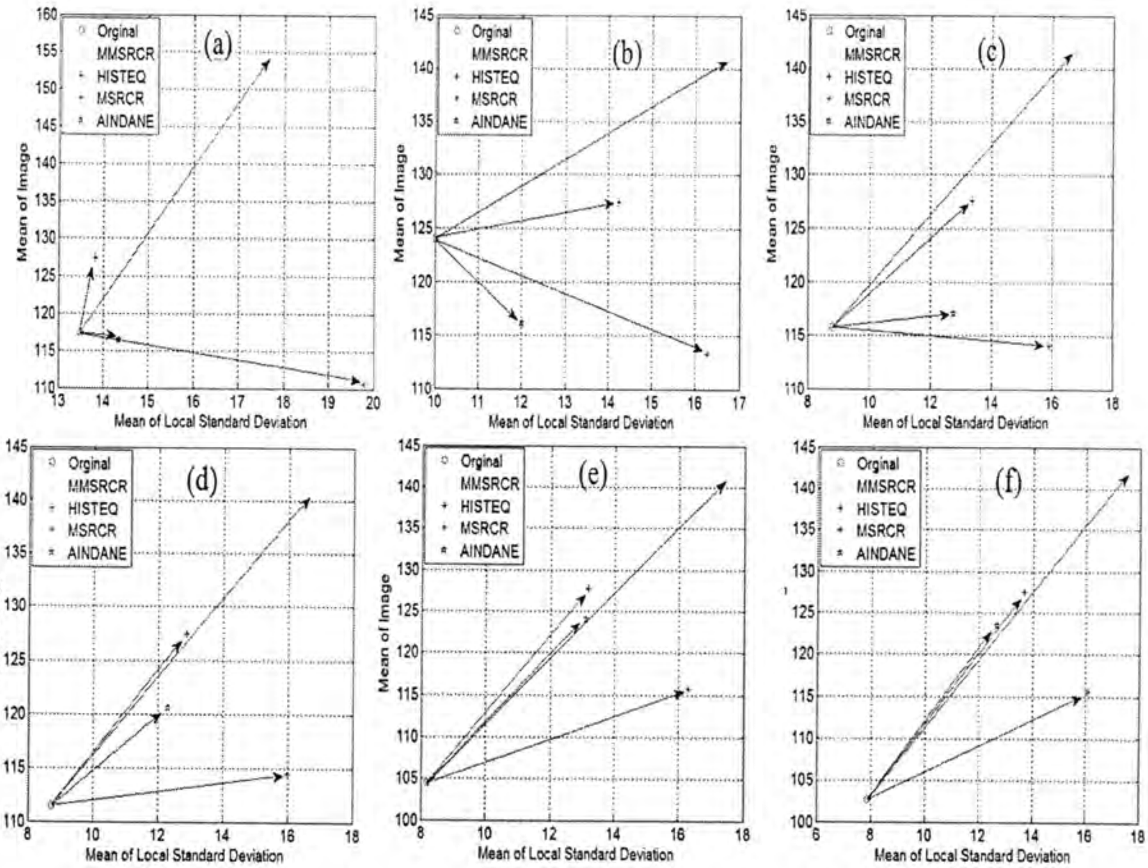

Figure -9:Relationship between mean of local standard deviations and mean of original and enhanced images (a) in air, (b) in depth 50 cm underwater, (c) in depth 100 cm underwater, (d) in depth 150 cm underwater, (e) in depth 200 cm underwater, (f) in depth 250 cm underwater.

7. REFERENCES

1. Singh, B., R.S. Mishra and P. Gour," Analysis of Contrast Enhancement Techniques for Underwater Image. Int. J. Comput. Technol. Elect. Eng., Vol. 1, pp. 190-194, 2011.
2. Anjali C., Bibhudendra A. and Mohammad I. K.," Retinex Image Processing: Improving the Visual Realism of Color Images", Int. J. Inform. Technol. Knowledge Management, Vol. 4, No. 2, pp. 371-377, 2011.
3. Foster, D. H., "Color Constancy" Vision Research Vol. 51, No.7, pp. 674-700, 2011.
4. In-Su J., Tae-Hyoung L., Wang-Jun K., and Yeong-Ho H., 2011. Local Contrast Enhancement Based on Adaptive Multi-Scaled Retinex using Intensity Distribution of Input Image. J. of Imaging Sci. and Technol. 55(4): 040502-1–040502-14, 2011. Society for Imaging Science and Technology 2011.
5. Hana H. K. Color image with Dim regions Enhancement Using Modified Histogram Equalization Algorithm. J. of Al-Nahrain Univ., Vol.15 No.3, September, pp.101-111, 2012.
6. Gonzales R. C. and Woods R. E., "Digital Image Processing Reading", MA: Addison-Wesley, 1987.
7. Jobson, D.J., Z. Rahman and G.A. Woodell, "Properties and Performance of a Center/Surround Retinex", IEEE Trans. Image Proc., Vol. 6, pp. 451-462, 1997.
8. Jabson, D.J., Z. Rahman and G.A. Woodel, "A Multi-scale Retinex for Bridging the Gap Between Color Images and the Human Observation of Scenes", IEEE Trans. Image Proc., Vol. 6, pp. 965-976, 1997.
9. Gupta, M., S.G. Narasimhan and Y.Y. Schechner, "On Controlling Light Transport in Poor Visibility Environments", Proceedings of the IEEE Conference on Computer Vision and Pattern Recognition, Jun. 23-28, IEEE Xplore Press, Anchorage, AK,p.p:1-8, 2008.
10. Jabson, D.J., Z. Rahman and G.A. Woodell, "Statistics of Visual Representation", Proceedings of the SPIE 4736, Visual Information Processing, Jul. 25-31, pp: 25-35, 2002.

The Glottal Modulation Components For Speaker Voice Recognition

Tariq A. Hassan and Rehab I. Ajel
College of Education, Al-Mustansuriay University
College of Science, Al-Mustansuriay University
Received 16/3/2013 – Accepted 15/9/2013

ABSTRACT

Glottal signals may carry more information about speakers than the speech signal itself when they used in the con- text of text-dependent speaker identification system. Source signals that came from voice-containing utterance appear to improve the system performance up to 10% comparing with the speech signal itself while those came from non-voiced utterance appear to have similar or pretty less accuracy comparing with the speech signals. Features are extracted from each speech/source signal by the method of AM-FM signal modulation. This method is able to introduce a set of descriptors that are encoded as a parameters for speaker identification. The purposes of this paper is to show that the voiced speech source signal contains more speaker dependence information than the speech signal in the context of speaker identification system. The speech signal and its source are parameterised in the method of AM-FM signal modulation. The results show that the source signal will give better performance just when it comes from voiced source.

1. INTRODUCTION

The task of speaker recognition can be divided into two fundamental parts: identification and verification [1]. Speaker identification is the task of assigning an unknown voice to one of the speakers known by the system; it is assumed that the voice must come from a fixed set of speakers. Speaker verification, on the other hand, refers to the case of accepting or denying a claim to be a particular speaker. In general, a speaker recognition system is composed of a speech parametrisation module and a statistical modelling module. These are responsible for the production of a machine readable parametrisation of the speech samples and the computation of a statis- tical model from the parameters [2]. During the past years the base model for speech parametrisation (the front-end of the recognition system) usually adopted is the source-filter model. This model has lead to the extraction of parameters such as linear predictive coding (LPC), mel-frequency cepstral coefficients (MFCCs) and perceptual linear prediction

(PLP) coefficients. These have proved highly successful in robust speech recognition, however the amplitude spectrum typically employed is highly sensitive to changes in speaking conditions such as changing channels and speaking style [3]. Also, this model is known to neglect some structure present in the speech signal, such as; unstable airflow, turbulence, and nonlinearities arising from oscillators with time-varying masses [4]. In recent years, new ways of modelling and characterising speech have been proposed. Of particular interest here is AM-FM modelling, which is used to decompose a speech signal into its modulated components of envelope (instantaneous amplitude) and phase (instantaneous frequency). However, AM-FM modelling becomes meaningless (containing many unaccepted negative frequencies) without breaking the signal down into its components, as the instantaneous frequency for a multicomponent real-valued signal is not well defined [5]. This model has adopted for many application related to the speech signal processing. Methods presented in [6, 7, 8] have employ this model in speaker parameters extraction for speaker recognition. The method in [6] used the AM-FM model to extract the nonlinear features carried by speech signal. In [7] the model has used to improve the speech spectrum of the reverberation sound. The model is also adopted with speech recognition area. In [9, 10] the AM-FM model has used to investigate the performance of the modulation components with the speech recognition. The short-time processing and the instantaneous band- width are used in the model to estimate the speech related features rather than the speaker person. This would open the door about more investigation to this model in the context of speech and speaker recognition. This paper explore the use of AM-FM source signal representation (rather than a speech signal) to introduce a new set of descriptors. This set is good descriptor of time-varying frequencies inherent in the speech signal that can be encoded as parameters for speaker identification. A popular statistical model in the context of text-independent speaker recognition, where there is no prior knowledge of what the speaker will say, is the Gaussian mixture model (GMM) [2]. This model is sufficiently powerful to discriminate among individual features, and so is used in this work.

2. GLOTTAL PARAMETERS ESTIMATION

In several important applications of speech processing, including speech analysis, speaker recognition, and speech coding, it is advantageous to extract features of the excitation signal. These features can contain speaker-specific and phoneme-specific properties that can be exploited in a targeted way to improve performance of several speech processing applications. For example, it has been shown in [11] that excitation features can be used to improve the speaker recognition task. Source signals, which in some application referrers to as glottal flow or excitation signal, can be achieved by inverse filtering of the speech waveform. According to the source-filter model view of speech production, in discrete time, the speech waveform s[n] is the output of the vocal tract filter with impulse response h[n], excited by the source signal u[n]. According to an all- pole representation of the vocal tract with transfer function in frequency domain:

$$H(z) = \frac{1}{1 - \sum_{i=1}^{p} a_i z^{-i}} \qquad (1)$$

The speech signal basically is a result of convolving between the source signal (excitation) and the vocal tract impulse response. Therefore, we have:

$$s[n] = \sum_{i=1}^{p} a_i s[n-i] + u[n] \qquad (2)$$

The speech signal in discrete time domain. To get the source from speech signal, the filter coefficients a_i should be estimated from the speech signal s[n]. To do so the covariance method of linear prediction is used. Covariance-based linear prediction is preferred over the autocorrelation method because, when the waveform follows the assumed all-pole model, the analysis window over which the prediction error is defined results in the correct solution for any window length greater than the prediction order [12]. After the filter coefficients are calculated, The source signal can be determined through the deconvolution operation. Simply, it is the convolution of the speech signal with an all-zero filter parameters obtained from the previous method. Figure 1 shows an example of the voiced speech signal waveform and its envelope (vocal tract transfer function) and the source signal (the excitation). The LPC order used in our method is equal to sampling frequency in kHz.

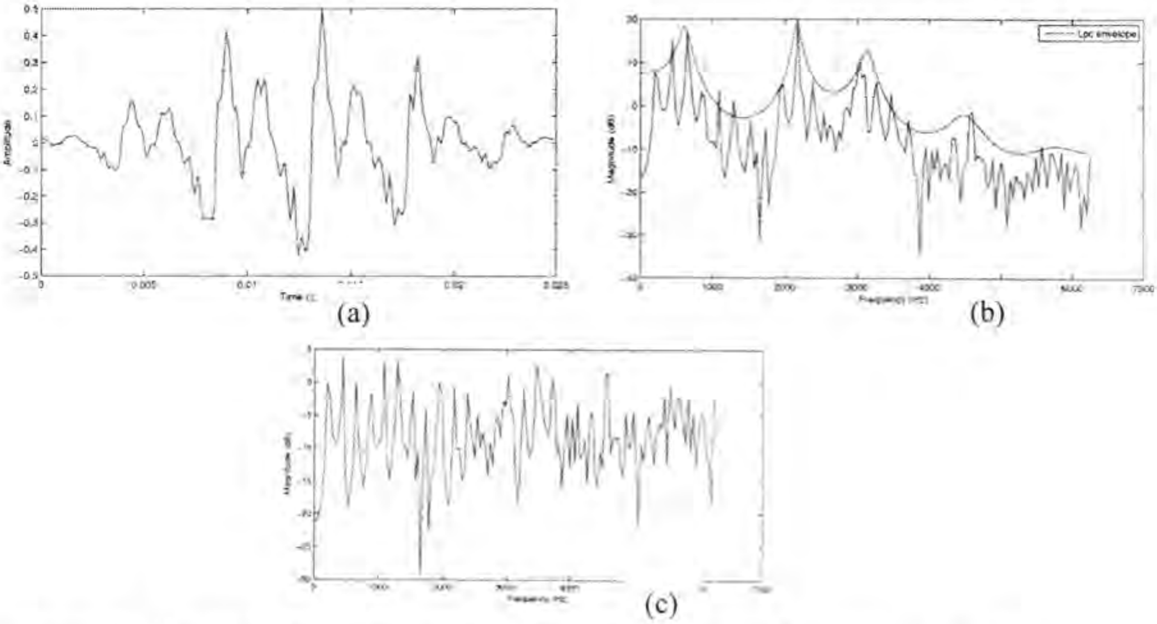

Figure-1: Segment of voiced speech (a), Signal spectrum and vocal tract envelope estimation (b), Glottal source signal(LP residual signal spectrum (c).

3. AM-FM MODEL

AM-FM speech signal modulation used to decompose a speech signal into its modulated components of envelope (instantaneous amplitude) and phase (instantaneous frequency). Subject to nonlinear and time-varying phenomena during speech production, i.e., the frequency content or spectrum changes with time, the AM-FM modulation model comes to seek and exploit the rich set of time-varying frequencies inherent in the speech signal and employed them in many speech signal applications. For example, in [13] AM-FM approach was used in the context on formant tracking, in [14] the model is employed in the speech recognition application. In [15] and [16] the AM-FM model is adopted for the purpose of speaker identification, both works used speech signal in the parameters encoding for speaker identification.

In order to characterise a modulation component for a speech signal, first, a single-valued frequency signal must be generated by breaking the signal down into its frequency components. To do that, a filterbank consist of set of bandpass filters are adopted. The idea is to perform the method of multi band demodulation analysis (MDA) as its described in [13]. We used the Gabor bandpass filters because they are optimally compact and smooth in both the time and frequency domains. This characteristic guarantees accurate amplitude and frequency estimates in the demodulation stage [13]. The analytic signal is then constructed for each bandpass output waveform; it is a transformation of the real signal into the complex domain and it is adopted because it permits the characterisation of the real input in terms of instantaneous amplitude and frequency [17]. Mathematically; given a real input signal s[n], its analytic signal can be computed as

$$s_a[n] = s[n] + jH[s[n]] = s[n] + j\hat{s}[n] \qquad (3)$$

where the quadrature signal sˆ[n] is the Hilbert transform of speech signal s(t). From the analytic and speech signal the phase φ(t) can be calculated as

$$\phi[n] = \arctan\left(\frac{\hat{s}[n]}{s[n]}\right) \qquad (4)$$

The instantaneous frequency (IF) of the signal can be computed directly from the phase as:

$$f[n] = \frac{1}{2\pi}.\frac{d\phi[n]}{dt} \qquad (5)$$

The instantaneous amplitude is computed as:

$$\hat{a}[n] = \sqrt{s^2[n] + \hat{s}^2[n]} \qquad (6)$$

To get the proper values of instantaneous frequency, instantaneous amplitude and instantaneous frequency are combined together to obtain a mean-amplitude weighted short-time estimate Fi of the instantaneous frequency for each bandpass filter output (waveform) [13].

$$F_i = \frac{\int_{n_0}^{n_0+\tau}[f[n].\hat{a}^2[n]]dt}{\int_{n_0}^{n_0+\tau}[\hat{a}^2[n]]dt} \qquad (7)$$

where τ is the selected length of the time-frame. The adoption of a mean amplitude weighted instantaneous frequency in (7) is motivated by the fact that it provides more accurate frequency estimates and is more robust for low energy and noisy frequency bands when compared with an unweighted frequency mean [13].

The computation of the short-time instantaneous frequency for each source signal leads to the extraction of the speaker descriptors set that used as a system parameters. Figure 2 shows a example of one channel output source signal and its instantaneous amplitude and frequency.

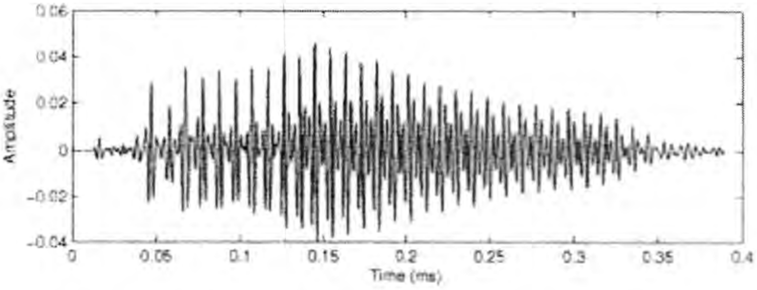

(a) Source signal and its instantaneous amplitude

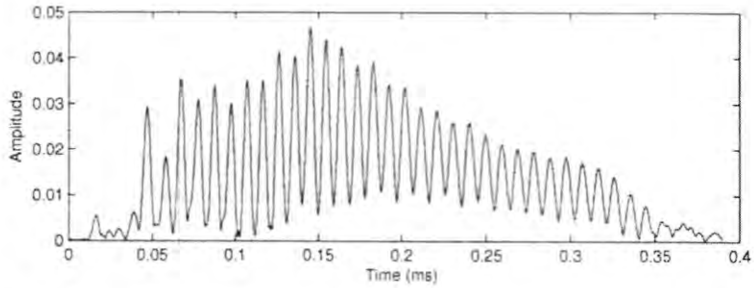

(b) The instantaneous amplitude of the source signal

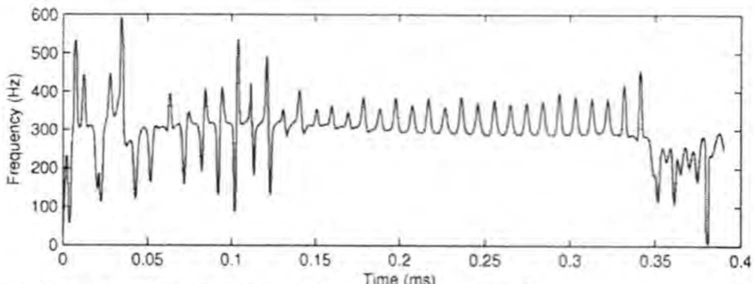

(c) The instantaneous frequency of the source signal

Figure-2: One channel source signal (a), The instantaneous amplitude (b), The instantaneous frequency (c).

4. THE MODULATION PARAMETERS OF THE GLOTTAL COMPONENTS

For our experiment, the filterbank adopted consist of 40-channels Gaussian filterbank with center frequencies that are Mel-scale spaced on the frequency axis and varying bandwidth follows the principles of constant-Q or Multiscale wavelet-like filterbank. Feature vector should be generated from each channel output of the band passed source signal with the use of a filterbank. The bandpassed waveform is then demodulated and its instantaneous amplitude and frequency computed. Through the application of AM-FM modulating schema on the source signal it has been found that the source signal firstly should be pre-emphasised (in order to balance the signal spectrum) by applying the following single-zero filter:

$$s[n] = x[n] - a.x[n-1] \qquad (8)$$

where the value of a is generally taken in the interval [.95,.98]; its .96 in our experiment. The instantaneous amplitude and frequency of each filter bank channel are then components together to obtain a mean-amplitude weighted short- time estimate of the instantaneous frequency of each source signal. As shown in equation (7) each frame with the length of τ will give one value represents the weighted instantaneous frequency of that length. Therefore, the output of each channel of the filter will be (with an overlap window of τ /2):

$$K = \left((\frac{2L}{\tau}) \right) - 1 \qquad (9)$$

where L represents the length of the signal.

After applying all channels of the filter bank and compute the feature vector of each channel output, the utterance of each individual can be represented by N ×K an matrix, where N is the number of filter channels, and K corresponds to the number of times that the input signal (one channel output) can be segmented into the short time segment with a given window length; the value τ in (7). The generating of the features vectors will be repeated for all that we used in the database. This will allow us to keep information about all the persons that we need to test their features.

5. SPEECH DATABASE

In our speaker identification experiments, a set of text- dependent British Telecom Millar database was used. The set contains the recordings of 60 speaker(46 male and 14 female) obtained in five different session with a time separation of about three months. The recordings were carried out in a quiet environment with high-quality microphone and each speaker participated in five recording sessions and spoke the digits 1 through 9, zero, oh and nought five times in each session. The first and second recording sessions (10 repetitions) were used for training while the rest of the data (15 repetitions) were used for testing.

6. SPEAKER IDENTIFICATION

The adopting experiment is not working on the frame-by- frame basis, instead the whole speech signal is taken as one segment passing through the Gabor filterbank. The wave- form of each channel is demodulated by Hilbert transform de- modulation (HTD)method and then its instantaneous ampli- tude and instantaneous frequency is computed. Then the two (instantaneous amplitude/frequency) are combined together to produce the mean amplitude weighted instantaneous frequency, which represent many values that describe the mod- ulating components of the signal at that filter channel. After passing the signal through the whole filter channels, a set of feature vectors (the model parameters for speaker identifica- tion) will be generated. The speaker identifiability based on the AM-FM signal modulation features is then determining through a Gaussian mixture model (GMM). Its adopted as is famously known of the most successful method in modeling human identity from speech [2]. Each Gaussian is characterized by a diagonal covariance matrix. This choice is based on the empirical evidence that diagonal matrices outperform full matrices and the fact that the probability density modeling of an Mth-order full covariance matrix can equally well be achieved using a diagonal covariance lager-order mixture [18]. Based on theGMMmodeling, each speaker (in both training and testing stages) is described by a mixture of ***M*** Gaussian models ; which are the weighted sum of the ***M*** component densities and called the mixture densities. Statistically, for each feature vector *~x*, the conditional probability is computed from the mixture equation:

$$p(\vec{x}|\Gamma) = \sum_{m=1}^{M} c_m.\gamma_m(\vec{x}) \qquad (10)$$

where cm are the mixture weights and γm (~x) an N-variate Gaussian function.

The dimensionality of the Gaussian function equal to the dimensionality of the feature vector or the filterbank channel used in the experiment.

For the values of mixture weights a special case of the expectation-maximization (EM) algorithm [18] is used, while for the number of component densities in the mixture model is chosen to be between (5 to 7) Gaussians. Our experiments showing that increasing the number of Gaussians beyond this values did not improve the performance of the classifier with AM-FM features. A set of S speakers {s1 , s2 , ..., sS } is represented by S Gaussian mixture models {Γ1 , Γ2 , ..., ΓS }.

A given observation sequence $X = [x_1, ..., x_K]$ is tested by finding the speaker model which has maximum a posteriori probability. By applying Bayes rule and using the logarithm [18], the probability can be computed as

$$\hat{S} = \arg\max \sum_{m=1}^{M} \log p(\vec{x}|\Gamma). \qquad (11)$$

To make the system more flexible, the process of feature vectors generation should focus only on the parts of utterance when frames contain meaningful and speaker dependent fea-tures (voiced segments in this case).

7. RESULTS

Many parameters can have an extremely important role in the computation of the signal modulating features as well as the system performance. These extend from the type of central frequencies scale employed in the experiment, the effective rms bandwidth of each filter channel, and the number of mod- els in the Gaussian mixture used in the decision-making step. In our experiment the filterbank adopted consist of a set of 30

Gabor bandpass filters with center frequencies that are evenly spaced on the Mel-scale frequency axis, while the bandwidth of the filters are set as:

$$\sigma_m = \frac{f_m}{3\sqrt{\ln 2}}. \qquad (12)$$

where f_m is the central frequencies. This is simply the constant-Q property or multiscale wavelet-like filter bank. It adopted because the error band across the filter channels should be made constant across the spectrum [19].

In terms of the number of mixture models of the GMM, 5 to 7 Gaussians is the proper number; the experiment shows that the increasing of Gaussian model component does not improve the performance. The speaker identification system construct of those parameters is employed in the calculation of modulating features of the speech and source signals. Based on the short-time energy function, where unvoiced regions have lower short-time energy than voiced regions, the rate of voiced regions (VR) that are embedded in each spoken word is referred to in each figure. Figure **3** show the result of digits zero, three, and eight for both source and speech signals respectively. They show how that the AM-FM source signal modeling features presented from voiced-containing utterance can achieve up to 10% accuracy over the results obtained from the speech signal of the same word. Figure **4** shows the result of digits one, two, and nougth for both source and speech signals respectively. Its clearly that the source signal of the voiced utterance can captured a more speaker dependence features than the speech signal in the context of AM-FM signal modulation approach.

Finally, Figure 5 shows speaker identification system performance for the whole database (all digits combined together) for both source and speech signal. This Figure will represent the voiced and unvoiced utterance in the speech database, which in term reflect the power of the

modulation components of both cases.
Form this Figure we can see that source and the signal components can hold lots of modulation information that can be used in estimation the speaker parameters that can be used in speaker recognition system.

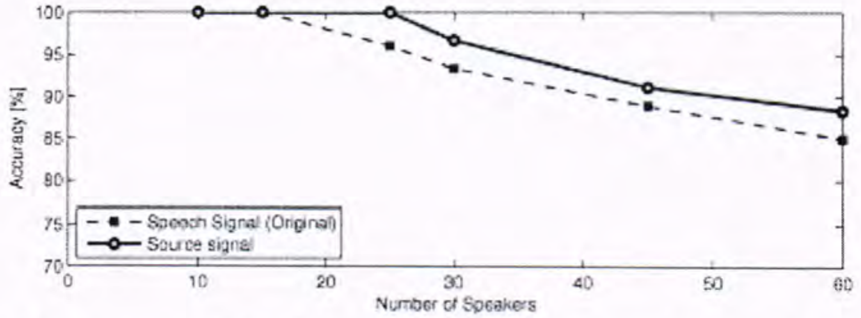

(a) Speaker identification accuracy of the reference GMM classifier for the word zero. VR=25%

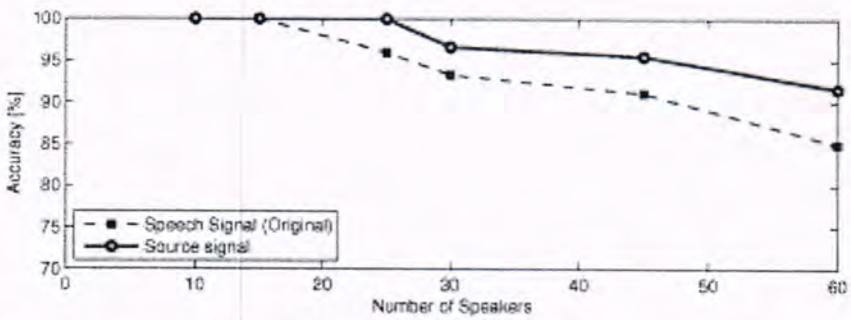

(b) Speaker identification accuracy of the reference GMM classifier for the word three. VR=35%

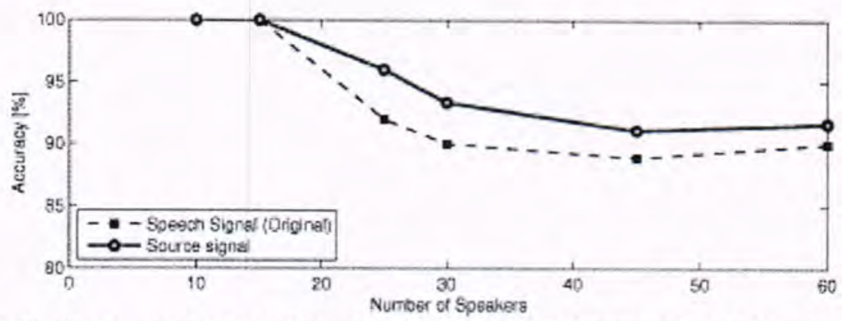

(c) Speaker identification accuracy of the reference GMM classifier for the word eight. VR=20%

Figure-3: Shows the effect of the source signal on speaker recognition in the case of voiced speech.

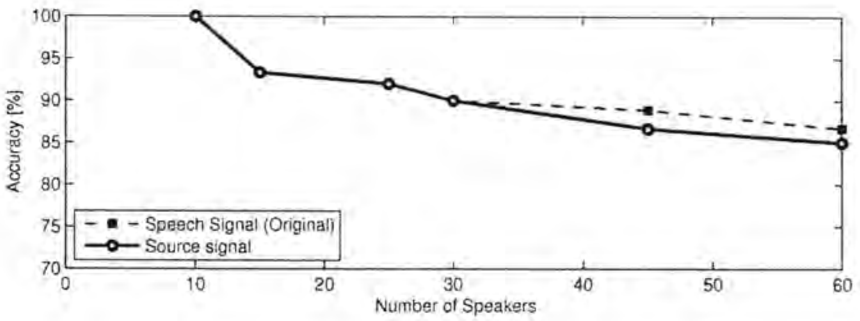

(a) Speaker identification accuracy of the reference GMM classifier for the word one. VR=10%

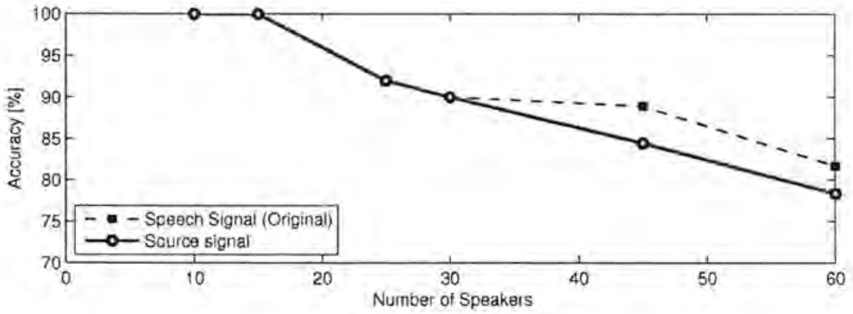

(b) Speaker identification accuracy of the reference GMM classifier for the word two. VR=5%

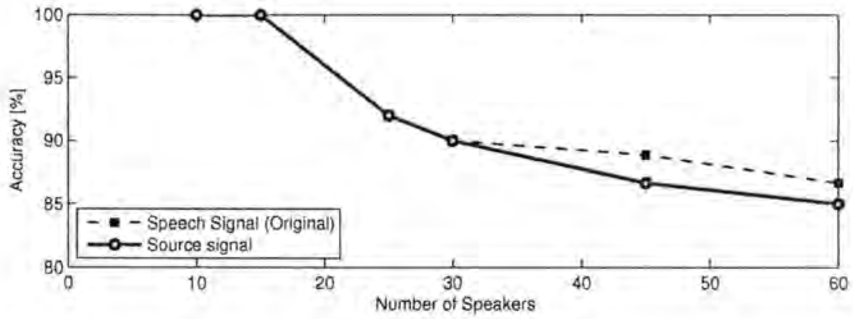

(c) Speaker identification accuracy of the reference GMM classifier for the word nought. VR=10%

Figure-4: Shows the effect of the source signal on speaker recognition in the case of unvoiced speech.

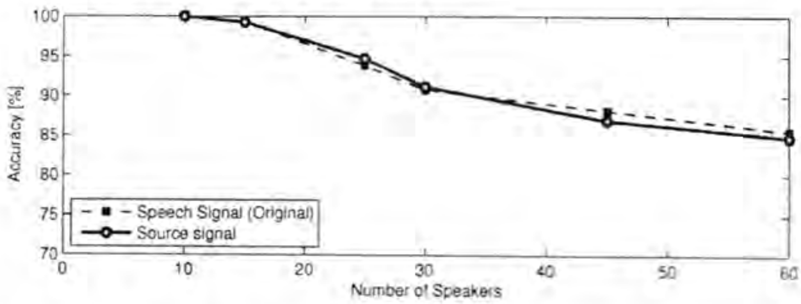

Figure-5:Speaker identification accuracy of the complete (all digits) database

8. CONCLUSION

In this paper, we showed that the source signal came from voiced-containing utterance contain speaker dependence features more than the speech signal itself. The result shows that the modulating features of the source signal extracted by the method of Hilbert transform demodulation (HTD) can improve the performance up to 10% when these sources came from voiced speech. However, the speech signals can give similar or beter result in the case of non-voiced speech. The only justify of this situation is, in the context of text- dependent speaker identification application, since the source signal can be assumed as a digital image of what happening in the vocal folds during speaking that can be reflected in the slitlike opening between the folds, which referred to as the glottis. Also, such glottal characteristics have been proven to contain speaker dependence [11]. Moreover, the phoneme classes are acoustically associated with the formant structure (central frequency and bandwidth), and the formant structures are relatively stable for a specific phoneme across different speakers [20]. Thus the features derived from the vocal tract spectrum carry the information useful for speech recognition and its just not pertinent to the speaker identity. In the case of non-voiced utterance, the source signal can be assumed as noise-like signal. So the features come from one individual can happen at the same class of the features come from another individual, and this case can profoundly degrade the performance of the speaker identification system.

9. REFERENCES

1. P. Joseph Campbell, "Speaker recognition: a tutorial," Proceedings of the IEEE, vol. 85, no. 9, pp. 1437–1462, 1997.
2. F. Bimbot, J-F. Bonastre, C. Fredouille, G. Gravier, I. Magrin-Chagnolleau, S. Meignier, T. Merlin, J. Ortega-Garc´ıa, D. Petrovska-Delacre´taz, and D. A. Reynolds, "A tutorial on text-independent speaker verification," EURASIP J. Appl. Signal Process., vol. 2004, pp. 430–451, 2004.
3. J. F. Bonastre, F. Bimbot, L. Boe, J. Campbell, D. Reynolds, and I. Magrin-Chagnolleau, "Person authentication by voice: A need for

caution," Eurospeech Processing, Genoe, Italy, pp. 33–36, Sep 2003.

4. M. Foundez-Zanuy, S. McLaughlin, A. Esposito, A. Hussain, J. Schoentgen, G. Kubin, W. B. Kleijn, and P. Maragos, "Nonlinear speech processing: Overview and applications," Int. J. Control Intelligent System, vol. 30, no. 1, pp. 1–10, 2002.
5. B. Boashash, "Estimating and interpreting the instantaneous frequency of a signal- part 1: Fundamentals," Proceedings of the IEEE, vol. 80, no. 4, pp. 540–568, Apr 1992.
6. M.S. Deshpande and R.S. Holambe, "Speaker identification based on robust am-fm features," in International Conference on Emerging Trends in Engineering and Technology (ICETET), 2009, pp. 880–884.
7. T.H. Falk and Wai-Yip Chan, "Modulation spectral features for robust far-field speaker identification," IEEE Transactions on Audio, Speech, and Language Processing, vol. 18, no. 1, pp.90–100, 2010.
8. S. Pandiaraj, D.S. Vinothini, H.N.R. Keziah, L. Gloria, and K.R.S. Kumar, "Speaker identification using pykfec and aann," in International Conference on Electronics Computer Technology (ICECT), 2011, vol. 3, pp. 313–316.
9. P. Tsiakoulis, A. Potamianos, and D. Dimitriadis, "Short-time instantaneous frequency and bandwidth features for speech recognition," in IEEE Workshop on Automatic Speech Recognition Understanding, 2009. ASRU 2009, 2009, pp. 103–106.
10. K.Gopalan and Tao Chu, "Keyword word recognition using a fusion of spectral, cepstral and modulation features," in International Conference on Electrical Communications and Computers (CONIELECOMP), 2012, pp. 234–238.
11. M.D. Plumpe, T.F. Quatieri, and D.A. Reynolds, "Modeling of the glottal flow derivative waveform with application to speaker identification," Speech and Audio Processing, IEEE Transactions on, vol. 7, no. 5, pp. 569–586, Sep 1999.
12. L. R. Rabiner and R. W. Schafer, Introduction to Digital Speech Processing, Now Publishers, USA, 2007.
13. Alexandros Potamianos, Ros Potamianos, and Petros Maragos, "Speech formant frequency and bandwidth tracking using multiband energy demodulation," J. Acoust. Soc. Amer, vol. 99, pp. 3795–3806, 1996.
14. D. Dimitriadis, P. Maragos, and A. Potamianos, "Robust am- fm features for speech recognition," Signal Processing Letters, IEEE, vol. 12, no. 9, pp. 621–624, Sept. 2005.
15. R. Jankowski, T. Quatieri, and D. Reynolds, "Measuring fine

structure in speech: application to speaker identification," in International Conference on Acoustics, Speech, and Signal Processing (ICASSP'95), May 1995, vol. 1, p. 325.
16. M. Grimaldi and F. Cummins, "Speaker identification using instantaneous frequencies," IEEE Transactions on Audio, Speech, and Language Processing, vol. 16, no. 6, pp. 1097– 1111, Aug. 2008.
17. A. Rao and R. Kumaresan, "On decomposing speech into modulated components," IEEE Transactions on Speech and Audio Processing, vol. 8, no. 3, pp. 240–254, May 2000.
18. D.A. Reynolds and R.C. Rose, "Robust text-independent speaker identification using gaussian mixture speaker models," Speech and Audio Processing, IEEE Transactions on, vol. 3, no. 1, pp. 72–83, Jan 1995.
19. A.C. Bovik, P. Maragos, and T.F. Quatieri, "Am-fm energy detection and separation in noise using multiband energy operators," Signal Processing, IEEE Transactions on, vol. 41, no. 12, pp. 3245, Dec 1993.
20. S. Umesh, L. Cohen, N. Marinovic, and D.J. Nelson, "Scale transform in speech analysis," Speech and Audio Processing, IEEE Transactions on, vol. 7, no. 1, pp. 40 –45, Jan. 1999.

Vol. 24
No. 5
2013

مجلة علوم المستنصرية

تصدر عن كلية العلوم الجامعة المستنصرية

عدد خاص ببحوث المؤتمر العلمي التاسع لكلية العلوم/ الجامعة المستنصرية للفترة من 6-7 ايار 2013

Mobile: 07711184399
e-mail: mustjsci@yahoo.com

مجلة علوم المستنصرية

هي مجلة علمية رصينة تصدر عن عمادة كلية العلوم في الجامعة المستنصرية في تخصصات الكيمياء والفيزياء وعلوم الحياة وعلوم الحاسبات وعلوم الجو. تقوم المجلة بنشر البحوث العلمية التي لم يسبق نشرها في مكان آخر بعد إخضاعها للتقويم العلمي من قبل مختصين وباللغتين العربية او الانكليزية وتُصدر المجلة عددين سنوياً بكلا اللغتين.

تعليمات النشر في المجلة

1. يقدم الباحث طلبا تحريريا لنشر البحث في المجلة ويكون مرفقا بأربع نسخ من البحث مطبوعة على ورق ابيض قياس (A4, 21.6×27.9 cm) مع ترك حاشية بمسافة انج واحد لكل اطراف الصفحة ومطبوعة بأستخدام برنامج (Microsoft Word, 97-2003) بصيغة (.doc).
2. يرفق مع البحث ملخص باللغة العربية وآخر باللغة الإنجليزية على ان لاتزيد كلمات الملخص عن (150) كلمة.
3. عدد صفحات البحث لاتتجاوز 10 صفحة بضمنها الاشكال والجداول على ان تكون الاحرف بقياس 14 نوع (Time New Roman) وبمسافة مزدوجة بين الاسطر. وينبغي ترتيب اجزاء البحث دون ترقيم وبالخط العريض (Bold) كالاتي: صفحة **العنوان، الخلاصة باللغة العربية، الخلاصة باللغة الإنجليزية، مقدمة، المواد وطرائق العمل (الجزء العملي)، النتائج والمناقشة، الاستنتاجات وقائمة المراجع.**
4. يطبع عنوان البحث واسماء الباحثين (كاملة) وعناوينهم باللغتين العربية والانكليزية على ورقة منفصلة شرط ان لاتكتب اسماء الباحثين وعناوينهم في أي مكان اخر من البحث ، وتعاد كتابة عنوان البحث فقط على الصفحة الاولى من البحث.
5. ترقم الجداول والأشكال على التوالي حسب ورودها في المخطوط، وتزود بعناوين، ويشار إلى كل منها بالتسلسل نفسه في متن البحث.
6. يشار الى المصدر برقم يوضع بين قوسين بمستوى السطر نفسه بعد الجملة مباشرة [1]، [2]، [3] وهكذا. تطبع المصادر على ورقة منفصلة ، ويستخدم الاسلوب الدولي المتعارف عليه عند ذكر مختصرات اسماء المجلات.
7. يتبع الاسلوب الاتي عند كتابة قائمة المصادر على الصفحة الاخيرة كالاتي: ترقيم المصادر حسب تسلسل ورودها في البحث ، يكتب الاسم الاخير (اللقب) للباحث او الباحثين ثم مختصر الاسمين الاولين فعنوان البحث ، مختصر اسم المجلة ، المجلد ، العدد ، الصفحات الاولى والاخيرة ، سنة نشر البحث. وفي حالة كون المصدر كتابا يكتب بعد اسم المؤلف او المؤلفين عنوان الكتاب ، الطبعة ، الصفحات ، سنة النشر ، المؤسسة الناشرة، الدولة مكان الطبع.

بخصوص اجور النشر يتم دفع مبلغ (50000) خمسون الف دينار عند تقديم البحث للنشر وهي غير قابلة للرد ومن ثم يدفع الباحث (25000) عشرون الف دينار اخرى عند قبول البحث للنشر.

جميع البحوث ترسل الى:
رئيس تحرير المجلة
أ. د. رضا ابراهيم البياتي
كلية العلوم- الجامعة المستنصرية
البريد الاليكتروني: mustjsci@yahoo.com

المحتويات

طريقة عامة لحل نظام المعادلات الخطية المضببة

أسماء زياد محمد الكاتب و باسل يونس ذنون
كلية علوم الحاسوب والرياضيات، جامعة الموصل
تاريخ تقديم البحث 2013/3/18 - تاريخ قبول البحث 2013/9/15

ABSTRACT

This paper deals with the issue of representation of a fuzzy linear system of equations and some methods of their solution. A short review is given of two methods available to solve these equations, these methods are fundamentally dependent on the prior identification of the used fuzzy numbers. A general method is then proposed for solving a system of linear fuzzy equations. An illustrative example the suggested method is given.

الخلاصة

يتناول هذا البحث مسألة تمثيل نظام من المعادلات الخطية المضببة وبعض طرائق حلها. وتستعرض أولاً طريقتين منشورتين لحل هكذا معادلات، وهذه الطريقتين تعتمد أساسا على تحديد مسبق لأشكال الأعداد المضببة المستخدمة. ثم تُقترح طريقة عامة لحل المعادلات الخطية المضببة لا تعتمد على أشكال الأعداد المضببة. ويقَدم مثال توضيحي للطريقة المقترحة .

1- المقدمة:

إن المعادلة الرياضية هي تمثيل رياضي يتضمن ثوابت constants ومتغيرات Variables ودوال رياضية. وتُستخدم المعادلة الرياضية عادة لوصف نظام معين باستعمال لغة الرياضيات بواسطة العلاقات بين المتغيّرات المختلفة، وعادة ما تحتوي المعادلة على مجهول واحد أو أكثر وهذه المجاهيل يطلق عليها المتغيرات أو الكميات الغير معينة. وتوصف المعادلة بأنها ذات متغير واحد أو متغيرين أو ثلاثة أو أكثر حسب عدد المتغيرات التي تحتويها، ويطلق على المعادلة أنها متحققة بالنسبة لقيم معينة من المتغيرات عندما يتم استبدال المتغيرات بهذه القيم [1].

تعدُّ المعادلات المضببة إحدى المجالات التي تتعامل معها نظرية المجموعات المضببة والتي تلعب فيها الأعداد المضببة والعمليات الحسابية عليها دوراً أساسياً. تُعرّف المعادلة المضببة بأنها معادلة رياضية تتضمن ثوابت أو متغيرات مضببة.

لنفرض أن لدينا المعادلة الرياضية:

$$A+X=B \qquad (1)$$

إذ إن A و B كميتان ثابتتان و X هو متغير. لقد بيّن [2] وجه الاختلاف في هذا النوع من المعادلات في حالة كون A و B عددان حقيقيان أو عددان مضببان: فكما هو معروف جيداً إذا كان **A** و B عددان حقيقيان فإن حل المعادلة (1) سيكون **X=B - A**. أما إذا كان A و B عددان مضببان فإن المقدار X=B - A لا يعدُّ حلا للمعادلة (1)، وكذلك إذا كانت لدينا المعادلة الرياضية:

$$X=B.A \qquad (2)$$

ولنفرض أن كل من A و B عدداً مضبباً، وكما هو الحال في النوع السابق من المعادلات فإنه ليس من الصعب إثبات أن **X=B/ A** ليس حلاً لهذا النوع من المعادلات المضببة.

يتناول هذا البحث بعض التعاريف الأساسية الخاصة بالمجموعات المضببة والأعداد المضببة والعمليات الحسابية عليها، كما يوضح مسألة تمثيل نظام من المعادلات الخطية المضببة وتذكر بعض طرائق حل مثل هكذا نظام. كما نقدم في هذا البحث خوارزمية مقترحة تعدّ طريقة عامة لحل النظام الخطي المضبب.

2- تعاريف أساسية:

سنذكر في هذه المبحث بعض التعاريف التي نحتاج إليها في المباحث اللاحقة وهذه التعاريف مقتبسة من المصادر [2]،[3]،[4]،[5].

التعريف (1): لتكن X هي المجموعة الشاملة فإن **المجموعة المضببة** A Fuzzy set من X هي مجموعة كل الأزواج المرتبة بالشكل: $A=\{ (x ,A(x)) \}$ لجميع قيم $x\in X$

إذ إن دالة العضوية A(x) هي درجة انتماء العنصر x إلى المجموعة A.

التعريف(2): إن **الداعم** Suppor للمجموعة المضببةA يُعرَّف على النحو الآتي:

$\text{Supp}(A) = \{x \in X : A(x) > 0\}$

التعريف(3): يقال للمجموعة المضببة A من X أنها **محدبة** Convex إذا كان لكل عنصرين $x_1, x_2 \in X$ ولكل $\lambda \in [0,1]$ يكون:

$A[\lambda x_1 + (1-\lambda)x_2] \geq \text{nim}\{A(x_1), A(x_2)\}$

التعريف(4): قطع-α للعدد المضبب C يعرَّف على $\mathbb{R}$ على النحو الآتي:

$C_\alpha = \{x \in \mathbb{R} : C(x) \geq \alpha\}\ ;\ \in \alpha\ (0,1)$

ويمكن كتابة قطع-α للعدد C بشكل فترة مغلقة على النحو الآتي: $C_\alpha = [c_1^\alpha, c_2^\alpha]$ لأي قيمة α حيث $\alpha \in (0,1]$.

التعريف(5): إن المجموعة الجزئية المضببة C من خط الأعداد الحقيقية $\mathbb{R}$ مع دالة الانتماء $C(x): \mathbb{R} \to [0,1]$ تسمى **عدداً مضبباً** Fuzzy Number إذا تحقق كل مما يأتي:

1. C هي مجموعة مضببة اعتيادية Normal ، أي إنه يوجد عنصر $x_0 \in \mathbb{R}$ بحيث إن $C(x_0) = 1$.
2. C هي مجموعة مضببة محدبة.
3. إن يكون C_α فترة مغلقة لجميع قيم $\alpha \in [0,1]$.
4. إن الداعم للمجموعة المضببة C يكون مقيداً Bounded.

التعريف(6): نرمز **للعدد المضبب شبه المنحرف** Trapezoidal Fuzzy Number بالرمز $C=(a,b,\gamma,\beta)$، إذ إن الفترة $[a-\gamma, b+\beta]$ هي الداعم للعدد C، وان $b > a$. إذا كان $\gamma = \beta$ فإن العدد C يسمى **عدد مضبب شبه منحرف متناظر** Symmetric Trapezoidal Fuzzy Number إن دالة الانتماء للعدد المضبب شبه المنحرف C تُعرَّف تحليلياً على النحو الآتي:

$$C(x) = \begin{cases} \frac{x-a+\gamma}{\gamma} & ; \quad a-\gamma \leq x < a \\ 1 & ; \quad a \leq x \leq b \\ \frac{b+\beta-x}{\beta} & ; \quad b < x \leq b+\beta \\ 0 & ; \quad \text{otherwise} \end{cases}$$

التعريف(7): نرمز **للعدد المضبب المثلثي** Triangle Fuzzy Number بالرمز $U=(a,b,c)$، إذ إن الفترة $[a,c]$ هي الداعم للعدد U، وان $c > b > a$. وإذا كان $b-a=c-b$ فان العدد U يسمى **عدد مضبب مثلثي متناظر** Symmetric Triangle Fuzzy Number. إن دالة الانتماء للعدد المضبب المثلثي U تُعرَّف تحليلياً على النحو الآتي:

$$U(x) = \begin{cases} \frac{x-a}{b-a} & ; \quad a \leq x \leq b \\ \frac{c-x}{c-b} & ; \quad b < x \leq c \\ 0 & ; \quad \text{otherwise} \end{cases}$$

التعريف(8): إن **تمثيل قطع- α** Representation -α للعدد المضببC هو زوج مرتب من الدوال $[L_c(\alpha), R_c(\alpha)]$ كلاهما معرَّف من الفترة [0,1] إلى $\mathbb{R}$ على النحو الآتي:

$L_c(\alpha) = \inf\{x : x \in C_\alpha\}$,

$R_c(\alpha) = \sup\{x : x \in C_\alpha\}$,

لكل $\alpha \in [0,1]$. وعلى ضوء ذلك يمكن كتابة العدد المضبب C بالشكل: $C_\alpha = [L_C(\alpha), R_C(\alpha)]$.

التعريف(9): لأي عددين مضببين X و Y إذ إن $X_\alpha = [L_x(\alpha), R_x(\alpha)]$ و $Y_\alpha = [L_y(\alpha), R_y(\alpha)]$ ولأي عدد حقيقي k تُعرف العمليات الحسابية حسب قاعدة لطفي زادة على النحو الآتي :

1. المساواة:

$Y = X$ إذا وفقط إذا كان $L_y(\alpha) = L_x(\alpha)$ و $R_y(\alpha) = R_x(\alpha)$ ، لكل $\alpha \in [0 , 1]$.

2. الجمع:

$$(Y + X)_\alpha = Y_\alpha + X_\alpha = [L_y(\alpha) , R_y(\alpha)] + [L_x(\alpha) , R_x(\alpha)] = [L_y(\alpha) + L_x(\alpha) , R_y(\alpha) + R_x(\alpha)]$$

3. الطرح

$$(Y - X)_\alpha = Y_\alpha - X_\alpha = [L_y(\alpha) , R_y(\alpha)] - [L_x(\alpha) , R_x(\alpha)] = [L_y(\alpha) - R_x(\alpha) , R_y(\alpha) - L_x(\alpha)]$$

4. الضرب:

$$(Y \times X)_\alpha = Y_\alpha \times X_\alpha = [L_y(\alpha) , R_y(\alpha)] \times [L_x(\alpha) , R_x(\alpha)]$$

$$= [\min \{L_y(\alpha).L_x(\alpha), L_y(\alpha).R_x(\alpha), R_y(\alpha).L_x(\alpha), R_y(\alpha).R_x(\alpha)\} , \max \{L_y(\alpha).L_x(\alpha), L_y(\alpha).R_x(\alpha), R_y(\alpha).L_x(\alpha), R_y(\alpha).R_x(\alpha)\}]$$

5. الضرب بعدد قياسي:

$$(kX)_\alpha = \begin{cases} [kL_x(\alpha) , kR_x(\alpha)] & ; k \geq 0 \\ [kR_x(\alpha) , kL_x(\alpha)] & ; k < 0 \end{cases}$$

التعريف(10): يكون العدد المضبب X عددا موجبا positive إذا كان $L_x(1) \geq 0$ ، ويكون عدداً موجباً صارماً strict positive إذا كان $L_x(1)>0$، ويكون عدداً سالباً negative إذا كان $R_x(1) \leq 0$ ويكون عدداً سالباً صارماً strict negative إذا كان $R_x(1)<0$. ونقول أن العددين المضببين X و Y لهما الإشارة نفسها إذا كان كلاهما موجب أو كلاهما سالب.

3- نظام المعادلات الخطية المضببة:

Fuzzy Linear System of Equations

لقد وضح [2] كيفية حل المعادلتين المضببتين (1) و (2) باستخدام قطع-α، فإذا كانت $A_\alpha = [a_1^\alpha, a_2^\alpha]$ و $B_\alpha = [b_1^\alpha , b_2^\alpha]$ و $X_\alpha = [x_1^\alpha , x_2^\alpha]$ تشير إلى قطع-α لكل من A و B و X، على التوالي، وبالتالي فإن المعادلة $A_\alpha + X_\alpha = B_\alpha$ يكون لها الحل $X_\alpha = [b_1^\alpha - a_1^\alpha , b_2^\alpha - a_2^\alpha]$ إذا وفقط إذا تحقق ما يلي:

1. $b_2^\alpha - a_2^\alpha \geq b_1^\alpha - a_1^\alpha$ لجميع قيم $\alpha \in (0,1]$ ،
2. إذا كان $\alpha \leq \beta$ فإن ذلك يؤدي إلى

$$b_2^\beta - a_2^\beta \leq b_2^\alpha - a_2^\alpha. \leq b_1^\beta - a_1^\beta \leq b_1^\alpha - a_1^\alpha$$

وبالتالي فإن حل المعادلة المضببة (1) يكون على النحو الآتي **[6]**:

$$X = \bigcup_{\alpha \in (0,1]} X^\alpha$$

حيث أن $X^\alpha = \alpha . X_\alpha$.

وكذلك يكون للمعادلة $A_\alpha . X_\alpha = B_\alpha$ الحل $X_\alpha = [b_1^\alpha / a_1^\alpha , b_2^\alpha / a_2^\alpha]$ إذا وفقط إذا تحقق كل مما يلي:

1. $b_2^\alpha / a_2^\alpha \geq b_1^\alpha / a_1^\alpha$ ، لجميع قيم $\alpha \in (0,1]$،
2. إذا كان $\alpha \leq \beta$ فإن ذلك يؤدي إلى

$$b_2^\beta / a_2^\beta \leq b_2^\alpha / a_2^\alpha. \leq b_1^\beta / a_1^\beta \leq b_1^\alpha / a_1^\alpha$$

حيث أن $a_1^\alpha \neq 0$ و $a_2^\alpha \neq 0$ ، لجميع قيم $\alpha \in (0,1]$.

وبالتالي فإن حل المعادلة المضببة (2) يكون على النحو الآتي:

$$X = \cup_{\alpha\in(0,1]} X^{\alpha}.$$

حيث أن $X^{\alpha} = \alpha \,.\, X_{\alpha}$.

التعريف(11): تسمى المصفوفة $A=[a_{ij}]$ **مصفوفة مضببة** fuzzy matrix إذا كان جميع عناصر A هي أعداد مضببة ، وتسمى المصفوفة A مصفوفة مضببة موجبة (سالبة) ويرمز لها $A > 0$ ($A < 0$) إذا كان كل عنصر من عناصر A هو عدد موجب (سالب) [3].

التعريف(12): يسمى المتجه $b=(b_i)$ **متجه مضبب** fuzzy vector إذا كان جميع عناصر b هي أعداد مضببة [3].

التعريف(13): لنفرض أن لدينا النظام الخطي الآتي:

$$\left.\begin{array}{l} a_{11}\times X_1 + a_{12}\times X_2 + \ldots + a_{1n}\times X_n = b_1 \\ a_{21}\times X_1 + a_{22}\times X_2 + \ldots + a_{2n}\times X_n = b_2 \\ \cdot \\ \cdot \\ \cdot \\ a_{n1}\times X_1 + a_{n2}\times X_2 + \ldots + a_{nn}\times X_n = b_n \end{array}\right\} \quad (3)$$

حيث أن مصفوفة المعاملات $A=[a_{ij}]$، $1 \le i,j \le n$ هي مصفوفة مضببة أو اعتيادية بسعة $n \times n$ ، وأن b_i و X_i ، $1 \le i \le n$ هي أعداد مضببة ، فإن هذا النظام يسمى **نظام المعادلات الخطية المضببة** ويكتب على النحو الآتي: $AX= b$ [4] .

4- الطريقة العامة لحل النظام الخطي المضبب كلياً

إذا كان لدينا النظام الخطي المضبب (3) حيث أن مصفوفة المعاملات $A=[a_{ij}]$، $1 \le i,j \le n$ هي مصفوفة أعداد مضببة، فإن هذا النظام يسمى **نظام المعادلات الخطية المضببة كلياً**.

لقد قدَّم الباحث[3] طريقة لحل النظام المضبب كلياً $AX=b$ بالاعتماد على فكرة الضرب التقاطعي، وهذه الطريقة تعالج حالة خاصة هي حالة كون جميع الأعداد المضببة في النظام هي أعداد مثلثية. فقد اعتمد في حل النظام الخطي المضبب كلياً على إشارة العدد المثلثي، اذ تتم المعالجة الرياضية أساساً على كون العدد المضبب موجباً أم سالباً. ولما كانت إشارة العدد المضبب تعتمد على تمثيل قطع- α للعدد المضبب عندما تكون $\alpha=1$، لذلك فرض الباحث [3] في طريقته للحل أن جميع أعداد النظام المضببة هي بشكل مثلثي. فإذا كان X مثلاً هو عدد مضبب مثلثي فإن $L_x(1) = R_x(1)$ فإذا كان X عددا موجباً /سالباً فإن ذلك يعني أن كل من $R_x(1)$ و $L_x(1)$ عدد موجب /سالب. لذلك يصبح من السهل اختبار إشارة العدد المضبب وبالتالي تحديد قاعدة الضرب التقاطعي. الآن ماذا لو كان العدد المضبب X بشكل شبه منحرف وكان $0 < L_x(1)$ و $R_x(1) > 0$ ؟ عندها يصبح من الصعوبة تحديد إشارة العدد المضبب وبالتالي من الصعوبة تحديد قاعدة الضرب التقاطعي. أما الباحث [7] فقد قدَّم طريقة لتحويل الأعداد المضببة بشكل شبه منحرف في النظام $AX=b$ إلى أعداد بشكل مثلثي باستخدام النظام الخطي المضبب المساعد، ثمّ يتم حل النظام الأخير بالطريقة السابقة نفسها ومن ثمّ إعادة الحل المثلثي الناتج إلى شكل شبه المنحرف، لكن هذه الطريقة تحتاج إلى عدد كبير من الحسابات. ولذلك سنقدم خوارزمية مقترحة لحل النظام الخطي المضبب كلياً تعالج مثل هذه المشكلات وتعدّ طريقة عامة لحل أي نظام خطي مهما كان شكل الأعداد المضببة فيه.

إذا كان لدينا النظام الخطي المضبب (3) حيث أن مصفوفة المعاملات $A=[a_{ij}]$، $1 \le i,j \le n$ هي مصفوفة أعداد مضببة بشكل شبه منحرف بسعة $n \times n$ وأن b_i و X_i ، $1 \le i \le n$ هي أعداد مضببة بشكل شبه منحرف، نعرّف المصفوفة الصميمة للمصفوفة A على النحو الآتي:

$$S=\begin{bmatrix} L(S_1) & L(S_2) \\ R(S_2) & R(S_1) \end{bmatrix}$$

حيث أن $L(S_1) + L(S_2)$ تمثل عناصر $L_{aij}(1)$ وإن $R(S_1) + R(S_2)$ تتمثل عناصر $R_{aij}(1)$ ، والعناصر s_{ij} تحدد قيمتها على النحو الآتي:

إذا كانت $0 \le L_{aij}(1)$ فإن:

$s_{ij} = L_{aij}(1),$

إذا كانت $0 > L_{aij}(1)$ فإن:

$s_{i,j+n} = L_{aij}(1),$

إذا كانت $0 \le R_{aij}(1)$ فإن:

$s_{i+n,j+n} = R_{aij}(1),$

إذا كانت $0 > R_{aij}(1)$ فإن:

$s_{i+n,j} = R_{aij}(1),$

وبقية عناصر المصفوفة S تساوي صفراً، لجميع قيم $1 \le i, j \le n$.

4-1 الخوارزمية (1): (الخوارزمية المقترحة)

1. نحل النظام الخطي الآتي (سعته $2n\times2n$) عندما $\alpha=1$:

$$\left.\begin{aligned} &\sum_{j=1}^{n} L_{(aij\times xj)}(1) = L_{bi}(1) \\ &\sum_{j=1}^{n} R_{(aij\times xj)}(1) = R_{bi}(1) \quad ,1 \le i \le n \end{aligned}\right\} \qquad (4)$$

وبالاعتماد على إشارة كل من $L_{aij}(1)$ و $L_{bi}(1)$ نجد قيمة $L_{xj}(1)$ و $1 \le i, j \le n$ على النحو الآتي:

إذا كان $L_{bi}(1) > 0$ و $L_{aij}(1) > 0$ و $1 \le i, j \le n$ فإن:

$L_{(aij\times xj)}(1) = L_{aij}(1) \times L_{xj}(1)$

وإذا كان $L_{bi}(1) < 0$ و $L_{aij}(1) > 0$ و $1 \le i, j \le n$ فإن:

$L_{(aij\times xj)}(1) = R_{aij}(1) \times L_{xj}(1)$

وإذا كان $L_{bi}(1) > 0$ و $L_{aij}(1) < 0$ و $1 \le i, j \le n$ فإن:

$L_{(aij\times xj)}(1) = L_{aij}(1) \times R_{xj}(1)$

وإذا كان $L_{bi}(1) < 0$ و $L_{aij}(1) < 0$ و $1 \le i, j \le n$ فإن:

$L_{(aij\times xj)}(1) = R_{aij}(1) \times R_{xj}(1)$

كذلك بالاعتماد على إشارة كل من $R_{aij}(1)$ و $R_{bi}(1)$ نجد قيمة $R_{xj}(1)$ ، $1 \le i, j \le n$ على النحو الآتي:

إذا كان $R_{bi}(1) > 0$ و $R_{aij}(1) > 0$ ، $1 \le i, j \le n$ فإن:

$R_{(aij\times xj)}(1) = R_{aij}(1) \times R_{xj}(1)$

وإذا كان $R_{bi}(1) < 0$ و $R_{aij}(1) > 0$ ، $1 \le i, j \le n$ فإن:

$R_{(aij\times xj)}(1) = L_{aij}(1) \times R_{xj}(1)$

وإذا كان $R_{bi}(1) > 0$ و $R_{aij}(1) < 0$ ، $1 \le i, j \le n$ فإن:

$R_{(aij\times xj)}(1) = R_{aij}(1) \times L_{xj}(1)$

و إذا كان $R_{bi}(1) < 0$ و $R_{aij}(1) < 0$ ، $1 \le i, j \le n$ فإن:

$R_{(aij\times xj)}(1) = L_{aij}(1) \times L_{xj}(1)$

وبالتالي سنحصل على القيمتين المختلفتين $L_{xj}(1)$ و $R_{xj}(1)$ لجميع قيم $1 \le j \le n$. فإذا كان $R_{xj}(1) \ge L_{xj}(1)$ لجميع قيم $1 \le j \le n$ فهذا يعني أن قيم $L_{xj}(1)$ و $R_{xj}(1)$ التي حصلنا عليها تمثل الحل المضبوط، أما إذا كان $R_{xj}(1) < L_{xj}(1)$ لبعض قيم $1 \le j \le n$ عندها نبدل قيمة $L_{xj}(1)$ فتأخذ قيمة $R_{xj}(1)$ و $R_{xj}(1)$ تأخذ قيمة $L_{xj}(1)$.

.2 باستخدام الحل الذي حصلنا عليه من الخطوة الأولى وبالاعتماد على إشارة هذا الحل وباستخدام المصفوفة الصميمة للمصفوفة A سنحل النظام الخطي الآتي لجميع قيم $\alpha \in [0, 1)$:

$$\sum_{j=1}^{n} L_{(aij\times xj)}(\alpha) = L_{bi}(\alpha) \quad (5a)$$

$$\sum_{j=1}^{n} R_{(aij\times xj)}(\alpha) = R_{bi}(\alpha) \quad ,1 \leq i \leq n \quad (5b)$$

فإذا كان $L_{xj}(1)$ و $R_{xj}(1)$ كلاهما عدد موجب (أو كلاهما عدد سالب) فهذا يعني أن العدد X_j موجب (أو سالب)، وبذلك سيكون حل النظام (5) باستخدام خطوات الحل نفسها كما في [3]. أما إذا كان $R_{xk}(1) > 0$ و $L_{xk}(1) < 0$، حيث ان $1 \leq k \leq n$ فإن حل النظام (5) سيكون على النحو الآتي:

نبدأ على اعتبار أن A مصفوفة مضببة موجبة و b متجه مضبب موجب، ولأجل إيجاد قيمة $L_{xi}(\alpha)$ نحل النظام الخطي (5a) على النحو الآتي:

$$\begin{aligned}\sum_{j=1}^{n} L_{(aij\times xj)}(\alpha) &= L_{bi}(\alpha)\\ &= L_{ai1}(1)\times L_{x1}(\alpha) + L_{ai1}(\alpha)\times L_{x1}(1) - L_{ai1}(1)\times L_{x1}(1)\\ &+\ldots+ L_{aik}(1)\times R_{xk}(\alpha) + L_{aik}(\alpha)\times R_{xk}(1) - L_{aik}(1)\times R_{xk}(1)\\ &+\ldots+ L_{ain}(1)\times L_{xn}(\alpha) + L_{ain}(\alpha)\times L_{xn}(1) - L_{ain}(1)\times L_{xn}(1).\end{aligned}$$

وبالتالي فإن:

$$\begin{aligned}&L_{ai1}(1)\times L_{x1}(\alpha) + \cdots + L_{aik}(1)\times R_{xk}(\alpha) + \cdots + L_{ain}(1)\times L_{xn}(\alpha) = L_{bi}(\alpha) -\\ &\{(L_{ai1}(\alpha) - L_{ai1}(1))\times L_{x1}(1)+\ldots+(L_{aik}(\alpha) - L_{aik}(1))\times\\ &R_{xk}(1)+\ldots+(L_{ain}(\alpha) - L_{ain}(1))\times L_{xn}(1)\}.\end{aligned}$$

لكل $\alpha \in [0, 1)$ و $1 \leq i \leq n$.

ولأجل إيجاد قيمة $R_{xi}(\alpha)$ نحل النظام الخطي (5b) على النحو الآتي:

$$\begin{aligned}\sum_{j=1}^{n} R_{(aij\times xj)}(\alpha) &= R_{bi}(\alpha)\\ &= R_{ai1}(1)\times R_{x1}(\alpha) + R_{ai1}(\alpha)\times R_{x1}(1) - R_{ai1}(1)\times R_{x1}(1)\\ &+\ldots+ R_{aik}(1)\times L_{xk}(\alpha) + R_{aik}(\alpha)\times L_{xk}(1) - R_{aik}(1)\times L_{xk}(1)\\ &+\ldots+ R_{ain}(1)\times R_{xn}(\alpha) + R_{ain}(\alpha)\times R_{xn}(1) - R_{ain}(1)\times R_{xn}(1).\end{aligned}$$

وبالتالي فإن:

$$\begin{aligned}&R_{ai1}(1)\times R_{x1}(\alpha) + \cdots + R_{aik}(1)\times L_{xk}(\alpha) + \cdots + R_{ain}(1)\times R_{xn}(\alpha) = R_{bi}(\alpha)\\ &- \{(R_{ai1}(\alpha) - R_{ai1}(1))\times R_{x1}(1)+\ldots+(R_{aik}(\alpha) - R_{aik}(1))\times\\ &L_{xk}(1)+\ldots+(R_{ain}(\alpha) - R_{ain}(1))\times R_{xn}(1)\}.\end{aligned}$$

لكل $\alpha \in [0, 1)$ و $1 \leq i \leq n$.

وفي حالة كون المصفوفة A سالبة أو المتجه b سالب أو كلاهما سالبين نحل المعادلتين (5a) و (5b)
حسب قاعدة الضرب التقاطعي وبالاعتماد على ما يأتي:
إذا كان العدد $W=X\times Y$ فإنه لدينا الحالات الآتية [3]:

a) إذا كان X و Y عددين مضببين موجبين فإن:

$$Lw(\alpha) = L_x(\alpha).L_y(1) + L_x(1).L_y(\alpha) - L_x(1).L_y(1)$$

$$Rw(\alpha) = R_x(\alpha).R_y(1) + R_x(1).R_y(\alpha) - R_x(1).R_y(1)$$

b) إذا كان X عدد موجب و Y عدد سالب فإن:

$Lw(\alpha) = R_x(\alpha).L_y(1) + R_x(1).L_y(\alpha) - R_x(1).L_y(1)$
$Rw(\alpha) = L_x(\alpha).R_y(1) + L_x(1).R_y(\alpha) - L_x(1).R_y(1)$

(c إذا كان X عدد سالب و Y عدد موجب فإن:

$Lw(\alpha) = L_x(\alpha).R_y(1) + L_x(1).R_y(\alpha) - L_x(1).R_y(1)$
$Rw(\alpha) = R_x(\alpha).L_y(1) + R_x(1).L_y(\alpha) - R_x(1).L_y(1)$

(d إذا كان X و Y عددين مضببين سالبين فإن:

$Lw(\alpha) = R_x(\alpha).R_y(1) + R_x(1).R_y(\alpha) - R_x(1).R_y(1)$
$Rw(\alpha) = L_x(\alpha).L_y(1) + L_x(1).L_y(\alpha) - L_x(1).L_y(1)$

2-4 مثال توضيحي:

إذا كان لدينا النظام الخطي المضبب كلياً الآتي:

$$\left.\begin{array}{l}(7,9,1,1)X_1 + (2,4,1,1)X_2 = (5,7,1,1)\\ (6,8,1,1)X_1 + (3,5,1,1)X_2 = (7,9,1,1)\end{array}\right\} \quad (6)$$

وباستخدام تمثيل قطع- α للأعداد المضببة بشكل شبه منحرف في النظام (6) نحصل على ما يأتي:

$$[6+\alpha, 10-\alpha] \times X_1 + [1+\alpha, 5-\alpha] \times X_2 = [4+\alpha, 8-\alpha]$$
$$[5+\alpha, 9-\alpha] \times X_1 + [2+\alpha, 6-\alpha] \times X_2 = [6+\alpha, 10-\alpha]$$

يمكن كتابة هذا النظام بالصيغة AX= b على النحو الآتي:

$$\begin{bmatrix}[6+\alpha, 10-\alpha] & [1+\alpha, 5-\alpha]\\ [5+\alpha, 9-\alpha] & [2+\alpha, 6-\alpha]\end{bmatrix}\begin{bmatrix}X_1\\ X_2\end{bmatrix} = \begin{bmatrix}[4+\alpha, 8-\alpha]\\ [6+\alpha, 10-\alpha]\end{bmatrix}$$

وحسب الخطوة (1) من الخوارزمية (1) وبما أن:

$L_{bi}(1) > 0$ و $L_{aij}(1) > 0$ ، كذلك $R_{bi}(1) > 0$ و $R_{aij}(1) > 0$ ، لجميع قيم $1 \le i, j \le n$

فإن المصفوفة الصميمة للمصفوفة A مع تمثيل قطع- α للمتغيرين X_1 و X_2 وعندما α =1 تكون على النحو الآتي:

$$\begin{bmatrix}7 & 2 & 0 & 0\\ 6 & 3 & 0 & 0\\ 0 & 0 & 9 & 4\\ 0 & 0 & 8 & 5\end{bmatrix}\begin{bmatrix}L_{x1}(1)\\ L_{x2}(1)\\ R_{x1}(1)\\ R_{x2}(1)\end{bmatrix} = \begin{bmatrix}5\\ 7\\ 7\\ 9\end{bmatrix}$$

وبالتالي نحصل على النظام الاعتيادي الآتي:

$$7L_{x1}(1) + 2L_{x2}(1) = 5$$
$$6L_{x1}(1) + 3L_{x2}(1) = 7$$
$$9R_{x1}(1) + 4R_{x2}(1) = 7$$
$$8R_{x1}(1) + 5R_{x2}(1) = 9$$

وبحل النظام الأخير نحصل على ما يأتي:

$L_{x1}(1) = 0.111$ و $R_{x1}(1) = -0.07$
$L_{x2}(1) = 2.111$ و $R_{x2}(1) = 1.9$

نلاحظ إن $R_{x1}(1) < L_{x1}(1)$، كذلك $R_{x2}(1) < L_{x2}(1)$ ، وحسب الخطوة (1) من الخوارزمية (1) سنقوم بإجراء التغيير الآتي:

$L_{x1}(1) = -0.07$ و $R_{x1}(1) = 0.111$
$L_{x2}(1) = 1.9$ و $R_{x2}(1) = 2.111$

وبالتالي فإن المصفوفة الصميمة للمصفوفة A ستكون على النحو الآتي:

$$\begin{bmatrix} 0 & 0 & 7 & 2 \\ 0 & 0 & 6 & 3 \\ 9 & 4 & 0 & 0 \\ 8 & 5 & 0 & 0 \end{bmatrix}$$

كما نلاحظ إن $L_{x2}\ (1)$ و $R_{x2}\ (1)$ كلاهما عدد موجب وهذا يعني (حسب التعريف (10)) أن العدد X_2 موجب، أما بخصوص العدد X_1 فإن $R_{x1}\ (1) > 0$ و $L_{x1}\ (1) < 0$ وحسب الخطوة (2) من الخوارزمية (1) سنحل النظام (6) على النحو الآتي:

$$\begin{bmatrix} 0 & 0 & 7 & 2 \\ 0 & 0 & 6 & 3 \\ 9 & 4 & 0 & 0 \\ 8 & 5 & 0 & 0 \end{bmatrix} \begin{bmatrix} L_{x1}\ (\alpha) \\ L_{x2}\ (\alpha) \\ R_{x1}\ (\alpha) \\ R_{x2}\ (\alpha) \end{bmatrix} = \begin{bmatrix} L_1 \\ L_2 \\ R_1 \\ R_2 \end{bmatrix}$$

حيث أن:

$$\begin{aligned} L_1 = {} & L_{b1}(\alpha) - [(L_{a11}(\alpha) - L_{a11}(1)).\, R_{x1}(1) + (L_{a12}(\alpha) - L_{a12}(1)).\, L_{x2}(1)] \\ = {} & (4+\alpha) - [(6+\alpha-7)(0.111) + (1+\alpha-2)(1.9)] \\ = {} & 6.011 - 1.011\,\alpha \end{aligned}$$

$$\begin{aligned} L_2 = {} & L_{b2}(\alpha) - [(L_{a21}(\alpha) - L_{a21}(1)).\, R_{x1}(1) + (L_{a22}(\alpha) - L_{a22}(1)).\, L_{x2}(1)] \\ = {} & (6+\alpha) - [(5+\alpha-6)(0.111) + (2+\alpha-3)(1.9)] \\ = {} & 8.011 - 1.011\,\alpha \end{aligned}$$

$$\begin{aligned} R_1 = {} & R_{b1}(\alpha) - [(R_{a11}(\alpha) - R_{a11}(1)).\, L_{x1}(1) + (R_{a12}(\alpha) - R_{a12}(1)).\, R_{x2}(1)] \\ = {} & (8-\alpha) - [(10-\alpha-9)(-0.07) + (5-\alpha-4)(2.11)] \\ = {} & 5.96 + 1.04\,\alpha \end{aligned}$$

$$\begin{aligned} R_2 = {} & R_{b2}(\alpha) - [(R_{a21}(\alpha) - R_{a21}(1)).\, L_{x1}(1) + (R_{a22}(\alpha) - R_{a22}(1)).\, R_{x2}(1)] \\ = {} & (10-\alpha) - [(9-\alpha-8)(-0.07) + (6-\alpha-5)(2.11)] \\ = {} & 7.96 + 1.04\,\alpha \end{aligned}$$

أي إن:

$$\begin{bmatrix} 0 & 0 & 7 & 2 \\ 0 & 0 & 6 & 3 \\ 9 & 4 & 0 & 0 \\ 8 & 5 & 0 & 0 \end{bmatrix} \begin{bmatrix} L_{x1}\ (\alpha) \\ L_{x2}\ (\alpha) \\ R_{x1}\ (\alpha) \\ R_{x2}\ (\alpha) \end{bmatrix} = \begin{bmatrix} 6.011 - 1.011\,\alpha \\ 8.011 - 1.011\,\alpha \\ 5.96 + 1.04\,\alpha \\ 7.96 + 1.04\,\alpha \end{bmatrix}$$

وبالتالي نحصل على النظام الخطي الاعتيادي الآتي:

$$\begin{aligned} 7R_{x1}(\alpha) + 2R_{x2}(\alpha) &= 6.011 - 1.011\,\alpha \\ 6R_{x1}(\alpha) + 3R_{x2}(\alpha) &= 8.011 - 1.011\,\alpha \\ 9L_{x1}(\alpha) + 4L_{x2}(\alpha) &= 5.96 + 1.04\,\alpha \\ 8L_{x1}(\alpha) + 5L_{x2}(\alpha) &= 7.96 + 1.04\,\alpha \end{aligned}$$

وبحل النظام الخطي الأخير نحصل على:

$L_{x1}(\alpha) = -0.15 + 0.08\alpha$ و $R_{x1}(\alpha) = 0.22 - 0.112\alpha$,

$L_{x2}(\alpha) = 1.832 + 0.08\alpha$ و $R_{x2}(\alpha) = 2.23 - 0.113\alpha$.

أي إن الحل المضبوط للنظام الخطي (6) هو:

$$X_{1_\alpha} = [L_{x1}(\alpha), R_{x1}(\alpha)] = [-0.15 + 0.08\alpha\ ,\ 0.22 - 0.112\alpha]$$

$$X_{2_\alpha} = [L_{x2}(\alpha), R_{x2}(\alpha)] = [1.832 + 0.08\alpha, 2.23 - 0.113\alpha\ ] .$$

إن هذا الحل هو بشكل تمثيل قطع-α، والصيغة الاعتيادية المقابلة للعددين X_1 و X_2 هي:

$X_1=$ (-0.07, 0.108 , 0.08 , 0.112) ,
$X_2=$ (1.912 , 2.117 , 0.08 ,0.113).

وهذين العددين المضببين موضحين في الشكلين(1) و(2) الآتيين:

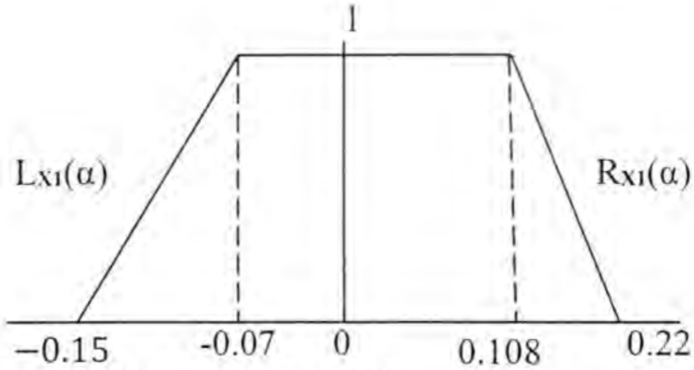

الشكل-1: العدد المضبب X_1.

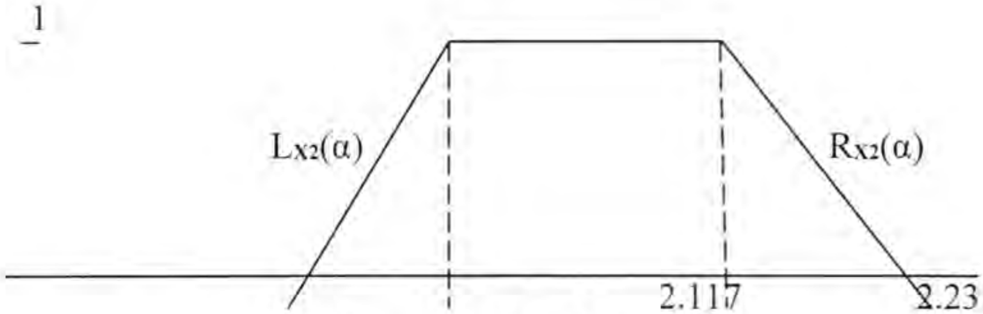

شكل-2: العدد المضبب X_2.

وكما هو واضح من الشكلين السابقين فإن X_1 على شكل شبه منحرف ويكافئ العدد المضبب "تقريبا 0"، في حين أن X_2 هو أيضا على شكل شبه منحرف ويكافئ العدد المضبب "تقريبا 2". وبالعودة الى النظام الخطي المضبب (6) والذي يمكن تمثيله بالمعادلة:

$$\begin{bmatrix} (7,9,1,1) & (2,4,1,1) \\ (6,8,1,1) & (3,5,1,1) \end{bmatrix} \begin{bmatrix} X_1 \\ X_2 \end{bmatrix} = \begin{bmatrix} (5,7,1,1) \\ (7,9,1,1) \end{bmatrix}$$

نجد أن b_1 يكافئ العدد المضبب شبه منحرف "تقريبا 6" و b_2 يكافئ العدد المضبب شبه منحرف "تقريبا 8" وأن عناصر المصفوفة A اعداد مضببة بشكل شبه منحرف على النحو الآتي:

a_{11} يكافئ "تقريبا 8" وa_{12} يكافئ "تقريبا 3" و a_{21} يكافئ "تقريبا 7" و a_{22} يكافئ "تقريبا 4"، فمن المعقول أن يكون حل النظام (6) هو العددان المضببان بشكل شبه منحرف X_1 الذي يكافئ "تقريبا 0" و X_2 الذي يكافئ "تقريبا 2".

5- الاستنتاجات:

إن الخوارزمية المقترحة تمكننا من حل أي نظام خطي مضبب مهما كان شكل الأعداد المضببة فيه، كما إن الحل بهذه الطريقة يكون أسهل من الطرق السابقة وذلك لإمكانية تحديد قاعدة الضرب التقاطعي باستخدام تمثيل قطع- α للعدد المضبب وبالاعتماد على إشارة الدالتين $R(\alpha)$ و $L(\alpha)$ عندما α تساوي واحد، وليس بالاعتماد على إشارة العدد المضبب نفسهُ كما هو عليه في الطرق السابقة إذ إنه من الصعوبة تحديد إشارة بعض الأعداد المضببة، كما أن هذه الطريقة تمكننا من إيجاد المصفوفة الصميمة

في حالة كون الأعداد بشكل شبه منحرف دون الحاجة إلى تحويلها إلى أعداد مثلثية كما في طريقة الحل باستخدام النظام المساعد، وبذلك تكون الطريقة المقترحة أكثر عمومية من الطريقتين السابقتين.

المصادر

1. الخياط، باسل يونس ذنون (2011) "مدخل إلى النمذجة الرياضية باستخدام MATLAB -الجزء الأول"، دار ابن الأثير للطباعة والنشر، جامعة الموصل.
2. Klir G.J. , Clair U. st. , and Yuan, Bo(1997). "Fuzzy Set Theory", Prentice Hall PTR.
3. Rouhparvar, H., Allahviranloo T., (2007)."A method for fully fuzzy linear system of equations", First Joint Congress on Fuzzy and Intelligent Systems Ferdowsi University of Mashhad, Iran, 29-31Aug.
4. Mosleh M. , Abbasbandy S., Otadi M., (2007)." Full fuzzy linear systems of the form Ax+b=Cx+d", First Joint Congress on Fuzzy and Intelligent Systems Ferdowsi University of Mashhad, Iran, 29-31Aug.
5. Amir Sadeghi, Ahmad Izani Md. Ismail and Ali F. Jameel. (2011)."Solving systems of fuzzy differential equation", International Mathematical Forum, Vol. 6 No.42, pp.2087-2100.Malay
6. Klir G.J. , and Yuan, Bo(1995). "Fuzzy Sets And Fuzzy Logic". Prentice Hall PTR.
7. Nasseri S.H., Gholami M., (2011). "Linear system of equations with trapezoidal fuzzy numbers", The Journal of Mathematics and Computer Science Vol.3 No.1, pp.71-79.

دراسة تأثير استخدام الصور الملتقطة والمحسنة بشدات اضاءة مختلفة على اخفاء البيانات باستخدام طريقة استبدال البت الاقل اهمية

علي عبد داود الزكي[1] و سجى علي ابراهيم [2] و سليمة سلطان سلمان[3] وانوار حسن مهدي[4]
[4,1] كلية العلوم / الجامعة المستنصرية
[2] معهد الصحة العالي / المنصور
[3] كلية الصيدلة / جامعة بغداد
تاريخ تقديم البحث 2013/3/23 - تاريخ قبول البحث 2013/9/15

ABSTRACT

The research aims to study the process of information hiding in a color image which taken with different lighting, which has been improved this image captured depend on technology Retinax, has been studying the effect of information hiding on the image and the amount of noise and distortion, which affects the image, which has been compared to histogram and characteristics of statistical image of the cover(captured and improved technology Retinax) before and after the hiding information , the results showed the efficiency of the use of imagery and improved with different in Lighting hide data using the method of LSB, this method worked to hidden data without a case of deformation of the original image, or the possibility note change occurring by the process of hidden information.

الخلاصة

يهدف البحث الى دراسة عملية اخفاء البينات النصية في صورة ملونة ملتقطة بشدات اضاءة مختلفة ، حيث تم تحسين هذه الصورة الملتقطة بالاعتماد على تقنية Retinax ، وتم دراسة تأثير عملية الاخفاء على الصورة ومقدار الضوضاء والتشوه الذي يصيب الصورة ،حيث تم مقارنة المخططات التكرارية والخصائص الاحصائية لصورة الغطاء (الملتقطة والمحسنة بتقنية Retinax) قبل وبعد اخفاء المعلومات فيها لقد بينت النتائج كفاءة استخدام الصور الملتقطة والمحسنة بشدات اضاءة مختلفة في اخفاء البيانات باستخدام طريقة استبدال البت الاقل اهمية ، نجحت هذه الطريقة في إخفاء البيانات النصية دون حدوث حالة تشوه للصورة الأصلية، أو إمكانية ملاحظة التغيرات الحاصلة فيها جراء عملية الإخفاء.

المقدمة

أن هناك ملفات عديدة في الحاسوب من الممكن أستخدامها كوسط لإخفاء الرسالة السرية ومن هذه الأوساط هي الصور الثابتة .يمكن اخفاء المعلومات بطرق مختلفة في الصور .لاخفاء المعلومات يتم ادخال الرسالة مباشرة قد يرمز كل بت من المعلومات في الصورة او يمكن تضمين الرسالة من خلال اختيار مكان الضوضاء والتي لا تلفت النظر – حيث يكون هناك اختلاف في اللون الطبيعي في هذه المناطق بكثرة [1] .

توجد عدد من الطرائق لاخفاء المعلومات في الصور الرقمية ومنها:

- ادخال البت الاقل اهمية LSB .
- التقنيع والترشيح Masking and Filtering
- الخوارزميات والتحويلات Algorithms and Transformations

بصورة عامة فان الحاسوب يتعامل مع الصورة على أنها مصفوفة ثنائية الأبعاد كل موقع فيها يمثل نقطة او ما يعرف بعنصر الصورة (pixel) وهي أصغر وحدة لتمثيل موقع معين على الشاشة ، وكلما زاد عدد عناصر الصورة (Pixel) ضمن حدود ثابتة ازداد تقارب هذه الصورة من الواقع لتحسس العين البشرية لحقائق هذه الصورة وهذا ما يسمى بـ (Resolution) والتجمع لهذه النقاط بقيمها الخاصة من الألوان (Red, Green, Blue) وتدعى بـ -(RGB) يكون لنا الصورة المرئية بحيث يمكن للعين المجرد إدراكها من نوع 24 bit/ pixel تمثيل كل نقطة من نقاط المصفوفة يكون من خلال استخدام ثلاث من الوحدات الخزنيه أو ما يدعى بالبايت، حيث يمكن لنا أن نحصل على مزيج لوني ما مقداره (255*255*255) من الألوان

الرئيسية الثلاث حيث يخصص بايت واحد لكل لون من الألوان وللبايت الواحد إمكانية تمثيل التدرج اللوني لكل لون من (255 – 0) الذي يمثل مدى التدرج لكل لون ، وبذلك نجد ان (3 byte) لها القدرة على توليد ما مقداره (16.777.216) من الالوان ومن خلال دمج هذه الـ (3 byte) أو إلحاقها مع بعضها نحصل على قيمة عددية تمثل لون تلك النقطة .أن هذه الصور الرقمية سوف تستخدم كحاوية للرسالة والمعلومات سوف تخزن على شكل رقم ثنائي يضاف الى الرقم الثنائي الاقل اهميةLeast Significant Bit لان الأرقام الثنائية السبع الأخرى تحتوي على معلومات كافية لتمثيل اللون الصحيح لتلك الوحدة الصورية ، وعند تغيير الرقم الثنائي الأقل أهمية لا يؤثرذلك على الصورة بشكل ملحوظ [1] ومن الأبحاث التي إهتمت بتطوير تقنيات الإخفاء.

- أقترح بسام حسن محمود في عام 2006 خوارزمية لتقييم عملية الإخفاء بتنفيذه الطرائق الأساسية للإخفاء(LSB,DCT and DWT) من خلال اخفاء نص في صورة . و استخدام تقنية رفع الضوضاء، وتقنية تخمين الضوضاء كأداة جديدة لقياس وتقييم عملية الاخفاء. وكذلك استخدم القوانين الاحصائية لمعرفة هل هناك شك بوجود إخفاء داخل الوسط (الصورة) ام لا ، ثم طبق عملية تخمين للضوضاء في الصورة ثم أجرى عملية رفع للضوضاء وطبق عملية استخلاص للمعلومات المخفية لفحص مدى رصانة طريقة الاخفاء [2].
- استخدمت سوزان صباح في 2007 للإخفاء ملفاً فديويا متداخلاً من نوع(AVI)، وقسّمت هذا الملف الى جزئين فديو و صوت، الفيديو عبارة عن سيل من الهياكل الصورية ، كل هيكل يخزن كملف صورة من نوع BMP ، ثم اختارت عدد الهياكل الصورية المطلوبة لغرض استخدامها كغطاء، جزء الصوت من الملف الصوتي الصوري المتداخل (AVI) يفصل كملف صوت من نوع WAV. وقد استخدمت طريقتين للإخفاء ، الطريقة الأولى هي البت الأقل أهميةLSB ، والطريقة الثانية هي نظام التحويل الموجي هار Haar]Wavelet Transform[3].

التباين والاضاءة

يشير مصطلح التباين إلى مقدار الاختلاف بين الإضاءة المختلفة لعناصر الصورة إذ على أنه النسبة بين إضاءة الأجسام وإضاءة الخلفية التي تقع" عليها الاجسام يعرف التباين Contrast إذ يعتمد التحسس للتباين على التوزيع ألحيزي للمناطق المضيئة والمعتمة إن شدة الإضاءة أو السطوع (Brightness)المتوافرعند التقاط الصورة الذي يعبر عن كمية الضوء المنعكس من أو المنتقل من خلال الكائن object الذي يلتقط بواسطة الكاميرا ، فالتباين الجيد هو الذي تتوافر فيه مستويات اضاءة تكون مختلفة فيما بينها بشكل يجعل الصورة واضحة المعالم فكلما توفرات الاضاءة الكافية تصبح الصورة واضحة المعالم وذات تباين لوني واضاءة مقبولة أما التباين السيئ(Bad Contrast) فينشأ عندما يكون الاختلاف بين مستويات الإضاءة إما قليلاً بحيث يجعل الصورة باهتة الألوان لا يمكن تمييزمعالمها وتسمى هذه الحالة بقلة التباين Low Contrast أو يكون الاختلاف كبيراً إلى درجة يجعل مناطق من الصورة معتمة جداً ومناطق أخرى ساطعة وتسمى هذه الحالة التباين العالي(High Contrast) وفي كلا النوعين تكون الصورة ذات ظهور مرئي غير جيد مما أدى إلى ضرورة معالجة هذه المشكلة.

اللـون

يستجيب نظام الرؤية في عين الإنسان لمدى واسع من مستويات الإضاءة وهذه الاستجابة تختلف اعتمادا على معدل الإضاءة الملاحظ والمحدد بحد العتبة للعتمة (Dark Threshold) وحد للسطوع (Glare Limited)فالكثافات الضوئية التي هي أقل من حد العتبة للعتمة تكون معتمة جداً بحيث لا تُرى أما الكثافات التي أكثر من حد السطوع تكون مضيئة جداً حيث يصعب على الناظر تمييز تفاصيل الصورة [4]. ويعرف اللون بأنه " صفة للإدراك المرئي لضوء ذو طول موجي معين يوصف كل طول موجي معين بصفة مثل(الأحمر، الأخضر، أبيض) ...وذلك

حسب تأثير الضوء في شبكية العين،[5]حيث يوجد بعض الألوان الرئيسية وبمزج هذه الألوان تنتج ألوان جديدة بتدريجات مختلفة ماعدا التدريجات الرمادية إذ لا تعد أحدى صفات اللون ، لذا يوجد تصنيفان للون [6] :-

1- (Chromatic colors): ويقصد أي لون ذي صبغة أي ألوان الطيف المعروفة ماعدا الأبيض والأسود والتدريجات الرمادية.

2- (Achromatic colors) : التي لا تعتبر لوناً نقياً ذا صبغة مثل (الأبيض والأسود والتدريجات الرمادية).

تحسين الصور باستخدام ريتنكس

تستخدم هذه الطريقة لتحسين الصور ذات الترددات العالية حيث تقوم بعملية توصيل الفجوة بين الصورة والعين . تعتمد هذه الطريقة على استخدام مرشح كاوس في بداية الأمر لكشف حافة الصورة ومن ثم يستخدم مرشح متماثل يمرر بشكل دائري لأجل إعادة صيغة الصور إلى شكل أفضل ، وذلك باستخدام ثلاث خوارزميات [7]:

الخوارزمية الأولى: تقوم بحساب القيم الجديدة لكل نقطه ضوئية من خلال الجمع المتتابع لمجموعة النقاط ألمحيطه بها وبمسار غير منتظم (عشوائي).

الخوارزمية الثانية: فانها تعمد على حساب القيم بطريقة تكرارية للنقاط التي يتم الحصول عليها

من الخوارزمية الأولى كما موضح بالمعادلة[7]

$$R = \sum_{n=1}^{N} \omega_n \{\log I_i(x,y) - \log[F_n(x,y) * I(x,y)]\}$$

حيث ان:

N : عدد نقاط التعيير التي تم الحصول عليها من الخوارزمية الأولى

ω : الوزن الذي يربط بين نقاط القياس

N=3, ωn=1/3,

$\boldsymbol{F_n}$: داله كاوس عند النقطة n.

$\boldsymbol{I_n}$:توزيع الصورة عند النقطة n (Image distribution) .

الخوارزمية الثالثة: وفي الثالثة يتم حساب النقاط الضوئية التي تم الحصول عليها من الخوارزمية الثانية وذلك بحساب الفرق بين لنقطة التي تمت معالجتها مع مجموع النقاط ألمحيطه به [7].

الشكل (1) يفيد مخطط خوارزمية الاخفاء المحسن.

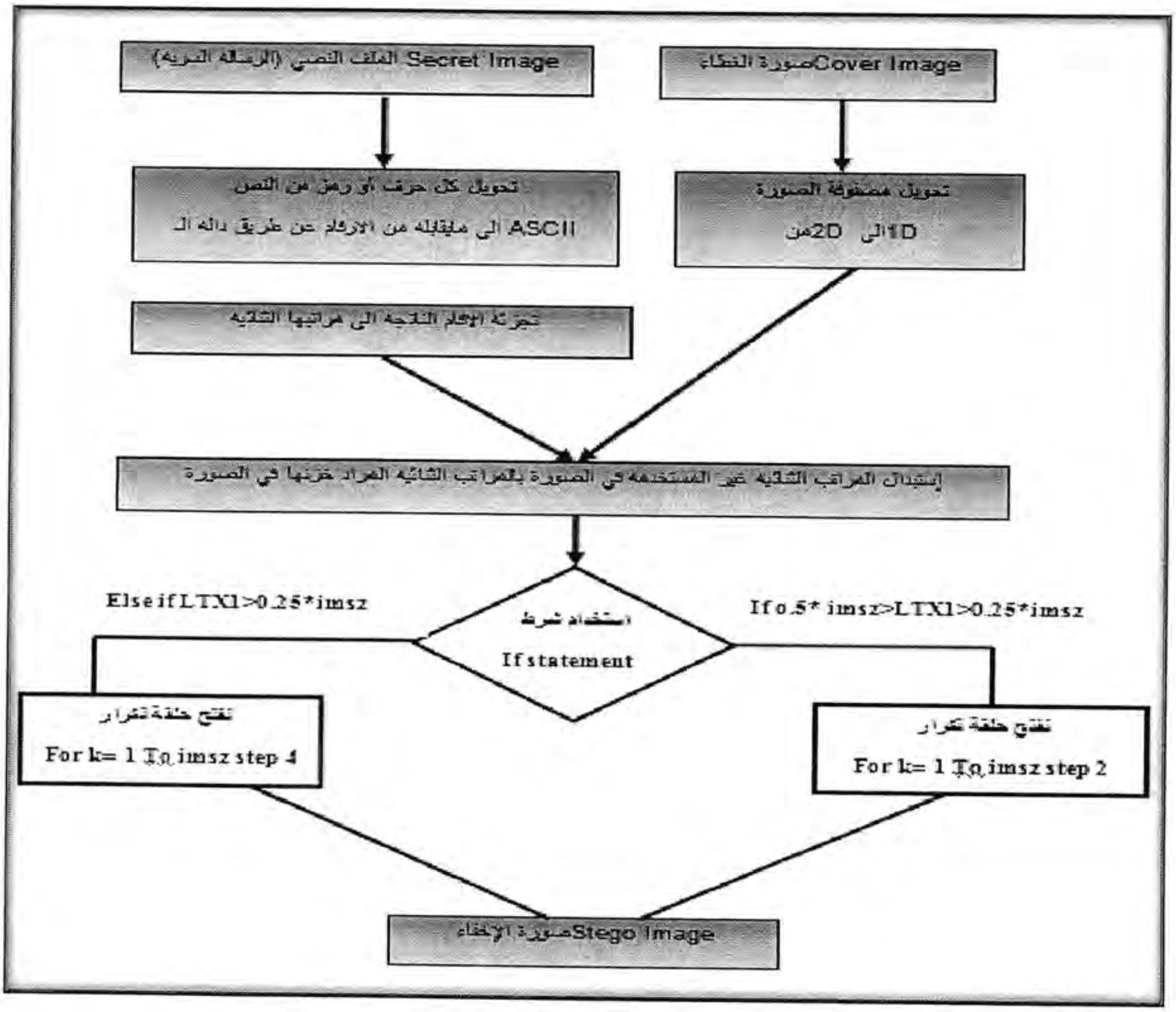

شكل-1:مخطط الخورازمية لتقنية الاخفاء المحسنة

منظومة العمل

تم تصميم منظومة التصوير الموضحة في الشكل (2) ، تتألف منظومة التصوير من صندوق مظلم يحتوي الصندوق في احد جوانبه على مصدر الإضاءة (مصباح من جهة اليمين و أخر من جهة اليسار) للحصول على إضاءة غير منتظمة وفي نفس الجانب أسفل مصدر الإضاءة توجد فتحة للتصوير توضع عليها الكاميرا وفي الجانب الاخر توضع الصورة المراد تصويرها تحت شروط الإضاءة المختلفة .

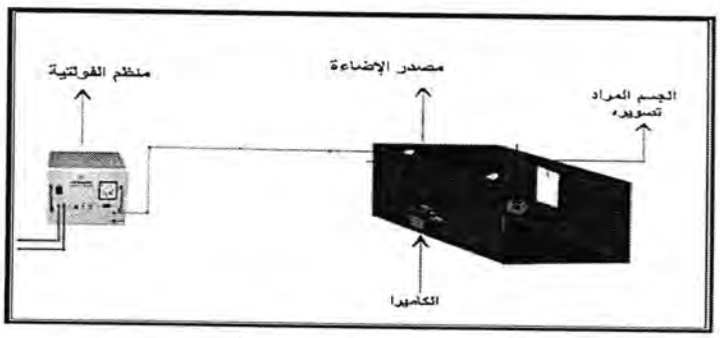

شكل-2: منظومــــــة التصوير المستخدمة

اعتمدت في هذه الدراسة على صورة تم التقاطها بوساطة الكاميرا الرقمية Sony Digital Camera ولشدات إضاءة مختلفة بالاعتماد على الفولتية المسلطة على المصدر الضوني وقد تم التقاط 11 صورة ولحالات إضاءة مختلفة لمصدر الإضاءة والشكل (3) يوضح الصور الناتجة لحالات الاضاءة المختلفة .

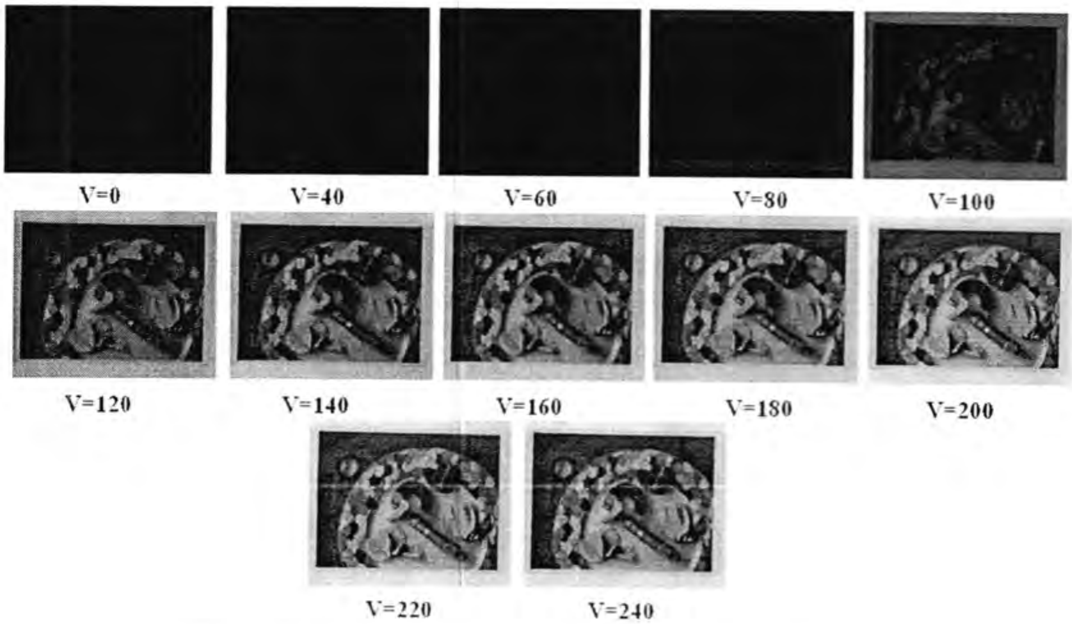

شكل-3: الصور الناتجة ذات فولتيات إضاءة مختلفة (شدات اضاءة مختلفة)

لتحسين الصور مختلفة الإضاءة الناتجة من منظومة التصوير تم الاعتماد على تقنية ريتنكس باستخدام مرشح كاوس وكانت نتائج التقنية موضحة بالشكل (4) لكافة حالات الاضاءة المختلفة

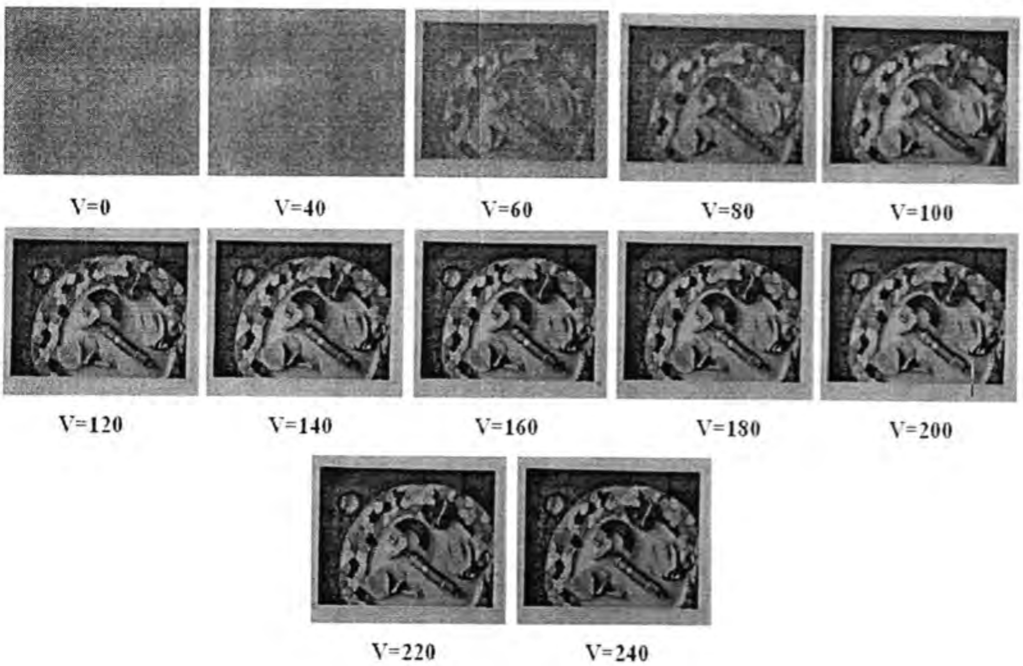

شكل-4: الصور مختلفة الإضاءة الناتجة من تقنية التحسين ريتنكس

تم اعتماد الصور الملتقطة بشدات اضاءة مختلفة والمحسنة في اخفاء البيانات وتم توضيح المخططات التكرارية للصور الملتقطة والمحسنة بشدات اضاءة مختلفة قبل وبعد اخفاء المعلومات حيث تم استخدام تقنية الاخفاء المحسن ، اذ يتم الاخفاء في عناصر معينة ويتم اختبارها وفق شرط محدد . الشكل (5) يوضح المخطط التكراري للصور الملتقطة والمحسنة بشدات اضاءة مختلفة قبل اخفاء المعلومات ، وكذلك يوضح المخطط التكراري لصور الملتقطة والمحسنة بشدات اضاءة مختلفة بعد اخفاء المعلومات ، وبمقارنة المخططات التكرارية للصور قبل وبعد الاخفاء تبين ان اغلب المخططات التكرارية بعد الاخفاء مقاربة الى حد كبير للمخطط الاصلي (قبل الاخفاء) .

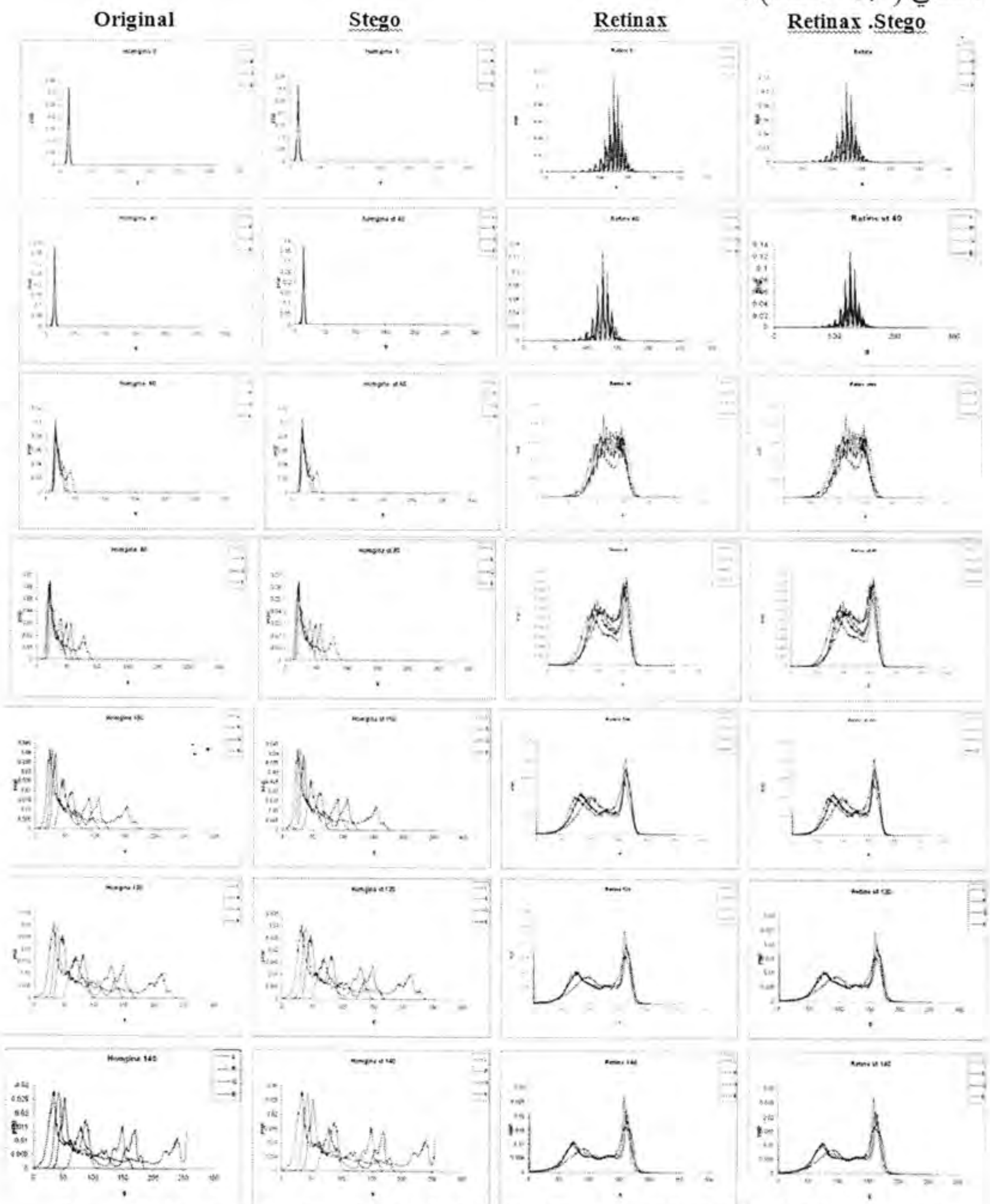

شكل-5: المخططات التكرارية للصور مختلفة الاضاءة الاصلية والمحسنة قبل وبعد اخفاء المعلومات

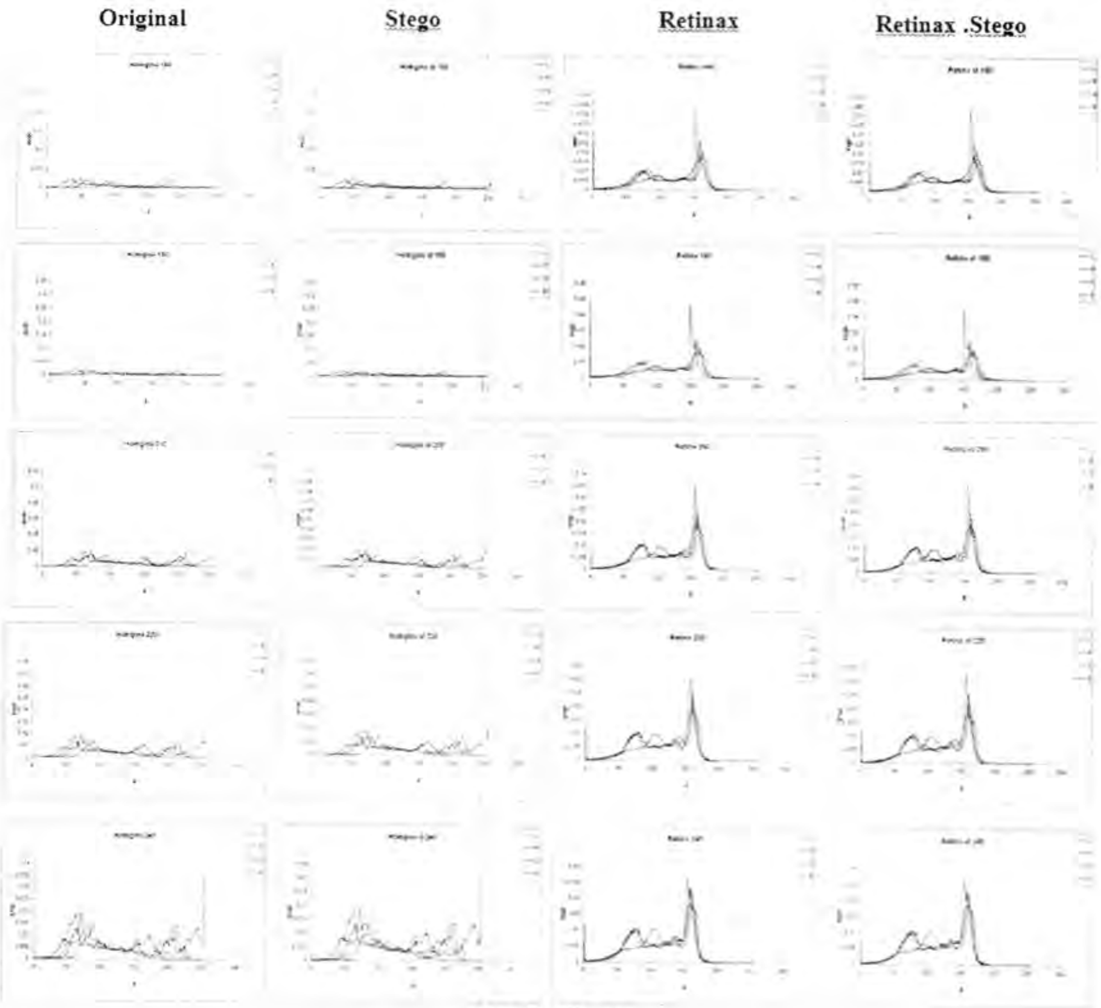

تابع للشكل (5)

الاستنتاجات

اثبت تقنية ريتنكس كفاءة عالية في تحسين الصور الملتقطة بشدات اضاءة مختلفة والمستخدمة في اخفاء المعلومات حيث يوضح المخطط التكراري للصور الملتقطة والمحسنة بشدات اضاءة مختلفة بعد اخفاء المعلومات ، وبمقارنة المخططات التكرارية للصور قبل وبعد الاخفاء تبين ان اغلب المخططات التكرارية بعد الاخفاء مقاربة الى حد كبير للمخطط الاصلي (قبل الاخفاء) ، وبشكل عام فان تقنية الاخفاء المحسن افضل من تقنية الاخفاء التقليدي ، لان اخفاء المعلومات بالتقنية المحسنة يسبب ضوضاء اقل مما لو استخدمت التقنية التقليدية .

المصادر

1. Cristobal, Patricia; “Steganography: A Privacy Protector or Just a Computer Security Trick?” SANS Institute FIRE 2003 as part of GIAC practical repository. Washington D. C. ‹2003.
2. Bassam, H., Mahmoud “Information Hiding Metrics" Thesis, the Informatics Institute for Postgraduate Studies of the Iraqi Commission for Computers and Informatics, 2006.
3. Susan, S., Ghazoul “Development of Information Hiding System Based on AVI Format" MSC. Thesis,Technology University 2007.

4. Umbaugh Cott E.,"Computer Vision and Image Processing Practical Approach using CVIP tools", Practice Hall، 1998.
5. Meylan, L.، "Color image enhancement using a Retinex-based adaptive filter" Master thesis in computer science at EPFL، 2002.
6. Tinku acharya and Ajoy k.Ray, "Image processing Principles and Applications", Prentice Hall, New jersey, 2005.
7. Cooper, "Modifications retinex to reset nonlinearity and implement segmentation constraints" The Human Vision and Electronic Imaging VII Conference, Vol 4662, pp. 349- 357, 2002.